CUK-H01186-15-P014370

AGRA UNIVERSITY JOURNAL OF RESEARCH

Vol. XV, Part I *SCIENCE* **January, 1966**

Index

Abbr.—*Agra Univ. J. Res. (Sci.)*

CALCUTT

15

PUBLISHED BY
THE REGISTRAR, AGRA UNIVERSITY,
AGRA, 1966.

Annual Subscription : Inland Rs. 15/- ; Foreign Rs. 20/-

P14370

Chancellor
Sri Biswanath Das, Gove r Pradesh State.
Vice-Chancellor
Dr. S. Ranjan, M. Sc. (C , D. Sc. (State France), F.N.I.
Registrar
Sri R. S. Agarwal
Editor
Dr. M. Ray, D. Sc., F. N. I.
Advisory Committee
Dr. S. P. Srivastava, M.S., F.R.C.S.
Dr. S. N. Singh, M. Sc., Ph. D.
Dr. A. Roy, M. Sc., Ph. D.
Dr. D. D. Pant, M. Sc., D. Sc.
Dr. P. I. Ittyerah, M. Sc., Ph. D.
Dr. V. Puri, D. Sc., F.N.I.
Dr. R. D. Saksena, M. Sc., Ph. D.
Dr. Mata Prasad, D. Sc., F. R. I. C., F. N. I.
The Registrar (*Ex-officio*)

Edited by Dr. M. Ray, D. Sc., F. N. I., Principal, Agra College, Agra, Published by Sri R. S. Agarwal, Registrar, Agra University, Agra, and Printed by Mr. H. K. Kapur, Agra University Press, Agra. (J-1486)

CONTENTS

PAGE

1. Steady flow in a straight tube; section—A hyperbolic sector. *By* J.P. AGARWAL 1
2. Morphology of the Head capsule and mouth parts of onitis philemon Fabr. (Coleoptera-Coprine). *By* P.S. VERMA 7
3. A Note on the kinetics of silver catalysed oxidation of glucose by potassium persulphate. *By* C. P. KHULBE & S. P. SRIVASTAVA 27
4. The alimentary canal of hister maindronii lewis (Coleoptera-Histeridae). *By* R. D. SAKSENA & P. S. VERMA .. 37
5. On a new species of the genus *Cranopygia* Burr (Dermaptera: Pygidicranidae) from South India. *By* V.C. KAPOOR .. 47
6. Absorption spectra of some new ketones Part II—Absorption spectra of α-bromo-α-formyl-p-bromo acetophenone. *By* D.D. PANT, O.N. PERTI, K.P. VERMA & G.C. SINGHAL 51
7. A note on the distribution of Indian collembola. *By* H.N. BAIJAL 55
8. Steady flow in a uniform straight tube of a particular type of section. *By* G. C. SHARMA 59
9. Influence of Presowing seed-treetment with NAA on early growth of Maize seedlings. *By* V. S. RATHORE & S.N. BHARDWAJ 67
10. Rotation of finite disc in Rotating fluid : Boundary layer growth : Motion started impulsively from rest. *By* HAR SWARUP SHARMA 71
11. The heart of fresh water Eel, *Macrognathus Aculeatus* (Bl). *By* V.P. AGRAWAL & R.C. DALELA 83
12. Circulatory system and associated tissues of *Syrphus Balteatus* De Geer (Syrphidae : Diptera). *By* J.L. NAYAR .. 91
13. A contribution to the aquatic and marshy plants of Kanpur. *By* S. BHAMBIE.. 99

ABSTRACT OF THESES

14. A study of soap gels in non-aqueous solvents. *By* R. C. SETH 115
15. Studies on pathogenesis of *clostridium chauvoei* infection in healthy, immunised and traumatised guineapigs. *By* S.N. DIXIT 121

CALCUTTA UNIVERSITY CENTRAL LIBRARY

PAGE

16. Study of aldosterone and its relationship with the changes in plasma volume and electrolytes in Pathogenesis of Human ascites due to cirrhosis of liver. *By* R.R. Bodkhe .. 125

17. Morphological studies in the family Flacourtiaceae. *By* G. GOPAL KRISHNA 131

18. Studies on Adsorption Indicators. *By* K.N. TANDON .. 135

19. Immune and antibody response in Rabbits and dairy cattle against staphylococcal vaccines. *By* B.S. MALIK .. 139

20. Studies on Indian araeopidae [=Delphacidae] (Homoptera, Fulgoroidea). *By* A.N.T. JOSEPH 141

21. Morphological and anatomical studies of the flower of Helobiae. *By* VIRENDRA SINGH 147

22. Studies on anthracnose diseases of Mango (*Mangifera Indica* L.), guava (*Psidium Guajava* L.) and citrus (*Citrus* Spp.). *By* B.B. SINGH 151

23. Factors affecting roughage utilisation in Ruminants. *By* NIRANJAN NATH PANDIT 157

24. Cytological, cytochemical and Histological studies in experimentally induced cancer of cervix in mice [With correlative studies on human patients]. *By* DR. (Km.) USHA KEHAR 165

25. Fractional integration and certain integral Transforms. *By* JAG MOHAN CHANDRA JOSHI 171

26. Absorption and fluorescence spectra, hyperfine structure and the Zeeman effect of Ho^{3+} in hexagonal $LaCl_3$ at very low temperatures. *By* BHUWAN CHANDRA PANDEY .. 183

27. Investigations on the Structure of the Hemicelluloses from bagasse. *By* BIMAL CHANDRA BANERJEE. 191

CALC
UNIVERS
CEN
LIBR

CONTENTS

PAGE

1. Action of Ultraviolet Radiations on aqueous solution of Ornithine and Lysine. *By* O. N. Perti & R. C. Rastogi .. 1
2. On a new species of Cockroach from North-West Himalayas. *By* H. N. Baijal & V. C. Kapoor 5
3. A study of the Fish fauna of Visakhapatnam district (Andhra Pradesh)—Its Disposal and Marketing. I. Scope for the Development of Inland fisheries in Visakhapatnam district. *By* M. V. Subba Rao & Ratan Singh 9
4. Study of the cooling curves of Gel-forming solutions of sodium oleate and sodium erucate in a fraction of Turpentine. *By* R. C. Seth 13
5. On the pathogenic significance of the Tapeworms hitherto reported from some of the fresh water fishes. *By* P. Rai .. 23
6. Studies on floral biology of Karaunda (*Carissa Carandas* Linn.) *By* Ayodhya Prasad 31
7. Morphological and Anatomical studies in Helobiae VIII. Vascular anatomy of the Flower of Hydrocharitaceae—Stratioideae and Thalassioideae. *By* V. Singh 43
8. Some Kernels in the Hankel Transform of two variables—I. *By* R. P. Gupta 61
9. Morphology of the male pink sugarcane Mealybug, *Saccharicoccus Sacchari* Cockerell (Pseudococcidae: Homoptera) Pt. I. Macropterous Form. *By* R. L. Yadava 71
10. Stress distribution in a Non-Newtonian Liquid in the presence of a Line Source. *By* Prem Dayal Narang 131
11. Studies on the Energy exponent of the primary Cosmic Ray spectrum in the Energy Interval 10^{14}—10^{16} E. volts through the medium of Air Showers at Nainital. *By* B. N. Srivastava .. 135
12. Maximum accelaration in two dimensional ideal fluid flow. *By* K. M. Agrawal & S. M. Garg 143
13. Morphological studies in Apocynaceae I. *Lochnera Pusilla* K. Schum. *By* Y. S. Murty & T. S. Chauhan.. 147
14. Absorption spectra of some new Ketones Part III-Synthesis and Absorption spectra of *p*-Chloro and *p*-Bromo Anilides of Bromo-Oxymethylene Acetophenone. *By* D.D. Pant, O.N. Perti, K. P. Verma & G. C. Singhal 163
15. Flow of a non-Newtonian fluid through a rectilinear pipe. *By* Radhey Shiam 'Shiam' 169

PAGE

16. Variational principle for Scalar Wave Equation Lagrange Formalism. *By* S. C. GUPTA 175
17. Studies in floral anatomy. VIII. Vascular anatomy of the Flower of certain species of the asclepiadaceae with special reference to Corona. *By* V. PURI & R. SHIAM 189
18. K° Meson production from K^+-P interaction at 2·26 BEV/C. *By* RANDHIR SINGH 217

Abstract of Theses

19. The Theory of Hankel Transform. *By* RAGHUNATH PRASAD GUPTA 243
20. Some problems in Fluid Dynamics. *By* HAR SWARUP SHARMA .. 263
21. Chemical effects of Nuclear Transformations in cobalt complexes. *By* MANOHAR LAL 269
22. Studies on infectious Laryngotracheities virus of Poultry with special reference to tissue culture system.. *By* PRAFULLA CHANDRA PANDA 275
23. Morphological studies in the Sapotaceae and some Allied families. *By* PADAM SARAN KAPOOR 277
24. The Evershed effect in sunspots. *By* ARVIND BHATNAGAR .. 281
25. Studies on growth and yield of two varieties of wheat as influenced by variations in plant density and soil fertility. *By* J. P. AGARWAL 285

CONTENTS

PAGE

1. Factors affecting the recurrence of postpartum oestrus in Murrah Buffaloes. *By* S. Basu 1
2. Morphological, histological and biochemical studies of corpus luteum during normal and abnormal oestrous cycle in Buffaloes. *By* D. J. Roy. 13
3. Respiration and rectal temperature as measures of adaptability of different breeds and crosses of lambs and kids to tropical environment. *By* O. N. Seth, K. C. Saraswat and A. Roy. 17
4. Action of mild doses of UV radiations on dilute aqueous solution of Glycine. *By* O. N. Perti and (Miss) V. Paul 31
5. Studies on the electrophoretic pattern of protein fractions of Colostrum and Milk Whey. *By* T. Prasad, J. S. Rawat and A. Roy. 35
6. Variable flow of a viscous incompressible fluid through a pipe of Rectangular Cross-section under a time dependent pressure gradient. *By* Prem Dayal Narang 43
7. A study of the fish fauna of Visakhapatnam district (Andhra Pradesh)—Its disposal and marketing. II. Fishery statistics of Visakhapatnam district. *By* M. V. Subba Rao and Ratan Singh .. 53
8. Boundary layer in some unseparated axisymmetrical flows. *By* Radhey Shiam 59
9. Morpho-histological studies on the alimentary canal of *Bagarius Bagarius* Ham. *By* Ratan Singh.. 69
10. Morphological and anatomical studies in Helobiae IX. Vascular Anatomy of the Flower of Hydrocharitaceae—Vallisnericideae and Halophiloideae. *By* V. Singh 83
11. Description of one new species of *Phytobia* Lioy (Agromyzidae: Diptera) from India. *By* Santokh Singh and Santosh K. Tandon.. 107
12. Studies on Indian Agromyzidae (Diptera) Part I. Description of two new species of *Phytagromyza* Hendel. *By* Santosh K. Tandon. 111
13. Monographic studies of *Cyperus Esculentus*. I. Growth habits and Tuberization. *By* R. Shiam 117
14. Variable flow in a Uniform Tube of a particular type of section. *By* J. P. Agarwal. 127

PAGE

15. Steady Poiseuille flows through straight channels bounded by parabolic walls. *By* G. C. Sharma 131

16. Appearance of short-wave radio signals in the morning hours indicating the concentration of the received energy near M.U.F. *By* R. R. Mehrotra, J. D. Garg and B. S. Shukla 137

17. A New apparatus for the measurement of the rate of syneresis by soap gels formed in Organic liquids, along with a review of previous literature. *By* Mata Prasad and R. C. Seth 145

18. Reactions between Ammonium chloride and Ammonium nitrate in solution and carbonates of Magnesium, Calcium, Strontium and Barium. *By* Kali Prasad Gupta and Suresh Singh 153

ABSTRACT OF THESES

19. Synthetic studies in the Cyclo-octane series. *By* Mahesh Prakash. .. 165

20. Chemical examination of Litsea Consimilis and Fraxinus Floribunda. *By* Kanaya Lal Dhar. 169

21. Biological availability of Calcium in growing ruminants from Indian feeds. *By* B. L. Agrawal. 171

22. Organic reagent in inorganic analysis with special reference to the use of the derivatives of Naphthoquinones. *By* Keshav Chandra Hajela 175

23. Chemical investigation on the structure of Commiphora Mukul Gum and other plant Gums. *By* K. C. Gupta. 181

STEADY FLOW IN A STRAIGHT TUBE, SECTION—A HYPERBOLIC SECTOR

J. P. AGARWAL
Agra College, Agra.

ABSTRACT

In this paper steady flow of an incompressible viscous fluid in a long uniform tube due to a constant pressure gradient has been considered. The section of the tube is a hyperbolic sector, bounded by the arc of a hyperbola and two straight lines passing through its centre. A method has been obtained covering a large variety of such hyperbolic sectors.

INTRODUCTION AND FORMULATION OF METHOD

The Hagen-Poiseuille theory of flow through a tube of circular section has been found to be well-founded as a result of experiments. It was applied to tubes with a circular annular section by Müller [3] and to rectangular pipes by Allen and Grunberg [1]. Here it is applied to tubes whose section is a hyperbolic sector.

Let the z-axis be taken along the axis of the tube and w be the velocity in this direction, the other components of velocity being assumed to be zero. Then by reference to the equation of continuity $\frac{\partial w}{\partial z}$ must be zero, so that w is a function of x and y only.

The equations of motion reduce to

$$\mu\left(\frac{\partial^2 w}{\partial x^2}+\frac{\partial^2 w}{\partial y^2}\right)=\frac{\partial p}{\partial z}$$

where $\frac{\partial p}{\partial z}$ is a constant.

Denoting this by $-\mathrm{P}$, the velocity w has to satisfy the equation

$$\frac{\partial^2 w}{\partial x^2}+\frac{\partial^2 w}{\partial y^2}=-\frac{\mathrm{P}}{\mu}$$

with a boundary condition

$w=0$, on the surface of the tube.

If we write $$w=\psi-\frac{\mathrm{P}}{4\mu}\left(x^2+y^2\right), \qquad ..(1)$$

then ψ has to satisfy the equation

$$\frac{\partial^2\psi}{\partial x^2}+\frac{\partial^2\psi}{\partial y^2}=0, \qquad ..(1A)$$

with a boundary condition

$\psi=\frac{P}{4\mu}(x^2+y^2)$ on the surface of the tube. Taking $\frac{P}{4\mu}=k$ this becomes

$$\psi=k(x^2+y^2) \quad ..(2)$$

Let us assume

$$\psi=A(x^4-6x^2y^2+y^4)+B\,xy\,(x^2-y^2)+C\,xy+D(x^2-y^2) \quad ..(3)$$

where each term is a plane harmonic.

This will satisfy the boundary condition on a curve whose equation is

$$A(x^4-6x^2y^2+y^4)+B\,xy\,(x^2-y^2)+C\,xy+D(x^2-y^2)-k(x^2+y^2)=0, \quad ..(4)$$

We shall determine the values of A, B, C and D so that the curve forms the boundary of a hyperbolic sector.

SOLUTION

The straight line $y=mx$ will form part of the curve (4) if $(y-mx)$ is a factor of the left hand side of equation (4).

For this it is necessary that

$$[A(1-6m^2+m^4)+Bm(1-m^2)]x^4+[Cm+D(1-m^2)-k(1+m^2)]x^2$$

should vanish for all values of x.

$$\therefore \quad A(1-6m^2+m^4)+Bm(1-m^2)=0 \quad ..(5)$$

and $$Cm+D(1-m^2)-k(1+m^2)=0 \quad ..(6)$$

Similarly the straight line $y=nx$ will form part of the curve (4) if

$$A(1-6n^2+n^4)+Bn(1-n^2)=0, \quad ..(7)$$

and $$Cn+D(1-n^2)-k(1+n^2)=0 \quad ..(8)$$

Now equations (5) and (7) can be satisfied by non zero values of A and B if

$$\begin{vmatrix} 1-6m^2+m^4, & m(1-m^2) \\ 1-6n^2+n^4, & n(1-n^2) \end{vmatrix}=0$$

or $$(n-m)(1+mn)(1-n+m+mn)(1+n-m+mn)=0, \quad ..(9)$$

If $n=m$ we can not form a sector for the two lines will coincide.

If $1+mn=0$, equation (8) becomes

$$Cm+D(1-m^2)+k(1+m^2)=0 \quad ..(10)$$

This is inconsistent with equation (6), for if we add (6) and (10), we get

$$k(1+m^2)=0$$

which is impossible.

Hence from (9), if follows that the relation connecting m and n can be

either $$1-n+m+mn=0, \quad ..(11)$$

or $$1+n-m+mn=0 \quad ..(12)$$

Thus choosing suitable straight lines so that m and n satisfy equations (11) or (12), we can determine the ratio between A and B and the values of C and D from equations (5), (6) and (8).

With these values, we can determine the function as well as the bounding curve from equations (3) and (4) respectively. The procedure will be clear from the particular cases given below. It would appear that by this procedure solutions can be found for an infinite number of hyperbolic sectors.

PARTICULAR CASES

Case I. Suppose $y=2x$ forms part of the boundary of the hyperbolic sector, so that

$$m=2.$$

Then from equation (11),

$$n=-3$$

so that $y=-3x$ is another straight line bounding the sector.

Substituting these values of m and n in equations (5), (6) and (8), we get

$$7A+6B=0 \qquad ..(13)$$

$$2C-3D=5k \qquad ..(14)$$

and $$-3C-8D=10k \qquad ..(15)$$

Here we have 4 arbitrary constants and 3 equations connecting them. So one constant is at our disposal.

Let $$A=\lambda k,$$

then $$B=-\frac{7}{6}\lambda k.$$

Also from equations (14) and (15)

$$C=\frac{2k}{5},$$

and $$D=-\frac{7}{5}k.$$

Substituting these values in equation (4), we get

$$\lambda k(x^4-6x^2y^2+y^4)-\frac{7}{6}\lambda k\,xy(x^2-y^2)+\frac{2k}{5}xy-\frac{7}{5}k(x^2-y^2)=k(x^2+y^2)$$

or $$(y-2x)(y+3x)\left(y^2+\frac{xy}{6}-\frac{x^2}{6}+\frac{2}{5\lambda}\right)=0$$

Thus the sector is bounded by

$$y=2x \qquad ..(16)$$

$$y=-3x \qquad ..(17)$$

and $$\frac{x^2}{6}-\frac{xy}{6}-y^2=\frac{2}{5\lambda} \qquad ..(18)$$

Now the hyperbola (18) is intersected by the lines (16) and (17) in real points only if λ is negative. So let $\lambda=-a^2$, then the equation of the hyperbola becomes

$$y^2+\frac{xy}{6}-\frac{x^2}{6}=\frac{2}{5a^2} \qquad ..(18\text{-A})$$

From equations (1) and (3) the corresponding value of velocity is given by

$$w=\frac{P}{4\mu}\Big[-a^2(x^4-6x^2y^2+y^4)+\frac{7}{6}a^2xy(x^2-y^2)+\frac{2}{5}xy-\frac{7}{5}(x^2-y^2)-(x^2+y^2) \qquad ..(19)$$

Case II.

With $y=2x$, we can take another sector also.

Taking $m=2$ from equation (12) we get $n=\frac{1}{3}$. Thus the sector is bounded by the lines

$$y=2x,$$

and $$y=\tfrac{1}{3}x.$$

With these values of m and n, from equations (5), (6) and (8) we get

$$7A+6B=0$$
$$2C-3D=5k$$
$$\frac{C}{3}+\frac{8}{9}D=\frac{10}{9}k.$$

Now taking $$A=ks,$$
$$B=-\frac{7}{6}ks$$
$$C=\frac{14}{5}k$$
and $$D=\frac{k}{5}.$$

substituting these values in equation (4) and simplifying we get

$$(y-x)\left(y-\frac{x}{3}\right)\left(y^2+\frac{7}{2}xy+\frac{3}{2}x^2-\frac{6}{5s}\right)=0,$$

so that the boundary consists of

$$\left.\begin{array}{l} y=2x \\ y=\dfrac{x}{3} \\ \text{and the hyperbola}\quad y^2+\dfrac{7}{2}xy+\dfrac{3}{2}x^2=\dfrac{6}{5s} \end{array}\right\} \qquad \ldots(20)$$

The straight lines will cut the hyperbola in real points if s is positive.

Putting $s=\beta^2$, the equation of the hyperbola becomes

$$y^2+\frac{7}{2}xy+\frac{3}{2}x^2=\frac{6}{5\beta^2} \qquad \ldots(21)$$

the corresponding value of velocity is given by

$$w=\frac{P}{4\mu}\left[\beta^2(x^4-6x^2y^2+y^4)-\frac{7}{6}\beta^2xy(x^2-y^2)+\frac{14}{5}xy+\frac{1}{5}(x^2-y^2)-(x^2+y^2)\right] \qquad \ldots(21\text{-A})$$

Case III.

To find out some characteristics of the flow, we shall derive a simple case.

Let $y=(\sqrt{2}-1)$ form part of the boundary,

so that $$m=\sqrt{2}-1.$$

Then from equation (11),

$$n=\sqrt{2}+1$$

Proceeding as before, we determine the boundary which consists of

$$\left.\begin{array}{l} y=(\sqrt{2}-1)x \\ y=(\sqrt{2}+1)x \\ \text{and the hyperbola}\quad x^2+y^2+2\sqrt{2}\,xy=\alpha^2 \end{array}\right\} \qquad \ldots(22)$$

The corresponding velocity is given by

$$w=\frac{P}{4\mu}\left[\frac{1}{\alpha^2}\,(x^4-6x^2y^2+y^4)+2\sqrt{2}\;xy-(x^2+y^2)\right] \qquad \ldots(23)$$

We shall now calculate the flux of the liquid across a section of the tube discussed in case (III) above.

Flux $=\int\int w.\, rd\,\theta\, dr$, over the area of the section

$$=\int_{\frac{\pi}{8}}^{\frac{3\pi}{8}} d\theta \int_0^{\frac{\alpha}{1+\sqrt{2}\sin 2\theta}} \frac{P}{4\mu}\left[\frac{1}{\alpha^2}(x^4-6x^2y^2+y^4)+2\sqrt{2}\;xy-(x^2+y^2)\right]rdr$$

$$=\frac{P}{4\mu}\int_{\frac{\pi}{8}}^{\frac{3\pi}{8}} d\theta \int_0^{\frac{\alpha}{1+\sqrt{2}\sin 2\theta}} \left[\frac{r^4(1-2\sin^2 2\theta)}{\alpha^2}+r^2(\sqrt{2}\sin 2\theta-1)\right]rdr$$

$$=\frac{P\alpha^4}{4\mu}\left[\frac{1}{8}\log_e 2-\frac{1}{12}\right]=\cdot 00083\,\frac{P\alpha^4}{\mu}\text{ approx.} \qquad \ldots(24)$$

Since the transverse axis of the hyperbola is proportional to α, it follows that the flux is proportional to the 4th power of the transverse axis in the case of the hyperbolic sectors of this particular type. This is an analogue to poiseuille's law in the case of circular tubes.

To compare this flux with the flux across a section of a circular tube of the same sectional area and with same pressure gradient.

Area of the hyperbolic sector

$$=\tfrac{1}{2}\int_{\frac{\pi}{8}}^{\frac{3\pi}{8}} r^2 d\theta \;=\tfrac{1}{2}\int_{\frac{\pi}{8}}^{\frac{3\pi}{8}} \frac{\alpha^2\, d\theta}{1+\sqrt{2}\sin 2\theta}=\frac{\alpha^2}{4}\log_e 2.$$

If ρ is the radius of a circle whose area is equal to that of this hyperbolic sector, we have

$$\pi\rho^2=\frac{\alpha^2}{4}\log 2 \qquad \ldots(25)$$

Now the flux through a section of a circular tube of radius ρ with pressure gradient P is, according to Lamb [2],

$$\frac{P}{\mu}\cdot\frac{\pi\rho^4}{8}\;\; i.\,e.\;\; \frac{P\pi}{8\pi}\alpha^4\left(\frac{\log 2}{4\pi}\right)^2 \qquad \text{from (25)}$$

$$=\cdot 0012\frac{P\alpha^4}{\pi}\text{approx.}$$

∴ the flux through a tube with this type of hyperbolic sector as a section bears to the flux through a circular tube of the same sectional area the ratio 0·7 approximately.

REFERENCES

1. Allen & Grunberg, 1937. *Phil. Mag.*, (7) **23**: 490-503.
2. Lamb, H. 1932. *Hydrodynamics*, p. 585.
3. Müller, W. 1936. Zun Problem der Anlaufstromung-eine- Flussig Kait in geraden Rohr mit Kreisring-und Kreisquerschnitt. *Zamm*, **16** : 227.

MORPHOLOGY OF THE HEAD CAPSULE AND MOUTH PARTS OF ONITIS PHILEMON FABR. (COLEOPTERA-COPRINE)

P.S. Verma
Department of Zoology, B.R. College, Bichpuri, Agra.

Introduction

The majority of the dung feeding beetles are included in the subfamily Coprinae of the family Scarabaeidae. The knowledge of this family is accredited to Arrow (1931). The members of this large subfamily have the peculiar habit of rolling dung balls and are, therefore, commonly known as dung rollers. They chiefly live upon dung, which is made into balls commonly seen to roll on the ground and stored in the sub-soil cells for the use of young ones.

Onitis philemon Fabr. is a medium sized, dark brown beetle, measuring from 1·5 to 2·0 cm. The insect feeds upon decaying organic matter (hence saprophagous) for which Cow and Buffalo dung is preferred.

There is not much information on Coprinae and no attempt has so far been made towards the study of the genus *Onitis*. Stickney ((1923) and Cook (1943) have given an account of the heads of some Coleoptera. The accounts dealing with the morphology of the head capsule in general are from Crampton (1921, 1932), Evans (1942), Ferris (1942, 1943), Duporte (1946) and Snodgrass (1947, 1960); while Crampton (1923, 1928), have dealt with various components of mouth parts of insects in general. Williams (1938) studied the comparative morphology of mouth parts of the order Coleoptera to establish their phylogeny.

Smith's (1892) study of mouth parts of *Copris Carolina* is a pioneer work in the family Scarabaeidae. Later Mathur *et al.*, (1958) described the head capsule and mouth parts of *Heliocopris bucephalus*; while Miller (1961) has given an account of mouth parts and digestive tract of adult dung beetles. In the present studies, the author has described in details the morphology of the head capsule and mouth parts with their musculature in relation to its saprophagous habit.

Material and Methods

The beetles were collected from the dung heaps of B. R. College Farm at Bichpuri (Agra) where they would be found in abundance from June to September. The beetles were killed in potassium cyanide bottle and preserved in 70% alcohol. The head capsule and mouth parts were treated with 10% solution of potassium hydroxide for several days till they became transparent. The boiling enhances the process. After treating with

Potassium hydroxide the material was transferred to glacial acetic acid and kept for few minutes, then transferred to Carbol-Xylol. The material was subsequently stained in Carbol-Xylol Fuchsin and finally mounted in Canada balsam. For musculature the beetles were first fixed in Bouin's fluid then kept in 70% alcohol for some time. The studies were made under the Bausch and Lomb Stereoscopic binocular microscope with the help of a powerful electric lamp.

OBSERVATIONS

Head Capsule. (Pl. Figs. 1, 2)

The head capsule of *Onitis philemon* Fabr. is a structure, strong, rigid, punctate and heavily sclerotized, without any visible suture. The fusion of dorsal, lateral and ventral sclerotized walls form the head capsule, which is held in prognathus condition.

Sulci or sutures of the head—The term sulcus has been used by Snodgrass (1960) for the suture, the same has been followed in the present studies. The head of *Onitis philemon* exhibits the following sulci :—

Epistomal or Frontoclypeal sulcus (eps)—The epistomal sulcus (eps) is very distinct and represented by a epistomal ridge. It divides the clypeus from the frons. The anterior arms of the tentorium arise from the epistomal ridge and their external pits, the anterior tentorial pits (atp) are well marked. Mathur *et al.*, (1958) did not observe the epistomal sulcus in *Heliocopris bucephalus*.

Clypeogenal sulcus (clp. gs.)—This sulcus is very peculiar in this insect, it separates the clypeus from the gena a condition not observed so far.

Subocular sulcus (sos.)—The subocular sulcus separates the frons from the gena.

Postfrontal sulcus (pfs)—The postfrontal sulcus is represented by a ridge, between the two eyes. It demarcates the frons from the vertex. Stickney (1923) while describing the heads of some Coleoptera and Mathur *et al.*, (1958) in *Heliocopris bucephalus* did not mention the postfrontal suture. Ferris (1943) while describing the insect cranium and Cook (1943) in the heads of some Coleoptera mentioned the postfrontal suture.

Postoccipital sulcus (pos)—The postoccipital sulcus sets off the narrow post occiput that arches over the occipital foramen (ocf).

Ocular sulcus (ocs)—This sulcus surrounds the compound eye on the ventral side of the head. Snodgrass (1935) called it as ocular suture but later on Snodgrass (1960) renamed it as circumocular sulcus.

Antennal sulcus (as)—This sulcus is a rounded structure in which the antenna is lodged and is situated on the ventral aspect of the head.

The epicranial suture is not visible in *O. philemon*. Before the investigations of Cook (1943) DuPorte (1946) and Snodgrass (1947, 1960), it was believed that the presence of the complete epicranial suture was a constant feature of the insect head and due to the presence of this suture various sclerites of the head capsule could be very easily identified. Snodgrass (1960) states that the so called "epicranial suture" which is no suture at all and does not form an internal ridge. It is merely a preformed line of weakness where the cuticle will split at the time of ecdysis and it has no morphological significance.

The areas of the head :

Clypeus (clp)—Clypeus is the anterior sclerite and is heavily chitinised. It completely covers the labrum, which is hinged to it. In the posterior region of the clypeus there is a small ridge. This ridge may be considered as remnant of the suture, which divides the clypeus into the ante and post-clypeus. The surface of the clypeus is granulated and the margins are provided with the bristles.

Frons (fr)—Frons is a roughly rectangular and the largest sclerite, extending between the two eyes. The surface of the frons is granulated. At the distal margin of the frons, just below the epistomal sulcus, there is a small frontal horn (frh). This is found in both the sexes. Mathur *et al.*, (1958) in *Heliocopris bucephalus* observed that the frontal horn is found only in males but in the insect under study there is no sexual dimorphism.

Genae (ge)—Genae are the lateral triangular plates of the head extending infront of the eyes, which are separated from the eyes by the ocular sulcus. The margins of the genae are provided with bristles or setae.

Vertex (v)—Vertex is an elongated smooth plate directed posteriorly in the middle and is demarcated from the postgenae on lateral side by a ridge and in the middle from the postocciput by the postoccipital sulcus.

Postgenae (pge)—On either side of the vertex is a triangular postgena which continues on the ventral side also. The surface of the postgenae is hairy on the dorsal and ventral side.

Postocciput (poc)—The postocciput is a narrow rim of the cranium separated by the occipital sulcus from the vertex and the postgenae. It articulates with the cervix and the prothoracic muscles which move the head capsule (Khatib 1946).

The caudal end of the head capsule is formed by the occipital foramen (ocf) surrounded by a distinct postocciput.

On the ventral surface the broad area between the occipital foramen and the post mentum forming the middle portion of the head, is known as gula (g). On either side it is separated from the postgena by a gular sulcus (gs).

Eyes (e)—The two large compound eyes, situated posterolaterally on each gena, are widely separate. Its one-fourth part projects dorsally through a slit and three-fourth below and continues with the midlateral edge. They are black, oval and convex consisting of large number of hexagonal ommatidia. No ocellus is found in *O. philemon* as observed by Stickney (1923) in other members of the group Coleoptera.

Antennae (ant) (Text. Fig. 1)—The position of the antennae is very interesting in *O. philemon*. It is situated neither on the gena nor on the frons but on the clypeogenal suture. Stickney (1923) did not mention such a position of the antennae in any member of the group of Coleoptera studied by him.

The two antennae, each measuring about 3 mm in length arise from the antennal socket on the ventral surface of the head adjacent to the eyes. Each antenna is lamellate (Essig 1942) and consists of nine segments *viz.*, an elongated basal scape (sc), a globular pedicel (pdc) followed by a flagellum (fl) or funiculus of seven segments of which four normal and three apical ones are lamellate. The normal segments of the flagellum are successively larger with the inner margin thrown into process to appear serrate. The apical three lamellate segments are many times broader than long profusely prolonged inwards although the last two apical segments equal in size are shorter than their proximal counterpart. They are provided with very small fine sensorial bristles very long on the mesial edge of the scape. Each segment is movably articulated to the other by antecoria membrane.

Tentorium—Each anterior tentorial arm is chitinised and opens to the exterior through a furrow, the anterior tentorial pits (atp) situated at the caudal end of each clypeogenal sulcus. Each anterior tentorial arm gives out a small tendon, the osteotendon from which the antennal muscle originates. The posterior tentorial arms; which are subchitinised and weaker than the anterior ones, unite to form the carpotentorium. From the lateral ends of the carpotentorium are given out the two tentorial arms which extend outwards and bifurcate at their caudal ends to meet the dorsal wall of the head capsule. The author agrees with Mathur *et al.*, (1958) regarding the structure of the tentorium.

Mouth parts—The mouth parts of *O. philemon*, a dung feeding beetle are of the mandibulate type for gathering, masticating, and injesting solid food. The mouth parts consist of an unpaired labrum, a pair of mandibles, a pair of maxillae and an unpaired labium. These parts extend in a horizontal plane on the ventral surface of the head which is of the prognathus type and are completely concealed from the above by the expended shovel shaped frontoclypeus.

Labrum (Text Figs. 2, 3)—The labrum forms the anterior or upper lip of the preoral cavity. It is moderately chitinised plate somewhat oval in outline and attached to the clypeus on a median line ventrad leaving anterior free lip; while highly chitinised margins of the posterior half provide attachment to well developed muscles originating from the frons. It is separated from the clypeus by a transverse clypeolabral suture (clp. ls) which gives mobility to the labrum. The anterior free edge is notched in the middle but the posterior is drawn out into lateral apodemes for the insertion of the labral muscles. The free edge of the labrum is fringed with a row of bristles longest in the middle and decreasing in size laterally. Four other rows of bristles starting from the anterior edge run posteriorly describing arcs over the dorsal surface converging towards the clypeolabral suture (clp. ls). The size of the bristles diminishes gradually anteroposteriorly. The presence of a beak like structure, curved to the right in between the lateral apodemes, is a unique structure in this beetle. Both the surfaces of the labrum are provided with innumerable large and small bristles and spines.

The presenee of numerous spines and bristles on the surfaces of the labrum probably serve to conduct the food material towards the buccal cavity. They are also tactile and gustatory and assist in discrimination of the food material.

The epipharynx represents a membranous structure stretched in between the highly sclerotized lateral apodemes of the labrum.

Mandibles. (Text Figs. 4,5,6)—The mandibles in O. *philemon* are mechanically adapted for their dual function of gathering and masticating the food material. Each mandible consists of a proximal basal supporting articular portion *viz.*, basalis (bp), a distal incisor lobe (in) viz terebra and an inner basal lobe *viz.*, the molar (ml).

The basalis (Smith 1892, or the basal portion (bp) (Miller 1961), is narrowly triangular bearing a distal socket and a ventral condyle articulating with the corresponding structures on the head capsule.

The terebra or piercer (Smith 1892), the incisor lobe (in) (Miller 1961) is a thin feebly chitinous elongated blade which projects forward horizontally beneath the labrum. It bears a comb of hairs proximally and branched fimbriated bristles distally along its inner edge with numerous setae on its dorsal, ventral and lateral surfaces.

On the ventral surface between the incisor lobe and the molar lobe there is an oval concavity full of longitudinal ridges. This structure has been termed as conjuctivus or connecting piece by Smith (1892) in *Copris carolina*, but Mathur *et al.*, (1958) name it as outer part of the prostheca in *Heliocopris bucephalus*. On the other hand Miller (1961) describes it as ventral oval flexible area consisting of a series of corrugated folds in adult dung beetles.

The molar or grinder (Smith 1892) or the molar lobe (ml) (Miller 1961) is massive, projects masad in a vertical plane and bears a molar area on the medial surface which lies in apposition to the other mandible. The medial molar areas of the two mandibles are not symmetrical but convex on the right and concave on the left so that the molar areas in two mandibles closely fit into each other. These areas grinding surfaces on the inner side nearly five times as high as broad. Each of these is provided with a series of parallel transverse cuticular ridges of uniform thickness inwards. Except the shape and curvatures on the surface, the mandibles are structurally similar. They form an efficient grinding apparatus that functions like a pair of opposed mill stones. The movement to the mandibles is imparted by contraction and relaxation of the mandibular muscles, the abductors swinging the mandible outward and the adductors inward. The alernate motion of the two mandibles being pulled apart and brought together, brings the incisor lobe into play to push the food medially assisted by the anteroposterior movements of the hypopharynx. Simultaneously molar lobes working against each other, result in grinding the food material.

Each mandible possesses two apodemes an inner intended for insertion of adductor and an outer for abductor muscle.

Maxillae. (Text Figs. 7, 8)—The maxillae are situated below the mandibles and lateral to the labium. Each maxilla articulates with the head capsule by means of three apodemes of the cardo.

The maxilla of *O. philemon* consists of the usual components *viz.*, cardo (ca), stipes (st), lacinia (lc), galea (ga) and maxillary palp (mx. p.).

Cardo (ca) is a small triangular sclerite and does not show any division into basi and disti cardo. Cardo looks like a deep cup shaped structure when seen from inside *i.e.*, anterodorsally. It is fitted into a shallow depression on either side of the labium. Proximal rim of the cardo bears three apodemes projecting into the head capsule, two of them are directed inwards (mesially) while the third one, which is the longest is directed outwards. The two mesial apodemes are situated more or less dorsoventrally to each other. These apodemes provide for the insertion of muscles. Distal end of the cardo is hinged movably with the stipital portion of the maxilla. They meet to form a transverse ridge, cardostipital ridge (Mathur *et. al.*, 1958).

The stipes (st) forms the main portion of the body of the maxilla and is divided into eustipes and parastipes. The eustipes may be devided into a basal region or basistipes (bs), a distal stipes or dististipes (ds) and median region or mediostipes (ms) on the basis of the sutures present. Crampton (1923) holds that the parastipes or parastipital region, which is distinct in many cases, tends to unite with the median region (ms) to form the larger median region in Dermaptera and Coleopteran beetles (*e.g.*, Staphylinid and Cicindellid beetles).

The stipes in *O. philemon* consist of basi stipes (bs) a mediostipes (ms) and a dististipes (ds). The mediostipes is a broad rectangular piece because it is formed by the fusion of parastipes and median region of eustipes. The basi and dististipes are small triangular pieces meeting together in the middle by their vertices. The longitudinal ridges are formed on both the lateral sides of the basi and dististipes which separate the mediostipes in the mesial side and the palpifer (pf) towards outerside.

The lacinia (lc) more or less club like with a stout stem which originates from the dorso-mesial proximal margin of the stipes and lodged in a long groove in the length of the mediostipes, is visible only from dorsal side. The distal membranous free end projects beyond and can be seen from the ventral side. The stem of the lacinia is beset with numerous long black stiff hairs (h) pointing towards the distal margin of the lacinia and a large number of long and fine setae form a fringe on the distal margin of the lacinia which are sensory in function.

The galea (ga) arises from the distal margin of the stipes ventral to the lacinia. It is divided into two parts by a transverse ridge. The proximal small chitinous subtriangular part is basigalea (bg) and the distal large and semicircular membranous part is the distigalea (dg). The distigalea is sparsely clothed with small setae and provided with large number of long and fine setae forming a fringe all round its free margin. The galea is separated from the stipes by a well developed ridge.

To the outer lateral margins of the basi and dististipes there is attached a long palpifer (pf) fully visible from the dorsal side. The palpifer is granulated on its dorsal and ventral surface. From the cephalic end of the palpifer is given out a four segmented maxillary palp (mx. p.). The first segment of the maxillary palp is short and narrow, its caudal end fitting into the cephalic concavity of the palpifer. The second and third segments are large and conical while the fourth segment is more or less clavate and cylindrical.

The entire surface of the cardo, stipes and palpifer is clothed with black and brown spine like bristles and bear various kinds of sensilla. The maxillary palp, lacinia, and galea probably function as olfactory and gustatory organs.

In the insect under study, the author has based his findings regarding maxillary components; on Crampton's (1923) observations on the phylogenetic comparison of the maxillae throughout the orders of insects, yet he feels that a confirmation of his views can be better arrived at by means of embryological evidences, which are beyond the scope of the present work.

Labium. (Text Fig. 9)—The labium in *O. philemon* consists of the free distal prementum bearing labial palpi, paraglossae and glossae and a proximal postmentum.

The free distal prementum (pr. mt.) is highly chitinised plate notched anteriorly to receive the ligula (lg). It is nearly half as long as broad. The entire surface of the prementum is provided with large number of long and small bristles. On its either lateral side there is present a distinct sclerite, the palpiger (pg), which bears a three- segmented labial palp (lp). The second segment of the palpus is the longest of all but the first slightly smaller than the second and the third very small appearing as a protuberance of the second segment. The first and second segments of the labial palpi bear numerous large and small bristles. The glossae of the ligula (lg) fuse to form a single compact lobe; while the paraglossae (pgl) are directed downwards and supported by the anterior prolongations of the labial endoskeleton. Its anterior and mesial margins are fringed with setae or bristles.

The postmentum (p.mt.) is a rectangular thickly chitinised plate which, though adnate to the gula (g), is demarcatèd from it by the presence of a transverse row of bristles, directed forwards. Its anterior lateral margins are extended to accommodate the inner posterior margins of the cardo of the maxilla. The postmentum is a single plate and does not manifest any subdivision into the mentum and submentum. The postmentum is separated from the prementum by the labial suture (ls).

The gula (g) is highly developed and is separated from the postgena by the gular sulcus (gs) on both the lateral sides. There are hairs on the gula known as gular hairs (gh.)

Endoskeleton of Labium—It is interesting to note that labium is supported by means of endoskeleton of sclerotized arms. From each lateral side of the prementum there arise two lateral sclerotized arms dorsad. The anterior sclerotized arms support the paraglossae and palpigers of both sides; while the posterior sclerotized arms are raised dorsally and unite by a transverse bar in the middle. At this junction there arises a long process which runs a short distance to the anterior and then curves to the dorsal side. To this is attached the dorsal part of the hypopharynx and is known as the suspensoria of the hypopharynx (Snodgrass 1935).

Musculature:

Musculature of the Antenna (Text Fig. 10). The antenna is moved by a set of three extrinsic muscles, arising from the tentorium.

The antennal flexor muscle (1) is a stout muscle arising distally from the tentorial arm and inserted on the inner margin of the base of scape. The contraction of this muscle draws the antenna inwards and a simultaneous action of both draws inwards.

The anterior extensor muscle (2) is a small muscle, the antagonist of the flexor, arising posteriorly on the tentorial arm and is inserted externally on the base of the scape. Its contraction moves the two antennae apart.

The antennal depressor muscle (3) is a small thin muscle arising ventrally on the tentorium and is inserted outwardly on the base of scape, when it contracts, the antenna is lowered.

Musculature of Labrum. (Text Fig. 11)

Lateral Labral muscles (4)—These muscles take their origin from the frons and are inserted on the lateral apodemes of the labrum. The contraction of these muscles brings about an upward movement of the labrum; while the relaxation bring about the downward movement of the same. The lateral movements can only take place when the muscles of one side contract and of the other side relax simultaneously. The insertion of muscles does not confirm Das's (1937) generalization that the lateral muscles are always inserted on the tormae.

Labro-epipharyngeal muscles (5)—The fibres of these muscles originate from underneath the middle of the clypeolabral suture and are inserted on the epipharynx. The contraction and relaxation of these muscles bring about the upward and downward movement of the epipharynx respectively. These muscles have not been observed by Snodgrass (1935), Das (1937), Pradhan (1938) and Verma (1964) in insects studied by them.

Musculature of Mandibles (Text Fig. 12)—Each mandible is provided with the following extrinsic muscles only *viz*:—

Adductor muscle (6)—The large stout, powerful and fan shaped adductor muscle originates from the dorsal and posterolateral wall of the cranium and is inserted on a large apodeme at the inner angle of the mandibular base. The contraction of this muscle brings about the molar area of the two mandibles together and serves to crush and grind the food.

Abductor muscle (7)—This is comparatively a thin muscle which takes its origin from a small area just below the adductor and is inserted upon a round convex apodeme at the outer angle of the base of the mandible. The contraction of these muscles bring about the two mandibles apart.

Musculature of the Maxilla (Text Figs. 13, 14):

The extrinsic musculature of the maxilla—There are five extrinsic muscles which impart movements to the maxilla. Three of them are inserted on the apodemes of the cardo and two on the stipital portion.

Dorsal flexor muscle of the maxilla (8)—This muscle originates partly from the posterior arm of the tentorium and partly from the lateral margin of the occipital foramen and is inserted on the dorsal apodeme of the cardo. This muscle brings about a withdrawal of this component proximally.

Ventral flexor muscle of the maxilla (9)—This muscle arises from the posterior arm of the tentorium and is inserted on the ventral apodeme of the cardo and also serves to pull the maxilla inwards.

Extensor muscle of the maxilla (10)—This muscle takes origin from the lateral wall of the cranium and is inserted on the longest apodeme of the cardo and serves the function of awarding a lateral movement.

Cranial flexor muscle of the lacinia (11)—The fibres of this muscle arise from the lateral rim of the occipital foramen and are inserted on the inner angle of the base of lacinia.

Pradhan (1938) and Verma (1964) in *Coccinella septempunctata* and *Chilomenes sexmaculata* respectively, named this muscle as an extensor of the lacinia. They also mentioned that the insertion of this muscle takes place on the outer angle of the base of lacinia. According to Pradhan (1938) the point of insertion of the lacinial muscle is not constant and that the muscle serves as a flexer or an extensor with respect to the insertion being on the inner or outer angle of the lacinia. But Snodgrass (1935) and Das (1937) mentioned this muscle as a cranial flexor of the lacinia with its insertion on the inner angle of the base of lacinia. The author, however, is inclined to agree with Snodgrass (1935) and Das (1937) regarding the insertion and function of this muscle.

Flexor muscle of the mediostipes (12)—This muscle originates from the posterior arm of the tentorium and is inserted on the proximal mesial corner of the mediostipes of the stipes.

Pradhan (1938) observed a flexor muscle of the subgalea in *Coccinella septempunctata*, the same observed by Verma (1964) in *Chilomenes sexmaculata*, but no part of the stipes fit to be called as subgalea exists in the insect under study. Snodgrass (1935), and Das (1937) also have not observed any muscle of this nature.

(ii) *The Intrinsic muscles of the maxilla*—The intrinsic musculature of the maxilla consists of the four muscles *viz*:—

Flexor muscle of the galea (13)—This muscle originates from the base of the stipes and is inserted on the proximal segment *i.e.*, basigalea of the galea passing through a chitinous ring shaped apodeme of the basigalea.

Das (1937) described the origin of this muscle from the mesial side of the stipes and its insertion on the base of the galea and named it as a cranial flexor of the galea. Pradhan (1938) in *Coccinella septempuntate* observed a similar muscle arising from the subgalea and inserting on the base of the distal segment of the galea and called it as subgalear flexor of the galea. The same was confirmed by Verma (1964) in *Chilomenes sexmaculata*. Both these authors considered subgalea as a distinct part of the stipes. But in the insect under study, no part of the stipes can be considered as subgalea, hence the author agrees with Snodgrass (1935) regarding the function and name of this muscle.

Stipital muscle of the maxillary palp (14)—This muscle takes its origin from the basal part of the palpifer and is inserted on the proximal rim of the basal segment of the maxillary palp. Accordiug to Pradhan (1938) this muscle acts as a levator and depressor simultaneously because the muscle fibres of both the types are mixed up in it and there can be no clear distinction between the fibres. The various movements of the maxillary palp are brought about by contraction of certain fibres and relaxation of others.

Proximal segmental flexor muscle of the maxillary palpus (15)—The fibres of this muscle arise from the second segment of the palpus and are inserted on the third segment of the same.

Distal segmental flexor muscle of the maxillary palpus (16)—The fibres of this muscle take their origin from the third segment of the palpus and are inserted on the fourth or the last segment of the same. This muscle is a true replica of the proximal segmental flexor of the palpus.

Musculature of labium. (Text Fig. 15):

Median muscles of the prementum (17)—In majority of insects this muscle originates from the posterior margin of the submentum, but since a plate of that designation does not exist in the insect under study, it is remarkable to note that this muscle takes its origin from a special phragma near the proximal margin of the gula, a condition not so far recorded. It is inserted ventrally on the middle of the proximal border of the prementum. These muscles serve as flexors of the prementum since the prementum has a definite hinge on the distal margin of the postmentum.

Flexor muscle of the ligula (18)—This muscle arises from the middle of the prementum and is inserted on the distal rim of the ligula.

Flexor muscle of the labial palp (19)—This muscle originates from the curved anterior sclerotized arm of the prementum and is inserted on the proximal rim of the first segment of labial palp. This muscle imparts various movements to the labial palp because there are no distinct levator and depressor muscles in this insect.

Flexor muscle of the paraglossa (20)—This muscle arises from the proximal margin of the prementum mesad and inserted on the base of the paraglossa. Such a muscle is very peculiar in this insect.

SUMMARY

1. Epicranial and coronal sulci in *Onitis philemon* are absent but epistomal, clypeogenal and postfrontal sulci are well developed.
2. The antennae are situated on the ventral surface of the clypeogenal sulcus.
3. Mouth parts are adapted for saprophagous habit and are consequently modified accordingly.
4. Food chiefly comprises of decaying organic matter for which preference is given to Cow and Buffalo dung.
5. The mandibles are provided with molar lobes which are convex on the right and concave on the left to fit closely to provide efficient surface for grinding of the food material.
6. The maxillary palp, lacinia and galea probably function as olfactory and gustatory organs due to the presence of bristles with various kinds of sensilla.

7. The labium is supported by means of an endoskeleton of sclerotized arms dorsad. The postmentum is a single plate not divided into mentum and submentum. Gula is well developed.

ACKNOWLEDGEMENTS

The author expresses his deep sense of gratitude to Dr. R. D. Saksena, M.Sc., Ph.D., F.Z.S.I., Professor and Head of the Zoology Department, B.R. College, Agra for his valuable guidance and painstaking correction of the manuscript, Dr. M. G. Ramdas Menon, Systematic Entomologist, I.A.R.I., New Delhi for the identification of insect. Thanks are also due to C.S.I.R., New Delhi for the award of fellowship and Dr. S.N. Singh, M.Sc., Ph.D., Principal, B. R. College, Agra for the research facilities.

REFERENCES

1. Arrow, C. J. 1931. Fauna of British India. *Coleoptera, Lamellicornia* Part III Vol. **13.**
2. Cook, E. F. 1943. The heads of some Coleoptera. *Microentomology*, **8** : 25-40.
3. Crampton, G. C. 1921. The sclerites of the head and Mouth-parts of Certain immature and adult insects. *Ann. Ent. Soc.* America **14** : 65-110.
4. Crampton, G. C. 1923. A phylogenetic study of the maxilla compared throughout the orders of insects. *Jour. N. Y. Ent. Soc.* **32** : 77-107.
5. Crampton G. C. 1923. A comparison of the labium in certain holometabolous insects from the standpoint of phylogeny. *Proc. Ent. Soc.* Washington **25** : 171-180.
6. Crampton, G. C. 1928. The eulabium, mentum and submentum and gular region of some insects. *Jonr. Ent. and Zool.*, **29** : 1-15.
7. Crampton, G. C. 1932. A phylogenetic study of head capsule in certain Orthopteroid. Pscoicid, Hemipteroid and holometabolous insects. *Bull. Brooklyn. Ent. Soc.* **27** : 19-49.
8. Das, G. M. 1937. The musculature of the mouth parts of insect larvae. *Quart. Jour. Micro. Sci.* London, **80** : 39-80.
9. DuPorte, E. M. 1946. Observation on the morphology of the face in insects. *Jour. Morpho.*, **79** : 371-417.
10. Essig, E. O. 1942. College Entomology. The Macmillan Company, New York.
11. Evans, J. W. 1942. Further notes on the morphology of insect head. *Trans. Roy. Soc.* South Australia., **66** (2) : 180-184.
12. Ferris, G. F. 1942. Some observations on the head of insects. *Microentomology*, **7** (2) : 25-62.
13. Ferris, G. F. 1943. The Basic material of insect cranium, *Ibid.*, **8** (1): 8-24.
14. Khatib, S.M.H. 1946. The external morphology of *Galerucella birmanica* (Jacoby) *Proc. Ind. Acad. Sci.* Sect. B. **23** (1) : 1-38.
15. Mathur, P. N., Khattar, N. & Mathur, V. D. 1958. Morphology of the head and mouthparts of *Heliocopris bucephalus* Fabr. *Proc. Ind. Acad. Sci.* Sect. B. **48** (4) : 137-153.
16. Miller, A. 1961. The mouth parts and *digestive* tract of adult dung beetles with reference to injestion of *helminth* eggs. *Jour. Parasitology*, **47** (5) : 735-744.
17. Pradhan, S. 1938. Neuromuscular study of the mouth parts of *Coccinella septempunctata* with a comparison of mouth parts in carnivorous and herbivorous Coccinellids. *Rec. Ind. Mus.*, **40** : 341-358.
18. Smith, J. B. 1892. The mouth parts of *Copris carolina* with notes on the homologies of the mandibles. *Trans. Amer. Ent. Soc.*, **19** : 83-87.

19. Snodgrass R.E. 1935. Principles of Insect Morphology. McGraw Hill Bolk Company, N. York.

20. Snodgrass, R. E. 1947. The insect cranium and epicranial suture. *Smith. Misc. Coll.,* **107** (7) : 1-52.

21. Snodgrass, R. E. 1960. Facts and theories concerning the insect head. *Smith Misc. Coll.,* **142** (1): 1-61.

22. Stickney, F. S. 1923. The heads of some *Coleoptera. Illinois. Biol. Mong.* **8** (1) : 1-105.

23. Verma, P. S. 1964. Study of mouth parts of *Chilomenes sexmaculata* Fabr. (Coleoptera : Cocinellidae) in relation to its cornivorous habit. *Agra Univ. J. Res. (Sci.),* **13** (2): 137-146.

24. Williams, I. W. 1938. The Comparative morphology of mouth parts of order Coleoptera treated from the standpoint of phylogeny. *Jour. N. Y. Ent. Soc.,* **46:** 245-267.

KEY TO LETTERING.

ant.	antenna.
arp.	articular process.
as.	antennal sulcus.
atp.	anterior tentorial pit.
bg.	basigalea.
bp.	basal portion.
bs:	basistipes.
ca.	cardo.
clp.	clypeus.
clp. gs.	clypeogenal sulcus.
clp. ls.	clypeolabral sulcus.
dg.	distigalea.
ds.	dististipes.
e.	eye.
eps.	epistomal sulcus.
fl.	flagellum.
fr.	frons.
frh.	frontal horn.
g.	gula.
ga.	galea.
ge.	gena.
gh.	gular hair.
gs.	gular sulcus.
h.	hair.
in.	inciser lobe.
lc.	lacinia.
lg.	ligula.
lp.	labial palp.
ls.	labial suture.
ml.	molar.
ms.	mediostipes.
mx.	maxilla.
mx. p.	maxillary palp.
oc.	occiput.
ocf.	occipital foramen.
ocs.	ocular sulcus.
pdc.	pedical.
pf.	palpifer.
pg.	palpiger.
pgl.	paraglossa.
pfs.	postfrontal sulcus.
pge.	postgena.
poc.	post occiput.
pos.	postoccipital sulcus.
pr. mt.	prementum.
p. mt.	postmentum.
r.	ridge.
sc.	scape.
st.	stipes.
sos.	subocular sulcus.
v.	vertex.

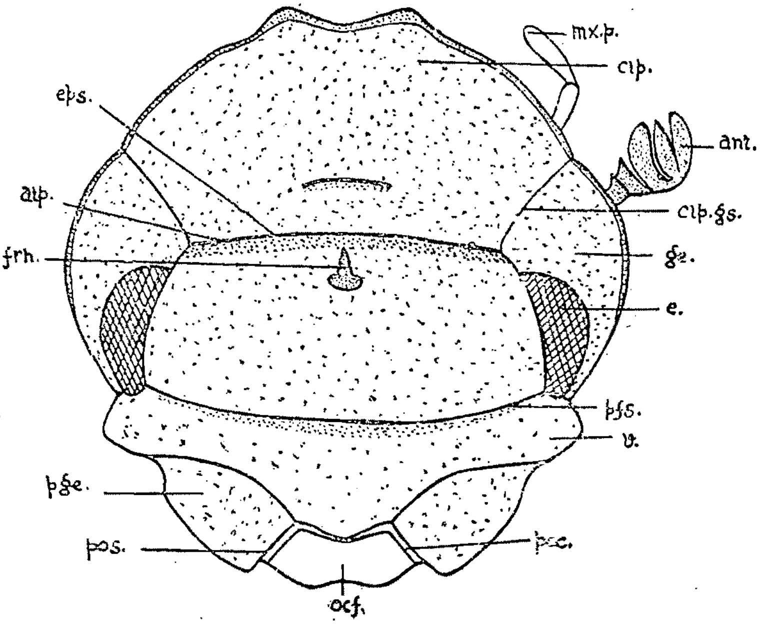

FIG. 1.

Fig. 1 Dorsal view of Head.

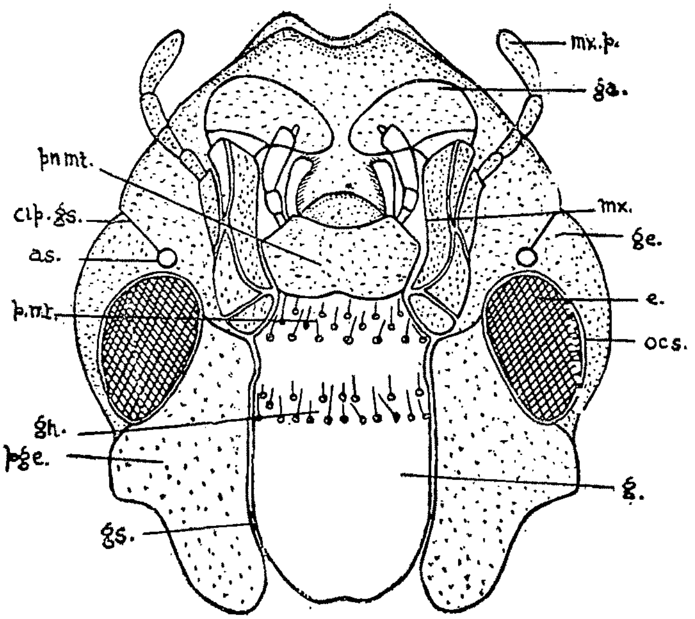

FIG. 2.

PLATE. I

Fig. 2 Ventral View of Head.

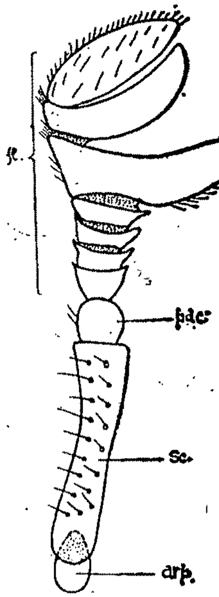

TEXT-FIG. 1

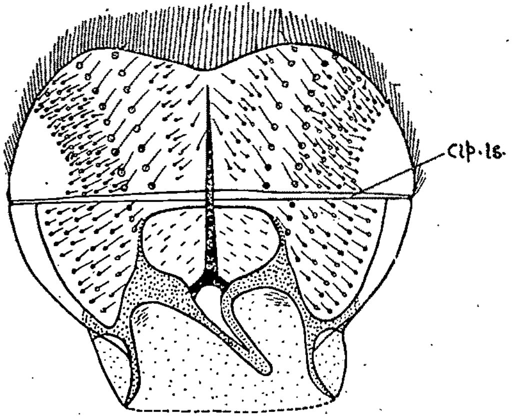

TEXT-FIG. 2

Text Fig. 1 Antenna.
Text Fig. 2 Dorsal view of labrum.

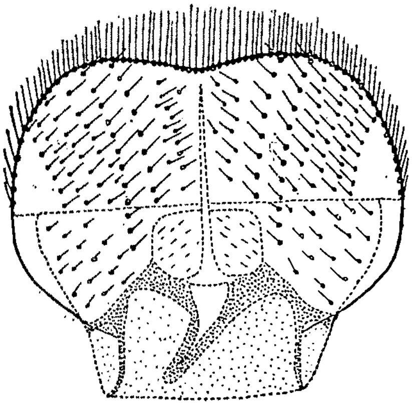

TEXT-FIG. 3

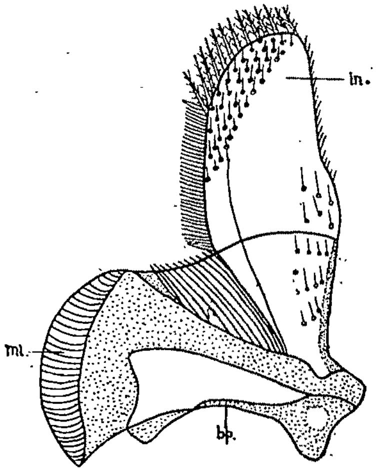

TEXT-FIG. 4

Text Fig. 3 Ventral view of labrum.
Text Fig. 4 Dorsal view of right mandible.

P14370

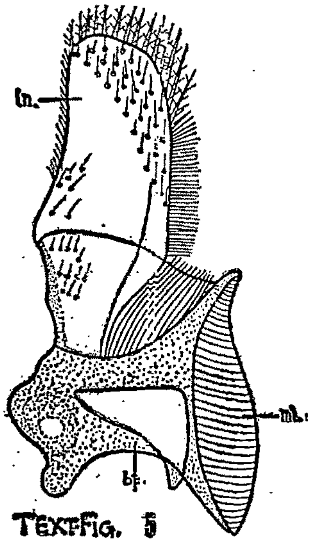

TEXT-FIG. 5

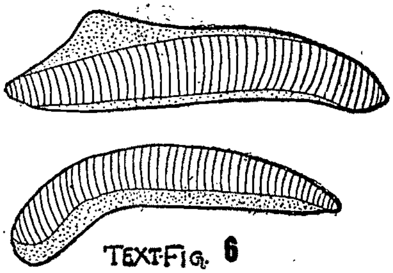

TEXT-FIG. 6

Text Fig. 5 Dorsal view of left mandible.
Text Fig. 6 Molars of grinders opposing faces.

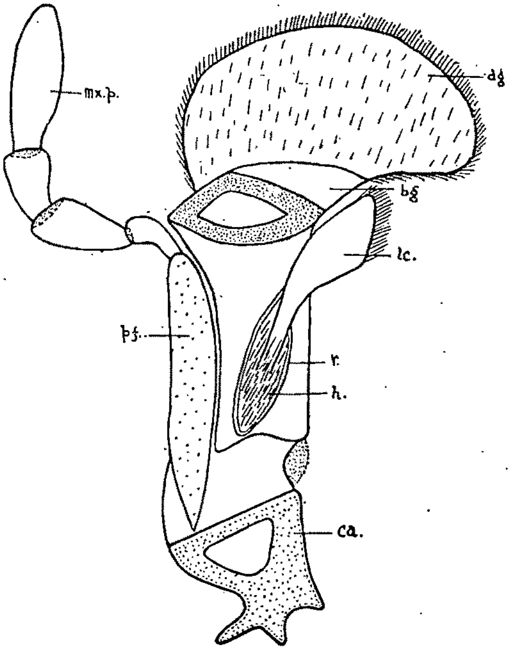

TEXT-FIG. 7

Text Fig. 7 Dorsal view of maxilla.

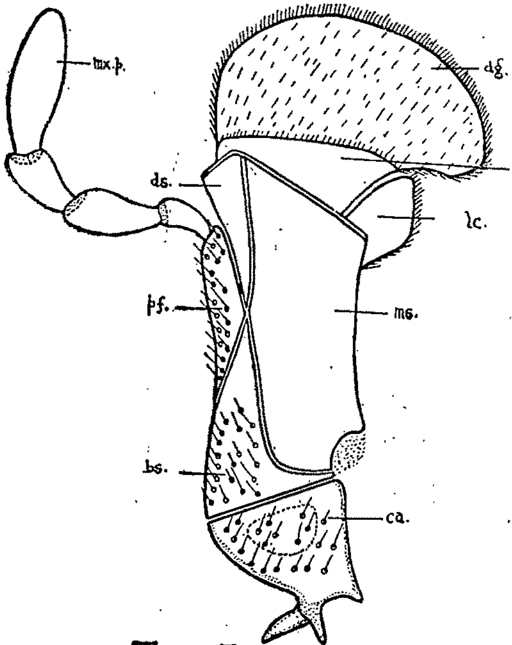

TEXT-FIG. 8

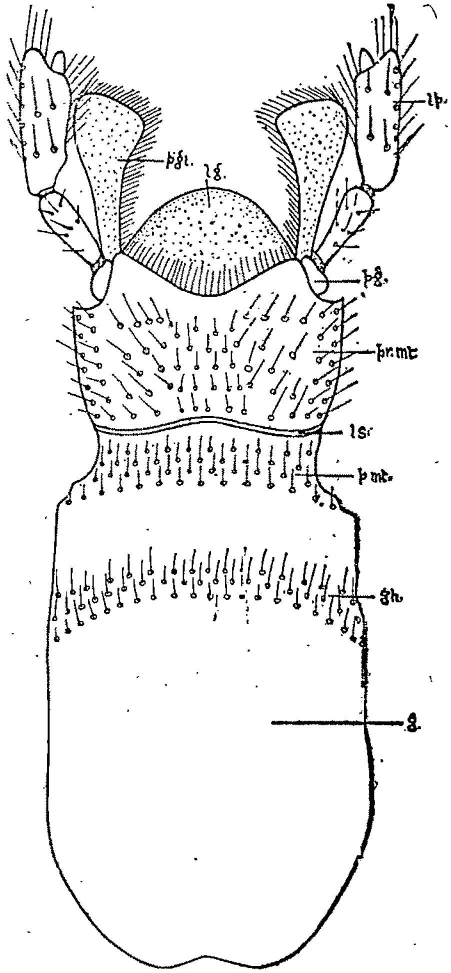

TEXT-FIG. 9

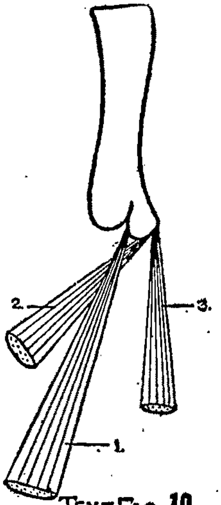

TEXT-FIG. 10

Text Fig. 8 Ventral view of maxilla.
Text Fig. 9 Ventral view of labium.
Text Fig. 10 Musculature of antenna.

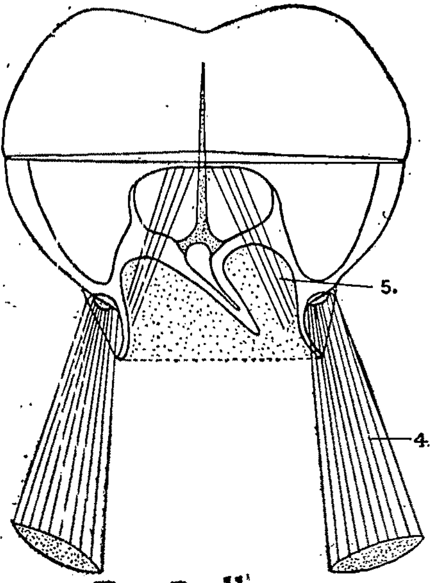

TEXT-FIG. 11

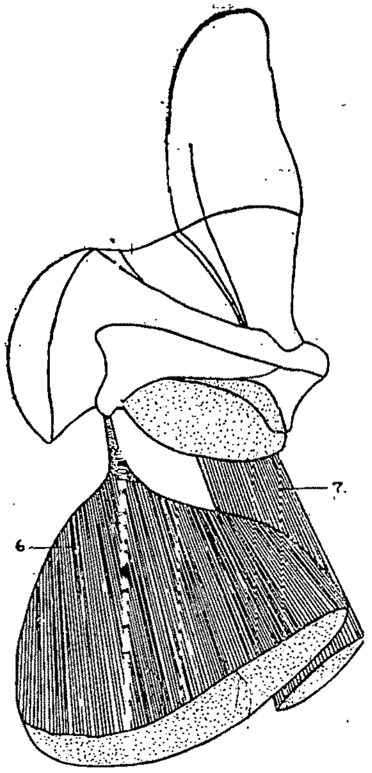

TEXT-FIG. 12

Text Fig. 11 Musculare of Labrum.
Text Fig. 12 Musculature of mandible.

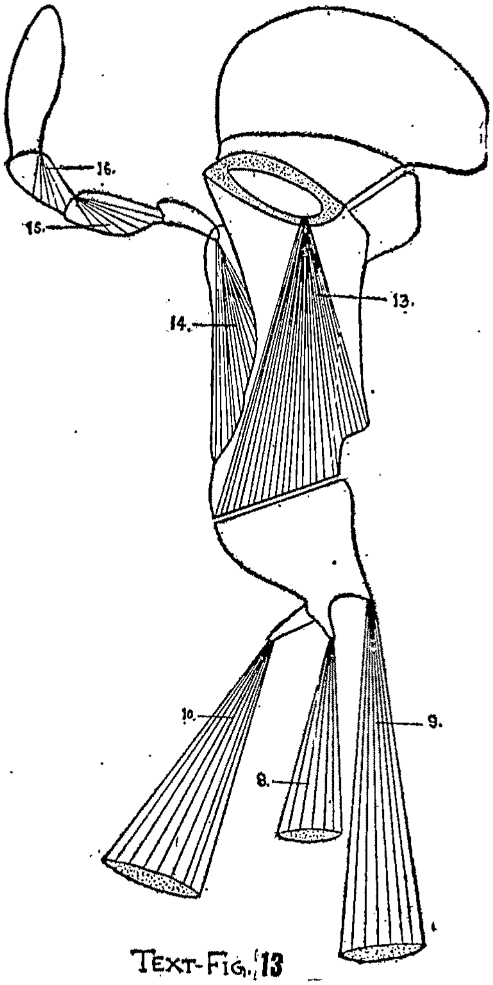

TEXT-FIG. 13

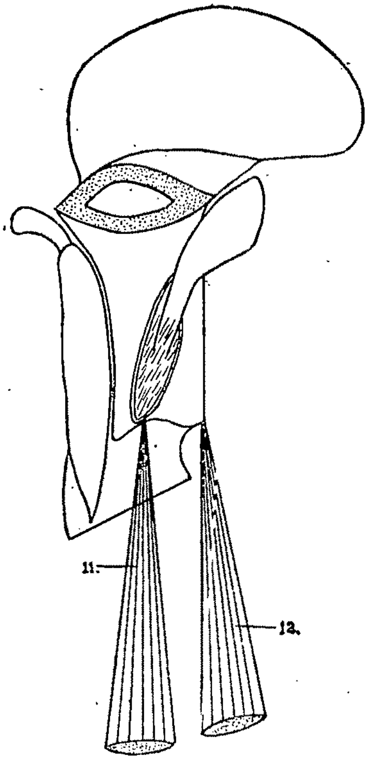

TEXT-FIG 14

Text Fig. 13 Musculature of maxilla.
Text Fig. 14 Musculature of maxilla.

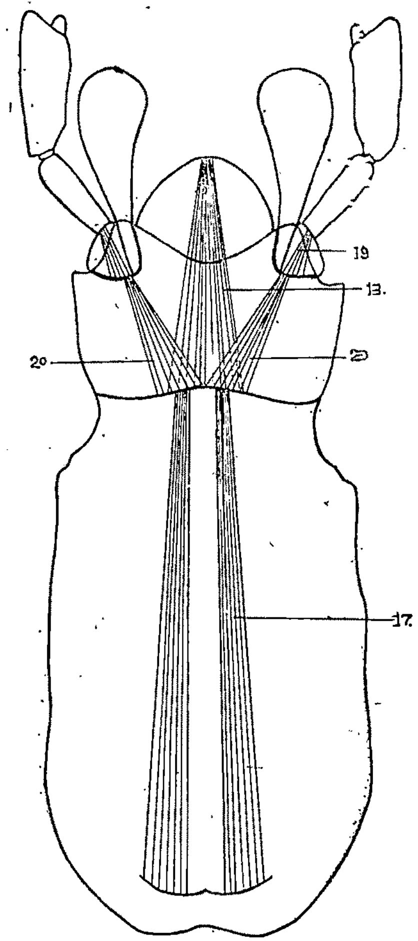

TEXT-FIG. 15

Text Fig. 15 Musculature of labium.

A NOTE ON THE KINETICS OF SILVER CATALYSED OXIDATION OF GLUCOSE BY POTASSIUM PERSULPHATE

C. P. KHULBE AND S. P. SRIVASTAVA*
Chemical Laboratories, Th. D. S. B. Govt. College, Naini Tal, India.

An earlier study[1,2] of this reaction in this laboratory by Purohit and Srivastava has shown that, unlike most of the redox reactions of persulphate ion, the oxidation of glucose by $K_2S_2O_8$ catalysed by silver ion is a bimolecular process; however, the order of the reaction with respect to each of reactants has not been precisely determined by these workers. Further, they have found that the reaction is greatly catalysed by Fe^{++} ion, the catalysed reaction showing a zero order behaviour and being greatly inhibited by Cl^- ion. In view of the peculiar behaviour of this reaction for which no plausible explanation can be given, the authors have reinvestigated this reaction kinetically. It has been shown that the reaction, when carried out in a buffered medium, follows an unimolecular behaviour like other Ag^+ catalysed oxidation reactions of S_2O_8'' ion. The apparent deviation from unimolecular behaviour has been attributed to the increase in H^+ ion concentration with the progress of the reaction which has a retarding effect. The energy of activation, frequency factor and entropy of activation of this reaction have also been calculated.

EXPERIMENTAL

G. R., E. Merck $K_2S_2O_8$ after recrystallisation, glucose and silver nitrate of A. R., B. D. H. quality were used. All the other chemicals used were also of A. R. grade. The standard solutions of $K_2S_2O_8$ and glucose were prepared by direct weighing of the salt and dissolving them in sodium acetate-acetic acid buffer where buffered medium was used; otherwise the solutions were made in redistilled water from a pyrex distilling still.

All reactions were carried out in a Pyrex Erlenmeyer flask coated with black japan and wrapped in a black cloth. Measured quantity of glucose, silver nitrate and buffer solution were kept in a thermostat maintained at the temperature of the experiment with an accuracy of ±0·1°C., and the reaction was started by running in the required volume of persulphate solution with a pipette. The progress of the reaction was followed by withdrawing 5 ml. of the reaction mixture and estimating the $K_2S_2O_8$ content by the procedure of Galiba, Csanyi and Szabo[3] modified by Khulbe and Srivastava.[4]

The sodium acetate-acetic acid buffer of pH 4·76 was used for preparing the solutions and for dilutions.

---

* Present address—Reader in Chemistry, University of Roorkee.

RESULTS OF MEASUREMENTS

The results of the kinetics of the reaction carried out in a non-buffered medium and in the presence of a high salt concentration are given in table 1.

TABLE 1

Glucose=$K_2S_2O_8$=*0·025M*; $AgNO_3$=*0·001M*; *Temperature—35°C.*

Time	Without Na_2SO_4			Na_2SO_4=0·25M		
	Vol. in ml. 0·02 N $Na_2S_2O_3$ equivalent to $K_2S_2O_8$	$k\times10^2$ uni.	$k\times10^4$ bimol. ml. $Na_2S_2O_3^{-1}$ min^{-1}	Vol. in ml. 0·02 N $Na_2S_2O_3$ equivalent to $K_2S_2O_8$	$k\times10^2$ uni.	$k\times10^4$ bimol. ml. $Na_2S_2O_3^{-1}$ min^{-1}
2	23·90	...	...	24·54	...	...
10	22·80	5·9014	2·5233	...	...	...
20	21·95	4·7339	2·0650	22·50	4·7595	2·0523
30	20·95	4·7047	2·1041	21·72	4·3674	1·8900
45	19·90	4·2578	1·9560	20·95	3·6794	1·6239
60	19·04	3·9190	1·8403	20·20	3·3300	1·5015
90	16·85	3·9724	1·9901	19·11	2·9049	1·3157
120	15·80	3·5071	1·8199	17·79	2·7265	1·3131
150	14·25	3·4949	1·9155	16·69	2·6076	1·2920
180	13·03	3·4092	1·9499	15·85	2·5556	1·2556
195	12·55	3·3387	1·9649	...	...	...
210	12·01	3·3094	1·9941	15·05	...	1·2383

The above data show that the rate slightly decreases with an increase in the ionic strength of the medium and that the unimolecular and the biomolecular rate constants fall off with time even in the presence of a high salt concentration. These show that the decrease in the rate constant values with time is not due to the increase in the ionic strength of the reaction mixture with the progress of the reaction, The reaction was then carried out at a constant pH of 4·76; the results obtained are given in table 2.

TABLE 2

Glucose=$K_2S_2O_8$=*0·025 M*, *AgNO*$_3$=*0·001 M*, *Temperature—35°C.*

Time	Vol. in ml. 0·02 N $Na_2S_2O_3$ equiv. to $K_2S_2O_8$	k × 10^2 uni.
2	23·70	...
5	22·90	1·1438
10	21·75	1·0709
15	20·05	1·2851
20	18·85	1·2723
25	17·80	1·2446
30	16·95	1·1967
35	16·00	1·1906
40	15·35	1·1430
50	14·10	1·0800
60	12·80	1·0621
70	11·70	1·0380
80	10·70	1·0195

The above data clearly show that the disappearance of $K_2S_2O_8$ in a buffered medium is first order with respect to the persulphate concentration and is not of second order as shown by Purohit and Srivastava (loc. cit.). The decrease in rate constant values with time observed by them in unbuffered medium is, therefore, due to the retarding effect of the increasing amount of acid formed with the progress of the reaction.

EFFECT OF PERSULPHATE CONCENTRATION

The effect of initial concentration of $K_2S_2O_8$ on its rate of disappearance was determined at a constant concentration of glucose (0·01 M).

The results obtained are represented graphically in fig. 1. The first order rate constant values evaluated from these curves are given in table 3.

TABLE 3

Glucose=0·01 M, $AgNO_3$=0·00075 M, Temperature=25°C.

Conc. of $K_2S_2O_8$	$k \times 10^3$
0·0050 M	6·8897
0·0075 M	5·9397
0·0100 M	5·6881
0·0150 M	4·5190
0·0200 M	4·0761
0·0250 M	3·6215
0·0300 M	3·5984
0·0400 M	2·9001
0·0500 M	2·7294

Although the rate constant is first order in a given experiment as shown by the linear curves given in fig. 1, its value decreases regularly with an increase in the initial concentration of persulphate. A similar behaviour has been reported by Eager and Winkler[5] in the oxidation of mercaptans, by Srivastava and Ghosh[6] in the oxidation of formate ion and by Khulbe and Srivastava[7] in the Ag^+ catalysed oxidation of iso-propyl alcohol by $K_2S_2O_8$. An increase in the rate constant value with an increase in $K_2S_2O_8$ concentration has been reported by Levitt and Malinowski[8] in the uncatalysed oxidation of iso-propyl alcohol. Since the rate does not fall appreciably with an increase of ionic strength or in the presence of high sulphate concentration (vide Table 1) and since the reaction has been carried out at constant pH., the most probable cause of the observed fall in rate constant value may b due to the specific inhibitory effect of K^+ ions, which is being investigated.

EFFECT OF GLUCOSE CONCENTRATION

The data corresponding to different initial concentrations of glucose are represented graphically in fig. 2, and the values of rate constant evaluated from these curves are given in table 4.

TABLE 4

$K_2S_2O_8=0{\cdot}01$ M; $AgNO_3=0{\cdot}00075$ M; Temperature=25°C.

Conc. of glucose	k×10³ (unimol.)
0·005 M	4·2035
0·010 M	6·0738
0·015 M	6·2809
0·020 M	7·2070
0·030 M	7·8824
0·040 M	8·9542
0·100 M	9·7210
0·200 M	10·9250

It is seen that the value of the rate constant increases with an increase in glucose concentration and does not become independent of glucose concentration even at 0·2 M glucose concentration (c. f. the effect of iso-propyl alcohol concentration on its oxidation reported by Levitt and Malinowski[9]).

EFFECT OF $AgNO_3$ CONCENTRATION

The results obtained in presence of different concentrations of $AgNO_3$ as catalyst are represented in fig. 3. From these data it is seen that the rate constant increases in a linear manner with an increase in $AgNO_3$ concentration.

EFFECT OF TEMPERATURE

The reaction was carried out at equimolecular concentration of the reactants and the values of the temperature coefficient, the energy of activation, frequency factor and entropy of activation calculated, are tabulated in table 5.

TABLE 5

$K_2S_2O_8$= glucose=0·01 M; $AgNO_3=0{\cdot}00075$ M.

Temp.	k×10³	Temp. Coeff.	E Energy of activation cals.	A Frequency factor litre mole. sec.⁻¹	ΔS≠ Entropy of activation E.S.U.
298°K	5·9494	1·57	8285	$1{\cdot}303\times10^2$	−48·85
303°K	7·2580			$1{\cdot}293\times10^2$	−48·89
308°K	9·3681	1·56	8418	$1{\cdot}301\times10^2$	−48·93
313°K	11·3378			$1{\cdot}287\times10^2$	−48·98
Mean		1·565	8351·5	$1{\cdot}296\times10^2$	−48·91

It is seen that the reaction is characterised by a low temperature coefficient, low energy of activation, a small frequency factor and by a large negative entropy of activation.

Further study of this reaction to identify the different products of oxidation and to elucidate the exact mechanism of this complex reaction is in progress.

ACKNOWLEDGEMENT

The authors are grateful to the authorities of Th. D. S. B. Govt. College, Naini Tal for the facilities provided for undertaking this work.

REFERENCES

1. Eager, R. L. & Winkler, C. A. 1948. *Can. J. Res. B.*, **26**, 527.
2. Khulbe, K. C. & Srivastava, S. P. 1961. *Proc. Nat. Acad. Sci., India.* **30**, 117.
3. Khulbe, K. C. & Srivastava, S. P. *Agra Univ. J. Res.* (*Sci.*), *India* Under print.
4. Levitt, S. & Malinowski, E. R. 1955. *J. Am. Chem. Soc.*, **77**, 4517.
5. Levitt, S. & Malinowski, E. R. 1958. *J. Am. Chem. Soc.*, **80**, 5334.
6. Purohit, G. B. & Srivastava, S. P. 1961. Vijnana Parishad, Allahabad, India. **4**, 199.
7. Purohit, G. B. & Srivastava, S. P. 1961. Vijnana Parishad, Allahabad, India. **4**, 303.
8. Srivastava, S. P. & Ghosh, S. 1953. *Zeit. Phys. Chem.*, **202**, 198.
9. Szabo, Csanyi & Galiba. 1952. *Z. anal. Chem.*, **155**, 269.

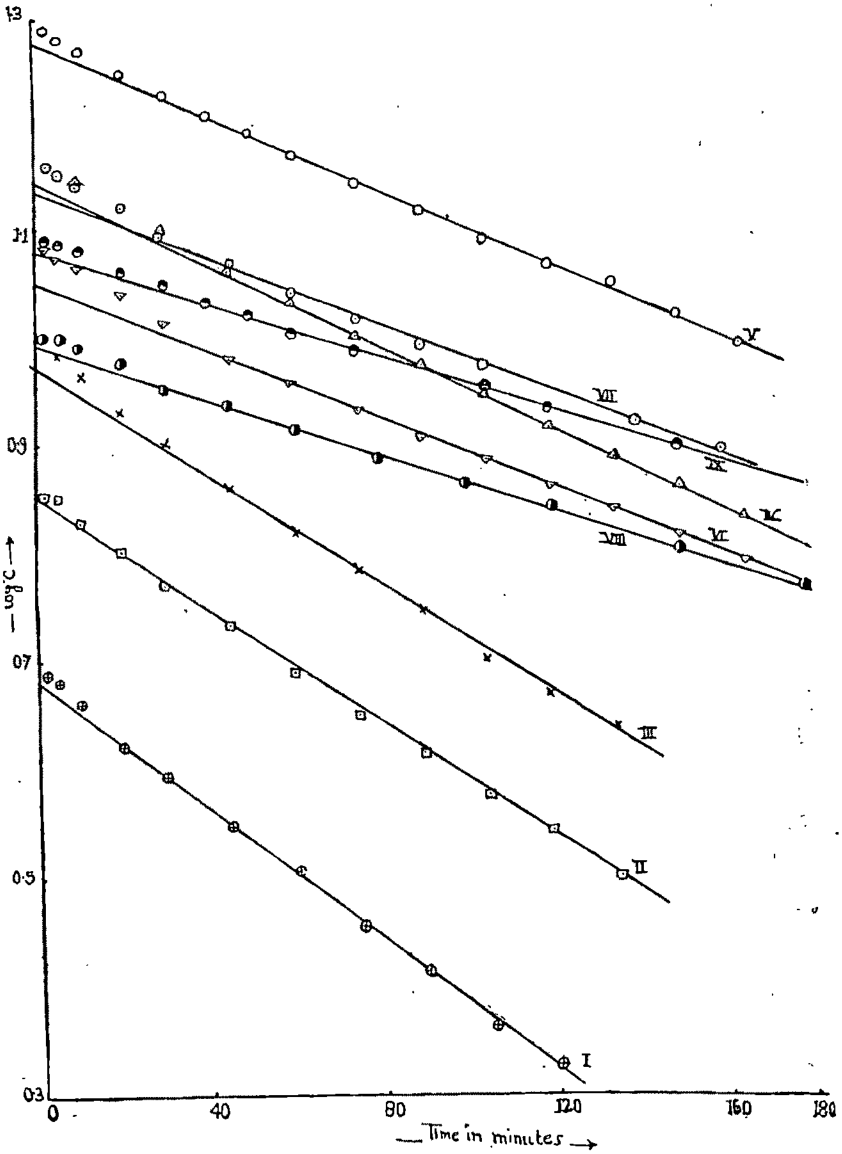

Fig. 1

Glucose $=0{\cdot}01$M, $AgNO_3=0{\cdot}00075$ M, Temp. $=25^oC$.

I, —, $K_2S_2O_8=0{\cdot}005$ M;
II, —, $K_2S_2O_8=0{\cdot}0075$ M;
III, —, $K_2S_2O_8=0{\cdot}01$ M;
IV, —, $K_2S_2O_9=0{\cdot}015$ M;
V, —, $K_2S_2O_8=0{\cdot}02$ M;
VI, —, $K_2S_2O_9=0{\cdot}025$ M;
VII, —, $K_2S_2O_8=0{\cdot}03$ M;
VIII, —, $K_2S_2O_8=0{\cdot}04$ M;
IX, —, $K_2S_2O^8=0{\cdot}05$ M;

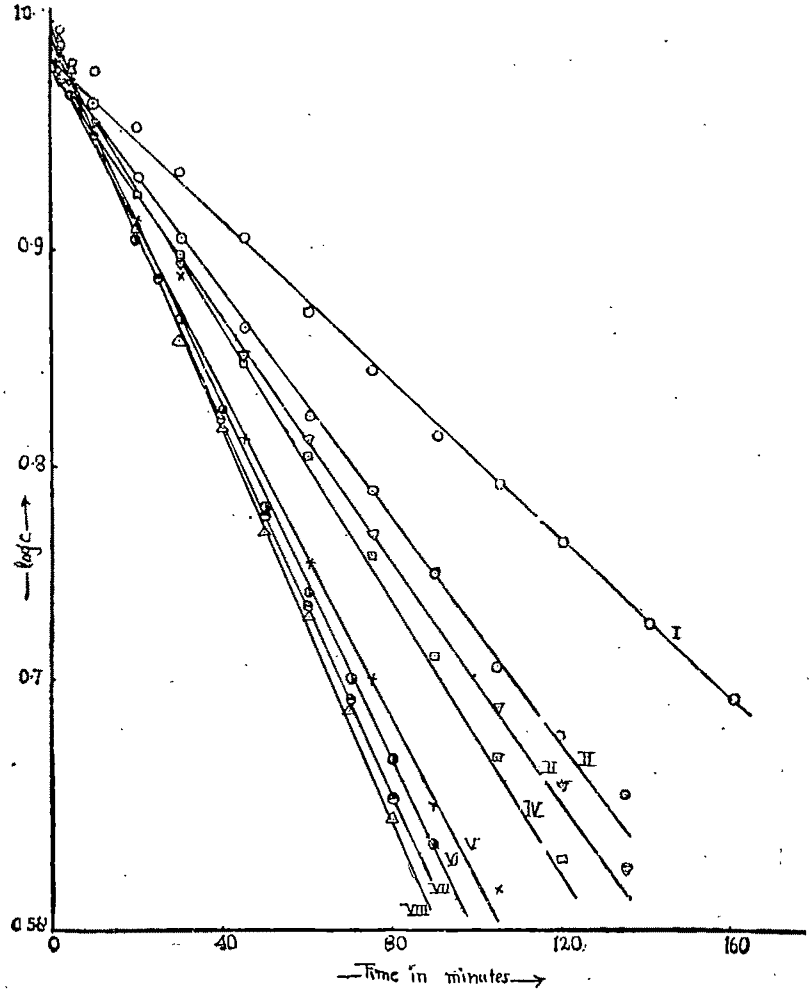

Fig. 2.

$K_2S_2O_8$=0·01 M; $AgNO_3$=0·005 M; Temp, —25°C.

I, —, Glucose=0·005 M;	II, —, Glucose=0·010 M;
III, —, Glucose=0·015 M;	IV, —, Glucose=0·020 M;
V, —, Glucose=0·030 M;	VI, —, Glucose=0·040 M;
VII, —, Glucose=0·100 M;	VIII, —, Glucose=0·200 M;

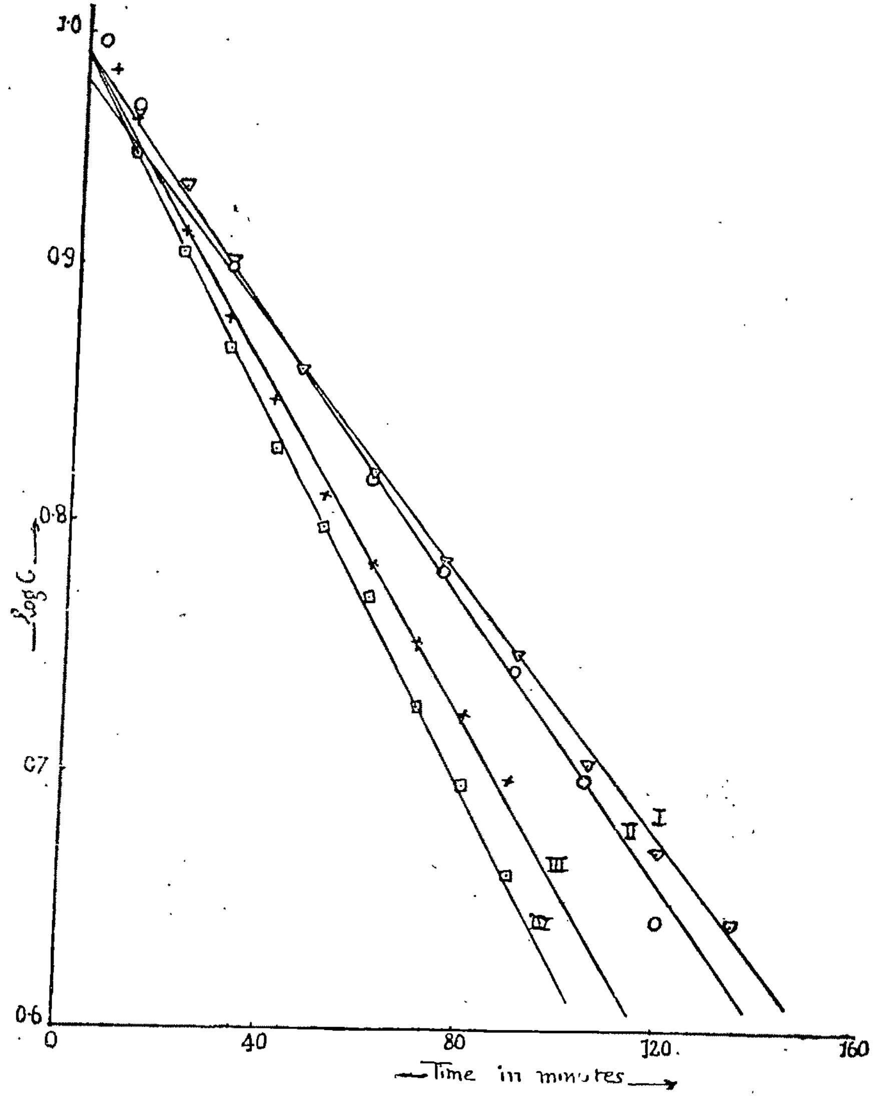

Fig. 3.

$K_2S_2O_8$=Glucose=0·01 M; Temperature—25_0C.
I, —, $AgNO_3$=0·00075 M; $k=6{\cdot}0738\times10^{-3}$.
II, —, $AgNO_3$=0·0008 M; $k=6{\cdot}5635\times10^{-3}$.
III, —, $AgNO_3$=0·0009 M; $k=7{\cdot}5612\times10^{-3}$.
IV, —, $AgNO_3$=0·0010 M; $k=8{\cdot}4440\times10^{-3}$.

THE ALIMENTARY CANAL OF HISTER MAINDRONII LEWIS (COLEOPTERA—HISTERIDAE)

R. D. Saksena and P. S. Verma
Department of Zoology, B. R. College, Agra.

Introduction

The studies of the alimentary canal of Histerid beetles have specially been undertaken in view of the fact that these beetles feed upon maggots which live and subsist on the dung of Cows and Buffaloes. Thus they exercise a definite control on the growing population of the developing maggots and contribute to mitigate the housefly menace to some extent. The alimentary canal of Coleoptera has been studied by various authors *viz.*, Fletcher (1930), Bigham (1931), Landis (1936), Pradhan (1936, 1939), Saksena (1951) and Sinha (1958) but the present authors mainly confined themselves to the study of these organs in *Hister maindronii* Lewis, chiefly for their special interest in acting as predators on the maggots inhabiting the cattle dung.

Material and Technique

The beetles were collected from the heaps of Cow and Buffalo dung in various localities of Bichpuri (Agra) and kept in a glass cage on a regular supply of fresh dung every day. Freshly killed specimens were dissected in normal saline under Bausch and Lomb stereoscopic binocular microscope. For the histological studies, the alimentary canal along with Malpighian tubules were dissected out of the body, fixed in Bouin's fluid for six to eight hours and washed in water. After dehydration in varying strengths of alcohol, they were cleared in cedarwood oil, embedded in paraffin wax as usual. Microtome sections of 5-6 microns thick were cut by a rotary microtome. Balsam mounts of the slides were prepared after staining in Ehrlich's acid haematoxylin and eosin.

Observations

The alimentary canal in *Hister maindronii* (Fig. 1) runs straight in the thorax but is thrown into a few convolutions in the abdomen. It is about twice as long as the body and is manifest into three usual divisions *viz.*, the fore-gut (stomodaeum), the mid-gut (mesenteron or ventriculus) and the hind-gut (proctodaeum). The fore-gut measures about 4 to 6 mm., mid-gut 10 to 13 mm. and the hind-gut 6 to 8 mm. A fine network of tracheae surrounds the alimentary canal, in addition to a thick layer of adipose tissues. The relative abundance or otherwise of this tissue varies with the time of the year. It was found that at the close of the active period when preparing to hibernate, the fat in the body increases considerably to engulf completely all the internal organs. The *Fore-gut* (stomodaeum) is comparatively a short straight thin tube almost exclusively confined to the head capsule and prothoracic region. It consist of the buccal cavity, the *Pharynx* the *oesophagus* the *crop*, and the *proventriculus*.

The mouth is anterior and the buccal cavity is merely a short space for the conduction of the food to the pharynx which follows it. The *pharynx* is a thin walled tube provided with extrinsic and intrinsic muscles, which arise from the walls of the pharynx and are inserted on the head sclerites and tentorium. The pharynx passes through the brain ring and can be consequently divided into the pre-cerebral and post-cerebral pharyngeal regions.

The *oesophagus* (OE) is a narrow thin walled tube which is followed by crop. The main function of the oesophagus is the conduction of food from the pharynx to the crop.

The *crop* (CR) is a pear shaped structure with a narrow anterior and wide posterior end, lying partly in the posterior region of the head capsule and partly in the region of the prothorax.

The crop is followed a small round proventriculus (PRVT) and opening into the mid-gut by the oesophageal valve. It is telescoped within the anterior end of the mid-gut.

Salivary or oesophageal glands are absent in this beetle.

HISTOLOGY OF THE FORE-GUT

A transverse section of the fore-gut shows two or three layers of the outer circular muscles (CM), while longitudinal muscles (LM) lie immediately below the circular ones in separate bundles. The epithelium (EPTH) is syncytial and the chitinous intima (INT) is well developed.

In the region of the *pharynx* (Fig. 2) the chitinous intima (INT) is very well developed. It is thrown into longitudinal folds of varying sizes and is devoid of spines and bristles. The epithelium (EPTH) is syncytial with distinct nuclei and finely granular cytoplasm. The musculature consists entirely two layers of moderately developed circular muscles (CM). Longitudinal muscles (LM) are not visible.

In the sections passing through the *oesophagus* (Fig. 3) the chitinous intima (INT) is somewhat thin and weaker than pharynx. But the chitinous intima forms two longitudinal folds, one dorsally placed and another ventrally, apparently dividing the lumen into two unequal halves. From the chitinous intima arise a number of spines which project into the lumen. These spines appear to act as a sieve for the food to pass into the mid-gut. The epithelium (EPTH) is syncytial with distinct nuclei and finely granular cytoplasm. The circular muscles (CM) consist of two layers comparatively thin than the pharyngeal region. The longitudinal muscles (LM) as usual are arranged in the form of bundles just below the circular muscles in this region.

In the region of *crop* (Fig.4) the structure is similar to that of the oesophagus except for a few differences. The chitinous intima (INT) is continued to be provided with bristles as in the oesophagus. The lumen enlarges to facilitate the storage of food material. The longitudinal muscles are altogether absent in this region.

Pradhan (1936) states that beside mixing and churning of food and secretions, it is also possible that when the major folds of the chitinous intima project into the lumen and their bristles stand erect, these bristles may form a good straining sieve. This statement holds good for the present insect too.

The *proventricular region* (Fig. 5) of the fore-gut is most important and hence has undergone a greater degree of specialization. Its walls are composed of thick circular (CM) and longitudinal muscles (LM) apparently for powerful peristaltic movements. The former are disposed off in circular layers of which as many as three layers can be seen, while the longitudinal muscles are arranged in bundles. The epithelial layer (EPTH) is thin with indistinct cell walls and nuclei. The chitinous intima is thrown into eight longitudinal folds, the four major and four minor. These longitudinal folds of chitinous intima (INT) are not provided with bristles or spines. By the contraction and the relaxation of the circular muscles the longitudinal folds of the intima meet in the lumen and crush the food particles finely.

The *Oesophageal valve* (Fig. 6) The fore-gut epithelium, as it decends down into the mid-gut is all round thrown into a fold before continuing into the mid-gut epithelium (MEPTH). This fold projecting into the lumen of mid-gut is located as a guardian without exercising any check to its entrance. Such a fold has been observed by various authors and named as oesophageal fold by some and oesophageal valve by others. The fold has an inner wall into which the thin layer of intima and epithelium of the fore-gut are continued. It is continued into an outer wall which has specialized elongated columnar glandular epithelial cells (GLEPTH) with distinct cell walls but devoid of chitinous intima. The inner wall of the fold is surrounded by three layers of circular muscles and a few bundles of longitudinal muscles; while the outer wall is surrounded by inner two layers of circular muscles and a few longitudinal muscles. The outer wall is later subsequently continued into the lining of the mid-gut.

The function of this structure is yet very controversial. Pradhan (1936), however, is of opinion that it does not act as a valve because the secretory globules from the mid-gut pass into the fore-gut.

The Mid-gut or (Mesenteron) (MG) is the longest portion of the alimentary canal extending from the posterior region of the prothorax to the fourth abdominal segment. It follows a straight course for some distance then coils and unites with hind-gut. It is remarkable that in males; it lies above the reproductive organs, while in females below them. There runs a close net work of tracheae and fat bodies on the walls of mid-gut which has a broad anterior portion and a narrow posterior portion. The former is thin walled and sac like and is very distensible. The latter is narrow and thick.

All along the outer surface of the mid-gut there arise a large number of slender evaginations of the wall forming finger like diverticula or crypts, which give the mid-gut a villous appearance. These diverticula are called regenerative crypts (Snodgrass, 1935). The number of regenerative crypts (RGCT) increases in the posterior region but they are shorter in length. These regenerative crypts perform the function of regeneration and make good the continuous disintegration of cells occurring in the mid-gut epithelium.

HISTOLOGY OF THE MID-GUT

The structure of the mid-gut is distinguished from the fore-gut by the size of epithelial cells, the reversal of muscular layers and the absence of chitinous intima. The outer longitudinal muscles are arranged in small bundles. The inner circular muscles are thin in the anterior region and thick in the posterior region of the mid-gut.

The cells of the epithelium (EPTH) are large and columnar with distinct cell walls and conspicuous centrally placed nuclei. The cytoplasm is granular. The epithelium of the mid-gut is continued in the regenerative crypts (Fig. 7). The cells of the regenerative crypts (Figs. 7, 8) are of the same nature as that of the mid-gut epithelium. At the distal ends of the regenerative crypts there is an aggregation of highly stained cells, the regenerative cells (RGC). The Similar regenerative crypts with distal regenerative cells have been observed by Sinha (1958) in *Tribolium castaneum*. The basement membrane is conspicuous throughout the length of the mid-gut.

The Hind-gut (Proctodaeum (is a much shorter tube than the mid-gut, though it is about twice the length of the fore-gut. It consists of an *ileum* (IL) the *colon* (COL) and the *rectum* (RECT). Ileum unites with the mid-gut. The junction between the mid-gut and hind-gut is marked off by the presence of pyloric valve.

The *ileum* (IL) is a coiled and thick walled tube extending between the fourth and fifth abdominal segements. The diameter of the ileum is similar throughout its length except at the posterior end where it gradually widens into the colon (COL). The *colon* is a thin walled pear-shaped structure. It has got a wrinkled appearance externally and narrows down posteriorly leading into the *rectum* (RECT) which has very thick walls.

HISTOLOGY OF THE HIND-GUT

The hind-gut has the usual histological details *i.e.*, the two muscle layers are lined by the basement membrane, epithelium and finally by chitinous intima.

The ileum (Fig. 9) has got comparatively thick walls. There is a single inner layer of circular muscles (CM), the outer longitudinal muscles (LM) are arranged in bundles. The epithelium (EPTH) forms six to seven longitudinal folds. The cells of the epithelium are columnar with distinct cell walls and centrally placed nuclei. The cytoplasm is finely granular. The chitinous intima (INT) is thin, bends sharply with the epithelium folds, provided with sharp spines or setae.

The wall of the colon (Fig. 10) is comparatively thin. The outer longitudinal muscles (LM) are arranged in bundles, while the inner circular muscles (CM) form a single layer. The epithelium form ten longitudinal folds. The lumen of the colon is enlarged, comparatively larger than that of the ileum. The epithelium cells (EPTH) are columnar with distinct cell-wall and centrally placed nuclei. The cytoplasm is finely granular. The chitinous intima (INT) is provided with densely placed spines or setae.

The wall of the rectum (Fig. 11) is thicker than ileum and colon. The arrangement of muscular layers is similar to that of the ileum and colon. The epithelium forms numerous longitudinal folds. The cells of the epithelium are flat and columnar. The epithelial folds are lined by chitinous intima (INT) which is devoid of spines or setae.

MALPIGHIAN TUBULES

Six Malpighian tubules (MT) arise separately at the junction of the mid and hind-gut. Two of these tubules are very long and coil round the mid-gut as far forward as the proventriculus. They very intimately adhere to the walls of the mid-gut and run through a number of trachae and fat bodies. Two others lie coiled under the alimentary canal and the rest two lie in association with the reproductive organs. In freshly dissected specimens the Malpighian tubules exhibit forward movements, which may be due to the excretory processes.

The disposition of Malpighian tubules in *Hister maindronii* differs markedly from other Coleopterous insect, in the fact, that there is a total absence of reassociation of these tubules with the proctodaeum.

A transverse section of the Malpighian tubule (Fig. 12) shows six to eight cells arranged in a circle surrounding a narrow central lumen. The nuclei of these cells are large, round or oval, take up a deep stain with Ehrlich's haematoxylin. No striated border has been observed. Sinha (1958) also did not observe striated border in *Tribolium castaneum*.

SUMMARY

1. The alimentary canal of *Hister maindronii* Lewis is about twice as long as the body.
2. Salivary or oesophageal glands are absent in this beetle.
3. In oesophagus and crop, the chitinous intima is provided with spines or bristles which project into the lumen and act as sieve for the food to pass into the mid-gut.
4. The proventriculus is provided with four major and four minor longitudinal folds of chitinous intima.
5. The outer surface of the mid-gut is provided with a large number of slender evaginations, the regenerative crypts.
6. The chitinous intima of ileum and colon is provided with sharp spines.
7. The Malpighian tubules are six in number and do not reassociate with the proctodaeum.

ACKNOWLEDGEMENTS

The authors have great pleasure to record their deep sense of gratitude to Dr. S. N. Singh, M. Sc., Ph. D., Principal, B. R. College, Agra, for the constant encouragement and facilities enjoyed by them. They are extremely grateful to Mr. E. O. Pearson, Director, Commonwealth Institute of Entomology, London for the identification of this insect. Thanks are also due to C. S. I. R. for the award of fellowship to the junior author.

REFERENCES

1. Bigham, J. T. 1931. The alimentary canal of *Asaphaes memnonius*, *Ohio. Jour. Sci.*, **31** (5) : 386-395.
2. Fletcher, F. W. 1930. The alimentary canal of *Phyllophaga gracilis*. *Ohio. Jour. Sci.*, **30**: 109-119.
3. Landis, B. J. 1936. Alimentary canal and Malpighian tubules of *Ceratomegilla fuscilabris* (Coccinellidae) *Ann. Ent. Soc. Amer.*, **29** (1) : 15-27.
4. Pradhan, S. 1936. The alimentary canal of *Epilachnc indica* (Coccinellidae : Coleoptera) with a discussion on the activity of the mid-gut epithelium. *Jour. Roy. Asiat. Soc. Bengal*, **11** : 127-156.
5. Pradhan, S. 1939. The alimentary canal and proepithelial regeneration in *Coccinella Septempunctata* with a comparison of carnivorous and herbivorous Coccinellids. *Quart. Jour. Micr. Sci.*, **81** : 451-475.
6. Saksena, R. D. 1951. Observations on the morphology and physiology of alimentary canal of *Aulacophora foveicollis*, *Proc. Natl. Acad. Sci. India*, **21** : 23-32.
7. Sinha, R. N. 1958. The alimentary canal of *Tribolium castaneum* (Coleoptera-Tenebrionidae) *Jour Kansas. Ent. Soc.*, **31** (2) : 118-125.
8. Snodgrass, R. E. 1935. Principles of Insect Morphology. *Mc Graw Hill Book Company, New York* and *London*.

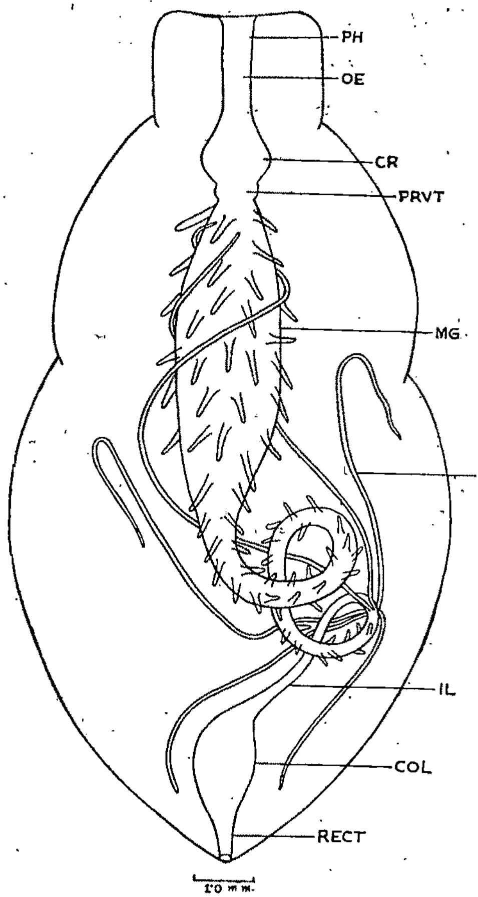

FIG. 1

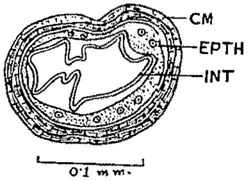

FIG. 2

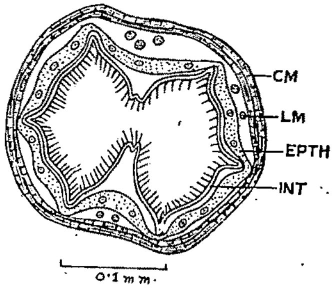

FIG. 3

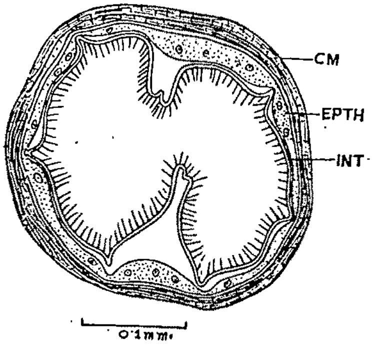

FIG. 4

Fig. 1—Alimentary canal in situ.
Fig. 2—T. S. of Pharynx.
Fig. 3—T. S. through the anterior region of Oesophagus.
Fig. 4—T. S. through the Crop.

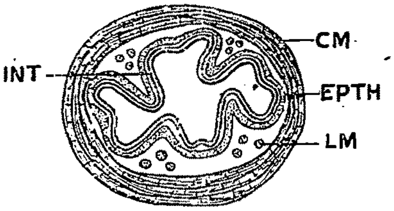

FIG. 5

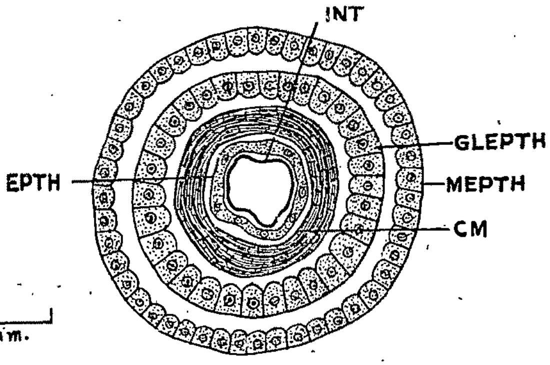

FIG. 6

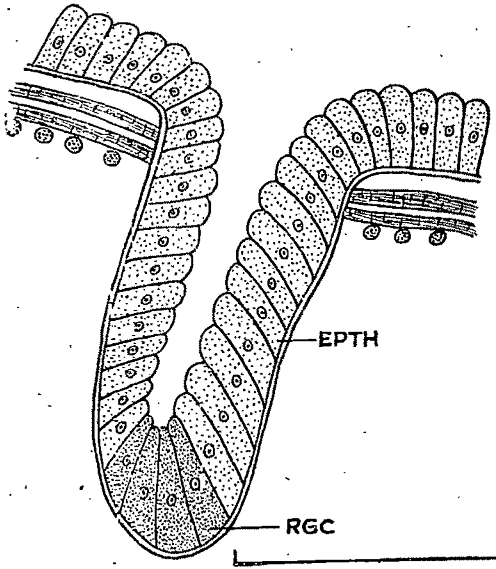

FIG. 7

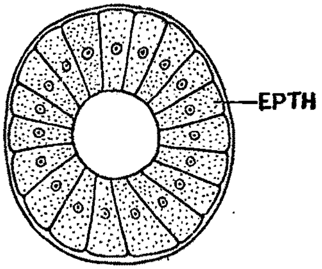

FIG. 8

Fig. 5—T. S. through Proventriculus.
Fig. 6—T. S. through Oesophageal valve.
Fig. 7—L. S. through Regenerative crypt.
Fig. 8—T. S. through Regenerative Crypt.

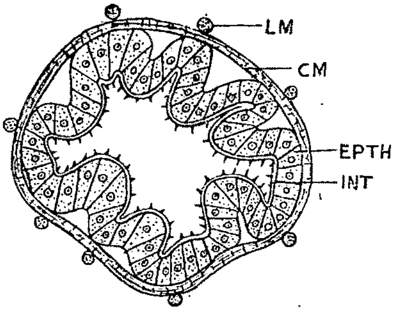

FIG.9

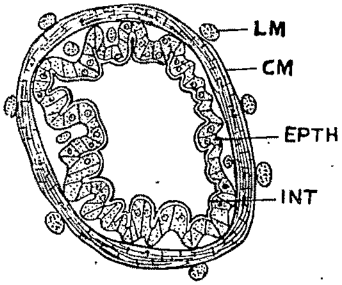

FIG.11

0·1 mm.

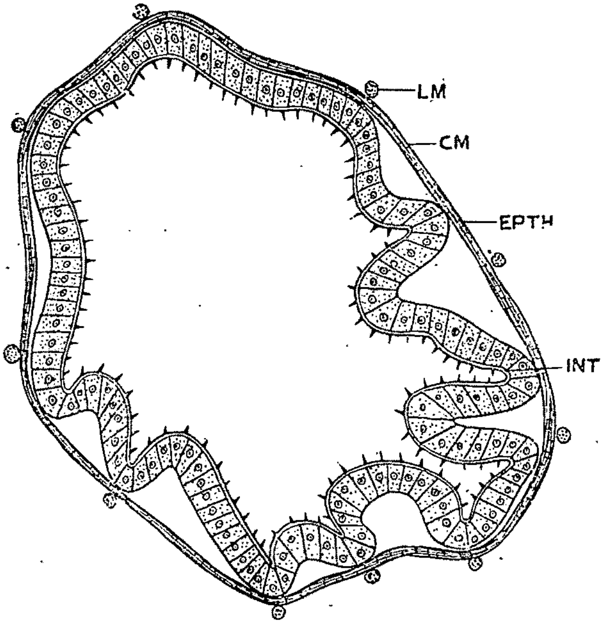

FIG. 10

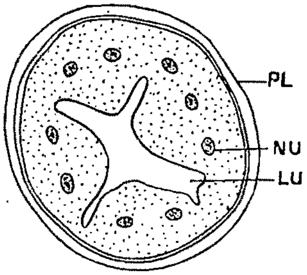

FIG.12

Fig. 9—T. S. through Ileum.
Fig. 10—T. S. through Colon.
Fig. 11—T. S. through Rectum.
Fig. 12—T. S. through Malpighian tubule.

ON A NEW SPECIES OF THE GENUS *CRANOPYGIA* BURR (DERMAPTERA : PYGIDICRANIDAE) FROM SOUTH INDIA

V. C. Kapoor

Research Scholar, Ministry of Education, Government of India,
Department of Zoology, Agra College, Agra.

This paper is the description of a new species belonging to the genus *Cranopygia* Burr, from South India, based upon the collections made by Dr. David Livingstone, School of Entomology, St. John's College, Agra. I offer my sincere thanks to him for placing this interesting collection at my disposal.

My thanks are due to Dr. H.N. Baijal, Zoology Department, Agra College, Agra, for guidance, Dr. M. Ray, Principal and Dr. C.P. Singh, Head of the Zoology Department, Agra College, Agra, for the facilities provided.

Cranopygia livingstoni sp. nov. (Figs. 1—4).

Male—Body reddish brown; head, pronotum, legs and tegmina pale yellowish marked with black and brown stripes.

Head—Dorso-laterally setaceous; sutures distinct; occiput slightly elevated; laterally black, median suture black, frons elevated in the centre with black stripe and lateral markings. Eyes black, well developed. Antenna broken.

Pronotum—Almost as long as the head, with two lateral stripes somewhat anastomosing caudad; prozona tumid, separated caudad from metazona by strongly impressed, crescentric sulcus; median sulcus distinct; metazona laterally depressed; anterior and lateral margins distinctly convex, caudal margin truncate.

Tegmina and Wings—Pubescent; pale yellowish with broad brown bands at the costal and sutural margins, anastomosing at the posterior margin; about two and a half times longer than broad; anterior margin oblique, exposing a prominent triangular whitish scutellum. Wings exposed posteriorly.

Legs—Femora compressed and longitudinally carinulate, mid- and hind-femora with anterio-laterally black, oval spots; tarsi simple, second tarsal segment shortest, a little less than one half the first.

Abdomen—Reddish brown, gradually widened to the ultimate tergite; setaceous.

Ultimate tergite—Transverse, rugose with abbreviated median sulcus.

Forceps—Asymmetrical, subcontiguous; left branch with broad base, curved, the inner basal margin with three prominent teeth, the outer basal margin with a small notch, middle inner margin smooth while the apical inner margin with a prominent tooth, crenulate and slightly hooked; the right branch with small base, straight, slightly hooked at the apex, inner margin homogeneously crenulate.

Pygidium—Indistinct.

Penultimate sternite—Lateral margin rounded, very feebly sinuate mesad.

Genitalia—Metaparameres mucronate; the inner processes indistinguishable from the outer angles of the metaparameres; the preputial sacs long; virga very long, much longer than the whole genital armature.

Length—Body............29·0 mm.
Forceps. .... 6·0 mm.

Female—Unknown.

Holotype—One male in spirit, labelled "On light, Thekkady, (Kerala State), South India, 27.V.1965, Coll. D. Livingstone." At present in author's collection.

This species comes near to *Cranopygia constricta* Hincks (1955) from Sikkim and Bhutan, from which it can be easily distinguished by more rugose ultimate tergite, its abbreviated median sulcus, asymmetrical forceps, form of penultimate sternite, differences in the metaparameres and genital armature.

REFERENCES

1. Burr, M. 1910. *Fauna of British India.* Dermaptera.
2. Hincks, W.D. 1955. New species of Pygidicranine Earwigs (Dermaptera: Pygidicranidae). *Ann. Mag. Nat. Hist.* (12) **8**: 806-827.
3. Hincks, W.D. 1959. Systematic monograph of the Dermaptera of the World. Part II. Pygidicranidae (excluding Diplatyinae). *British Museum (Natural History) London.*

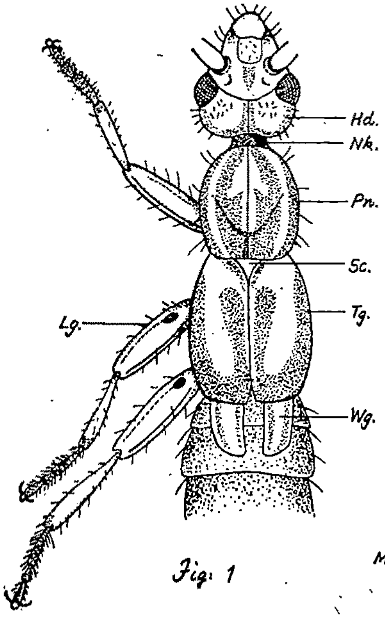

Fig: 1

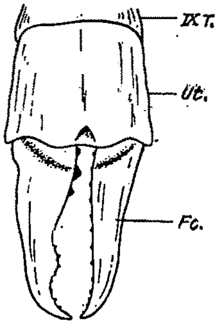

Fig: 2

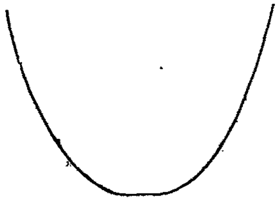

Fig: 3

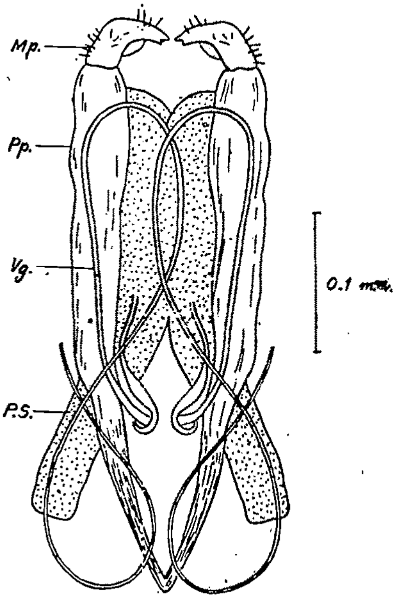

Fig: 4

Fig. 1. Male (Head, pronotum, tegmina and wings).
Head—Hd; Leg—Lg; Neck—Nk; Pronotum—Pn; Scutellum—Sc; Tegmina—Tg; Wings—Wg.

Fig. 2. Ultimate tergite and forceps.
Forceps—Fc; Ninth tergite—IXT; Ultimate tergite—Ut.

Fig. 3. Distal portion of male penultimate sternite

Fig. 4. Male Genitalia.
Metaparameres—Mp; Proparameres—Pp; Preputial Sac—P.S; Virga—Vg.

ABSORPTION SPECTRA OF SOME NEW KETONES

PART II—ABSORPTION SPECTRA OF α-BROMO-α-FORMYL-P-BROMO ACETOPHENONE

D. D. PANT, O. N. PERTI, K. P. VERMA AND G. C. SINGHAL
Physics and Chemical Laboratories, D. S. B. Govt. College, Nainital.

ABSTRACT

(Absorption spectra of α-bromo-α-formyl-p-bromo acetophenone has been studied in n-hexane. The bathochromic shift observed appears to be due to the formyl group.)

INTRODUCTION

Bokadia and Verma[2,3] studied the UV absorption spectrum of chloro ethyl acetate, chloro formyl ethyl acetate, α-bromo acetophenone, α-formyl -α-bromo acetophenone and α-bromo-α-formyl-p-chloro acetophenone in water, n-hexane, alcohol, ether, hydrochloric acid and caustic potash. In this paper we are reporting the UV absorption spectra of α-bromo-α-formyl -p-bromo acetophenone in n-hexane.

EXPERIMENTAL

Para bromo acetophenone was prepared by the method already reported in literature[8].

Starting from this compound α-bromo-α-formyl-p-bromo acetophenone was prepared by the method described by earlier workers[3,1] M. P. 114°C.

Absorption measurements were made with a Hilger Uvispek photo electric spectrophotometer with quartz optics. Solvent used was purified n-hexane. The strength of solution was $0{\cdot}5 \times 10^{-4}$ M. Results are recorded in Fig 1.

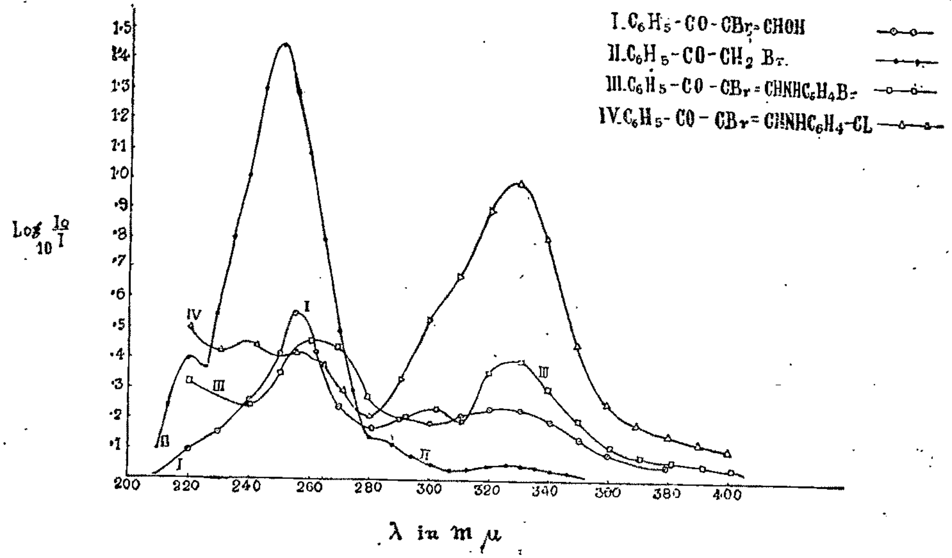

From the graph λ_{max} and ε_{max} are noted in table 1.

TABLE 1

Compounds	λ_{map}	ε_{max}	λ_{max}	ε_{max}	λ_{max}	ε_{max}	λ_{max}	ε_{max}
I. 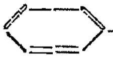—CO–CBr=CHOH	255	11,000	285	3,400	320	1600	—	—
II. Cl—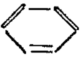CO–CBr=CHOH	255	5,600	—	—	330	1080	378	7800
III. 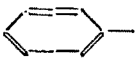—CO—CH_2Br	250	29,000	—	—	320	840	—	—
IV. Br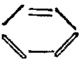CO–CBr=CHOH	260	18,000	—	—	335	2200	385	600
α:bromo-α-formyl-p-bromo acetophenone								

Note : I, II, III studied previously[2,3]

DISCUSSION

One of us[1] had studied previously the absorption spectra of formyl chloro ethyl acetate 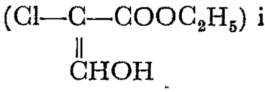 $(Cl—\underset{\underset{CHOH}{\|}}{C}—COOC_2H_5)$ in different solvents and noticed that the absorption band in this ester is due to $-COOC_2H_5$ which undergoes a bathochromic displacement in chloro ethyl acetate.[5,6] Formyl chloro ethyl acetate exists mostly in enol form and the presence of an electron repelling—OH group at one end of the conjugated system of the enol causes a bathochromic displacement to about 245 mμ.

In case of α–bromo-α–formyl acetophenone the three maxima are 255, 285 and 320 mμ. A comparison of this with acetophenone[7] (242, 278 and 320 mμ) shows that by introducing a formyl radical =CHOH the effect is bathochromic. Likewise if we compare the three maxima of α–bromo–α–formyl acetophenone with those of phenacyl bromide a new band is observed at 222mμ. However, when we compare α–bromo–α–formyl –p– chloro acetophenone (255, 330 and 378 mμ) with α–bromo–α– formyl acetophenone and phenacyl bromide it is noticed that the band due to phenyl group (namely 270–280 mμ) is absent indicating that as suggested by us earlier a quinonoid type structure is the contributory factor.

Structure of α–bromo–α–formyl–p– bromo acetophenone from the method of preparation can be suggested as follows :—

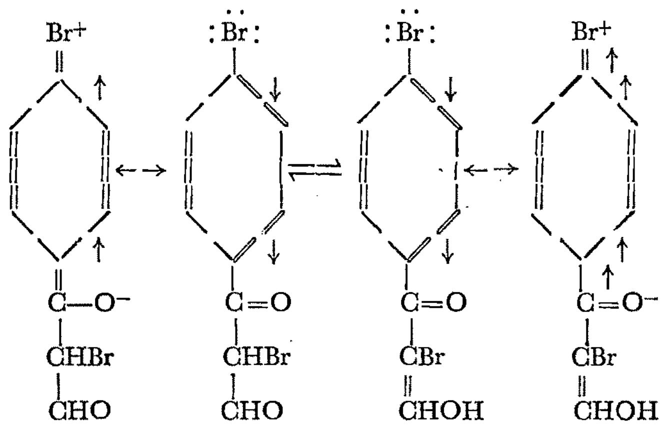

α–bromo–α–formyl–p–bromo aceptophenon (IV) is a purely enol form and is a stable compound (M.P.114°C). On comparison of its absorption with that of α–bromo–α–formyl acetophenone, α–bromo–α–formyl–p–chloro acetophenone and phenacyl bromide it is found that here also the formyl radical has a bathochromic effect. Here again the absorption band (280 mμ region) due to phenyl radical is absent and so quinonoid type of contributing structures are suggested.

ACKNOWLEDGEMENTS

Authors are grateful to the authorities of D. S. B. Govt. College, Nainital for providing research facilities and also to the C. S. I. R. for senior research fellowship to one of us (G. C. S.).

REFERENCES

1. Agrawal, Gupta & Deshpande, 1949. *J. Ind., Chem. Soc.*, **26** : 55.
2. Bokadia & Verma, 1957-58. *J. Sci. Res. B.H.U.*, **VIII** (2) : 133.
3. Bokadia & Verma, 1958. *Agra Univ. J. Res (Sci).*, **VII** (2) : 119.
4. Bokadia & Garg, 1957. *J. Ind. Chem. Soc.*, **34** : 286.
5. Hantzsch, 1914. *Z. Physik. Chem.*, **96** : 624.
6. Hantzsch, 1917. *Ber.*, **50** : 1422.
7. Mortan, Hassan, & Calloway, 1934. *J. Chem. Soc.*, 883.
8. Vogel : *Practical Organic Chemistry*, Longmans Green & Co., London 1948, p. 696.

A NOTE ON THE DISTRIBUTION OF INDIAN COLLEMBOLA

H. N. Baijal
Zoology Department, Agra College, Agra.

The Collembola, which are popularly known as "bristles tails" or "spring tails" have been practically ignored in India. Apart from the numerous remarkable characters of purely scientific interest in their general organisation and habits as compared with other insects they form a group of very great importance in various other ways. They have attained a stage of being pests in Europe and other countries; the greatest damage is being done to young, tender plants, specially to seedlings by making irregular holes in the leaves, gradually piercing them through and through, characteristically leaving the epidermis intact at the bottom of the punctures. Many species attack the stems of plants just below the ground level and often cut through them. On roots of Sugarcane, spring tails cause injury by gnawing pits and by destroying rootlets. In North America a single species of Collembola *Bourletiella hortensis* (Fitch) has earned sufficient importance to receive its popular name as the garden springtail, a pest of great though local importance on seedlings of flowers of dandelion. Some forms are major pest of edible mushroom in U.S.A. *Sminthurus viridis* (L) is the most important pest of field crops. This "lucerene flea, as it is called, damages the foliage of many winter fodder plants particularly *alfaalfa* and clovers besides attacking wheat, oats and barley.

Collembola have a world wide distribution. About 2,000 species have been described and 137 of these have been recorded from India. The first important contribution on the distribution of Collembola was made by Womersley(1939) in his publication dealing with Apterygota of Australia. Salmon (1941) discussed the Zoogeography of New Zealand Collembola and subsequently (1947) circumscribed their distribution to cool and moist environments. The author has herein given a complete analysis of these small soil inhabiting forms from India with a note on their distribution. A discussion on Zoogeography leads to very great interest because of their small size, apterous condition and difficulties of migration as large tracts of water and swift flowing rivers form almost an impassable barriers to them. Presently land animals like reptiles, bird and mammals which can easily migrate over long distances mainly form the basis of the world land mass into Zoogeographical regions but the distribution of small organisms as Collembola, neglected so far would be likely to throw a flood of light on the prehistoric divisions of the World.

The peculiarities of the composition of Collembolan fauna of India exhibit high degree of endemism *viz.*, 75% of the total species belonging to India. Even some of the genera like *Idiomerus*, *Dicranocentroides*, *Cyphoderopsis*, *Pseudocyphoderus*, *Himalanura* and *Salmonomia* are confined totally to Indian limits. The majority of these endemics occur particularly in Western and North Western part of India. This leads one to believe that species represent the Palearctic elements and along with non endemic Palaearctic species constitute 47% of the total Collembola known so far from India. The oriental elements including endemics comprise about 39% of the total fauna. The dominant oriental genera include *Hypogastrura*, *Seira*, *Aphysa* and *Handschinphysa*.

**Zoogeographical Relationship of Indian Collembola*

Subfamilies	Total	Endemic	Oriental	Ethiopion	Palaearctic	Nearctic	Australian	Wide spread
1. Poduridae	1	1	...	...	...	...	...	...
2. Onychiurinae	3	1	...	...	...	...	...	2
3. Hypogastrurinae	10	7	1	...	...	...	...	2
4. Brachystomellinae	2	2	...	...	...	...	...	...
5. Neanurinae	5	4	1	...	...	...	...	...
6. Pseudachorutinae	2	2	...	...	...	...	...	...
7. Proisotominae	11	10	...	...	...	...	...	1
8. Isotominae	10	6	...	1	1	1	...	1
9. Tomocerinae	2	...	1	...	...	...	...	1
10. Entomobryinae	47	39	4	1	2	1	...	...
11. Paronellinae	25	20	3	...	...	...	2	...
12. Cyphoderinae	7	4	1	1	...	...	...	1
13. Sminthuridinae	4	2	...	...	...	1	...	1
14. Sminthurinae	8	5	...	...	...	...	...	3
Total	137	103	11	3	3	3	2	12
Percentage out of total species		75%	8·0%	2 0%	2·0%	2·0%	1·5%	9%

* Subfamilies *Tulberginae, Anuridini, Oncopoduridae, Anurophorinae,* and *Lepidophrelline* are not represented in India.

The Ethiopian, Holarctic and Australian groups are 2%; 2% and 1·5% respectively.

Ethiopian

1. *Rhodonella minos* (Denis)
2. *Lepidocyrtinus ethiopicus* (Denis)
3. *Cyphoderus limboxiphious* Borner

HOLARCTIC

1. *Entomobrya multifasciata* Tulb
2. *Isotoma fenica* Reuter
3. *Sminthurdies violaceous* (Reuter)

AUSTRALIAN

1. *Pseudoparonellides bulbosa* Salmon
2. *Aphysa fissisetosa* Handschin

In addition to the Oriental, Palaearctic, Ethiopian and Australian faunal elements, following 12 widely distributed species also occur in India, of these *Hypogastrura armata* (Nicolet); *Onychiurus fimetarias* (L. Tulb); *Onychiurus armatus* Tulberg; *Folsomia fimetaria* (L) Tulb; *Bourletiella hortensis* (Fitch); and *Sminthurus viridis* Linne are of economic importance in India, for the reason that they attack various kinds of crops and vegetables.

WIDE SPREAD

1. *Hypogastrura armata* (Nicolet)
2. *Hypogastrura hirtellus* (Borner)
3. *Onychiurus fimetarias* (L. Tulb)
4. *Onychiurus armatus* Tulberg
5. *Folsomia fimetaria* (L) Tulb
6. *Isotomurus palustris* Muller
7. *Tomocerus vulgaris* Tulberg
8. *Cyphoderus assimilis* Borner
9. *Sminthurides aquaticus* (Bourlet)
10. *Bourletiella hortensis* (Fitch)
11. *Bourletiella arvalis* (Fitch)
12. *Sminthurus viridis* Linne

DISCUSSION

The above data indicate that Indian Collembola exhibit high degree of endemism and oriental elements. Further Indian regions show most remarkable and extensive affinities with Ethiopian regions owing to the occurrence of genus *Rhodonella* and *Cyphoderus* in both the regions. Since the migration facilities are totally wanting it is likely that these must have spread far and wide in prehistoric times before the continental drift. Next it shows affinities with Australian and Indo Malayan regions over the basis of distribution of genus *Entomobrya*, *Lepidocyrtus* and *Aphysa*. It is also remarkable that the number of cosmopolitan species is very high in India which simultaneously occur throughout the world. A detailed study of Collembolan distribution throughout the Indian limits may reveal some interesting facts about their cosmopolitan distribution. The primitive form of Collembola with very low structural organisation may have caused their wide distribution in very ancient time in very early geological periods. The comparatively lower grade of percentages of Ethiopian, Palaearctic, Nearctic and Australian elements is due to the unequality of the research done in India.

CONCLUSION

In this paper the author has stressed that Collembola are really very important for studying the Zoogeographical relationship of world regions because they are limited by their poor means of dispersal. More accurate knowledge of distribution of Collembola from various parts of Indian limits is required to arrive at substantial conclusions but author feels that this group furnishes a basis upon which real picture of Zoogeography may be built in future.

ACKNOWLEDGMENTS

I am indebted to Dr. R. D. Saxena, M. Sc., Ph. D., F. Z. S. I., Professor and Head of Zoology Department, B. R. College, Agra for most helpful discussions on various points that arose during the course of the work. I am also grateful to Principal M. Ray, D. Sc., F. N. I. and Dr. C. P. Singh, Head of Zoology Department, Agra College, Agra for facilities for work and constant encouragement.

REFERENCES

1. Salmon, J. T. 1941. The Collembolan Fauna of New Zealand including a Discussion on its distribution and Affinities. *Trans. Roy. Soc. N. Z.*, **70**: 282-431.
2. Salmon, J. T. 1949. The Zoogeography of the Collembola. *Brit. Sc. News*, **2**(19): 196-198.
3. Uchida, Hajime. 1955. Historical Reviews of the Study on the Apterygota of the Far East and Remarks on the Geographical Distribution of the Far Eastern Collembola. *Bull. Biogeog. Soc.* Japan **16-19**: 197-203.
4. Womersley, H. 1939. Primitive insects of South Australia. Adelaide Government Printer, 322 pp.

STEADY FLOW IN A UNIFORM STRAIGHT TUBE OF A PARTICULAR TYPE OF SECTION

G. C. SHARMA
Agra College, Agra.

ABSTRACT

In this paper the steady flow of an incompressible viscous fluid in a long uniform straight tube due to a constant pressure gradient has been considered. The section of the tube is a curvilinear quadrilateral bounded by the arcs of two confocal ellipses and two confocal hyperbolas. The exact solution for the velocity has been obtained by the application of finite Fourier Transform. Three particular cases have also been derived.

INTRODUCTION

The steady flow of an incompressible viscous fluid in a pipe of rectangular cross-section has been considered experimentally and theoretically by R. J. Cornish [2]. J. P. Agrawal [1] has considered the flow through pipes, section—a hyperbolic segment.

In the present paper the steady flow due to a constant pressure gradient has been considered when the section of the tube is the curvilinear quadrilateral PQRS shown in the figure.

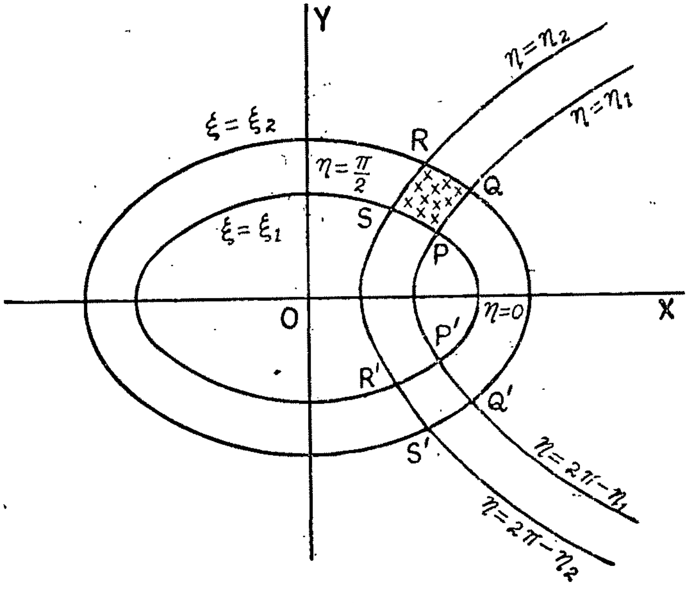

FIG. NO. 1

EQUATION OF MOTION

Using a rectangular cartesian coordinate system the equation of motion for steady flow is

$$\nu\left(\frac{\partial^2\omega}{\partial x^2}+\frac{\partial^2\omega}{\partial y^2}\right)=\frac{1}{\rho}\frac{\partial p}{\partial z} \quad ..(1)$$

where ω is the velocity in the direction of z, other components of the velocity are assumed to be zero, ν is the kinematic viscosity and $\frac{\partial p}{\partial z}$ is a constant.

For the present case put $x+iy=c\cosh(\xi+i\eta)$ ..(2)

Then $\xi=\xi_1$, $\xi=\xi_2$ are two confocal ellipses and $\eta=\eta_1$ and $\eta=\eta_2$ are two confocal hyperbolas.

If the cartesian equations of the confocal ellipses and confocal hyperbolas are

$$\left.\begin{aligned}\frac{x^2}{a^2}+\frac{y^2}{b^2}&=1\\ \frac{x^2}{a^2-k^2}+\frac{y^2}{b^2-k^2}&=1\end{aligned}\right\}$$

$$\left.\begin{aligned}\frac{x^2}{\alpha^2}-\frac{y^2}{\beta^2}&=1\\ \frac{x^2}{\alpha^2+l^2}-\frac{y^2}{\beta^2-l^2}&=1\end{aligned}\right\}$$

respectively, then the values of ξ_1, ξ_2, η_1, η_2 and c will be determined from the following equations:—

$$\left.\begin{aligned}c\cosh\xi_1&=a\\ c\sinh\xi_1&=b\\ c\cosh\xi_2&=\sqrt{a^2-k^2}\\ c\sinh\xi_2&=\sqrt{b^2-k^2}\end{aligned}\right\}$$

$$\left.\begin{aligned}c\cos\eta_1&=\alpha\\ c\sin\eta_1&=\beta\\ c\cos\eta_2&=\sqrt{\alpha^2+l^2}\\ c\sin\eta_2&=\sqrt{\beta^2-l^2}\end{aligned}\right\}$$

Equation of motion with the help of (2) becomes

$$\frac{\partial^2\omega}{\partial\xi^2}+\frac{\partial^2\omega}{\partial\eta^2}=-\frac{Pc^2}{2\mu}[\cosh 2\xi-\cos 2\eta] \quad ..(3)$$

where $-P$ is the value of $\frac{\partial p}{\partial z}$.

The boundary conditions are:

$$\left.\begin{aligned}\omega=0 \text{ when } \xi=\xi_1 &\text{ and } \xi=\xi_2\\ \omega=0 \text{ when } \eta=\eta_1 &\text{ and } \eta=\eta_2\end{aligned}\right\} \quad ..(4)$$

SOLUTION OF THE EQUATION

Putting $\eta = \mathrm{A}q + \mathrm{B}$ where

$$\mathrm{A} = \frac{\eta_2 - \eta_1}{\pi} \text{ and } \mathrm{B} = \eta_1 \qquad ..(5)$$

equation (3) becomes

$$\frac{\partial^2 \omega}{\partial \xi^2} + \frac{\pi^2}{(\eta_2 - \eta_1)^2} \cdot \frac{\partial^2 \omega}{\partial q^2} = -\frac{\mathrm{P}c^2}{2\mu} \Big[\cosh 2\xi - \cos 2\,(\mathrm{A}q + \mathrm{B}) \Big] \qquad ..(6)$$

subject to the conditions:—

$$\omega = 0 \text{ when } \xi = \xi_1 \text{ and } \xi = \xi_2 \text{ and } 0 \leqslant q \leqslant \pi \qquad ..(7)$$

$$\omega = 0 \text{ when } q = 0 \text{ and } q = \pi \text{ and } \xi_1 \leqslant \xi \leqslant \xi_2 \qquad ..(8)$$

Now we use a finite sine transform and write

$$\bar{\omega}(s) = \int_0^{\pi} \omega \sin sq.\, dq \qquad \text{where } s \text{ is a positive integer.}$$

Since ω vanishes at $q = 0$ and $q = \pi$,

$$\int_0^{\pi} \frac{\partial^2 \omega}{\partial q^2} \sin sq \,.\, dq = -s^2 \bar{\omega}$$

Applying this finite transform to equation (6), we get,

$$\frac{d^2 \bar{\omega}}{d\xi^2} - \frac{\pi^2 s^2}{(\eta_2 - \eta_1)^2} \cdot \bar{\omega} = -\frac{\mathrm{P}c^2}{2\mu} \int_0^{\pi} \Big\{ \cosh 2\,\xi - \cos 2\,(\mathrm{A}q + \mathrm{B}) \Big\} \sin sq.\, dq$$

$$= -\frac{\mathrm{P}c^2}{2\mu s} \Big[\cosh 2\,\xi\, (-\cos sq) \Big]_0^{\pi}$$

$$+ \frac{\mathrm{P}c^2}{4\mu} \left[\frac{\cos\,(\overline{2\mathrm{A} - s}.\, q + 2\mathrm{B})}{2\,\mathrm{A} - s} - \frac{\cos\,(\overline{2\mathrm{A} + s}.\, q + 2\mathrm{B})}{2\mathrm{A} + s} \right]_0^{\pi}$$

$$\therefore \frac{d^2 \bar{\omega}}{d\xi^2} - \frac{\pi^2 s^2}{(\eta_2 - \eta_1)^2} \cdot \bar{\omega} = \frac{\mathrm{P}c^2 s}{2\mu\,(4\mathrm{A}^2 - s^2)} \Big\{ \cos 2\,(\mathrm{A}\pi + \mathrm{B}) - \cos 2\,\mathrm{B} \Big\} \quad \text{when } s \text{ is even} \qquad ..(9a)$$

$$\frac{d^2 \bar{\omega}}{d\xi^2} - \frac{\pi^2 s^2}{(\eta_2 - \eta_1)^2} \cdot \bar{\omega} = -\frac{\mathrm{P}c^2}{\mu s} \cosh 2\,\xi - \frac{\mathrm{P}c^2 s}{2\mu(4\mathrm{A}^2 - s^2)} \Big\{ \cos 2(\mathrm{A}\pi + \mathrm{B}) + \cos 2\mathrm{B} \Big\} \quad \text{when } s \text{ is odd} \qquad ...(9b)$$

with conditions $\bar{\omega} = 0$ when $\xi = \xi_1$ and $\xi = \xi_2$ ..(10)

For even values of s the solution of equation (9a) is

$$\bar{\omega} = c_1 e^{\frac{\pi s}{(\eta_2 - \eta_1)}\xi} + c_2 e^{-\frac{\pi s}{(\eta_2 - \eta_1)}\xi} - \frac{\mathrm{P}c^2\,(\eta_2 - \eta_1)^2}{2\mu\pi^2 s\,(4\mathrm{A}^2 - s^2)} \Big\{ \cos 2(\mathrm{A}\pi + \mathrm{B}) - \cos 2\mathrm{B} \Big\} \qquad ..(11)$$

where c_1 and c_2 are to be determined by the help of conditions (10)

$$\left.\begin{aligned} \therefore\ c_1 e^{\frac{\pi s}{(\eta_2-\eta_1)}\cdot\xi_1} + c_2 e^{-\frac{\pi s}{(\eta_2-\eta_1)}\cdot\xi_1} &= k[\cos 2\ (A\pi+B)-\cos 2B] \\ \text{and} \qquad & \\ c_1 e^{\frac{\pi s}{(\eta_2-\eta_1)}\cdot\xi_2} + c_2 e^{\frac{-\pi s}{(\eta_2-\eta_1)}\cdot\xi} &= k[\cos 2\ (A\pi+B)-\cos 2B] \end{aligned}\right\} \quad ..(12)$$

$$\text{where } k=\frac{Pc^2\,(\eta_2-\eta_1)^2}{2\mu\pi^2 s\,(4A^2-s^2)}. \qquad ..(13)$$

From (12) the values of c_1 and c_2 can be obtained and inserted in (11) to determine $\bar{\omega}$ completely.

Now we proceed to find the solution of (9b) for odd values of s

$$\bar{\omega}=c_3 e^{\frac{\pi s}{(\eta_2-\eta_1)}\cdot\xi} + c_4 e^{\frac{-\pi s}{(\eta_2-\eta_1)}\cdot\xi} + k\{\cos 2\ (A\pi+B)+\cos 2B\} - \frac{Pc^2\cosh 2\xi}{\mu s\left[4-\frac{\pi^2 s^2}{(\eta_2-\eta_1)^2}\right]} \qquad ..(14)$$

where c_3 and c_4 are to be determined by the help of conditions (10)

$$\left.\begin{aligned} \therefore\ c_3 e^{\frac{\pi s}{(\eta_2-\eta_1)}\xi_1} + c_4 e^{\frac{-\pi s}{(\eta_2-\eta_1)}\cdot\xi_1} &= -k\{\cos 2\ (A\pi+B)+\cos 2B\} \\ &\quad + \frac{Pc^2}{\mu s}\cdot\frac{\cosh 2\ \xi_1}{\left[4-\frac{\pi^2 s^2}{(\eta_2-\eta_1)^2}\right]} \\ \text{and} \qquad & \\ c_3 e^{\frac{\pi s}{(\eta_2-\eta_1)}\xi_2} + c_4 e^{\frac{-\pi s}{(\eta_2-\eta_1)}\cdot\xi_2} &= -k\{\cos 2(A\pi+B)+\cos 2B\} \\ &\quad + \frac{Pc^2}{\mu s}\cdot\frac{\cosh 2\xi_2}{\left[4-\frac{\pi^2 s^2}{(\eta_2-\eta_1)^2}\right]} \end{aligned}\right\} \quad ..(15)$$

c_3 and c_4 can be determined from (15) and substituted in (14) to determine $\bar{\omega}$. Now by the inversion of the transform

$$\omega=\frac{2}{\pi}\sum_s \bar{\omega}\sin sq, \text{ where } s \text{ is a positive integer}$$

$$=\omega_1+\omega_2, \text{ where}$$

$$\omega_1=\frac{2}{\pi}\sum_s\left[c_1 e^{\frac{\pi s}{(\eta_2-\eta_1)}\cdot\xi} + c_2 e^{\frac{-\pi s}{(\eta_2-\eta_1)}\cdot\xi} - k\{\cos 2\ (A\pi+B)-\cos 2B\}\right]\sin sq$$

$$=\frac{2}{\pi}\sum_{s}\left[c_1e^{\frac{\pi s}{(\eta_2-\eta_1)}\cdot\xi}+c_2e^{\frac{-\pi s}{(\eta_2-\eta_1)}\cdot\xi}-k\{\cos 2\,(\mathrm{A}\pi+\mathrm{B})-\cos 2\mathrm{B}\}\right].\sin s\frac{\eta-\mathrm{B}}{\mathrm{A}}\quad ..(16)$$

when s is even positive integer.

and

$$\omega_2=\frac{2}{\pi}\sum_{s}\left[c_3e^{\frac{\pi s}{(\eta_2-\eta_1)}\cdot\xi}+c_4e^{\frac{-\pi s}{(\eta_2-\eta_1)}\cdot\xi}+k\{\cos 2(\mathrm{A}\pi+\mathrm{B})+\cos 2\mathrm{B}\}-\frac{\mathrm{P}c^2}{\mu s}\cdot\frac{\cosh 2\xi}{\left[4-\frac{\pi^2s^2}{(\eta_2-\eta_1)^2}\right]}\right]\sin sq$$

$$=\frac{2}{\pi}\sum_{s}\left[c_3e^{\frac{\pi s}{(\eta_2-\eta_1)}\cdot\xi}+c_4e^{\frac{-\pi s}{(\eta_2-\eta_1)}\cdot\xi}+k\{\cos 2(\mathrm{A}\pi+\mathrm{B})+\cos 2\mathrm{B}\}-\frac{\mathrm{P}c^2}{\mu s}\cdot\frac{\cosh 2\xi}{\left[4-\frac{\pi^2s^2}{(\eta_2-\eta_1)^2}\right]}\right].\sin s\frac{\eta-\mathrm{B}}{\mathrm{A}}.\quad ..(17)$$

when s is odd positive integer.

where A & B, k, c_1 & c_2, c_3 & c_4 are given by (5), (13), (12) and (15) respectively.

PARTICULAR CASES

Case No. 1. If $\eta_1=0$, $\eta_2=\frac{\pi}{2}$, then $\mathrm{A}=\frac{1}{2}$, $\mathrm{B}=0$, $q=2\eta$

The section of the tube is in the form of a quadrant of the annular space between the ellipses $\xi=\xi_1$ and $\xi=\xi_2$ (See fig. 2)

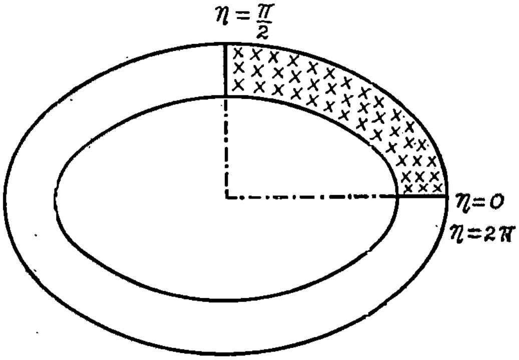

FIG. NO. 2

$\therefore\ \omega=\omega_1+\omega_2$, where

$$\omega_1=\frac{2}{\pi}\sum_{s}\left[c_1e^{2s\xi}+c_2e^{-2s\xi}+2k\right]\sin 2s\eta,\ \text{when } s \text{ is even positive integer}$$

and

$$\omega_2=\frac{2}{\pi}\sum_s\left[c_3e^{2s\xi}+c_4e^{-2s\xi}-\frac{Pc^2\cosh 2\xi}{4\mu s\,(1-s^2)}\right]\sin 2s\eta;\ \text{when } s \text{ is odd positive integer}$$

c_1, c_2 and c_3, c_4 can be determined from (12) and (15) by putting these values of η_1, η_2, A and B.

Case No. 2. Here we consider the section of the tube to be the portion of the elliptical annulus symmetrical about the major axis so that $\xi=\xi_1$, $\xi=\xi_2$, $\eta=\eta_1$ and $\eta=2\pi-\eta_1$ according to Milne [3].

Then $A=\frac{2(\pi-\eta_1)}{\pi}$, $B=\eta_1$, $q=\frac{(\eta-\eta_1)\pi}{2(\pi-\eta_1)}$ (See fig. 3)

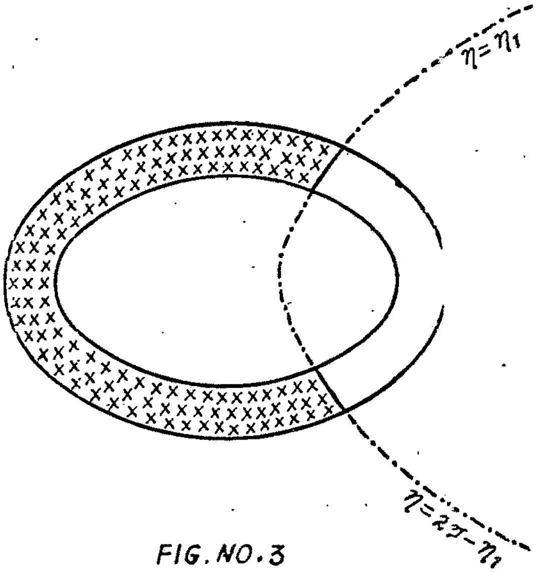

FIG. NO. 3

$\therefore\ \omega=\omega_1+\omega_2$ where

$$\omega_1=\frac{2}{\pi}\sum_s\left[c_1e^{\frac{\pi s}{2(\pi-\eta_1)}\xi}+c_2e^{-\frac{\pi s}{2(\pi-\eta_1)}\xi}-k\{\cos 2(A\pi+B)-\cos 2B\}\right]\times\sin s\frac{(\eta-\eta_1)\pi}{2(\pi-\eta_1)}\ \text{when } s \text{ is even,}$$

and

$$\omega_2=\frac{2}{\pi}\sum_s\left[c_3e^{\frac{\pi s}{2(\pi-\eta_1)}\xi}+c_4e^{-\frac{\pi s}{2(\pi-\eta_1)}\xi}+k\{\cos 2(A\pi+B)+\cos 2B\}-\frac{Pc^2}{\mu s}\,\frac{\cosh 2\xi}{\left(4-\frac{\pi^2s^2}{4(\pi-\eta_1)^2}\right)}\right]\sin s\,.\,\frac{(\eta-\eta_1)\pi}{2(\pi-\eta_1)}\ \text{when } s \text{ is odd.}$$

c_1, c_2, c_3, and c_4 can be determined from (12) and (15) by putting the values of A and B and $\eta_2=2\pi-\eta_1$

Case No. 3. Putting $\eta_1 = \frac{\pi}{2}$ in case No. 2, the section of the tube becomes left half of the annulus between the ellipses $\xi = \xi_1$, $\xi = \xi_2$ and y—axis (See fig. 4)

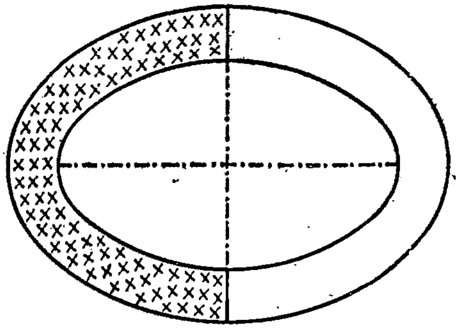

FIG. NO. 4

In this case $A = 1$, $B = \frac{\pi}{2}$, $q = \eta - \frac{\pi}{2}$

Hence, $\omega = \omega_1 + \omega_2$ where

$$\omega_1 = \frac{2}{\pi} \sum_s \left[c_1 e^{s\xi} + c_2 e^{-s\xi} \right] \sin s\left(\eta - \frac{\pi}{2}\right) \text{ when } s \text{ is even.}$$

and

$$\omega_2 = \frac{2}{\pi} \sum_s \left[c_3 e^{s\xi} + c_4 e^{-s\xi} - 2k - \frac{Pc^2 \cosh 2\xi}{\mu s\,(4 - s^2)} \right] \sin s\left(\eta - \frac{\pi}{2}\right) \text{ when } s \text{ is odd.}$$

c_1, c_2, c_3 and c_4 can be determined as in case No. 2 by putting $\eta_1 = \frac{\pi}{2}$.

ACKNOWLEDGEMENT

In the end I wish to thank Dr. J. P. Agrawal for the help in the preparation of this paper.

REFERENCES

1. Agrawal, J. P. 1959, *Uttar Bharti*, **VI** (2): 117-126.
2. Cornish, R. J. 1928. *Proc. Royal Soc.*, A. **120:** 619-700.
3. Milne—Thomson's hydrodynamics, p. 157.

INFLUENCE OF PRESOWING SEED-TREATMENT WITH NAA ON EARLY GROWTH OF MAIZE SEEDLINGS

*V. S. RATHORE[1] AND S. N. BHARDWAJ[2]
Botany Department, Agra College, Agra.

INTRODUCTION

Investigations on maize relating to the influence of presowing soaking the seeds with NAA (continuous soaking for 24 hours in 5 ppm aqueous solution) revealed that the treatment enhanced the oxygen-uptake and enzymatic activities during sprouting, yet the carbon-dioxide-release was decreased; the values for respiratory quotient were lowered (Rathore and Bhardwaj 1963). It was considered of interest to study the impact of the above metabolic events on early seedling growth, especially of roots, upto the emergence of first leaf from the coleoptile. The results obtained are embodied in this paper.

METHODS AND MATERIALS

Seeds of maize variety T. 41 were partially immersed in 5 ppm solution of NAA and were kept there for 24 hours at 30°C in dark. These were transferred to test-tubes (150 × 18 mm) fitted with rolls of Whatman No. 1 filter paper for subsequent growth, adopting the technique described earlier (Bhardwaj 1960). Seedlings raised from the seeds soaked in distilled water served as control. Observations in respect of total root length (in mm), number of roots, average length (in mm) per root and coleoptile length (in mm) were recorded at 24 hour intervals till 96 hours after sowing. Twelve replicates were maintained for each treatment and the data were analysed statistically, following the analysis of variance on factorial basis. Critical differences at 5 per cent probability were calculated wherever the treatment was significant.

EXPERIMENTAL FINDINGS AND DISCUSSION

The data recorded on early seedling growth are presented in table 1 below:—

TABLE 1

Effect of NAA on early growth of maize seedlings (Mean per seedling)

Age (hrs.)	Treatment	Total root length (mm)	Number of roots	Average root length	Coleoptile length (mm)
48	Cont.	12·8	1·3	10·0	7·3
	NAA	7·1	1·3	5·8	3 9
72	Cont.	73·3	3·4	20·4	17·0
	NAA	53·3	3·1	9·4	15·5
96	Cont.	196·6	4·5	45·5	48·8
	NAA	188·5	4·4	41·1	48·6

C. D. at 5 per cent probability :—

Age :	38·4	0·9	10·7	10·5
Seed treatment :	N.S.	N.S.	8·9	8·7
Interaction	N.S.	N.S.	N.S.	N.S.

---

* Present address: 1. Botany Department, Christ Church College, Kanpur.
2. Botany Division, Indian Agricultural Research Institute, New Delhi-12.

From the above, it is seen that retardation in the total length of roots and of coleoptile due to the hormone treatment was the maximum at 48 hours followed by a recovery later on, and reached almost to the level of control by the end of 96 hours. Average length per root was also lowered but the number of roots per seedling was not affected. These results are in close agreement with the observations of Burstrom (1953) and Aberg (1957) that hormonal applications even down to the concentration of 10^{-11} to 10^{-12}M have often resulted in suppression of root growth. It may be mentioned here, the present study relates to the residual effect of hormone application at $2{\cdot}7 \times 10^{-6}$M (5ppm solution) for 24 hours in contrast to the results of continuous feeding of seedlings referred to by the above workers.

Earlier work carried out by the authors (Rathore and Bhardwaj 1963) indicated the depletions in the amount of total available carbohydrates, non reducing sugars and soluble nitrogen in NAA-treated seeds during sprouting. It is plausible that the depletions in carbohydrates and nitrogenous contents of the seedling might lead to slowing down of growth as observed at 48 hours after sowing. In this connection, the differential response in respect of 0_2-uptake and Co_2 output was interesting.

The occurrence of oxidative anabolism was suggested in normal maize seedlings owing to very low R. Q. values (0·57). The above response leads to further lowering of R. Q. to 0·45. This might result in accentuated accumulation of the products of oxidative anabolism and consequently in improvement of growth, as would be seen by the relative growth rates, expressed as log values between 24-48, 48-72 and 72-96 hours furnished in table 2.

TABLE 2

Relative growth rates of NAA-treated and 'control' seedlings of maize (expressed per seedling basis)

Observation	Between hours after sowing					
	24–48		48–72		72–96	
	Cont.	NAA	Cont.	NAA	Cont.	NAA
Total root length	1·1072	0·8513	1·7818	1·6646	2·0910	2·1306
Average length per root	1·0000	0·7634	1·0170	0·55563	1·3997	1·5011
Coleoptile length	0·8633	0·5911	0·9868	1·0645	1·5024	1·5198

It appears that the hormone uptake during soaking takes place in supra-optimal concentration resulting in suppressed seedling growth. This concentration goes down reaching the optimal level with the passage of time and the relative growth rate increases. Another interesting feature is the alteration in metabolic patterns during the ontogeny; differences in respect of chlorophyll synthesis (Rathore 1964) carbohydrate and nitrogen metabolisms (Rathore and Bhardwaj 1963) have been observed. Experiments to follow the variations in synthetic-oxidative processes at different stages of plant growth are in progress.

SUMMARY

The residual effect of soaking maize seeds in 5 ppm solution of NAA on early seedling growth was studied. The total length of roots and of coleoptile was retarded initially but complete recovery was obtained at 96 hours after sowing. The number of roots per seedling was not influenced by the treatment. The implications of the results have been discussed.

ACKNOWLEDGEMENTS

We are grateful to Professor S. Sinha, Head of the Department for the facilities and keen interest shown during the progress of work. We are also thankful to Dr. A. B. Gupta, Head of Botany Department, Christ Church College, Kanpur for suggestions and encouragement in the preparation of manuscript.

REFERENCES

1. Aberg, B. 1957. *Ann. Rev. Plant Physiol.*, **8** : 153-80.
2. Bhardwaj, S. N. 1960. *Proc. Nat. Acad. Sci.*, **31** (B) : 143-55.
3. Burstrom, H. 1953. *Ann. Rev. Plant. Physiol.*, **4** : 237-52.
4. Rathore, V. S. 1964. *Current Sc.*, **33** (6) : 190.
5. Rathore, V. S. & Bhardwaj, S. N. 1963. *J. Indian Plant Physiol.*, **6** : 129-34.

ROTATION OF FINITE DISC IN ROTATING FLUID : BOUNDARY LAYER GROWTH: MOTION STARTED IMPULSIVELY FROM REST

HAR SWARUP SHARMA
Department of Mathematics, Agra College, Agra.

SUMMARY

The growth of motion of revolving flow in the earlier stages of its development caused by a finite circular plane lamina which at $t=0$ is suddenly made to rotate with constant angular spin is discussed. Those various cases also have been studied when the angular velocity of the disc is greater than or less than the angular velocity of the rotating fluid. The cases in which the disc rotates in the opposite sense to that of the external flow has also been considered.

INTRODUCTION

T. V. Kármán[3] (1921) has solved the problem of rotation of an infinite plane lamina in a viscous fluid. He assumed that the motion is steady and the lamina rotates with a constant angular velocity Ω about the axis $r=0$. He has found exact solutions of the equations of motion which satisfy all the boundary conditions of the problem. The axial velocity does not vanish at infinity, but tends to a finite limit which signifies a steady axial flow towards the rotating lamina. T. V. Kármán interprets that it is necessary to preserve continuity, since the rotating lamina acts like centrifugal fan, the fluid moving radially outwards especially near the lamina.

The axisymmetric flow of a rotating incompressible viscous fluid over a fixed infinite plane has been studied by Bodewadt[2] (1940) using a similarity solution which is a solution both of the full Navier-Stokes equations and of the appropriate boundary layer equations of the problem. At a large distance from the plane the radial pressure gradient balances the centrifugal acceleration, but in the immediate vicinity of the plane the effect of viscosity is to reduce the zonal velocity and accordingly there is radial inflow of fluid accompanied by an outflow in the axial direction. Thus the boundary layer is losing fluid, and on the axis of the symmetry both the radial and zonal velocities vanish.

Batchelor[1] (1951), Stewartson[9] (1958), Rogers and Lance[6] (1960) investigated the more general problem of a fluid in rigid-body rotation over a rotating disc. A common feature of the above-mentioned flows is that they have similarity solutions, where the velocity components take the form

$$v=rG(z),\ u=rF(z),\ w=H(z).$$

Ludwieg[4] (1951) and Squire[8] (1953) linearized the boundary layer equations for the case of small disturbances about a state of rigid rotation. In the linearized form, the equations reduce to a set of ordinary differential equations, which are linear. In a recent paper the axisymmetric boundary layer on a finite circular disc due to a rotating fluid has been examined numerically by Rogers and Lance[7] (1964).

Nigam[5] (1951) discussed the growth of motion in the earlier stages of its development caused by an infinite lamina which at $t=0$ is suddenly made to rotate with a constant angular velocity Ω about the axis $r=0$.

In the present problem we have discussed the case of revolving flow over a rotating finite circular disc. We have considered the growth of motion in the earlier stages of its development caused by a finite circular plane lamina which at $t=0$ is suddenly made to rotate with a constant angular spin. We have also discussed the various cases when the angular velocity of the disc is greater or less than the angular velocity of the rotating fluid. The cases when the disc rotates in the opposite direction to the fluid have also been studied.

EQUATIONS GOVERNING THE MOTION

Cylindrical polar coordinates (r, ϕ, z) are used, with the disc $0 \leqslant r \leqslant a$ in the plane $z=0$, with the origin at the centre of the disc. If the Reynolds number of the flow is large, viscous effects become dominant only in the region at a small distance z from the plate. Hence we have a thin boundary layer over the surface of the disc. Denoting the radial, zonal, and axial components of the fluid velocity by (u, v, w) respectively and taking the independent variables such that t denotes the time from the start of the motion the appropriate boundary layer equations of motion are: (as in reference 7)

$$\frac{\partial u}{\partial t} + u\frac{\partial u}{\partial r} + w\frac{\partial u}{\partial z} - \frac{v^2}{r} = -r\Omega^2 + \nu\frac{\partial^2 u}{\partial z^2} \qquad \ldots(1)$$

$$\frac{\partial v}{\partial t} + u\frac{\partial v}{\partial r} + w\frac{\partial v}{\partial z} + \frac{uv}{r} = \nu\frac{\partial^2 v}{\partial z^2} \qquad \ldots(2)$$

The equation of continuity is

$$\frac{\partial}{\partial r}(ru) + \frac{\partial}{\partial z}(rw) = 0 \qquad \ldots(3)$$

where ν is the kinematic viscosity and Ω the angular velocity of the fluid at a great distance from the disc. The radial pressure gradient has been computed from the frictionless flow at a large distance from the disc from the condition

$$\frac{1}{\rho}\frac{\partial p}{\partial r} = \frac{V^2}{r}$$

or with $V = r\,\Omega$

$$\frac{1}{\rho}\frac{\partial p}{\partial r} = r\Omega^2$$

If the disc is made to rotate with angular velocity $\sigma\Omega$ the boundary conditions to be satisfied are

$$\left.\begin{array}{l} \left.\begin{array}{l} u=w=0 \\ v=r\sigma\,\Omega \end{array}\right\} \text{ on } z=0,\ 0\leqslant r\leqslant a,\ t>0, \\ u=0,\ v=a\Omega \quad \text{ on } r=a,\ z>0 \\ \text{together with} \\ u\to 0,\ v\to r\Omega;\ 0\leqslant r\leqslant a,\ z\to\infty,\ t>0. \end{array}\right\} \qquad \ldots(4)$$

SIMPLIFICATION OF THE DIFFERENTIAL EQUATIONS

Let us assume

$$\left.\begin{aligned} u&=\Omega^2 r\, t f(\eta)\\ v&=\Omega r\, g\ (\eta)\\ w&=-4\nu^{\frac{1}{2}}\Omega^2 t^{\frac{3}{2}} h\ (\eta)\end{aligned}\right\} \qquad \ldots(5)$$

where

$$\eta=\frac{z}{2(\nu t)^{\frac{1}{2}}} \qquad \ldots(6)$$

Substituting these values of u, v, w in equations (1), (2) and (3) we get

$$f''+2\eta f'-4f=4-4g^2+4t^2\,\Omega^2\,(f^2-2hf') \qquad \ldots(7)$$

$$g''+2\eta g'=8\Omega^2 t^2(fg-hg') \qquad \ldots(8)$$

$$f-h'=0 \qquad \ldots(9)$$

During early stages of motion when t is small (or in boundary layer theory terminology : when the thickness of the boundary layer is small) we may neglect the terms in the equations of motion containing higher orders of t. Therefore by omitting terms of order t^2 in the equations of motion and continuity, we get a first order of approximation, the following equations:

$$f''+2\eta f'-4f=4-4g^2 \qquad \ldots(10)$$

$$g''+2\eta g'=0 \qquad \ldots(11)$$

$$f=h' \qquad \ldots(12)$$

where dashes denote the differentiations with respect to η.

The boundary conditions now are

$$\left.\begin{aligned} &\left.\begin{aligned} f&=0=h\\ g&=\sigma\end{aligned}\right\} \text{ when } \eta=0\\ &f=0,\ g=1 \quad \text{ when } \eta\to\infty\end{aligned}\right\} \qquad \ldots(13)$$

SOLUTIONS OF EQUATIONS

Integrating (11) we get

$$g=\mathrm{A}\ erf\ (\eta)+\mathrm{B} \qquad \ldots(14)$$

where $erf\ (\eta)$ stands for

$$\frac{2}{\sqrt{\pi}}\int_0^{\eta} e^{-\eta^2}\,d\eta\ .$$

Applying the boundary conditions (13) we get

$\sigma=\mathrm{B}$ and $1=\mathrm{A}+\mathrm{B}$

whence $\mathrm{A}=(1-\sigma)$ and $\mathrm{B}=\sigma$.

Thus equation (14) becomes

$$g=(1-\sigma)\ erf\ \eta+\sigma \qquad \ldots(15)$$

Substituting this value of g, equation (10) becomes

$$f''+2\eta f'-4f=(4-4\sigma^2)-8\sigma(1-\sigma)\ erf\,\eta-4(1-\sigma)^2\ erf^2\eta \qquad \ldots(16)$$

Let equation (16) be written in the form

$$f''+2\eta f'-4f=F(\eta) \qquad \ldots(17)$$

where

$$F(\eta)=K+F_1(\eta)+F_2(\eta)$$

and

$$K=4(1-\sigma^2),\ F_1(\eta)=-8\sigma(1-\sigma)\ erf\ \eta$$
$$F_2(\eta)=-4(1-\sigma)^2\ erf^2\ \eta.$$

The two particular integrals of (17) are [as Wadhwa[10] (1958)]

$$p=\sum_{r=0}^{m} A_{2r}\ \eta^{2r}$$

$$q=p\ erf\ \eta+\sum_{r=0}^{m-1} B_{2r+1}\ \eta^{2r+1}\ \frac{2}{\sqrt{\pi}}e^{-\eta^2}$$

$$A_{2r+2}=\frac{2(m-r)}{(r+1)(2r+1)}\ A_{2r},$$

$$B_{2r+1}=\frac{2(m+r)\ B_{2r-1}\ -2r\ A_{2r}}{r(2r+1)}$$

$$B_{2m+1}=0.$$

Hence the complete solution of (17) is

$$f=Ap+Bq+p\int\frac{qF}{p'q-pq'}\ d\eta+q\int\frac{pF}{pq'-p'q}\,d\eta \qquad \ldots(18)$$

where A and B are arbitrary constants to be determined from the boundary conditions.

Here we find that

$$p=1+2\eta^2$$
$$q=(1+2\eta^2)erfc\ \eta-\frac{2}{\sqrt{\pi}}\eta e^{-\eta^2}$$

where

$$erfc\ \eta=1-erf\ \eta=1-\frac{2}{\sqrt{\pi}}\ exp\ (-\eta^2).$$

The complete solution of (10) or (16) is

$$f=A(1+2\ \eta^2)+B\left[(1+2\eta^2)erfc\ \eta-\frac{2}{\sqrt{\pi}}\eta\ e^{-\eta^2}\right]$$
$$+2(1-\sigma^2)\eta^2-2\sigma(1-\sigma)\left[\eta^2\ erf\ \eta-\tfrac{1}{2}\ erf\ \eta+\ \frac{\eta e^{-n^2}}{\sqrt{\pi}}\right]$$
$$-2(1-\sigma)^2\left[\frac{2}{\sqrt{\pi}}e^{-\eta^2}\eta\ erf\eta+\frac{1}{\pi}\ e^{-2\eta^2}+\eta^2\ erf^2\eta\right] \qquad \ldots(19)$$

Now the constants A and B are to be determined by applying the boundary conditions (13). So we have

$$0=A+B-2(1-\sigma)^2\frac{1}{\pi}$$

$$0=A(1+2\eta^2)+2(1-\sigma^2)\eta^2-2\sigma(1-\sigma)(\eta^2-\tfrac{1}{2})-2(1-\sigma)^2\eta^2 \text{ when } \eta\to\infty$$

$$0=[A+\sigma(1-\sigma)]+2\eta^2[A+1-\sigma^2-\sigma(1-\sigma)-(1-\sigma)^2] \qquad \text{when } \eta\to\infty$$

which can be satisfied *i. e.*, the terms in both the brackets vanish if

$$A=-\sigma(1-\sigma)$$

and therefore

$$B=\frac{(1-\sigma)[2-2\sigma+\pi\sigma]}{\pi}$$

Substituting the values of A and B the equation (19) becomes

$$f=-\sigma(1-\sigma)(1+2\eta^2)+\frac{(1-\sigma)\{2+\sigma(\pi-2)\}}{\pi}\left[(1+2\eta^2)\,erfc\,\eta-\frac{2}{\sqrt{\pi}}\eta e^{-\eta^2}\right]$$
$$+2(1-\sigma^2)\,\eta^2-2\sigma(1-\sigma)\left[\eta^2\,erf\,\eta-\tfrac{1}{2}\,erf\,\eta+\frac{\eta e^{-\eta^2}}{\sqrt{\pi}}\right]$$
$$-2(1-\sigma)^2\left[\frac{2}{\sqrt{\pi}}e^{-\eta^2}\eta\,erf\,\eta+\frac{1}{\sqrt{\pi}}e^{-2\eta^2}+\eta^2\,erf^2\,\eta\right] \qquad \ldots(20)$$

Since from equation (12) $f=h'$, hence function h is obtained by a quadrature of f.

Under the complicated process we get

$$h=-\sigma(1-\sigma)\,(\eta+\tfrac{2}{3}\eta^3)+\frac{(1-\sigma)\{2+\sigma(\pi-2)\}}{\pi}$$
$$\left[(\eta+\tfrac{2}{3}\eta^3)\,erfc\,\eta-\frac{2}{3\sqrt{\pi}}(1+\eta^2)e^{-\eta^2}\right]$$
$$+\tfrac{2}{3}(1-\sigma^2)\eta^3-2\sigma(1-\sigma)\left[(\tfrac{1}{3}\eta^3-\tfrac{1}{2}\eta)\,erf\,\eta+\frac{1}{3\sqrt{\pi}}\eta^2e^{-\eta^2}-\frac{2}{3\sqrt{\pi}}e^{-\eta^2}\right]$$
$$-2(1-\sigma)^2\left[\eta\left(\frac{1}{\sqrt{\pi}}e^{-\eta^2}+\eta\,erf\,\eta\right)^2-\frac{1}{3\sqrt{\pi}}erf\,\eta\,e^{-\eta^2}-\frac{2}{3\sqrt{\pi}}erf\,(\sqrt{2}\,\eta)\right.$$
$$\left.-\tfrac{2}{3}\eta^3\,erf^2\,\eta-\frac{4}{3\sqrt{\pi}}\eta^2\,erf\,\eta\,e^{-\eta^2}-\frac{2}{3\pi}\eta\,e^{-2\eta^2}\right]$$
$$+\text{ constant} \qquad \ldots(21)$$

Applying the boundary condition (13) *i. e.*, $h=0$ when $\eta=0$ we get

$$\text{constant}=\frac{2(1-\sigma)}{3\sqrt{\pi}}\left\{\frac{2-c(\pi+2)}{\pi}\right\}.$$

Hence (21) finally becomes

$$h=-\sigma(1-\sigma)(\eta+\tfrac{2}{3}\eta^3)+\frac{(1-\sigma)\{2+\sigma(\pi-2)\}}{\pi}$$
$$\left[(\eta+\tfrac{2}{3}\eta^3)erfc\,\eta-\frac{2}{3\sqrt{\pi}}(1+\eta^2)e^{-\eta^2}\right]$$
$$+\tfrac{2}{3}(1-\sigma^2)\,\eta^3-2\sigma(1-\sigma)\left[(\tfrac{1}{3}\eta^3-\tfrac{1}{2}\eta)\,erf\,\eta+\frac{1}{3\sqrt{\pi}}\eta^2e^{-\eta^2}-\frac{2}{3\sqrt{\pi}}e^{-\eta^2}\right]$$
$$-2(1-\sigma)^2\left[\eta\left(\frac{1}{\sqrt{\pi}}e^{-\eta^2}+\eta\,erf\,\eta\right)^2-\frac{1}{3\sqrt{\pi}}\,erf\,\eta\,e^{-\eta^2}\right.$$

$$+\frac{2}{3\sqrt{\pi}}erf\,(\sqrt{2}\,\eta)-\tfrac{2}{3}\,\eta^3\,erf^2\eta-\frac{2}{3\pi}\eta\,e^{-2\eta^2}-\frac{4}{3\sqrt{\pi}}\eta^2\,erf\,\eta.\;e^{-\eta^2}\Bigg]$$

$$+\frac{2(1-\sigma)}{3\sqrt{\pi}}\left\{\frac{2-\sigma(\pi+2)}{\pi}\right\} \qquad \ldots(22)$$

GRAPHICAL REPRESENTATION

Here we discuss the functions f, g, h graphically for various values of σ.

Function $g\ (\eta)\ =\ (1-\sigma)\ erf\ \eta+\sigma$

(*i*) When $\sigma=0$.

This case does not arise as the disc does not start rotating impulsively. However function g becomes only $erf\ (\eta)$ and the table for the graph is

η	0	0·5	1	1·5	2	2·5	3	∞
g	0	0·5205	0.842701	0·966105	0·995322	0·999593	0·999978	1

(*ii*) When $\sigma=0·25$

$g\ (\eta)=0·25+0·75\ erf\ \eta$

η	0	0·1	0·2	0·5	1	2	3	∞
g	0·25	0·334347	0·417027	0·640375	0·882025	0·996491	0·999983	1

(*iii*) When $\sigma=0·5$

$g\ (\eta)=\frac{1}{2}\ erf\ \eta+0·5$

η	0	0·1	0·2	0·5	1	2	3	∞
g	0.5	0·5562315	0·611351	0·760250	0·921350	0·997661	0·999989	1

(*iv*) When $\sigma=1$.

In this case

$g\ (\eta)=1$

i.e., the function becomes a straight line parallel to the η-axis. In this case the disc is rotating with the angular velocity of the liquid.

(*v*) When $\sigma=1\cdot5$.

In this case the angular velocity of the disc is 1·5 times the velocity of the fluid (the disc is rotating faster than the fluid), hence we have

$$g\,(\eta)=-\tfrac{1}{2}\,erf\,\eta+1\cdot5$$

η	0	0·1	0·2	0·5	1	2	3	∞
g	1·5	1·443768	1·388649	1·239750	1·078650	1·002339	1·000011	1

(*vi*) When $\sigma=2$.

In this case

$$g\,(\eta)=-erf\,\eta+2$$

η	0	0·1	0·2	0·5	1	2	3	∞
g	2	1·887537	1·777297	1·479500	1·157299	1·004678	1·000022	1

(*vii*) When $\sigma=-1$, *i. e.*, when the angular velocity of the disc is in the opposite direction to that of the fluid, that is to say, the disc has been given a spin in the opposite direction to that of the fluid.

In this case we have

$$g\,(\eta)=2\,erf\,\eta-1$$

η	0	0·1	0·2	0·5	1	2	3	∞
g	–1	–0·775074	–0·554594	0·041000	0·685402	0·990644	0·999956	1

(*viii*) When $\sigma=-2$.

In this case we have

$$g\,(\eta)=3\,erf\,\eta-2$$

η	0	0·1	0·2	0·5	1	2	3	∞
g	–2	–1·662611	–1·331891	–0·438500	0·528103	0·985966	0·999934	2

GRAPHS OF THE FUNCTION $g(\eta)$ FOR VARIOUS VALUES OF σ

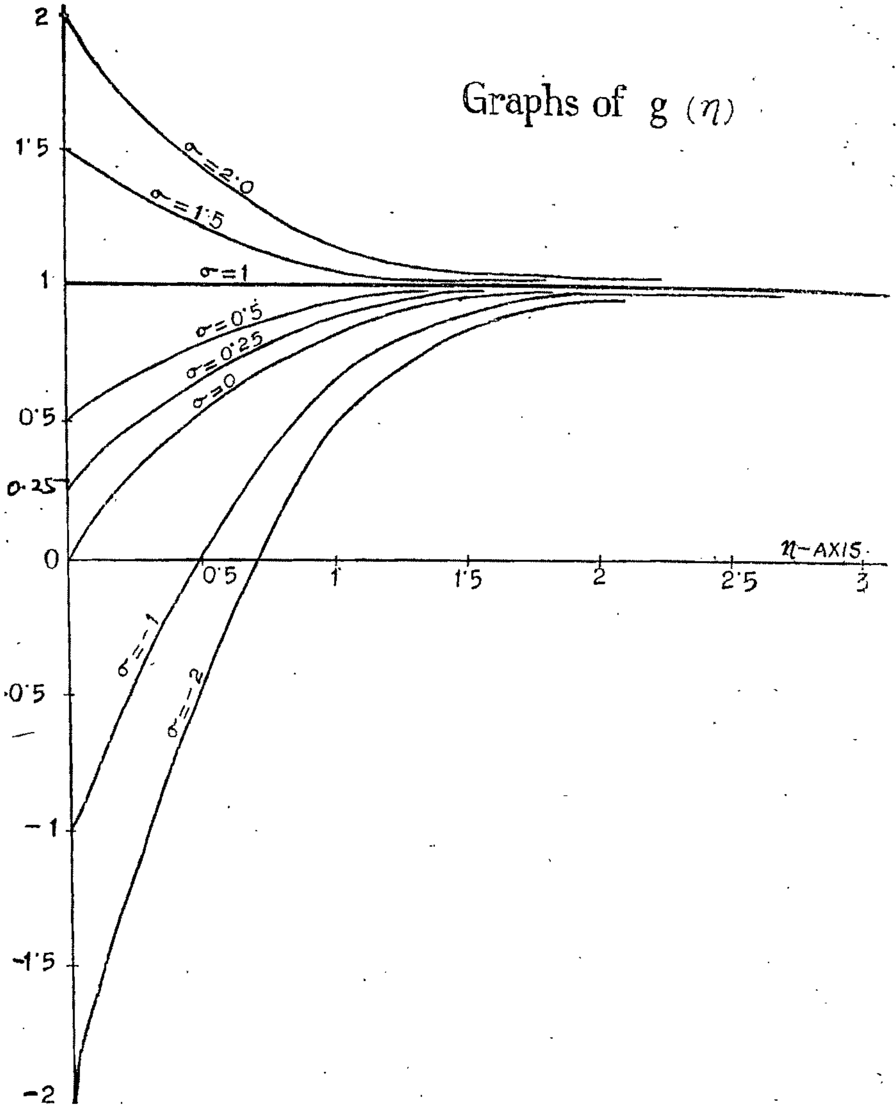

INTERPRETATION OF THE RESULTS OF g

It is quite clear from the graphs of $g(\eta)$ that when the angular velocity of the disc is less than that of the rotating fluid, zonal velocity increases and it decreases when the angular velocity of the disc is greater than that of the liquid.

When the disc rotates in the opposite direction of the fluid, zonal velocity for some values of η *i. e.*, of z remains negative but for great values of η it becomes positive. In case when σ is equal to -1, the zonal velocity becomes positive when η is slightly less than 0·5. In case when $\sigma=-2$ the zonal velocity becomes positive when η is nearly equal to 0·7.

Thus in the vicinity of the disc some fluid moves along with the disc in the direction opposite to the main stream.

GRAPHS OF $f(\eta)$

(*i*) When $\sigma=0$

$$f(\eta) = \frac{2}{\pi}\left[(1+2\eta^2)\, erfc\, \eta - \frac{2}{\sqrt{\pi}}\eta\, e^{-\eta^2}\right] + 2\,\eta^2 - 2\left[\frac{2}{\sqrt{\pi}}\eta\, e^{-\eta^2} erf\, \eta + \frac{1}{\pi}\, e^{-2\eta^2} + \eta^2\, erf^2\, \eta\right]$$

η	0	0·1	0·2	0·5	1	2	3	∞
f	0	–0·101619	–0·21584	–0·300860	–0·170438	–0·002485	+0·002074	0

(*ii*) When $\sigma=\frac{1}{2}$

$$f(\eta) = -\tfrac{1}{4}(1+2\eta^2) + \left(\frac{1}{2\pi} + \tfrac{1}{4}\right)\left[(1+2\eta^2)\, erfc\, \eta - \frac{2}{\sqrt{\pi}}\eta\, e^{-\eta^2}\right]$$
$$+1\cdot5\,\eta^2 - \tfrac{1}{2}\left[\eta^2\, erf\, \eta - \tfrac{1}{2} erf\, \eta + \frac{\eta\, e^{-\eta^2}}{\sqrt{\pi}}\right]$$
$$-\tfrac{1}{2}\left[\frac{2}{\sqrt{\pi}}\, e^{-\eta^2}\eta\, erf\, \eta + \frac{1}{\pi}\, e^{-2\eta^2} + \eta^2\, erf^2 \eta\right]$$

η	0	0·1	0·2	0·5	1	2	3	∞
f	0	0·068922	–0·022275	–0·130649	–0·083685	–0·003492	–0·000066	0

(*iii*) When $\sigma=1$.

In this case $f(\eta)=0$, hence $f(\eta)$ is represented by the η-axis.

(*iv*) When $\sigma=2$.

$$f(\eta) = 2\,(1+2\,\eta^2) - \left(2 - \frac{2}{\pi}\right)\left[(1+2\,\eta^2)\, erfc\, \eta - \frac{2}{\sqrt{\pi}}\eta\, e^{-\eta^2}\right]$$
$$-6\eta^2 + 4\left[\eta^2\, erf\, \eta - \tfrac{1}{2}\, erf\, \eta + \frac{\eta e^{-\eta^2}}{\sqrt{\pi}}\right]$$
$$-2\left[\frac{2}{\sqrt{\pi}}\eta\, e^{-\eta^2}\, erf\, \eta + \frac{1}{\pi}\, e^{-2\eta^2} + \eta^2\, erf^2 \eta\right]$$

η	0	0·1	0·2	0·5	1	2	3	∞
f	0	0·274148	0·322189	0·497538	0·232121	0·009109	–0·005473	0

(*v*) When $\sigma=-1$.

$$f(\eta) = 2\,(1+2\eta^2) + 2\left(\frac{4}{\pi} - 1\right)\left[(1+2\eta^2)\, erfc\, \eta - \frac{2}{\sqrt{\pi}}\eta\, e^{-\eta^2}\right]$$
$$+4\left[\eta^2\, erf\, \eta - \tfrac{1}{2}\, erf\, \eta + \frac{\eta\, e^{-\eta^2}}{\sqrt{\pi}}\right]$$

$$-8\left[\frac{2}{\sqrt{\pi}}\eta\, e^{-\eta^2} erf\,\eta + \frac{1}{\pi}\, e^{-2\eta^2} + \eta^2\, erf^2\,\eta\right]$$

η	0	0·1	0·2	0·5	1	2	3	∞
f	0	–0·030732	–0·326681	–0·405666	–0·277580	–0·016655	0·000949	0

The graphs of the function $f(\eta)$ for various values of sigma are shown here.

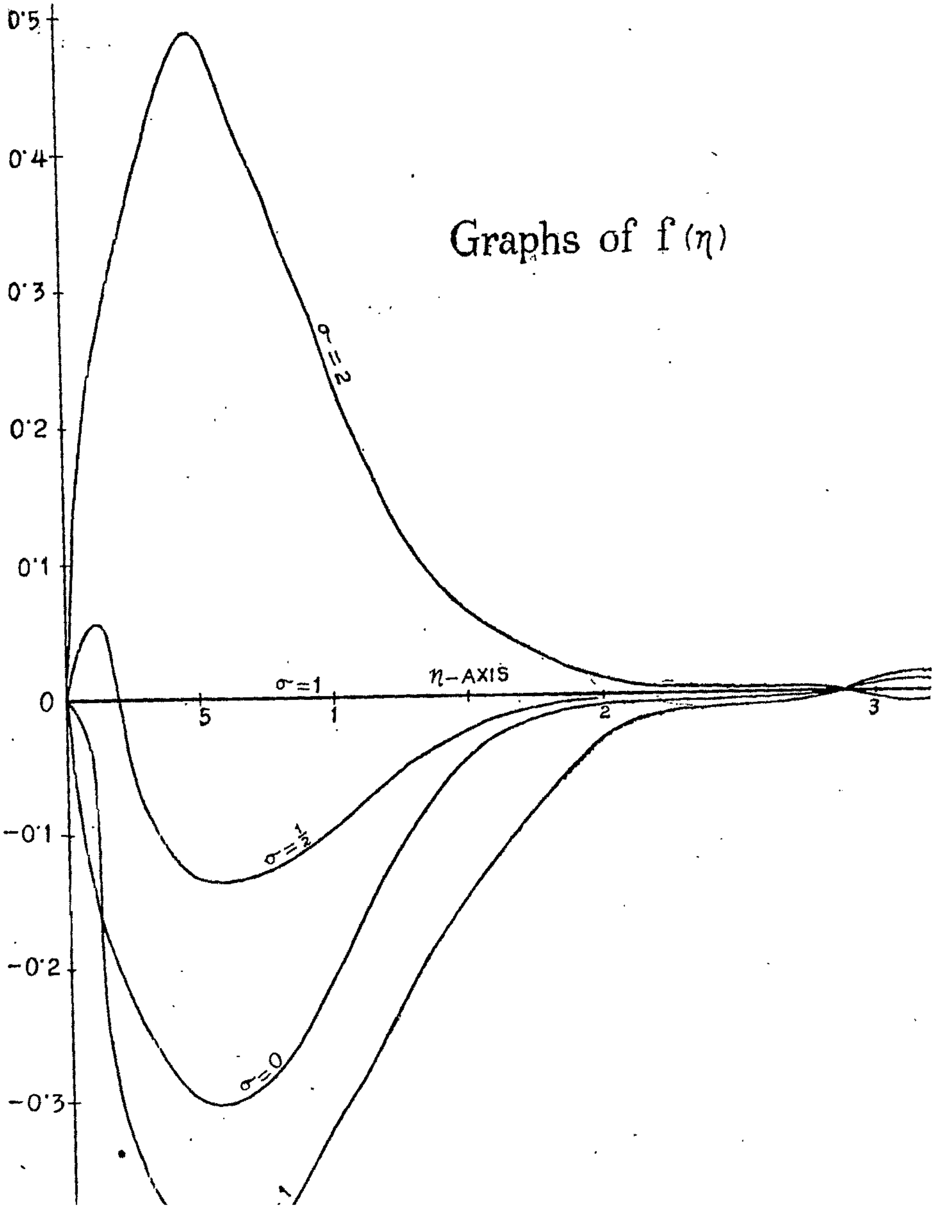

INTERPRETATION OF THE GRAPHS OF $f(\eta)$

When $\sigma=0, f(\eta)$ remains negative between $\eta=0$ and $\eta=$slightly less than 3, at $\eta=3$ it has become positive. Thus the fluid moves radially inwards between $\eta=0$ and $\eta=$slightly less than 3. At $\eta=3$ the fluid moves radially outwards.

When $\sigma=\frac{1}{2}$ fluid moves radially outwards in the beginning and afterwards it begins to flow radially inwards.

When $\sigma=1$ *i.e.*, when the disc is rotating with the angular velocity of the fluid, there is no radial flow.

When $\sigma=2$, *i. e.*, when the disc rotates faster than the rotating fluid, the fluid moves radially outwards. The radial velocity increases upto $\eta=0{\cdot}5$ and then the velocity begins to decrease and at $\eta=3$, fluid moves radially inward.

When $\sigma=-1$, *i.e.*, when the disc rotates in the opposite direction of the fluid, there is radially inward flow and reaches the maximum when $\eta=0{\cdot}5$. The velocity then begins to decrease and ultimately the fluid moves radially outwards at $\eta=3$.

FUNCION OF $h(\eta)$.

As $h(\eta)$ is a complicated function, we find its limit when $\eta\to\infty$

We already know that $h=0$ when $\eta=0$.

$$h(\infty)=-\frac{2(1-\sigma)}{3\sqrt{\pi}}\left\{2-\sigma-\frac{2-2\sigma}{\pi}\right\}$$

Thus when $\sigma=0$, $h(\infty)=-\dfrac{2}{3\sqrt{\pi}}\left\{2-\dfrac{2}{\pi}\right\}=-0{\cdot}51271$

when $\sigma=\frac{1}{2}$, $h(\infty)=-\dfrac{1}{3\sqrt{\pi}}\left\{1{\cdot}5-\dfrac{1}{\pi}\right\}=-0{\cdot}22219$

when $\sigma=1$, $h(\infty)=0$

when $\sigma=2$, $h(\infty)=\dfrac{2}{3\sqrt{\pi}}\left\{0+\dfrac{2}{\pi}\right\}=0{\cdot}239407$

when $\sigma=-1$, $h(\infty)=-\dfrac{4}{3\sqrt{\pi}}\left\{3-\dfrac{4}{\pi}\right\}=-1{\cdot}29795$

when $\sigma=-2$, $h(\infty)=-\dfrac{2}{\sqrt{\pi}}\left\{4-\dfrac{6}{\pi}\right\}=-2{\cdot}35752$

INTERPRETATION OF THE RESULTS OF $h(\eta)$

From the above results we note that $h(\eta)=0$ when $\sigma=1$ *i.e.*, when the disc rotates with the angular velocity of the fluid, there is no axial flow. In case the angular velocity of the disc is greater than that of the fluid, the axial flow is directed outwards and in all other cases there is an axial flow towards the disc.

STREAM FUNCTION

A stream function may be defined by the equations

$$u=-\frac{1}{r}\cdot\frac{\partial\psi}{\partial z}$$

$$w=\frac{1}{r}\ \frac{\partial\psi}{\partial r}$$

whence the stream function may be expressed

$$\psi=-2\nu^{\frac{1}{2}}\Omega^{2}t^{\frac{3}{2}}r^{2}h(\eta)$$

This gives stream surfaces which are surfaces of revolution.

ACKNOWLEDGEMENTS

In conclusion I express my deep sense of gratitude to Dr. M. Ray, D.Sc., F.N.I. for his kind help in preparation of this paper.

REFERENCES

1. Batchelor, G. K. 1951. *Quart. J. Mech. Appl. Math.*, **4:** 29.
2. Bodewadt, U. T. 1940. *Z. angew. Math. Mech.*, **20:** 241.
3. Kármán, T. V. 1921. *Zeitschr. f. angew. Math. u. Mech.* **1:** 244-247.
4. Ludwieg, H. 1951. *Ingenieur—Archiv.*, **19:** 296.
5. Nigam, S.D. 1951. *Quart. of Appl. Maths.* IX **1** 89-91.
6. Rogers, M. H. & Lance, G. N. 1960. *J. Fluid Mech.* **7:** 617.
7. Rogers, M. H. & Lance, G. N. 1964. *Quart. J. of Mech. & Appl. Maths.* XVII **3:** 319-330.
8. Squire, H.B. 1953. *Aero. Res. Counc., Lond.*, 16021.
9. Stewartson, K. 1958. Boundary Layer Research Symposium, Freiburg Berlin : Springer Verlag, 59-71.
10. Wadhwa, Y.D. 1958. *Philosophical Mag.* **3** (26) : 154-155.

THE HEART OF FRESH WATER EEL, *MACROGNATHUS ACULEATUS* (Bl)

V. P. Agrawal and R. C. Dalela
Department of Zoology, D. A. V. College, Muzaffarnagar.

INTRODUCTION

The *Macrognathus aculeatus* (family, Mastacembelidae; order, Mastacembeliformes), a fresh water eel, is of frequent occurence in the rivers and ponds of Muzaffarnagar. This fish is burrowing in habit for which it is well adapted. For a detailed account of the general structure of the heart reference may be made to Danforth (1912) on the heart of *Polyodon*, Gegenbaur (1891), Smith (1918) and Parson (1929) on the conus arteriosus of fishes. The latter author studied a few fishes including an eel, *Symbranchus* with special reference to the musculature and endocardiac ridges or valves of the conus. Mott (1950) studied the heart of *Anguilla*, and Singh (1960) described the heart of a few fresh water teleosts. Recently, Chaudhry and Das (1963) have described the heart of *Amphipnous cuchia*. However, no account is yet available of the blood vascular system of the fish, *Macrognathus aculeatus*.

MATERIAL AND METHODS

The structure of the heart was studied by injecting 4% formaline in the heart of freshly dissected fish through hepatic sinuses so as to fix the tissue of the heart. The specimens were then preserved in 4% formaline for a few days to ensure the hardening of the heart. The hand cut sections of the heart were prepared to study the internal structure. Serial transverse and longitudinal sections of 10 microns thickness were also studied.

OBSERVATIONS

The heart of a fish is a specialised part of the ventral aorta, which has become muscular and modified for the propulsion of blood. In *Macrognathus aculeatus*, the heart is comparatively small and tubular. It lies ventrally in the body cavity in front of the pectoral girdles. It is surrounded by a membranous pericardial sac which is filled with colourless pericardial fluid. The pericardium is attached anteriorly to the proximal end of the bulbus aorta, while posteriorly it encloses the heart all round. In a fish, measuring 28·9 cm in body length, the heart was found to be only 0·9 cm. long and 0·6 cm wide in the middle. The heart consists of the sinus venosus, the auricle, the ventricle, and the bulbus aorta.

The Sinus Venosus:

The sinus venosus (s. v.) is a small, thin walled, roughly triangular chamber forming the hinder most part of the heart. The sinus collects venous blood from the body of the fish through paired lateral ductus cuvieri (d.c.), a pair of large and spacious hepatic sinuses (h. s.) and a single inferior jugular vein (i. j. v.). Anteriorly, the sinus venosus empties itself into the auricle through sinu-auricular aperture which is guarded by a pair of well developed, flap-like sinu-auricular valves (sa. v.) the distal ends of which project freely into the auricle; the other end of each valve is joined with the wall of the sinus venosus.

The sinu-auricular aperture is slightly oblique in position so that the dorsal sinu-auricular valve hangs vertically from the wall of the auricle while the ventral valve forms the lower margin of the aperture. The lumen of the sinus venosus is quite spacious with smooth inner surface.

The Auricle:

The auricle (au.) is a relatively thick-walled lobulated chamber lying anterior to the sinus venosus. Dorsally, it covers the ventricle and a part of the bulbus aorta. It extends laterally so as to embrace the dorso-lateral sides of the ventricle. The internal cavity of the auricle is occupied by a number of contractile muscle fibres which cris cross with one another in such a way that the internal space of the auricle becomes spongy in texture. The auricle opens into the ventricle through a median, auriculo-ventricular aperture, which is guarded by two pairs of valves. The first pair is situated along the anterior and posterior margins (a.v; p.v.), while the second pair (l.v.) is located along the lateral margins of the aperture. The valves of the first pair are large and pocket-shaped, and are mainly responsible for controlling the flow of blood, where as the valves of the second pair are small and triangular structures. These valves allow the flow of blood from the auricle to the ventricle and not vice versa.

The Ventricle:

The ventricle (vn.) is roughly triangular with highly muscular wall. It is covered dorsally by the auricle and the sinus venosus and dorso-laterally with the auricle. The muscles of the ventricle are thrown internally into ridges and folds which enclose a number of narrow pits. The small lumen of the ventricle is restricted to the region where the bulbus aorta and auricle open. Anteriorly, the ventricle opens into the bulbus aorta through ventriculobulbar aperture which is guarded by a pair of semi-lunar valves (v.l.v.). The valves, which are placed upright on the right and left sides of the aperture, are thin hemispherical structures, projecting into the lumen of bulbus aorta. The convexities of the valves lie towards the ventricle.

The Bulbus Aorta:

The bulbus aorta (b.a.) is a tubular structure with a swollen base. It lies anterior to the ventricle and continues forwards as ventral aorta which is comparatively long in this fish. The outer surface of the bulbus aorta is smooth while its inner margin is raised into a number of muscular ridges or trabeculae (trb) so that the lumen of the bulbus aorta becomes very small.

The venous blood from the body is collected into the sinus venosus through the hepatic sinuses and ductus cuvieri. From the sinus venosus the venous blood passes through the auricle and ventricle into the long ventral aorta which gives out four pairs of afferent branchial arteries for the gills.

DISCUSSION

The heart of *Macrognathus aculeatus* as also of *Anguilla* (Mott, 1950) and *Mastacembelus armatus* (Singh, 1960), is tubular with well developed auricle. Internally the auricle is spongy in texture while Chaudhry and Das (1963) reported that in *Amphipnous cuchia*, it is smooth and without any muscle fibres. The ductus cuvieri is reduced in *Anguilla* and *Monopterus* (Wu and Liu, 1943), while it is quite large and spacious in the present case. The number of sinu-auricular valves differs in different fishes. Mott (1950) described three asymmetrically placed sinu-auricular valves in *Anguilla*, while Chaudhry and Das (1963) observed only one such valves in *Amphipnous cuchia*. In *Macrognathus*, two distinct valves are present.

In the presence of four auriculo-ventricular valves (two big and two small), the heart of *Macrognathus* closely resembles with the heart of *Mastacembelus armatus* (Singh, 1960) but differs with that of *Anguilla* (Mott, 1950) and *Amphipnous cuchia* (Chaudhry and Das, 1963) where only two such valves have been reported. The accessory valves, as observed by Sen (1928) in *Labeo*, are not found in this fish.

In the presence of a pair of ventriculo-bulbar valves, the heart of *Macrognathus* shows similarity with the hearts of *Anguilla* (Mott, 1950), *Mastacembelus armatus* (Singh, 1960), *Amphipnous cuchia* (Chaudhry and Das, 1963), and *Chaudhuria caudata* (Mitra and Ghosh, 1931).

The studies of Gegenbaur (1891), Smith (1918) and others show that in almost all the teleosts, contractile conus arteriosus undergoes great reduction. Parson (1929) suggested the bulbus arteriosus in the teleost as a part of the original conus arteriosus. Danforth (1912) noted the presence of a well developed conus arteriosus in the *Polyodon* with three rows of transverse valves. Karandikar and Thakur (1954) described the absence of conus in *Sciaenoides brunneus*. In *Macrognathus aculeatus*, as also in *Anguilla* (Mott, 1950) the conus is replaced by an elastic bulbus aorta. The internal cavity of bulbus contains the muscular trabeculae, a condition similar to that of *Symbranchus* (Parson, 1929).

The heart of *Macrognathus aculeatus* shows a great resemblance with that of *Mastacembelus armatus*, another fresh water spiny-eel of the same family, while it differs in many respects with the heart of *Anguilla anguilla*, a marine eel as well as with the amphipinid eel, *Amphipnous cuchia*.

SUMMARY

The heart of *Macrognathus aculeatus* is a small and tubular structure with well developed sinus venosus, auricle, ventricle and bulbus aorta.

The sinus venosus is rather small and has a pair of sinu-auricular valves; it is smooth internally.

The auricle is proportionately large, with four auriculo-ventricular valves, one pair being larger than the other. Its lumen is filled with contractile muscle fibres.

The ventricle is a thick walled structure with a narrow lumen and is provided with a pair of ventriculo-bulbar valves.

The bulbus aorta is thick walled with swollen base. The lumen of the bulbus is occupied by a large number of trabeculae.

REFERENCES

1. Chaudhry, H. S. & Das, A. B. 1963. The heart of Indian cuchia Eel, *Amphipnous cuchia* (Ham). *Proc. Ind. Acad. Sci.* India, **33 B** (4) : 647-650.
2. Danforth, C. H. 1912. The heart and arteries of *Polyodon. J. Morph.* **23** : 409-454.
3. Gegenbaur, C. 1891. Conus arteriosus der fische. *Morph. Jahrb.*, **17**: 596-610.
4. Karandikar, K. R. & Thakur, S. S. 1954. *Sciaenoides brunneus* Day. Anatomy with notes on distribution and Bionomics. *The Univ. Bombay Zoological memoirs.* **3** : 1-92.
5. Mitra, B. K. & Ghosh, E. 1931. On the internal anatomy of the families of Opisthomi. *Rec. Ind. Mus.*, **33** : 291-300.
6. Mott, J. C. 1950. The gross anatomy of the blood vascular system of the Eel. *Anguilla anguilla. Proc. Zool. Soc. Lond.*, **120** : 503-510.
7. Parson, C. W. 1929. The conus arteriosus in fishes. *Quart. Jour. Micr. Soc.*, London, **73**: 145-176.
8. Sen, P. 1928. On the branchiocephalic system of blood vessels, together with a note on the dorsal aorta of a common Indian fresh water carp "Rohu" *Labeo rohita. J. Deptt. Science Univ.* Calcutta, **9** : 1-20.
9. Singh, G. P. 1960. The structure of the heart of some fresh water teleosts. *Ind. Jour. Zoot.*, **1** : 1-26.
10. Smith, W. C. 1918. On the process of disappearance of the conus arteriosus in teleosts. *Anat. Rec.* **15** : 65-71.
11. Wu, H. W. & Liu, C. K. 1943. On the blood vascular system of *Monopterus javenensis*, an air breathing fish. *Sinensia,*, Nanking, **14** : 61-87.

PLATE I

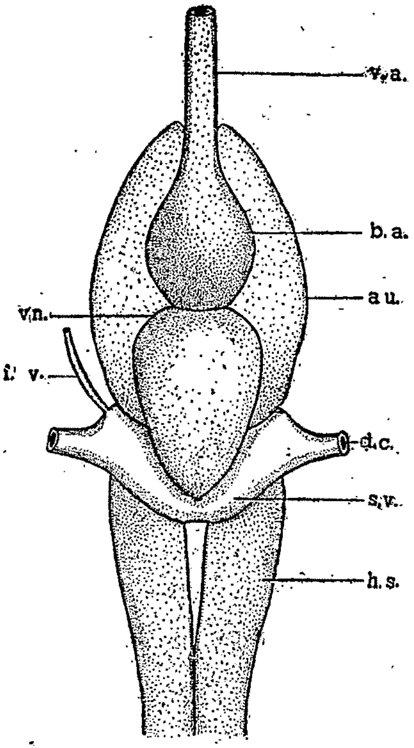

Fig. I

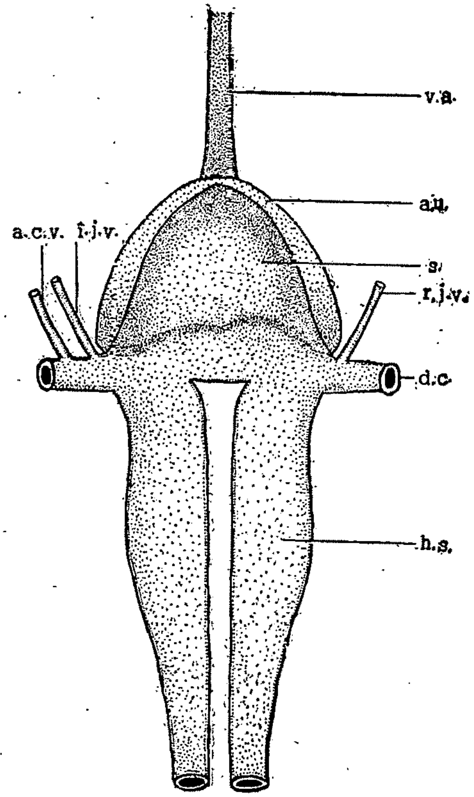

Fig. II

Fig. I. Ventral view of heart x10.
Fig. II. Dorsal view of heart x10.

a. c. v., anterior cardinal vein; au., auricle; b.a., bulbus aorta; d.c., ductus cuvieri; h.s., hepatic sinus; i.j. v., infra juglar vein; r. j. v., right infra juglar vein; s. v., sinus venosus; v. a., ventral aorta; vn., ventricle.

PLATE II

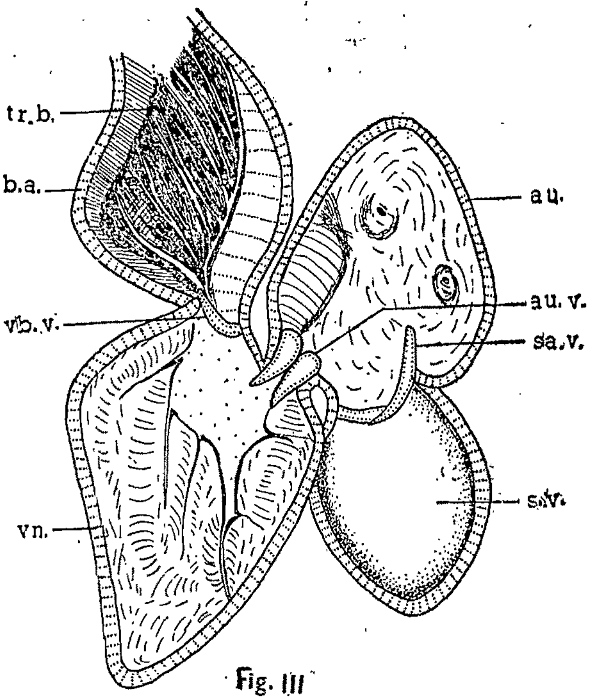

Fig. III

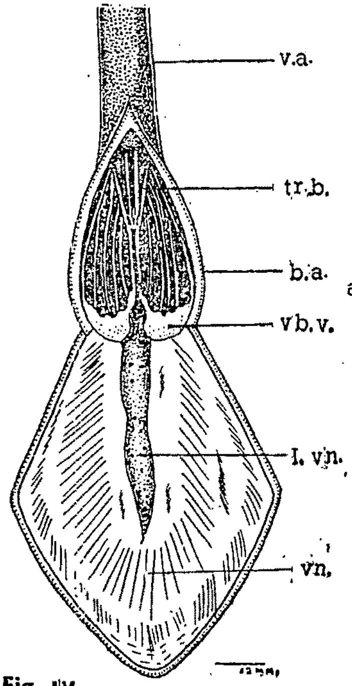

Fig. IV

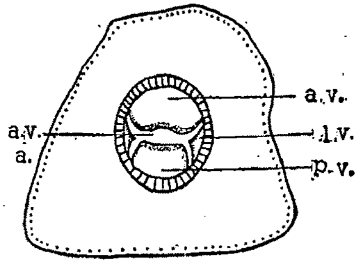

Fig. V

PLATE II

Fig. III. Sagittal section of sinus venosus, auricle and ventricle x30.
Fig. IV. Horizontal section of ventricle and bulbus aorta.
Fig. V. Auriculo-ventricular valves seen from ventricle.

au., auricle; au. v., auriculoventricular valve; av., anterior valve; a. v. a., auriculo-ventricular aperture; b. a., bulbus aorta; l. v., lateral valve; l. vn., lumen of ventricle; p. v., posterior valve; sa.v., sinu-auricular valve; s. v., sinus venosus; trb., trabeculae; va., ventral aorta; vb.v., ventriculo-bulbar valve; vn., ventricle.

CIRCULATORY SYSTEM AND ASSOCIATED TISSUES OF *SYRPHUS BALTEATUS* DE GEER (SYRPHIDAE: DIPTERA)*

J. L. NAYAR†
Senior Research Scholar, C. S. I. R., Ministry of Education,
School of Entomology, St. John's College, Agra.

INTRODUCTION

The circulatory system of the flies has been scarcely attempted by workers. Lowne (1890-95) described the structure of heart in *Calliphora erythrocephala* L. while Hewitt (1914) worked on house fly. Hase (1927) contributed on the heart beat of *Hippobosca*. Miller (1950) gave a detailed account of circulatory system in *Drosophila melanogaster* Meigen. Jones (1952) dealt with the aortic sinuses in *Anopheles*, *Culex* and *Aedes* while in (1954) he gave a detailed structure of heart and associated tissues of *Anopheles quadrimaculatus* Say. There is absolutely no work on the circulatory system of Syrphidae and this paper deals with the detailed anatomy of heart and associated tissues of the syrphids.

MATERIAL AND METHOD

The freshly chloroformed flies were fixed in wax-dish and dissected in Ringer's solution both from the dorsal and ventral sides. For the study of alary muscles; the diaphragm and the chambers of the heart, eosin stained mounted slides were studied under Ortholux built-in-Illumination microscope with the Phase contrast attachment. The diagrams were drawn with the help of camera lucida.

Circulatory system and associated tissues—The circulatory system comprises a dorsal vessel, the haemocoel and the blood. The associated structures performing specific functions through the medium of blood are the pericardial cells, oenocytes, corpus allatum and the fat tissue.

Dorsal Vessel—It is differentiated into an anterior (Fig. 1; AO) and the posterior pulsatile organ, the heart (HT). The latter is confined to the abdominal cavity while the former extends from the posterior extremity of the thorax into the head.

The Heart—As mentioned above the heart lies in the abdomen and extends from the anterior margin of the second abdominal segment (Fig. 1; ABDSEG$_2$) up to the anterior portion of the sixth abdominal segment (ABDSEG$_6$) in both the sexes. It occupies the pericardial sinus which is marked off from the perivisceral cavity by a thin perforated dorsal diaphragm (Figs. 1

---

* Contribution No. 107 from the School of Entomology, St. John's College, Agra.

† Present address : S. G. T. B. Khalsa College, Delhi—5.

and 2; DDPH). The diaphragm and four pairs of rather ill developed alary muscles (Fig. 1; $ALMSC_{1-4}$) keep the heart suspended.

The heart is divided into five chambers and measures 5·25 mm in length. The posteriormost chamber or the fifth chamber (Figs. 1 and 2; HTC_5) which ends blindly in the anterior part of the sixth abdominal segment (Fig. 1; $ABDSEG_6$) is relatively narrower than the others. In the fifth abdominal segment ($ABDSEG_5$) it bulges slightly before narrowing down anteriorly. The fourth chamber (Figs. 1 and 2; HTC_4) is about one and a half times as long as the fifth and stretches throughout the length of the fourth abdominal segment (Fig. 1; $ABDSEG_4$). The third chamber (Figs. 1 and 2; HTC_3) is as long as the fifth and occupies the posterior three-fourths of the third abdominal segment (Fig. 1; $ABDSEG_3$). The second chamber (Fig. 1; HTC_2) is as long as the fourth but widens out abruptly before its anterior extremity to constitute a part of the so-called "aortic bulb" (Figs. 1 and 3; AOBLB). The remaining part of the "aortic bulb" is formed by the first chamber (HTC_1)along with the posterior widened end of the aorta.

Hewitt (1914) in house-fly and Miller (1950) in *Drosophila* have reported the presence of only four chambered heart. Lowne (1890-95) in *Calliphora*, on the other hand, believes that heart consists of five chambers. The existence of a pair of ostia in the "aortic bulb" induced Lowne to consider its portion posterior to the ostia as an additional chamber which he named as the anterior chamber. Apart from this anterior chamber, he recognised four other chambers making the total five during his investigations on *Calliphora*. Hewitt (1914) and Miller (1950) did not report the presence of ostia on the aortic bulb. It is interesting to note here that in *Syrphus balteatus*, there are present two pairs of ostia (Figs. 1 and 3; OST_1 & OST_2) on the dorso-lateral walls of the aortic bulb. The portion of the aortic bulb between the two pairs of the ostia is narrow and extremely thick-walled. It is suggested here to name this narrow portion as the anterior chamber or the first chamber (HTC_1). The anterior and posterior limits of this chamber are marked by transverse grooves ($TGRV_1$ and $TGRV_2$) on the outer surface.

The wall of the heart is formed by delicate, circular striated fibrillae, which are invested internally and externally by thin membranes. The muscular layer in the anterior chamber (HTC_1) and the swollen part of the second chamber (HTC_2) is extremely well developed. This strong musculature enables the "aortic bulb", to function as a powerful pulsating organ to push the blood right up to the head capsule. The absence of any pulsatile organ in the thoracic region necessitates the development of a powerful pumping apparatus that should be capable of driving blood up to the head capsule. Accessory pulsatile organs have been reported in the thorax of *Drosophila* by Miller (1950).

Each chamber of the heart is marked by the presence of a pair of vertical slit-like openings, the ostia. The first two pairs (OST_1 and OST_2), are situated on the aortic bulb, the third (Fig. 1; OST_3) in the anterior one-fourth of the third abdominal segment ($ABDSEG_3$) the fourth (Figs. 1 and 2; OST_4) occupies an inter-segmental position between the third and fourth abdominal segments (Fig. 1; $ABDSEG_3$ & $ABDSEG_4$) while the fifth pair of ostia (Figs. 1 and 2; OST_5) are situated on the inter-segmental position of the fourth and fifth abdominal segments (Fig. I; $ABDSEG_4$ and $ABDSEG_5$). Each ostium is situated at the bottom of the ostial pouch formed by the inflection of the heart wall. The margin of the slit-like ostium projects into the lumen of the heart and serves as the ostial valve allowing the flow of the blood from the haemocoel into the heart and checking the reflux. The heart beats could be observed for nearly ten minutes on dissecting living *Syrphus* flies in Ringer's solution. The cells (Fig. 3; C) of the cardiac wall just posterior to the swollen portion of the second chamber have assumed a characteristic columnar shape and bulge into the lumen of the heart. By the contraction of the strongly developed circular musculature of the swollen anterior end of the second chamber (Fig. 3; HTC_2), these cells presumably are brought closer to occlude the lumen of the heart thereby functioning as a valve to prevent the backward flow of the blood.

The dorsal diaphragm—The diaphragm (Figs. 1 and 2; DDPH) or the pericardial septium lying below the heart extends from the anterior part of the second abdominal segment to the posterior border of the fifth abdominal segment. It consists of delicate longitudinal and transverse fibrillae (LFB and TFB) interwoven into fenestrated gauze-like sheath. Along its lateral margins the diaphragm is attached to the dorso-lateral tergal margin. The diaphragm also contains four pairs of alary muscles (Fig. 1; $ALMSC_{1-4}$) which are inserted on the latero-ventral wall of the heart. Each alary muscle consists of 7-8 delicate fibrillae at the place of its insertion and converge to a single thick band at its origin on the lateral tergal margin lateral to the attachment of the diaphragm. The first pair of alary muscles ($ALMSC_1$) take the origin form the antero-lateral margin of third abdominal segment and fan-out medially to become inserted on the heart precisely in the region of the third pair of ostia; the second pair (Figs 1 and 2; $ALMSC_2$) originates from the antero-lateral margin of the fourth abdominal segment to become inserted at the heart in the intersegmental region between the third and fourth abdominal segments; third pair ($ALMSC_3$) arises from the postero-lateral margin of the fourth abdominal segment to become inserted on the heart in the posterior region of the same segment and the last pair ($ALMSC_4$) has its origin slightly posterior to the latero-anterior margin of the fifth abdominal segment and is inserted almost at the same level in the same segment.

The Aorta—It (Fig. I; AO) is a long thin-walled tube about 4·50 mm long extending from the posterior part of the first abdominal segment to the bases of the antennae in the head. At its junction with the heart, the aorta slightly swells up to constitute the anterior portion of the aortic bulb (the other portion is formed by the first chamber of the heart and the anterior end of the second chamber). After the aortic bulb the aorta proper dips ventrally and passes below the mesophragma to enter into the thorax. In the thorax, it runs above the alimentary canal lying underneath the extremely developed median longitudinal muscles and forms a small aortic funnel (AOFNL) dorsal to the oesophagus in the cervical region. The aortic funnel is termed by Jones (1952) as the aortic sinus in the adults of *Anopheles*, *Culex* and *Aedes*. To this funnel is attached dorsally the corpus allatum (CA). Anteriorly, the aorta passes through the oesophageal canal of the brain (BR) and terminates at the bases of the antennae forming an antennal pulsating organ (ANTPO). Clements (1956) has reported the antennal pulsating organ at the bases of antennae in mosquito and other Diptera, but Day (1955) claims it to be a sense organ in nematocerous Diptera. On injecting the flies with carmine, it was observed that this pulsating organ stains similar to the dorsal vessel. It is, therefore, suggested that the structure should be considered as the pulsating organ.

Course of blood in circulation—The haemocoelomic cavity in the abdomen is divided into a dorsal pericardial sinus by the diaphragm (Fig. I; DDPH) and the ventral perivisceral sinus whereas in the thorax and the head it remains undivided. The ventral diaphragm is absent thereby eliminating the further subdivision of the perivisceral cavity into a ventral sinus. The blood from the perivisceral cavity reaches the dorsal sinus through the fenestrae of the diaphragm and also through the narrow openings at the anterior and posterior ends of the latter. From the dorsal sinus, through the paired ostia the blood flows to the heart. By the contractions of the cardiac walls the blood is pushed into the head through the aorta, where it bathes the internal structures of the head capsule. From the head it follows a backward course through the thorax and locomotory appendages to reach again into the perivisceral cavity of the abdomen.

The cells associated with the circulatory system include the pericardial (Figs. 1, 2 & 4; PCLS) cells, the oenocytes (Figs. 5 and 6; OEN), the corpus allatum (Fig. 1; CA) and the fat cells (Fig. 6: FTC).

Pericardial cells—These (Figs. 1, 2 and 4; PCLS) are large, oval eosinophilic, uninucleate or binucleate cells sticking to the dorsal diaphragm in the dorsal sinus and in the surrounding region of the cardia (Fig. 1; CD). In the dorsal sinus, they form a row of cells along the lateral wall of the heart from the first abdominal segment to the posterior border of the fifth abdominal segment, while in the thorax in the vicinity of the cardia few of them are found widely scattered along the tracheae and the muscle fibres. The pericardial cells are structurally similar in both thorax and abdomen except that the latter are comparatively larger in size than the former. These cells exhibit a distinct affinity towards the carmine stain. Their carmine absorbing nature has been reported by Kowalevsky (1892). The pericardial cell cytoplasm (Fig. 4; CTM) is granular with a well developed almost central, spherical, single nucleus (N) or two subcentral small ovoid nuclei. Tiny basophilic inclusions are present in the cytoplasm of the pericardial cells, the true nature of which is not yet properly understood. Leydis, (1866) referred by Wigglesworth (1930) showed their mesodermal origin and Hollande (1922) reported their role in excretion. These observations could not be confirmed under the present investigations.

Oenocytes—The oenocytes (Figs. 5 and 6; OEN) lie widely scattered in the abdomen and mixed with the fat cells, in the posterior abdominal segment. These have been observed metamerically placed in *Drosophila* (Koch, 1945) and irregularly scattered throughout the fat body in Muscids (Perez, 1910). Snodgrass (1935), however, is of the view that these are not known to occur in adult Diptera, whereas Zavrel (1938) termed these as "Synoenocytes" in adult Diptera to distinguish them from the larval oenocytes.

The oenocytes are small in size as compared to the large size of the pericardial cells and closely adhere to one another. Their small size has been reported by Hosselet (1925) in adult *Culex*. Each oenocyte is almost a minute oval, eosinophilic structure with granular cytoplasm (Fig. 5; CTM) and a distinct nucleus (N). Nothing is certain about their functions though Hollande (1914) believes them to be the organs of intermediary metabolism, which discharge their secretion into the blood. Zavrel (1933) during his studies on Chironomids suggested their endocrinal activity.

Corpus allatum—(Fig. 1; CA). It is a single, small, compact oval mass of tissue lying upon the dorsal wall of the aorta in the prothorax just near the aortic funnel. The component cell boundaries forming this granular mass of protoplasmic tissue are not distinct. Slightly bigger granules (G), acidophilic in nature lie at the periphery of this body and the rest of the protoplasm is uniformly granulated. Strindberg (1913) has observed its endocrinal function. Brilliant experiments conducted by Wiggleworth (1934) have demonstrated that the corpora allata are the source of hormones that induce moulting.

Fat-bodies—The fat tissue mainly lies among the viscera in the abdomen and rather scarce in the thorax and the head. The compact fat cell masses are situated in the posterior region of the abdomen, where same oenocytes are also intermingled with this tissue. The fat cell (Fig. 6; FTC) is small, distinctly uninucleated with granular inclusions in its interior.

SUMMARY

The diaphragm and four pairs of alary muscles support the heart. The heart is five chambered and five pairs of distinct ostia are recognised. The long thin-walled aorta extends from the posterior part of the first abdominal segment to the bases of the antennae. The aorta forms a small aortic funnel dorsal to the oesophagus and terminates at the base of the antennae forming an antennal pulsating organ. The pericardial cells, oenocytes and fat cells have been separately described.

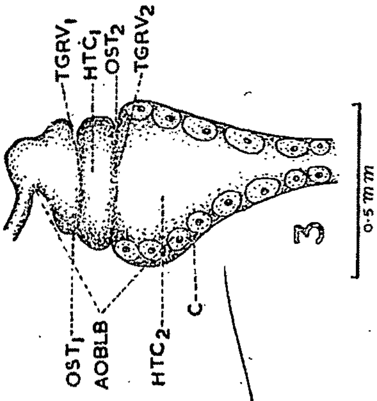
TGRV$_1$
HTC$_1$
OST$_2$
TGRV$_2$
OST$_1$
AOBLB
HTC$_2$
C
0·5 mm

3

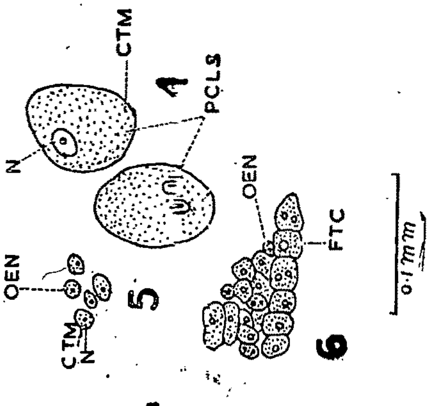
CTM
N
PCLS
OEN
CTM
N
OEN
FTC
0·1 mm

4

5

6

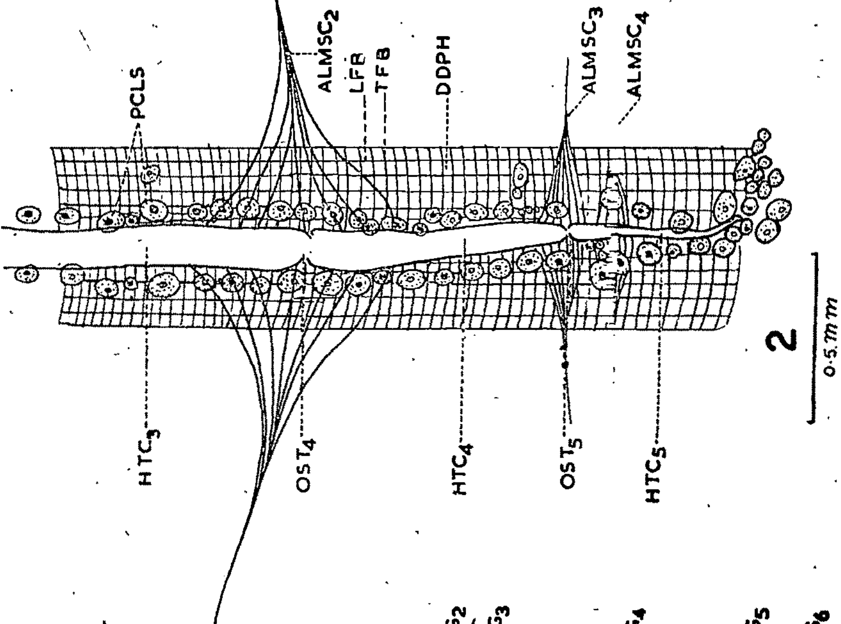
PCLS
ALMSC$_2$
LFB
TFB
DDPH
ALMSC$_3$
ALMSC$_4$
HTC$_3$
OST$_4$
HTC$_4$
OST$_5$
HTC$_5$
0·5 mm

2

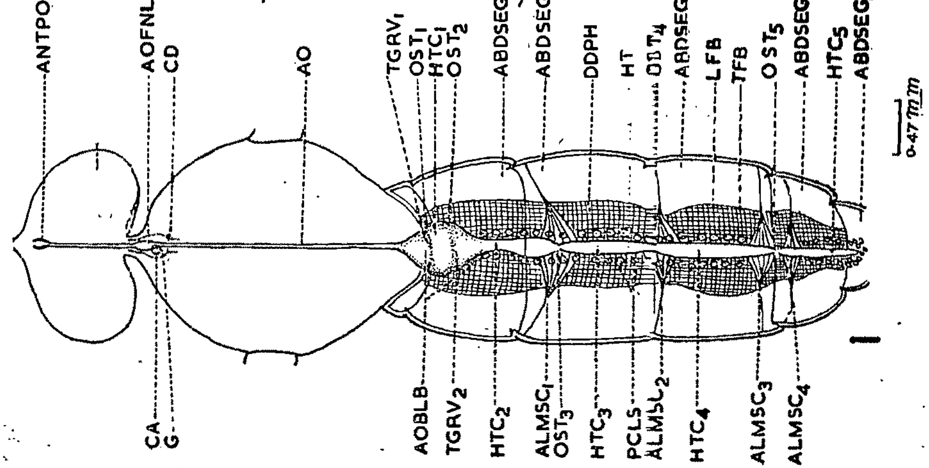
ANTPO
AOFNL
CD
AO
TGRV$_1$
OST$_1$
HTC$_1$
OST$_2$
ABDSEG$_2$
ABDSEG$_3$
DDPH
HT
OST$_4$
ABDSEG$_4$
LFB
TFB
OST$_5$
ABDSEG$_5$
HTC$_5$
ABDSEG$_6$
0·47 mm
CA
G
AOBLB
TGRV$_2$
HTC$_2$
ALMSC$_1$
OST$_3$
HTC$_3$
PCLS
ALMSC$_2$
HTC$_4$
ALMSC$_3$
ALMSC$_4$

1

EXPLANATION OF FIGURES

Fig. 1. Circulatory system in situ.
Fig. 2. Posterior part of the circulatory system (Highly magnified).
Fig. 3. Aortic bulb (Highly magnified)
Fig. 4. Pericardial cells.
Fig. 5. Oenocytes.
Fig. 6. Fat cells.

$ABDSEG_2$—Second abdominal segment; $ABDSEG_3$—Third abdominal segment; $ABDESG_4$—Fourth abdominal segment; $ABDSEG_5$—Fifth abdominal segment; $ABDSEG_6$—Sixth abdominal segment; $ALMSC_{1-4}$—Alary muscle$_{1-4}$; $ALMSC_1$—Alary muscle$_1$; $ALMSC_2$—Alary muscle$_2$; $ALMSC_3$—Alary muscle$_3$; $ALMSC_4$—Alary muscle$_4$; *ANTPO*—Antennal pulsating organ; *AO*—Aorta; *AOBLB*—Aortic bulb; *AOFNL*—Aortic funnel; *BR*—Brain; *C*—Cell; *CA*—Corpus allatum; *CD*—Cardia; *CTM*—Cytoplasm; *DDPH*—Dorsal diaphragm; *FTC*—Fat cells; *G*—Granules; *HT*—Heart; HTC_1—First chamber of the heart; HTC_2—Second chamber of the heart; HTC_3—Third chamber of the heart; HTC_4—Fourth chamber of the heart; HTC_5—Fifth chamber of the heart; *LFB*—Longitudinal fibrillae; *N*—Nucleus; *OEN*—Oenocytes; OST_1—Ostium$_1$; OST_2—Ostium$_2$; OST_3—Ostium$_3$; OST_4—Ostium$_4$; OST_5—Ostium$_5$; *PCLS*—Pericardial cells; *TFB*—Transverse fibrillae; $TGRV_1$—Transverse groove$_1$; $TGRV_2$—Transverse groove$_2$.

ACKNOWLEDGEMENTS

I express my deep gratitude to Dr. T. Singh, Professor of Zoology and Entomology, School of Entomology, St. John's College, Agra, for valuable guidance and facilities for work. My thanks are due to Dr. Santokh Singh for apt suggestions and assistance.

REFERENCES

1. Clements, A. N. 1956. The antennal pulsating organs of mosquitoes and other Diptera. *Quart. Journ. Micr. Sci.*, **97** : 429-433.
2. Day, M. F. 1955. A new sense organ in the head of the mosquito and other Nematocerous flies. *Australian Journ. Zool.*, **3**(3) : 331-335.
3. Hase, A. 1927. Heart beat, *Hippobosca* (*Diptera*). *Zeit. Morphl. Okol. Tiere,* **8**: 187.
4. Hewitt, C. G. 1914. The House fly. Cambridge Univ. Press.
5. Hollande, A. C. 1914. Oenocytes : review and original. *Arch. Anat.* Microsc., **16**: 1-64.
6. Hollande, A. C. 1922. Pericardial cells : review and original. *Arch. Anat. Microsc.*, **18** : 85-307.
7. Hosselet, C. 1925. Cytology of oenocytes : *Culex* Diptera. *C. R. Acad. Sci.*, Paris. **180** : 399-401.
8. Jones, J. C. 1952. Prothoracic aortic sinuses in *Anopheles*, *Culex* and *Aedes*. *Proc. ent. Soc.* Washington, **54** : 244-246.
9. Jones, J. C. 1954. The heart and associated tissues of *Anopheles quadrimaculatus* Say. (*Diptera : Culicidae*) *J. Morph*, Philadelphia, **94** : 71-123.
10. Koch, J. 1945. Oenocytes : *Drosophila*. *Rev. Suisse Zool.*, **52** : 415-420.
11. Kowalevsky, A. 1892. Pericardial cells and Storage excretion. *Congr. internat. Zool*,. Moscow, **1** : 187-234.
12. Lowne, B. T. 1895. The anatomy, Physiology, Morphology and development of the blow fly (*Calliphora erythrocephala*) R. H. Porter, 18, Princes Street, Cavendish Square, London.
13. Miller, 1950. The internal anatomy and histology of Imago of *Drosophila melanogaster* given in the biology of *Drosophila*. Edited by M. Demerec. N. Y. John Wiley and Sons, Inc. London.

14. Perez, C. H. 1910. Histology, metamorphosis, *Calliphora. Arch. Zool. Exptl. et. Gen.*, **4** : 1-274.

15. Snodgrass, R. E. 1935. Principles of Insect Morphology. McGraw-Hill Book Company, Inc. New York and London.

16. Strindberg, H. 1913. Embryologische studies an inseckten. *Z. Wiss. Zool.*, **106** : 1-227.

17. Wigglesworth, V. B. 1934. Factors controlling moulting and metamorphosis. *Quart. Journ. Micr. Sci.*, **77** : 191-221.

18. Wigglesworth, V. B. 1950. Principles of Insect Physiology. Methuen & Co., Ltd., London.

19. Zavrel, J. 1938. Oenocytes in Syndiamesa, Chironomid. *Publ. Fac. Sci. Univ.*, Masaryk, **257** : 1-23.

A CONTRIBUTION TO THE AQUATIC AND MARSHY PLANTS OF KANPUR

S. Bhambie
Christ Church College, Kanpur.

The literature on the data of the systematics of hydrophytes of different localities of India is meagre. So far as the author is aware, the available accounts for particular localities are by Misra (1946), Lakshman (1950), Mirashi (1954, 57), Patnaik & Patnaik (1956), Srivastava (1956), Puri & Mahajan (1958), Sen (1959), Murty & Singh (1960), Chavan & Sabins (1961), Vyas (1964) etc. Recently Subramanyam (1962) has published a treatise entitled 'Aquatic Angiosperms' dealing with some common and important hydrophytes of our country.

There has been no record of the aquatic and marshy vegetation of Kanpur—a centrally placed city of Uttar Pradesh. The luxuriant growth of hydrophytes in several permanent ponds and banks of the Ganges and Ganges canal attracted the attention of the author. Therefore, a study of these plants was undertaken and several collections were made during 1961-1964 in different seasons. This paper places on record a list of aquatic and marshy plants of this locality, yet it is not claimed to be a complete list as occasional floods in the Ganges every year change the vegetation to some extent.

TOPOGRAPHY AND CLIMATE

Kanpur has a subtropical location (26°, 28′ N latitude and 80° 21′ E longitude) and is situated in Upper Gangetic Plain on the west bank of Ganges. Its height above sea level is 122 m. having an average rainfall of 104 cm. (1959-62). The temperature of the air may reach a maximum of 46°C and a minimum of 4°C and that of water 38°C to 8°C. There are three marked seasons of the year, *i.e.*, rainy, winter and summer. The surface of this locality is more or less evenly plain with slight undulations. There are no hills.

Several ponds, both temporary and permanent, and marshes abound round the city. Ganges canal which originates from Hardwar also terminates here passing through the heart of the city. Among the permanent ponds, the following were visited by the author on every alternate week. They are Allen forest pond, which is known as Allen forest lake as its circumference is quite large, Ganges pond, which is situated on Kanpur-Lucknow road just by the side of Ganges bridge and Kalyanpur pond, which is just opposite the Kalyanpur Police Station. Monthly collections were also made from some of the temporary ponds of Rawatpur and Panki, from the banks of Ganges and Ganges canal and from such temporary ponds and ditches which come into existence during rainy season. A map of Kanpur has been given to show the localities from where the plants have been collected mainly.

TAXONOMIC DATA

Besides, a large number of algal forms such as species of *Chara*, *Nitella*, *Spirogyra*, *Nostoc* etc., and a few pteridophytes such as *Marsilea minuta* (L.) Mant., *Salvinia auriculata* (Aublet) Hist., *Azolla pinnata* R. Br., and *Ceratopteris thalictroides* (L.) A. Brongn. etc., which are found in association with angiosperms, the aquatic and marshy vegetation of Kanpur consists of a varied assemblage. On the basis of author's own collections the following taxonomic data have been presented adopting Hooker (1872-1897) :—

RANUNCULACEAE

1. **Ranunculus sceleratus** Linn.

An erect winter annual with yellow flowers. Common in marshy and wet places particularly on the banks of Ganges and near Allen forest lake. A large variation in size; a plant of an inch having flower was recorded. Fl. Dec.—March. Bhambie 42.

NYMPHAEACEAE

2. **Nymphaea nouchali** Burm. f.

Nymphaea lotus non Linn.

Leaves sharply toothed; flowers white or sometimes pink, 5-24 cm. in diameter. Common in Kalyanpur pond and Ganges pond Hindi:—Chota Kamal. Fl. July—Nov. Bhambie 1.

3. **Numphaea stellata** Willd.

Leaves entire with rose or purple floweres reaching upto 25 cm. in diameter. Very common in Allen forest pond. Hindi—Kamal. Fl. July—Feb. Bhambie 43.

4. **Nelumbo nucifera** Gaertn.

Nelumbium speciosum Willd.

Leaves and rosy or pinkish flowers high above the water; common in Kamla Retreat—a part of Allen forest pond. Hindi—Kamal. Fl. Rainy season. Bhambie 71.

PAPILIONACEAE

5. **Aeschynomene indica** Linn.

Tall annual with yellowish white flowers. Frequent in Allen forest near the pond and in rice fields but common in marshy places near the ponds of Rawatpur. Hindi—Sola. Fl. Aug.—Oct. Bhambie 11.

ROSACEAE

6. **Potentilla supina** Linn.

A small herb having compound leaves and yellow flowers Common on the banks of Ganges and Ganges canal. Fl. Feb.—April. Bhambie 75.

LYTHRACEAE

7. **Ammannia baccifera** Linn.

Erect herb with usually apetalous flowers in dense spikes. Common in rice fields and on the banks of Ganges. Fl. July—Jan. Bhambie 3.

ONAGRACEAE

8. **Ludwigia adscendens** (Linn.) Hara.

Jussieua repens Linn.

Plants creeping or floating, petals five, white with yellow veins. Quite common in Allen forest pond, Kalyanpur pond and Ganges pond. Fl. Sept.—March. Bhambie 25.

9. **Ludwigia octavolvis** (Jacq.) Raven.

Jussieua suffruticosa Linn.

Plants erect, petals four, yellow. Frequent in wet places near Allen forest pond. Fl. Sept.—Jan. Bhambie 26.

10. **Ludwigia perennis** Linn.

Ludwigia Parviflora Roxb.

Plants erect, stamens as many as calyx lobes, petals yellow. Very common in the marshy localities near Ganges pond, Rawatpur and Panki. Fl. Sept.—Nov. Bhambie 27.

TRAPACEAE

11. **Trapa bispinosa** Roxb.

Fruit bony with two spines. Abundant in Kalyanpur pond and in all the ponds of Rawatpur, Panki etc. Hindi—Singhara. Fl. July—Nov. Bhambie 4.

UMBELLIFERAE

12. **Centella asiatica** (Linn.) Urban.

Hydrocotyle asiatica Linn.

Prostrate herb, leaves remiform, crenate. Frequent in wet places on the banks of Ganges canal. Hindi—Brahmi. Fl. Nov.—March Bhambie 41.

COMPOSITAE

13. **Eclipta prostrata** Linn.

Eclipta erecta Linn.

Eclipta alba (Linn.) Hassk.

Prostrate or erect perennial herb with axillary or terminal heads, petals white. Common in marshy and wet places and collected from the edges of all the ponds as well as from the banks of Ganges canal and Ganges. Fl. Throughout the year. Bhambie 56.

14. **Caesulia axillaris** Roxb.

A glabrous semi-aquatic herb with axillary heads; flowers white or bluish. Frequent in Typha belt of Panki and on the banks of Rawatpur ponds. Fl. Oct.—Jan. Bhambie 52.

15. **Cotula anthemoides** Linn.

Small perennial herb with dissected leaves and solitary heads. Common on the banks of Ganges canal and Ganges ponds. Fl. Feb. March. Bhambie 44.

ASCLEPIADACEAE

16. **Oxystelma esculentum** R. Br.

A glabrous twiner with deciduous leaves and pink flowers Fl. Sept. — Oct. Bhambie 74.

GENTIANACEAE

17. **Nymphoides cristatum** (Roxb.) O. Krnze.

Limnanthemum cristatum Griseb.

Aquatic herb with alternate floating leaves and white flowers. Common in Allen forest, Ganges and Kalyanpur ponds. Fl. throughout the summer but occasionally flowers were found in the beginning of summer.

HYDROPHYLLACEAE

18. **Hydrolea zeylancia** (Linn.) Vahl.

Annual herb rooting at nodes, flowers blue. Common in wet ground of Ganges pond, sometimes the major part of the plant is submerged. Fl. Dec.—Feb. Bhambie 66.

CONVOLVULACEAE

19. **Ipomoea aquatica** Forsk.

An aquatic herb forming a net work of vegetation over the surface of water with companulate corolla. Very common in ponds of Allen forest 'Ganges' Kalyanpur and Panki etc. Hindi—Nali-Ka-Sag. Fl. Most part of the year. Bhambie 58.

SCROPHULARIACEAE

20. **Bonnaya verenicaefolia** Spreng.

A creeping herb with purple flowers. Frequently seen near Typha belt on the banks of Ganges and Allen forest. Fl. Aug.—Dec. Bhambie 73.

21. **Bacopia monnieri** (Linn.) Pennell.

Moniera cuneifolia Michx.

A creeping herb with axillary flowers having blue or purple petals Fairly common in wet places of Allen forest and on the edges of Ganges pond. Fl. Sept.—Dec. Bhambie 28.

22. **Veronica anagalis** Linn.

An erect herb with white or pale purple flowers in lax axillary racemes. Very common in marshy localities of Allen forest, Rawatpur, Panki etc., and on the banks of Ganges canal. Fl. Feb.—April. Bhambie 45.

LENTIBULARIACEAE

23. **Utricularia inflexa** var. *stellaris* (Linn.f.) Taylor.

U. stellaris Linn. f.

A submerged aquatic herb with inflorescence projecting above water; peduncle with a whorl of spongy floats; flowers yellow. Common in Kalyanpur pond and frequently found in ponds of Rawatpur and Panki. Fl. Sept.—Nov. Bhambie 29.

24. **Utricularia flexuosa** Vahl.

Similar to U. inflexa but the peduncle lacks spongy float at the base. Common in Kalyanpur pond only. Fl. Oct.—Dec. Bhambie 67.

ACANTHACEAE

25. **Astercantha longifolia** (Linn.) Nees.

Hygrophila spinosa T. Anders.

A stout herb with sessile axillary flowers surrounded by rigid spines with purple white petals. Common on the bank of Ganges canal and in ditches of Panki, Rawatpur, etc. Fl. Sept.—Dec. Bhambie 30, 68.

26. **Justicia quinqueangularis** Koen.

A slender herb with flowers in terminal spikes having rose-coloured bilipped flowers. Fl. Sept.-Nov. Bhambie 31,69.

VERBENACEAE

27. **Phyla nodiflora** (Linn.) Greene

Lippia nodiflora A. Rich.

A creeping much branched herb with pale pink or white flowers arranged in dense globose axillary heads. Very common on the banks of Ganges and Ganges canal and in wet soil near all the ponds. Fl. almost throughout the year. Bhambie 60

LABIATAE

28. **Mentha piperata** Linn.

A small aromatic herb with white flowers. Occasionally met near the ponds of Panki and Rawatpur. Fl. Aug.-Oct. Bhambie 12.

AMARANTHACEAE

29. **Alternanthera sessilis** (Linn.) R. Br. ex DC.

Alternanthera triandra Lamk.

A prostrate branched herb with shinning flowers arranged in axillary sessile heads. Very common on wet places near Ganges canal and other ponds. Fl. Aug. Feb. Bhambie 13.

POLYGONACEAE

30. **Polygonum orientale** Linn.

A tall silky villous annual with white red or pale green flowers in spikes and scarious stipules; leaves up to 8 in. long. Found only in Allen forest pond in association with *Eichhornia crassipes*, etc. Fl. Oct.-Feb. Bhambie. 53.

31. **Polygonum glabrum** Willd.

An erect glabrous herb with pink flowers and ochcreate stipules. Frequently seen on wet soil near Allen forest pond and the ponds and ditches of Rawatpur. Fl. Sept.-Jan. Bhambie 54.

32. **Polygonum serrulatum** Lagasc.

An annual herb with white flowers and long britsles over stipules. Commonly seen on the banks of the ponds of Rawatpur, Allen forest and Panki, etc. Fl. Sept.-Feb. Bhambie 32.

33. **Rumex dentatus** Linn.

An annual herb with white flowers in distant whorls. Fl. Feb.-April. Bhambie 46.

URTICACEAE

34. **Pouzolzia pentandra** (Roxb.) Benn.

An erect herb without stining hairs and white flowers in axillary clusters. Common on wet soil near Allen forest pond and Ganges pond. Fl Aug.-Dec. Bhambie 14.

SALICACEAE

35. **Salix tetrasperma** Roxb.

A medium sized tree or shrub with young parts silky and female flowers in catkins; both male and female flowers lack perianth. Frequent on the bank of Allen forest pond. Fl. Aug.-Sept. Bhambie 15.

36. **Salix babylonica** Linn.

A big tree with weeping branches. Cultivated near an artificial pond in Government Agriculture College. Fl. Aug.-Oct. Bhambie 16.

CERATOPHYLLACEAE

37. **Ceratophyllum demersum** Linn.

A free submerged aquatic herb with sessile axillary greenish leaves and nut like fruit; male and female flowers in separate axils. Abundant in most of the ponds and ditches forming association along with *Hydrilla verticillata* and *Potamogeton crispus*, etc. Fl. July-Oct. Bhambie 5.

HYDROCHARITACEAE

38. **Hydrilla verticillata** (Linn. f.) Royle.

A submerged fresh water herb with whorled leaves and dioecious greenish flowers. Abundant in most of the ponds and ditches. Fl. July-Sept. Bhambie 6.

39. **Nechemandra alternifolia** (Roxb.) Thw.

Lagrosiphon roxburghii Benth.

A submerged fresh water herb with alternate or opposite leaves upto 4 cm. and dioecious white flowers. Common in Ganges pond. Fl. Sept.-Oct. Bhambie 34.

40. **Vallisneria spiralis** Linn.

A submerged tufted herb with linear strap-shaped leaves and greenish white dioecious flowers; female flowers having long spiral stalk which bring them to the surface of water. Common in Allen forest, Ganges and Rawatpur ponds. Fl. Feb.-April. Bhambie 47.

PONTEDERIACEAE

41. **Eichhornia crassipes** (Mart.) Solms-Laub.

An erect free floating or marshy herb with blue flowers and spongy petiole. Common in pond of Allen forest, Rawatpur, Kalyanpur and Panki. Hindi—Samunder-Sokh. Fl. Feb.-March. Bhambie 48.

42. **Monochoria hastata** (Linn.) Solms-Laub.

An aquatic herb with creeping root stock and whitish blue flowers Frequent in Allen forest pond. Fl. Aug.-Sept. Bhambie 17.

43. **Monochoria vaginalis** (Burm. f.) Kirk.

An aquatic herb with sub-erect root stock and blue flowers. Frequent in rice fields. Fl. Aug.-Oct. Bhambie 18.

ARACEAE

44. **Pistia stratiotes** Linn.

A floating stemless herb with obovate, cuneate, sessile leaves in rosette; flowers, unisexual monoecious. Common in the ponds of Kalyanpur. Fl. Late winter. Bhambie 74.

COMMELINACEAE

45. **Cyanotis axillaris** Schult. f.

An annual sub-erect herb with violet blue flowers in axillary scorpiod cymes having six stamens. Common in wet places and on the bank of Ganges and Ganges canal. Fl. Aug.-Nov. Bhambie 9.

TYPHACEAE

46. **Typha elephantina** Roxb.

A tall bulrush 8-12 ft. high with trigonous leaves above the sheath and flowers in cylindrical spikes. Frequent in marshy areas of Allen forest and Panki pond and common on the banks of Ganges. Fl. July-Oct. Bhambie 7.

47. **Typha angustata** Bory & Chaub.

A tall bulrush 5-10 ft. high with semicylindrical leaves above the sheath. Frequent in marshy areas of Allen forest pond. Fl. Aug.–Oct. Bhambie 20.

LEMNACEAE

48. **Spirodela polyrhiza** (Linn.) Schleid.

Plants red on the lower surface with each joint having several roots. Common in ponds and ditches during the rainy season and winter. Fl. Not observed. Bhambie 62.

49. **Lemna paucicostata** Hegelm.

Plants green on the lower surface with each joint having one root. Common in ponds and ditches during rainy season and winter. Fl. Not observed. Bhambie 63.

50. **Wolffia arrhiza** (Linn.) Wimm.

Plants globular. Common in ponds and ditches during rainy season. Fl. Not observed. Bhambie 64.

ALISMACEAE

51. **Sagittaria guayanesis** H. B. K. sub sp. *lappula* (D. Don.) Bogin.

Erect stemless aquatic herb with floating broadly ovate leaves and white flowers. Frequent in Kalyanpur pond. Fl. Aug.–Oct. Bhambie 21.

52. **Sagittaria sagittifolia** Linn.

Erect stemless herb with leaves rising above the surface of water hastate or sagittate and white flowers having a purple claw. Common in the ponds of panki and Kalyanpur. Fl. April–May. Bhambie 51.

APONOGETONACEAE

53. **Aponogeton natans** (Linn.) Engl. & Krause.

Perennial aquatic herb with stoloniferous root stock and floating leaves showing variations; flowers light blue in dense terminal spikes. Fl. Aug.-Nov. Bhambie 70.

54. **Aponogeton crispum** Thunb.

Perennial aquatic herb with submerged linear lanceolate or oblong leaves and flowers in lax spikes. Fl. Oct.-March. Bhambie 55.

POTAMOGETONACEAE

55. **Potamogeton nodosus** Poir.

P. natans Linn. Proparte.

An aquatic herb with upper brown, ovate, multiveined, floating alternately arranged leaves, basal leaves linear; flowers in dense spike. Common in Ganges pond and frequent in ponds of Kalyanpur. Fl. After rainy season. Bhambie 72.

56. **Potamogeton pectinatus** Linn.

An aquatic herb with much dichotomously branched stem and filiform or thread like three nerved, opaque, alternately arranged leaves having long tapering leaf tips; bisexual flowers in lax and long spikes. Common in running water of Ganges canal and in Allen forest pond. Fl. Sept.—Dec. Bhambie 35.

57. **Potamogeton crispus** Linn.

An aquatic herb with submerged, linear or linear oblong, three nerved, translucent alternately arranged leaves having finely toothed margin; bisexual flowers in lax spikes. Fl. Feb.—April. Bhambie 49.

58. **Zannichellia palustris** Linn. Subsp. *Pedicellate* Wahlenberg & Rosen.

Aquatic Slender herb with submerged, linear, oppositely arranged leaves and unisexual flowers. Frequent in ditches of Rawatpur. Fl. Feb.—March. Bhambie 50.

NAJADACEAE

59. **Najas minor** Allione

An aquatic herb with narrowly linear finely toothed alternately arranged leaves: flowers unisexual, monoecious. Frequent in ditches of Rawatpur and Kalyanpur. Fl. Sept.—Oct. Bhambie 36.

ERIOCAULACEAE

60. **Eriocaulon sieboldianum** Sieb. & Zucc.

Marshy herb with linear grass like leaves having sheathing leaf base; flowers minute in globose heads. Frequent in paddy fields of Panki and Kalyanpur. Fl. Oct.—Nov. Bhambie 40.

CYPERACEAE

61. **Cyperus alopecuroides** Rottle.

Juncellus alopecuroides Clarke.

A tall pale herbaceous plant with brown spikelets in globose heads with flowering glumes alternate; fruit a laterally compressed nut. Common in Panki along with Typha and near Ganges pond. Fl. Most part of the year. Bhambie 57.

62. **Cyperus laevigatus** Linn.

Juncellus laevigatus Clarke

A small pale herbaceous plant similar to *C. alopecuroides.* Abundant on muddy soil near Ganges canal. Fl. Aug.—Sept. Bhambie 22.

63. **Cyperus distans** Linn.

Perennial stoloniferous herb with three angled solid stem; bracts in two rows; fruit a trigonous nut. Frequent in marshy places near Kalyanpur pond and on wet marshy soil of Ganges canal. Fl. July—Sept. Bhambie 8.

64. **Cyperus alulatus** Kenn.

Similar to *C distans.* Common on wet and muddy soil of Ganges and Ganges canal. Fl. July—Sept. Bhambie 9.

65. **Eleocharis plantaginea** R. Br.

An annual herb with cylendrical leaves. Common on wet and muddy soil near Ganges pond.

66. **Fimbristylis littoralis** Gaud.

Fimbristylis millacea non Vahl

An annual herb with three angled stem having scales all round the spikelets clustered in corymbose inflorescence; flowering glumes spirally arranged. Frequent in marshy places near Kalyanpur pond and Rawatpur ponds. Fl. July—Sept. Bhambie 10.

67. **Fimbristylis menestachya** Hassk.

Caespitose marshy herb with flat short leaves and hairy glumes. Other characters are similar to *F. milacea.* Fairly common on the banks of Ganges canal and Typha producing area of Allen forest. Fl. rainy season. Bhambie 61.

GRAMINEAE

68. **Paspalum scrobiculatum** Linn.

A perennial grass with lanceolate leaves and laterally compressed spike, basal glume absent. Common on wet soil particularly at water edges of the ponds of Allen forest, Kalyanpur and on the banks of Ganges canal. Fl. Sept.—Oct. Bhambie 37.

69. **Paspalidium punctatum** (Burm. f.) A. camus.

An annual erect grass with linear ciliated leaves; spikelets awnless and dorsally convex. Common on the edges of Allen forest lake and Ganges canal. Fl. Sept.-Nov. Bhambie 38.

70. **Echinochloa crusgalli** (Linn.) Beauv.

Panicum crusgalli Linn.

An annual grass with flat leaves; spikelets two flowered and glumes with hairs. Common along with Typha plants in Allen forest and Panki. Fl. Aug.-Nov. Bhambie 23.

71. **Oryza sativa** Linn.

A tall marshy or aquatic grass with flat long leaves; spikelets deciduous always awaned apparently one flowered but have three flowers. Cultivated in Kalyanpur and Rawatpur area and growing wild in many marshy lecalities. Fl. Oct.-Nov. Bhambie 65.

72. **Vetiveria zizanioides**(Linn.) Nash ex Small.

A rigid perennial grass with fragrous roots, spikelets awanless in whorled raceme surrounded by silky hairs. Common in open plains near Ganges, Allen and Kalyanpur ponds in dense tufts. Fl. Aug.-Oct. Bhambie 24.

73. **Arundo donax** Linn.

A very tall grass with flat leaves in which ligules represented by hairs only; spikelets laterally compressed lemmas with silky hairs on the back. Frequently seen on the banks of Ganges canal and cultivated in Memorial garden and Medical College garden near marshy habitat. Fl. Oct.-Dec. Bhambie 39.

ECOLOGICAL CLASSIFICATION

The hydrophytes of Kanpur can be classified into the following five categories on the basis of their contact with soil, water and air. A few important plants of each category are listed below although the plants marked with an asterisk show different behaviour in different environment.

Free floating—The plants of this category remain floating on the surface of water and are in contact with water and air only. They may be with roots or rootless.

Spirodela polyrhiza, *Lemna minor*, *Eichhornia crassipes**, *Pistia stratiotes*, *Azolla pinnata*, *Wolfia arrhiza*, *Salvinia auriculata.*

Free submerged—The plants of this category are free but they remain submerged and are in contact with water only. In *Utricularia* the inflorescence, however, comes out of water.

Ceratophyllum demerum, Utricularia flexuosa, Utricularia inflexa var. *stellaris, Najas minor.**

Attached submerged—These plants are firmly attached to the bottom but they are submerged and are in contact with soil and water only. The inflorescence in some species of *Potamogeton* comes out of the water.

Hydrilla verticillata, Potamogeton crispus, Potamogoton pectinatus, Potamogeton natans, Zannichellia palustris, Vallisneria spiralis.

Attached with floating leaves—In this category the leaves of the plants completely come up on the surface of water although they are rooted in the soil and are in contact with the soil, water and air.

Nymphoides cristatum, Nymphaea nouchali, Nymphaca stellata, Nelumbo nucifera, Trapa bispinosa, Ludwigia adscendens, Sagittaria guayanesis.*

Occurring on marshy soil or on moist soil—Plants of this category are usually confined to shallow waters or marshy habitat. The roots, the lower part of the stem and in some cases even lower leaves are submerged. Some of them may be referred to as amphibious plants as they can grow in water as well as on moist soil while others grow on the margins of the moist grounds near the ponds on the banks of rivers and canals.

Typha elephantina, Typha angustata, Ranunculus scleratus, Monochoria hastafolia. Sagittaria sagittifolia, Aeschynomene aspera, Ipomoea aquatica*, Cyporus alopecruoides, Cyperus alulatus, Bacopa monnieri*, Veronica anagalis, Alternanthera sessilis*, Phyla nadiflora*, Paspalum scrobioulatum, Cyanotis axillaris.*

SUMMARY

The paper describes the aquatic and marshy vegetation of Kanpur—a centrally placed city of Uttar Pradesh. In total 73 species have been recorded. Out of these, 37 belong to families of Dicotyledons and 36 species belong to families of Monocotyledons. Cyperaceae, Gramineae, Potomogetonaceae, Polygonaceae and Lythraceae are somewhat dominant families represented by 7, 6, 5, 5, 4 species respectively. *Alternanthera sessilis, Phyla nodiflora, Polygonum glabrum, Eichhornia crassipes, Potamogeton pectinatus, Potamogeton crispus and Paspalum scrobiculatum* are the most dominant plants occuring in abundance.

Among the Pteridophytes only *Marsilea minuta* and *Azolla pinnata* are growing wildely. *Salvinia auriculata* and *Ceratopteris thalictroides* are cultivated in educational institutions. A brief description of individual plant and an ecological classification of some of the common plants are presented.

ACKNOWLEDGEMENTS

I express my sincere gratitude to Dr. K. Subramanyum, Jt. Director, Botanical Survey of India, Calcutta for going through the manuscript and giving some valuable suggestions, Professors V. Puri, A.B. Gupta and Y.S.

Murty for encouragement, continuous interest and for the facilities. I am also thankful to Dr. V. Singh for his numerous acts of kindness and help in various ways and to my pupil Mr. K. C. Kurian for helping in the collection of plants.

REFERENCES

1. Chavan, A.R. & Sabins, S.D. 1961. A study of the hydrophytes of Baroda and environs. *J. Indian Bot. Soc.*, **40** : 121-130.
2. Hooker, J.D. 1872-1897. Flora of British India, London.
3. Lakshman, C. 1950. Studies in the hydrophytic vegetation of South India. *Proc. Indian Sci. Cougr.*, Poona Part III : 11.
4. Mirashi, M.V. 1954. Studies in the hydrophytes of Nagpur. *J. Indian Bot. Soc.*, **33**: 299-308.
5. Mirashi, M.V. 1957. Studies in the hydrophytes of Umerd. Ibid. **36** : 396-407.
6. Misra, R.D. 1946. The ecology of low-lying lands. *Indian Ecol.*, I : 11.
7. Murty, Y.S. & Singh, V. 1960. Aquatic and marsh plants of Hastinapur. *Uttar Bharati*, **8** : 89-100.
8. Patnaik, H. & Patnaik, N.K. 1956. The hydrophytes of Cuttak. *J. Indian Bot. Soc.*, **35** : 167-170.
9. Puri, G. S. & Mahajan, S.D. 1958. The vegetation of marshes and swamps in Poona District. *Proc. Indian Inst. Sci.*, **24** (B) : 159-164.
10. Sen, D.N. 1959. Hydrophytes of Gorakhpur. *Agra Univ. J. Res.* (*Sci.*), **8** : 17-29.
11. Srivastava, M.P. 1956. Hydrophytes of Sagar Lake. *Bull. Bot. Soc. University Saugar*, **8** (B) : 34-37.
12. Subramanyum, K. 1962. Aquatic Angiosperms. Delhi.
13. Vyas, L.N. 1964. A study of hydrophytes and marsh plants of Alwar and environs. *J. Indian Bot. Soc.*, **44** : 17-30.

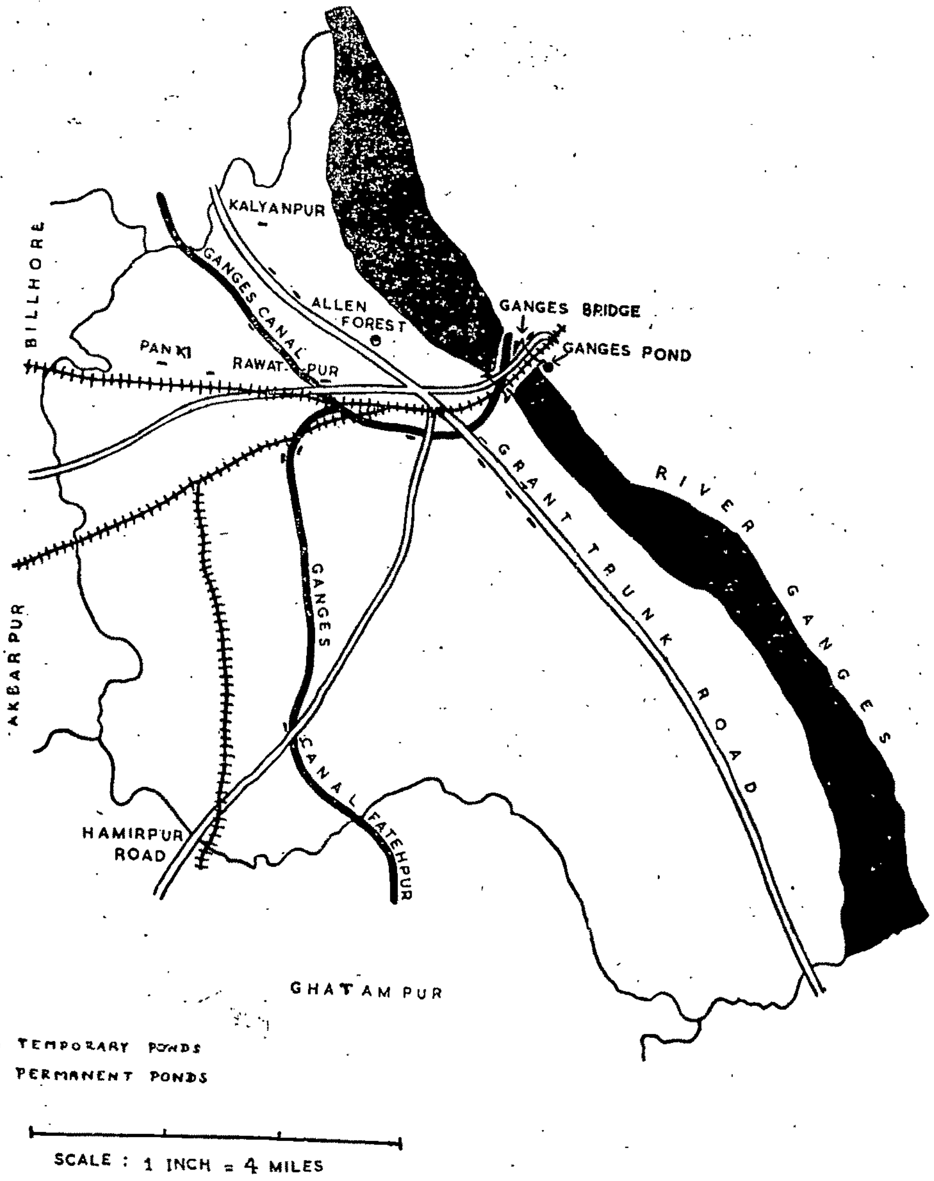

A map of Kanpur showing the main localities from where the plants have been collected

Abstract of Theses

A STUDY OF SOAP GELS IN NON-AQUEOUS SOLVENTS*

R. C. Seth
Chemical Laboratories, St. John's College, Agra.

Gels of sodium oleate and sodium erucate in the fraction of turpentine, called as liquid A, have been prepared for the first time by the author by cooling the gel-forming solutions prepared at 140°C., and are found to be syneretic. The author has measured the time and temperature of setting of these gels, the rate of cooling of the gel-forming solutions, the opacity and the depolarisation of the light scattered by the solutions during and after setting and the rate of syneresis of the set gels of these soaps. The results obtained and the conclusions drawn from these studies are given in the following:—

1. *Time and temperature of setting of gel-forming solutions:*

It has been found that the time of setting (t_s) measured by Fleming's method, according to the definition given by Prasad, decreases as the amount (c) of soaps in gels increases and the temperature (T) at which gel-forming solutions (prepared at 140°C) are allowed to cool, is lowered; no gels are obtained if this temperature is 110°C., or higher. The relation between t_s and c is given by $(t_s - k_1 c^{-m_1})(t_s - k_2 c^{-m_2}) = 0$, where k_1, k_2, m_1 and m_2 are constants for a particular temperature. The generality of this relation has been established by its applicability to soap gels in other media studied by previous workers.

It has been further shown that Arrhenius equation is applicable to these gel-forming systems; hence the heats of activation of the gelation process have been calculated; they are negative for both gels.

The time of setting of gel-forming solutions of the same concentration has been found to increase as the columns of the solutions of the same diameters or the diameters of the solutions of the same heights, are increased. This has revealed that the time of setting of these gels is also a function of the volume of the gel-forming solution.

The effect of the addition of sodium stearate, sodium palmitate and potassium stearate to the gel-forming solutions of both soaps on the time of setting is specific and follows the order sodium stearate >sodium palmitate> potassium stearate.

An important observation has been made that the gelation temperature (t_g) is a characteristic property of these gels and is a function of their concentrations only.

---

* Abstract of the thesis for which Ph. D. degree has been awarded by this University.

2. *Cooling of the gel-forming solutions:*

Systematic study of the rate of cooling of gel-forming solutions of several concentrations from the temperature at which they are prepared to several lower temperatures has revealed that it is lowered by the increase in concentration. In the earlier part, the cooling curves for the solution coincide with that for the liquid A cooling under the same conditions, but their course changes at gelation temperatures (t_g) in a direction which indicates that heat is evolved on gelation. The actual values of the heats (H) evolved and of the ratio of molar heats of gelation (MH) to (t_g+273)have been calculated; former increase with the increase in the soap contents of the gel and decrease with the increase of temperature of surroundings, but the latter decrease with increase of both the concentration of the gels and the temperature of surroundings.

The parts of the curves above and below the gelation temperatures obey Newton's law of cooling; this behaviour has enabled the author to calculate the specific heats of gel-forming solutions (S_1) and of the set gels (S_2) in all cases, S_1 has been found to be greater than S_2 and both S_1 and S_2 increase with increase in soap content.

3. *Opacity measurements during and after the setting of gel-forming solutions, that is, during the syneresis of the set gels:*

It has been found that opacity of these gels during setting and during syneresis, which commences soon after the gels have set, measured on Klett Summerson Colorimeter, increases for some time and then reaches an almost constant value after about six hours. It increases when (1) the concentration of the soaps is increased, (2) substances mentioned below are added to the gel-forming solutions and (3) the amounts of the added substances are increased. The effectiveness of the addition agents is in the order potassium erucate> potassium palmitate> potassium stearate> sodium palmitate> sodium stearate.

4. *Turbidity, dissymmetry and depolarisation measurements during the setting and the syneresis of gels:*

The measurements have been made on Brice Phoenix Light Scattering Photometer at 20°C., at 45°, 90° and 135°. The values of F(G/G′), assumed to represent the turbidities, have been found to decrease during the cooling of the gel-forming systems from 140° to 20°C., this includes the period during which these systems set to gels and synerise to a great extent. These observations lead to the conclusion that the particles in these systems prior to gel-formation are fairly large and reduce in size during the syneresis, probably by disintegration, and the disintegrated parts go to compose the sol which is exuded as syneretic liquid. The increase in the values of F(G/G′) on increasing the amount of the two soaps has shown that the size of the particles in systems containing larger amounts of the gel-forming substances are larger and remain larger throughout the period of investigation, but there is no simple relation between the two. The addition of sodium stearate, potassium stearate, and sodium palmitate to the two gel-forming systems affects the size of the original particles differently. Generally it increases in sodium oleate and decreases in sodium erucate systems, the order of their effectiveness being sodium stearate> potassium stearate> sodium palmitate.

The values of dissymmetry decreases slowly during the setting and rapidly during the syneresis of both gels. They increase on increasing the amounts of the gel-forming substances in the two systems and thus support the conclusions drawn from the values of $F(G/G')$. The effect of the addition of sodium and potassium stearates and sodium palmitate on the dissymmetry values of the two gel-forming systems is specific in individual cases, and hence no general conclusions have been drawn regarding their effects.

The depolarisation factors (ρ_u, ρ_v and ρ_h) of the transversely scattered light have been measured at 45°, 90° and 135° with light unpolarized, and vertically and horizontally polarised in the case of the gel-forming systems containing different amounts of the gel-forming substances in the absence and presence of sodium and potassium stearates and sodium palmitate. The values of ρ_h have shown that (1) initially the particles in the gel-forming systems are only slightly anisotropic, (2) the anisotropy of the particles remains practically unaffected during the formation of gels, and (3) the anisotropy of the particles in the set gels increases rapidly in the case of sodium oleate and slowly in the case of sodium erucate gels, due to the syneresis of the set gels. The values of ρ_b have shown that (1) initially the particles in the two gel-forming systems are small and their size is comparable with the wave-length of light, (2) the size of the particles remains practically unaltered until the gels set and (3) the size of particles decreases on account of the syneresis of the set gels. This conclusion has been confirmed from the study of the values of $\triangle\ \rho_u$. The author has consequently classified the changes observed in the values of ρ_u, ρ_v and ρ_h into two types: (1) those which take place during the formation and the setting of the gels and (2) those which take place subsequently on account of syneresis; their values are fairly small in the former and fairly large in the latter stages. The values of ρ_u, ρ_v and ρh do not change in any regular manner with either the change in the amount of the gel-forming substance or the angle at which the measurements are made. The effects of the addition agents are also very irregular, but the values of $\triangle\ \rho_u$ calculated for these systems show that generally the size of the particles decreases with time in the presence of these agents.

5. *Syneresis of sodium oleate and sodium erucate gels:*

It has been found that the rate of syneresis decreases with increase in time, but the graphs between the amount of syneresis and time are smooth rising curves, and not S-shaped as found by Fergusson and Applebey with gels of silicic acid. These graphs thus show that the rate of syneresis is large in the initial period and falls off continuously with time and the process of syneresis is not autocatalytic in nature. The process of syneresis does not follow the unimolecular law of chemical reactions, as found by Lipatov with geranin gels as the values of the unimolecular constant (Km) decrease with increase in time; however, the plots of R/t(R=x or y) against Km show a linear relation between the two. The syneresis of these gels is not the exact reverse of the imbibition of liquids by gels, as the plots of log x or log y, in the case of gels of sodium oleate or sodium erucate, respectively, against log *t*, are not single straight lines. The plotted points lie on a pair of intersecting straight lines which indicate that two different processes are involved in the syneresis of these gels.

The rate of syneresis decreases with an increase of temperature at which the gels synerise. This is shown by the fact that the values of unimolecular constant (Km) at a given interval of time are large for low temperatures and decrease as the temperature is increased; however, the plots of R/t (R=x or y) against Km for gels of the same concentration synerising at different temperatures lie on the same straight lines. Similarly the plots of the values of log x or log y against those of log t appear to lie on the same pair of intersecting straight lines, showing thereby that this characteristic behaviour of these gels is not affected by change in temperature.

The amount of syneresis in any given interval of time at a given temperature has been found to be greater for the dilute gels than for the concentrated ones. Also the plots of R/t ($R=x$ or y) against Km for all concentrations of gels used in this investigation lie on the same straight lines.

The syneresis of these gels has been found to increase with increase of diameter and length of the gel column. It is retarded by the addition of sodium stearate, sodium palmitate, potassium stearate and potassium palmitate to the gel-forming mixtures, and the retardation is greater, larger is the amount of the added substance. The retarding effect of these agents is in the order sodium stearate > sodium palmitate > potassium stearate > potassium palmitate. The external pressure of the surroundings in which the gels are placed has a pronounced effect on their syneresis; it increases with decrease in the external pressure.

6. *The effect of the size of the molecule of the gel-forming substance on the several properties of the gels:*

The increase in the length of the molecule of the gel-forming substance on changing it from sodium oleate ($CH_3(CH_2)_7CH{:}CH.(CH_2)_7COONa$) to sodium erucate ($CH_3(CH_2)_7CH{:}CH(CH_2)_{11}COONa$) has been found to exert a pronounced influence on the several properties of gel-forming systems studied in this investigation.

Under the same conditions of the surrounding temperatures the gel-forming systems of sodium erucate take longer time to set than the systems of sodium oleate having the same concentration, expressed in grams in a fixed volume of the dispersing liquid A; probably the increase in the length of the chain of the molecule of the gel-forming substance hinders the process of setting. It therefore follows that the gelation temperatures for sodium erucate gels of different concentrations are lower than those for sodium oleate gels of the same concentrations; this has actually been found.

The specific heats of gel-forming solutions of sodium oleate have been found to be greater than those for sodium erucate having the same concentration; reverse happens with the specific heats of the set gels of these soaps. However, in both cases heat is evolved on gelation. It follows, therefore, that (1) the specific heats of the gel-forming systems of both soaps in the sol state are greater than those in the gel state, and (2) the heat evolved on the gelation of sodium erucate is less than the heat of gelation of sodium oleate gels; these conclusions have been actually found to be true.

The higher specific heats of solutions of sodium oleate than those of sodium erucate are not in accordance with Kopp's law which requires that reverse should happen on account of larger number of atoms in sodium erucate. However, the results obtained lead to the conclusion that in the pre-gel-forming stage the complexities of the particles in sodium oleate systems are greater than those in sodium erucate systems and the reverse happens in the post-gel-forming stage. These inferences are supported by the light scattering measurements of these systems. It has been found that the size of the particles in gel-forming systems of sodium erucate is smaller than those in sodium oleate systems of the same concentrations in the pre-gel-forming stage, while the reverse happens in the post-gel-forming stage.

The opacities of solutions of sodium erucate throughout the process of gelation have been found to be slightly higher than those of sodium oleate solutions of the same concentration, because the size of the molecules of sodium erucate is larger than those of sodium oleate and, since the particles in the pre-gelation stage in the gel-forming system of sodium erucate are smaller than those in sodium oleate system, the number of the particles in sodium erucate gels is greater than in gels of sodium oleate.

Another feature brought out from the study of opacity is that the opacities of the two gel-forming systems increases with increase in concentration, showing thereby that the compactness or the denseness of gels increases with increase in the concentration of the gel-forming substance in the gel. This goes to show that the speed of syneresis of these gels depends upon the compactness of the set gels; more compact the gels are, lower is their speed of syneresis; this has actually been observed.

The results obtained in this investigation conducted by the author are interesting as they correlate the behaviour of gel-forming systems with the constitution of the gel-forming substances.

STUDIES ON PATHOGENESIS OF *CLOSTRIDIUM CHAUVOEI* INFECTION IN HEALTHY, IMMUNISED AND TRAUMATISED GUINEAPIGS*

S. N. Dixit†

Department of Pathology, Post-graduate College of Animal Sciences,
Indian Veterinary Research Institute, Mukteshwar (Kumaon).

In the present study pathogenesis and progressive pathology of experimental *Clostridium chauvoei* infection in healthy and immunised guineapigs was studied by inoculating *Cl. chauvoei* spores suspended in normal saline or culture filtrate into normal or traumatised area.

For experimental work a total number of 55 guineapigs including 7 controls for different groups of artificial infection were used. A group of 12 guineapigs were inoculated each with 0·8 ml. of concentrated standardised spore suspension in culture filtrate and destroyed in pairs at various intervals post infection. Another group of 8 healthy guineapigs were inoculated with the same number of spores in normal saline and the guineapigs were destroyed in pairs at various intervals. Six immunised guineapigs were destroyed at each of the six different intervals. Twentytwo traumatised animals were divided into two sub-groups. First sub-group of 11 guineapigs were inoculated with spores of *Cl. chauvoei* in culture filtrate 4 hours after injection of traumatic agent (Aluminium sulphate-albumin mixture) to initiate mild inflammatory reaction. In the other group of 11 guineapigs *Cl. chauvoei* spore suspension in culture filtrate was inoculated 18 hours post trauma. In all the guineapigs, spore suspension was inoculated always by intramuscular route in thigh region. Traumatic agent was also given intramuscularly in thigh region.

For specific immunisation, two injections of Blackquarter composite broth vaccine were inoculated, first injection 0·5 ml of vaccine was followed by another injection of 1 ml of vaccine after a week. Guineapigs were challenged with virulent spore suspension 3 weeks after the first injection.

Blood from the heart was collected just prior to sacrifice or immediately after for haematological studies which included total erythrocyte count, total leukocyte count, haemoglobin estimation, differential leucocytic count, and for cultural study. Liver, heart, skeletal muscle from the site of inoculation, adrenal, kidneys and spleen pieces were collected and processed for histopathological studies.

---

* Abstract of thesis approved for the award of M. V. Sc. degree of Agra University (1963).

† Present address—Senior Research Fellow, Division of Experimental Medicine, Central Drug Research Institute, Lucknow.

It was found that in the initial stages of infection there was progressive oligocythemia, a sharp leukopenia of neutrophilic type and a relative lymphocytosis. In later stages due to haemoconcentration erythrocyte count tended to return to normal values. The symptoms exhibited by guineapigs in healthy and traumatised groups were alike. By about 12 hours of infection symptoms of distress, rise of temperature and marked swelling at the site of inoculation were noticed. By 24 hours and onwards the guineapigs were very dull and showed sticky purulent discharge at the eyes and nervous symptoms. Immunised groups of guineapigs and those that received spores in saline were apparently healthy and did not manifest any symptoms of sickness.

Post-mortem lesions in healthy guineapigs receiving spore suspension in saline and in immunised guineapigs receiving spores in culture filtrate were essentially similar and had a localised disposition rather than of generalised nature as observed in other groups. At the site of inoculation animals of both groups exhibited only mild gelatinous oedema without much blackening of muscles. Other internal organs such as liver, heart, skeletal muscles, adrenals, spleen and kidneys, did not show any abnormality. The other groups of healthy guineapigs receiving spore suspension of *Clostridium chauvoei* in culture filtrate and those receiving infective agent after variable intervals post trauma manifested generalised lesions of toxaemic nature differing only in degree of severity. Lesions were more severe in traumatised groups of animals.

In the initial stages of infection muscles at the site of inoculation showed slight blackening together with accumulation of gelatinous oedematious fluid. By 12 hours, the lesion extended to the muscles of abdomen, shoulder and back. They were dull black in colour, swollen and contained gas pockets in between the muscle bundles. The affected muscles emitted a characteristic rancid butter odour. There was extensive accumulation of haemorrhagic exudate in muscles and subcutaneous tissue of abdomen. The swelling crepitated on pressure. In the terminal stages of infection there were splitting of muscle bundles and extensive haemorrhagic exudate in the subcutaneous tissues.

In liver and spleen the only changes perceptible to the eyes were slight darkening and sometime swelling of the organ. On sectioning of liver tissue, some grey foci were seen. Kidneys appeared to be slightly congested.

Microscopic changes were well marked and characteristic. In healthy traumatised animals receiving spore suspension in culture filtrate, in the initial stages muscles at the site of inoculation showed separation of muscle bundles and individual fibers due to congestion of blood vessels and accumulation of haemorrhagic exudate. In advance stages the changes were characterised by myonecrosis, transverse splitting, fragmentation and dissolution of muscle fibers. Haemorrhagic exudate consisted of erythrocytes, polymorphonuclear leucocytes and a few mononuclear cells.

In liver there was congestion of blood vessels in the portal area, tributary sinusoids and central veins. Mild degenerative changes in the hepatic cells occasionally accompanied with disorganisation of hepatic cell column were seen in most of the specimens. Focal necrotic areas were seen only in a few specimens.

Spleen, heart muscle and kidneys presented congestion of blood vessels. Kidneys showed hydropic degeneration of tubular cells. Some of the adrenal specimens showed depletion of fat from the cells of zona fasciculata.

In healthy animals receiving spore suspension in saline and in the immunised groups of animals, the muscle at the site of inoculation showed congestion of blood vessels in the endo- and epymysial connective tissue, areas of haemorrhagic exudate, separation of muscle bundles and polymorphonuclear infiltration. Inflammatory reaction did not spread to other muscles as seen in the previous group. Other internal organs did not show any marked changes from normal structure.

These findings, in the light of available literature have been briefly discussed and the literature on the history, incidence, pathogenecity in animals, mode of infection, pathology of disease in animals together with immunization against *Cl. chauvoei* infection has been briefly reviewed.

ACKNOWLEDGEMENTS

Thanks are due to Sri S. S. Khera, B. Sc., M. V. Sc., Dip. Bact. (Lond.) for his guidance and going through the manuscript and to Dr. G. L. Sharma, L. V. P., M. S., Ph. D. (Michighan), Head, Division of Pathology & Bacteriology, I. V. R. I., Mukteshwar for the facilities provided.

STUDY OF ALDOSTERONE AND ITS RELATIONSHIP WITH THE CHANGES IN PLASMA VOLUME AND ELECTROLYTES IN PATHOGENESIS OF HUMAN ASCITES DUE TO CIRRHOSIS OF LIVER*

R. R. Bodkhe†
Liver Diseases Research Unit, S. N. Medical College, Agra.

The pathogenesis of ascites in human liver cirrhosis is a multifaceted complex problem. In spite of daily additions to the already vast literature on this subject, the exact cause of this condition still remains a challenge to the investigators in the field of liver disease. From time to time several factors have crept up as playing significant role in the process of ascites formation though it has all along been difficult to incriminate any one of them playing the major role in all these cases. It has also become apparent that different patients with cirrhosis of liver vary greatly in both the number and relative importance of causal agents inducing cirrhosis.

Elevated urinary aldosterone excretion in cases of cirrhosis with ascites has been reported by some workers. The factors responsible for an initial accumulation of ascites in these patients are not yet definitely known, but the isolated results of various studies carried out so far suggest that aldosterone plays a secondary, compensatory role in ascites formation. The exact mechanism of increased secretion and excretion of aldosterone in this disease is, however, not fully understood. The mechanisms controlling aldosterone secretion in man under physiologic conditions are also poorly known. At the present state of knowledge, it is supposed that the production of aldosterone is controlled partly by changes in extracellular fluid volume, partly by blood sodium and potassium concentration and to some extent by neurohormone mechanism, although it is evident that the various changes in aldosterone secretion can not be accounted for by these known mechanisms. No clear relationship is available between any one of these factors and the increased excretion of aldosterone observed in patients with cirrhosis and ascites.

The present work was undertaken to obtain a clearer picture of the mechanism of the regulation of aldosterone output in decompensated liver cirrhosis and to further extend our knowledge about the mechanism of ascites formation in the light of the increased aldosterone secretion in this disease.

The work reported here was carried out on a total of sixty patients of cirrhosis of liver. Of these fifty were cases of cirrhosis with ascites, and ten without ascites. Twenty normal subjects under moderate sodium restriction (50 — 70 mEq/day) served as controls for these patients who were also submitted to the same diet.

---

* Abstract of the thesis approved for the degree of Doctor of Philosophy to the Agra University, Agra.

† Present Address—Department of Biochemistry, G.R. Medical College, Gwalior, (M. P.).

The following estimations were carried out in these patients:—

(1) Total (and also free and conjugated fractions in some cases) urinary aldosterone excretion in 24 hour specimen.
(2) Urinary 17-hydroxycorticoids in 24 hour urine specimen.
(3) Plasma volume.
(4) Plasma sodium.
(5) Urinary sodium.
(6) Serum potassium.
(7) Urinary potassium.
(8) Endogenous creatinine clearance, and
(9) Red blood cell water, sodium and potassium in some cases.

These estimations were carried out in view of the observed influence of volume and electrolyte concentration of intravascular fluid on the physiological regulation of aldosterone output in experimental studies. In the patients of cirrhosis with ascites these estimations were repeated during the periods ending 24, 48, 72 and 96 hours after abdominal paracentesis during the reaccumulation of fluid into peritoneal cavity. The object was to study the changes in aldosterone excretion and to correlate them with the plasma volume and sodium and potassium concentration of blood and urine during the formation of ascites.

The methods used in this study were described in brief with their theoretical aspects and normal healthy individuals were first studied to obtain the normal values with these methods.

The following were the observations and results obtained in this study.

Urinary aldosterone excretion in patients of cirrhosis with ascites when compared to the normal healthy subjects kept on a similar moderate salt restriction as that of the patients, has been found to be increased in 36 cases. In the remaining cases, it was at the higher side of the normal range. In the patients of cirrhosis without ascites, six out of ten showed an increased aldosterone excretion but this increase was much less than the patients of cirrhosis with ascites.

Urinary sodium excretion has been found to be low in 41 patients of cirrhosis with ascites. In the remaining it was at the lower side of the normal range. In patients of cirrhosis without ascites urinary sodium excretion was not so much decreased as that of the patients with ascites.

The concentration of plasma sodium was found to be lower in 15 patients of cirrhosis with ascites as compared to control subjects. In the remaining 35 cases it was within the normal range. In patients of cirrhosis without ascites there was no significant change in plasma concentration as compared to normal individuals.

In patients of cirrhosis with ascites serum potassium was low in 36 cases and in the remaining it was within the normal range. In patients of cirrhosis without ascites it does not show any difference from normal individuals.

Endogenous creatinine clearance was found to be reduced in 31 cases of cirrhosis with ascites and in the remaining cases it was within the normal range.

The changes observed in urinary aldosterone, plasma volume, plasma sodium, serum potassium, urinary sodium and endogenous creatinine clearance after abdominal paracentesis in patients of cirrhosis with ascites during the reaccumulation of fluid into peritoneal cavity were statistically analysed. It shows: (i) urinary aldosterone which was already high in these patients was further increased at the end of 48, 72 and 96 hours after paracentesis with a maximum at 48 hours. At the end of 24 hours urinary aldosterone excretion was somewhat decreased than the preparacentesis levels. All these changes in the urinary aldosterone were statistically significant ($P<0{\cdot}001$). (ii) Plasma volume showed a decrease after paracentesis. At the end of 48 hours and 72 hours, this decrease was highly significant ($P<0{\cdot}001$). At the end of 24 hours and 96 hours it was less significant, P being $<0{\cdot}01$ and $<0{\cdot}05$ respectively. (iii) Plasma sodium was decreased upto the end of 48 hours after paracentesis. It then started rising and reached to near preparacentesis levels. However, all these changes except at the end of 48 hours ($P<0{\cdot}05$) were statistically insignificant. (iv) Serum potassium was found to be slightly increased after paracentesis with a maximum at 48 hours. The changes observed in it were also statistically insignificant. (v) Urinary sodium showed a decrease after paracentesis with a maximum at the end of 48 hours. At the end of 96 hours it had nearly reached to the preparacentesis levels. All these changes, however, were statistically insignificant. (vi) Changes observed in the endogenous creatinine clearance after paracentesis were also statistically insignificant.

The changes of urinary aldosterone level show inverse correlation with that of plasma volume after 48, 72 and 96 hours at which time the changes among both these factors were statistically significant. Though there was a general inverse correlation between the changes in plasma sodium and urinary aldosterone and direct correlation between the changes in serum potassium and urinary aldosterone, it was statistically insignificant. However, at 48 hours after paracentesis the correlation between plasma sodium and urinary aldosterone was significant. Urinary sodium changes also show a general inverse correlation with urinary aldosterone which was not significant statistically.

In an effort to study the impaired destruction and conjugation of aldosterone by the functionally damaged liver, as a cause of increased aldosterone excretion in these patients, proportion of free and conjugated fractions of excreted aldosterone has been studied and compared with that of normal subjects. It has been observed that urinary excretion of free or readily hydrolysable aldosterone constitute 35·6 to 72·8 per cent of the total urinary aldosterone in the patients of cirrhosis with ascites and 38·0 to 61·0 per cent of the total urinary aldosterone in the patients of cirrhosis without ascites, as compared to 22 to 44 per cent in normal subjects.

The previous observations that prednisone therapy depresses urinary aldosterone excretion and causes sodium and water diuresis in subjects of cirrhosis with ascites, suggesting that the deficiency of cortisone-like steroids which has been shown to occur in this disease may lead to increased aldosterone secretion by some unknown mechanism. In view of this, 17-hydroxycorticoid excretion which represent the true index of cortisone-like steroids (glucocorticoids) has been estimated to find out its correlation, if any, with aldosterone excretion. It has been found that 17-hydroxycorticosteroids excretion was subnormal in these patients. However, it has not shown any consistant correlation with urinary aldosterone in individual cases during the period of study following paracentesis. The changes observed in urinary aldosterone after abdominal paracentesis could not be correlated with the changes in 17-hydroxycorticosteroid excretion.

Changes in red blood cell electrolytes and water content, and sodium, potassium and protein content of ascitic fluid has been also studied in a limited number of patients.

The various possible mechanisms involved in the relationship between urinary aldosterone excretion and plasma volume, blood and urinary electrolytes and G. F. R. have been discussed. From the data collected in the present study, it has been suggested that intravascular volume seems to be the most immediate stimulus to aldosterone secretion. Plasma electrolytes may also be of importance as a stimulus for aldosterone secretion in this disease but to a lesser extent. Among plasma electrolytes sodium is of more importance than. potassium. It may be possible that small changes in plasma electrolytes might be bringing large reciprocal changes in urinary aldosterone.

It appears from the present work that liver damage alone is not of much importance, in causing increased urinary aldosterone excretion as campared to changes in the volume of intravascular compartment. This conclusion is supported by the following observations of this study (1) Urinary aldosterone excretion has been found to be significantly increased only in patients of decompensated liver cirrhosis in whom the fluid is passing into peritoneal cavity and thus reducing the intravascular volume, (2) in patients of compensated liver cirrhosis having no ascites, though there was liver damage, urinary aldosterone excretion is normal or only slightly elevated as compared to control subjects, and (3) the patients of decompensated cirrhosis accumulating ascites, show the marked increases in their aldosterone excretion after abdominal paracentesis, though the liver damage is not much enhanced by this process.

In the light of the findings observed in the present study, an attempt was made to explain the mechanism of ascites formation in this disease. These studies of rapid production of ascites following abdominal paracentesis may serve as a model outlining the retention mechanism in spontaneous production of ascites, when patients with liver cirrhosis enter the stage of decompensation.

MORPHOLOGICAL STUDIES IN THE FAMILY FLACOURTIACEAE*†

G. Gopal Krishna
School of Plant Morphology, Meerut College, Meerut.

The present investigation is based on the results of 38 species of which 36 belong to the family Flacourtiaceae and one each to the Bixaceae and Cochlospermaceae.

The nodal anatomy of *Flacourtia ramontchi* var. *occidentalis*, *F. indica* and *Casearia tomentosa* has been worked out. It is observed that the node in the two species of *Flacourtia* is unilacunar with one broad arc like leaf trace leaving a single gap in the stele. *Casearia* has trilacunar node with 3 distinct traces entering the leaf. The trilacunar node is believed to be primitive. A correlation between trilacunar nodes and the presence of stipules has been observed from the nodal anatomy of *Casearia* and *Flacourtia*.

The sepals in the majority of the genera in the Flacourtiaceae are observed to be three trace organs. The traces are either derived from a single source or from different sources. In some cases (female flowers of *Flacourtia*, *Laetia*, etc.) it is interesting to note that the number of traces to each sepal varies from 1 to 4. However, the traces are reduced to two (*Xylosma*) or even one in the male flowers of *Flacourtia*, the members belonging to section Euhydnocarpus and *Bixa orellana*. In *Cochlospermum gossypium* while the outer sepals receive one trace each, the inner sepals are supplied by three traces each. The reduction in the number of traces is believed to be due to fusion of lateral traces. In *Flacourtia sepiaria*, one of the sepals receives two traces instead of usual one. Saunders (1934) suggested a similar condition in *Veronica* to be a case of "Congenital concrescence" where two organs are incorporated into one.

Some tribes of the family Flacourtiaceae (Flacourtieae, Casearieae) are apetalous. In others the petals are found to be usually one traced. Three traced condition is seen in a few cases (*Scolopia buxiflora*, *Bixa*, *Cochlospermum*, etc.). In *Hemiscolopia* while the petals in the male flowers receive one trace each, they are three traced in the female flowers.

The tribe Pangieae of this family is distinguished by the presence of fleshy and densely hairy, scaly structures lying inside at the base of the petals. Rendle (1938) described the scales as outgrowths of the floral axis and Sleumer (1955) as staminodal like structures, inserted on the inner side of the base of petals. The present study of six species of *Hydnocarpus* and

---

* Abstract of the thesis approved for the degree of Doctor of Philosophy of the Agra University.

† Research contribution No. 75 from the School of Plant Morphology, Meerut College, Meerut.

Pangium edule, however, reveals that the scales, which posess inversely oriented vascular bundles are mere enations from the inner faces of "double bladed" petals.

The stamens show a great diversity in their number as well as in their mode of vascular supply. They are either few (*Erythrospermum*, *Hydnocarpus*, *Casearia*, and *Gossypiospermum*) or numerous in other members studied. Wherever they are numerous, they arise either independently (*Pangium* and *Flacourtia inermis*), or in small groups (Male flowers of *Flacourtia* and *Xylosma* and *Laetia* and *Bixa*) or conjointly with those of outer floral organs. Formation of sepal-stamen; petal-stamen; sepal-petal-stamen-fascicle traces is observed in *Lindackeria, and Scolopia, Pleuranthodendron, Prockia, Hasseltia, Hemiscolopia* and *Cochlospermum.* The presence of the stamen fascicle traces seems to favour the fusion hypothesis put forward by Wilson (1937).

The bifurcation of stamen bundle in the connective is seen in a number of cases (*Erythrospermum, Pangium, Hydnocarpus anthelmintica,* etc.). Wilson (1942) regarded such a case as evidence to support the telomic interpretation of the stamen. But the present study does not support such a conclusion.

Nectariferous glands occupying various positions have been observed in the members of the family except in the tribes Oncobeae, Pangieae and Casearieae and in *Bixa* and *Cochlospermum.* They are met within the male, female as well as in bisexual flowers. In the male flowers of *Flacourtia, Xylosma* and *Hemiscolopia* they are in the form of a lobed extrastaminal disc. These glands are found inner to each sepal and alternating with the petals in the species of *Homalium.* In the female flowers of *Flacourtia* and *Xylosma* the glandular disc spreads around the base of the ovary and is lobed above. On the basis of the vascular supply they are interpreted as staminodal.

The placentation is parietal in all members (except in *Hasseltia,* and *Prockia*). The placentae are borne on the margins of two adjacent carpels and the vascular supply is received from either ventral bundles or fused products of placental strands. In *Hasseltia* and *Prockia,* the dorsals and ventrals lie on the same radii. The ovules are borne on the fused margins of the same carpel and receive their vascular supply from the ventrals (or ventral strands of the same carpel). Hence in these species the placentation is axile. However, in the upper regions unilocular condition is present and at this level the placentation appears to be parietal. Thus multilocular condition with axile placentation at the base and unilocular with parietal placentation in the upper regions of the same gynoecium in *Hasseltia* and *Prockia,* fits in very well with the classification of gynoecium put forward by Troll (1928, see Wilson and Just, 1939).

The protrusions in the ovary in *Flacourtia* and *Cochlospermum* are regarded to be formed by the fusion of carpellary margins themselves. These protrusions do not bear any ovules on the sides of their truncate apex and they are borne more or less far removed from the apex. The sterile surface on either side of the placental apex is interpreted as representing the thickness of the carpellary margin or rather its lateral face (Puri, 1961). The placental strands in *Flacourtia*, *Casearia papauna* and *Bixa* are inversely oriented. The bundles are concentric at the base (or become concentric in *Bixa*) from which a number of branches are given off towards the periphery. As a result of this branching the xylem in the ventral strands faces more towards the periphery and ultimately the ventral strands become inversely oriented. In *Laetia* an interesting case is seen where each ventral strand consists of a number of bundles which are arranged in a ring appearing like a cylindrical stele. The inner bundles, which are inverted with respect to the centre of the flower, are the first to supply the ovules. Then the laterals and even the outer bundles contribute to ovular supply. For the present the connection between the condition in *Laetia* and that in other genera is not clear. It is believed that the inversion of placental strands in parietal placentae may be brought about in a number of ways although its morphological significance may still be the same.

In the majority of the genera ovary is superior but in *Homalium* it is either half inferior or completely inferior (*H. nepalense*). No conclusive interpretation is given as it is difficult to prove the strands in the 'floral cup' whether they are 'traces' or 'bundles'.

A correlation between the number of vascular bundles in the style and the lobes of stigma has been observed. In those members where each stigma lobe is undivided (*Homalium*, *Prockia*, *Hasseltia*, etc.) the number of bundles is equal to the number of carpels. In these cases each bundle represents the fusion product of dorsal and ventrals and the stigma is carinal. In others (*Flacourtia*, *Hydnocarpus*, etc.) each stigma lobe is bifid and the dorsal bundle divides radially into two branches which before entering the stigma, fuses with the corresponding ventrals. Thus here the stigma is not typically carinal.

The course and movement of the vascular bundles in the style in *Scolopia* are of some interest. Each dorsal bifurcates into two branches which diverge towards the ventral of their respective side and fuse with it. This fusion product moves towards the centre and then takes an outward course reaching the inner side of the dorsal suture. In the species of *Scolopia* an intermediate condition between carinal and commissural stigma is observed. But, in *Bixa* the stigmas are commissural as they lie on the ventral sutures.

Further evidence for the separation and independent status of the three allied families Bixaceae, Cochlospermaceae and Flacourtiaceae, is afforded by their anatomical studies. From the material of *Hemiscolopia trimera*, sent by two persons from the same place, it is felt that it is not monotypic but it may have two species. From the anatomical differences noted, further study on different aspects of the problem is necessary to find out whether *Flacourtia ramontchi* and *F. sepiaria* should be included in *F. indica* or should be treated separately.

STUDIES ON ADSORPTION INDICATORS*

K. N. TANDON

Lecturer in Chemistry, University of Rajasthan, Jaipur.

The applicability of a number of new adsorption indicators in the argenometric titrations of halides and thiocyanate has been described. These new indicators are methyl orange, resorcinol-3:6-endomethylene-Δ^4-tetrahydrophthalein, resorcinolthiophene-2:3-dicarboxylein, sulphonefluorescein, dicholorosulphonefluorescein, dibromosulphonefluorescein, diiodosulphonefluorescein, pyrocatechol-sulphonephthalein (catechol violet), pyrogallol-sulphonephthalein (pyrogallol red), ammonium purpurate (murexide), phthaleincomplexone, xylenol orange, calcein, benzene-azo-l-naphthylamine and ethyl red. These dyes include besides acid alkali indicators some important metal indicators used in complexometric titrations, the dyes of sulphonefluorescein series—a series analogous to fluorescein series discovered by schools of Fajans and Kolthoff as adsorption indicators, and the basic dyes such as benzene-azo-l-naphthylamine and ethyl red. These also include the dyes recently isolated *viz.*, resorcinol-3:6-endomethylene-Δ^4-tetrahydrophthalein and resorcinol-thiophene-2:3-dicarboxylein, the applicability of which was tested mainly to throw some light on the mechanism of colour change in this class of indicators.

Further, new applications of well known adsorption indicators have been described. These indicators have been applied to the systems in which they were found unsuitable by the previous workers by altering the conditions of those systems. Thus eosin has been described for the titration of chloride with silver ions in the pH range (1-3), the erythrosin has been applied in the argentometric titrations of halides and thiocyanate in presence of IN-2N nitric acid, the p-ethoxychrysoidine has been applied for the titration of silver with halide and thiocyanate ions in slightly acidic medium (pH 4-5), and the phenosafranine has been applied in the argentometric titrations of iodide and thiocyanate in slightly alkaline medium in presence of dilute sodium hydroxide. Besides these, the new applications include the use of congo red in fractional separations, *viz.*, titration of iodide in presence of chloride with silver ions, and the titration of silver with bromide or iodide ions in presence of lead after sequestering the latter with EDTA. Congo red has also been described as metal indicator in the determination of mercury (II) with EDTA and potassium thiocyanate. The use of diiodosulphonefluorescein and erythrosin has been extended to the titrations of chloride and bromide with mercurous ions. Most of the new uses have been described in the process of testing certain conclusions arrived at in the preliminary investigations to understand the mechanism of this class of indicators. For example, a study of the changes in pH produced when iodide and chloride ions respectively are titrated against silver ions led to the conclusion that in the pH range 5·0-5·5, congo red should mark the equivalence point for iodide ions alone (in presence of chloride ions); on putting to test, this expectation was proved fully correct.

---

* Abstract of the thesis submitted for the degree of Doctor of Philosophy of the University of Agra.

The theories of the mechanism of adsorption indicators have been reviewed and it has been observed that Mehrotra's theory of chemical adsorption is in better agreement with the observed facts whereas the older theories of Fajans and Kolthoff are unable to explain all the observed behaviour of adsorption indicators. Mehrotra's theory has been supported by various lines of experimental evidence which have been obtained in the present studies. The studies include (i) the actual isolation of silver compounds of adsorption indicators and an investigation of their properties, (ii) the pH measurements during the argentometric titrations in dilute solutions using a little excess of the adsorption indicators, (iii) the light absorption studies of eosin, congo red and bromophenol blue adsorbed on silver iodide sol and (iv) the adsorption and coprecipitation studies.

The silver compounds of congo red, p-ethoxychrysoidine, benzene-azo-1-naphthylamine, methyl orange, fluorescein, dichlorofluorescein, dibromofluorescein, eosin, bromophenol blue and ethyl red have been isolated and it has been observed that the properties of these compounds explain well the indicator action of these dyes. For instance, the compounds have been found to show the same colour which are developed and observed on the precipitate of silver halides in presence of excess silver ions when the dyes are adsorbed on the precipitate; the compounds are generally stable only in the same pH range in which the titrations are possible—in more acidic solutions the undissociated and the less soluble dye molecules are formed and in more alkaline solutions silver oxide (or silver-ammonia complex in presence of ammonia) is formed. The silver dye compounds are in general less stable than the silver halide or thiocyanate and are, therefore, not formed so long as the corresponding halide or thiocyanate ions are in excess, but as soon as the silver ions are added in excess the silver dye compound is formed on the surface of silver halide or thiocyanate precipitate.

The studies on pH measurements during argentometric titrations of dilute solutions using adsorption indicators have been carried out with methyl orange, resorcinol-3:6-endomethylene-Δ^4—tetrahydrophthalein, resorcinol-thiophene-2:3-dicarboxylein, sulphonefluorescein, murexide, catechol violet, pyrogallol red, congo red, p-ethoxychrysoidine benzene-azo-I-naphthylamine, ethyl red, phenosafranine, rhodamine 6G, phthalein-complexone, xylenol orange and calcein. No pH changes during the titrations or at the end point have been observed with purely anionic dyes. These dyes form anions under the conditions in which the titrations are carried out and the colour change at the equivalence point is caused by the adsorption of the dye anions in the form of the silver dye compound. The pH changes during titrations have been observed with congo red, the basic dyes such as p-ethoxychrysoidine, benzene-azo-I-naphthylamine, ethyl red, phenosafranine and rhodamine 6G as well as the metal indicators—phthaleincomplexone, xylenol orange and calcein under the conditions in which these dyes are applicable as adsorption indicators. These pH changes have been satisfactorily explained and lend strong support to the theory of surface compound formation of the mechanism of adsorption indicators.

The light absorption studies of dyes adsorbed on silver iodide sol have been carried out with eosin, congo red and bromophenol blue. These dyes and the silver iodide sol have been found particularly suitable for these studies. A comparison of the absorption curves of the dye solution, the dye adsorbed on silver iodide sol in presence of a slight excess of iodide ions, the dye adsorbed on silver iodide sol in presence of a slight excess of silver ions and the dye in presence of a concentrated silver nitrate solution has been made. The concentration of the dye and the silver iodide sol in each case was the same. It has been observed that the absorption maximum of the dye adsorbed on silver iodide sol in presence of excess silver ions is nearly the same as the absorption maximum of the dye in presence of a concentrated solution of silver nitrate. It supports the view that the colour change at the equivalence point during the argentometric titrations using adsorption indicators is due to the formation of the silver dye compound.

The adsorption and coprecipitation studies have been carried out with fluorescein, dichlorofluorescein, sulphonefluorescein and dibromofluorescein. It has been shown in these studies that the formation of silver dye compound on the surface of the silver halide precipitate in presence of excess silver ions is mainly a coprecipitation phenomenon. The silver dye compound has been coprecipitated along with silver halide or thiocyanate by slowly adding halide or thiocyanate solution to an excess of silver nitrate containing the dye solution so that maximum coprecipitation may occur. The supernatant solution has been analysed for excess silver ions and excess dye. The amounts of silver ions and the dye adsorbed on the precipitate have been calculated and it has been observed that they are adsorbed in equivalent proportions. The coprecipitation of silver dye compounds with silver halide or thiocyanate precipitate supports the theory of chemical adsorption or surface compound formation of the mechanism of adsorption indicators. Coprecipitation of more soluble compounds along with less soluble compounds is a widespread phenomenon. Even highly soluble substances are often coprecipitated. Thus it becomes quite understandable that silver fluoresceinate is not precipitated when a few drops of sodium fluoresceinate are added to a dilute silver nitrate solution, but the same gets coprecipitated along with silver halide in presence of just a slight excess of silver ions. This is confirmed by the stoichiometric ratio (1:1) of the silver ions and the dye in the coprecipitated silver-dye compounds.

The factors which determine the extent of adsorption or coprecipitation have been ascertained. The main factors which govern the extent of adsorption or coprecipitation are (i) the surface area of the precipitate, (ii) the primarily adsorbed ions on the precipitate, (iii) the insolubility of the adsorbed or coprecipitated compound. The amount of the primarily adsorbed ions on the precipitate is, evidently, directly proportional to its surface area. Thus the greater would be the surface of the precipitate exposed to the solution, the more would be the concentration of the primarily adsorbed ions on the precipite and the corresponding adsorption orcoprecipitation of the ions or molecules which would form the next most insoluble compound with the primarily adsorbed ions would take place. It clearly explains as to why the adsorption indicators are better applicable to systems which are more colloidal.

The various observed facts which are inexplicable on the theories of Fajans and Kolthoff have thus been explained in the light of the new theory. The conditions under which a dye would be suitable as an adsorption indicator in a particular titration have been laid down. These are summarised below:—

(i) The dye must form a sparingly soluble metal-dye complex which should be differently coloured than the dye ions.

(ii) The metal dye complex should be more soluble than the main precipitate produced by the reaction of the metal ion and precipitating anion.

(iii) The main precipitate should separate in a finely divided state.

(iv) The concentration of the dye used as indicator in the titration should be such that it should be almost completely coprecipitated so that a sharp colour change may be observed at the equivalence point.

IMMUNE AND ANTIBODY RESPONSE IN RABBITS AND DAIRY CATTLE AGAINST STAPHYLOCOCCAL VACCINES*

B. S. Malik†
Department of Microbiology,
University of New Hampshire, Durban, N. H. (U.S.A.).

Maximum yield of alpha and beta toxins and coagulase was obtained when cultures of *Staphylococcus aureus* were shaken on a rotary shaker with an atmosphere of 50 per cent O_2 and 50 per cent CO_2 at 37°C. The optimal incubation period for alpha and beta toxin production was 48 hours and 72 hours respectively. With the exception of trypticase soy broth, other media tested, namely extract broth, veal infusion broth, heart infusion broth and N. Z. amine broth gave good yield of both alpha and beta toxins. In general optimum incubation period for coagulase was 16 to 24 hours under static conditions, 12 to 16 hours on the shaker and 8 to 12 hours on the shaker under 50 per cent O_2 and 50 per cent CO_2. Prolonged incubation under the latter conditions appeared to denature the coagulase previously produced in the culture medium. Extract broth and N. Z. amine broth gave maximum coagulase yield. Temperature ranges of 34 and 40 C had no effect on the yield of coagulase.

S. aureus cells disrupted by various physical and biological means were compared with formalin and beta-propiolactone (BPL) treated cells for antigenic analysis. In rabbits disrupted cell vaccines gave higher antibody response than whole cell vaccines. On the other hand when rabbits were challenged with strains of *S. aureus*, best protection was produced with formalinized whole cell vaccines. BPL treated cell toxoids produced higher antibody response in rabbits than similar preparations inactivated with formalin, but in cows a higher antibody response was obtained with formalin treated cell toxoids.

Five polyvalent cell toxoid vaccines different from each other either in the method of inactivation or in the potencies of different toxins were tested in rabbits for immune and antibody response. Rabbits vaccinated with Vaccine PV-12, a preparation containing formalin treated cells, BPL inactivated toxin and a high coagulase titre developed higher antileucocidin levels and were more resistant to challenge with *S. aureus* than rabbits injected with the other vaccines tested.

Three polyvalent vaccines were used to immunize 15 cows equally divided into three groups. Vaccine PV-C (formalinized N.Z. amine whole broth culture) stimulated the highest levels of antibodies, although the difference from the cows of other groups was statistically significant only for antileucocidin. The antisera from the cows vaccinated with vaccine PV-C also showed higher mouse protection power. Cows in this group also were more resistant to challenge with *S. aureus* via the teat canal. It is concluded that high antileucocidin titre and mouse protection power of antisera is perhaps the best *in vitro* criteria of resistance against staphylococcal infections.

---

* This is an abstract of the dissertation submitted to the University of New Hampshire in partial fulfilment of the requirements for the degree of Ph. D. in Microbiology.

† Present address—Department of Bacteriology, U. P. College of Veterinary Science & Animal Husbandry, Mathura, INDIA.

STUDIES ON INDIAN ARAEOPIDAE[=DELPHACIDAE] (HOMOPTERA, FULGOROIDEA.)

A. N. T. JOSEPH
Lecturer in Zoology, Lohia Colloge, Churu, Rajasthan.

Araeopidae is one of the most neglected families of Homoptera. From time to time the students of Fulgoroidea, Distant (1906), Lefroy (1909), Muir (1915) and Metcalf (1943), have pointed out the necessity of a detailed study of these insects. Very little is known regarding the morphology of araeopids save for the recent publications of Mathur and Joseph (1961) and Joseph (1961). The need for the study of systematics of Indian Araeopidae is easily conceivable from the fact that many of our common species belonging to this family are unrecorded. Hence the author has taken up the studies of the morphology and systematics of these insects. Some of the salient features of these studies are illustrated below.

Araeopids are small, delicate insects never measuring more than a centimetre in length from the vertex to the tip of the tegmina, although some forms measure even less than two millimetres. They can be easily identified from other members of the superfamily Fulgoroidea by a large mobile spur borne on the inner side of the apex of the hind tibiae. The most striking feature of the family as a whole is its great homogeneity in general aspect and appearence. They are polymorphic, their tegmina are found to occur in three different forms, *viz.*, brachypterous—very short with reduced venation covering only the basal segments of the abdomen; koelopterous—moderate length covering most part of the abdomen with fairly developed venation; macropterous—longer than the abdomen with well developed venation. Of the many collections made during the course of this study the author has got only one species of dimorphic araeopid, *Delphacodes propinqua*, which occurs in koelopterous as well as macropterous forms.

The head is generally simple, relatively small, but in a few genera it is extremely developed, *e.g.*, *Embalophora* and *Pseudoembalophora*, and is opisthognathous. It is decorated with keels, the keels varying in number, extent and prominence. The compound eyes are reniform occupying considerable area of head and surround the posterior part of antennae. The antennae are usually simple with a short basal segment, a short sometimes elongate second segment and a terminal flagellum. Occasionally either the first or second or both the segments are greatly elongated and considerably flattened (*e. g.*, *Perkinsiella*) or the basal segment is triangular in cross section with its length

---

* Abstract of the thesis submitted for the degree of Doctor of Philosophy of Agra University.

1. Present address—Asstt. Zoologist, Zological Survey of India, 34, Chittaranjan Avenue, Calcutta-12.

considerably exceeding the next segment (*e. g.*, *Parohita*). There are two ocelli, each on either side between the compound eye and the lateral carina.

Three species of araeopids belonging to two tribes—*Liburnia pallescens*, *Delphacodes propinqua* (tribe Delphacini) and *Purohita cervina* (tribe Tropidocephalini)—were selected for detailed morphological studies. The head capsule is devoid of clypeolabral and epicranial sutures. The epistomal suture is well developed bearing a highly developed epistomal ridge. The occipital suture is intercepted at the dorsolateral sides by the compound eyes. The mandibular plates are homologised to the pleurostoma of generalised insect cranium. The anterior pair of arms of tentorium exhibits varying degrees of reduction, whereas the posterior as well as the dorsal pairs are well developed. The anterior arms are atrophied in the tribe Delphacini; in the tribe Tropidocephalini they are complete but are much reduced. It is interesting to observe the fate of the anterior arms in these two tribes under study as they are either atrophied or reduced but at the same time the dorsal arms are well developed. The normal function of the anterior arms is the strengthening of the facial region in insects which is secondarily taken up by the highly developed epistomal ridge in araeopids and consequently this reduction. The musculature of the head capsule follows the general pattern of Fulgoroidea.

The mouth parts are of typical hemipterous type. There is no distinction between the lever and the inner arm of the mandibular stylet. The maxillary stylet is devoid of a maxillary lever. The labium is four segmented and extends beyond the forecoxae. The apex of the fourth segment has undergone special modifications to form a temporary ring around the stylets when the intrinsic muscles of the labium contract. The chaetotaxy and apical clamp are similar in Delphacini and Tropidocephalini. The lora of hypopharynx show variation in size from species to species. The membrane connecting the labium with the maxillary plates, designed here as the labio-maxillary membrane, is homologised with the hypostomal bridge of Heteroptera.

Araeopids exhibit great morphological modifications in the thorax and particularly marked in the metathorax. The pro- and mesothorax very much resemble those of other fulgoroids except for a number of sutures in the latter. The development of the sutures in the thorax of these insects is interesting as it follows a similar course in the araeopids suggesting similar lines of evolution. In araeopids a jumping mechanism is developed in connection with the hind legs, although curiously enough, the metathorax lacks furca. In order to compensate this loss, the metathorax has developed a complicated system of ridges to form an internal skeletal frame work at the lateral sides to withstand the extra stresses and strains shouldered by it. The hind legs are remarkable for their large size in comparison to the pro- and mesothoracic legs and also for the development of the spur on the hind tibiae. From the ventral side of the trochanter arises an apodeme projecting into the metathorax through the coxa for the insertion of muscles coming from the thorax. This is a new development come across in connection with the jumping mechanism. The wing venation is comparatively well developed. Unlike that of certain Fulgoroidea, such as the members of the families Flatidae and Ricaniidae etc., there is no precostal region in araeopids. In the tegmen all along the course of veins are provided with macrotrichiae except second cubitus.

The abdomen is composed of eleven segments, the eighth and ninth in female and the ninth alone in the male represent the genital segments. The tenth and eleventh are fused together. In male the tenth segment bears a pair of anteriorly directed processes, the anal processes, which are absent in *Peregrinus maidis*. The females are devoid of them.

The alimentary canal is an almost straight tube with the crop arising from the stomodaeum as a sideways diverticulum. It is similar in histology to that of other Homoptera. The mesenteron is simple and without filter chamber. The malpighian tubules are four in number, the two of each side join together before opening into the alimentary tract. There is a pair of well developed salivary glands, whose principal glands are lobulated.

The respiratory system consists of two pairs of thoracic and eight pairs of abdominal spiracles. The thoracic spiracles and the first two pairs of abdominal spiracles have an external closing apparatus; the remaining have an internal closing type. There is no transverse commissure in the abdomen except for the eighth in female.

The female reproductive organs show some interesting modifications in the position of common oviduct and vagina. The vagina is deflected to the left side and due to this deflection the region immediately anterior to it, namely the common oviduct, comes to occupy the left side. The number of ovarioles constituting the ovary vary not only from species to species but also within the species. The egg tube is acrotropic type. The spermatheca and the accessory gland open almost at the same level to the vagina. The ovipositor is well developed and of typical homopterous type. The first pair of valvulae themselves and these and the second pair of valvulae are articulated by ridge-and-groove method.

The internal male reproductive organs are of generalised insect type. Each testis is composed of two sperm tubes in the two species under ovservation namely *Delphacodes propinqua* and *Liburnia pallescens*. The sperm tube has a number of apical cells. The vas deferens is devoid of a distinct seminal vesicle. The ejaculatory duct has one median and two lateral parts. The 'sheath', 'chamber' and part of the basal plate bridge are variously modified regions of the ejaculatory duct. The pygofer or ninth segment in araeopids is ring-shaped and is without any distinction into tergum, laterotergites or pleurosternite. The length and breadth of the opening of pygofer, the outgrowth of its ventral margin, the anal angles and the development of the diaphragm etc., vary with the species. The parameres vary in shape and size in different species. The aedeagus periandrum may be entire or may be decorated with spines.

During the course of the study of systematics, it has been observed that the external male genitalia is the most reliable specific character. They help not only for specific identification but also afford generic criteria. The characters of female genitalia can be utilised with advantage as has been done by Hassan (1948) and is followed here. In the present study, the author has followed the general trend of notable araeopidan systematists for the sake of convenience. However, he feels that since the male and female genitalia form the chief basis of reliable specific characters they would gain preference over other characters, *viz.*, vertex, carination, spur and colouration etc. It would, therefore, be advisable to arrive at specific identification on the basis of genitalia and confirm the same by other subsidiary characters.

Collections of araeopids were made from various parts of India—Uttar Pradesh, Rajasthan, Delhi, Orissa, Maharashtra, Madras and Kerala. Of the twentyone species collected, twelve—*Tropidocephala signata* (Distant), *Purohita cervina* Distant, *Perkinsiella insignis* (Distant), *Perkinsiella sinensis* Kirkaldy, *Delphacodes propinqua* Fieber, *Phyllodinus pulchellus* (Distant), *Liburnia pallescens* (Distant) *Liburnia furcifera* (Horvath), *Liburnia purana* (Distant), *Peregrinus maidis* (Ashmead), *Sardia rostrata* Melichar and *Nilaparvata lugens* (Stal)—are already reported, eight species—*Sogata rhodesi* Muir, *Chloriona paludum* (Kirkaldy), *Coronacella krikaldyi* (Muir), *Delphacodes albovitta* (Matsmura), *Delphacodes crawfordi* Muir and Giffard, *Phyllodinus sauteri* Muir, *Dicranotropis muiri* Kirkaldy and *Dicranotropis cognata* Muir—are reported here for the first time from India and the remaining one—*Stenocranus ajmerensis*—is a new species. A key to the identification is given wherever more than one species is described in a single genus.

ACKNOWLEDGEMENTS

The author wishes to express his gratitude to Dr. R. D. Saksena, Prof. of Zoology, Balwant Rajput College, Agra, under whose able guidance the work has been carried out. He is also thankful to Dr. P. N. Mathur, Prof. of Zoology, Government Colloege, Ajmer, for the help he has rendered during the course of this work.

LITERATURE CITED

1. Distant, W. L. 1906. Fauna of British India, 3, Rhynchota. Thacker Spink & Co., Calcutta & London.
2. Hassan, A. I. 1948. The significance of genitalia in generic classification of Araeopidae. *Bull. De La Societe Fouad Ler D' Entomologie*, **32**: 85-93.
3. Joseph, A. N. T. 1961. Studies on the external morphology of *Peregrinus maidis* (Ashmead), (Homoptera, Fulgoroidea, Araeopidae=Delphacidae), Part III, Abdomen. *J. Anim. Morph. Physiol.*, **8** (2): 93-99.

4. Lefroy, H. M. 1909. Indian Insect Life, 728-729. Thacker Spink & Co., Calcutta.
5. Mathur, P. N. & Joseph, A. N. T. 1961. Studies on the external morphology of *Peregrinus maidis* (Ashmead), (Homoptera, Fulgoroidea, Araeopidae=Delphaciae), Part I, Head capsule and mouth parts. *J. Anim. Morph. Physiol.*, **8** (1): 1-10.
6. Mathur, P. N. & Joseph, A. N. T. 1961. Studies on the external morphology of *Peregrinus maidis* (Ashmead) (Homoptera, Fulgoroidea, Araeopidae=Delphacidae), Part II, Thorax. *Ibid.*, **8** (2): 81-92.
7. Metcalf, Z. P. 1943. General Catalogue of Hemiptera, Fasc. IV, Part-3, Delphacidae. Smith College, Northampton, Mass, U. S. A., 522 pp.
8. Muir, F. 1915. A contribution towards the taxonomy of Delphacidae. *Canadian Ent.*, **47**: 208-212, 261-270, 296-302, and 317-320.

MORPHOLOGICAL AND ANATOMICAL STUDIES OF THE FLOWER OF HELOBIAE*†

VIRENDRA SINGH
School of Plant Morphology, Meerut College, Meerut.

The present work embodies the results of investigation of 42 species belonging to the seven families—Potamogetonaceae, Najadaceae, Aponogetonaceae, Scheuchzeriaceae, Alismaceae, Butomaceae and Hydrocharitaceae of the order Helobiae.

The vegetative anatomy of about 20 species has been attempted. Vascular cylinder of the stem shows a reduction series. The axial position of the cylinder is considered to have been attained phylogenetically by a gradual shifting of the peripheral bundles towards the centre of the axis where they unite to form a single concentric 'bundle'.

The basal sheath of the leaf is either completely fused, adnate at the base or completely free from the leaf base. It is evident from the vascular supply that the membranous sheath of monocotyledonous leaves is equivalent to the stipules of dicotyledons.

A variable number of small scale like structures—the squamulae intravaginales are associated with the leaf bases. The squamulae do not belong to the leaf in whose axil they appear to arise but they originate from the surface of the internode separating this leaf from next leaf above. The tubers of *Potamogeton pectinatus* and *Sagittaria sagittifolia* have been studied. They develop at the tips of the stolons and are formed by the enlargement of the cells of the ground tissue of the stolons.

The vascular anatomy of the flower of three genera of Potamogetonaceae has been studied. While there are numerous bisexual flowers in a spike of *Potamogeton*, the number is reduced to two in *Ruppia*. The unisexual flowers of *Zannichellia* are described as axillary but vascular anatomy shows that they terminate the main axis. The "flower" of *Potamogeton* and *Ruppia* which has been considered by some authors as 'reduced inflorescence' is regarded here as a normal flower. Consistent with our understanding of the flower we have considered the 'perianth' as true perianth and not as bracts or expansions from the connective of the stamens. The triangular outgrowth present in between the two anther lobes of a stamen of *Ruppia* shows homology with the perianth part of *Potamogeton*.

---

* Abstract of the thesis approved for the degree of Doctor of Philosophy of the Agra University.

† Research contribution No. 74 from the School of Plant Morphology, Meerut College, Meerut.

The vascular supply of a carpel of *Potamogeton* and *Ruppia* consists of two bundles—one dorsal and one placental strand. While the dorsal bundle extends up to the base of the stigma in *Potamogeton*, it only traverses for about half the length of the carpel in *Ruppia*. The only bundle in the carpel of *Zannichellia* is used up in supplying the solitary ovule.

Three species of *Najas* have been studied. The male and female flowers are represented by a single stamen and pistil respectively, and are enclosed in a bottle-shaped spathe. In *N. graminea* the staminate flower is nacked. The vascular supply of the gynoecium of *Najas* consists of a single bundle which gives off a very small dorsal trace in *N. fleixilis* before entering the base of the solitary ovule, which is described as basal. It appears that the so-called basal ovule in *Najas* too, as in many other cases, is a derived one. The presence of two stigmas gives some indication towards the pseudomonomerous and bicarpellary nature of the gynoecium.

Three species of *Aponogeton* of the monogeneric family Aponogetonaceae have been studied. Vascular supply of each carpel consists of a dorsal and two ventral bundles. However, in *A. distachyon* in addition to these, secondary marginals are also present.

The three carpels of *Aponogeton* are basally and adaxially connate and thus the gynoecium shows axile placentation in the basal region. But when the carpels become free they show marginal placentation. The carpels are open in young condition and thus they show some resemblance with the primitive ranalian carpels. The present study also substantiates the placing of Aponogetonaceae close to Scheuchzeriaceae.

The only member of the family Scheuchzeriaceae studied is *Lilaea subulata*. The flowers are polygamous. Each perfect flower consists of a perianth segment, a sessile stamen and a closely appresed carpel. The perfect flower of *Lilaea* has been considered by some authors as a secondary inflorescence consisting of one staminate and one pistilate flower. However, the present investigation shows that it is a normal bisexual flower.

The presence of three dorsal bundles in the carpel of *Lilaea* suggests its tricarpellary nature and so called monocarpellary condition has been brought about by the suppression of two of the three carpels. It appears logical that the ventral strand is the fusion product of the ventrals of the only surviving carpel. The apparently basal position of the ovule in *Lilaea* is considered as derived one. The present investigation also gives some support for removing *Lilaea* to a separate family.

The vascular supply of the perianth segments shows variations in the genera *Alisma, Luronium, Baldellia, Limnophyton* and *Sagittaria* of the Alismaceae, investigated. *Alisma* stands apart from other genera in that the marginal bundles of the inner perianth segments arise conjointly with those of the outer.

The numerous free carpels are arranged spirally (*Sagittaria*) or in a single whorl (*Alisma* and *Luronium*). However, in genera like *Alisma* and *Luronium* the carpels are connate at the base. Each carpel receives its vascular supply from a single bundle, which branches below the locule into a dorsal bundle and a ventral strand. It is interesting to note in *Alisma* that the dorsal bundle bifurcates at a little higher up of its origin.

Probably the achenes in the family the Alismaceae have been derived from follicles like those in the Aponogetonaceae and Scheuchzeriaceae. Thus, the basal position of the ovule in this family also appears to be a derived one.

Only one species of the Butomaceae, *i.e.*, *Butomus umbellatus* has been studied. The perianth and the stamens remain fused with the gynoecium for some distance and separate only at the level of the appearance of locules of the carpels. Thus the flowers of *Butomus* show a tendency towards epigyny. The six carpels remain coherent at the base for some distance but become free higher up. Vascular supply of a carpel consists of a dorsal bundle and numerous branches of ventral bundles, the latter which are distributed on walls of the carpel.

The placentation in *Butomus* has been described as 'superficial' since the ovules are distributed almost throughout the inner carpel wall except the dorsal suture. It is considered that in cases like *Butomus* where carpels are free, the superficial placentation might have originated from marginal placentation by the unequal extension of the ventral surface of the carpellary margins. The present study also brings out certain resemblances in between Butomaceae and Hydrocharitaceae, while on the other hand vasculature of the flower of Butomaceae hardly shows any resemblance to that of Alismaceae.

Ten genera (*Ottelia*, *Bootia*, *Hydrocharis*, *Enhalus*, *Nechamandra*, *Blyxa*, *Vallisneria*, *Hydrilla*, *Elodea* and *Halophila*) of the family Hydrocharitaceae have been studied. The flowers are generally unisexual with a few exceptions like *Ottelia* and *Blyxa* where they are bisexual. Several staminate or a solitary pistillate flower is surrounded by a spathe.

The perianth is generally in two whorls of three each, but reduction in their size, number and vascular supply have been observed in different genera investigated. In certain genera like *Nechamandra*, *Vallisneria* and *Hydrilla*, though the perianth segments are present, they do not show any vascular supply. It is, therefore, interesting to note that during the course of reduction, the organ is not completely reduced but its vascular supply is lost.

Reduction in the number of carpels has been observed in different members of the family studied. While there are six carpels in *Ottelia*, *Hydrocharis* and *Enhalus*, there are three in *Blyxa*, *Vallisneria* and *Hydrilla*. In *Nechamandra* and *Halophila* apparently there are only two carpels. The vascular supply of a carpel normally consists of a dorsal bundle and a ventral (placental) strand, which lie on different radii. In some genera (*Hydrocharis* and *Enhalus*) secondary marginals are also present. On the other hand some reduction in normal vascular supply is also seen, while the dorsals continue only for a very short distance in *Vallisneria*, they are totally absent in *Hydrilla*.

The placentation is normal parietal in majority of genera but in some cases such as *Hydrocharis*, *Ottelia* and *Enhalus* the condition becomes rather interesting since the ovary is incompletely divided into six segments and most of the internal surface of ovary wall, except along the dorsal suture, is covered with ovules.

It appears that the bicarpellary condition in *Halophila* and *Nechamandra* has been brought about by the suppression of one of the carpels in the ovary region. Similarly tricarpellary condition in the family also appears to have been derived from hexacarpellary condition which still prevails in several genera of the family. The present observations reveal that the nectary in *Hydrocharis* is of "stylar type" and represents the expanded bases of styles.

The hydrocharitaceae is the only family of the Helobiae where the ovary is inferior. The internal region of the ovary wall is truly carpellary in nature. Regarding the outer region of the ovary wall, which has been a centre of controversy, the present observations give support to appendicular view.

An attempt has been made to trace the trends of specialization in placentation in Helobiae. The marginal placentation appears to be the basic condition and specialization progressed from this condition along three different lines, leading to axile, superficial and basal placentation. Further specialization in axile placentation has resulted in parietal placentation.

STUDIES ON ANTHRACNOSE DISEASES OF MANGO (*MANGIFERA INDICA* L.), GUAVA (*PSIDIUM GUAJAVA* L.) AND CITRUS (*CITRUS* SPP.)*

B. B. Singh

Govt. Horticultural Research Institute, Saharanpur.

The anthracnose diseases of mango, guava and citrus are world wide in distribution and produce varying types of symptoms in different parts of the world depending upon the humidity, temperature and other environmental conditions. In view of serious losses caused by these diseases in the Saharanpur (India) region, the present investigation was undertaken with the object of studying the symptoms caused by these diseases in this region as well as to find out, on the basis of detailed comparative morphological, physiological and pathological characters, of the various isolates, whether all these diseases were caused by only one or several species. The physiological studies include the enzymatic and biochemical studies of the metabolites which have not been studied so far. Attempts have also been made to find out control measures against some of the important phases of the disease on these fruit crops including the hitherto untackled phases, namely, the fruit spot of guava, fruit drop of sweet orange and the post harvest decay of mango fruits in cold storage.

In mango, the disease attacks leaves, twigs, flowers and fruits. Whenever the inflorescence is attacked and the temperature and humidity are favourable for the development of the disease, complete deblossoming may occur. In humid places like Florida, Hawaii and Cuba, fruit spots and fruit drop are the most common symptoms of the disease which are rarely observed in India. In this region, young and green fruits on the tree are infected, but the infection remains latent and develops only in storage producing brown to black, roundish spots, varying from 10 to 15 mm in diameter, which are scattered all over the fruit surface. The spots are slightly sunken and several of them may coalesce to form bigger lesions. The fungus also attacks the stem of young seedlings producing brownish spots which gradually enlarge and girdle the stem resulting in the death of the entire plant.

On guava, the disease appears as brownish spots on the rainy season fruits, winter crop being free. Both green and ripe fruits are attacked. Small spots of the size of pin-head first appear on the unripe fruits, which gradually enlarge and attain a size of 5 to 6 mm in diameter. They are dark brown to black in colour, sunken, circular, and bear minute black stromata in the centre of the lesions which produce creamy spore masses in moist weather. The disease sometimes produces leaf spots and has been reported to cause die-back and death of the entire plant which has not been observed in this region.

---

* Abstract of the thesis submitted to the Agra University for the degree of Doctor of Philosophy.

Among citrus, the disease is most serious on sweet orange and kaghzi-lime, causing wither tip of young as well as old twigs in both the cases and pre-harvest fruit-drop in sweet orange.

Cross inoculation studies showed that the isolate from any one of the hosts can infect all the four hosts *viz.*, mango, guava, sweet orange and lime.

The effect of temperature and humidity on the development of anthracnose spots on mango and guava fruits have been studied. On mango, the disease developed from 10°-30°C., the spread being most rapid at 25°-27°C. On guava, the minimum temperatures for the spread of the disease on ripe as well as unripe fruit were 10° and 15°C., respectively whereas the maximum and optimum temperatures for the development of the disease were 35° and 30°C, respectively in both the cases.

The maximum spread of the disease occurred at 96·1 per cent relative humidity followed by 100 per cent. At 75·6 per cent and below, the disease did not develop either in mango or in guava.

All the available important varieties of mango and guava were tested for their resistance against the causal organisms. Among the mango varieties tested, Gopal Bhog and Taimuria were fairly resistant, whereas Fazari White was slightly resistant and the rest were all susceptible. All the eight varieties of guava and four species of *Psidium* tested for resistance took the infection, but Apple Guava Red Fleshed was slightly resistant.

All the four isolates were capable of infecting *Aegle marmelos, Carica papaya, Diospyros kaki, Eriobotrya japonica, Grewia asiatica, Linum grandiflorum, Lupinus hartwegii, Malus sylvestris, Matthiola incana, Musa sapientum, Petunia hybrida, Prunus persica, Viola tricolour-maxima* and *Ziziphus jujuba* whereas *Achras zapota, Ayerrhoa carambolla, Carissa carandas, Phlox drummondii, Phyllanthus emblica, Ricinus commnuis* and *Tagetes erecta* were not infected by any of the isolates.

The growth of all the isolates was best on potato-dextrose agar and poorest on Czapek's agar, except that of lime isolate which had the poorest growth on Richard's agar. Sporulation, in general, was the best on corn meal agar followed by Richard's, potato-dextrose, Oats and Czapek's agar.

The growth of all the four isolates increased slightly with the increase in depth of the medium. The mycelial growth was profuse in plates containing 60 ml of the medium, whereas Sporulation was best in plates containing 15 ml of the medium.

In Richard's medium, sugar was the most important constituent of the medium for all the four isolates, without which very little growth took place. Potassium nitrate was next to sugar in importance for all the isolates, except the lime isolate for which magnesium sulphate was more important. The third in importance was magnesium sulphate, though it was least important for the sweet orange isolate. Potassium monobasic phosphate and ferric chloride were last in importance, though their presence was essential for their normal growth in the Richard's medium. The sporulation, in general, was scanty, but lime and guava isolates had profuse sporulation in the absence of magnesium sulphate and ferric chloride, respectively.

On modified Richard's medium containing different sources of carbon, the mango isolate grew best on media containing xylose, whereas sweet orange and lime isolates showed their maximum growth on maltose. All the isolates grew profusely on media containing maltose, dextrose, sucrose, xylose, fructose and sorbitol; moderately on raffinose, soluble starch, glucose, rhamnose and inulin, and poorly on mannitol, dulcit and lactose. The sporulation, in general, was profuse on sucrose, fructose, raffinose, dulcit; moderate on maltose, glucose, mannose, xylose, rhamnose, starch, sorbitol and scanty on lactose, dextrose, inulin, mannitol as well as in media without carbon.

All the four isolates of *Colletotrichum* sp. were capable of deriving their nitrogen requirement from a variety of organic and inorganic sources. All the isolates except the sweet orange had the best growth on the media containing potassium nitrate followed by alanine. The sweet orange isolate grew best on alanine followed by asparagine and potassium nitrate. The growth of all the isolates on media containing arginine, asparagine, creatinine, glycine, kreatine, valine, ammonium nitrate and sodium nitrate was moderate, whereas on ammonium dihydrogen orthophosphate and ammonium sulphate as well as on media with no source of nitrogen, it was scanty.

The minimum, optimum and maximum temperatures for the growth of the four isolates was 10°, 25° and 35°C. There was no sporulation at 10° and 35°C., scanty at 15°C., moderate at 20°C., and abundant at 25° and 30°C.

The maximum growth of all the isolates occurred at a relative humidity of 90 per cent followed by 80, 70, 100 and 50 per cent.

They could grow at a pH range of 3 to 9 with an optimum of pH 6.

The thermal death point of the culture of the four isolates lay between 56° to 58°C., and all the isolates died at 58°C., even when they were exposed for 5 minutes. The mango and sweet orange isolates were killed by 15 minutes exposure even at 54°C., whereas at 56°C., all the isolates were killed by 15 minutes' exposure.

The pectinolytic enzymes *i. e.*, protopectinase, polygalacturonase and pectin methylesterase were produced by all the isolates in culture as well as on the hosts.

The conidia of all the four isolates did not germinate at and below 5°C., and at 40°C., and above. At 10°C., the spores of all the isolates germinated except that of mango. The minimum temperature for the germination of mango isolates lay between 10° and 15°C. The optimum temperature for germination of mango, sweet orange and lime isolates was 25°C., whereas that for the guava isolate it was 30°C. The conidia of all the isolates except the lime one germinated upto as high a temperature as 38°C. The germination started after six hours in all the isolate, the percentage being highest in the guava isolate.

The oganisms on all the four hosts can survive the varying weather conditions of Saharanpur for atleast a year and can provide sufficient inoculum for reinfection in the next year.

On the basis of morphological, physiological and cultural characters, it was established that the causal organisms of anthracnose of mango, guava, sweet orange and lime in this region are the same, that is, *Colletotrichum gloeosporioides* Penz., whose perfect state is known to be *Glomerella cingulata* (Stonem.) S. & v. S.

In order to check the anthracnose disease of mango in cold storage, the pre-harvest as well as post-harvest treatments were tried. Experiments have been carried out to control the anthracnose of mango by spraying the trees with various fungicides as well as by the application of various post-harvest treatments including the hot water treatment, just after harvesting and before storing in cold storage. The disease was reduced significantly by spraying the trees with 0·3% Fytolan, Bordeaux mixture 4:4:50 or with 0·2 per cent Dithane Z-78. From the present studies it was found that two sprayings should be given during the flowering period, that is between February and March and thereafter spraying may be started just before the onset of monsoon and continued till harvest. A total of about 8 sprayings were necessary. As a post-harvest treatment, a number of fungicides like Flit 406, Fungi copper, Sodium orthophenyl-phenate were tried as a dip with little success. A 2 per cent solution of Sodium orthophenyl-phenate checked the disease, but caused necrotic spots on the fruits, thereby rendering them useless for consumption. Exposure of infected fruits to ammonia, sulphurdioxide, carbon dioxide gases or to hot air was also unsuccessful in controlling the disease. The most effective treatment was the hot water wherein the fruits were kept at a temperature of 50° to 55°C., for 15 minutes. The treatment did not affect the appearance or the quality of the fruits and prolonged the life of the fruits in cold storage at 9-10°C., to 8 weeks, which could hardly be stored for about 3 weeks without this treatment.

The guava anthracnose causes severe loss due to fruit spot on the rainy season crop. It was considerably reduced by spraying the trees with Fytolan 0·3 per cent, or Fungi copper 0·3 per cent at weekly intervals commencing from the 1st week of July and continuing till harvest. Bordeaux mixture

3 : 3 : 50 was more effective in checking the disease, but this produced an unwashable spot on the surface of the fruit which reduced its market value.

The wither tip and fruit-drop of sweet orange was reduced by pruning the diseased twigs in January and June. The first pruning was followed by 2 sprayings of Bordeaux mixture 5:5:50 or 0·2 per cent Dithane Z-78 whereas the second was followed by sprayings with the same fungicide at 14 days' interval till September.

For the control of wither tip of lime, pruning of disease twigs was carried out in June followed by spraying with 0·2 per cent Dithane Z-78 at 14 days interval till the last week of September. Dithane Z-78 was the most effective fungicide, followed by Fytolan 0·3 per cent, Bordeaux mixture 5:5:50 Fungi copper 0·3 per cent and Ferbam 0·3 per cent.

FACTORS AFFECTING ROUGHAGE UTILISATION IN RUMINANTS*

NIRANJAN NATH PANDIT
Assistant Professor of Animal Husbandry & Dairying,
Balwant Rajput College, Agra.

The importance of livestock to shoulder the burden of Indian Agriculture will remain of ever great significance. To recondition and shape the genital worth of some of our best existing strains of livestock, the provision for a balanced nutrition demands priority. Buffaloes—a promising class of animals have excelled during recent years by virtue of their square adaptability under the variable climatic conditions as well as high butter fat yield. Among the many sided developments envisaged to lift this class of animals, a study of the nutritional aspect is the immediate need. This study becomes all the more essential when the shortage of feed supply and rapid multiplication of livestock are taken into consideration.

The present day Indian economy does not permit the allocation of more land to be put under fodders because there exists an acute competition between man and animal for the same acre of land. The livestock man thus looks for guidance from the nutritionist to suggest means of increasing the efficiency of the coarse roughages which are the by-products of grain industry and constitute the bulk of the ration. The present study is an endeavour in this direction, wherein it has been envisaged to study the "Effect of different factors on the utilisation of roughages in ruminants".

Programme of work :

This investigation is spread over two parts:—

Part I—Studies on the utilisation of nutrients in intact animals,

Part II—An evaluation of the roughage utilisation in ruminants employing fistula technique.

Two levels of stipulated D.C.P.—0·40 lb. and 0·80 lb./1000 lb. body weight to represent both the field and ideal conditions were studied in the two parts.

PART I

To begin with, a preliminary trial was conducted to assess the nutritional status of the experimental animals at 0·40 lb./1000 lb. body weight of D.C.P. intake. The results showed that animals were running short of Ca in the ration and, therefore supplementation of mineral mixture @ 35 gm./head/day was deemed necessary for the subsequent experimentation barring phase VI.

---

* Abstract of the thesis approved for the degree of Doctor of Philosophy of the Agra University

The programme of study under this part was detailed into six phases as below:—

Phase I : The role of molasses as an energy supplement fed at two levels *viz.*, 2 and 4 lb./head/day in association with low D.C.P. intake (0·40 lb. D.C.P./1000 lb. body weight).

Phase II : The role of molasses as an energy supplement fed at levels as in phase I in association with high D.C.P. Intake (0·80 lb. D.C.P./1000 lb. body weight).

Phase III : The effect of starch (sago) supplementation at isocaloric levels to molasses as in phase I in association with high D.C.P. Intake (0·80 lb. D.C.P./1000 lb. body weight).

Phase IV : The impact of urea substitution levels—25 and 50 per cent replacements for cake protein in association with molasses at high D.C.P. intake (0·80 lb./1000 lb. body wieght).

Phase V : The impact of urea substitution levels as part replacements for cake protein as in phase IV in association with maize starch at high D.C.P. intake.

Phase VI : The influence of mineral supplements *viz.*, Ca and P, Ca and P with trace element mixture but devoid of cobalt and Ca and P in addition to trace element mixture with cobalt.

PART II

The experimental variables remaining the same as in Part I, under this part of the investigation the extent of the dry matter and fibre utilisation—the latter measured in terms of crude fibre and cellulose, in relation to time, was studied in the rumen. In addition to these studies, tentative observations on ruminal pH and temperature were also made.

MATERIALS AND METHODS

Animals (male buffaloes) procured from the villages were conditioned for a reasonable period of time on the college dairy farm and prepared for experimentation.

One of the farm raised male buffaloes was fistulated for the second part of these investigations.

During the whole course of these studies wheat bhusa constituted the sole source of roughage. The protein need of the animals was met through rape cake. The supplements for energy comprised molasses, starch (sago) and maize. The urea was tried at two different levels as part replacements for conventional cake protein. The animals were given free salt and a vit. A supplement. In phase VI Ca and P were supplemented through pure

$CaCO_3$ and $NaH_2PO_4 . 12 H_2O$. Trace element mixture was the one recommended from I.V.R.I. For the most part standard A.O.A.C. techniques were followed. However, the fistula technique as suggested by Van Keuren and Heinemann (1962) was employed. The cellulose and the crude fibre in the feed, faeces and the rumen contents were estimated following the methods suggested by Crampton and Maynard (1938). For the study of blood picture of the animals, the technique given by Napier and Das Gupta (1935) was adopted.

RESULTS

Part I : The molasses as an energy supplement when accompanied with low D.C.P. intake did not alter the total dry matter intake of the animals materially, although a consistently lower consumption of dry matter through wheat bhusa occurred. The appetising influence of the molasses as suggested by some earlier workers was not visible at low level of D.C.P. intake. However, the supplementation of molasses with high D.C.P. not only enhanced the dry matter intake, but also affected a significant improvement in its digestibility.

Replacement of molasses by starch (sago) on isocaloric levels resulted in an insignificant fall both in the dry matter intake as well as its digestibility, suggesting thereby a parity in between the two sources of energy. When cost is a consideration molasses will score over starch.

With the replacement of cake protein by urea at 25 and 50% levels in association with 2 lb. molasses, an insignificant elevation in dry matter intake occurred. This increase, however, was accompanied by a proportionate decrease in its digestibility. This status quo continued even when the energy supplement was changed from molasses to maize.

With both molasses and maize 25% urea substitution gave consistently better results than the higher level (50% R.)

Virtually no improvement with regard to the total dry matter intake was noted when minerals were supplemented, although the digestibility of dry matter indicated a positive response, which was more marked with Ca and P supplements alone rather than the additional fortification of the ration with trace minerals.

The S.E. consumption of animals was significantly more when molasses was the energy supplement. A proportionate increase was noted in T.D.N also. When the level of stipulated D.C.P. was raised to 0·80 lb. D.C.P./1000 lb. body weight, a positive response for increased energy consumption resulted. However, when the source of energy was changed from molasses to starch (sago) on isocaloric levels, no supplementary effect could be noted. This again signifies that starch claims no superiority over molasses as an energy supplement.

Substitution of cake protein by urea when associated with molasses did not influence any material alteration in the energy intake, although an insignificant increase with the two experimental groups resulted. In combination with maize the same substitution levels affected a slight improvement notably in case of lower one (25% R). The toxicity of high urea intake was guessed.

The supplementary intakes of Ca and P through $CaCO_3$ and NaH_2PO_4. 12 H20 influenced a marked positive change in the energy consumption. This improvement receded with the inclusion of trace element mixture with or without cobalt in the ration.

With low level of D.C.P. intake (0·40 lb. D.C.P./1000 lb. body weight) significant impairment in the fibre utilisation occurred when high level of molasses (4 lb./head/day) was included in the ration. With lower level (2 lb./head/day), however, an insignificant improvement was noted. This impairing influence of high molasses supplementation as mentioned above could be checked by raising the level of D.C.P. in the ration.

The high level of D.C.P. remaining the same, replacement of molasses by starch on isocaloric basis depressed the fibre utilization, although the mean differences were insignificant.

A virtual improvement in the fibre digestibility occurred when urea at lower level (25% R) in association with molasses, was included in the ration. The higher substitution level (50% R) was found to be relatively less efficient. In association with maize, however, both the substitution levels resulted in consistent, though insignificant improvements.

Mineral supplements, particularly Ca and P through $CaCO_3$ and NaH_2PO_4. 12 H20 materially improved the fibre digestibility when associated with molasses. This improvement was considerably masked when trace element mixture with or without cobalt was also included in the ration.

At lower level of D.C.P. intake, consistent and positive response in the digestibility of crude protien and its subsequent utilisation with the increasing level of molasses supplementation was noted. The digestibility of crude protein increased significantly when the level of stipulated D.C.P. intake was raised from 0·40 to 0·80 lb./1000 lb. body weight. The increase in digestibility which was in proportion to the level of energy supplement also, was invariably accompanied by lowered biological values.

As against molasses supplementation starch (sago) at isocaloric levels indicated decreased digestibility of crude protein which was accompanied by an increase in its utilisation, thus establishing the same logical relationship between digestion and assimilation.

The substitution of urea at 25 and 50% levels for cake protein, when accompanied by molasses, indicated a proportionate increase in the digestibility of crude protein. The subsequent utilisation, however, expressed an irregular trend. With the ingestion of maize starch, fed isocaloric to molasses levels, the increase in the digestibility of crude protein remained unarrested. The subsequent biological values, however, indicated a fall thus, confirming again the inverse correlation between digestibility and the biological values.

Significant impairment in the digestibility of crude protein was noted when trace element mixture with or without cobalt was included in the ration. Such ill effects were not visible when Ca and P together constituted the only mineral supplement. The inverse relation between digestibility and biological value was once more affirmed.

As against control or the high level of molasses (4 lb./head/day), the lower level *i.e.*, 2 lb./head/day improved the digestibility of crude fat when the D.C.P. level was low. With an increase in the D.C.P. level, however, a fall in crude fat digestibility was noticeable. This fall, which remained unabated even with the energy change over from molasses to starch (sago), was proportionate to the level of energy supplements.

Irrespective of the source of energy supplement when urea at different levels (25 and 50% substitution) was included in the ration, an apparent fall in the digestibility of crude fat occurred. This depression was invariably associated with the lowered intake of crude fat in the two experimental groups, as the cake—the principal supplier of fat—was replaced by urea. In general, the studies conclude that higher fat intake accompanies higher digestibility.

Inclusion of minerals along with molasses did not put in any material advantage for crude fat digestibility, although the supplementation of cobalt had a positive response.

Irrespective of the level of D.C.P. intake significant differences were observed in the digestibility of both T.C. and N.F.E., when molasses at 2 and 4 lb./head/day was included in the ration. Such a trend underwent almost no deviation when molasses was replaced by starch (sago) on isocaloric levels. The starch supplementation, however, did not indicate any significant difference in experimental means as compared to control.

A fall in the N.F.E. digestibility was witnessed when urea was substituted partly for cake—the low level of molasses intake remaining the same. This position, however, could be restored when molasses was replaced by maize. 50% substitution of urea was not of any benefit even when associated with maize.

Marked improvements in the digestibility of total carbohydrates occured with the supplementation of Ca and P in association with lower level of molasses. This improvement underwent partial regression with additional supplementations of trace element mixture with or without cobalt.

The ingestion of molasses was invariably accompanied by negative Ca balances, which continued to mount with the passage of time so long as molasses was a component of the ration. A change in the source of energy from molasses to starch restored the situation appreciably. This suggests with reasonable emphasis that there is something in molasses which interferes with Ca absorption. The utilisation of these two mineral constituents usually showed an inverse correlation.

When urea was included in the ration, the position with regard to Ca and P balances got reversed. The positive Ca and negative P balances were characteristically marked in association with molasses. This indicates that the interfering effect of molasses on Ca utilisation can be obviated by inclusion of urea particularly at the lower level of substitution. This encouraging effect of urea was masked when molasses was replaced by maize, the animals going into negative Ca balances again and showing tendency to recover from negative P balance.

The mineral supplementations *viz.*, Ca and P; Ca, P and trace element mixture without cobalt and Ca, P and trace element mixture with cobalt in association with molasses improved the Ca balances markedly and P balances sparingly. Maximum advantage was noted in case of Ca/P supplementation alone.

No significant variations in the haematological behaviour of the animals due to experimental variables were observed.

Part II : At 0·40 lb. stipulated level of D.C.P. intake, maximum dry matter as well as crude fibre digestibility was observed with 2 lb. molasses supplementation. Higher level of molasses (4 lb./head/day) depressed the digestibility of all the constants significantly. No advantage could be seen even when the level of D.C.P. was raised.

The digestibility of both crude fibre and cellulose was markedly improved when 25% of cake protein was replaced by urea and associated with 2 lb. level of molasses. With 50% replacement a regression in digestibility of these constituents ensued. Associating maize in place of molasses indicated equally beneficial results with regard to digestibility of dry matter and the fibre. 50% replacement of protein by urea along with maize was equally effective.

The digestion of dry matter and cellulose was markedly improved when molasses at 2 lb. level was associated with Ca and P supplementation. Further supplements of trace elements depressed the fibre digestibility, but the inclusion of cobalt improved it considerably. The findings revealed that cobalt as also Ca and P are intimately associated with the cellulolytic acivity in the rumen.

During the course of these observations, it was seen that maximum shifts in dry matter and fibre digestibility occur within a time interval of

24 to 48 hours with a declining upward trend upto 72 hours, after which the values invariably level off.

The pH of the rumen was noted to shift above the neutral point with the inclusion of molasses in the ration. The values reconciled when other sources of energy *viz.*, starch (sago) and maize were brought in. Minimum pH was recorded in case of the control. No conclusive variations could be noted with regard to the rumen temperature.

From the experimental evidences gathered during the course of this study, it may be safely concluded that molasses is the cheapest yet efficient energy supplement. However, one should get familiar with the implications of its inclusion in the rations of ruminants. It involves a few very vital considerations.

A provision for high level of D.C.P. intake and supplementation of Ca is inevitable to get the optimum results from molasses supplementation. Since high level of D.C.P. may involve prohibitive cost it can be replaced by 25% urea without undermining the efficiency of molasses, but in such a case both Ca and P will have to be supplemented to prevent the animals from running into negative balances. 2 lb. of molasses as against 4 lb./head/day has proved more beneficial. On the basis of total dry matter intake molasses can safely contribute about 12·0% to dry matter which for practical purposes comes to 1 lb. of molasses for every 8·3 lb. of dry matter ingestion.

CYTOLOGICAL, CYTOCHEMICAL AND HISTOLOGICAL STUDIES IN EXPERIMENTALLY INDUCED CANCER OF CERVIX IN MICE*

[WITH CORRELATIVE STUDIES ON HUMAN PATIENTS]

Dr. (Km.) USHA KEHAR
Department of Pathology, Medical College, Agra.

Carcinoma cervix is the commonest malignant tumour in Indian women. Epidemiological studies have yielded interesting findings *i.e.*, the age incidence being a decade earlier than in the women in western countries, and majority of the cases when first seen in the hospital are in an advanced clinical stage beyond any useful surgery or radiotherapy. Follow-up studies have shown that if these cases are detected at their earliest stage (or preinvasive stage) when clinically the disease is symptomless, the prognosis is very encouraging.

In order to save humanity from this scourage, it is absolutely essential to investigate the possibility of early detection of this disease. Study of vaginal smears for exfoliated cells affords such a technique, which is reasonably reliable, comparatively easy of performance, and agreeable to the patients.

The biological behaviour of cervical carcinoma is still not clearly understood. However, there is universal agreement that it arises from an atypical or dysplastic epithelium and not in a normal epithelium. To have a real preventive approach against cervical carcinoma, one has to concentrate on these epithelial atypias and preinvasive stage.

The study of the nature of these epithelial dysplasias has thus attracted considerable attention of cancer biologists in recent years. Each of the cervical dyaplasia presents a different biological behaviour depending on its age of onset and severity of the process. Furthermore, it is not clearly understood at this stage that which of these would progress, persist or regress when followed for sufficient length of time. For the better understanding of various earlier phases of cervical carcinogenesis and the resulting morphological changes in the cervix, it is essential that the natural history of the disease be studied in specially bred mice which show a striking biologic and pathologic resemblance to human cervical carcinoma.

A correlative study in human cases of cervical epithelial dysplasias and cervical carcinoma was also carried out.

The work reported here consists of:—

1. Experimental studies.
2. Studies on human cases.

---

* Abstract of the thesis approved for the degree of Doctor of Philosophy by the Agra University.

Experimental studies:

Mice cervices were painted with 3:4 benzpyrene for varying length of periods, after which the painting was discontinued and animals followed till their sacrifice or death. Smears from experimental and control mice were stained with Papanicolaou's staining technique and various non-enzymatic and enzymatic cytochemical reactions carried out. Fresh cellular samples for phase contrast microscopic studies were collected. A total of 4,000 vaginal smears were studied each by Papanicolau's and cytochemical staining reactions. Papanicolaou's stained smears were subjected to detailed cytologic differential and cytodifferential counts.

(1) Cytologic studies revealed changes in the morphology of exfoliated cells in the vaginal smears during various phases of experimental carcinogenesis. On the basis of both cytologic and histologic changes the following distinct lesions were recognized:—

(a) acute inflammation of cervical and vaginal epithelium.

(b) epithelial dysplastic changes—these were graded according to their severity into mild dysplasia or dysplasia grade I, moderate dysplasia or dysplasia grade II, and marked dysplasia grade III.

(c) intraepithelial carcinoma

(d) invasive carcinoma

All the mice painted with 3:4 benzpyrene showed dysplastic changes. On following these animals till their sacrifice or death, 17 of these *i.e.*, 21:2 per cent belonging to group A developed invasive carcinoma after a latent period of 8 to 33 weeks of the experimental study, 8 *i.e.*, 10 per cent belonging to group B developed intraepithelial carcinoma following a latent period of 8 to 19 weeks of experimental study.

Intraepithelial carcinoma showed a shorter induction period as compared to invasive carcinoma. Yield of both intraepithelial and invasive carcinoma increased with the increase in the period of carcinogenic treatment.

7 mice *i.e.*, 8·7 per cent belonging to group C, progressed to higher grades of dysplasia, 42 *i.e.*, 52·5 per cent of group D showed persistent dysplastic changes till the time of their sacrifice or death and lastly 6 mice *i.e.*, 7·5 per cent of group E showing moderate dysplastic changes regressed cytologically and histologically to normal. None of the mice showing marked dysplastic changes regressed to normality. On the contrary these invariably progressed to preinvasive or invasive carcinoma.

(2) On carrying out detailed cytologic differential and cytodifferential counts some important differences were discerned between the counts of various groups of dysplasias which showed varied biological behaviour on follow up studies *viz.*, group A—Dysplasia→Invasive carcinoma, group

B—Dysplasia→Intraepithelial carcinoma, Group C—Dysplasia→progressing, group D—Dysylasia→persisting and group E—Dysplasia→regressing.

There was a statistically significant difference in the number of malignant cells in group A and B. Similarly, the number of spindle-shaped squamoid cells differed statistically in these two groups.

The interrelationship between various components of cytologic differential counts between various groups showed that the abnormal cell counts were helpful in differentiating the prognostic viewpoint of the cervical dysplasias. Abnormal cell counts in the vaginal smears showed significant difference between groups A & D, B & D, and C & D, whereas these counts were more or less similar in groups A, B and C.

Thus those animals which ultimately progressed to invasive or preinvasive carcinoma or to higher grades of dysplasias, showed similar cytologic differential counts, which were different when compared with the counts of those animals who revealed persistence of dysplastic lesions without significant progression or regression.

Among the cytodifferential counts of the various abnormalities in the cells macronuclei, hyperchromasia, macro and multiple nucleoli, number of spindle shaped-squamoid cells and the chromatin pattern of the cells were found to be most helpful in establishing the diagnosis of dysplasias or preinvasive or invasive carcinoma.

(3) The significant cells encountered in animals with intraepithelial carcinoma were the malignant basal cells, atypical parabasal type of cells and small basal type of cells showing atypical cytoplasmic keratinization. Along with these, the general cellular pattern of vaginal smears in these animals, helped to differentiate intraepithelial from invasive carcinoma.

Histologically, the whole thickness of the epithelium showed neoplastic change limited by an intact basement membrane in all the animals, except in one *viz.*, Mouse No. 11 with well differentiated intraepithelial carcinoma, where some degree of superficial surface keratinization was recognized.

(4) Amongst the non-enzymatic cytochemical reaction there was a gradual increase of DNA and RNA and DNA (later more constantly) during progressive experimental carcinogenesis. Amount of glycogen, polysaccharides and disulphide groups showed a gradual decrease during progressive experimental carcinogenesis, except that disulphide showed strongly positive reaction when epithelial pearl formation was present. Sulfhydryl groups gave irregular reactions.

Amongst the enzymatic reactions, practically all of them showed a quantitative increase during progressive experimental carcinogenesis, being more pronounced with acid phosphatase, phosphamidase, glucuronidase and esterase.

(5) Phase contrast microscopic studies revealed similar stages of development during experimental carcinogenesis as seen with Papanicolaou's staining technique. This method was found useful in the rapid interpretation of fresh cellular samples with practically the same accuracy as by the Papanicolaou's staining technique. However, it was considered useful as a rapid screening procedure rather than a replacement for Papanicolaou's staining technique.

Studies on Human cases:

33,095 women with or without gynaecological symptoms were examined for detailed clinical history, single or multiple cervical smear examination by Papanicolaou's technique and cervical biopsy studies whenever indicated. A total of 36,955 smears were studied.

(1) Out of these 649 cases were detected to be of cervical carcinoma, either by cytology or by cytology and biopsy both. The age peak incidence of these patients was between 46-50 years. Early marriage, early age of first childbirth and multiparity seemed to be of etiological significance. Bleeding per vagina was the commonest symptomatology. Majority of the patients were first seen in the clinical stage III and IV. 68 patients *i. e.* (10·4 per cent) of the cases were not suspected of malignancy on clinical grounds and were diagnosed as cases of cervical erosion. Histologically majority of the cervical carcinoma cases were epidermoid carcinomas, predominantly grade III.

(2) 695 cases out of the total women screened revealed dysplastic changes in their cervical smears. 136 of these *i.e.*, 19·5 per cent were associated with pregnancy at one or more occasions. Dysplastic changes were divided into three grades *viz.*, mild dysplasia or dysplasia grade I, moderate dysplasia or dysplasia grade II and marked dysplasia or dysplasia grade III, depending on their severity of cytomorphological and histomorphological characteristics.

Gradual increase in age incidence of patients with increasing grades of dysplasias, intraepithelial and invasive carcinomas was found. Early marriage, early age of first childbirth and multiparity seemed to be frequently associated with cervical dysplastic lesions. Discharge per vagina was the commonest symptom present in these cases and next common being bleeding per vagina. Majority of the cases *i.e.*, 53·9 per cent gave a clinical impression of cervical erosion. Interestingly, 21·3 per cent showed healthy looking cervices and 6 were suspected of malignancy. Histologically, dysplastic lesions of grade II were seen most commonly *i.e.*, in 60·5 per cent of cases. A close correlation was found in the cytological and histological diagnoses of grading dysplastic lesions.

(3) 104 cases of cervical dysplasia were followed up for varying length of periods. Corresponding to the groups in experimental study *viz.*, groups A, B, C, D and E, the human cases also showed different biological behaviour

of these dysplastic lesions on follow up studies. 5 cases each progressed to invasive and intraepithelial carcinomas, 11 to higher grades of dysplasias, 68 showed persistence of dysplastic changes and 15 showed regression of dysplastic changes.

(4) Various cell types and cellular pattern corresponding closely to that observed in experimental intraepithelial carcinoma were seen in human cases. Histologically the whole thickness of the epithelium showed neoplastic changes within an intact basement membrane.

(5) Cytological differential and cytodifferential counts showed similar observations as seen in the experimental studies.

FRACTIONAL INTEGRATION AND CERTAIN INTEGRAL TRANSFORMS*

JAG MOHAN CHANDRA JOSHI†

Head of Mathematics Department, Govt. Degree College, Pithoragarh.

In the thesis on "Fractional Integration and Certain Integral Transforms" we have discussed the various properties of the transform.

$$(i)\quad F(x)=\frac{\Gamma(\beta+\eta+1)}{\Gamma(\alpha+\beta+\eta+1)}\times$$

$$\times\int_0^\infty (xy)^\beta\, {}_1F_1(\beta+\eta+1;\alpha+\beta+\eta+1;-xy)\,f(y)\,dy$$

whose nucleus has been obtained (in the Introductory Chapter) by using properties of Kober's Operators of Fractional integration.

We have also used fractional integration and differentiation to develop the theory of generalized Hankel transform

$$(ii)\quad F(x)=\left(\tfrac{1}{2}\right)^\lambda\int_0^\infty J^\mu_\lambda\left(\tfrac{1}{4}x^2y^2\right)(xy)^{\lambda+\frac{1}{2}}f(y)\,dy$$

and

$$(iii)\quad F(x)=\int_0^\infty (xy)^\nu\, J^\mu_\lambda(xy)\,f(y)\,dy$$

In chapter one we have given a brief account of the three integral transforms *viz.*, Laplace, Stieltjes and Hankel, and their generalizations with which we have been concerned in the course of our investigations. We have also defined operators of fractional integration and differentiation which have been used to develop a Kernel for transform (i).

In chapter two the following theorems have been proved:

Theorem 1. If the integral

$$(iv)\quad F(x)=\frac{\Gamma(\beta+\eta+1)}{\Gamma(\alpha+\beta+\eta+1)}\times$$

$$\times\int_0^\infty (xy)^\beta\, {}_1F_1(\beta+\eta+1;\alpha+\beta+\eta+1;-xy)\,d\psi(y)$$

converges for $x=x_0$ then it converges for every x provided that Re $\beta\geqslant0$ Re $\eta>0$ with an additional condition Re $x>$ Re x_0 in case $\alpha=0$ or Re $x<0$.

---

* Abstract of the thesis approved by the Agra University for the degree of Doctor of Philosophy submitted in 1963.

† Home address—S/o Dr. S. M. Joshi, Ranikhet, (India).

In the latter case, we also have

$$\frac{\Gamma(\beta+\eta+1)}{\Gamma(\alpha+\beta+\eta+1)} \times$$

$$\times \int_0^\infty (xy)^\beta {}_1F_1(\beta+\eta+1;\alpha+\beta+\eta+1;-xy)\,d\psi(y)$$

$$= \frac{\Gamma(\beta+\eta+1)}{\Gamma(\alpha+\beta+\eta+1)} \left(\frac{x}{xo}\right)^\beta \int_0^\infty \chi(x,y)\,\phi(y)\,dy$$

where

$$\chi, (x,y) = \frac{\left\{ \begin{array}{l} x\,{}_1F_1(a+1,b+1,-xy)\,{}_1F_1(a,b,-x_0 y) - \\ \qquad -x_0\,{}_1F_1(a+1,b+1,-x_0 y)\,{}_1F_1(a,b,-xy) \end{array} \right\}}{[{}_1F_1(a,b,-x_o y)]^2}$$

$$a=\beta+\eta+1,\ b=a+\alpha$$

and

$$\phi(t) = \frac{\Gamma(\beta+\eta+1)}{\Gamma(\alpha+\beta+\eta+1)} \times$$

$$\int_0^t (x_0 y)^\beta {}_1F_1(\beta+\eta+1;\alpha+\beta+\eta+1;-x_0 y)\,d\psi(y)$$

Theorem 2. If the integral (*iv*) converges absolutely for $x=x_0$ then it converges uniformly provided that Re $\beta \geqslant 0$, Re $\eta > 0$ with an additional condition Re $x=$Re x_0 in case $\alpha=0$ or Re $x<0$.

Theorem 3. If for some real number ξ

$$\psi(y)=0\left(y^{\eta+1-\xi}\right) \quad (y\to\infty)$$

(*v*) when Re $x>0$ or

$$\psi(y)=0\left(y^{\alpha-\beta} e^{\xi y}\right) \qquad (y\to\infty)$$

(*vi*) when Re $x<0$ or $\alpha=0$ or both then the integral (*iv*) converges for $\xi>0$ under conditions (*v*) and for Re $x>\xi$ under conditions (*vi*), provided that Re $\beta\geqslant 0$, Re $\eta>0$.

Theorem 4. If the integral (*iv*) converges for $x=x_0$ then, provided that Re $\beta\geqslant 0$, Re $\eta>0$,

$$\psi(y)=0\left(y^{\eta+1}\right)$$

if Re $x>0$ or

$$\psi(y)=0\left(y^{\alpha-\beta} e^{y \,\mathrm{Re}\, x_0}\right)$$

if Re $x_0>0$, $\alpha=0$.

In chapter three the following Abelian theorem has been proved for the transform (*iv*).

Theorem 5. If (*iv*) converges for $x>0$ then for any constant A

$$\mathop{\overline{\mathrm{Lim}}}_{\substack{x\to\infty\\ y\to 0}} \left| x^{\gamma+\alpha-\beta} - \mathrm{A} \right| \leqslant \mathop{\overline{\mathrm{Lim}}}_{\substack{y\to 0\\ y\to\infty}} \left| \frac{\psi(y)}{c\,y^{\nu+\alpha-\beta}} - \mathrm{A} \right|$$

Provided that $\mathrm{Re}.\beta>0$ $\mathrm{Re}\ \eta>0$, $\mathrm{Re}\,(\beta+\eta+1)>\mathrm{Re}\,(\nu+\alpha)>0$ and $\psi(y)=0\left(y^{-\beta}\right)$ $(y\to 0)$

where $$c=\frac{\Gamma(\beta+\eta+1-\nu)}{\Gamma(\beta+\eta+1-\gamma-\alpha)\,\Gamma(\gamma+\alpha)}\,(\nu+\alpha-\beta)^{-1}$$

In chapter four the following complex inversion theorem has been developed.

Theorem 6. If $\mathrm{F}(x)$ is given by (i) then

$$\tfrac{1}{2}[f(y+)+f(y-)]=$$

$$=\frac{1-}{2\pi i}\lim_{\tau\to\infty}\int_{c-i\tau}^{c+i\tau}\frac{\Gamma(\alpha+\eta+s)}{\Gamma(\beta+1-\xi)\,\Gamma(\eta+s)}\,y^{-s}\,\phi(s)\,ds.$$

where

$$\phi(s)=\int_0^{\infty}x^{-s}\,\mathrm{F}(x)\,dx$$

Provided that $t^{c-1}(t)\in\mathrm{L}(0,\infty)$

$t^{-s}\,\mathrm{F}(t)\in\mathrm{L}(0,\infty)$, $(\mathrm{S}=c+i\tau, -\infty<\tau<\infty)$

$\mathrm{F}(t)$ is of bounded variation in the neighbourhood of the point $t=y$ $(y>0)$

$f(t)=0\left(t^{\rho-\beta}\right)\mathrm{Re}\,\rho>0\ (t\to 0)$

$=0\left(s^{-tv}\right)$, $\mathrm{Re}\,\nu>0$, $(t\to\infty)$

Chapter Five deals with a singular integral and a real inversion theorem. We prove

Theorem 7. If $a<a+\xi<b$, $\phi(y)\in c^2$
$(a\leqslant y\leqslant a+\xi)$, $\phi'(a)=0$ $\phi''(a)<0$
ϕ is non decreasing in $(a\leqslant y\leqslant b)$ then

$$\int_a^b e^{n\phi(y)}\,y^{\beta-\alpha}\,ay\sim e^{n\phi(a)}\,a^{\beta-\alpha}\{-\pi|\,2n\,\phi''(a)\}^{\frac{1}{2}}$$

Theorem 8. If $a<a+\xi<b$, $\phi(y)\in c^2$ $(a\leqslant y<a+\xi)$ $\phi(y)$ is non decreasing in $(a\leqslant y\leqslant b)$, $\phi'(a)=0$, $\phi''(a)<0$
then

$$\int_a^b e^{n\phi(y)}\,y^{\beta-\alpha}\,dy\sim e^{n\phi(a)}\,a^{\beta-\alpha}\left(\frac{-\pi}{2n\,\phi''(a)}\right)^{\frac{1}{2}}$$

Theorem 9. If $a<a+\xi<b$, $\phi(y) \in c^2\ (a\leqslant y\leqslant a+\xi)$ $\phi'(a)=0$, $\phi''(a)<0$, $\phi(y)$ is non increasing $(a\leqslant y\leqslant b)$ $\psi(y) \in L\ (a\leqslant y\leqslant b)$, $\psi(a)\neq 0$.

$$x_1(y)\equiv\int_a^y [\psi(u)-\psi(a)]\,du=0\,(y-a)\quad(y\to at)$$

then

$$\int_a^b \psi(y)\, e^{n\phi(y)} y^{\beta-\alpha} dy \sim \psi(a) e^{n\phi(a)}\, a^{\beta-\alpha}\left(\frac{-\pi}{2n\,\phi''(a)}\right)^{\frac{1}{2}}$$
$$(n\to\infty)$$

Theorem 10. If $f(y) \in L\ (1/R\leqslant y\leqslant R)$ for every $R>1$.

$\int_1^\infty f(y)\, e^{-cy}\, dy$ converges for a fixed $c>0$.

$\int_{0+}^1 y^r f(y)\, dy$ converges for fixed r

$$\int_x^y [f(u)-f(u)]\, du=0\,(|x-y|)\quad(y\to x)$$

then

$$\frac{1}{\Gamma(\beta-\alpha+n+1)}\left(\frac{n}{u}\right)^{\beta-\alpha+n+1}\int_0^\infty e^{\frac{-xy}{x}}\, y^{\beta-\alpha+n} f(y)\,dy \sim f(x)\quad(n\to\infty)$$

Theorem 11. If $f(y) \in L$ in $0\leqslant y\leqslant R$ for every positive R and is such that the integral (i) converges for some $x(=x_0$ say),

then
$$\lim_{n\to\infty} Q_{n,t}[F(x)]=f(t)$$

for all positive t in the Lebesgue set for $f(y)$, where

$$Q_{n,t}[F(x)]=\frac{(-)^n}{\Gamma(x+1+\beta-\alpha)}x^{-\eta+1}\times D^{(n)} x^{-\alpha} D^{(-n)} x^{\alpha+\beta+\eta+n}\times$$
$$\times D^{(n)}[x^{-\beta}F(t)]\Big|_{x=\frac{n}{t}}$$

Theorem 12. If (iv) converges then, provided that
Re $s\geqslant 0$, Re $\eta>0$

$$\lim_{r\to 0+}\frac{n^{\beta+n+1}\,\Gamma(\beta+\eta+2n+1)}{\Gamma(n+1+\beta-\alpha)\,\Gamma(\beta+\eta+2n+1+\alpha)}\frac{1}{r^{n+\beta}}\times$$
$$\times\int_0^\infty y^{n+\beta}\,{}_1F_1\left(\beta+\eta+2n+1,\ \alpha+\beta+\eta+2n+1,\ -\frac{ny}{r}\right)\psi(y)\,dy$$
$$=\frac{n\,\Gamma(\beta+n)\,\Gamma(\eta+n+1)}{\Gamma(n+1+\beta-\alpha)\,\Gamma(\alpha+\eta+n+1)}\psi(0+)$$

Theorem 13. If $\psi(y)$ is a normalized function of bounded variation in $0 \leqslant y \leqslant R$ for every positive R and if the integral (iv) converges for some x, then

$$\lim_{n \to \infty} \int_{0+}^{u} Q_{n1t}\,[F(x)]\,dt = \psi(u) - \psi(0+)$$

In Chapter Six we have thrown generalized laplace transform (i) into the form of a Convolution transform in order to obtain an inversion formula for the same and have proved the theorem.

Theorem 14. If $f(t) \in$ C.B. on $0 < t < \infty$ and if the integral (i) converges then the relation

$$\lim_{n \to \infty} \frac{(-)^{n+1}}{\Gamma(n+2+\beta-\alpha)} x^{-\eta+1} D^{(n+1)} x^{-\alpha} D^{(-n-1)} x^{\alpha+s+\eta+n+1}$$

$$D^{(n+1)}\Big[x^{-s}F(x)\Big]\Big|_{x=n/t} = f(t)$$

holds for $0 < x < \infty$.

In Chapter seven fractional integration has been used to obtain inversion and representation theorems for the transform (i). We have proved.

Theorem 15. Let $f(y) \in L\,p\,(0, \infty)$

$1 \leqslant p < \infty$, $x > 0$ If $\eta > -1/p$, $\beta > -1/q$ When $\alpha > 0$ when $\alpha > 0$ and $\eta + \alpha > -1/p$, $\beta > -1/q$ when $\alpha < 0$ then $I_{\eta+\alpha,\,-\alpha}\,[\phi(x)]$ exists and is equal to $F(x)$ where $\phi(x)$ is given by

$$\phi(x) = \int_0^\infty (xy)^\beta\, e^{-xy} f(y)\, dy$$

Theorem 16. Let $f(y) \in L\,(0, \infty)$ $1 < p < \infty$ in $0 \leqslant y \leqslant R$ for every positive R. If integral given by (i) converges for $x > 0$ and $\eta > -1/p$ when $\alpha > 0$ and $\eta + \alpha > -1/p$ if $\alpha < 0$ ($\beta > -1/q$ in both the cases) then for almost all positive t

$$\lim_{n \to \infty} Q_{n1t} \left\{ I_{n+\alpha_1-\alpha}\Big(F(x)\Big)\right\} = f(t)$$

Theorem 17. The necessary and sufficient conditions for a function $F(x)$ to have the representation (i) with $f(y)$ belonging to $L_p\,(0, \infty)$, $p \geqslant 1$ $x > 0$ $\beta > -1/q$ and with $\eta > -1/p$ when $\alpha > 0$ and $n + \alpha > -1/p$ when $\alpha < 0$, are $I_{n+\alpha,-\alpha}\,[F(x)] \equiv \psi(x)$

exists, has derivatives of all orders in $0 < x < \infty$ and vanishes at infinity and there exist constants M and p ($p > 1$) such that

$$\int_0^\infty \left| Q_{n,\,t} \left\{ \psi(x) \right\} \right|^p dt < M \quad -(A)$$

Theorem 18. If F (x) has the representation (i), with the conditions $f(y) \in L_p\ (0, \infty)$, $p \geqslant 1$, $x > 0$ $\beta > -1/q$ and $\eta > -1/p$ if $\alpha > 0$ or $\eta + \alpha > -1/p$ if $\alpha < 0$, and if the fractional derivatives or integrals $I_{\eta+\alpha_1-\alpha}[F(x)]$ exists then

$$\lim_{n\to\infty} \int_0^\infty \left| Q_{n,t}\left\{ \psi(x) \right\} \right|^p dt = \left\{ \left\| f \right\|_p \right\}^p \quad \ldots..(A)$$

Theorem 19. If the function F (x) has the representation (i) with $f(x) \in L_p\ (0, \infty)$ $p \geqslant 1$, $x > 0$ $\beta > -1/q$ and $\eta > -1/p$ if $\alpha > 0$ or $\eta + \alpha > -1/p$ if $\alpha < 0$ then

$$\lim_{n\to\infty} \int_0^\infty \left| Q_{n,t}\left\{ F(x) \right\} \right|^p dt = \int_0^\infty \left| \overline{K}_{n1\alpha}\left\{ f(t) \right\} \right|^p dt$$

Theorem 20. If the fractional derivatives or integrals $I_{\eta+\alpha_1-\alpha-r}$ $\{F(x)\}$ exists for $r = 0, i, 2, \ldots.$ then the integral in condition (A) of theorems 18, and 17 can be replaced by

$$\int_0^\infty \left| \frac{1}{\Gamma(n+\beta+1)} \sum_{0}^{n} (-)^r A_r \left(\frac{n}{t}\right) I_{n+\alpha_1-\alpha-r} \left\{ F\left(\frac{n}{t}\right) \right\} \right|^p dt$$

where

$$A_r = n_{C_r} (\beta+\eta)(\beta+\eta+1) \ldots\ldots (\beta+\eta+n-r-1) \quad (r=0, 1, \ldots.n-1)$$

$$A_n = 1$$

Theorem 21. If $f(t)$ is bounded in $0 < t < \infty$ then, provided that integral (i) converges,

$$f(t) = \lim_{n\to\infty} Q_{n,t}\ [F(x)]$$

for all positive t provided that Re $\eta > 0$, Re $\beta \geqslant 0$, where Q_{n1t} $[F(x)]$ is defined by the relation

$$Q_{n1t}\{F(x)\} = \frac{(-)^n}{\Gamma(n+1+\beta-\alpha)} x^{\beta+n+1} \left(\frac{d}{dx}\right)^n \left\{ x^{-\beta} F(x) \right\} \Big|_{x=n/t}$$

Theorem 22. The necessary and sufficient condition s that a given function F (x) may have the representation (i) with $f(y)$ bounded and Re $\beta \geqslant 0$ Re $\eta > 0$ Re $\alpha < 0$ are that F (x) has derivatives of all orders in $0 < x < \infty$, $F(x) \to 0$ as $x \to \infty$,

$$|Q_{n,t}\{F(x)\}| < M \text{ for all } n \ (0 < t < \infty).$$

In Chapter Eight we have found out a new generalization of the well known Stieltjes transform

$$\text{(vi) } \phi(s) = \int_0^\infty \frac{f(y)}{s+y}\, dy$$

in the form

$$\text{(vii)} \quad \phi(s) = \frac{\Gamma(\beta+\eta+1)\,\Gamma(\beta+1)}{\Gamma(\alpha+\beta+\eta+1)\,S} \times$$

$$\times \int_0^\infty (s/y)^{-\beta}\, {}_2F_1\left(\beta+\eta+1,\, \beta+1;\, \alpha+\beta+\eta+1; -\frac{y}{s}\right) f(y)\, dy$$

named as Dr. S. M. Joshi's Generalized Stieltjes Transform after my father who instilled in me love for research. We have also found out an invertion theorem for (vii) using it to obtain an inversion theorem for the transform (i). We have proved.

Theorem 23. If $\phi(s) = \int_0^\infty e^{-sx} F(x)\, dx$

where F (x) is given by the convergent integral (i)

then $\phi(s) = \dfrac{\Gamma(\beta+\eta+1)}{\Gamma(\alpha+\beta+\eta+1)} \times \dfrac{1}{s}$

$$\int_0^\infty \left(\frac{s}{y}\right)^{-\beta} {}_2F_1\left(\beta+\eta+1,\, \alpha+\beta+\eta+1;\, -\frac{y}{s}\right) f(y)\, dy$$

provided that Re $\beta \geqslant 0$ Re $\eta > 0$ and $(\alpha+\beta+\eta+1) \neq 0, -1, -2, \ldots\ldots$

Theorem 24. If $f(s) \in$ C. B. on $0 < s < \infty$ and if the integral (vii) converges then the relation

$$\lim_{n\to\infty} (-)^n \frac{\Gamma(n+\alpha)}{\Gamma(n)\,\Gamma(n+\beta)\,\Gamma(n+2)} S^{\alpha+\eta} D^{(-n-1)} S^{-\alpha} D^{(n+1)} S^{-(\beta+\eta)}$$

$$D^{(n+1)} S^{2n+\beta+1} \phi^{(n)}(S) = f(s)$$

for all positive s.

Theorem 25. If $f(y) \in$ L in $0 < y < \infty$ and if $f(x)$ is defined by the convergent integral (i) then the relation

$$\lim_{n\to\infty} (-)^n \frac{\Gamma(n-1+\alpha)}{\Gamma(n-1+\beta)\Gamma(n-1)\Gamma(n+1)} \int_0^\infty e^{-sx} s^{n-1} x^{-\eta-\alpha-1} \times$$

$$D'^{(-n)} x^{\alpha} D'^{(n)} x^{\beta+\eta+2n} D'^{(n)} \{x^{\beta} F(x)\}\, dx \qquad = f(s)$$

holds for all positive values of s.

In Chapter Nine we have defined a generalization of Laplace transform in two variables known as Dr. S. M. Joshi Generalized two variable Laplace Transform. We have given a convergence theorem for it together with certain rules in operational calculus for this transform. We have proved.

Theorem 26. If the integral

$$F(p,q) = \left\{ \frac{\Gamma(\beta+\eta+1)}{\Gamma(\alpha+\beta+\eta+1)} \right\}^2 \times$$

$$\times \int_0^\infty \int_0^\infty {}_1F_1(\beta+\eta+1;\, \alpha+\beta+\eta+1; -xp) \times$$

$$\times\ {}_1F_1\,(\beta+\eta+1,\ \alpha+\beta+\eta+1;-yq)\quad (xpyq)^{\beta}\,f(x,y)\,dx\,dy.$$

converges boundedly at the point (p_0, q_0) then it converges at all points (p, q) provided that Re $\beta \geqslant 0$ Re $\eta > 0$ with an additional condition Re $(p-p_0) > 0$ Re $(q-q_0) > 0$ in case $\alpha = 0$ or Re $p < 0$ Re $q < 0$.

In Chapter Ten we have used operators of fractional integration and differentiation to develop the theory of Generalized Hankel transforms (2) and (3) written in slightly changed forms

$$\text{(viii)}\quad F(x) = (\tfrac{1}{2})^{\lambda}\int_0^{\infty} (xy)^{\lambda+\frac{1}{2}} J_{\lambda}^{\mu}\left(\tfrac{1}{4}x^2\,y^2\right)^{\mu} f(y)\,dy$$

$$\equiv H^{\mu}_{\lambda+\frac{1}{2},\ \lambda}\, f(y)$$

$$\text{(ix)}\quad F(x) = \int_0^{\infty} (xy)^{\nu} J_{\lambda}^{\mu}(xy)\, f(y)\,dy$$

$$\equiv h^{\mu}_{\nu,\ \lambda}\, f(y)$$

we prove.

Theorem 27. If n is a positive integer

$f(x) = 0\ (x^{\alpha})\ (x \to 0)$

$0\ (x^{\beta})\ (x \to \infty)$

(a) $F(x) + H^{\mu}_{x+\frac{1}{2},\lambda}\ F,\ g(z) = I^{-}_{x+\frac{1}{2},\ n}\ F$

$G = I^{-}_{\lambda+\frac{1}{2},\ n}\ F$ then

$G = \mu\, H^{\mu}_{\lambda+\frac{1}{2}}\ {}^{+2\mu n_1}\ \lambda + (\mu+1)n^{g}$

provided that

$$\lambda + \alpha + \frac{3}{2} > 0,\ \lambda + \frac{3}{2} < 0,\ \beta + 1 < 0,\ 0 < \mu \leqslant 1$$

(b) $F = \mu\, H^{\mu}_{\lambda+\frac{1}{2}}\ +2\mu n,\ \lambda+(\mu+1)_{n}f$

$G = K^{+}_{\lambda+\frac{1}{2},\ n} F,\ G = K^{+}_{\lambda+\frac{1}{2},\ n} F$ then $G = H^{\mu}_{\lambda+\frac{1}{2},\ \lambda}\, g.$

Theorem 28. If F (x) is given by the relation (iii) and $f(y)$ belongs to $L_2\,(0, \infty)$ then F (x) exists and also belongs to $L_2\,(0, \infty)$.

Theorem 29. If n is a positive integer $0 < \mu \leqslant 1$,

$f(y) \in L_2\,(0, \infty)$ and $F = h^{\mu}_{\frac{\lambda}{2},\lambda} f\ g = I^{+}_{\frac{\lambda}{2},\ x} f$

$G = I^{-}_{\frac{\lambda}{2},\ n}$ F then $G = h^{\mu}_{\frac{\lambda}{2}+\mu n,\ \lambda+(\mu+1)_n}$

(*b*) $F=\mu\, h^{\mu}_{\frac{\lambda}{2}+\mu n,\ \lambda+\ (\mu+1)n}\, f$

$g=K^{-}_{\frac{\lambda}{2},n}\, f$, $G=K^{-}_{\frac{\lambda}{2},n}\, F$ then $G=h^{\mu}_{\frac{\lambda}{2},\lambda}$

Theorem 30. If $g\,(t) \in L_2\,(0,\infty)$ and $\tau^{n}\, g_1\,(\tau) \in L_2\,(-\infty,\infty)$

Also if (*a*) $G=\mu h^{\mu}_{\frac{\lambda}{2}+\mu n,\ \lambda+\ (\mu+1)n}\, g$

then the functions $f=(I^{+}_{\frac{\lambda}{2},n})^{-1} g$ and $F=(I^{+}_{\frac{\lambda}{2},n})^{-1} G$

exists, belong to $L_2\,(0,\infty)$ and $F=h^{\mu}_{\frac{\lambda}{2},\ \lambda}\, f$.

(*b*) $G=h^{\mu}_{\frac{\lambda}{2},n}\, g$ then $\tau^{n}\, G,\ (\tau) \in L_2\,(-\infty_1\,\infty)$ the functions $f=(K^{+}_{\frac{\lambda}{2}}, n)^{-1} g$

and $F=(K^{+}_{\frac{\lambda}{2},n})^{-1} G$ exists, belong to $L_2\,(0,\infty)$ and $F=h^{\mu}_{\frac{\lambda}{2}+\mu n,\,-7+(\mu+1)n}\, f$

provided that in both the cases Re $(\lambda)-1$.

Theorem 31. If the conditions of Theorem 28 are satisfied and

(*a*) $G=\mu H^{\mu}_{\lambda+\frac{1}{2}+2\mu\, n,\ \lambda+\ (\mu+1)n}\, g$

g is given representable in the form $g=I^{-}_{\lambda+\frac{1}{2},n}\, f$

then also G is representable in the form $G=I^{-}_{\lambda+\frac{1}{2},n}\, F$

where $F=H^{\mu}_{\lambda+\frac{1}{2},\ \lambda}\, f$.

(*b*) $G=H^{\mu}_{\lambda+\frac{1}{2},\ \lambda}\, g$, g is representable in the form $g=K^{+}_{\lambda+\frac{1}{2},n}\, f$, then also G is representable in the form $G=K^{+}_{\lambda+\frac{1}{2},n}\, f$ and $F=\mu H^{\mu}_{\lambda+\frac{1}{2}+2\mu\, n,\ \lambda+(\mu+1)\, n}\, f$

Theorem 32. If $F\,(x)=h^{\mu}_{\frac{2}{\mu},\lambda}\, f$ then

$$x^{l}\ F\,(x)=h^{\mu}_{\frac{2}{\mu},\,\lambda-\frac{l}{\mu}} \left(\frac{\partial}{\partial y}\right)^{l} f\,(y)$$

Theorem 33. If

$$\phi(s) = \int_0^\infty S^{\nu - \frac{\lambda+1+r}{\mu}} F(x) \times$$

$$\sum_0^\infty \frac{\Gamma(\mu+2m+1-\nu+r)}{\Gamma(\frac{3}{2}+\mu+m-n-\gamma+r)} \times \frac{\Gamma(\mu+1-\gamma+r)}{\Gamma\left\{\frac{1+\lambda+r}{\mu}\right\}} x^{\frac{\lambda+1+r}{\mu}-\nu-1} dx$$

where F (x) is defined by the convergent integral (iii) then for almost all positive t

$$\underset{n\to\infty}{l.\overset{p}{i}.m.}\ L_{n1t}\ [\bar{K}_{\frac{1}{2}+m-k_1-\frac{1}{2}+m+k}\{\phi(s)\}] = f(t)$$

provided that $\frac{1}{2} \leqslant \mu \leqslant 1$, Re $\lambda > -1$ with an additional condition Re $(\frac{1}{2}\lambda + \frac{3}{4} - m + \nu + |m|) < \frac{1}{2}$ $f(y) \in Lp$ $(1 \leqslant p < \infty)$ in $0 \leqslant t \leqslant R_1$ $2m > -\frac{1}{\surd}$ when $\frac{1}{2} - m - k > 0$

$\frac{1}{2} + m - k > -\frac{1}{q}$ when $\frac{1}{2} - m - k < 0$, $\int_0^\infty e^{-yx} f(y)\, dy$ converges

and

$$L_{n1t}\ [G(x)] = \frac{(-)^n}{n!}\left(\frac{n}{t}\right)^{n+1} G^{(n)}\left(\frac{n}{t}\right)$$

Theorem 34. If $\phi(s) = \int_0^\infty S^{+\gamma - \frac{\lambda+1+r}{\mu}} \times$

$$\times \sum_0^\infty \frac{\Gamma(k+m+2+\mu-\gamma+\lambda)\ \Gamma(k-m+2+\mu-\gamma+r}{\Gamma(\mu+2-\gamma+r)\ \Gamma\left\{\frac{(1+\lambda+r)}{\mu}\right\}} \times$$

$$\times\ x^{\frac{\lambda+\mu r}{\mu} - \gamma - 1} F(x)\, dx$$

where F (x) is given by the convergent integral (iii) then for almost all positive t

$$\lim_{q\to\infty} V_{q_1 t}\ \{\phi(s)\} = f(t)$$

provided that $\frac{1}{2} \leqslant u \leqslant 1$, Re $\lambda > -1$ with an additional condition

Re $\left(\frac{\lambda}{2} + \gamma - k - \frac{1}{4}\right) < \frac{1}{2}$ in case $\mu = 1$, $0 < k + m < 1 V_{q,\,t}[f(x)] = \frac{(-)^q t^{-1}}{\Gamma(q)}$

$$\left[x^{q-k-m}\left(\frac{d}{dx}\right)^q \left\{x^{k+m} f(x)\right\}\right]_{x=\frac{q}{t}} \qquad u = 1_1\ 2_1 -$$

Theorem 35. If $\phi(s) = \int_0^\infty S^{\gamma - \frac{\lambda+1+r}{\mu}} \times$

$$\times \sum_{0}^{\infty} \frac{\Gamma(\mu+2m+1-\gamma+r)\Gamma(\mu+1-\gamma+r)}{\Gamma(\frac{1}{2}+\mu+m-k-\gamma+r)\,\Gamma\left\{\frac{1+\lambda+r}{\mu}\right\}}\, x^{\frac{\lambda+1+r}{\mu}-\gamma-r}\, F(x)\, dx$$

where $F(x)$ is given by the convergent integral (iii) then for almost all positive u.

$$\lim_{\mu\to\infty} V_{q,u}[\phi(s)] = f(u)$$

where

$$V_{q,u}[f(x)] = \frac{(-)^{q} u^{-1}}{\Gamma(q+k+m-\frac{1}{2})} \left[x^{m-q-\frac{1}{2}-\frac{1}{2}} D^{q} \left\{ x^{k-m+\frac{1}{2}} f(x) \right\} \right]_{x=\frac{q+k+m-\frac{1}{2}}{n}}$$

provided that

$\frac{1}{2} \leqslant \mu \leqslant 1$, Re $\lambda > -1$ with an additional condition Re $(\frac{1}{2}+\lambda+\frac{3}{4}-m-\gamma+|m|) < \frac{1}{2}$ in case $\mu=1$, $f(y)$ is integrable in $0 \leqslant y \leqslant R$ for every positive R, $\int_{0}^{t} f(u)\, du = 0\, (e^{\gamma t})$ for some γ $(t\to\infty)$.

Theorem 36. If $\phi(s) = \frac{S^{2\gamma}}{\mu} \int_{0}^{\infty} x^{-2\gamma-\lambda-\frac{3}{2}} \times$

$$\times\, G^{\mu}_{1+\lambda+\mu\nu} \left(\frac{S^2}{x^2}\right) \gamma - (x)\, dx$$

where $F(x)$ is given by the convergent integral (ii) then

$$f(u) = \frac{1}{i}\left(\frac{1}{2\pi}\right)^{\frac{1}{2}} \int_{c-i\infty}^{c+i\infty} (ux)^{\frac{1}{2}}\, I_{\nu}(xu)\, \phi(x)\, dx$$

provided that Re $\lambda > -1$, $f(x) = 0(x^{\alpha})$ $(x\to 0)$ $f(x) = 0(x^{\beta})$ $(x\to\infty)$ Re $(2\gamma+\alpha+\lambda+\frac{3}{2}) > 0$ and $f(y)$ such that $\phi(s)$ exists and the conditions of Meijer's complex inversion formula are satisfied.

ABSORPTION AND FLUORESCENCE SPECTRA, HYPERFINE STRUCTURE AND THE ZEEMAN EFFECT OF Ho^{3+} IN HEXAGONAL $LaCl_3$ AT VERY LOW TEMPERATURES*

Bhuwan Chandra Pandey†
Department of Physics,
The Johns Hopkins University, Baltimore, Maryland, 21218 U. S. A.

Summary

In this thesis the author has obtained experimentally the fluorescence and absorption spectra of Ho^{3+} in hexagonal $LaCl_3$ at temperatures from 2° to 77°K. The Zeeoman effect in magnetic fields from 150 to 35000 gauss, both parallel and perpendicular to the crystal axis, and the nuclear hyperfine structure of many lines, with and without magnetic field, have been studied. The results have been interpreted by means of the crystal field theory and the theory of complex atoms.

The object of this work has been to identify the energy levels of Ho^{3+} in $LaCl_3$. The crystal spectra of Ho^{3+} arise due to the transitions within the states of the well-shielded $4f^{10}$ configuration. At very low temperatures the energy levels become very sharp, and this results in sharp spectral lines. In crystals, a free ion state splits into a number of levels, depending upon the J-value of that state and the summetry of the crystal field; these levels are called the Stark components. Classification of these crystal field levels can be made empirically by studying the absorption, fluorescence spectra, hyperfine structure and the Zeeman effect of this crystal. In conjunction with the experimental results, crystal field calculations are of great help.

Crystals of 0·1%, 1%, 2%, and 2·5% Ho^{3+} in $LaCl_3$ were used in this investigation, of which the first three were from 1 to 2 mm thick, the last was 9 mm. These crystals were sealed separately, inside quartz tubes, in an atmosphere of dry helium gas.

The absorption spectra were photographed with a 21-ft concave grating in a Paschen mounting; this grating was 7″ wide, with 30000 lines per inch. The dispersion of this instrument was 1·2 Å/mm in the first order, and in this order the resolving power was at least 150000. It was used in the first order above 5000 Å and below this in the second order. Spectra between 2700 and 3300 Å were photographed in the third order also.

For the 0·1% and 1% crystals, the absorption spectra were photographed at 4·2°K, from 3200 to 6700 Å and 3200 to 9200 Å, respectively. The spectra of the 2% crystal were photographed from 2450 to 9200 Å at 2°K, and those of the 2·5% crystal, from 2600 to 9200 Å at 4·2°K and to 6700 Å at 77°K.

---

* Abstract of the thesis approved for the degree of Doctor of Philosophy by the Agra University.

† Present address—Department of Physics, Punjab University, Chandigarh.

For photographing the absorption spectrum in the range 10800 to 12600 Å, a 3·4-meter, plane grating, Fastie spectrograph was used. The dispersion of this instrument was 4·5 Å/mm in the first order. The absorption spectrum of only the 2·5% crystal was recorded in this range at 4·2°K.

The spectra were studied in both σ and π polarizations. For the 2·5% crystal and one of 2% Ho^{3+}, the helium pressure inside the tube containing the crystals was low—from 1 to 2 cm—while for the other crystals the pressure was about 40 cm. Using a low pressure of helium gas results in some conduction of heat between the crystal and the coolant; the crystal was therefore at a little higher temperature.

The light source for the absorption experiments between 2450 and 3000 Å was a xenon arc, and between 2600 and 6700 Å, a high pressure mercury (GE-AH6) lamp. A tungsten lamp was used for experiments from 5000 to 12600 Å, and in some experiments between 9200 and 12600 Å, a zirconium lamp was also used. Overlapping of the orders was avoided by using suitable Corning filters.

At 4·2°K there are 70 lines in the π polarization and 107 in the σ polarization. These lines constitute 23 groups, which are designated by A, B, C, etc., through W. At 2°K some of these lines disappear, while at 77°K many extra lines appear, and the lines become very broad.

Most of the fluorescence work and some absorption work was done with a 21-foot concave grating in a Wadsworth mounting. It was used in the first order above 5300 Å; the dispersion in this order was 5Å/mm. In a few cases the spectra were photographed in the second order up to 6200 Å.

The fluorescence spectra of the 2% crystal were photographed at 77° and 4·2°K in the range 4000-10600 Å and 3500-10600 Å, respectively. The spectrum of this crystal was also photographed with the Paschen spectrograph from 3500-7800 Å at 4·2°K. In the earlier fluorescence spectrum there were many impurity lines of Sm^{2+}, Sm^{3+} Nd^{3+} and Pr^{3+}, and purer chemicals were therefore used for other crystals.

The fluorescence spectra of the 0·1% and 1% crystals were photographed with the Wadsworth spectrograph in the range 4000 Å to 10600 Å at 4·2°K. No fluorescence studies were made for the 2·5% crystal.

A high pressure mercury lamp (GE-AH6) was used for exciting the fluorescence spectrum. In some special experiments a 6V 108W tungsten ribbon filament lamp was used for exciting the fluorescence spectrum. The exciting band was selected by suitable filters.

Monochromatic excitation experiments were very often necessary, and in such cases either an interference filter or a 1-meter Ebert monochromator was used. Such experiments were made when the temperature of the crystal had to be kept very low, or when fluorescence groups having different upper and lower states fell upon one another and had to be separated. Due to the weak intensity, no polarization experiments were made in fluorescence.

At 4·2°K, 354 lines were observed in fluorescence, and 249 of these constitute 30 groups: the B, D, E, F, J, and M to the Z state; the D, E, F, K, M, P and Q to the Y state; the F, J, K, M, P and Q to the A state; the J, K, M, and Q to the B state; K, P and Q to the C state; and Q to the D, E, and G states. Z is the ground state and Y is the first excited state.

Moncochromatic excitation experiments were made to study the energy transfer in the excited states of Ho^{3+}; in these a f/6 plane grating spectrograph with a focal length of 30″ was used to photograph the spectra. The dispersion of this instrument was 16 Å/mm in the first order, with a range of 3700 Å in one setting. The fluorescence was obtained for the 1% crystal from 3500 Å to 7200 Å at 4·2°K; and for the 2% crystal, in the range 3500-7200 Å and 3000-9100 Å at 77° and 4·2°K, respectively. All the levels from D to S were excited monochromatically one by one for these experiments.

Energy transfer studies yielded evidence of ion-pair resonance process. Energy transfer to a lower level was conspicuous whenever these two levels were separated by almost the same energy as that of the Y state. This could be understood if the ion pair had a transition to the Y state.

The Zeeman effect studies were made in absorption for the 2% crystal in both parallel and transverse orientation at 2° and 4·2°K, from 3000-6700Å, at various field strengths from 6000 to 35000 gauss. A temperature of about 20°K was used for parallel orientation.

The electromagnet used for the Zeeman effect work was supplied by Messrs. Arthur D. Little, Cambridge, Massachusetts, U.S.A. The field could be varied by varying the current through its coils.

The 2°K temperature was obtained by pumping liquid helium at 3 to mms; and a temperature of around 20°K was obtained by enclosing the crystal in low-pressure helium (1—2 cm) within a quartz tube, immersing this tube in liquid helium (4·2 K), and focusing the light from a zirconium lamp on the crystal.

In the parallel Zeeman effect, most of the lines were split into two components and the higher wavelength component became weak with increasing magnetic field and was absent for fields above 15000 gauss. In some cases extra lines also appeared in the magnetic field and showed shifts with the change in field strength.

In the transverse Zeeman effect, the polarization rules were violated. The field free lines were split into two or four components; in addition, a few extra lines also appeared, and their intensity increased with the field. These lines, very conspicuous in the I, J, and M groups, show the two-line pattern in a transverse magnetic field.

Existence of the hyperfine structure in some of the absorption lines was first revealed in the Paschen plates taken for the 2% crystals. These experiments were repeated for a 0·1% crystal, and the hyperfine structure was found to be resolved for even some of those lines for which it was unresolved for the 2% crystal.

The hyperfine structure of the 0·1% and 2·5% crystals was re-photographed at 4·2°K with a 5-meter, plane grating, Ebert-Fastie spectrograph. The width of the grating was 10″, with 7500 lines per inch, and it was blazed at 5·9μ. The dispersion of this spectrograph was 2Å/mm in the first order, and it had a resolving power of 600,000 in the 9th order. The hyperfine structure was photographed from 3850—9200Å, from the 15th to 7th order, depending upon the wavelength of the absorption group. For strong lines the 0·1% crystal was very suitable; for the weaker lines, the 2·5% crystal was used.

The hyperfine structure of a line consisted of eight components. It was measured for 26 lines. In various lines, the hyperfine structure splitting interval, or the separation between two successive hyperfine structure components, varied from 0·072 cm^{-1} to 0·232 cm^{-1}. The hyperfine structure components were very sharp (line width, 0·04 cm^{-1}) for some lines, for others they were less sharp, and in some cases very broad. In the J_1 line, besides the usual eight components, there were a few extra lines.

In addition to the lines showing hyperfine structure, there were other types of lines; one of which was a very sharp, single line, nearly as wide as the single component of a line showing hyperfine structure with sharp components. There were also wide lines with sharp edges; a few with diffuse edges; and a few lines which were very broad and diffuse (line width, 10 cm^{-1} or more).

The Zeeman effect of the hyperfine structure in absorption was studied for the D and J groups at 4·2°K, at various magnetic fields from 150 to 35,000 gauss, with the 5-meter, plane grating, Fastie spectrograph. Studies were made in great detail for the parallel orientation and in somewhat lesser detail for the transverse orientation.

The point group symmetry of $LaCl_3$ is C_{3h}, and the energy levels of Ho^{3+} in it split into a number of Stark components. The ground state of Ho^{3+}, according to Hund's rule, is $^5I_8$ and the higher groups up to M can be easily identified with the corresponding free ion groups. The various Stark components of a state can be designated by the crystal quantum number, μ, where μ can have values 0^+, 0^-, ± 1, ± 2, 3^+ and 3^-. From the Zeeman effect and the crystal field calculations, the lowest Stark component of the ground state, Z_1, should have $\mu=1$. From the calculations, the next higher Stark component, Z_2, has $\mu=0^+$.

At very low temperatures only Z_1 is populated and absorption takes place from this state to the Stark components of the excited states. If the temperature is raised, some of the higher Stark components of the ground state are also populated and absorption takes place from these levels also.

In the fluorescence emission at very low temperatures, only the lowest Stark component of an upper state is populated, and from it transitions take place to the Stark levels of the lower states. If the temperature is higher, the higher Stark components of the upper state are also populated and participate in the fluorescence emission. The transitions in both fluorescence and absorption are predominantly electric dipole. The following are the selection rules.

Electric dipole: $\Delta\mu=\pm3(\pi), \Delta\mu=\pm2, \pm4(\sigma)$

with the subsidiary rules that only the following transitions are allowed :—

$0^+ \longleftrightarrow 3^+ \quad 0^- \longleftrightarrow 3^- \quad (\Delta J=\text{odd})$

$0^+ \longleftrightarrow 3^- \quad 0^- \longleftrightarrow 3^+ \quad (\Delta J=\text{even})$

Magnetic dipole: $\Delta\mu=\pm1, \pm3(\pi), \Delta\mu=0, \pm5(\sigma)$ $(\Delta J=0, \pm1)$

with the subsidiary rules allowing :—

$0^+ \longrightarrow 0^+, \quad 0^- \longrightarrow 0^- \quad (\Delta J=\text{even})$

$0^+ \longrightarrow 0^-, \quad 0^- \longrightarrow 0^+ \quad (\Delta J=\text{odd})$

One of the surest methods for determining the assignment of μ values to the various Stark components is the Zeeman effect. In a parallel magnetic field a level should split† into two components separated by $\Delta E=2M^*g$, where $M^*=\sum_i |a_i|^2 M_i$, a_i are the mixing coefficients and M_i are the corresponding M values. For a level with $\mu=0$ or 3, $M^*=0$, and for a level with $\mu=1$ or 2, $M^*\neq0$.

The ground state of Ho^{3+} in $LaCl_3$ has $M^*=6{\cdot}477$, according to the calculations. If the upper state has $M^*>0$ or $=0$ or <0, then a single line should split in a parallel magnetic field into two lines separated by the sum of the splittings of the upper and ground states, equal to that of the ground state or to the difference of the splittings of the upper and lower states.

Holmium consists of only one isotope, with mass 165, spin $I=\frac{7}{2}$, and the nuclear magnetic moment of 3·3 nuclear units. It can be shown that the hyperfine structure splitting of a Ho^{3+} level is given by $\Delta E_{hfs}=qM^*I_z$, where q is approximately constant for a configuration, I_z assumes eight values from $-\frac{7}{2},\ldots+\frac{7}{2}$, so that the spacing of eight equidistant components is given by M^*, the same quantity which also determines the Zeeman splitting in a parallel magnetic field.

---

† Lorentz units.

If the upper level has $M^*>0$, or $=0$ or <0, the resulting line should show a hyperfine structure having a separation equal to the sum of the hyperfine splitting of the two levels, or equal to that of the ground level or to the difference of the two levels, respectively.

The hyperfine structure splitting interval of the ground state varies from 0·162 cm^{-1} between the two lowest components, to 0·187 cm^{-1} between the highest ones.

An analysis of the fluorescence spectrum is very helpful in the classification. In some cases there are many transitions to the same final state, and complete information about this state is often obtained from fluorescence. The level with $\mu=0$ cannot be observed in absorption under ordinary conditions, but it can be obtained easily from fluorescence, since the upper level can have $\mu=3$ or 2, both of which can combine with a $\mu=0$ level.

Once the μ values for the various Stark components of the states of Ho^{3+} are known, the causes of line widths and many other interactions observed in the magnetic field can be understood.

The sharpest levels are the Stark components of long-lived fluorescing states, since $\Delta\nu\Delta t \sim 1$, and if Δt is larger, $\Delta\nu$ will naturally be narrow. Even the lowest Stark components of non-fluorescing states are decidedly less sharp, although the hyperfine structure is still distinct. The origin of single sharp lines, which appear at slightly elevated temperatures, can be understood from a different reasoning. Such sharp lines are due to a transition from the $Z_2(0^+)$ state to an upper state with $\mu=3$. For both these states, $M^*=0$, they have a vanishing hyperfine structure, and the resulting lines should be sharp.

In the parallel Zeeman effect, two states having the same μ values interact and give rise to nonlinear effects. If one of these levels can combine with a lower state, the other level can also combine with the latter, even if it is a forbidden line. The shift in energy due to this interaction is given by

$$\varepsilon'=\pm\frac{\delta}{2}\left(1-\sqrt{1+a^2}\right)$$

where δ is the energy difference between the two interacting levels, $a=\frac{2H}{\delta}$ $H_{1,11}=g\beta BM^{**}$, $M^{**}=\Sigma_1 a_1' a_1'' M_1$, and a_1', a_1'' are the mixing coefficients, β is the Bohr magneton, B the magnetic field and g the Landé splitting factor.

Similarly the M^* value, which is zero in zero magnetic field, changes to

$$\pm\frac{3a}{\sqrt{1+a^2}}$$

for the $\mu=3^{\pm}$ states; where $a=\frac{2H}{\delta}$ and $H=3\beta gB$. Thus the upper state has a nonvanishing hyperfine structure in a magnetic field and it changes with the field.

Some of the lines show an anomalous behaviour in that they have only seven components instead of the usual eight in the magnetic field. In this disturbed pattern, one of the lines is usually stronger and is isolated by a wider than normal interval from its neighbors.

For some lines the anomalies consist of irregular structure and blurring of lines, and the virtual disappearance of a line for a wide range of fields. These anomalies are due to the interaction of two levels in a transverse magnetic field. These interacting levels, with μ and $\mu \pm 1$, come very close to one another for a certain range of magnetic field and interact strongly.

The appearance of extra lines with $\mu=0$ is also due to the interaction with a $\mu=1$ level in a transverse magnetic field.

The crystal field calculations were made with a computer and the use of the free ion wave functions of Ho^{3+} in intermediate coupling. The crystal field parameters were found by using the empirical values of the ground state Stark components and varying the parameters to give the best fit between the empirical and calculated values. The crystal field parameters are

$$B_2^0=122,\ B_4^0=-45,\ B_6^0=-28,\ B_6^6=286$$

With these parameters calculations were made for the states up to the J group. The calculations were not satisfactory for higher states and only the calculated values for the Z, Y, A, B and C states are given.

INVESTIGATIONS ON THE STRUCTURE OF THE HEMICELLULOSES FROM BAGASSE*

BIMAL CHANDRA BANERJEE†
Department of Organic Chemistry, National Sugar Institute, Kanpur.

The present investigations had been carried out, primarily to isolate a homogeneous polysaccharide from the bagasse hemicellulose and establish its chemical constitution, by graded hydrolysis, methylation and periodate oxidation studies.

ANALYSIS OF THE BAGASSE

The bagasse was dried in the sun and powdered. The powdered material (40 mesh) was used for all the investigations carried out. The analytical data of the bagasse are given in table 1.

TABLE 1

		Original Bagasse %	*Defatted Bagasse%*
1.	Alcohol-benzene soluble portion	7·6	—
2.	Water soluble portion	6·6	3·6
3.	Carbonated ash/Sulphated ash	7·2/8·0	3·2/3·2
4.	Nitrogen	0·3	0·2
5.	Pentosans	23·2	26·2
6.	Available furfuraldehyde	13·4	15·4

ISOLATION OF THE HEMICELLULOSE

The hemicellulose was isolated, by first defatting the bagasse (alcohol-benzene 2 : 1) and then subjecting it to sodium chlorite oxidation in a slightly acidic medium (pH 4·5), and extracting the holocellulose produced with increasing concentrations of alkali. Each alkali extract was separately acidified (pH 4·5) with glacial acetic acid and precipitated with rectified spirit (3—4 volumes). Three fractions of the hemicellulose were thus isolated (2% Na_2CO_3, 4% KOH and 10% KOH fractions; yields, 3·1%, 17·5% and 8·6% respectively). Each fraction was separately soxhletted with 50%, 80%, 95% and finally absolute ethanol (4 hours each), dried and powdered, when the three fractions of the hemicellulose were obtained as milk-white powders. The 4% caustic potash fraction, which was obtained in the highest yield

---

* Abstract of the thesis approved for the degree of Doctor of Philosophy by the Agra University, Agra.
For details, please consult the papers under references 1 to 4.

† Present address—Department of Chemistry, D. A. V. College, Kanpur.

(analytical results : methoxyl 2·1%, carbonated ash 1·7%, sulphated ash 1·9%, pentosans 90·1%), had been used in these investigations.

THE NATURE OF THE SUGARS PRESENT IN THE BAGASSE HEMICELLULOSE

The hemicellulose (18 gms.) was completely hydrolysed with 2N-sulphuric acid and the hydrolysate, after neutralisation with barium carbonate was concentrated to a syrup. Treatment of the syrup with absolute methanol gave two fractions. Fraction I was the precipitate of the barium salt of the uronic acid (yield 0·46 gms.), while Fraction II (17·5 gms.) consisted of the methanolic solution of the neutral sugars.

Fraction I—The uronic acid gave a single pink spot on paper chromatography (p-anisidine phosphate spray reagent), indicating that the fraction might be galacturonic acid.[5] The fraction was identified by converting it into the brucine galacturonate (m. p. 177° *d*, Lit.[6] m. p. 180° *d*). The presence of galacturonic acid in this fraction was confirmed, by refluxing it with 5% methanolic hydrogen chloride, and reducing the derived methyl glycoside with sodium borohydride[7], and subsequent hydrolysis, when galactose was identified by paper chromatography (Solvent[8]: Ethyl acetate pyridine-water, 1 : 2 : 2).

Fraction II—The methanolic solution of the neutral sugars was concentrated to a thin syrup, and a portion of it was subjected to cellulose column chromatography (Solvent : *n*-butanol, half-saturated with water), when four sugars were obtained in the pure state, which were identified as detailed below :

1. *DL—Xyloketose*—The ketonic nature of the sugar was established by paper chromatography, using specific spray reagents for ketoses. Thus *p*-anisidine phosphate[9], sodium meta-periodate benzidine B-benzidine A[10], and resorcinol-ethanolic hydrogen chloride[11] gave lemon-yellow, yellow against grey back-ground, and blue spots respectively. The last colour is specific for a Keto-pentose[11].

The osazone of the sugar showed the characteristic crystalline features of xylosazone. The melting point of the osazone (202°—204°) was considerably depressed (140°—150°) by mixing with authentic samples of D-xylosazone (m. p. 160°—161°) and L-arabinosazone (m. p. 156°). The high melting point of the osazone indicated that it might be the DL-xylosazone, (Lit.[12] m.p. 207°). The identity of the osazone was established by conducting its paper chromatography on a borax-buffered (pH 9·6) Whatman No. 1 filter paper, using 75% dioxan-hexane-water-benzene (55 : 50 : 25 : 20, upper layer), as the irrigating solvent[13], when the osazone moved at the same rate as an authentic sample of D-xylosazone. The corresponding sugar was thus identified as DL-Xyloketose, (DL-xylulose, DL-threo-pentulose).

Xyloketose is one of the rare sugars, which has considerable importance in the biochemistry of plants,—in its influence on the germination of seeds, and also as an intermediary in the biosynthesis of ascorbic acid. However, no reference is found in the Literature for the isolation of xyloketose from plant polysaccharides. Hence the isolation of DL-xyloketose from bagasse hemicellulose is of considerable importance from theoretical considerations.

2. *D-Xylose*—The sugar, $\left[\alpha\right]_D^{30}+17{\cdot}5°$, m.p. 143°—144°, was identified by converting it into (a) D-xylosazone, m.m.p. 160°—161°; (b) the *p*-nitro phenyl hydrazone of D-xylose, m.m.p. 154°—155°; and (c) the di-O benzylidene dimethyl acetal of D-xylose[14], m.m.p. 206°—207°.

3. *L-Arabinose*—The sugar, $\left[\alpha\right]_D^{30}+78{\cdot}4°$, was identified as the *N*-(*p*-nitro phenyl)-*L*-arabinosyl amine, m.m.p. 200°.

4. *D-Glucose*—The sugar, $\left[\alpha\right]_D^{30}+47{\cdot}4°$, was identified as the *N*-(*p*-nitro phenyl)-*D*-glucosyl amine, m.m.p. 179°.

ISOLATION OF THE ALDOBIOURONIC ACID

The hemicellulose (30 gms.) was hydrolysed with 0·1 *N*-sulphuric acid, the course of the hydrolysis being followed by iodometric titrations[17]. The hydrolysate on being worked up[15], gave the barium salt of the aldobiouronic acid in low yield (2·6%, Ba as $BaSO_4$, 17·3%).

Attempts were also made for isolating the aldobiouronic acid by following the procedure described by Srivastava and Adams[8], by hydrolysing the powdered bagasse with 0·5 *N*-sulphuric acid. The aldobiouronic acid (R-xylose 0·6, Solvent[8] : ethyl acetate—acetic acid—formic acid—water, 20 : 3 : 1 : 4) was obtained in very low yield 0·9%).

It was then concluded that the uronic acid was not present as a regular building unit of the bagasse hemicellulose. This pointed out the possibility that the bagasse hemicellulose might be a neutral polysaccharide of the xylan type, (percentage of D-xylose in the bagasse hemicellulose was found to be 83·7%).

ISOLATION OF THE XYLAN

The xylan was isolated from the bagasse hemicellulose (4% KOH fraction, 18 gms.), by following the procedure described by Chanda, *et al*[16]. The xylan was soxhletted with increasing concentrations of ethanol (*loc. cit.*) and dried, (sulphated ash 0·33%, pentosans 98·6%, methoxyl 0·25%; yield 8·0 gms.). The xylan on hydrolysis gave a single spot, corresponding to D-xylose only on paper chromatographic examination; no other sugar or uronic acid could be detected. The amount of xylose obtained by the complete hydrolysis of the xylan was estimated[17,18] and corresponded to 98·3%. Since β-methyl xyloside on being treated with dilute sulphuric acid, under the experimental conditions of hydrolysis, results in the loss of 2% xylose[16], the whole of the polysaccharide had been accounted for as a xylan of at least 99·5% purity.

METHYLATION OF THE XYLAN

The xylan (5·6 gms.) was methylated nine times with dimethyl sulphate and caustic soda, followed by fractionation with petroleum ether containing increasing concentrations of chloroform[16]. One of the fractions (1·6 gms.), having $\left[\alpha\right]^{20}_{D}$ 14·6°—14·6° (in chloroform), had the methoxyl value of 37·8%. This fraction on two more methylations with Purdie's reagent in acetonic solution gave the fully methylated xylan, having $\left[\alpha\right]^{20}_{D}$ —14·6° and methoxyl value of 38·2%, (calc. for $C_7H_{12}O_4$, OMe 38·7%); yield 1·35 gms.

HYDROLYSIS OF THE METHYLATED XYLAN

The methylated xylan was subjected to methanolysis with 2% methanolic hydrogen chloride. The methanol and hydrogen chloride were removed by distillation, and the resulting methyl glycosides of the methylated xyloses were hydrolysed with aqueous (0·5 N) hydrochloric acid. The hydrolysate after the usual treatments[16], gave a syrup (1·3 gms.), which showed the presence of five sugars. The sugars were separated by paper chromatography and estimated by the hypoiodite oxidation method[17]. The results of the analysis were, (a) trimethyl xylose; (b) dimethyl xylose; (c) mono-methyl xylose; (molar percentages 2·86, 93·7, and 3·26 respectively). The yields of an unidentified sugar and D-xylose, being very small were neglected. Since the tri-methyl xylose could be obtained only from the non-reducing end-groups, the amount of the tri-methyl xylose obtained indicated the presence of one non-reducing end group in a straight chain of 35 xylose units, or 70 xylose units, if the polymer had one branch.

Similar results were obtained by separating the different methylated sugar components on Whatman No. 3 MM filter papers, eluting the filter paper strips with water, weighing and identifying the different methylated xyloses by measuring the optical rotations and noting the melting points of their characteristic aniline derivatives. The constituent methylated xyloses were thus identified as (a) 2 : 3 : 4-tri-O-methyl-D-xylopyranose; (b) 2 : 3-di-O-methyl-D-xylopyranose; and (c) 2 : 0-methyl-D-xylopyranose; (molar percentages 2·98, 93·1 and 3·93 respectively). The molar percentage of the tri-methyl xylose (yield 0·039 gms.) indicated the presence of 33—34 xylose units in an assumed straight chain, or 66—68 xylose units, if the polymer had one branch.

The presence of the 2 : 3-di-O-methyl-D-xylopyranose indicated that the xylose units were linked through the 1→4′ glycosidic bonds. The negative optical rotation of the methylated xylan indicated that the xylose moieties were linked by the β-glycosidic linkages. Since this particular sugar (yield 1·13 gms.) was obtained in an overwhelmingly large quantity, the 1→4′ β-glycosidic linkage might be considered to be the main structural feature of the xylan isolated from the bagasse hemicellulose.

The presence of 2 : 0 methyl-D-xylopyranose (yield 0·044 gms.) indicated the presence of at least one branch in the macro-molecule and the branching took place from the position C (3) of a xylose unit, the serial number of which could not be ascertained.

THE HYPOIODITE OXIDATION OF THE XYLAN

The average molecular weight of the xylan by the hypoiodite oxidation method (Ingles and Israel[19], as modified by Chanda, *et al*[16]) gave the mean value of the molecular weights as 8800, indicating one reducing end-group per 66/67 xylose units.

THE PERIODATE OXIDATION OF THE XYLAN

(*a*) *The Uptake of the Periodate*—Just a little over a mole of periodate was consumed per xylose unit in the high polymer, in confirmity with the 1→4′ glycosidic linkages between the constituent xylose units. This result confirmed the findings of the methylation studies, that the 1→4′-β-glycosidic linkages were the main structural features of the xylan under discussion.

(*b*) *The Liberation of the Formic Acid*—One mole of formic acid was liberated by the periodate oxidation of the xylan per 17—18 xylose units, the reaction being completed in 168 hours (7 days). Since 1 mole of formic acid is liberated from the non-reducing end and 2 moles from the reducing end, this result indicated 51—54 xylose units in an assumed straight chain; or 68—72 xylose units in a single branched structure. The former conclusion seemed untenable, in view of the results of the methylation studies (presence of 2 : 0-methyl-D-xylopyranose) and the hypoiodite oxidation studies (molecular weight 8800, D.P. 66—67). The latter conclusion, which agreed well with the methylation and hypoiodite oxidation studies, had been further substantiated by the study of the degradation products of the periodate oxidised xylan.

THE DEGRADATION PRODUCTS OF THE PERIODATE OXIDISED XYLAN

(*a*) *Detection and Estimation of the Residual Xylose*—The periodate oxidised xylan was treated with a few drops of ethylene glycol, to destroy the excess of the periodate, and then dialysed to remove the inorganic matter. The resulting solution was concentrated and then hydrolysed with N-sulphuric acid. After the usual treatments, a faint spot corresponding to D-xylose was observed on paper chromatographic examination. This result showed the presence of at least one branch in the macromolecule—the xylose unit from which the branching occurred, being immune to periodate oxidation. The amount of xylose left unaffected by the periodate oxidation was estimated[18] and corresponded to 69-70 xylose residues, (molecular weight 9150; D. P. 69-70).

(*b*) *Reduction of the Periodate Oxidised Xylan*—The 1→4′ glycosidic linkage in the xylan had been definitely established by reducing the periodate oxidised xylan with sodium borohydride and subsequent hydrolysis, when glycerol and glycollic aldehyde, together with a trace of xylose were identified by paper chromatography.

The 1→3′ linked xylan was immune to periodate oxidation, while the 1→2′ linked xylan would also consume 1 mole of periodate per xylose unit. The latter would, however, give rise to glyceraldehyde (which would change to pyruvic acid by the treatment with dilute sulphuric acid[20]) and glycol.

(*c*) *Isolation of the Pyruvic Acid from the Periodate Oxidised Xylan*—The 1→4′ glycosidic linkage in the xylan had been further confirmed by hydrolysing the periodate oxidised xylan and isolating the pyruvic acid from the product. The pyruvic acid had obviously been formed by the loss of the elements of water from glyceric aldehyde with dilute sulphuric acid, and subsequent molecular rearrangement into methyl glyoxal[20] (pyruvic aldehyde), which was oxidised to pyruvic acid by air, during distillation.

The pyruvic acid was identified by converting it into (a) iodoform, m.m.p. 114°, and (b) the 2 : 4-dinitro-phenyl-hydrazone of pyruvic acid, m.m.p. 206°.

The 1→2′ linked xylan under similar treatments would have given the tartronic aldehyde (glucic acid, reductone), and glycollic aldehyde.

CONCLUSION

From the foregoing discussions it seems justifiable to assign to the xylan from bagasse hemicellulose, a structure containing about 65-75 D-xylopyranose units joined together by the 1→4′ β-glycosidic linkages with a single branch point formed by the 3→1′ union at some point as yet undetermined along the chain. Thus the main structural features of the xylan from the bagasse hemicellulose can be represented by the formulae shown in plate I.

REFERENCES

1. B. C. Banerjee, S. Bose & S. Mukerjee, The Hemicelluloses from Bagasse, Part I—Nature of the Sugars Present, *Sharkara*, Vol. 3, (1960), 125 to 129.
2. *Idem.*, Isolation of DL—Xyloketose from Bagasse Hemicellulose. *Science & Culture*, Vol. **27**, (1961), 498 to 499.
3. *Idem.*, The Xylan from Bagasse Hemicellulose, *Labdev*, Vol. **1**, April 1964. pp. 155 to 156.

4. *Idem.*, The Xylan from Bagasse Hemicellulose, *J. Ind. Chem. Soc.*, Vol. **41**, May 1964, pp. 323-329.
5. Mildred Gee & R.M. McReady, *Anal. Chem.*, **29**, (1957), 257.
6. I. Heilborn & H. M. Banbury, Heilborn's Dictionary of Organic Compounds, II, (1953), page 579.
7. E. L. Hirst & A. S. Perlin, *J. Chem. Soc.*, (1954), 2622.
8. H. C. Srivastava & G. A. Adams, *J. Amer. Chem. Soc.*, **81**, (1959), 2409.
9. S. Mukherjee & H.C. Srivastava, *Nature*, **169**, (1952), 330.
10. J. A. Cifonelli & F. Smith, *Anal. Chem.*, **26**, (1954), 1132.
11. L. Hough & J.K.N. Jones, *J. Chem. Soc.*, (1951), 3191.
12 *Idem.*, *ibid.*, (1952), 4047.
13. B. Arreguin, *Anal. Chem.*, **31**, (1959), 1371.
14. L. J. Breddy & J.K.N. Jones, *J. Chem. Soc.*, (1945), 738.
15. S. Mukherjee & A.N. Srivastava, *J. Amer. Chem. Soc.*, **80**, (1958), 2536.
16. S. K. Chanda, E. L. Hirst, J.K.N. Jones & E.G.V. Percival, *J. Chem. Soc.*, (1950), 1289.
17. E.L Hirst, L. Hough & J K.N. Jones, *J. Chem. Soc.*, (1949), 928.
18. E.L. Hirst & J.K.N. Jones, *ibid.*, (1949), 1659.
19. O.G. Ingle & G.C. Israel, *ibid.*, (1948), 810.
20. G. Jayme & M. Satre, *Ber.*, **75**, (1942), 1840.

Plate 1.

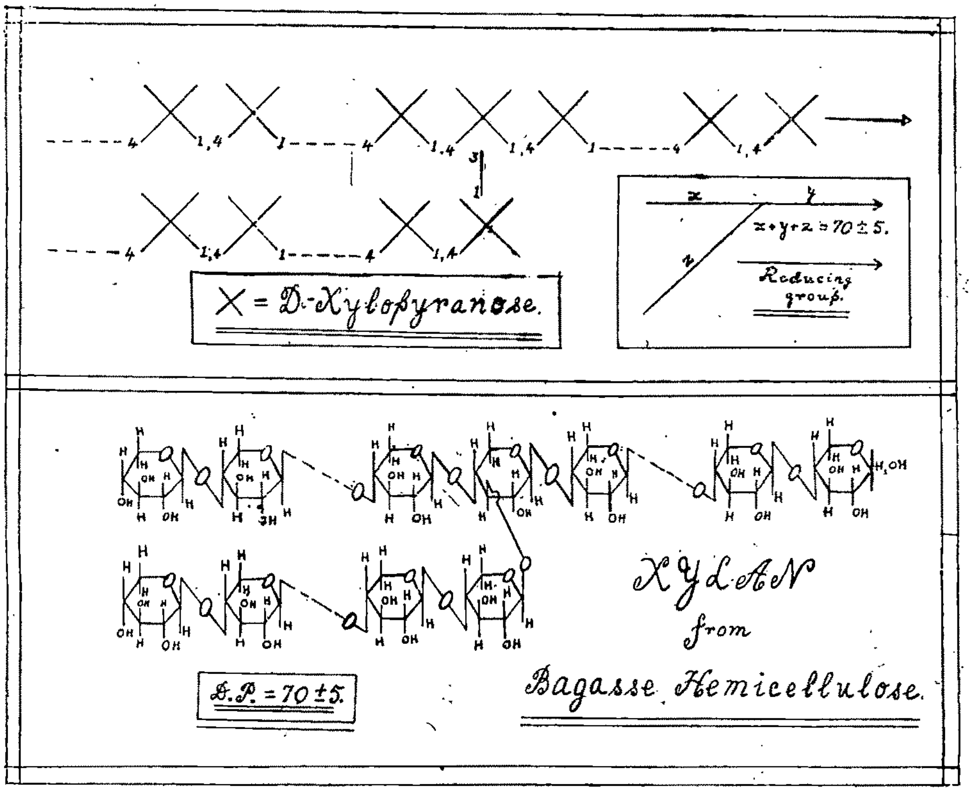

AGRA UNIVERSITY JOURNAL OF RESEARCH

Vol. XV, Part II *SCIENCE* **May, 1966**

Abbr.—*Agra Univ. J. Res. (Sci.)*

UNIVERSITY OF CALCUTTA
GENERAL LIBRARY

PUBLISHED BY
THE REGISTRAR, AGRA UNIVERSITY,
AGRA, 1966.

Annual Subscription : Inland Rs. 15/- ; Foreign Rs. 20/-

Chancellor
Sri Biswanath Das, Governor, Uttar Pradesh State.
Vice-Chancellor
Dr. S. Ranjan, M. Sc. (Cantab), D. Sc. (State France), F.N.I.
Registrar
Sri R. S. Agarwal
Editor
Dr. M. Ray, D. Sc., F. N. I.
Advisory Committee
Dr. S. P. Srivastava, M. S., F.R.C.S.
Dr. S. N. Singh, M. Sc., Ph. D.
Dr. A. Roy, M. Sc., Ph. D.
Dr. D. D. Pant, M. Sc., D. Sc.
Dr. P. I. Ittyerah, M. Sc., Ph. D.
Dr. V. Puri, D. Sc., F.N.I.
Dr. T. Singh, M. Sc., Ph. D.
Dr. Mata Prasad, D. Sc., F. R. I. C., F. N. I.
The Registrar (*Ex-officio*)

Edited by Dr. M. Ray, D. Sc., F. N. I., Principal, Agra College, Agra, Published by Sri R. S. Agarwal, Registrar, Agra University, Agra, and Printed by Mr. H. K. Kapur, Agra University Press, Agra. (J.- 1764)

ACTION OF ULTRAVIOLET RADIATIONS ON AQUEOUS SOLUTION OF ORNITHINE AND LYSINE

O. N. Perti AND R. C. Rastogi
Professor of Chemistry, *Department of Chemistry,*
M. L. N. R. E. College, Allahabad. *Th. D. S. B. Govt. College, Nainital.*

Abstract

When dilute aqueous solutions of ornithine and lysine are exposed to ultraviolet radiations from 5 minutes to 45 hours interesting changes are observed. Ornithine can give rise to glutamic acid, alanine and amino-n-butyric acid while lysine shows the formation of aspartic acid, glycine, alanine, amino-n-butyric acid, valine and leucine.

Introduction

Several workers have reported the evolution of ammonia or deamination when amino acids are irradiated with ultraviolet light[1], x-radiations[2,3,4,5] cathode rays[6] or radon[7]. Lieben and Urban[8] pointed out that only the α-amino group in amino acids undergoes this type of change. Recently Perti and Pathak[9], Perti, Bahadur and Pathak[10,11,12] have noticed that when aqueous solution of amino acids are exposed to sunlight or light from a 1000 watt bulb, they undergo interesting changes—new amino acids are formed and in several cases peptides also are detectable.

It may be mentioned that other workers have noticed that when dilute solutions of certain amino acids are exposed to ultraviolet radiations other amino acids are also formed. Alanine[13], lysine[14], ornithine[15], phenyl alanine[16], proline[17] tryptophane[18] tyrosine[19] when exposed to ultraviolet radiation give rise to different amino acids which could be detected under suitable conditions. It was observed that lysine in alkaline medium gives rise to aspartic acid, glutamic acid, alanine, norvaline and norleucine[14]. In the case of ornithine formation of proline, glutamic acid and aspartic acid could be detected[15].

Experimental

Aqueous solutions of chromatographically pure ornithine and lysine were kept in beakers at a distance of 62 cms. from a source of ultraviolet radiations (1500 watt Elvak 'Universal' lamp).

Periodically a portion of the solution was taken out and analysed for amino acids and peptides by chromatographic methods described earlier by Perti et al.,[9,10,11,12]. At the end of each experiment a test was made for infection by using aseptic potato dextrose medium and incubating it for 48 hours at 25°C. Results are recorded in the table given below.

TABLE 1

Exposure of amino acids solution to ultraviolet light.

(*i*) Concentration of lysine mono hydrochloride=0·2000 g/100 ml. water
(*ii*) Concentration of ornithine hydro-bromide=0·2000 g/100 ml. water.
(*iii*) Distance of solution from the source of light=62 cms.

Exposure time	Results of chromatographic analysis for amino acids	
	Ornithine	Lysine
5 minutes	Ornithine	Lysine
30 ,,	Ornithine	do-
2 hours	Ornithine+glutamic acid	-do-
4 ,,	Ornithine+glutamic acid	-do-
6 ,,	Ornithine+glutamic acid+ amino-n-butyric acid	-do-
10 ,,	-do-	Lysine+aspartic acid+glycine+ alanine
15 ,,	Ornithine+glutamic acid+alanine+ amino-n-butyric acid.	-do-
20 ,,	-do-	-do-
25 ,,	-do-	Lysine+aspartic acid+glycine+ alanine+amino-n-butyric acid+ valine+leucine
30 ,,	-do-	-do-
35 ,,	-do-	-do-
45 ,,	-do-	-do-

DISCUSSION

When ornithine solution was exposed to ultraviolet radiations no change was seen for 5 and 30 minutes. However, after an exposure of 2 hours formation of glutamic acid could be detected. When the exposure time was increased to 6 hours besides glutamic acid, formation of amino-n-butyric acid was also indicated. On increasing the exposure time from 15-45 hours formation of glutamic acid, alanine and amino-n-butyric acid could be detected chromatographically. In the case of lysine, an exposure from 5 minutes to 6 hours to ultraviolet radiations gave no indication of the formation of new amino acids. When the exposure time was increased to 10 hours aspartic acid, glycine and alanine could be identified. On prolonging the exposure to 25 hours aspartic acid, glycine, alanine, amino-n-butyric acid, valine and leucine was indicated. Increase of exposure time to 45 hours indicated no further change.

It appears that when aqueous solutions of ornithine and lysine are exposed to ultraviolet radiations, they also undergo changes which can give rise to other amino acids. The mechanism of the reaction is obviously complicated and no attempt has been made to trace it.

Further work along these lines is in progress.

ACKNOWLEDGEMENT

Authors are grateful to the authorities of Th.D.S.B. Government College, Naini Tal (India) for research facilities.

REFERENCES

1. Henry, V., Weizmann, C. & Hirschberg, 1934. *Compt. rend*, **198** : 168.
2. Stenstrom, W. 1929. *Radiology*, **13**: 437.
3. Stenstrom, W. & Lohmann, A. 1931. *Radiology*, **17**: 432.
4. Maxwell, C. R., Peterson, D.C. & Sharpless, N.E. 1954. *Radiation Research*, **1** : 530.
5. Sharpless, N.E., Blair, A.E. & Maxwell, C.R. 1955. *Radiation Research*, **2**: 135.
6. Allen, A.J., Steiger, R. E., Magill, M. A. & Franklin, R. G. 1937. *Biochem. J.*, **31**: 195.
7. Loiseleur, J. 1933. *Compt. rend, soc. biol.*, **114**: 589.
8. Lieben, F. & Urban, F. 1931. *Biochem. Z.*, **239**: 250.
9. Perti, O. N. & Pathak, H.D. 1961. *Agra Univ. J. Res (Sci.)*, **X** (2): 265-278.
10. Perti, O.N., Bahadur, K. & Pathak, H. D. 1961. *Proc. Natl. Acad. Sci. (Indian)*, **30A**: 216-220.
11. Perti, O.N., Bahadur, K. & Pathak, H. D. 1962. *Indian J. Appl. Chem.*, **25**: 90-96.
12. Perti, O.N., Bahadur, K. & Pathak, H. D. 1962. *Biokhimia*, **27**(4): 708-714.
13. Watanabe, J. 1960. *Nagasaki Igakkai Zasshi*, **35**: 22.
14. Morokuma, T. 1954. *Nagasaki Igakkai Zasshi*, **29**: 813; *Chem. abst.*, **49**, 4051 g.
15. Mukai, I. 1959. *Nagasaki Igakkai Zasshi*, **34** : 577; *Chem. abst.*, **53**, 18138 d.
16. Matsuda, G. Maekawa, T., Ohkawa, I. & Yamada, M. 1954. *Nagasaki Igakkai Zasshi*, **29**: 10; *Chem. abst.*, **48**, 6842 d.
17. Yamada, M. *Nagasaki Igakkai Zasshi*, **31**: 999; *Chem. abst.* **51**, 6359 b.
18. Matsuda, G. 1953. *Nagasaki Igakkai Zasshi*, **28**: 438; *Chem. abst.*, **48**, 7660 c.
19. Suzatani, E. 1958. *Nagasaki Igakkai Zasshi*, **33**: 507; *Chem. abst.*, **52**, 12030 h.

ON A NEW SPECIES OF COCKROACH FROM NORTH-WEST HIMALAYAS

H. N. Baijal and V. C. Kapoor
Department of Zoology, Agra Colloge, Agra.

While making a Dermaptera survey in the North-Western regions of Himalayas in June 1965, the authors came across with some cockroaches, which appeared to them to be new species described with following lines:—

Calolampra simlansis sp. nov. (Figs. 1-8)

Holotype Male—Smaller in size than female with specifically elliptical form.

Head—Slightly longer than broad; the narrowest inter-ocular distance nearly equal to that between antennal sockets. Eyes reduced, not projecting. Antenna long, reaching nearly upto the IXth tergite.

Pronotum—Very feebly and evenly convex; lateral margins slightly convex divergent, greatest width at the caudal margin; thinly transparent texture; cephalic margin above head and caudal margin subsinuate; latero-caudal angles rounded.

Tegmina and wings—Absent.

Mesonotum and metanotum—With latero-caudal angles strongly produced, acute, their apices sharply rounded; the caudal margins, as a result, strongly concave, showing a minute angulate process on the posterior side of the metanotum only.

Legs—Front femur with five spines in each row on the ventral side, middle and hind-femora with four well-developed spines in each row on the ventral side; hind legs abnormal; hind tarsus with basal segment longer than the remaining segments including claws and arolium.

Abdomen—Caudal margins of tergites with distinct longitudinal furrows, latero-caudal angles acute angulate but produced into increasing processes distad upto eighth tergite, supra-anal plate somewhat rounded, feebly notched caudo-mesad; cerci small, stout, margin entire with round acute apices. Sub-genital plate quadrate, the lateral sides gently arcuate, latero-caudal angles strongly produced, caudal margin subsinuate mesially. Styles small, cylindrical, feebly inset and nearly one-third as long as the distance between their bases.

Colouration—Head blackish-brown, vertex and frons brown, antennal sockets, clypeus and labrum yellow; maxillary palp dirty greyish-brown; antennae reddish-brown, darker near base. Pronotum, mesonotum and metanotum blackish-brown, extreme lateral margins brown. Coxae, femora, tibiae and first tarsal segment brown; rest tarsal segments and claws yellow brown; tips of claws reddish. Cercus blackish-brown, pale at apex; styles brown.

Measurements (in mm)—Length of body, 28·0; pronotum, 7·0; right hind tibiae, 9·0; left hind tibiae, 8·0; right tarsal segments, 6·2; left tarsal segments 5·3; width of pronotum, 11·0; right hind tibiae, 0·14; left hind tibiae, 0·14.

Allotype Female—Larger than male, differing in the following features:—

Antennae—Reaching upto the VIIIth tergite.

Pronotum—Somewhat convex, lateral portions slightly declinant latero-cephad, greatest width mesad, cephalad margin subtruncate, latero-caudal margins moderately convex convergent, then gently concave to the distinct, small and bluntly rounded meso-caudal process.

Tegmina—Punctate, elongate, projecting beyond the body, costal and sutural margins nearly straight, apex and anal margin oblique.

Wings—As long as the tegmen, with well-developed veins.

Legs—Having the same texture as in male; hind legs normal.

Abdomen—Dorsal surface of abdomen with lateral stigmata distinctly marked; supra-anal plate round, strongly depressed dorso-laterad leaving a triangular portion, with blunt spine on either side anteriorly, very slightly notched meso-caudad; cerci slightly longer than that of male, sub-genital plate convex posteriorly and rugose.

Colouration—Head blackish-brown, frons black; Pronotum blackish brown. Tegmina and wings brown. Ventral side of abdomen blackish-brown with white tinge except the sub-genital plate.

Measurements (in mm)—Length of body, 30·0; pronotum, 7·0; hind tibia; 10·0; tegmen, 30·0; width of pronotum, 8·0; hind tibia, 0·14.

Material examined—Holotype one male and *allotype* one female in spirit, *paratypes* one male and one female on pins, labelled "under stones in the running water, Glen fall, Alt. 6,000 ft., Simla (Himachal Pradesh), 17. VI. 1965, Collected by V. C. Kapoor." At present in author's collection and ultimately to be deposited in the Zoological Survey of India.

Variations—A very interesting anomaly has been observed in the length of the tibiae and tarsal segments of the hind legs of the *holotype*. The tibia and the tarsal segments of the left hind leg are smaller than that of the right hind leg and these variations are clearly visible in the specimen.

ACKNOWLEDGMENTS

We are very grateful to the Principal Dr. M. Ray and Dr. C. P. Singh, Head of the Zoology Department, Agra College, Agra, for the facilities enjoyed by us. Grateful thanks are due to Dr. R. D. Saksena, Head of the Zoology Department, B. R. College, Agra, for his valuable suggestions. The authors are also very thankful to Dr. S. K. Tandon, Zoological Survey of India, Calcutta, for valuable assistance.

REFERENCES

*1. Brunner, C. de Wattenwyl. 1893. Rèvision du systéme des *Orthopteres* et description des espèces rapportées par M. Leonardo Rea de Birmanie. *Ann. Mus. Genova,* **XIII** (2) : 1-230, pls. 1-6.

2. Gurney, Ashley B. 1965. Two new cockroaches of the genera *Pelmatosilpha* and *Henchoutedenia,* with a Key to the West Indian species of *Pelmatosilpha* (Dictyoptera :Blattaria) *Proc. R. ent. Soc. Lond.* (*B*). **34** (1-2) : 5-11.

3. Hanitsch, R. 1915. Malayan Blattidae, *J. R. Asiatic Soc. Straits Branch,* **69:** 17-178.

4. Hanitsch, R. 1923. On a collection of Blattidae from the Buitenzorg Museum. *Treubia Buitenzorg.* **3** : 197-221, 8 Figs.

5. Hanitsch, R. 1923. Malayan Blattidae. Part II. *J. Malayan Br R. Asiat. Soc.,* **1** : 393-474, 2 pls.

6. Hebard, M. 1929. Studies in Malayan Blattidae. *Proc. Acad. nat. Sci. Philadelphia,* **8:** 1-109.

7. Mani, M. S. 1955. Introduction to Entomology. *Agra University Press, Agra.* 229-234.

8. Rehn, J. A. G. 1904. Studies in Old World *Forficulids* or earwigs, and *Blattids* or Cockroaches. *P.U.S. Mus.* **XXVII,** No. 1363 : 539-560.

9. Rehn, J. A. G. 1916. Dermaptera and Orthoptera I. *Trans. Am. ent. Soc.,* **XIii,** No. 753: 215-308

10. Schroder, Ch. 1925. Handbuch der Entomologie. **3**: 471-493.

11. Shelford, R. 1910. Genera Insectorum. **101** : 1-21, pls. 2.

PLATE I

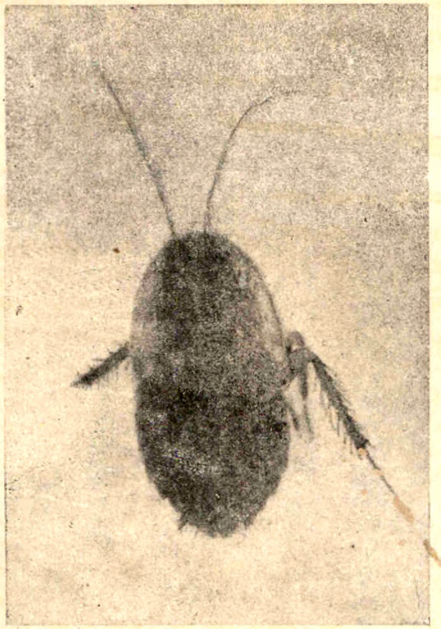

Fig. 1. *Holotype Male*

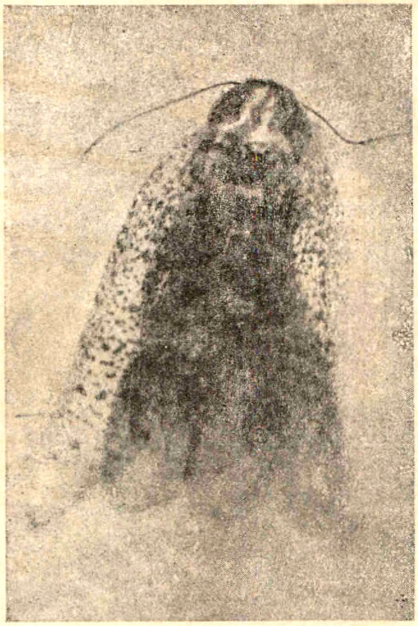

Fig. 2. *Allotype Female*

---

* Not Consulted in Original.

Plate II.

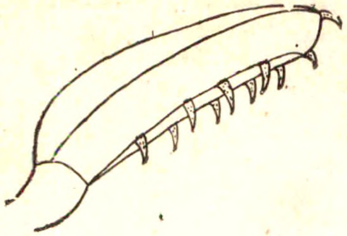

Fig. 3

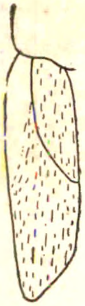

Fig. 6

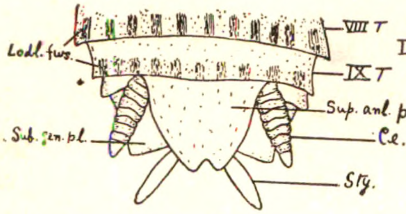

Fig. 4

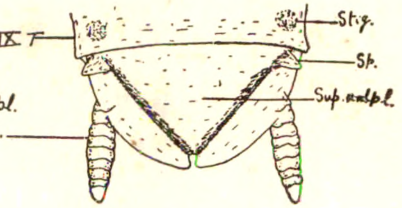

Fig. 7

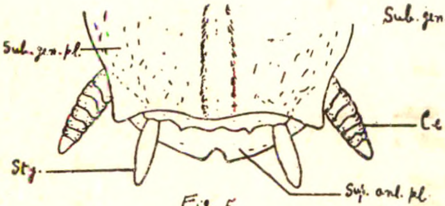

Fig. 5

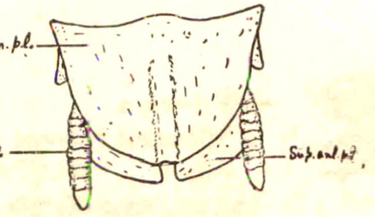

Fig 8

Holotype Male

Fig. 3. Hind femur.

Fig. 4. Supra-anal plate.
Cerci............Ce; Longitudinal furrows............Lodl. fws; Style.............Sty; Sub-genital plate............Sub. gen. pl; Supra-anal plate............Sup. anl. pl; VIII T............Eighth tergite; IX T............Ninth tergite.

Fig. 5. Sub-genital plate.
Cerci............Ce; Style............Sty; Sub-genital plate............Sub. gen. pl. Supra-anal plate......... ..Sup. anl. pl.

Allotype Female

Fig. 6. Left tegmen.

Fig. 7. Supra-anal plate.
Cerci...............Ce; Spine...............Sp; Stigmata............Stig; Supra-ana plate............Sup. anl. pl; IX T............Ninth tergite.

Fig. 8. Sub-genital plate.
Cerci...............Ce; Sub-genital plate...............Sub. gen. pl; Supra-anal plate............Sup. anl. pl.

A STUDY OF THE FISH FAUNA OF VISAKHAPATNAM DISTRICT (ANDHRA PRADESH)—ITS DISPOSAL AND MARKETING

I. SCOPE FOR THE DEVELOPMENT OF INLAND FISHERIES IN VISAKHAPATNAM DISTRICT[1]

M. V. SUBBA RAO
Department of Zoology,
S. V. University, Tirupati, (A. P.)

AND

RATAN SINGH
Department of Zoology,
B. R. College, Agra, (U. P.)

(Communicated by R. D. Saksena, M.Sc., Ph.D., F.Z.S.I.)

Most of the rivers in Visakhapatnam district yield good fisheries. There are three rivers and two small channels in the district. All these are the natural homes of a number of quick growing fishes.

Due to the avaricious and unthoughtful exploitation of the fishermen, the fisheries of the rivers have been dwindling at a rapid rate year after year. Excessive exploitation of the breeders tends to eliminate or reduce their intensity on whose protection the success of the future fisheries depends. Besides fishing adults excessively, our fishermen and farmers in paddy fields kill young fishes which are the potential sources for future fisheries. It is, therefore, necessary to enforce suitable legislation to protect the young ones and the breeders without which no success is possible.

Fish like *Hilsa* ascend into our rivers during the floods for breeding and contributing for river fishery. But to obstruction caused by barrages and anicuts, they cannot go back to their old haunts which lie in the upper reaches where they can breed unmolested. The construction of the barrages leads to the congregation of breeders in large numbers below them. This arouses the greed of fishermen who fish indiscriminately in tide and drain water during low tide.

Estuaries and backwaters have a low salinity compared to the adjoining sea. Several estuarine fishes such as *chanos* and *Mugil cephalus* have been successfully acclimatised to fresh water. There are large number of backwater lagoons which can be converted into estuarine and backwater fish farm by which their present fishery can be enriched and enhanced.

TANKS AND PONDS

There are about 4,118 minor tanks and 547 major tanks in Visakhapatnam district. (Statement No. 3). The ponds are innumerable. Some of the tanks are perennial and others seasonal. Many of them, which can be advantageously utilised for the production of a good crop fish remain fallow. The first step in their development is to find out the existing physical, chemical and biological features of the pond. Then all defects that are noticed have to be removed wherever possible and stocked with suitable types of fish. By proper planning the pond-fisheries can also be developed enormously.

New varieties of fishes from other countries have been added to the original ones. This has not only left to depletion but has prevented the normal breeding fishes which inspite of the limitations placed on the length of the course of their journey, have learnt to breed below the dams and anicuts. In order to allow migratory fishes to breed unmolested, steps should be taken wherever possible to construct fish passes, fish ladders etc., to enable the fish to cross the barriers and to ascend to their original places of breeding. As a secondary step suitable legislation has to be introduced to check the intensity of fishing and to protect the breeders.

A record of fish landing from rivers with all necessary details should be maintained in an efficient manner. Statistical data on the types and numbers of each type of net used, the number of fishermen dependent on river fisheries etc., should also be maintained. This information will be highly useful before deciding on conservation measures.

ESTUARINE AND BACKWATER FISHERIES

There are five estuaries, two backwaters and four rivers in Visakhapatnam district. (Statement Nos. 1 and 2) A great deal of work has to be done to improve estuarine and backwater fisheries.

During high tide, water overflows into adjoining low lying areas, taking fish along with it. This feature, wherever present, can be taken advantage of and developed into estuarine or backwater ponds or fish farms. Necessary arrangements to let in water into the ponds during high tides is one of the ways of improving the pond fisheries. Chinese carps such as the gross, Black silver, Big head, and Mud carps, can be considered for transplantation into lentic water with advantage.

ACKNOWLEDGEMENT

We are grateful to Dr. R. D. Saksena, Professor and Head of the Zoology Department, B. R. College, Agra for providing all facilities during the course of this work.

REFERENCES

1. Alkunhi, K. H. 1954. "On ponds and fishes." *Indicn Farming*, June, 1954.
2. Chopra, B. N. 1951. "Hand Book of Indian Fisheries." Prepared for the third meeting of the Indo-Pacific Fisheries Council, Madras.
3. Hyder, H. M. W. 1949. "Development of fish farms in Hyderabad State." *Bulletin No.* 4.
4. Kesteven, G. L. 1954. "The Scope of Fishery Biology." F. A. O. Publication. Proceedings and Technical Papers No. 2, 1954.
5. Rounsfell, G. A. & Everhart, W. H. 1953. "Fisheries Science, its methods and applications." John Wiley & Sons, Inc. New York., Chapman & Hall Ltd., London.

STATEMENT 1

Estuarine Fisheries, fish production in Visakhapatnam District.

I. *Estuarine Fisheries*	Type of water and location	Approximate fish production
1. Visakhapatnam	Backwaters	1,50,000 lbs.
2. Champavathi river	Near Kondada-backwaters	1,20,000 lbs.
3. Gosthani river	Near Bhimilipatnam backwaters	1,25,000 lbs.
4. Sarada river	Near Polavaram backwaters	1,20,000 lbs.
5. Ravia-Peta	Small backwater	60,000 lbs.
	Total	5,75,000 lbs.
	Valued at Rs. 1,00,000/-	
II. *Riverine Fisheries*		
6. Three rivers above Nos. 2, 3 & 4 7. Varaha river		50,000 lbs.
	Valued at Rs. 17,500/-	

STATEMENT 2

Total Inland Fish production in Visakhapatnam District.

Estuaries	Fish production	Amount
1. Five Estuaries & backwaters	5,75,000 lbs.	Rs. 1,00,000/-
2. Four Rivers	50,000 lbs.	Rs. 7,500/-
3. 4,665 Tanks	17,00,000 lbs.	Rs. 2,50,000/-
Approximately 1,000 tons	22,25,000 lbs.	Rs. 3,57,500/-

STATEMENT 3

Statement showing the Tank Fisheries in Visakhapatnam District.

Location	Minor irrigation No. of Tanks	Major irrigation No. of Tanks
Anakapalli Taluk	509	83
Elamanchili Taluk	280	259
Chintapalli	80	...
Lakavarapukota area	375	...
Gajapatinagaram S. Taluk	527	...
Gajapatinagaram Estate area	18	64
A. Koduru Sub Taluk	410	...
Madugala	298	...
Chodavaram Taluk	133	40
Srungavarapu Kota Taluk	378	21
Narasipatnam Taluk	268	54
Visakhapatnam Taluk	159	...
Bhimilipatnam Taluk	388	26
Bhogapuram Taluk	295	...
Total Tanks	4,118	547

STATEMENT 4

Statement showing the Tank area and Fish production of Visakhapatnam.

	Minor irrigation	Major irrigation
Approximate area	50,000 acres	1,20,000 acres
Total Tanks area (Approximate)	1,70,000 acres	
Fish production (Approximate)	1,70,000 lbs.	
	Valued at Rs. 2,50,000/-	

STUDY OF THE COOLING CURVES OF GEL-FORMING SOLUTIONS OF SODIUM OLEATE AND SODIUM ERUCATE IN A FRACTION OF TURPENTINE

R. C. Seth
Department of Chemistry, St. John's College, Agra.

Several workers have emphasized the importance of the study of the cooling process during the sol-gel transformation of organic and inorgano-organic gels, since most of these gels are prepared either by cooling or heating a solution of the gel-forming substance. These studies have been made mostly by Freundlich[2], Lottermoser and Matthaes[6], Pleass[7], Hollemann and co-workers[3], Fischer[1], Laderer[5], Lawrence[4], and Prasad and co-workers[8] for various systems. All these workers have observed a sudden change in the cooling curves at the point of setting in a direction which indicates that heat is evolved during gelation.

The author has prepared gels of sodium oleate and sodium erucate in a fraction of turpentine for the first time. Hence in consonance with the previous studies of such systems, the author has also investigated the cooling process of solutions containing several amounts of sodium oleate and sodium erucate in a given volume of the fraction of turpentine from the temperature at which they are prepared to several lower temperatures.

EXPERIMENTAL

1. *Preparation of gel-forming solutions:*

Solutions of sodium oleate and sodium erucate in the fraction of turpentine, called as liquid A whose particulars are published elsewhere, were prepared in pyrex glass test-tubes of the same internal diameter (2·10 cm.). For this purpose a known amount of the soap was weighed out in a test-tube and 10 ml. of the liquid A were added to it. The test-tube with its contents was then electrically heated to 140°C; the upper end of the tube was attached to an air condenser to prevent the evaporation of the liquid. After all the soap had dissolved, the test-tube was placed in an air thermostat maintained at a constant temperature.

2. *Determination of cooling curves :*

The fall in temperature of solutions on cooling was read on a thermometer dipping in the solutions. The observations were taken with solutions containing 0·30, 0·40 and 0·50 gram of sodium oleate cooled at 30°, 60° and 90°C and 0·30, 0·40 and 0·50 gram of sodium erucate cooled at 30° and 60°C. In order to get comparable results, the liquid A was also heated in the test-tube of the same size to the same temperature as the solutions, was allowed to cool in the same air thermostat maintained at the same temperature, and the fall in temperature was read in the same manner as in the case of gel-forming solutions.

3. *Results:*

The results obtained are given in Figs. 1-6 in which the following notations have been used:—

T=Temperature in degrees in centigrade at which the solution or the solvent was allowed to cool;

t=Time in minutes;

Q=Weight in grams of sodium oleate or sodium erucate in 10 ml. of the gel-forming solution;

T_1=Temperature in degrees centigrade of the solvent and the solution undergoing cooling.

DISCUSSION

It will be seen from Figs. 1-6 that the curves for the two soaps in the liquid A containing 0·30, 0·40 and 0·50 gram of the soaps are very similar in general characteristics; however, the higher the concentration of the soap, the lower is the rate of cooling. It will also be seen that the course of cooling of the solutions coincides in the earlier part with that for the liquid A. These curves also show that subsequently, under the same conditions, the liquid A cools more rapidly than the gel-forming solutions.

Further, the curves for all soap solutions show definite arrests at the point of setting. The initial rate of cooling is followed by a change in direction of the curves which continues regularly later on. These changes in direction, constituting a kink, clearly indicate that heat is evolved on gelation. The temperatures of setting of these gels lie in the temperature range of the kink.

It has been found that the parts of the curves above and below the arrest points (kinks) obey Newton's law of cooling. Hence this finding has been utilised for calculating the specific heats of gel-forming solutions (S_1) and of the set gels (S_2) by means of standard relation; the values obtained are given in columns 3 and 4 of the tables 1 and 2. It will be seen from the tables that the specific heats of the solutions and of the set gels increase as the soap content in the system is increased, and that for a system of a particular soap content, the specific heat is greater in the solution or sol state than in the gel state.

Prasad and co-workers[8] have calculated the actual amount of heat of gelation (H) of soap-pinene systems from the relation, $H=\frac{S_1\theta_1+S_2\theta_2}{2}t$, where S_1 and S_2 are the specific heats in the sol and gel states, θ_1 and θ_2 are their rates of cooling and t is the time in seconds over which the heat is evolved. The heats of gelation of the gels of sodium oleate and sodium erucate in the liquid A have been calculated in the same manner by the author; the values obtained are given in column 5 of the tables 1 and 2. It will be observed that the amount of heat evolved during gelation increases as the soap content of the gel is increased and decreases with the increase of temperature of the surrounding.

Prasad and co-workers[8] have calculated the molar heat of gelation (MH) of soap systems in pinene. They have also calculated the ratios of molar heat of gelation (MH) to the temperature of setting (T_g), expressed in absolute units ($T_{A=273+T_g}$) for the soap systems in pinene, and have found that this ratio is fairly constant and is independent of the concentration of the solution and its rate of cooling. The molar heats of gelation (MH) and their ratios to temperatures of setting in absolute units (T_A) have been calculated by the author for the systems of sodium oleate and sodium erucate in the liquid A and the values obtained are given in columns 6 and 8 of tables 1 and 2. It is seen from these tables that the values of the ratio MH/T_A are not constant but decrease with increase in the concentration and of the temperature of the surroundings.

SUMMARY

The study of the rate of cooling of solutions of sodium oleate and sodium erucate in the fraction of turpentine, called as liquid A, of different concentration from the temperature at which they are prepared to several lower temperatures, has revealed that their rate of cooling is identical with the rate of cooling of the liquid A until the solutions begin to set to gels. Subsequently the gel-forming solutions cool at a slower rate than the liquid A, thus showing definite arrests at temperatures which corresponds to the setting temperatures of the gels; the changes in direction indicate that heat is evolved on gelation. The curves above and below the arrest points obey the law of cooling; these observations have been utilised to calculate of specific heats of the gel-forming solutions and the set gels, and the heats of gelation of gel-forming systems.

ACKNOWLEDGEMENTS

The author is grateful to Dr. Mata Prasad, D. Sc., F. R. I. C., F. N. I., for suggesting the problem and guidance during this investigation. He is also thankful to Dr. P. I. Ittyerah, Ph. D. (Agra), Ph. D. (Cantab), F. R. I. C., Head of the Chemistry Department, St. John's College, Agra, for giving him all facilities for the conduct of this investigation, and to the C. S. I. R., for awarding him the Research Fellowship which enabled him to carry out this work.

REFERENCES

1. Fischer, 1929. *Koll. Z.*, 46, 359.
2. Freundlich, 1926. Colloid and Capillary, *Chem. Eng. Edn.*, P. 701.
3. Hollemann & Co-workers, 1934. *Koll. Chem. Beih.*, 40, 211.
4. Lawrence, 1938. *Trans. Farad. Soc.*, 34, 660.
5. Lederer, 1931. *Koll. Z.*, 57, 16.
6. Lottermoser & Matthaes, 1929. *Z. Physical Chem.*, 141, 129.
7. Pleass, 1930. *Proc. Roy. Soc.*, 126A, 406.
8. Prasad & Co-workers, 1940, *Curr. Sci.*, 9, 119, 459 ; 1945, *Proc. Indian Acad. Sci.*, 21A, 1; 1945, *J. Univ. Bom.*, 14, part 3, 23; 1956, *J. Indian Chem., Soc.*, 33, 346; 1958, *J. Univ. Vikram,*, 2, No. 1, 91.

TABLE 1

Sodium Oleate

Q	T	S_1	S_2	H	MH	T_A	$\frac{MH}{T_A}$
0·30	30°	1·3440	0·8011	33·095	2185·0	375·0	5·828
0·40	,,	1·5840	0·9128	41·230	2041·0	378·0	5·399
0·50	,,	1·7600	0·9446	47·235	1871·0	381·0	4·910
0·30	60°	1·2050	0·9226	20.420	1348·0	375·0	3·595
0·40	,,	1·4950	0·9822	25·780	1276·0	378·0	3·375
0·50	,,	1·6860	0·9931	29·885	1184·0	381·0	3·109
0·30	90°	1·1980	0·7630	8·710	575·0	375·0	1·533
0·40	,,	1·2660	0·9482	9·727	481·6	378·0	1·274
0·50	,,	1·3470	1·0280	12·236	484·5	381·0	1·272

TABLE 2

Sodium Erucate

Q	T	S_1	S_2	H	MH	T_A	$\frac{MH}{T_A}$
0·30	30°	0·9766	0·9596	19·380	1516·0	348·0	4·356
0·40	,,	1·3600	0·9956	27·395	1605·0	360·5	4·452
0·50	,,	1·4970	1·0080	30·405	1426·0	361·5	3·946
0·30	60°	1·1370	1.0710	19·463	1522·0	348·0	4·373
0·40	,,	1·1520	1·0960	21·680	1271·0	360·5	3·526
0·50	,,	1·1740	1·1240	23·295	1375.0	361·5	3·804

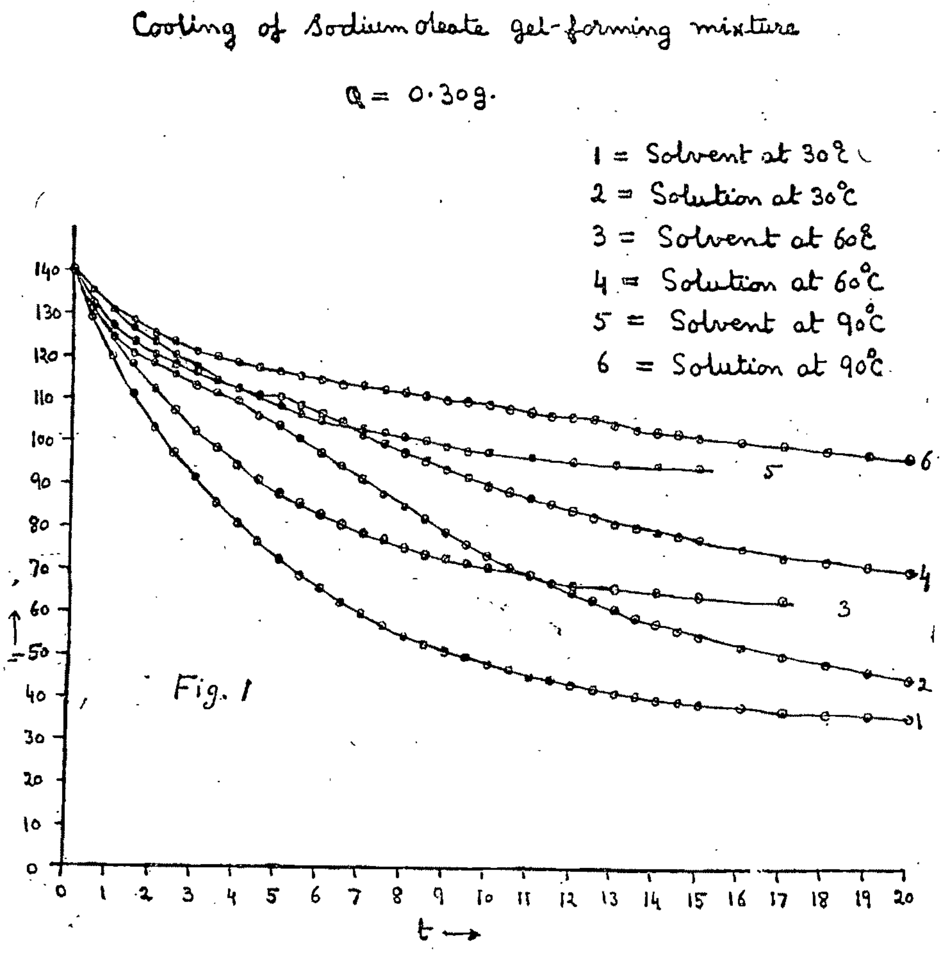

Fig. 1

Cooling of Sodium oleate gel-forming mixture
Q = 0.30g.
1 = Solvent at 30°C
2 = Solution at 30°C
3 = Solvent at 60°C
4 = Solution at 60°C
5 = Solvent at 90°C
6 = Solution at 90°C
140
130
120
110
100
90
80
70
60
50
40
30
20
10
0
0
1
2
3
4
5
6
7
8
9
10
11
12
13
14
15
16
17
18
19
20
t →
1
2
3
4
5
6

Cooling of sodium oleate gel-forming mixture.

Q = 0.40 g.

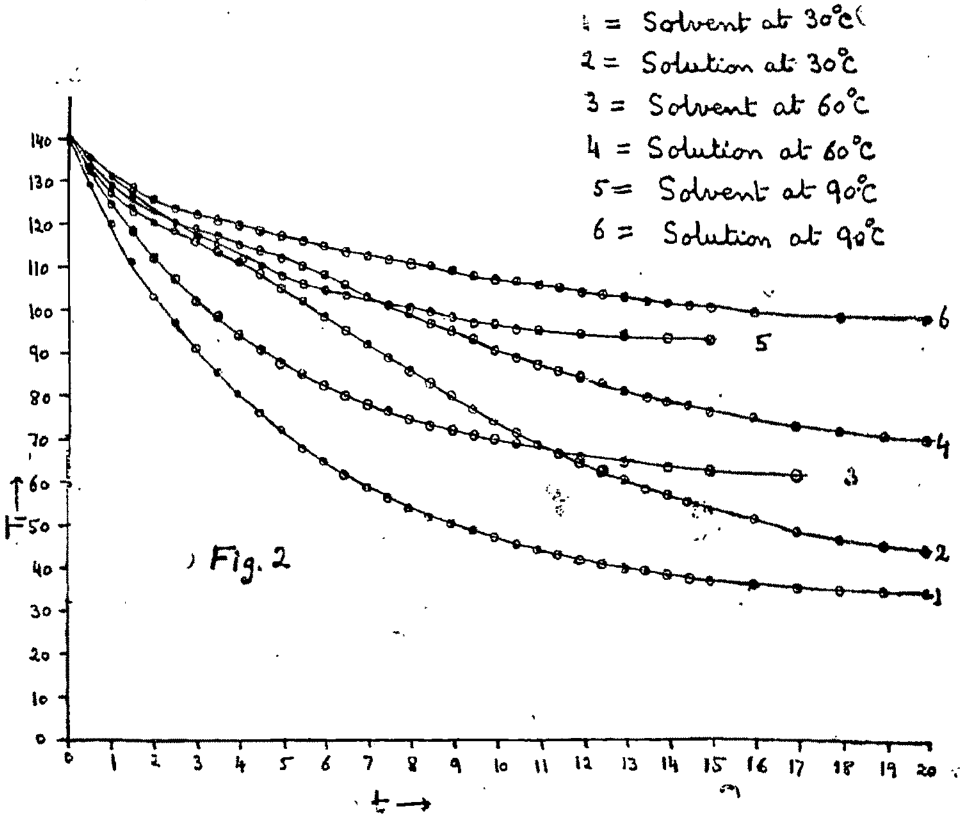

Fig. 2

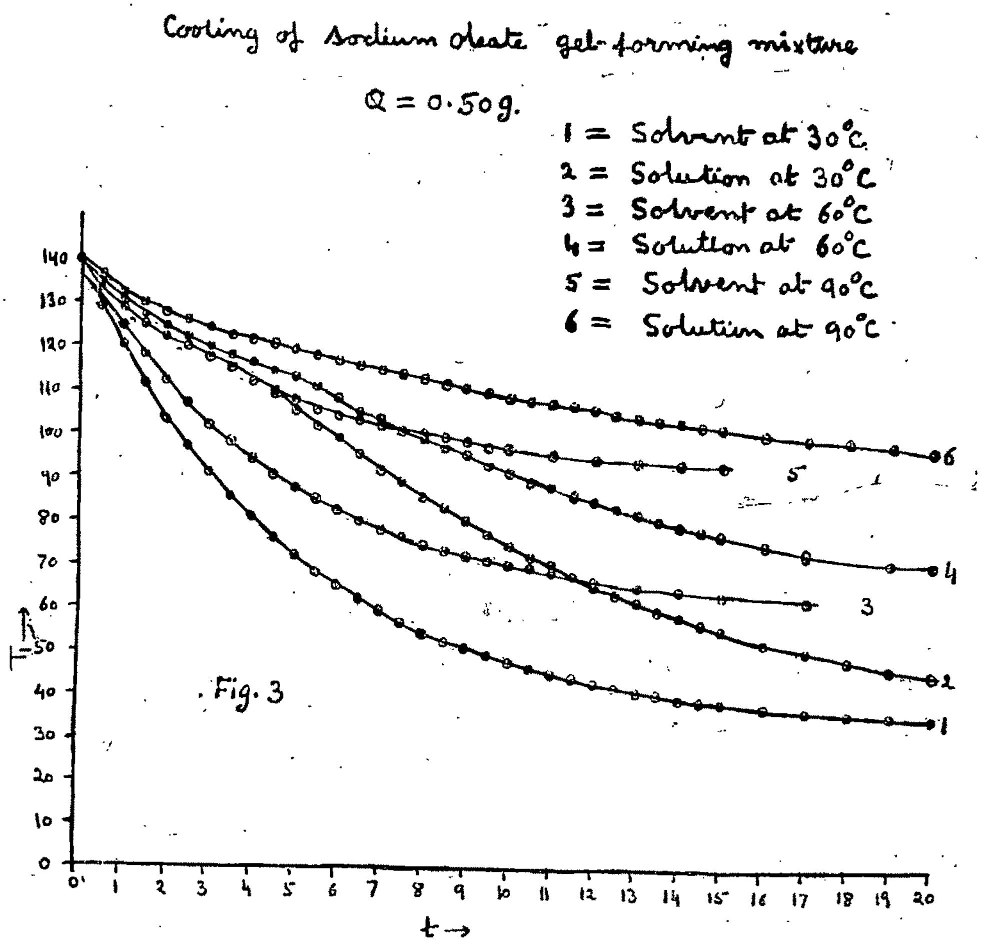
Cooling of Sodium oleate gel-forming mixture
Q = 0·50g.
1 = Solvent at 30°C
2 = Solution at 30°C
3 = Solvent at 60°C
4 = Solution at 60°C
5 = Solvent at 90°C
6 = Solution at 90°C
140
130
120
110
100
90
80
70
60
50
40
30
20
10
0
T ↑
0'
1
2
3
4
5
6
7
8
9
10
11
12
13
14
15
16
17
18
19
20
t →
1
2
3
4
5
6

Fig. 3

Cooling of Sodium erucate gel-forming mixture

Q = 0·30g.

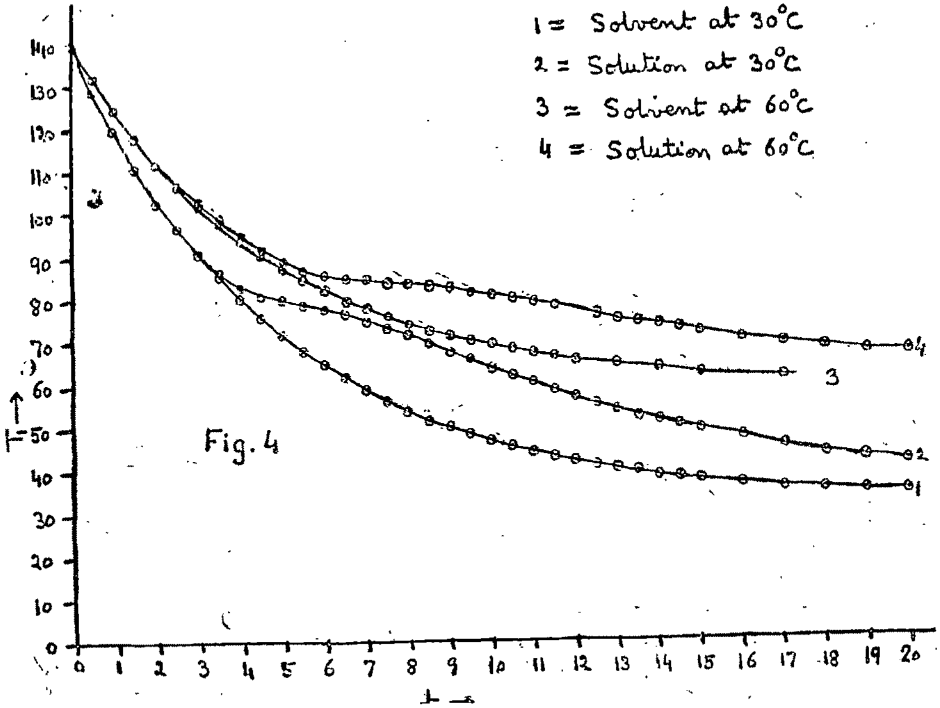

Fig. 4

Cooling of Sodium erucate gel-forming mixture

Q = 0·40 g.

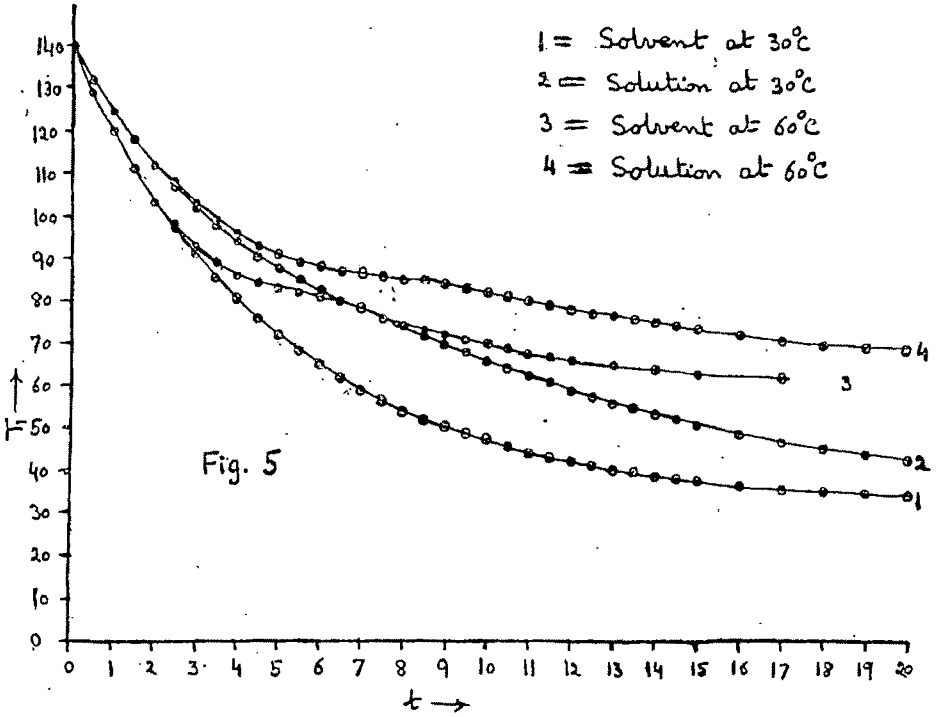

Fig. 5

Cooling of sodium erucate gel-forming mixture.

Q = 0.50g.

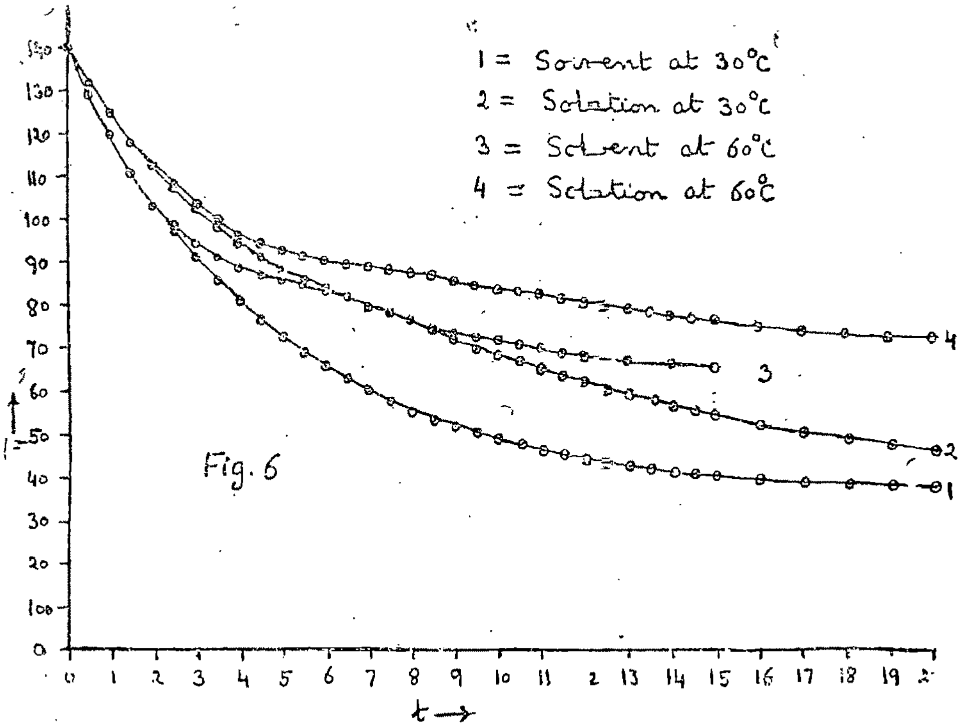

Fig. 6

ON THE PATHOGENIC SIGNIFICANCE OF THE TAPEWORMS HITHERTO REPORTED FROM SOME OF THE FRESH WATER FISHES

P. Rai
Department of Parasitology,
U. P. College of Vet. Sci. & A. H., Mathura.

The eucestodan tapeworms parasitic in some of our fresh water siluroids are represented by *Proteocephalus* Weinland, 1859; *Gangesia* Woodland, 1928 and *Vermaia* Wardle and McLeod, 1952, under Proteocephalidea Mola, 1928, and *Bothriocephalus* Rudolphi, 1808 and *Senga* Dollfus, 1934, under Pseudophyllidea Carus, 1863. The first three genera have been studied by Southwell (1913 and 1930), Woodland (1924 and 1925), Verma (1926 and 1928) and Singh (1948) and the latter two by Woodland (1924) and Johri (1956).

Proteocephalus, with its characteristically unarmed scolex and the testes lying in one continuous field, has the two species: *P. ritai* Verma, 1926, from *Rita rita* and *P. vitellaris* (Verma, 1928) Southwell, 1930, from *Bagarius yarrelli* (originally included by Verma in *Ichthyotaenia* Löenberg, 1894). The armed character of the scolex, with a single or double row of hooks, distinguishes *Gangesia* in which the type species, *G. bengalensis* (Southwell, 1913) Woodland, 1924, originally included by its author under *Ophryocotyle* Friis, 1870 was collected from *Ophiocephalus striatus*—the three other Indian species being *G. macrones* Woodland, 1924, from *Mystus seenghala*; *G. wallago* Woodland, 1924, from *Wallago attu*; and *G. agreansis* Verma, 1928, from *W. attu*, the last two were made a synonym of *G. bengalensis* by Southwell (1930). *G. pseudotropii*, described by Verma (1928) from *Pseudotropius garua*, and *G. lucknowia*, reported from *Euctropiicthys vacha* by Singh (1948) were added. Wardle and McLeod (1952) removed *G. pseudotropii* and made it the type of his new genus, *Vermaia*, because of the presence of a single crown of rostellar hooks, the cup-shaped character of the rostellum and the vitellaria being confined to short preovarian lateral fields. Yamaguti (1959) also maintained *Vermaia*.

Bothriocephalus pycnomerus Woodland, 1924, from *Ophiocephalus marulius*, was removed by Dollfus, (1934) to his new genus *Senga* in which the other Indian species, *S. lucknowensis* Johri, 1956, has been described from *Mastacembalus armatus*.

The tapeworms collected from the siluroid fishes, *W. attu*, *M. seenghala*, *B. yurrelli*, *E. vacha*, *Clupisoma garua*, *M. armatus* and *O. punctatus*, belonged to the species: *P. vitellaris*, *G. bengalensis*, *V. pseudotropii* and *S. lucknowensis*. During examinations of the numerous stained permanent mounts and from a study of the living specimens, *G. bengalensis* exhibited several features intergrading between *G. lucknowia* and *G. bengalensis.* Numerous developmental forms, in varying grades of development, occurred in deeper locations in the intestinal lining of *W. attu, O. punctatus* and *B. yarrelli.* The distinctive character of the scolex, visible in the stained serial sections, provided identification criteria. These sections were also studied for an evaluation of the pathological changes.

1. *P. vitellaris,* parasitic in small intestine of *W. attu, B. yarrelli* and *M. armatus,* was collected on many occasions. The intestinal mucosa, in case of *W. attu,* was covered with a thick, tenacious and yellowish exudate of a slimy consistency chiefly at the places the embedded scolices occurred with the immediately following anterior region of the strobila lying, for some distance, under the mucosa. An extensive damage, observed at such areas during histological study, consisted of a marked denudation of the mucous membrane in which, with broken villi, there was a heavy infiltration with cells and a copious congestion of the blood vessels, both in the mucosa and sub-mucosa. Haemorrhage, at some places, was also observed (Fig. 1).

2. In case of *V. pseudotropii,* collected from *E. vacha* at Mathura, and *C. garua* at Gorakhpur, the detached segments numbering 50 or more were found packing up the lumen—a feature suggestive of impaction. The mucosa, at such places, was covered with a thick slimy exudate of a pale yellow colour. In the sections of a portion of the intestine with the contained segments, a severe damage to the mucous membrane, with the broken villi around the segments, was observed with a few eggs, from the disintegrated segments, having reached the mucosal layer. Marked cellular infiltration, mostly with eosinophils, and a congestion of blood vessels were also in evidence. The submucosa, however, did not reveal any pathological change (Fig. 2).

3. Commenting on the systematic position of *G. lucknowia,* Singh (1948) believed that his species differed from *G. bengalensis* in the size of the scolex, the number of rows of the rostellar spines, the large suckers, the small-sized testes being fewer, the smaller-size of the cirrus sac and the greater number of the uterine diverticula. From the other Indian species, *G. macrones,* it was differentiated because of its larger scolex, the character of rostellum and the sucker, and the hooks being 50 in number.

G. bengalensis, according to Southwell, has the 28-42 rostellar hooks arranged in a single row. In a revised account of this species, Verma (1928) stated that the rostellar hooks, all of one kind, were in two circular rows and also depicted this feature in the diagram. Singh's contention that *G. lucknowia* was different from *G. bengalensis* because of its double row of the alternating hooks of the same size and shape is, therefore, not correct. The other differential characters relating to the comparative sizes would not provide sound differences as, in the present collection, specimens with varying body-sizes and in differences in the number of segments, the shape and size of scolex, rostellum, suckers and hooks were visible. Thus, in the differently developed and aged specimens which share in common the rostellar character of two rows of similar hooks, the scolex was from 0·37-0·58 mm in size, the rostellum measured 0·16-0·29 mm., the suckers were 0·14-0·21 mm in diameter and the hooks of 0 025-0·041 mm length. Some or more of the hooks get commonly lost in processing. *G. lucknowia* does not seem to be a valid species and is herein suppressed as a synonym of *G. bengalensis.*

In infection with *G. bengalensis*, both adults and immature forms were obtained—the scolex in the mature worms lying embedded in the mucosa with the rest of the body hanging free in the lumen. A copius thick exudate was, however, absent in such areas (Fig. 3). The immature worms, lying deeply embedded in the mucosa, did not reveal any part of the body in gross examination but, on careful examination, the scolex could be detected as a small, opaque and pinhead-sized spot. The stained sections, from the small intestine of *B. yarrelli*, showed lysis around the embedded scolex—the cellular structures being dissolved. A heavy infiltration with reactionary cells and some exudate were also in evidence. The blood vessels had become congested but there was no haemorrhage (Fig. 4).

4. Of the bothriocephalids represented by the four known species of *Senga*, the two Indian forms are: *S. pycnomerus* (Woodland, 1924) Dollfus 1934, from *Ophiocephalus marulius*, and *S. lucknowensis* Johri, 1956, from *M. armatus.*

The examinations of *W. attu*, *M. armatus*, *B. yarrelli* and *O. punctatus* yielded numerous developing and fully mature specimens of *S. lucknowensis*, locally and at Gorakhpur, on many occasions. The scolex was mostly embedded fairly deeply and showed no visible gross lesions. But, from histological study, this species appeared sufficiently significant. The typical feature of the rostellar spicule/spines, the bothria and the character of developing gonads provided the diagnostic clues in examinations of the stained serial sections. The pathological changes, in the vicinity, included marked infiltration with reactionary cells, a denudation of the epithelial layer and presence of mucous shreds (Fig. 5). Pronounced haemorrhage, around the embedded rostellum, was also observed.

Heavy infection with this species could possibly produce lesions of enteritis which, from undermining of the health, could lead to lowered production. Experimental life-cycle study with clean and laboratory raised fishes, keeping adequate control, would confirm these suspicions on the true nature of their role.

SUMMARY

The known proteocephalidan and bothriocephalidan tapeworm parasite of some of our siluroid fresh-water fishes, representing four species under

Proteocephalus, *Vermaia*, *Gangesia* and *Senga*, have been studied in relation to their pathological role in naturally occurring infections. *G. lucknowia* has been suppressed as a synonym of *G. bengalensis*. The information, available during this study, stresses the need to undertake life cycle studies on these tapeworms in order to evaluate the true nature of their deleterious effects in lowering the production.

ACKNOWLEDGEMENTS

Grateful thanks are due to Dr. B. P. Pande, M. Sc., D. Sc., F. N. A. Sc., Professor of Parasitology for supervision, guidance and going through the manuscript. Thanks are also due to the Principal for the facilities provided.

REFERENCES

1. Dollfus, R. Ph. 1934. Sur un Cestode pseudophyllide parasite de poisson d'ornement. *Bull Soc. Zool.*, France, **59** : 476-490.
2. Johri, G. N. 1956. A new cestode *Senga lucknowensis* from *Mastacembellus armatus* Lacep. *Curr. Sc.*, **25** (6): 193-195.
3. Singh, K. S. 1948. On a new cestode, *Gangesia lucknowia* (Proteocephalidae) from a fresh water fish *Eutropiicthys vacha* Day, with a revised key to the species of the genus. *Indian J. Helm.*, **1** (1): 41-46.
4. Southwell, T. 1913. Parasites from fish. Notes from the Bengal fisheries Laboratory. *Rec. Indian Mus.*, **9**: 79-103.
5. Southwell, T. 1913. On some Indian cestode. Pt. I. *Ibid.* **9**: 279-300.
6. Southwell, T. 1930. The fauna of the British India including Ceylon and Burma. Cestoda, Part I Taylor and Francis, Red Lion court, Fleet street London. 394 pp.
7. Verma, S. C. 1926. On a new proteocephalid cestode from an Indian fresh water fish. *Allahabad Univ. Stud.*, **2**: 353-362.
8. Verma, S. C. 1928. Some cestodes from Indian fishes, including four new species of Tetraphyllidea and revised keys to the genera *Acanthobothrium* and *Gangesia*. *Ibid*, **4**: 119-176.
9. Woodland, W. N. F. 1924. On a new *Bothriocephalus* and a new genus of the Proteocephalidae from Indian fresh water fishes. *Parasitol.*, **16**: 265-279.
10. Woodland, W. N. F. 1925. On three new proteocephalids (Cestoda) and revision of the genera of the Family. *Ibid.*, **17**: 370-374.
11. Yamaguti, S. 1959. Systema Helminthum Volum II. The Cestodes of Vertebrates. Interscience Publishers, New York. 860 pp.

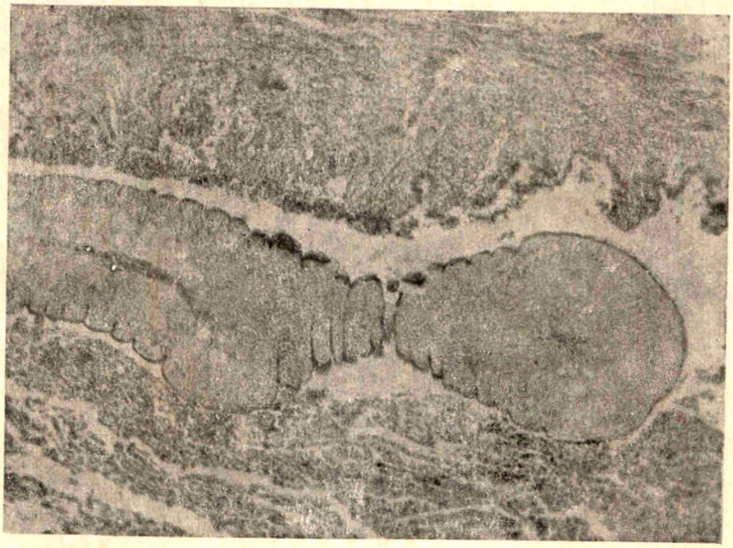

Fig. 1. Photomicrograph of cross section of small intestine of *W. attu* showing *P. vitellaris* infection (70 x).

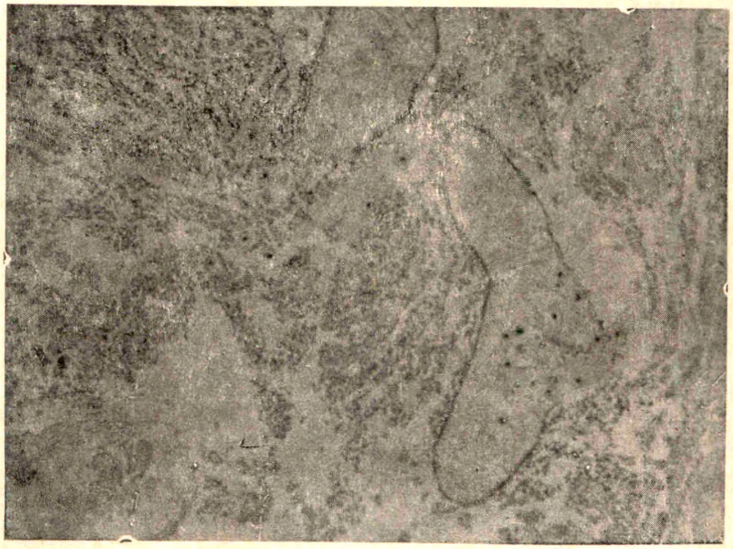

Fig. 2. Photomicrograph of cross section of small intestine of *E. vacha* showing *V. pseudotropii* infection (65 x).

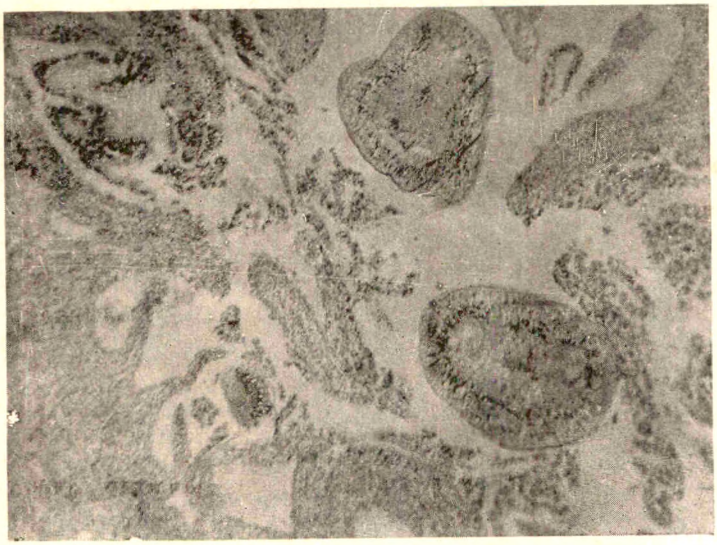

Fig. 3. Photomicrograph of cross section of small intestine of *W. attu* showing *G. bengalensis* infection (80 x).

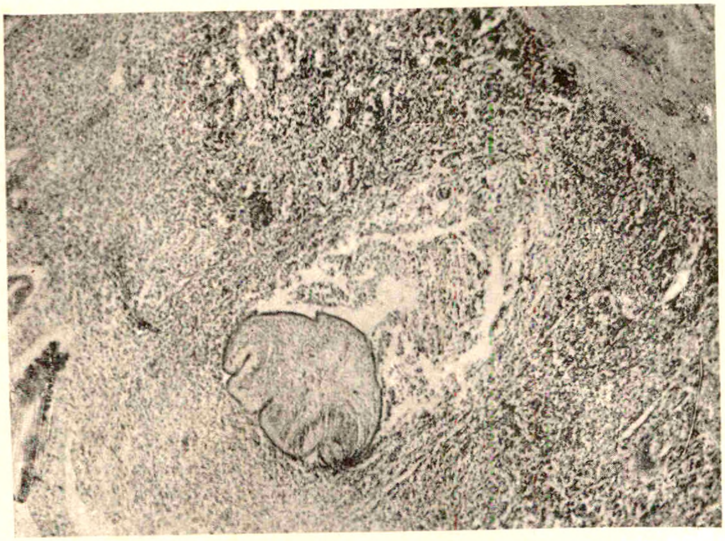

Fig. 4. Photomicrograph of cross section of small intestine of *B. yarrelli* showing *G. bengalensis* infection (85 x).

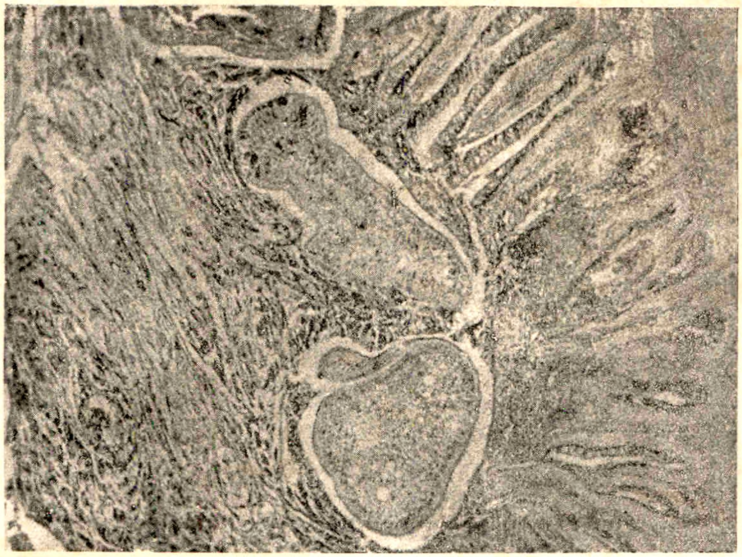

Fig. 5. Photomicrograph of cross section of small intestine of *O. punctatus* showing *S. lucknowensis* infection (95 x).

STUDIES ON FLORAL BIOLOGY OF KARAUNDA
(*CARISSA CARANDAS* Linn.)

AYODHYA PRASAD
*Department of Botany, Govt. Agricultural College, Kanpur.**

Carissa carandas Linn. (Karaunda) of the family Apocynaceae is commonly found in many parts of India. The plant is of very hardy nature and has got its adaptability to wide range of soils and climatic conditions. It provides a good protective and evergreen hedge. Even as a hedge plant, Karaunda bears heavily. Its fruits are used for making pickles and other preserves. The fruits are also used for jelly preparation. Besides, the leaves are used for making decoction which is given in remittent fevers.

No systematic efforts have yet been made for improvement of this crop. Before the programme of improvement in the Karaunda through selection, hybridization and other means is initiated the knowledge regarding anthesis, dehiscence of anthers, pollen morphology and fertility, respectivity of stigma, mode of pollination and extent of fruit set is necessary. Therefore, it was considered desirable to undertake in detail the study of floral biology of two varieties of Karaunda *viz.*, Amara and Dulcis, with a view to have a better understanding of the factors contributing to the improvement of this plant. These investigations will also be helpful in breeding work of this fruit crop.

Karaunda with dark purple greenish fruits are called Amara and those with cream coloured fruits are known as Dulcis. Ten years old 14 Karaunda seedling plants, uniform in growth and Productivity, were selected for the material of this investigation at Botanical Garden, Govt. Agricultural College, Kanpur, in the year 1961. All the experimental plants were of similar vigour and received similar cultural and manurial treatments.

(a) *Time, duration and mode of flowering*—In spring, the flower buds develop in the axils of the leaves. There are 1-3 peduncles and a peduncle has 2—3 pedicellate flower buds. The corolla is twisted to the left in the bud. The flower buds near the base are usually the first to mature and there is progression towards later blossoming. The central flower of the cluster is the first to open, while others may open 1 to 4 days later. The flowering begins in the first week of March and usually reaches its peak from 4 to 5 weeks later but sporadic flowering on some plants continues until the end of June.

The short pedicelled white flowers are arranged in Corymbose cymes. The flowers are actinomorphic, hermaphrodite, hypogynous and pentamerous. The corolla is gamopetalous, salverform while androecium is epipetalous, has short filaments and introse anthers which are in linear and tapering form. The gynoecium consists of two carpels—syncarpous and filiform below the stigmatic head.

---

* Present address—Asstt. Horticulturist, Incharge, National Hortorium, Circuit House, Meerut, U. P., India.

(b) *Anthesis*—The flower bud opens rather quickly in Karaunda. Just before anthesis the buds become plumpy and form slit on the top. Soon after the slit is gradually widened by the pressure of the petals as they unfold and form a cup like shape. At first, one petal separates at the apex and the rest remain united which separate later on. As the inner angle of the apices of the petals increases, the tendency of the petals to fall apart, becomes greater and consequently the process is hastened. This tendency continues till the bud is fully opened. The androecium and gynoecium remain enclosed in the basal tube of corolla. These various phases of anthesis take about one hour. The mode of anthesis is the same in both the varieties under study. After anthesis the flower remains in open condition for about 2 days till it fades or drops its accessary parts.

For determining the time of anthesis uniform branches were tagged and the number of flowers which opened between 4 p.m. and 11 p.m. were recorded at hourly interwals. The opened flowers were removed after every observation to avoid recounting in next observation. The data regarding anthesis of Amara variety are presented in table 1.

TABLE 1

Time of opening of flowers in Amara.

Dates of observation	Percentage of flowers opened at hours							Total No. of flowers recorded
	4–5 p. m.	5–6 p. m.	6–7 p. m.	7–8 p. m.	8–9 p. m.	9–10 p. m.	10–11 p. m.	
24–3–61	...	5·8	12·7	78·5	3·0	...	...	210
25–3–61	...	6 3	14·2	75·6	3·9	...	...	316
26–3–61	...	6·0	18·5	72·1	3·4	...	...	285
27–3–61	...	3·9	11·0	76·1	9·0	...	...	297
28–3–61	...	2·8	10·6	78·3	8·1	0·2	...	312
29–3–61	...	3·4	9·2	76·8	9·5	1·1	...	308
30–3–61	...	5·0	11·2	77·1	6·1	0·6	...	326
31–3–61	...	7·0	12·5	76·5	3·1	0·9	...	390
1–4–61	...	7·0	15·9	70·8	5·1	1·2	...	377
2–4–61	...	9·2	16·5	69·8	4·5	...	...	382
3–4–61	...	6·8	18·0	70·6	4·6	...	...	417
4–4–61	...	10·7	21·4	66·5	1·4	...	...	425
5–4–61	...	9·4	20·6	68·5	1·5	...	...	436
6–4–61	...	10·0	19·3	70·0	0·7	...	...	419
7–4–61	...	9·6	18·5	71·4	0·5	...	...	363

A perusal of table 1 shows that the anthesis started in the evening at 5. p. m. and the maximum percentage of flowers opened between 7 and 8 p. m. while the anthesis continued upto 10 p. m., but the percentage of flowers which opened after 8 p. m. was less than 11 per cent.

(c) *Dehiscence*—Dehiscence of anthers in Karaunda starts about 4 to 9 hours before anthesis and is completed within 4 to 5 hours. The general idea about time and mode of dehiscence was taken by opening the flowers by hand.

(i) *Mode of dehiscence*—Before dehiscence the anthers become shiny, and beginning of dehiscence is marked by the appearance of longitudinal slits in the anther-lobe. The slit widens and after some time the epidermis falls apart, exposing the whitish mass of pollen grains. A transverse section of an anther showed that there were two layers of thicker cells in pollen sac walls. At places where there was only one layer of these cells, the endothecium raptured from base towards the top probably on account of the effect of humidity, heat and the internal pressure of pollen grains.

(ii) *Time of Dehiscence*—To study the time of dehiscence, 100 flower buds were tagged at 6 a. m. each day for two weeks and the number of completely dehisced anthers were then counted at hourly intervals from 6 a. m. to 2 p. m. All anthers completely dehisced in the period of 5 hours (table 2). The dehisced anthers were removed in each observation for avoiding recounting.

TABLE 2

Time of dehiscence in Amara.

Dates of observation	Percentage of anthers dehisced at hours							Total No. of anthers recorded
	7–8 a. m.	8–9 a. m.	9–10 a. m.	10–11 a. m.	11–12 a. m.	12–1 p. m.	1–2 p. m.	
24–3–61	...	1·50	51·14	35·70	11·66	...	...	216
25–3–61	...	3·05	52·06	44·12	0·77	...	...	205
26–3–61	...	7·16	43·25	48·60	0·99	...	...	236
27–3–61	...	5·22	47·06	43·96	2·15	1·61	...	212
28–3–61	...	8·06	56·62	33·16	1·01	1·15	...	228
29–3–61	...	8·73	51·97	38·01	1·29	...	...	225
30–3–61	...	11·0	59·26	29·74	...	...	...	234
31–3–61	...	7·18	66·84	24·09	1·89	...	...	242
1–4–61	...	7·82	68·70	23·48	...	...	...	217
2–4–61	...	10·27	65·11	23·60	1·02	...	...	238
3–4–61	...	12·50	65·75	21·05	0·70	...	...	203
4–4–61	...	9·45	61·85	28·16	0·54	...	...	227
5–4–61	...	13·08	62·12	24·29	0·51	...	...	210

It is evident from table 2 that the dehiscence started at 8 a. m. and completed in a period of about 5 hours. The data indicate that the peak period of dehiscence was 9 to 10 a. m. Thus it is clear from tables 1 and 2 that the dehiscence takes place about 4 to 9 hours prior to anthesis.

POLLEN STUDIES I

(a) *General appearance and shape:*

Morphological features of the pollen grains were studied by aniline oil gentian violet and Methyl green glycerine jelly methods described by Erdtman[7] and Wodehouse[21].

The pollen grains appeared as fine whitish powdery mass when seen with the naked eye. The natural form of the pollen grains was best observed in the aniline oil gentian violet. They appeared elliptical in shape in equatorial view and triangular and spherical types in polar view which were shrivelled and compressed from the sides. In methyl green glycerine jelly they expended and appeared oblong in equatorial view with 2-4 germpores, which are placed equidistantly. The normal grain looks almost spherical in shape. The exine is much thicker and transparent than the intine.

(b) *Pollen size in different media:*

The pollen grains were mounted in different media and the size was measured with micrometer. The size in these two varieties does not vary much within the same medium. The average size of 200 pollen grains was recorded during the peak period of flowering and is presented in table 3.

TABLE 3

Size of pollen grains in different media.

Varieties	Aniline oil gentian-violet (μ)	Acetocarmine with glycerine (μ)	Methyl green glycerine jelly (μ)	Water (μ)
Amara	32·70	28·25	27·52	29·76
Dulcis	42·26	40·35	38·27	34·50

A perusal of table 3 shows that the size of pollen grains is quite large with a range of 27·52 to 42·26 μ in different media.

(c) *Pollen fertility:*

The pollen fertility was determined by stainability of pollen with acetocarmine and on stigmas of different ages. The deeply stained, normal looking pollen grains were counted fertile while shrivelled and weakly stained grains were recorded as sterile ones. They were recorded in 60 random fields on the different slides and the data are summarized in table 4.

TABLE 4

Pollen fertility in different varieties.

Vareities	Total number of pollen grains studied	Number of fertile pollen grains	Number of sterile pollen grains	Percentage of fertile pollen grains
Amara	1278	1085	193	84·89
Dulcis	1190	1016	174	85·37

It is clear from table 4 that pollen fertility was 85·37 and 84·89 per cent in Dulcis and Amara varieties of Karaunda respectively.

(*d*) *Artificial germination of pollen grains:*

The pollen grains are monosiphonous. Their germination studies were made in different concentrations sucrose solutions by hanging drop method described by Prasad[10]. The results are given in table 5.

TABLE 5

Germination of pollen grain in sucrose media.*

Varieties	Per cent Germination in sucrose media of					
	5%	10%	15%	20%	25%	30%
Amara	6·11	12·58	38·50	68·10	40·13	29·06
Dulcis	9·75	14·19	44·82	77·05	46·95	34·52

* About 200 to 230 pollen grains were examined in each observation after 4 hours of pollen planting.

From a perusal of table 5 it is clear that Karaunda pollen showed some germination in all the concentrations tried but the best germination of 68·10 per cent in Amara and 77·05 per cent in Dulcis was recorded in 20 per cent concentration.

POLLEN STUDIES II

(*a*) *Receptivity of stigma:*

The stigma receptivity was studied only in Amara variety. From visual observation the stigma was considered to be healthy and receptive when it was fully developed, shiny and sticky due to the secretion of stigmatic fluid. The stigma was recorded as unhealthy and non-receptive when it was undeveloped, dry and dull green in colour. The visual observations were compared with the actual condition of receptivity, as indicated by the presence of germinating pollen grains on the stigmas of different age, after controlled pollination. The controlled pollinations on emasculated flowers were made at different intervals of 12, 8, and 4 hours before anthesis, at anthesis and 4, 8, 10, and 12 hours after anthesis. Stigmas thus pollinated were removed alongwith styles after 6 hours of pollination and were fixed in aceto-alcohol (1: 3) for 10-12 minutes. These were then preserved in 30 per cent alcohol until they were finally examined. They were then transferred to a vial containing lactic acid for 24 hours. They were stained with cotton blue and kept in an oven for 2 hours at 50°C and were macerated on a slide after putting a cover slip (Darlington and La Cour, 6). It was found that the stigmas pollinated 12 hours before anthesis and 10 hours after anthesis had no pollen tubes in the styles while the stigmas pollinated from 8 hours before to 8 hours after anthesis had the pollen tubes in the styles. These observations regarding the receptivity of stigma are more or less in agreement with the corresponding data obtained by microscopic examination of macerated stigmas.

(*b*) *Duration of Receptivity of Stigma:*

(i) *Visual observation*—The stigmas were examined with the help of hand lens (X 10) for their receptive stage. Shiny yellowish green stigmas were considered to be receptive, while dried, yellowish and greenish white stigmas were treated as non-receptive. They became receptive from eight hours prior to anthesis. Beyond this period the stigmas became greenish white and styles began to dry up, therefore, they were considered as non-receptive. Consequently the corolla with androecium dropped off and calyx remained persistant.

(ii) *Fruit set method*—The confirmation of the visual observations for the receptivity of stigma was also made. Artificial controlled pollinations were made of the previously bagged and emasculated flowers at different stigmatic ages and fruit set was recorded eight days after pollination. The results are summarized in table 6.

TABLE 6

Receptivity of stigma in Karaunda based on fruit set studies.

Varieties	Before anthesis						At anthesis		After anthesis					
	12 hours		8 hours		4 hours				4 hours		8 hours		12 hours	
	a*	b*	a	b	a	b	a	b	a	b	a	b	a	b
Amara	50	0	50	52	50	84	50	42	50	12	50	4	50	0
Dulcis	50	0	50	66	50	92	50	48	50	20	50	6	50	0

a*=Number of flowers pollinated.

b*=Percentage of fruit-set.

It is evident from table 6 that 12 hours before or after anthesis the stigmas were found to be non-receptive The maximum receptivity of stigmas, 92 per cent and 84 per cent were recorded in Dulcis and Amara varieties respectively, in the flowers which were pollinated 4 hours prior to anthesis.

(*c*) *Germination of pollen on the stigmatic surface:*

To determine the correlation between the receptivity of stigma and extent of pollen germination and tube growth on the stigmatic surface, controlled pollination of emasculated flower buds was carried out in the Amara variety at different stigmatal ages. Ten pollinated flowers were taken every time at the different intervals of 4, 8, 10 and 12 hours after pollination in each case. The stigmas of pollinated flowers were examined for pollen germination by the method described by Darlington and La Cour[6]. The results are presented in table 7 on page 38.

A perusal of table 7 indicates that the stigma has maximum receptivity 4 hours prior to anthesis while it decreases afterwards. It is also clear that the maximum pollen germination (90 per cent) was noted for 4 hours prior to anthesis.

POLLINATION AND FRUIT-SET STUDIES IN AMARA VARIETY

The different modes of pollination in Amara variety were tested and their effectiveness was ascertained on fruit-set. The fruit was considered set after eight days when the style dropped, ovary swelled to small pea size and turned greenish in colour.

(1) *Self-pollination*—120 flower buds were tagged and bagged 10 hours prior to anthesis for self-pollination.

(2) *Hand-pollination*—120 flower buds were emasculated and bagged 10 hours before anthesis. The stigmas of the emasculated flowers were pollinated with the pollen of the me tree. After pollination these flowers were carefully bagged again.

(3) *Natural open pollination*—150 flowers were tagged and left as such for the open pollination.

(4) *Natural cross-pollination*—10 hours prior to anthesis 120 flower buds were emasculated and left to be pollinated by natural agencies such as bees, flies, insects and wind. The data are presented in table 8 on page 39.

It is apparent from table 8 that there is least fruit-set under natural cross-pollination (47·50%) but when pollens were dusted on each stigma by hand, the fruit-set increased to 61·66 per cent. The maximum fruit-setting (82·00%) was found in natural open pollination.

TABLE 7

Pollen germination on stigma in Amara vareity.

Stigmatal age in relation to anthesis	Stigma examination after hours of pollination												Total stigma examined	Stigmatal receptivity	
	4 hours			8 hours			10 hours			12 hours				Stigma with pollen tubes	Receptivity (per cent)
	a	b	c	a	b	c	a	b	c	a	b	c			
(1) 12 hours before	10	0	0	10	0	0	10	0	0	10	0	0	40	0	...
(2) 8 hours before	7	3	0	5	5	0	4	3	3	3	4	3	40	21	52·5
(3) 4 hours before	2	5	3	1	5	4	1	6	3	0	4	6	40	36	90·0
(4) At anthesis	5	4	1	4	4	2	4	4	2	5	3	2	40	22	55·0
(5) 4 hours after	6	2	2	5	3	2	4	5	1	5	4	1	40	20	50·0
(6) 8 hours after	7	3	0	6	3	1	6	3	1	7	2	1	40	14	35·0
(7) 10 hours after	8	2	0	7	3	0	7	2	1	9	1	0	40	9	22·5
(8) 12 hours after	10	0	0	10	0	0	10	0	0	10	0	0	40	0	...

a=No germination of pollen.

b=Fair germination of pollen.

c=Good germination of pollen.

TABLE 8

Fruit-set as affected by various modes of pollination in Amara vareity of Karaunda.

S.No.	Modes of pollination	Number of flowers pollinated	Number of fruit set	Percentage of fruit set
1.	Self-pollination	120	66	55·00
2.	Hand-pollination	120	74	61·66
3.	Natural open pollination	150	123	82·00
4.	Natural cross-pollination	120	57	47·50

DISCUSSION

In the present studies it was observed that anthesis and dehiscence were not related to each other and were completed on the same day. Anthesis generally started between 5 and 6 p.m. and the peak of anthesis took place between 7 and 8 p. m. Similar short durations for anthesis have been reported by Bajpai[2], Randhawa and Dass[13] and Sen *et al.*,[15] in the case of Aonla (*Phyllanthus emblica* L.), Phalsa (*Grewia asiatica* L.) and Mango (*Mangifera indica* L.) respectively. It was interesting to note that anthesis required very short period for its completion. In the studies on Karaunda it was seen in general observations that there was no correlation between anthesis and the atmospheric temperature and humidity. More or less similar observations have been reported by Musahib-uddin and Dinsa[8], Popenoe[9], Randhawa and Damodaran[12], Singh[16], Torres[19] and Wagle[20] in the case of mango.

Dehiscence of anthers starts prior to anthesis and occurs as a continuous process till all the anthers dehisced. All the anthers in a flower require about 4 to 5 hours to complete dehiscence. Most of the anthers dehisce between 9 a. m. and 11 a. m. though dehiscence starts at about 8 a. m. and continues till 1 p.m. It is interesting to note that anthesis and dehiscence take place at different timings and complete within a short period. Such a short duration in case of dehiscence has also been reported by Bajpai[2], Balsubrahmanyam[3] and Randhawa and Sharma[14] in Aonla (*Phyllanthus emblica* L.), Guava (*Psidium guajava* L.) and grape *Vitis vinifera* L.) respectively.

These investigations also show that there is not much difference in the morphology of the pollen grains of Amara and Dulcis varieties of Karaunda. Normal pollen grain looks almost spherical in shape having 2 to 4 germpores placed equidistantly. Pollen grain size varies with a range of 27·52 to 42·26 microns in different media. The fertility of pollen grains, as observed by acetocarmine stainability was 85·37 and 84·89 per cent in Dulcis and Amara varieties respectively. Artificial germination of pollen grains showed that maximum germination was 77·05 and 68·10 per cent in Dulcis and Amara varieties respectively, in 20 per cent sucrose medium. Maximum percentage of pollen germination and tube growth in 20 per cent sucrose medium have also been reported by Prasad[11] and Singh[17] in custardapple (*Anona squamosa* L.). However, Addicot[1] reports that pollen germination and tube growth are two different processes which depend upon the physiological conditions of the pollen grains at the time of testing.

In the present studies the maximum pollen germination obtained was 68·10 per cent in the case of Amara variety, while the fertility obtained by acetocarmine stainability test was 84·89 per cent. It is, however, evident that the low germination obtained in artificial media does not represent the maximum germination that occurs on stigmatic surfaces in natural conditions. The studies on stigma receptivity in Amara variety of Karaunda lead to the conclusion that stigma becomes fairly receptive on the day of anthesis and receptivity lasts for 10 hours after opening of the flower. The most receptive period was from 8 hours prior to 4 hours after anthesis though visual observation did not reveal the receptivity of stigma before the anthesis yet germinated pollen grains and fruit-set were obtained by pollination. This might be due to the fact that pollen remains viable till the stigma remains receptive and consequently pollen germination and tube growth take place. Such results of stigma receptivity have been reported by Climenko[5] and Singh and Tomar[18] in oranges (*Citrus sinensis* Swingle) and Kagzilime (*Citrus aurantifolia* Swingle) respectively.

The results of self, cross and open pollination (table 8) reveal that there is a great deal of difference among the different modes of pollination, as far as the fruit-set is concerned. This shows that there is no self-sterility in the varieties under study, nor is there any cross incompatibility. It is possible to obtain as high as 82·00 per cent of fruit-set in Amara variety by natural open pollination while natural cross-pollination gives very poor fruit-setting (47 50 per cent). These findings of fruit-set clearly show that natural open pollination is quite predominant in Karaunda. The present studies on pollination are more or less in accordance with the observations of Randhawa and Dass[13] and Bajpai and Prasad[4] in Phalsa (*Grewia asiatica* L.).

SUMMARY

(1) The investigations were carried out on anthesis, dehiscence, pollen morphology, pollen germination and receptivity of stigma in Amara and Dulcis varieties of Karaunda while the pollination and fruit-set studies were done only in Amara variety.

(2) The mode of anthesis and dehiscence is similar in both Amara and Dulcis varieties of Karaunda.

(3) Anthesis started in the evening. Maximum percentage of flowers opened between 7 and 8 p.m. in both the varieties.

(4) Dehiscence of anthers started 5 to 8 hours before opening of the flowers and was over within a period of 5 hours. Maximum percentage of anthers dehisced between 9 and 10 a. m.

(5) The pollen grains in both the varieties were almost identical in morphology, however, their size varied from 27·52 to 42·26μ in different media.

(6) Maximum percentage of artificial pollen germination was recorded in 20 per cent sucrose solution.

(7) Stigma attained maturity 8 hours prior to anthesis and remained receptive for about 10 hours after opening of the flower.

(8) Maximum percentage of fruit-set (82·00%) was found in natural open pollination and minimum fruit-set (47·50%) was recorded in natural cross-pollination.

REFERENCES

1. Addicot, F. T. 1943. Pollen germination and pollen tube growth as influenced by pure growth substances. *Plant Physiol,* **18** : 270-79.
2. Bajpai, P. N. 1957. Blossom biology and fruit-set in (*Phyllanthus emblica* L. *Indian J. Hort.*, **14** (2) : 121-25.
3. Balsubrahmanyam, V. R. 1959. Studies on blossom biology of guava (*Psidium guajava* L.) *Indian J. Hort.* **16** (2) : 69-75.
4. Bajpai, P. N. & Prasad, A. 1962. Studies on blossom biology of Phalsa (*Grewia asiatica* L.). *Agra Univ. J. Res.* (*Sci.*), **XI** (iii) : 173-84.
5. Climenko, C. T. 1936. Period of the receptivity of stigma on oranges. *Bull. Batum Entrop. Bot. Gdn.* No. 1 : 127-129.
6. Darlington, C. D. & La Cour, L. T. 1947. Handing of chromosomes. George Allen & Unwin, London.
7. Erdtman, G. 1952. Pollen morphology and plant taxonomy : Angiosperms. Almqvist & Wiksell, Stockholm.
8. Musahib-uddin & Dinsa, H. S. 1946. The floral count and fruit-set studies in some of the North Indian mangoes. *Punjab Fruit J.*, (37) **10** : 35-42.
9. Popenoe, W. 1917. The pollination of Mango. *U. S. D. A. Bur. Ind. Bull.* 542.
10. Prasad, A. 1962 Studies in the artificial germination of pollen of *Zizyphus mauritiana*. *Madras Agri. J.*, **49** (10) : 351.
11. Prasad, A. 1963. Studies on the pollen germination of Anona in artificial media. *Sci. & Cult.*, **29** (2) : 96-97.
12. Randhawa, G. S. & Damodaran, V. K. 1961. Studies on floral biology and sex-ratio in mango (*Mangifera indica* L.) var. Chausa, Dashehari and Krishnabhog. II. Flowering habit, flowering season, panicle development and sex-ratio. *Indian J. Hort.*, **18** (1) : 36-45.
13. Randhawa, G. S. & Dass, H.C. 1962. Studies on floral biology of Phalsa (*Grewia asiatica* L.) *Indian J. Hort.*, **XIX** (1-2) : 10-24.
14. Randhawa, G.S. & Sharma, R. L. 1960. Studies on flowering and pollination of grapes. *Hort. Adv.*, **4** : 21-37.
15. Sen, P.K., Malik, P.C & Ganguly, B. D. 1946. Hybridization of the Mango. *Indian J. Hort.*, **4** (1-2) : 4-15.
16. Singh R. N. 1954. Studies on floral biology and subsequent development of fruit in the mango (*Mangifera Indica* L.) Varieties Dashehari and Langra. *Indian J. Hort.*, **11** (3) : 69-88.

17. Singh, S.N. 1957-59. Germination of Custard apple pollen in artificial medim. *Annu.. Rep. Fr. Res. Sta*. Saharanpur, 73-78.

18. Singh, S.N. & Tomar, B.S. 1949. Bearing habits of Kagzilime. *Ind. Fmg.* **10** : 532-36.

19. Torres, J. P. 1931. Some notes on the Carabao Mango flower. *Phillipp. J. Agric.*, **2** : 395-98.

20. Wagle, P.V. 1928. Studies in the shedding of Mango flowers, and fruits. *Memoris. Dep. Agri. India (Bot.)*, **15** (8) : 259-63.

21. Wodehouse, R. P. 1935. Pollen grains, McGraw hill Company, New York.

MORPHOLOGICAL AND ANATOMICAL STUDIES IN HELOBIAE VIII.

VASCULAR ANATOMY OF THE FLOWER OF HYDROCHARITACEAE—STRATIOIDEAE AND THALASSIOIDEAE*

V. SINGH
School of Plant Morphology, Meerut College, Meerut.

INTRODUCTION

Hydrocharitaceae comprising 13 genera and 80 species (Willis, 1951) is chiefly distributed in the tropical regions of the world. The majority of species are fresh water but a few are marine. The plants are partly or completely submerged or rarely floating herbs and show great variation in the vegetative organization and structure of the flower.

Certain aspects of the family such as biology of the flower, cytology, embryology, etc., have received considerable attention from earlier workers. Saunders (1929) also touched this family in connection with her theory of carpel polymorphism. She envisiged that in Hydrocharitaceae there are two types of carpels one of which is sterile and the other fertile. Troll (1931) made a study of the gynoecium in the family. However, a perusal of literature reveals that the vascular anatomy of the flower of this family did not receive any attention at the hands of earlier workers except for a short note by Kaushik (1940) describing the vascular anatomy of the pistillate flower of *Enalus acoroides*. Further, Hydrocharitaceae is one of those few monocotyledonous families with an inferior ovary which is yet to receive adequate attention. Appreciating this Eames (1961) remarks that, "The morphology of gynoecium in this family needs anatomical study; the relation of the carpels to the receptacle is obscure and has been variously interpreted." In the same way the so called superficial placentation in the family also deserves further attention.

The present investigation has been undertaken with a view to have a better understanding of the morphological problems of the family.

Engler and Prantl (1889) divided the family in the four tribes—Stratioideae, Thalassioideae, Vallisnerioideae and Halophiloideae. The present paper embodies the results of observations on some five genera of the family, of these *Ottelia*, *Bootia* and *Hydrocharis* belong to the tribe Stratioideae and *Enhalus* and *Nechamandra* to Thalassioideae

MATERIAL AND METHODS

The material that includes inflorescences, flowers and flower buds of different ages has been procured from various sources (table 1). It was fixed in formalin-acetic acid-alcohol and dehydrated in ethyl alcohol and xylol grades and embedded in paraffin. Serial microtome sections, both transverse and longitudinal, were cut 10-12 microns thick and generally stained with crystal violet and erythrosin. Floral parts cleared by potassium hydroxide, lactic acid and methyl salicylate were also studied. Basic fuchsin proved to be a very good stain for such cleared preparations.

---

* Research contribution No. 77 from the School of Plant Morphology, Meerut College, Meerut.

TABLE 1

Species	Place	Collector (s)
1. *Ottelia alismoides* (Linn.) Pers.	Indore Varanasi	Mr. R. Sharma Dr. Y.S.R.K. Sharma
2. *Bootia cordata* Wall.	Varanasi	Dr. Y.S.R.K. Sharma
3. *Hydrocharis dubia* (Bl.) Baker.	Leiden (Netherlands)	Dr. W.A. van Heel
4. *Enhalus acoroides* (Linn. f.) Rich. ex. Steud.	Madras	Dr. K.K. Lakshmanan
5. *Nechamandra alternifolia.* (Roxb.) Thw.	Madras	Dr. K.K. Lakshmanan

OBSERVATIONS

Ottelia Pers.

Ottelia alismoides (L) Pers. is a submerged, flaccid, annual fresh water herb, common in slow running streams and water. The hermaphrodite flowers are sessil and solitary within a long peduncled tubular elliptic to ovate spathe with two acute tips and 5-10 flat or crisped wings of which 2-3 are more prominent. The perianth is of six free segments. The outer three are green and persistent while the inner three are petaloid and larger than the outer. The six stamens are of unequal heights and are arranged in three pairs. The filaments are flattened and the anthers are dithecous and basifixed. The pollen grains are densely set with numerous minute tubercles. There are also present three staminodes, each alternating with a pair of stamens. The narrowly oblong, beaked, inferior, and hexacarpellary ovary is unilocular and bearing numerous small anatropous ovules. Each of the six styles is bifid with two unequal papillose arms. The oblong-elliptic fruit, enclosed in a 5-10 winged spathe, bursts irregularly near the top. The seeds are many, minute, oblong or fusiform.

Anatomy of the Flower—The peduncle is 3-6 angular in a cross-section and the cortex shows a large number of lacunae. The vascular supply consists of numerous scattered vascular bundles of which the three central bundles are large (Fig. 2). The bundles are collateral and the xylem is very much reduced and is represented by a channel formed by the obliteration of vessels.

In the peduncle and leaf stalk of *Ottelia alismoides* Majumdar (1938) has noticed polystely and that each meristele is surrounded by its own endodermis and pericycle. In the present investigation no endodermis and pericycle have been observed surrounding the vascular bundles of the peduncle.

The spathe receives all the peripheral bundles of the peduncle and also a trace from each of the three central bundles (Fig. 3). In a transverse section the spathe is generally 3-4 cells in thickness and the wings show a large number of small lacunae. In between the spathe and the ovary are present small scaly structures—the squamulae intravaginales—generally 2-3 cells in thickness. The three larger bundles branch and anastomose to form an almost complete vascular cylinder (Figs. 4, 5). At this level some thick-walled elements also appear in the xylem.

A little higher up, at the base of the ovary, the vascular cylinder splits up into a large number of vascular bundles (Figs. 6,7). As the locules make their appearance some of the bundles begin to fade out except the 12 peripheral ones which are arranged in a ring and constitute gynoecium supply (Figs. 8,9). Out of these, six are the carpellary dorsals* and the alternating six are the ventral strands. At the base the ovary is perfectly six-locular, but slightly higher up it becomes unilocular being incompletely divided into six cells by protruding placentae. Each placenta is formed by the fusion of two half placentae of the two adjacent carpels. In very young buds the two adjacent half placentae are in intimate contact with one another. But in the older buds each placenta splits up at the tip along the original line of the union of the two half placentae and finally separating the two half placentae of the adjacent carpels. A large number of lacunae are present in the ovary wall and the placentae. Each placental strand supplies many anatropous ovules borne on the two half placentae of the two adjacent carpels.

Both the dorsal bundles and the remaining placental strands continue up to the top of the ovary where they show anastomosing (Fig. 1) and form an incomplete vascular cylinder (Figs. 10,11) which gives rise to traces for the outer and inner perianth and the stamens successively.

The traces for the outer and inner whorl of the perianth segments arise in alternating whorls (Figs. 12,13). The vascular supply of each perianth segment consists of three bundles, of which the median remains undivided while the two marginals may divide further. A large number of lacunae are present in the perianth segments of the outer whorl.

After the departure of the traces for the perianth the remaining vascular tissue breaks up into 12 bundles, the six outer supply the stamens while

---

* The terms dorsal bundles and ventral strands (placental strands) have been used in topographic sense but they also carry the bundles of other floral organs adnated to them.

the six inner extend into the six styles (Fig. 14). The anthers lie in pairs, each opposite a perianth segment of the outer whorl. The filaments are covered with unicellular papillose hairs formed by the prolongation of the epidermal cells. Alternating with each pair of stamens are present three staminodes (Fig. 15). In transverse section of the flower they can be easily distinguished from the filaments of the fertile stamens by their dark staining cells. Generally the staminodes are without any vascular supply, but in some flowers traces to the staminodes have been observed and in such cases the bundle of a staminode extends only for a very short distance.

The stylar bundle continues as such for some distance, and then it bifurcates into two branches extending into two unequal arms of the style (Figs. 16,17). The two arms of the style are often adhering together with the flat side. The inner side of these arms is covered with papillose outgrowths of the epidermal cells.

Flowers with 5,7,8 or 9 stamens and carpels were also observed. In such cases gynoecium supply of the flower consists of bundles double the number of the carpels.

Bootia Wall.

Bootia cordata Wall. is similar to *Ottelia alismoides* in habit and vegetative characters. It can be distinguished from the latter only in flowering condition. The plants are dioecious. Only staminate flowers were available for study. Numerous staminate flowers are enclosed in a spathe. There are six perianth segments in two whorls of three each, the outer are green while the inner are white with an yellowish tinge. The twelve stamens that are of unequal heights are arranged in four whorls. The filaments are flattened; the anthers are 2-locular dehiscing laterally. Six styllodia are also present in two whorls of three each.

Anatomy of the Male Inflorescence—The vascular supply of the peduncle consists of three larger bundles in the centre and many smaller and poorly developed bundles in the peripheral region of the cortex (Fig. 18). The xylem of the bundles is reduced to a cavity bounded by a layer of thin-walled cells.

At the base of the spathe, the three central bundles expand and unite to form an almost complete vascular cylinder. The xylem elements of this cylinder show spiral thickenings. Three traces arise from this vascular cylinder for the spathe which encloses the inflorescence (Fig. 19). All the three bundles extend unbranched to the top of the spathe. A large number of air cavities are present in the spathe.

After the departure of the traces for the spathe, the remaining vascular cylinder constitutes the vascular supply of the flowers (Fig. 20). It gives off a mass of vascular tissue for the pedicel of each flower which soon breaks up into 3-5 larger bundles in the centre and many smaller bundles in the peripheral region of the cortex (Figs. 21, 22). In between the spathe and pedicels of the flowers a large number of squamulae are present (Figs. 20-22).

Anatomy of the Staminate Flower—Higher up in the pedicel the vascular bundles expand and at the base of the receptacle of the flower they anastomose to form an almost complete vascular cylinder (Figs. 23, 24). This cylinder gives off nine traces almost simultaneously for the perianth segments of the outer whorl (Fig. 25). Thus each perianth segment receives three bundles—one median and two marginals—which continue unbranched throughout their length. Closely above nine more traces are given off from the central cylinder, three for each of the three perianth segments of the inner whorl (Fig. 25). During their outward course the lateral traces bifurcate.

The mesophyll cells of the outer perianth segments are loosely arranged and show a number of air cavities, while that of the inner are rather compact. The perianth segments of the inner whorl show some foldings in the upper region.

After the departure of the perianth traces the vascular cylinder again becomes almost complete (Fig. 26). It gives off twelve traces in four successive and alternate whorls of three each for the stamens (Figs. 27, 28). The single concentric bundle of each stamen extends throughout the filament and connective undivided.

The remaining vascular tissue reorganises into a somewhat three lobed vascular cylinder (Fig. 28). This constitutes the vascular supply of the styllodia. Three traces move outwards from this vascular cylinder corresponding to the median bundles of the perianth segments of the outer whorl (Fig. 29). They enter the three styllodia of the outer whorl which separate form one another at a slightly higher level. The remaining vascular tissue splits up into three bundles which alternate with those of the outer whorl. They form the vascular supply of the three styllodia of the inner whorl (Fig. 31). The single bundle of each styllodium continues as such for some distance (Fig. 33) and then it bifurcates (Figs. 33, 34). The two branches extend but for a short distance into the two lobes of a styllodium (Figs. 32, 34,35). The cytoplasm of the cells of the styllodia is densely staining with centrally placed prominent nuclei. The styllodia reach only up to the level of the anthers of the inner whorl of stamens.

Hydrocharis Linn.

Hydrocharis dubia (Bl.) Baker (syn. *H. morus-ranae* (non Linn.) F.V.M. Fragm), commonly known as Frog-bit, occurs in ponds and ditches. The plants are stoloniferous herbs, free floating or rooting at the bottom in shallow water.

The plants are monoecious. The unisexual flowers are borne in 2-leaved membranous spathes. The female spathe is pedicelled and one-flowered. The outer perianth is sepaloid and consists of three persistent segments. The three inner perianth segments are petaloid and larger than the outer. They are broadly ovate, crumpled and white with a yellow spot near the cuneate base. A nectary is present opposite each perianth segment of the inner whorl. In the female flowers there are three pairs of linear yellow staminodes, each pair lying opposite a perianth segment of the outer whorl. The ovary is inferior, hexa-carpellary, oblong, elliptic and unilocular with six parietal placentae. The styles are six, flat, each splitting half way into two yellow hairy arms.

Anatomy of the Pistillate Flower—Since this species reproduces vegetatively the flowering is not very common. Only a few pistillate flowers were available for study from the material obtained from Netherlands. The present observations are based only on one series each of transverse and longitudinal sections. In the material studied two whorls of carpels were observed in the gynoecium of the pistillate flowers. But due to the shortage of material it could not be ascertained whether it is a normal feature for *Hydrocharis* or the flowers studied are showing some abnormality.

The vascular supply of the pedicel consists of a large number of scattered vascular bundles evenly distributed in the ground tissue. The four bundles which lie towards the centre are large while the peripheral bundles are comparatively much smaller (Fig. 36). The xylem is represented only by a few lignified elements in the smaller bundles, however, in the larger bundles the protoxylem is obliterated to form a narrow channel bordered by a lining of thin-walled cells.

At the base of the receptacle, except for some of the outer paripheral bundles, others branch and anastomose freely and form a broken vascular cylinder (Figs. 37, 38). At this level the vascular supply of the flower consists of 15 peripheral bundles and an incomplete central vascular cylinder. All the peripheral bundles continue as such up to the top of the ovary. The central vascular cylinder soon breaks up into a large number of small scattered vascular bundles. Some of the bundles of the central region reorganise to form a small incomplete vascular cylinder in the centre of the axis (Fig. 39). The bundles which are outer to the central cylinder constitute the vascular supply of the outer whorl of the carpels of the gynoecium.

Soon after, six locules make their appearance successively one after another (Fig. 40). The ovary is incompletely divided by six placentae which project towards the centre of the ovary. The six prominent bundles take median position in the six carpels as dorsal bundles of the carpels. The remaining bundles are the ventrals and are distributed throughout the placental region (Fig. 40). They supply the numerous ovules which are scattered all over the surface of the placentae (Figs. 42, 50).

The latter formed vascular cylinder continues as such in the centre of the axis for some distance. At a slightly higher level, where the locules of the outer-whorl make their appearance, it also breaks up into numerous scattered bundles (Fig. 40). Three locules (of the three carpels of the inner whorl) make their appearance successively. Higher up the three locules merge into one another forming a single large locule (Fig. 41) with three placentae which project towards the centre. The vascular supply of the carpels of the inner whorl is similar to that of the outer whorl *i.e.*, each carpel is supplied by a single dorsal and many ventral bundles. The carpels of the inner whorl are poorly developed and bear only a few ovules. They extend for about 2/3rd the length of the ovary. Only after the disappearance of the carpels of the inner whorl the six locules of the carpels of the outer whorl merge into one another to bring about the unilocular condition (Fig. 42).

The ovary wall is differentiated into two distinct regions. The outer, through which the peripheral bundles extend, is made up of closely packed large cells with small intercellular spaces. The inner consists of small very loosely arranged cells enclosing numerous air spaces. The air spaces are also present in the placentae. In the outer region of the ovary wall some circular canals are also present which are bounded by a distinct layer of thin-walled cells.

Alongwith the peripheral bundles the dorsal and ventral bundles of the outer whorl of the carpels also extend in the ovary wall up to the top of the ovary (Fig. 43). At the top of the ovary the 15 peripheral bundles constitute the vascular supply of the outer whorl of the perianth segments (Figs. 44-47), each of which receives five bundles of which except the median one the others may divide further.

The carpellary branches (dorsal and ventral bundles) come closer in the upper region of the ovary and show some branching and anastomosing (Fig. 44). Then three traces diverge out on the radii alternating with those of the outer perianth segments for each of the three perianth segments of the inner whorl (Fig. 45). The median bundle of the perianth segment remains undivided while the marginals branch freely (Figs. 46, 47). The perianth segments of both the whorls have a large number of air cavities.

After the departure of the perianth traces six traces pass outwards for the six staminodes (Fig. 47). The concentric bundle of the staminode extends throughout its length. The three large nectaries, present opposite the perianth segments of the inner whorl (Figs. 48,49), are quite distinct because of their dark staining cells. Each nectary generally receives one to three traces which branch freely on entering it (Fig. 48). The bundles left after giving rise to the traces for inner perianth segments, staminodes and nectary continue into the styles. Generally 3-5 bundles extend into each style (Figs. 48,49). The styles are bifid and the arms are covered with unicellular glandular hairs.

Enhalus Rich.

Enhalus is a monotypic genus, *E. acoroides* (Linn. f.) Rich. ex Steud. is a submerged salt water herb, distributed throughout the tropical belt of Indian ocean.

The plants are dioecious. The numerous, minute, pedicelled male flowers are enclosed in a compressed peduncled spathe consisting of two connate blades. There are two whorls of perianth, each with three free, white and reflexed segments. The three stamens are opposite the outer perianth; the anthers are dithecous, sub-sessile oblong and dehiscing latrorsely. The pollen grains are large and spherical with very fine reticulate surface. The female flowers are much larger, solitary and sessile in a peduncled spathe consisting of two nearly free persistent blades, the outer embracing the inner. The blades are strongly keeled and covered with long rough hairs. The outer three perianth segments are reddish and imbricate, while the inner three are white wrinkled and subvalvate. The gynoecium is hexacarpellary and syncarpous; the ovary is inferior, ovoid with six papillose ridges and densely set with long finger-like hairs (Fig. 59). It is unilocular with six protruding parietal placentae almost meeting in the centre and incompletely dividing the ovary into six chambers. There are a few anatropous ovules on each placenta. The styles are six, each bipartite from the base. The fruit, which is enclosed in a persistent spathe and raised above the surface of water, is ovate acuminate and bursting irregularly at the apex.

Anatomy of the Male Inflorescence and Flower—The cortex of the peduncle shows many lacunae and scattered tannin cells. The vascular supply consists of a large number of scattered vascular bundles. The peripheral bundles are small in size while the two central ones are large. Each bundle is bounded on outer side by a sheath made up of three or four layers of lignified cells.

At the base of the spathe each of the two central bundles gives off a trace successively in opposite directions. They traverse the cortex and enter the spathe segments of their sides. Besides these two bundles a large number of peripheral bundles also enter into the two spathe segments.

The central mass of the vascular tissue formed after the departure of the spathe traces gives off one trace to each flower. The single bundle in the pedicel of the staminate flower is centrally disposed (Fig. 52). At the base of the flower the bundle splits into three (Fig. 53). Three traces arise, one from each of the three resultant bundles, for the perianth segments of the outer whorl (Fig. 54). Close above three more traces pass off almost simultaneously alternating with those of the first for the three perianth segments of the inner whorl (Fig. 55). The single bundle of each perianth segment traverses unbranched to the tip. The inner epidermal cells of the inner whorl of perianth segments are conspicuously papillate (Fig. 58).

The three bundles left after the departure of the perianth traces constitute the androecial supply (Figs. 56,57). Each stamen receives a single bundle which extends throughout the length of the filament and connective unbranched (Fig. 51). Tannin cells are present in the different parts of the flower.

Anatomy of the Pistillate Flower—In a short note Kaushik (1940) has described the vascular anatomy of the pistillate flower of *Enhalus acoroides*. The present observations agree with his description except for some minor details.

The internal structure and vascular supply of the inflorescence axis is similar to that of the staminate flower. After the departure of the traces for the spathe the two central bundles before or after their fusion give off a number of traces that move outwards. As a result of this and also because of the splitting of central vascular tissue, there are two rings of bundles at the base of the ovary—the peripheral with nine and the central with six bundles.

The peripheral bundles extend as such in the outer region of the ovary wall while the central ring constitute the vascular supply of the six carpels. Just below the level where the locules make their appearance each bundle of the inner ring splits up into five—one dorsal, two secondary marginals and two ventrals (Fig. 60).

The six locules make their appearance successively, but immediately they merge into one another. A little higher up the six placentae that protrude towards the centre of the ovary and incompletely dividing it into six chambers, also get differentiated. The two half placentae of juxtaposed carpels are free from each other throughout their length (Figs. 60, 61). A few anatropous ovules are borne on each half placenta. A large number of lacunae gradually appear in the placentae. The ovary wall is clearly differentiated into two regions. The outer with many layers of loose parenchyma surrounding the peripheral ring of the bundles and the inner enclosing a large number of air cavities.

The two ventral bundles, one of which is restricted to each half placenta, are completely used up in giving rise to traces for the ovules. The secondary marginals, each of which may split into two during its course in the ovary wall, fade out at the top of the ovary. Each dorsal bundle bifurcates and the two branches extend into a pair of stigmatic lobes of each carpel (Fig. 63). The stigmatic lobes of all the six carpels are arranged in a circle enclosing the pollen collecting cavity and they are densely covered with the unicellular papillose outgrowths. Tannin cells are present in the ovary wall, placentae, style and stigma.

The outer whorl of nine bundles which are the combined traces of the two whorls of the perianth segments continue as such in the outer region of the ovary wall up to the top of the ovary (Fig. 62). Then each of these bundles splits into two, thus the nine outer form the vascular supply of the three perianth segments of the outer whorl and nine inner that of the three inner perianth segments (Fig. 63). The median bundle extends unbranched to the tip of the perianth segment while the marginals divide freely. The mesophyll of the perianth segment contains air cavities and large number of tannin cells. The tannin cells are much more in the outer perianth than the inner. The perianth segments of the inner whorl show foldings and their inner epidermal cells are conspicuously papillate like that of the staminate flowers.

Nechamandra Planch.

Nechamandra alternifolia (Roxb.) Thw. (syn. *Lagerosiphon roxburghii* Benth.) is distributed in India and Ceylon. The plants are submerged, fresh water perennial herbs, occuring commonly in ponds, tanks and lakes. The stems are filiform with alternate or opposite, sessile and amplexicaul leaves.

The plants are dioecious. Numerous minute and pedicellate staminate flowers are enclosed in an ovoid 2-fid spathe. The pistillate flowers are solitary and sessile in a narrow oblong spathe. The perianth of the male flowers consists of an outer whorl of three petaloid segments enclosing the two antero-posteriorly placed segments of the inner whorl. The perianth segments reflex after flowering. The two stamens are divergent with short filaments and dithecous anthers dehiscing transversely. The perianth tube in the female flowers is filiformly attenuated above into a neck with 3-partite limb. The inferior ovary is produced into a filiform, flexuous beak. It is unilocular with numerous orthotropous ovules irregularly distributed on parietal placentae. The styles are three, each terminating into a cuneate bilobed stigma covered by papillose hairs. The fruit which is an ovoid and indehiscent utricle has a membranous pericarp and is included in the spathe.

Anatomy of the Male Inflorescence and Flower—The ground tissue of the peduncle shows many air cavities, raphides, and tannin cells. The vascular supply of the inflorescence axis consists of a centrally disposed stele with a lacuna in the centre representing the reduced xylem. The remaining of the stele is of more or less undifferentiated mass of phloem and parenchyma. At the base of the spathe the stele expands and the xylem lacuna is replaced by elongated lignified cells. This central mass of the vascular tissue gives rise to two traces successively in opposite directions for the sheathing spathe. The bundles extend throughout the length of the spathe unbranched. Squamulae have been observed in between the spathe and the floral axis. After the departure of the spathe traces, the stele extends into the elongated conical axis and gives off one trace for each of the numerous small flowers (Fig. 64) which are arranged in a somewhat spiral fashion.

The centrally disposed stele (Fig. 66) of the pedicel is similar in structure to that of the peduncle. The stele extends as such for some distance without giving rise to any vascular supply to the perianth segments. After the perianth segments are separated from the central axis the single bundle bifurcates into two and these branches extend into the filaments of the two divergent stamens and continue up to the base of the connective (Figs. 65, 67,68). Tannin cells are present in the perianth segments and filaments.

Anatomy of the Female Inflorescence and Flower—The structure and vascular supply of the peduncle of the female flower is similar to that of the male. The vascular supply of the spathe is also derived in a similar fashion (Figs. 69-72). Squamulae have also been observed in between the ovary and the spathe.

The central mass of the vascular tissue left after the departure of the spathe traces forms the gynoecium supply. Two prominent traces diverge out almost simultaneously on the same radii on which the traces for the spathe were given off. These are the dorsal bundles of the carpels. A little higher up the remaining vascular tissue splits into two bundles which move outwards and become ventral strands (Fig. 71). They lie on the radii alternating with those of the carpellary dorsals. The single locule makes its appearance in the centre of the ovary (Fig. 72). There is no distinct placental region and the ovules are scattered throughout the inner surface of the ovary wall. The ventral strands give traces for the ovules (Fig. 73) and are completely used up in supplying the ovules (Fig. 74). Tannin cells are also present in the ovary wall and the parenchymatous tissue of the style.

The two dorsal bundles continue through the ovary wall as such (Fig. 81) and on reaching the top of the ovary they show some flattening and then one of them splits into two (Figs. 75-77). The three resultant bundles continue one in each of the three styles (Fig. 78). At the base of the stigma the bundle of the style bifurcates (Fig. 79) and extends into the two lobes of a stigma. A somewhat 3-angular stylar canal extends up to the ovarian cavity. The stigma is covered with long unicellular glandular hairs (Fig. 80) which are densely filled with cytoplasm and have prominent nuclei. In the female flowers too, like the male flowers, no vascular supply could be traced to the perianth segments.

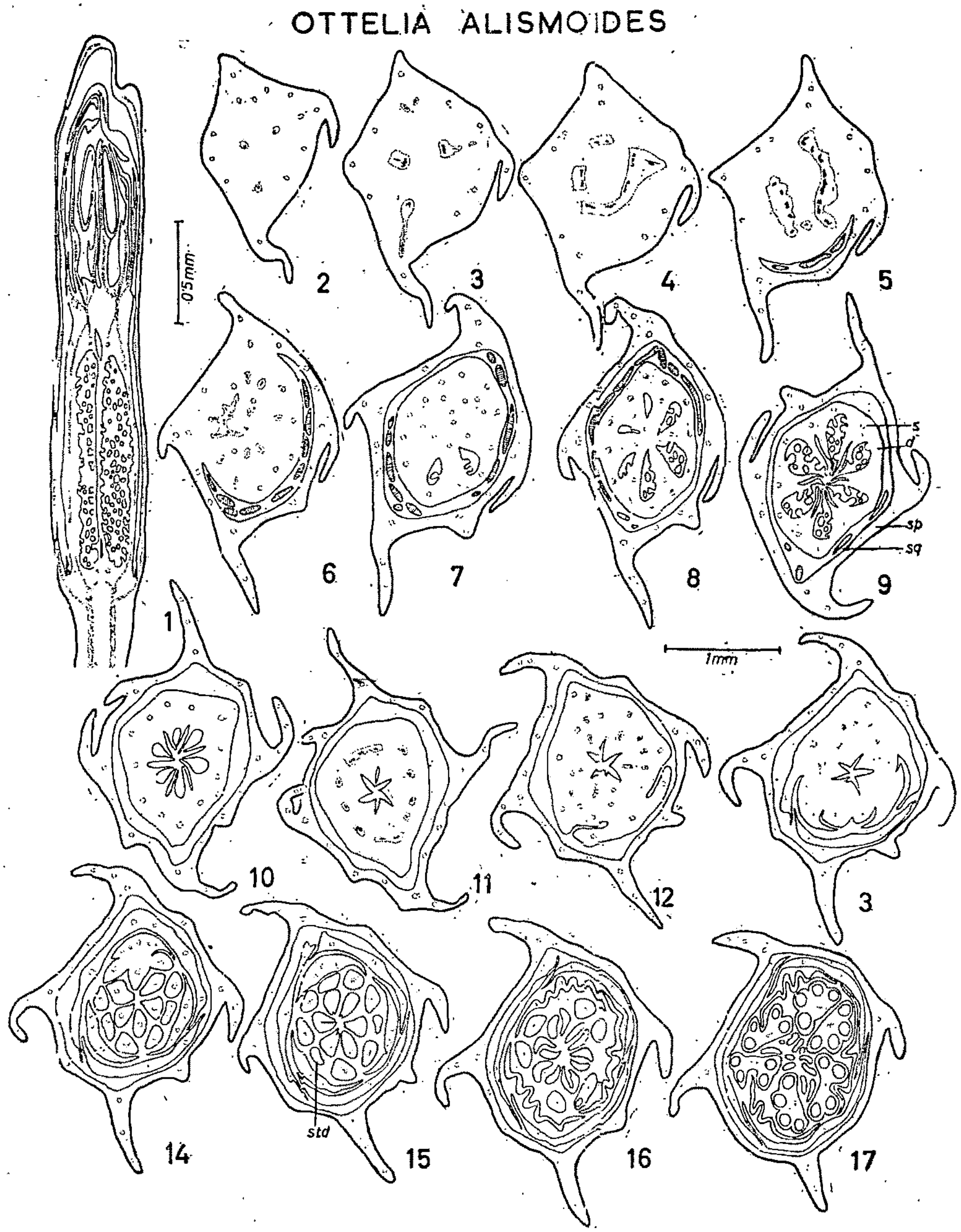

Figs. 1–17. *Ottelia alismoides* Fig. 1. Semidiagrammatic longitudinal section of a flower bud showing vascular ground plan. Figs. 2-17. Serial cross sections of flower bud from base upward showing vascular supply at different regions.

d—dorsal bundle; sp—spathe; sq—squamulae;
std—staminode; s—ventral strand.

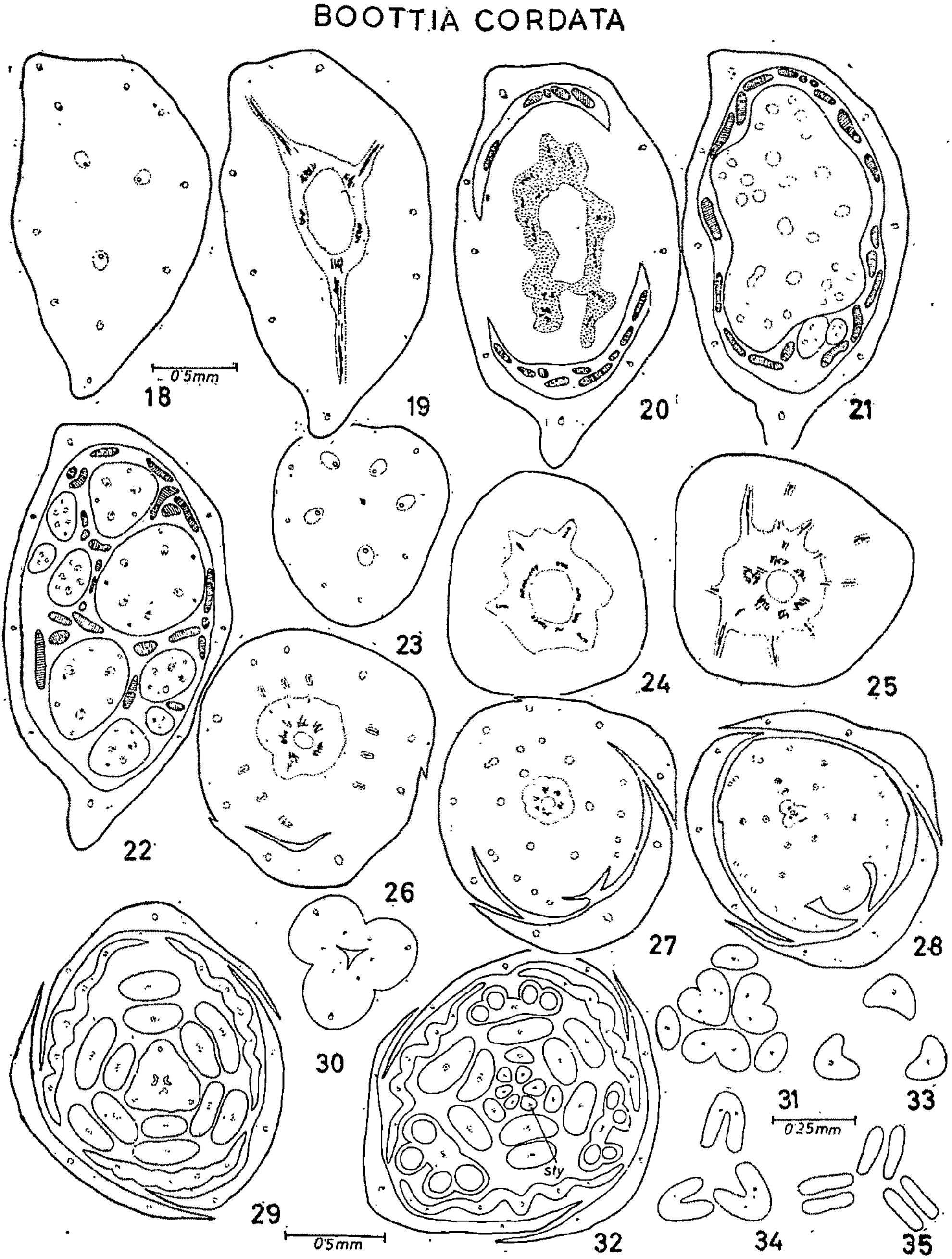

Figs. 18-35. *Bootia cordata*. Figs. 18-22. Serial cross sections of male inflorescence. Figs. 23-29 and 32. Serial cross sections of male flower from base upward showing vascular supply to different organs. Figs. 30,31,33-35. Serial cross sections through styllodia of the same flower.

sty—styllodia.

HYDROCHARIS DUBIA

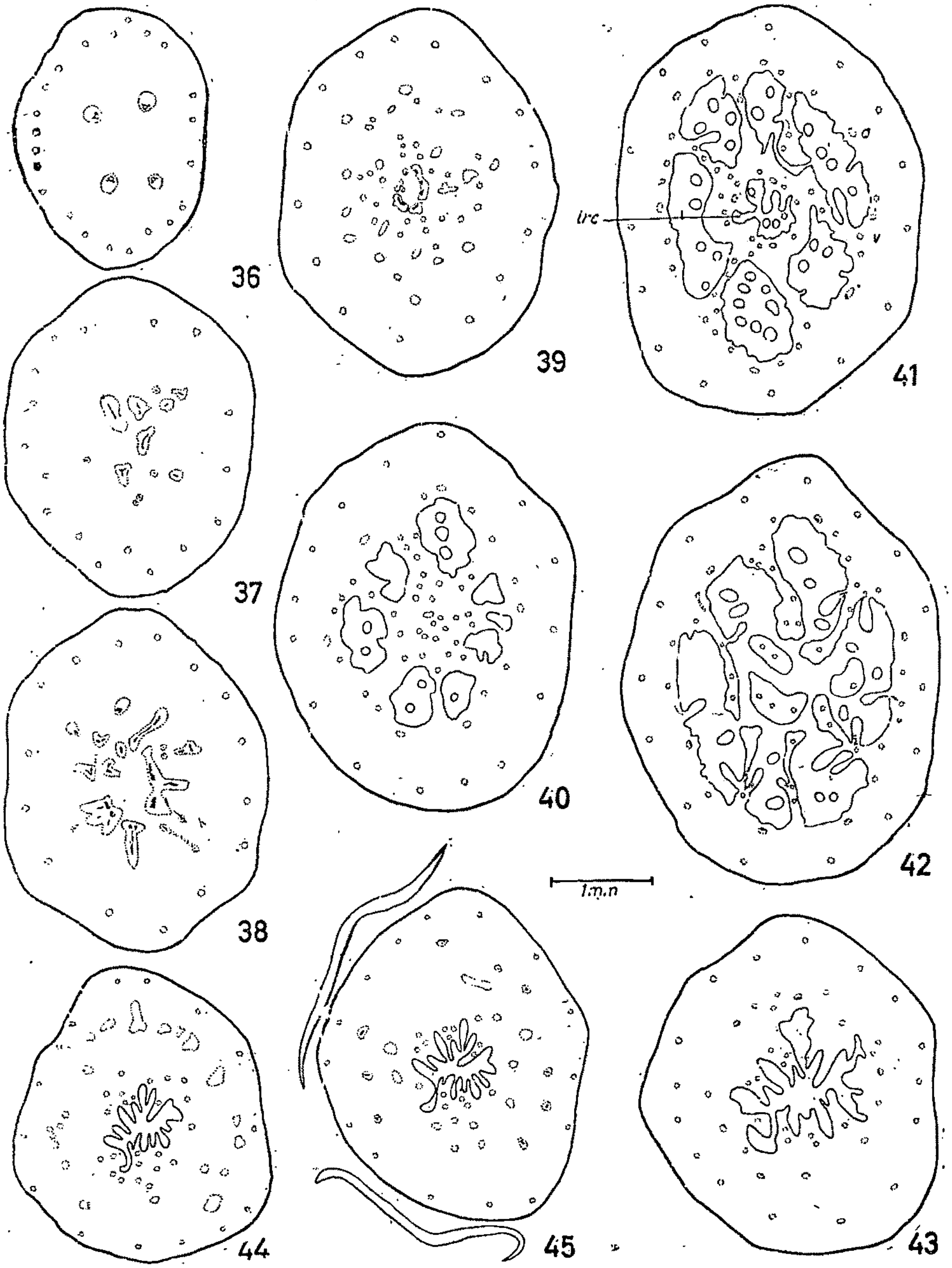

Figs. 36-45 *Hydrocharis dubia.* Serial cross sections of pistillate flower from base upward showing vascular supply at different levels.

d—dorsal bundle; irc—inner ring of carpels; V—ventral bundles.

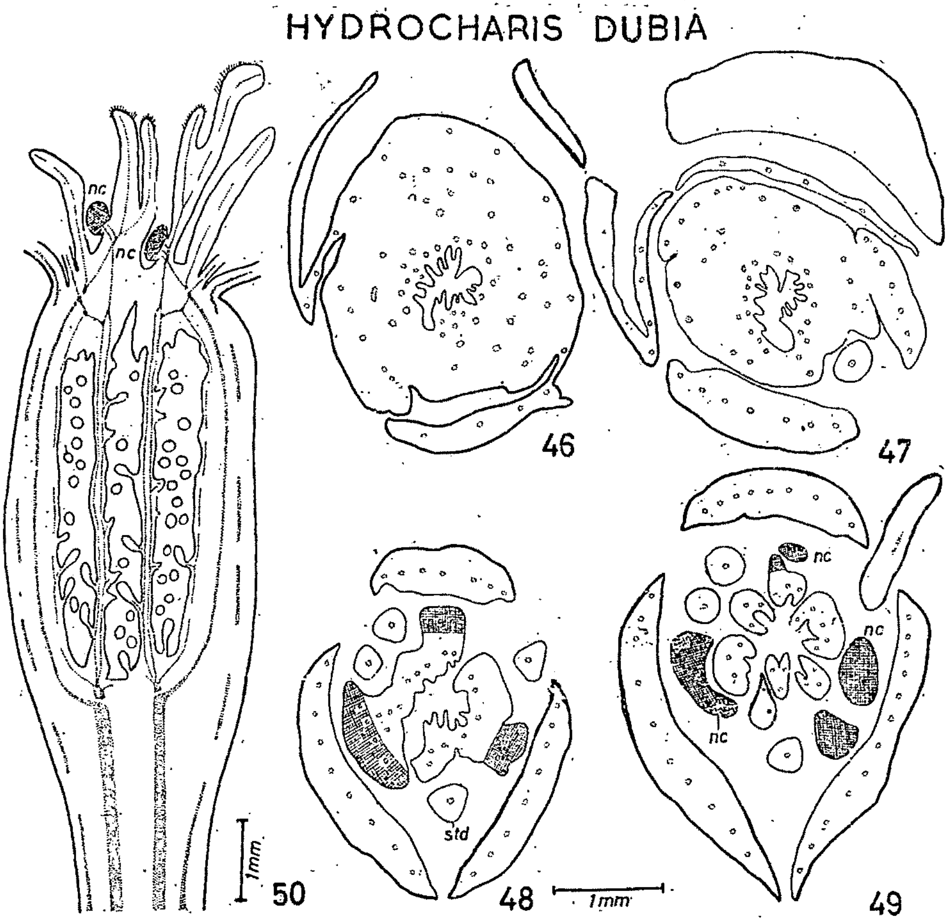

Fig. 46-50. *Hydrocharis dubia*. Figs. 46-49. Serial cross sections of pistillate flower above the level in Fig. 45. Fig. 50. Semidiagrammatic representation of vascular ground plan in a longitudinal section of pistillate flower.

nc—nectary; std—staminode.

ENHALUS ACOROIDES

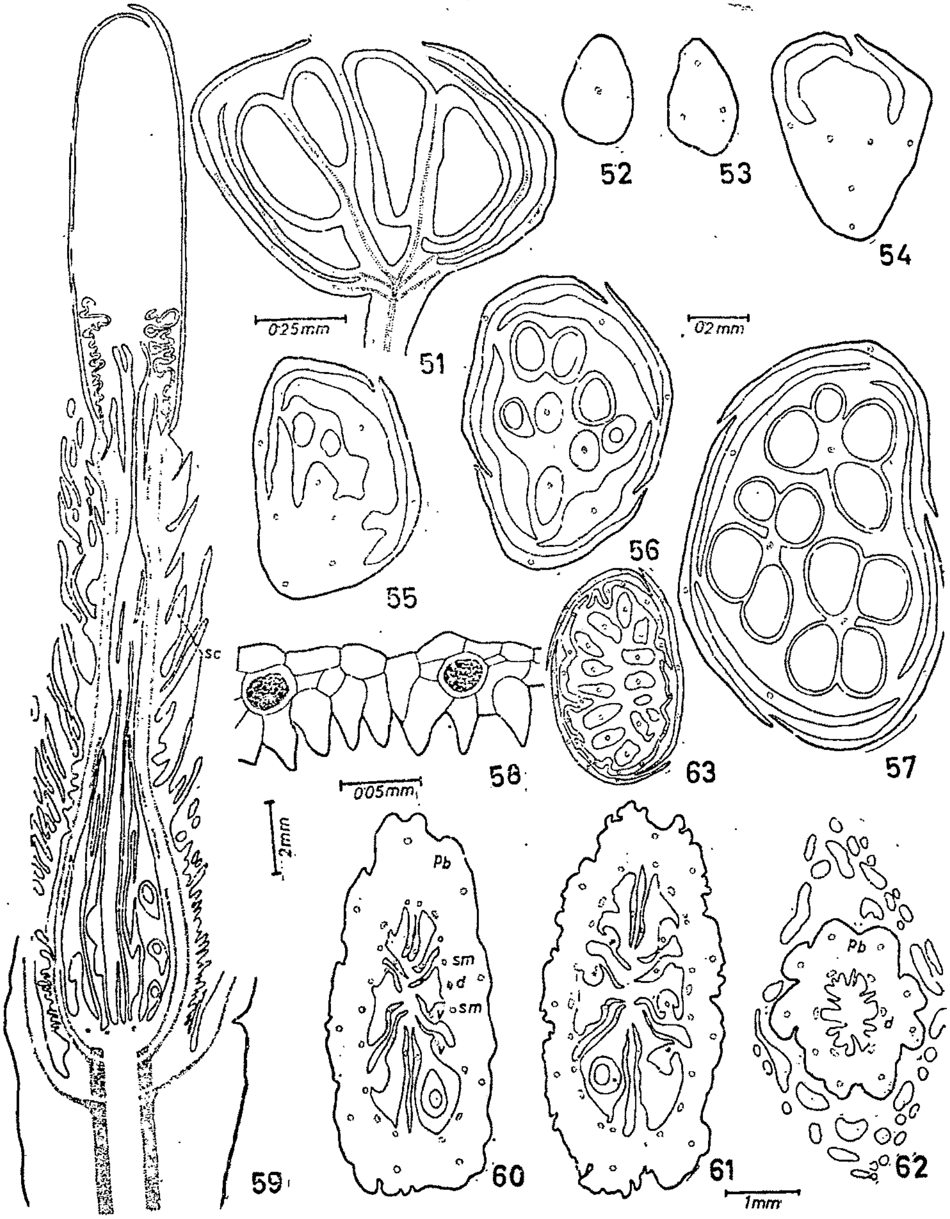

Figs. 51-63. *Enhalus, accoroides.* Fig. 51. Longitudinal section of a staminate flower. Figs. 52-57. Serial cross sections of the same. Fig. 58. A portion of vertical section of perianth showing papillate outgrowths from lower epidermal cells. Fig. 59. Semidiagrammatic longitudinal section of pistillate flower showing vascular ground plan. Figs. 60-63. Cross sections of pistillate flower at four different levels.

d—dorsal bundle; Pb—Peripheral bundles; sc—scales; sm—secondary marginal; v—ventral bundle.

NECHAMENDRA ALTERNIFOLIA

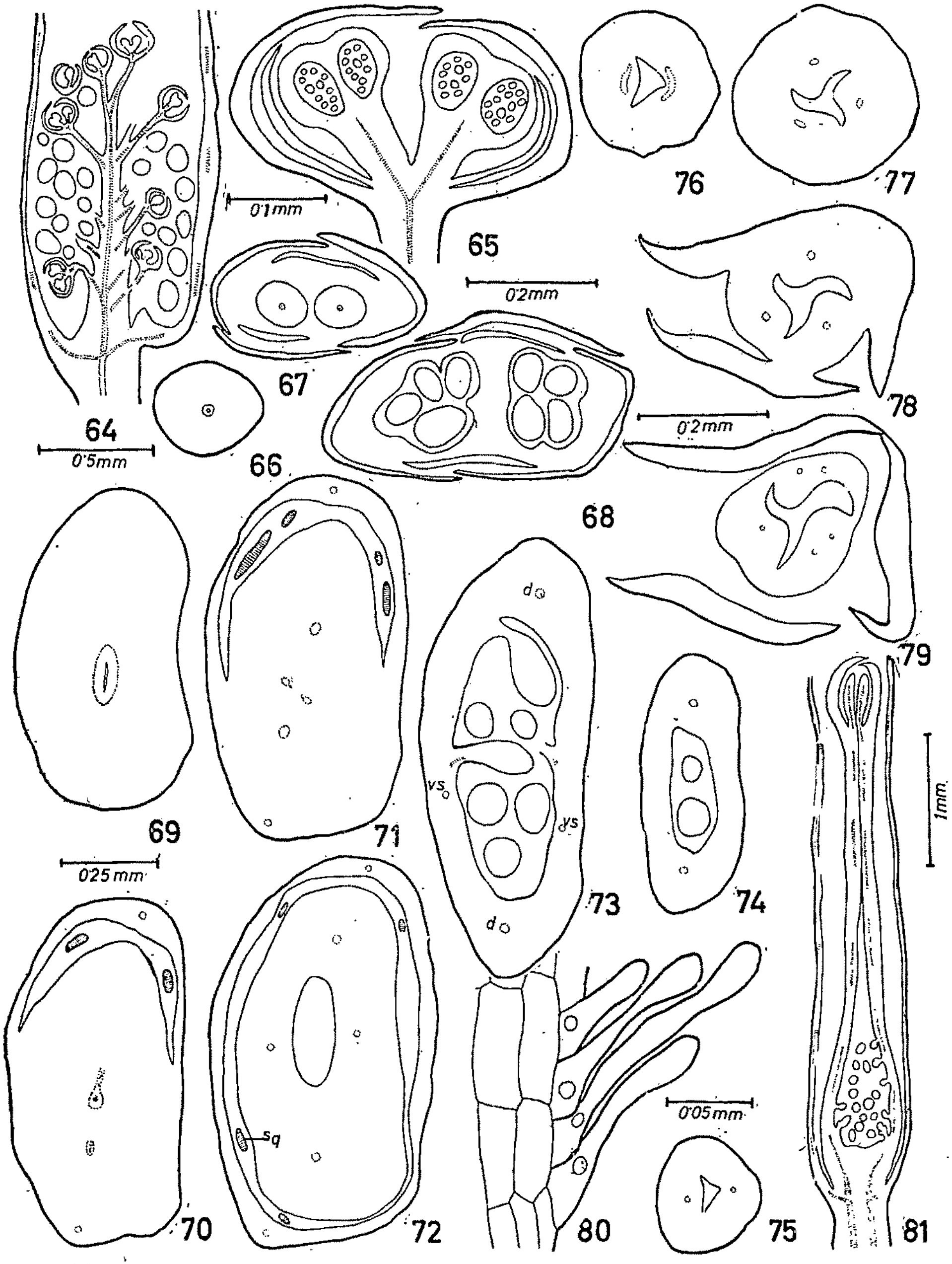

Figs. 64-81. *Nechamendra alternifolia.* Fig. 64. Longitudinal section of male inflorescence. Figs. 65. Longitudinal section of staminate flower. Figs. 66-68. Serial cross sections of the same. Figs. 69-79. Serial cross sections of pistillate flower from base upwards showing vascular supply to different organs. Figs. 80. A portion of longitudinal section of stigma showing glandular hairs. Fig. 81. Semidiagrammatic representation of vascular ground plan of pistillate flower in longitudinal section.

d—dorsal bundle, sq—squamulae; vs—ventral strend.

SOME KERNELS IN THE HANKEL TRANSFORM OF TWO VARIABLES—I

R. P. Gupta
D. S. B. Govt. College, Naini Tal.

1. The wellknown Hankel transform in one variable, *viz.*,

$$g(x)=\int_0^\infty (xy)^{\frac{1}{2}} J_\nu(xy) f(y)\, dy$$

has been extended to two variables and is defined by the integral equation

$$g(x,y)=\int_0^\infty\int_0^\infty (x\xi y\eta)^{\frac{1}{2}} J_\rho(\eta y) J_\nu(\xi x) f(\xi,\eta)\, d\xi\, d\eta$$

Gray[4], Erdelyi[2] and Owen[6] have investigated some self-reciprocal functions involving two complex variables under this transform. R.P. Agarwal[1] has given two formulae connecting different classes of self-reciprocal functions of different orders in two variables. Following the analogy of self-reciprocal function of one variable, we define the kernel in two variables in the following manner.

If two functions $f(u, u')$ and $g(x, y)$ are connected by the relation

$$g(x,y)=\int_0^\infty\int_0^\infty P(xu, yu') f(u, u')\, du du',$$

where $f(u, u')$ is $R_{\nu,\rho}$ and $g(x, y)$ is $R_{\mu,\lambda}$; then $P(x, y)$ is called the kernel in two variables for transforming $R_{\nu,\rho}$ into an $R_{\mu,\lambda}$ and vice-versa.

The object of this paper is to investigate some such kernels with the help of the theorems of § 2[5] and employ them to derive some new self-reciprocal functions.

2. Consider the Integral

$$I = \int_0^\infty\int_0^\infty x^{s+\gamma+n\beta-1} y^{\alpha+\beta-1} e^{-\frac{1}{2}x}\, {}_1F_1(k+m+\tfrac{1}{2}; 2m+1; x) W_{k,m}(x) \times I_\nu(\tfrac{1}{2}x^n y) K_\rho(\tfrac{1}{2}x^n y)\, dx\, dy$$

Evaluating, we get

$$I=\frac{\Gamma(2m+1)\Gamma\left(\frac{1}{4}+\frac{m}{2}+\frac{\gamma}{2}+\frac{n\beta}{2}+\frac{s}{2}\right)\Gamma\left(\frac{1}{4}-\frac{m}{2}+\frac{\gamma}{2}+\frac{n\beta}{2}+\frac{s}{2}\right)}{2^{\frac{7}{2}+m-\gamma-n\beta-s-\alpha-\beta}\cdot\pi\Gamma(1+m-k)\,\Gamma\left(\frac{3}{4}-\frac{m}{2}-k+\frac{\gamma}{2}+\frac{n\beta}{2}+\frac{s}{2}\right)}$$

$$\frac{\Gamma\left(\frac{3}{4}-\frac{m}{2}+\frac{\gamma}{2}+\frac{n\beta}{2}+\frac{s}{2}\right)}{\Gamma\left(\frac{3}{4}+\frac{3m}{2}-\frac{\gamma}{2}-\frac{n\beta}{2}-\frac{s}{2}\right)}\times$$

$$\times\frac{\Gamma\left(\frac{1}{4}+\frac{m}{2}-k-\frac{\gamma}{2}-\frac{n\beta}{2}-\frac{s}{2}\right)\Gamma\left(\frac{\nu}{2}+\frac{\beta}{2}+\frac{\rho}{2}+\frac{\alpha}{2}\right)}{\Gamma\left(1+\frac{\nu}{2}-\frac{\beta}{2}+\frac{\rho}{2}-\frac{\alpha}{2}\right)}$$

$$\frac{\left(\frac{\nu}{2}+\frac{\beta}{2}-\frac{\rho}{2}+\frac{\alpha}{2}\right)\Gamma\left(\frac{1}{2}-\frac{\alpha}{2}-\frac{\beta}{2}\right)\Gamma\left(1-\frac{\alpha}{2}-\frac{\beta}{2}\right)}{\Gamma\left(1+\frac{\nu}{2}-\frac{\beta}{2}-\frac{\rho}{2}-\frac{\alpha}{2}\right)}$$

provided Re $(\gamma+n\beta+s\pm m+\frac{1}{2})>0$ and Re $(-\nu\pm\rho)<$Re $(\alpha+\beta)<1$. Since the integrals involved are absolutely convergent, it follows by Reed's theorem[7],

$$x^{\gamma+n\beta}\,y^{\beta}\,e^{-\frac{1}{2}x}\,{}_1F_1\,(k+m+\tfrac{1}{2};\,2m+1;\,x)\;\;W_{k,m}(x)\;I_{\nu}(\tfrac{1}{2}\,x^{n}y)K_{\rho}(\tfrac{1}{2}\,x^{n}y)$$

$$=\frac{2^{\gamma+n\beta-m+\beta-\frac{7}{2}}\Gamma(2m+1)}{\pi\,\Gamma(1+m-k)}\cdot\frac{1}{(2\pi i)^2}\int_{c-i\infty}^{c+i\infty}\int_{c'-i\infty}^{c'+i\infty}2^{\alpha+s}\frac{\Gamma\left(\frac{1}{4}+\frac{m}{2}+\frac{\gamma}{2}+\frac{n\beta}{2}+\frac{s}{2}\right)}{\Gamma\left(\frac{3}{4}-\frac{m}{2}-k+\frac{\gamma}{2}+\frac{n\beta}{2}+\frac{s}{2}\right)}$$

$$\frac{\Gamma\left(\frac{1}{4}-\frac{m}{2}+\frac{\gamma}{2}+\frac{n\beta}{2}+\frac{s}{2}\right)}{\Gamma\left(\frac{3}{4}+\frac{3m}{2}-\frac{\gamma}{2}-\frac{n\beta}{2}-\frac{s}{2}\right)}\times\frac{\Gamma\left(\frac{1}{4}+\frac{m}{2}-k-\frac{\gamma}{2}-n\beta-\frac{s}{2}\right)\Gamma\left(\frac{\nu}{2}+\frac{\beta}{2}+\frac{\rho}{2}+\frac{\alpha}{2}\right)}{\Gamma\left(\frac{\nu}{2}-\frac{\beta}{2}+\frac{\rho}{2}-\frac{\alpha}{2}+1\right)}$$

$$\frac{\Gamma\left(\frac{\nu}{2}+\frac{\beta}{2}-\frac{\rho}{2}+\frac{\alpha}{2}\right)\Gamma\left(\frac{1}{2}-\frac{\alpha}{2}-\frac{\beta}{2}\right)\Gamma\left(1-\frac{\alpha}{2}-\frac{\beta}{2}\right)}{\Gamma\left(\frac{\nu}{2}-\frac{\beta}{2}-\frac{\rho}{2}-\frac{\alpha}{2}+1\right)}x^{-s}y^{-\alpha}\,ds\,d\alpha$$

Case 1. For $\gamma=3\varepsilon-2$, $k=\frac{1}{2}-\varepsilon$, $m=2\varepsilon-1$, $\beta=0$, $\gamma=-\rho=-\frac{1}{4}+\frac{1}{2}\mu$; then

$$x^{3\varepsilon-2}e^{-\frac{1}{2}x}\,{}_1F_1\,(\varepsilon;\,4\varepsilon-1;x)W_{\frac{1}{2}-\varepsilon,\,2\varepsilon-1}(x)\;I_{\frac{1}{2}\mu-\frac{1}{4}}(\tfrac{1}{2}x^{n}y)\;K_{\frac{1}{4}-\frac{1}{2}\mu}(\tfrac{1}{2}x^{n}y)$$

$$=\frac{1}{(2\pi i)^2}\int_{c-i\infty}^{c+i\infty}\int_{c'-i\infty}^{c'+i\infty}2^{\alpha+s}\Gamma[\tfrac{1}{4}+\tfrac{1}{2}\,(5\varepsilon-3)+\tfrac{1}{2}s]\Gamma(\tfrac{1}{4}+\tfrac{1}{2}\varepsilon+\tfrac{1}{2}s)\Gamma[\tfrac{1}{4}+\tfrac{1}{2}(\mu-1)]$$

$$\Gamma(\tfrac{1}{4}+\tfrac{1}{2}\mu+\tfrac{1}{2}\alpha)\,\chi(s,\,\alpha)x^{-s}y^{-\alpha}\,ds\,d\alpha$$

where

$$\chi(s,\,\alpha)=\frac{2^{\varepsilon-\frac{9}{2}}\,\Gamma(4\varepsilon-1)\,\Gamma\left(\frac{\alpha}{2}\right)\Gamma\left(\frac{1}{2}-\frac{\alpha}{2}\right)\Gamma\left(-\frac{1}{4}+\frac{\varepsilon}{2}+\frac{s}{2}\right)\Gamma\left(\frac{1}{4}+\frac{\varepsilon}{2}-\frac{s}{2}\right)}{\pi\Gamma(3\varepsilon-1)\,\Gamma\left(-\frac{1}{4}+\frac{3\varepsilon}{2}+\frac{s}{2}\right)\Gamma\left(\frac{1}{4}+\frac{3\varepsilon}{2}-\frac{s}{2}\right)\Gamma\left(\frac{1}{4}+\frac{\mu}{2}+\frac{\alpha}{2}\right)\Gamma\left(\frac{3}{4}+\frac{\mu}{2}-\frac{\alpha}{2}\right)}$$

$$=\chi\,(1-s,\,1-\alpha)$$

Thus the function

$$x^{3\varepsilon-2}\, e^{-\frac{1}{2}x}\, {}_1F_1\,(\varepsilon\,;\,4\varepsilon-1\,;\,x)\,W_{\frac{1}{2}-\varepsilon;\;2\varepsilon-1}(x)\,I_{\frac{1}{2}\mu-\frac{1}{4}}(\tfrac{1}{2}x^{n}y)\,K_{\frac{1}{4}-\frac{1}{2}\mu}(\tfrac{1}{2}x^{n}y)$$

is a kernel transforming

$$R_{5\varepsilon-3,\,\mu-1} \text{ to } R_{\varepsilon,\,\mu}$$

provided $2/5<\mathrm{R}e\,\varepsilon<\frac{3}{4}$, $\mathrm{R}e\,\mu\geqslant\frac{1}{2}$.

Case 2. For $\gamma=3\varepsilon+3/2$, $k=-1-\varepsilon$, $m=2\varepsilon+3/2$, $\beta=0$, $\nu=-\rho=-\frac{1}{4}+\frac{1}{2}\mu$, we get

$$x^{3\varepsilon+3/2}e^{-\frac{1}{2}x}\,{}_1F_1\,(\varepsilon+1,\,4\varepsilon+4;x)\;W_{-1-\varepsilon,\;2\,\varepsilon+3/2}(x)\,I_{\frac{1}{2}\mu-\frac{1}{4}}(\tfrac{1}{2}x^{n}y)\,K_{-\frac{1}{4}\mu+\frac{1}{2}}(\tfrac{1}{2}x^{n}y)$$

as a kernel transforming

$$R_{5\varepsilon+3,\,\mu-1} \text{ to } R_{\varepsilon,\,\mu}$$

provided $-4/5<\mathrm{R}e\,\varepsilon-\frac{1}{2}$, $\mathrm{R}e\,\mu\geqslant\frac{1}{2}$.

Case 3. For $\gamma=\frac{1}{2}\varepsilon-9/4$, $k=\frac{1}{2}$, $m=\frac{1}{2}\,\varepsilon-\frac{3}{4}$, $\beta=0$, $\nu=-\rho=-\frac{1}{4}+\frac{1}{2}\mu$; we get

$$x^{\frac{1}{2}\varepsilon-\frac{9}{4}}e^{-\frac{1}{2}x}\,{}_1F_1\,(\tfrac{1}{2}\varepsilon+\tfrac{1}{4};\varepsilon-\tfrac{1}{2};x)\,W_{\frac{1}{2},\;\frac{1}{2}\varepsilon-\frac{3}{4}}(x)\;I_{\frac{1}{2}\mu-\frac{1}{4}}(\tfrac{1}{2}x^{n}y)\;K_{\frac{1}{4}-\frac{1}{2}\mu}(\tfrac{1}{2}x^{n}y)$$

as a kernel transforming

$$R_{\varepsilon-3,\,\mu-1} \text{ to } R_{\varepsilon,\,\mu},$$

provided $2<\mathrm{R}e\,\varepsilon<5/2$, $\mathrm{R}e\,\mu\geqslant\frac{1}{2}$.

Case 4. For, $\gamma=2\varepsilon-3$, $k=-\varepsilon+3/2$, $m=\varepsilon-1$, $\beta=0$, $\nu=-\rho=\frac{1}{2}\mu-\frac{1}{4}$, we get

$$x^{2\varepsilon-3}e^{-\frac{1}{2}x}\,{}_1F_1\,(1;\,2\varepsilon-1\,;x)\,W_{-\varepsilon+\frac{3}{2},\;\varepsilon-1}(x)\,I_{\frac{1}{2}\mu-\frac{1}{4}}(x^{n}y)\,K_{\frac{1}{4}-\frac{1}{2}\mu}(x^{n}y)$$

as a kernel transforming

$$R_{\varepsilon-1,\,\mu-1} \text{ to } R_{\varepsilon,\,\mu},$$

provided $\frac{1}{2}<\mathrm{R}e\,\varepsilon<\frac{3}{2}$, $\mathrm{R}e\,\mu\geqslant\frac{1}{2}$.

Case 5. For $\gamma=-1$, $k=\frac{1}{2}$, $m=-\varepsilon$, $\beta=0$, $\nu=-\rho=\frac{1}{2}\mu-\frac{1}{4}$, we get

$$x^{-1}e^{-\frac{1}{2}x}\,{}_1F_1\,(1-\varepsilon;\;1-2\varepsilon;\;x)\,W_{\frac{1}{2},-\varepsilon}(x)\,I_{-\frac{1}{4}+\frac{1}{2}\mu}(\tfrac{1}{2}x^{n}y)\;K_{\frac{1}{4}-\frac{1}{2}\mu}(\tfrac{1}{2}x^{n}y)$$

as a kernel transforming

$$R_{1-3\varepsilon,\,\mu-1} \text{ to } R_{\varepsilon,\,\mu}$$

provided $-\frac{1}{2}<\mathrm{R}e\,\varepsilon<0$, $\mathrm{R}e\,\mu\geqslant\frac{1}{2}$.

Case 6. For $\gamma=m-\frac{1}{2}$, $k=\beta=0$, $\nu=-\rho=-\frac{1}{4}+\frac{1}{2}\mu$, we get

$$I_m\,(\tfrac{1}{2}x)\;K_m\,(\tfrac{1}{2}x)\;I_{\frac{1}{2}\mu-\frac{1}{4}}\,(\tfrac{1}{2}x^{n}y)\,K_{\frac{1}{4}-\frac{1}{2}\mu}\,(\tfrac{1}{2}x^{n}y)$$

as a kernel transforming

$$R_{2m-\frac{1}{2},\, \mu-1} \text{ to } R_{2m+\frac{1}{2},\, \mu},$$

provided $-\frac{1}{4}<\mathrm{R}e\, m<\frac{1}{2}$, $\mathrm{R}e\, \mu \geqslant \frac{1}{2}$.

Case 7. For $\gamma=-\frac{1}{2}$, $k=\beta=0$. $\nu=-\rho=-\frac{1}{4}+\frac{1}{2}\mu$, we get

$$x^{-m} I_m\left(\tfrac{1}{2}x\right) K_m\left(\tfrac{1}{2}x\right) I_{\frac{1}{2}\mu-\frac{1}{4}}\left(\tfrac{1}{2}x^n y\right) K_{\frac{1}{4}-\frac{1}{2}\mu}\left(\tfrac{1}{2}x^n y\right)$$

as a kernel transforming

$$R_{3m+\frac{1}{2},\, \mu-1} \text{ to } R_{-(m+\frac{1}{2}),\, \mu}$$

provided $-\frac{1}{2}<\mathrm{R}e\, m<\frac{1}{2}$, $\mathrm{R}e\, \mu \geqslant \frac{1}{2}$.

Case 8. For $\gamma=3\varepsilon-n/6+\frac{n\mu}{3}-2$, $k=1-\varepsilon$, $m=2\varepsilon-1$, $\beta=\frac{1}{6}-\frac{\mu}{3}$, $\nu=\rho=\frac{\mu}{3}-\frac{1}{6}$; we get

$$x^{3\varepsilon-2} y^{\frac{1}{6}-\frac{\mu}{3}} e^{-\frac{1}{2}x} {}_1F_1\left(k+m+\tfrac{1}{2};\, 2m+1;\, x\right) W_{1-\varepsilon,\, 2\varepsilon-1}(x)\, I_{\frac{\mu}{3}-\frac{1}{6}}\left(\tfrac{1}{2}x^n y\right)$$
$$K_{\frac{\mu}{3}-\frac{1}{6}}\left(\tfrac{1}{2}x^n y\right)$$

as a kernel transforming

$$R_{5\varepsilon-3,\, -\frac{\mu+1}{3}} \text{ to } R_{\varepsilon,\, \mu},$$

provided $2/5<\mathrm{R}e\, \varepsilon<\frac{3}{4}$, $\frac{1}{2} \geqslant \mathrm{R}e\, \mu \geqslant -\frac{1}{2}$.

Case 9. For $\gamma=3\varepsilon-\frac{n}{6}+\frac{n\mu}{3}+\frac{3}{2}$, $k=-1-\varepsilon$, $m=2\varepsilon+\frac{3}{2}$, $\beta=\frac{1}{6}-\frac{\mu}{3}$, $\nu=\rho=\frac{\mu}{3}-\frac{1}{6}$, we get

$$x^{3\varepsilon+\frac{3}{2}} y^{\frac{1}{6}-\frac{\mu}{3}} e^{-\frac{1}{2}x} {}_1F_1\left(1+\varepsilon;\, 4\varepsilon+4;\, x\right) W_{-1-\varepsilon,\, 2\varepsilon+\frac{3}{2}}$$
$$(x)\, I_{\frac{\mu}{3}-\frac{1}{6}}\left(\tfrac{1}{2}x^n y\right) K_{\frac{\mu}{3}-\frac{1}{6}}\left(\tfrac{1}{2}x^n y\right)$$

as a kernel transforming

$$R_{5\varepsilon+3,\, -\frac{\mu+1}{3}} \text{ to } R_{\varepsilon,\, \mu}.$$

provided $-4/5<\mathrm{R}e\, \varepsilon<-\frac{1}{2}$, $\frac{1}{2} \geqslant \mathrm{R}e\, \mu \geqslant -\frac{1}{2}$.

Case 10. For $\gamma=\frac{1}{2}\varepsilon+\frac{n\mu}{3}-\frac{n}{6}-\frac{9}{4}$, $k=\frac{1}{2}$, $m=\frac{1}{2}\varepsilon-\frac{3}{4}$, $\beta=\frac{1}{6}-\frac{\mu}{3}$, $\nu=\rho=\frac{\mu}{3}-\frac{1}{6}$, we get

$$x^{\frac{1}{2}\varepsilon-\frac{9}{4}}\, y^{\frac{1}{6}-\frac{\mu}{3}}\, {}_1F_1(\tfrac{1}{4}+\tfrac{1}{2}\varepsilon;\varepsilon-\tfrac{1}{2};x)\, W_{\frac{1}{2},\,\frac{1}{2}\varepsilon-\frac{3}{4}}(x)\, I_{\frac{\mu}{3}-\frac{1}{6}}(\tfrac{1}{2}x^{n}y)\, K_{\frac{\mu}{3}-\frac{1}{6}}(\tfrac{1}{2}x^{n}y)$$

as a kernel transforming

$$R_{\varepsilon-3,\,-\frac{\mu+1}{3}} \text{ to } R_{\varepsilon,\,\mu},$$

provided $2<\mathrm{Re}\,\nu<5/2,\ \tfrac{1}{2}\geqslant \mathrm{Re}\,\mu\geqslant-\tfrac{1}{2}$.

Case 11. For $\gamma=2\varepsilon+\frac{n\mu}{3}-\frac{n}{6}-3,\ k=-\varepsilon+\frac{3}{2},\ m=\varepsilon-1,\ \beta=\frac{1}{6}-\frac{\mu}{3},$ $\nu=\rho=\frac{\mu}{3}-\frac{1}{6}$, we get

$$x^{2\varepsilon-3}\, y^{\frac{1}{6}-\frac{\mu}{3}}\, e^{-\frac{1}{2}x}\, {}_1F_1(1;2\varepsilon-1;x)\, W_{-\varepsilon+\frac{3}{2},\,\varepsilon-1}(x)\, I_{\frac{\mu}{3}-\frac{1}{6}}(\tfrac{1}{2}x^{n}y)\, K_{\frac{\mu}{3}-\frac{1}{6}}(\tfrac{1}{2}x^{n}y)$$

as a kernel transforming

$$R_{\varepsilon-1,\,-\frac{\mu+1}{3}} \text{ to } R_{\varepsilon,\,\mu},$$

provided $\tfrac{1}{2}<\mathrm{Re}\,\varepsilon<\tfrac{3}{2},\ \tfrac{1}{2}\geqslant \mathrm{Re}\,\mu\geqslant-\tfrac{1}{2}$.

Case 12. For $\gamma=-1+\frac{n\mu}{3}-\frac{n}{6},\ k=\frac{1}{2},\ m=-\varepsilon,\ \beta=\frac{1}{6}-\frac{\mu}{3},\ \nu=\rho=\frac{\mu}{3}-\frac{1}{6}$, we get

$$x^{-1}\, y^{\frac{1}{6}-\frac{\mu}{3}}\, e^{-\frac{1}{2}x}\, {}_1F_1(1-\varepsilon;\ 1-2\varepsilon;x)\, W_{\frac{1}{2},\varepsilon}(x)\, I_{\frac{\mu}{3}-\frac{1}{6}}(\tfrac{1}{2}x^{n}y)\, K_{\frac{\mu}{3}-\frac{1}{6}}(\tfrac{1}{2}x^{n}y)$$

as a kernel transforming

$$R_{1-3\varepsilon,\,-\frac{\mu+1}{3}} \text{ to } R_{\varepsilon,\,\mu},$$

provided $-\tfrac{1}{2}<\mathrm{Re}\,\varepsilon<0,\ \tfrac{1}{2}\geqslant \mathrm{Re}\,\mu\geqslant-\tfrac{1}{2}$.

Case 13. For $\gamma=m+\frac{n\mu}{3}-\frac{n}{6}-\frac{1}{2},\ k=0,\ \beta=\frac{1}{6}-\frac{\mu}{3},\ \nu=\rho=\frac{\mu}{3}-\frac{1}{6}$, we get

$$y^{\frac{1}{6}-\frac{\mu}{3}}\, I_m(\tfrac{1}{2}x)\, K_m(\tfrac{1}{2}x)\, I_{\frac{\mu}{3}-\frac{1}{6}}(\tfrac{1}{2}x^{n}y)\, K_{\frac{\mu}{3}-\frac{1}{6}}(\tfrac{1}{2}x^{n}y)$$

as a kernel transforming

$$R_{2m-\frac{1}{2},\,-\frac{\mu+1}{3}} \text{ to } R_{2m+\frac{1}{2},\,\mu},$$

provided $-\tfrac{1}{4}<\mathrm{Re}\,m<\tfrac{1}{2},\ \tfrac{1}{2}\geqslant \mathrm{Re}\,\mu\geqslant-\tfrac{1}{2}$.

Case 14. For $\gamma=\frac{n\mu}{3}-\frac{n}{6}-\frac{1}{2}, k=0, \beta=\frac{1}{6}-\frac{\mu}{3}, \nu=\rho=\frac{\mu}{3}-\frac{1}{6}$, we get

$$x^{-m}y^{\frac{1}{6}-\frac{\mu}{3}}\,\mathrm{I}_m(\tfrac{1}{2}x)\,\mathrm{K}_m(\tfrac{1}{2}x)\,\mathrm{I}_{\frac{\mu}{3}-\frac{1}{6}}(\tfrac{1}{2}x^{n}y)\mathrm{K}_{\frac{\mu}{3}-\frac{1}{6}}(\tfrac{1}{2}x^{n}y)$$

as a kernel transiorming

$$\mathrm{R}_{3m+\frac{1}{2},\,\mu} \text{ to } \mathrm{R}_{-\frac{1}{2}(m+1),-\left(\frac{\mu+1}{3}\right)},$$

provided $-\frac{1}{2}<\mathrm{R}e\, m<\frac{1}{2}, \frac{1}{2}\geqslant\mathrm{R}e\,\mu\geqslant-\frac{1}{2}$.

3. Consider the Integral

$$\mathrm{I}=\int_0^\infty\int_0^\infty x^{s+\gamma+n\beta-1}y^{\alpha+\beta-1}e^{-\frac{1}{2}x}\,{}_1\mathrm{F}_1(k+m+\tfrac{1}{2};2m+1;x)\mathrm{W}_{k,m}(x)\,\mathrm{J}_\rho(\sqrt{\tfrac{1}{2}}x^{n}y)\,\mathrm{K}_\rho(\sqrt{\tfrac{1}{2}}x^{n}y)\,dxdy$$

$$=\frac{2^{\alpha+\gamma+n\beta-m+\beta-\frac{7}{2}+s}\Gamma(1+2m)\Gamma\left(\frac{1}{4}+\frac{m}{2}+\frac{\gamma}{2}+\frac{n\beta}{2}+\frac{s}{2}\right)}{\Gamma(1+m-k)\Gamma\left(\frac{3}{4}-\frac{m}{2}-k+\frac{\gamma}{2}+\frac{n\beta}{2}+\frac{s}{2}\right)}\times$$

$$\frac{\Gamma\left(\frac{1}{4}-\frac{m}{2}+\frac{\gamma}{2}+\frac{n\beta}{2}+\frac{s}{2}\right)\Gamma\left(\frac{3}{4}-\frac{m}{2}+\frac{\gamma}{2}+\frac{n\beta}{2}+\frac{s}{2}\right)\Gamma\left(\frac{1}{4}+\frac{m}{2}-k-\frac{\gamma}{2}-\frac{n\beta}{2}-\frac{s}{2}\right)}{\Gamma\left(\frac{3}{4}+\frac{3m}{2}-\frac{\gamma}{2}-\frac{n\beta}{2}-\frac{s}{2}\right)\Gamma\left(\frac{\rho}{2}+\frac{\beta}{4}+\frac{\alpha}{4}+\frac{1}{2}\right)}$$

$$\frac{\Gamma\left(\frac{\alpha}{2}+\frac{\beta}{2}+\rho\right)\Gamma\left(\frac{\alpha}{2}+\frac{\beta}{2}\right)}{\Gamma\left(\frac{\rho}{2}-\frac{\alpha}{4}-\frac{\beta}{4}+1\right)}$$

for $\mathrm{R}e\,(\gamma+n\beta+s\pm m+\frac{1}{2})>0$ and $\mathrm{R}e\,(\alpha+\beta+\rho)>|\mathrm{R}e\,\rho|$.

Since the integrals involved are absolutely convergent, it follows by Reed's theorem

$$x^{\gamma+n\beta}y^{\beta}e^{-\frac{1}{2}x}\,{}_1\mathrm{F}_1(k+m+\tfrac{1}{2};2m+1;x)\mathrm{W}_{k,}(x)\,\mathrm{J}_\rho(\sqrt{\tfrac{1}{2}}x^{n}y))\mathrm{K}(\sqrt{\tfrac{1}{2}}x^{n}y)$$

$$=\frac{2^{\gamma+n\beta-m+\beta-\rho-\frac{7}{2}}\Gamma(2m+1)}{\Gamma(1+m-k)(2\pi i)^2}\int_{c-i\infty}^{c+i\infty}\int_{c'-i\infty}^{c'+i\infty}2^{\alpha+s}\frac{\Gamma\left(\frac{1}{4}+\frac{m}{2}+\frac{\gamma}{2}+\frac{n\beta}{2}+\frac{s}{2}\right)}{\Gamma\left(\frac{3}{4}-\frac{m}{2}-k+\frac{\gamma}{2}+\frac{n\beta}{2}+\frac{s}{2}\right)}$$

$$\frac{\Gamma\left(\frac{1}{4}-\frac{m}{2}+\frac{\gamma}{2}+\frac{n\beta}{2}+\frac{s}{2}\right)}{\Gamma\left(\frac{3}{4}+\frac{3m}{2}-\frac{\gamma}{2}-\frac{n\beta}{2}-\frac{s}{2}\right)}\times\frac{\Gamma\left(\frac{3}{4}-\frac{m}{2}+\frac{\gamma}{2}+\frac{n\beta}{2}+\frac{s}{2}\right)\Gamma\left(\frac{1}{4}+\frac{m}{2}-k-\frac{\gamma}{2}-\right.}{\Gamma\left(\frac{\rho}{2}+\frac{\beta}{4}+\frac{\alpha}{4}+\frac{1}{2}\right)}$$

$$\frac{\left.\frac{n\beta}{2}-\frac{s}{2}\right)\Gamma\left(\rho+\frac{\beta}{2}+\frac{\alpha}{2}\right)\Gamma\left(\frac{\alpha}{2}+\frac{\beta}{2}\right)}{\Gamma\left(\frac{\rho}{2}-\frac{\alpha}{4}-\frac{\beta}{4}+1\right)}x^{-s}y^{-\alpha}\,ds\,d\alpha$$

Case 1. For $\gamma=3\varepsilon=\frac{1}{2}n-2$, $k=\frac{1}{2}-\varepsilon$, $m=2\varepsilon-1$, $\beta=\frac{1}{2}$, then

$$x^{3\varepsilon-2}y^{\frac{1}{2}}e^{-\frac{1}{2}x}\,{}_1F_1(\varepsilon;4\varepsilon-1;x)W_{\frac{1}{2}-\varepsilon,\,2\varepsilon-1}(x)J_\rho(\sqrt{\tfrac{1}{2}}\,x^n y)K_\rho(\sqrt{\tfrac{1}{2}}\,x^n y)$$

$$=\frac{1}{(2\pi i)^2}\int_{c-i\infty}^{c+i\infty}\int_{c'-i\infty}^{c'+i\infty}2^{a+s}\Gamma[\tfrac{1}{4}+\tfrac{1}{4}(5\varepsilon-3)+\tfrac{1}{2}s]\Gamma(\tfrac{1}{4}+\tfrac{1}{2}\varepsilon+\tfrac{1}{2}s)\Gamma(\tfrac{1}{4}+\rho+\tfrac{1}{2}a)\Gamma(\tfrac{1}{4}+\tfrac{1}{2}a)$$

$$\chi(s,a)x^{-s}y^{-a}\,ds\,da$$

where
$$\chi=(s,a)=\frac{2^{\varepsilon-\rho-4}\,\Gamma(4\varepsilon-1)\Gamma\left(-\frac{1}{4}+\frac{\varepsilon}{2}+\frac{1}{2}s\right)}{\Gamma(3\varepsilon-1)\,\Gamma\left(-\frac{1}{4}+\frac{3}{4}\varepsilon+\frac{1}{2}\,\varepsilon\right)\Gamma\left(\frac{1}{4}+\frac{3}{2}\varepsilon-\frac{1}{2}s\right)}$$
$$\frac{\Gamma\left(\frac{1}{4}+\frac{1}{2}\,\varepsilon-\frac{1}{2}s\right)}{\Gamma\left(\frac{5}{8}+\frac{\rho}{2}+\frac{a}{4}\right)\Gamma\left(\frac{7}{8}+\frac{\rho}{2}-\frac{a}{4}\right)}=\chi(1-s,1-a)$$

Thus the function

$$x^{3\varepsilon-2}y^{\frac{1}{2}}e^{-\frac{1}{2}x}\,{}_1F_1(\varepsilon;4\varepsilon-1;x)\,W_{\frac{1}{2}-\varepsilon,\,2\varepsilon-1}(x)J_\rho(\sqrt{\tfrac{1}{2}}\,x^n y)K_\rho(\sqrt{\tfrac{1}{2}}\,x^n y)$$

is a kernel transforming

$$R_{5\varepsilon-3,\,2\rho}\text{ to }R_{\varepsilon,\,0},$$

for $2/5<\mathrm{Re}\,\varepsilon<\frac{3}{4}$, $\mathrm{Re}\,\rho>-\frac{1}{2}$.

Case 2. For $\gamma=3\varepsilon-\frac{1}{2}n+3/2$, $k=-1-\varepsilon$, $m=2\varepsilon+3/2$, $\beta=\frac{1}{2}$, we get

$$x^{3\varepsilon+\frac{3}{2}}y^{\frac{1}{2}}e^{-\frac{1}{2}x}\,{}_1F_1(\varepsilon+1;4\varepsilon+4;x)W_{-1-\varepsilon,\,2\varepsilon+\frac{3}{2}}(x)J_\rho(\sqrt{\tfrac{1}{2}}\,x^n y)K_\rho(\sqrt{\tfrac{1}{2}}\,x^n y)$$

as a kernel transforming

$$R_{5\varepsilon+3,\,2\rho}\text{ to }R_{\varepsilon,\,0},$$

provided $-4/5<\mathrm{Re}\,\varepsilon<-\frac{1}{2}$, $\mathrm{Re}\,\rho>-\frac{1}{2}$.

Case 3. For $\gamma=\frac{1}{2}\varepsilon-\frac{1}{2}n-9/4$, $k=\frac{1}{2}$, $m=\frac{1}{2}\varepsilon-\frac{3}{4}$ and $\beta=\frac{1}{2}$, we get

$$x^{\frac{1}{2}\varepsilon-\frac{9}{4}}y^{\frac{1}{2}}e^{-\frac{1}{2}x}\,{}_1F_1(\tfrac{1}{2}\varepsilon+\tfrac{1}{4};\varepsilon-\tfrac{1}{2};x)W_{\frac{1}{2};\,\frac{1}{2}\varepsilon-\frac{3}{4}}(x)J_\rho(\sqrt{\tfrac{1}{2}}\,x^n y)K_\rho(\sqrt{\tfrac{1}{2}}\,x^n y)$$

as a kernel transforming

$$R_{\varepsilon-3,\,2\rho}\text{ to }R_{\varepsilon,\,0},$$

provided $2<\mathrm{Re}\,\varepsilon<5/2$, $\mathrm{Re}\,\rho>-\frac{1}{2}$.

Case 4. For $\gamma=2\varepsilon-\frac{1}{2}n-3$, $k=-\varepsilon+\frac{3}{2}$, $m=\varepsilon-1$, $\beta=\frac{1}{2}$, we get

$$x^{2\varepsilon-3}y^{\frac{1}{2}}e^{-\frac{1}{2}x}\,{}_1F_1(1;2\varepsilon-1;x)\,W_{-\varepsilon+\frac{3}{2},\,\varepsilon-1}(x)J_\rho(\sqrt{\tfrac{1}{2}}\,x^n y)K_\rho(\sqrt{\tfrac{1}{2}}\,x^n y)$$

as a kernel transforming

$$R_{\varepsilon-1,\,2\rho}\text{ to }R_{\varepsilon,\,0},$$

provided $\frac{1}{2}<\mathrm{Re}\,\varepsilon<\frac{3}{2}$, $\mathrm{Re}\,\rho>-\frac{1}{2}$.

Case 5. For $\gamma=-1-\frac{1}{2}n$, $k=\frac{1}{2}$, $m=-\varepsilon$, $\beta=\frac{1}{2}$, we get

$$x^{-1}y^{\frac{1}{2}}e^{-\frac{1}{2}x}\,{}_1F_1\,(1-\varepsilon;\,1-2\varepsilon;\,x)W_{\frac{1}{2},\,-\varepsilon}(x)\,J_\rho(\sqrt{\tfrac{1}{2}}\,x^n y)K_\rho(\sqrt{\tfrac{1}{2}}\,x^n y)$$

as a kernel transforming

$$R_{1-3\varepsilon,\,2\rho} \text{ to } R_{\varepsilon,\,0}\,,$$

provided $-\frac{1}{2}<Re\,\varepsilon<0$, $Re\,\rho>-\frac{1}{2}$.

Case 6. For $\gamma=m-\frac{1}{2}n-\frac{1}{2}$, $k=0$, $\beta=\frac{1}{2}$, we get

$$y^{\frac{1}{2}}I_m(\tfrac{1}{2}x)\,K_m\,(\tfrac{1}{2}x)\,J_\rho\,(\sqrt{\tfrac{1}{2}}\,x^n y)\;K_\rho(\sqrt{\tfrac{1}{2}}\,x^n y)$$

as a kernel transforming

$$R_{2m-\frac{1}{2},\,2\rho} \text{ to } R_{2m+\frac{1}{2},\,0}\,,$$

provided $-\frac{1}{4}<Re\,m<\frac{1}{2}$, $Re\,\rho>-\frac{1}{2}$.

Case 7. For $\gamma=-\frac{1}{2}-\frac{1}{2}n$, $k=0$, $\beta=\frac{1}{2}$, we get

$$x^{-m}y^{\frac{1}{2}}I_m(\tfrac{1}{2}x)\,K_m\,(\tfrac{1}{2}x)\,J_\rho(\sqrt{\tfrac{1}{2}}\,x^n y)K_\rho\,(\sqrt{\tfrac{1}{2}}\,x^n y)$$

as a kernel transforming

$$R_{3m+\frac{1}{2},\,2\rho} \text{ to } R_{-(m+\frac{1}{2}),\,0}\,,$$

provided $-\frac{1}{2}<Re\,m<\frac{1}{2}$, $Re\,\rho>-\frac{1}{2}$.

Case 8. For $\gamma=3\varepsilon-(\frac{5}{2})\,n-2$, $k=\frac{1}{2}-\varepsilon$, $m=2\varepsilon-1$, $\beta=\frac{5}{2}$, we get

$$x^{3\varepsilon-2}y^{\frac{5}{2}}e^{-\frac{1}{2}x}\,{}_1F_1\,(\varepsilon;\,4\varepsilon-1;\;x)\,W_{\frac{1}{2}-\varepsilon,\,2\varepsilon-1}(x)\,J_\rho(\sqrt{\tfrac{1}{2}}\,x^n y)K_\rho(\sqrt{\tfrac{1}{2}}\,x^n y)$$

as a kernel transforming

$$R_{5\varepsilon-3,\,2\rho} \text{ to } R_{\varepsilon,\,2}\,,$$

provided $\frac{2}{5}<Re\,\varepsilon<\frac{3}{4}$, $Re\,\rho>\frac{1}{2}$.

Case 9. For $\gamma=3\varepsilon-(\frac{5}{2})n+\frac{3}{2}$, $k=-1-\varepsilon$, $m=2\varepsilon+\frac{3}{2}$, $\beta=\frac{5}{2}$, we get

$$x^{3\varepsilon+\frac{3}{2}}y^{\frac{5}{2}}e^{-\frac{1}{2}x}\,{}_1F_1\,(\varepsilon+1\,;4\varepsilon+4;\,x)W_{-1-\varepsilon,\,2\varepsilon+\frac{3}{2}}(x)\,J_\rho(\sqrt{\tfrac{1}{2}}\,x^n y)K_\rho\Big(\frac{x^n y}{\sqrt{2}}\Big)$$

as a kernel transforming

$$R_{5\varepsilon+3,\,2\rho} \text{ to } R_{\varepsilon,\,2}\,,$$

provided $-\frac{4}{5}<Re\,\varepsilon<-\frac{1}{2}$, $Re\,\rho>\frac{1}{2}$.

Case 10. For $\gamma=\frac{1}{2}\varepsilon-(\frac{5}{2})\,n-\frac{9}{4}$, $k=\frac{1}{2}$, $m=\frac{1}{2}\varepsilon-\frac{3}{4}$, $\beta=\frac{5}{2}$, we get

$$x^{\frac{1}{2}\varepsilon-\frac{9}{4}}y^{\frac{5}{2}}e^{-\frac{1}{2}x}\,{}_1F_1\,(\tfrac{1}{2}\varepsilon+\tfrac{1}{4};\,\varepsilon-\tfrac{1}{2};\,x)W_{\frac{1}{2},\,\frac{1}{2}\varepsilon-\frac{3}{4}}(x)\,J_\rho(\sqrt{\tfrac{1}{2}}\;x^n y)K_\rho(\sqrt{\tfrac{1}{2}}\,x^n y)$$

as a kernel transforming

$$R_{\varepsilon-3,\,2\rho} \text{ to } R_{\varepsilon,\,2}\,,$$

provided $2<Re\,\varepsilon<\frac{5}{2}$, $Re\,\rho>\frac{1}{2}$.

Case 11. For $\gamma=2\,\varepsilon-(\frac{5}{2})\,n-3$, $k=(\frac{3}{2})-\varepsilon$, $m=\varepsilon-1$, $\beta=\frac{5}{2}$, we get

$$x^{2\varepsilon-3}y^{\frac{5}{2}}e^{-\frac{1}{2}x}\,{}_1F_1\,(1;2\varepsilon-1;x)\;W_{-\varepsilon+\frac{3}{2},\,\varepsilon-1}(x)\,J_\rho(\sqrt{\tfrac{1}{2}}\,x^n y)K_\rho(\sqrt{\tfrac{1}{2}}\,x^n y)$$

as a kernel transforming

$$R_{\varepsilon-1,\,2\rho}\ \text{to}\ R_{\varepsilon,\,2}\,,$$

provided $\frac{1}{2}<\mathrm{R}e\,\varepsilon<\frac{3}{2}$, $\mathrm{R}e\,\rho>\frac{1}{2}$.

Case 12. For $\gamma=-1-(\frac{5}{2})\,n$, $k=\frac{1}{2}$, $m=-\varepsilon$, $\beta=\frac{5}{2}$, we get

$$x^{-1}y^{\frac{5}{2}}e^{-\frac{1}{2}x}\,{}_1F_1\,(1-\varepsilon;1-2\varepsilon;x)W_{\frac{1}{2},\,-\varepsilon}\,(x)\,J_\rho(\sqrt{\tfrac{1}{2}}\,x^n y)K_\rho(\sqrt{\tfrac{1}{2}}\,x^n y)$$

as a kernel transforming

$$R_{1-3\varepsilon,\,2\rho}\ \text{to}\ R_{\varepsilon,\,2}\,,$$

provided $-\frac{1}{2}<\mathrm{R}e\,\varepsilon<0$, $\mathrm{R}e\,\rho>\frac{1}{2}$.

Case 13. For $\gamma=m-(\frac{5}{2})\,n-\frac{1}{2}$, $k=0$, $\beta=\frac{5}{2}$, we get

$$y^{\frac{5}{2}}I_m\,(\tfrac{1}{2}x)K_m\,(\tfrac{1}{2}x)\,J_\rho(\sqrt{\tfrac{1}{2}}\,x^n y)K_\rho(\sqrt{\tfrac{1}{2}}\,x^n y)$$

as a kernel transforming

$$R_{2m+\frac{1}{2},\,2\rho}\ \text{to}\ R_{2m-\frac{1}{2},\,2}$$

provided $-\frac{1}{4}<\mathrm{R}e\,\varepsilon<\frac{1}{2}$, $\mathrm{R}e\,\rho>\frac{1}{2}$.

Case 14. For $\gamma=-\frac{1}{2}-(\frac{5}{2})\,n$, $k=0$, $\beta=\frac{5}{2}$, we get

$$x^{-m}y^{\frac{5}{2}}I_m\,(\tfrac{1}{2}x)K_m\,(\tfrac{1}{2}x)\,J_\rho(\sqrt{\tfrac{1}{2}}\,x^n y)K_\rho\,(\sqrt{\tfrac{1}{2}}\,x^n y)$$

as a kernel transforming

$$R_{3m+\frac{1}{2},\,2\rho}\ \text{to}\ R_{-(m+\frac{1}{2}),\,2}\,,$$

provided $-\frac{1}{2}<\mathrm{R}e\,m<\frac{1}{2}$, $\mathrm{R}e\,\rho>\frac{1}{2}$.

Example. We know that

$$(xy)^{\frac{1}{2}(\nu-\rho+1)}J_{\frac{1}{2}\,(\nu+\rho)}\,(xy),\ \mathrm{R}e\,\rho>\mathrm{R}e\,\nu>-1$$

is $R_{\nu,\,\rho}$.

Hence considering the case 1 of § 2, we have

$$G\,(x,y)=\int_0^\infty\int_0^\infty (xu)^{3\nu-2}e^{-\frac{1}{2}xu}\,{}_1F_1\,(\nu;4\nu-1;xu)W_{\frac{1}{2}-\nu,\,2\nu-1}\,(xu)$$

$$(uu')^{\frac{1}{2}(\nu-\rho+1)}I_{\frac{1}{2}\rho-\frac{1}{4}}\,(\tfrac{1}{2}x^n yu')\,K_{\frac{1}{2}\rho-\frac{1}{4}}\,(\tfrac{1}{2}x^n yu')\,J_{\frac{1}{2}(\nu+\rho)}\,(uu')\,du\,du'$$

$$=\frac{2}{\pi}\,2^{\frac{3\nu}{2}-\frac{\rho}{2}-3}\,\frac{\Gamma(2-2\nu)}{\Gamma(3\nu-1)}\left(\frac{x^{2n+2}y^{2}}{4}\right)$$

$$G^{5,3}_{5,7}\left(\frac{x^{2n+2}y^{2}}{4}\left|\begin{matrix}-\frac{3}{4}-\frac{\nu}{2},-\frac{1}{2},-\frac{1}{4}-\frac{\nu}{2},\frac{3\nu}{2}-\frac{5}{4},-\frac{3}{4}+\frac{\rho}{2}\\ -\frac{5}{4}+\frac{\rho}{2},-1,\frac{\nu}{2}-\frac{5}{4},\frac{\nu}{2}-\frac{3}{4},\frac{5\nu}{2}-\frac{9}{4},-\frac{1}{4}-\frac{3\nu}{2},-\frac{3}{4}-\frac{\rho}{2}\end{matrix}\right.\right)$$

provided $3/10<Re\,\nu<Re\,\rho$; on using the results [3; pp. 91, 430 & 422].

Thus the function

$$G^{5,3}_{5,7}\left(\frac{x^{2n+2}y^{2}}{4}\left|\begin{matrix}\frac{1}{4}-\frac{\nu}{2},\frac{1}{2},\frac{3}{4}-\frac{\nu}{2},\frac{3\nu}{2}-\frac{1}{4},\frac{1}{4}+\frac{\rho}{2}\\ -\frac{1}{4}+\frac{\rho}{2},0,-\frac{1}{4}+\frac{\nu}{2},\frac{1}{4}+\frac{\nu}{2},\frac{5\nu}{2}-\frac{5}{4},\frac{3}{4}-\frac{3\nu}{2},\frac{1}{4}-\frac{\rho}{2}\end{matrix}\right.\right)$$

is $R_{5\nu-3,\,\rho-1}$.

ACKNOWLEDGEMENT

I wish to express my thanks to Dr. Ram Kumar, D.Sc., for his kind help in the preparation of this paper.

REFERENCES

1. Agarwal, R. P. 1950. Ganita, **1**.
2. Erdelyi, A. 1936-37. *Atti della Reale Academia della Sc.* di Torino, 721.
3. Erdelyi, A. 1954. *Tables of Integral Transform*, **I** & **II**.
4. Gray, M. C. 1931. *Jour. Lond. Math. Soc.*, **6** : 247.
5. Gupta, R. P. 1965. In press.
6. Owens, Mac, 1939. *Proc. Lond. Math. Soc.*, **45** : 458.
7. Reed, I. S. 1944. *Duke Math. Jour.*, **2** : 565.

MORPHOLOGY OF THE MALE PINK SUGARCANE MEALYBUG, *SACCHARICOCCUS SACCHARI* COCKERELL (PSEUDOCOCCIDAE : HOMOPTERA)—Pt. I. MACROPTEROUS FORM.

R. L. YADAVA
Department of Zoology, B. R. College, Agra.

INTRODUCTION

The morphology of the male Pseudococcidae has largely been neglected and almost all attention has been focussed on the anatomy and taxonomy of the females. Most of the available papers on the male coccids, deal primarily with taxonomy and consist mainly of brief notes on the more obvious features of their anatomy. Berlese's (1893, 1896) paper contains many details of the anatomy of male coccids but his descriptions are somewhat incomplete and inaccurate. Nel's (1933), Stickney's (1934) and Balachowsky's (1937) papers are not very informative. The paper by Mäkel (1942) on *Pseudococcus*, though a very elaborate work, is more concerned with musculature than with external morphology. Jancke's (1955) paper on the male coccids seems to be of relatively little morphological significance. The papers by Suter (1932), Geier (1949), Mac Gillivray (1921), Mahdihassan (1931), Morrison (1928), Pesson (1941), Oguma (1919), Misra (1931), and Sulc (1932, 1943) are devoted to the general anatomy of the male coccids. The structure of the eyes has been studied by Krecker (1909) and Pflugfelder (1936). The wing venation is described by Patch (1909). Ezzat's (1956) paper on the morphology of male coccids lacks details. Recently Theron (1958) made a comparative morphological study of the male scale insects and established the homologies of the various structures. Ghauri's (1959) paper contains many morphological details of the males of the family Diaspididae. Beardsley (1960) briefly described the males of thirty species of the Hawaiian Pseudococcidae (including *S. Sacchari*) and has discussed only the broad outline of the morphological aspects of the family. But his descriptions lack details. Giliomee (1961) has described the morphology, including chaetotaxy, of the males of three species of the genus *Pseudococcus* and has discussed the relationship of the family Pseudococcidae with other sub-divisions of the Coccoidea. No attempt has so far been made towards the morphological study of the Indian Pseudococcidae and the present study has been undertaken in an attempt to remedy this. There occur three forms, *i. e*, apterous, brachypterous and macropterous of the male pink sugarcane mealybug.

The present investigation is devoted: (1) to study the morphology of the macropterous male pink sugarcane mealybug, *Saccharicoccus sacchari* Cockerell and (2) to determine the possible relationships of the Pseudococcidae with other subdivisions of the Coccoidea.

MATERIAL AND TECHNIQUE

The males of *Saccharicoccus sacchari* were obtained by breeding the insects on pieces of soft sugarcane stem. The cut surfaces of the pieces of cane stem were sealed with wax and they were kept in petridishes containing about half an inch of water. Whenever males appeared they were removed and preserved in 70% alcohol.

For the microscopic examination the specimens were at first kept in 10% KOH for 6 hours at 60°C until the internal organs were dissolved, then they were washed in distilled water and dehydrated by passing them slowly through a graded series of alcohols upto 70% and further cleared in chlorophenol (1 part chloral hydrate + 2 parts phenol) for 16-22 hours. They were then stained in basic fuchsin (1·5 gm in 100 cc. absolute alcohol) for 15 minutes and afterwards transferred to alcohol-terpineol mixture. They were left in this medium until the excess stain was removed and afterwards transferred to pure terpineol and were finally mounted in cavity slides in Canada-balsam.

All drawings were made to scale on graph paper by using a squared eyepiece micrometer. In all the drawings internal ridges are indicated as thick black lines as wide as the ridge, sclerotized areas are stippled, and membranous areas are left blank. Where the limits of a sclerotized area were not very definite, as is often the case in weakly sclerotized areas, they were indicated by dots. Internal structures, or structures which could not be seen through overlapping by another structure, were drawn in broken lines. Heavily sclerotized ridges are drawn in thick lines.

The drawings were all made from specimens which were cleared in KOH and are presumably slightly distended when compared with living specimens.

All the measurements were taken in microns by using an ocular micrometer calibrated with the help of a stage micrometer.

GENERAL MORPHOLOGY

The macropterous males are very minute and fragile. They possess pink coloured elongated body, with white transparent fore wings covered with waxy powder. Total body length is 1049·54-1240·85 (av. 1119·76) μ including genital segment which is 83·49-106·26 (av.95·38) μ long.

A—THE HEAD : (Figs. 1, 2, 4, 5, & 6):

The head of the male Pseudococcidae has been described by Berlese (1893), Vaney and Conte (1908), Uichanco and Villanueva (1932), Cottier (1936), Betrem ((1937), Mäkel (1942), Sulc (1943), Janke (1955), Theron (1958), Beardsley (1960) and Giliomee (1961). Berlese (1893) has given some morphological details, while Mäkel's paper gives many details of the cephalic structures beside the musculature. The papers by Vaney and Conte (1908), Uichanco and Villanueva (1932), Cottier (1936), Betrem (1937) and Janke (1955) contribute little of morphological value. Theron (1958) has clearly established the homologies of various structures. Beardsley's paper contains a brief description of the head of *Pseudococcus adonidum.* Giliomee's paper contains many morphological details of the head and its dermal structures of the three species of the genus *Pseudococcus* (*i.e.*, *P. fragilis, P. adonidum* and *P. maritimus*).

Weber (1928, 1935) has described the three distinct regions in the homopteran head, *i. e.*, (*i*) the epicranium, bearing the antennae, eyes and ocelli, (ii) the "Vorderkopf", consisting of the clypeus, labrum and mandibular and maxillary plates with their respective stylets, and (iii) the labium which is usually partially fused with the prothorax. Theron (1958) has observed that in *Pseudococcus citri* the epicranium consists of the entire head capsule; "Vorderkopf" is very much reduced and is represented by a small area around the vestigial mouth opening; the labium is completely wanting.

The most striking features of the head of *S. sacchari* are: (i) the loss of functional mouth parts and their musculature; (ii) the pronounced sclerite degeneration; (iii) the opisthognathy; (iv) the undivided condition of the epicranium, *i.e.*, the vertex and frons are not separated; (v) the invaginated apophysis of the ventral surface; (vi) the loss of the dorsal ocelli.

1. HEAD CAPSULE : (Figs. 4, 5 & 6):

The head is roughly inversely conical, roundly constricted posteriorly. This is separated from the thorax by a shallow cervical groove (cv). The length and width of the head in microns are given in the following table :—

TABLE 1

	Length		Width
	From apex to the post-occipital ridge	From apex to the cervical groove	across genae
Maximum (Max.)	154·3	169·5	199·8
Minimum (Min.)	134·0	151·8	164·4
Mean	140·7	160.6	183·4
Standard Error of Mean (S.E.)	1·93	2·39	4·16
Standard Deviation (S.D.)	5·47	6·767	11·78
Coefficient of variation (C. V.)	3·88	4·21	6·42

The dorsomedial part of the epicranium (dmep) is only very weakly sclerotized and is slightly raised. No demarcated triangular sclerite as that of *Pseudococcus citri* (Theron, 1958) is found. Posteriorly this area is bounded by a distinct V-shaped ridge (por) which may be regarded as a remnant of the postoccipital ridge (pocr). The anterior arms of the V-shaped postoccipital ridge (por) almost reach the preocular ridges (procr) as in *P. fragilis* (Giliomee, 1961). The Mäkel's interpretation that the anterior extensions of the V-shaped ridge are continuous with the preocular ridges, has been shown to be incorrect by Theron (1958), although her observations speak of the condition found in *P. fragilis* (Giliomee, 1961) and *S. sacchari.* Medially the postoccipital ridge is closely approximated by a faintly demarcated median ridge which is regarded by Theron (1958) as a detached dorsal part of the midcranial ridge (mcr). The ridge terminates anteriorly between the antennal bases. The ventral extension of the midcranial ridge (mcr) is completely separated from the dorsal part of midcranial ridge. The former gives off two lateral branches (lmcr), which run towards the bases of the antennae and thus assumes Y-shaped appearance. The lateral branches (lmcr) do not articulate with the base of the scape (scp). Posteriorly the ventral stem continues towards the ventral eyes and disappears infront of them. Similar conditions of midcranial ridge and its lateral branches have been found by Theron (1958) in *P. citri* and *Eulecanium* and Giliomee (1961) in *P. fragilis*, *P. adonidum* and *P. maritimus.* However, this is contrary to Mäkel's (1942) observations. The frontal apophysis (Berlese, 1893), which originates anteriorly between the antennae and to which antennal muscles are attached, does not exist in *Saccharicoccus sacchari.* Theron (1958) pointed out that Berlese (1893) had mistaken the ventral part of the midcranial ridge for the frontal apophysis.

The ocular sclerites (ocs), each of which is separated from the dorsomedial part of the epicranium (dmep) by a membrane, comprise most of the ventral surface and part of the lateral surface of the cranium. There is also a large rounded membranous area, corresponding topographically to the genae (g), behind the postocular ridge (pocr) extending upto the cervical groove. The ocular sclerites are bounded posteriorly on each side by a ridge named the postocular ridge (pocr), which originates behind the dorsal eyes and runs ventrally posterior to the lateral ocellus (o) and then in a posteromedian direction, finally ending in a sclerotic area near the anterior proximity of the proepisternum+cervical sclerite (pepcv). According to Theron (1958) these ridges correspond to the postocular ridges of *Pseudaspidoproctus* and *Eulecanium* as they have the same relationships to neighbouring structures. Mäkel (1942) refers to these postocular ridges as the dorsal and the ventral branches of two ridges which bifurcate below the ocelli. Berlese (1893) describes these postocular ridges in *P. citri* without giving any particular name to them and according to Theron (1958), he incorrectly considers them to be connected with each other and dorsally with the posterior margin of the head.

Each ocular sclerite (ocs) is bounded anterodorsally by the preocular ridge (procr) which carries a small anterior process for articulation with the scape (scp). It cuts across the ocular sclerite (ocs) ventral to the point where it articulates with the scape (scp) and fuses with the postocular ridge (pocr) below the lateral ocellus (o). According to Theron (1958) the pre- and postocular ridges of the pseudococcids correspond to Sulc's (1943) "para ocular bars" of *Phenacoccus*. Dorsal to the lateral ocellus (o) the two ridges are joined together by a transverse ocellar ridge (ocr). This transverse ocellar ridge is absent in *P. citri* (Theron, 1958), but is described by Mäkel as part of the "Sclerotized ring" which surrounds the lateral ocellus. Anteroventrally the ocular sclerites are not bounded by ridges and they are indistinguishably fused with one another ventromedially. Posteroventrally the ocular sclerites are bounded by the preoral ridges (pror) as also found in *P. citri* (Theron, 1958), and *P. adonidum, P. fragilis* and *P. maritimus* (Giliomee, 1961).

Each ocular sclerite bears a pair of large dorsal and ventral simple eyes and a pair of lateral ocelli (o). The dorsal simple eyes (dse) are borne on the ocular sclerites (ocs) between the ocular ridges (procr and pocr), while the ventral simple eyes (vse) are situated ventrally on two conical prominences. Each lateral ocellus (o) occurs as a tubercle where the pre- and postocular ridges coalesce. Berlese (1893) has described the simple dorsal and ventral eyes of *Pseudoccus*, as accessory eyes and the lateral ocelli as lateral eyes, which according to him, are the persisting larval eyes. Krecker (1909) fully agrees with Berlese's views. Beardsley (1960) describes three pairs of simple eyes in *S. sacchari*, regarding the lateral ocelli as the simple eyes. From Pflugfelder's (1936, 1937) work on the nervous connections and the development of the eyes of *Eulecanium*, it appears that the simple dorsal and ventral eyes of *S. sacchari* and other coccids and the row of simple eyes in *Steingelia* and some lecaniids (Theron, 1958) are all homologous with the compound eyes of other insects. The lateral ocelli (o) of the adult were shown by Pflugfelder (1936, 1937) to be the persistent larval ocelli, and these in turn must be regarded not as homologues of the dorsal ocelli of some exopterygote nymphs (which are apparently absent from all Coccoidea), but as corresponding to a surviving group of ommatidia of the compound eye of more primitive exopterygote nymphs (Theron, 1958).

The dorsal eyes of *S. sacchari* are widely separated from one another—70·84-93·61 (av. 83·12) μ apart, while the ventral eyes are somewhat approximated—the distance between them being only 12·65-15·18 (av. 14·09) μ. The dorsal and ventral eyes each have a well developed cornea, of which the diameter is slightly larger in the ventral than in the dorsal eyes (see the following table). The distances between and diameters of the dorsal and ventral eyes are (in microns):—

TABLE 2

	Distance		Diameter	
	Between ventral eyes	Between dorsal eyes	Ventral eye	Dorsal eye
Max.	15·18	93·61	27·83	25·30
Min.	12·65	70·84	25·30	22·77
Mean	14·09	83·11	26·14	24·45
S.E.	0·510	3·103	0·623	0·614
S.D.	1·35	8·31	1·527	1·504
C.V.	9·64	10·00	5·821	6·151

On the median line the ventral wall of the epicranium is invaginated to form a narrow slit-like ventral cavity (vc) the external opening of which is situated behind the ventral eyes. From this ventral cavity a fairly short and dorsoventrally flattened apophysis (ca) stretches internally and, according to Mäkel (1942) and Berlese (1893), four pairs of antennal muscles are attached to it. Berlese (1893) calls it the occipital apophysis, but Theron (1958) more accurately named it as the cranial apophysis (ca). The anterior tentorial arms (ata) originate in the ventral cavity posterior to the craniāl apophysis. Due to narrowness of the ventral cavity, the anterior tentorial pits get merged and the arms are, therefore, fused for a short distance and then run posteriorly as two separate thread-like structures. The tentorial arms (ata) are extremely fine and can hardly be recognised. They are posteriorly fused with the stouter posterior tentorial arms (pta) which invaginate from two small posterior tentorial pits (ptp) situated in the membrane surrounding the vestigial mouth opening (mo). The two posterior tentorial arms (pta) are connected by means of an arcuate tentorial bridge (tb). Mäkel (1942) failed to recognise the extremely fine anterior tentorial arms and her interpretations of the ventral cranial wall are, therefore, partly erroneous. Beardsley (1960) has not referred to the tentorium.

Just behind the ventral cavity (vc) the two slightly sclerotized preoral ridges (pror) form an inverted V-shaped structure. Medially the two arms fuse with one another and laterally each arm is connected with the postocular ridge of its side by means of an intermediate sclerotized plate (ip). Ghauri (1959) describes a similar connection between the preoral and postocular ridges in most of the aspidotines (Diaspididae), and Giliomee (1961) in the three species of *Pseudococcus*, but Theron (1958) and Beardsley (1960) have not described such a connection in *P. citri* and *P. adonidum* respectively.

The vestigial mouth opening (mo) is situated in the membrane between the preoral ridges (pror).

Mäkel (1942) is of the opinion that the cervical groove does not represent the posterior margin of the head ventrally, because the parts of the so-called "Vorderkopf", and especially the labium, lie behind this groove. Theron (1958) totally disagrees with her views and regards the cervical groove to represent the posterior margin of the head.

Dermal Structures : (Figs. 1 and 2)—The chaetotaxy of the male Pseudococcidae has been studied by Sulc (1943), Beardsley (1960) and Giliomee (1961). Two types of setae are found on the head capsule of *S. sacchari*: (i) a thick-set, "fleshy" type (fs) which tapers only slightly and has a blunt apex, and (ii) a slender "hair-like" type (hs) which tapers quite notably so as to have an acute apex. The fleshy setae of *S. sacchari* are slender and much like the hair-like setae as in *P. fragilis* (Giliomee, 1961). It is, therefore, difficult to separate the two types of setae. The setae and other dermal structures of the head are :

TABLE 3

Region	Description	Max.	Min.	Mean	S.E.	S.D.	C.V.
Dorsal	Fleshy setae	4	4	4	0	0	0
	Hair-like setae	28	23	25·5	1·04	2·08	8·15
	Simple derm pores	8	3	4·5	1·19	2·38	52·88
	Trilocular disc pores	...	...	...	...	...	...
	Quadrilocular disc pores	6	4	5	0·575	1·150	23·00
	Quinquelocular disc pores	2	2	2	0	0	0
	Hexalocular disc pores	...	...	...	...	...	...
Ventral	Fleshy setae	2	2	2	0	0	0
	Hair-like setae	30	25	27·25	1·105	2·21	8·11
	Simple derm pores	...	...	...	...	...	...
	Trilocular disc pores	...	...	...	...	...	...
	Quadrilocular disc pores	...	...	...	...	...	...
	Quinquelocular disc pores	...	...	...	...	...	...
	Hexalocular disc pores	...	...	...	...	...	...

The cephalic setae may be arranged in the following groups :

(i) *Dorsal Head Setae* (*dhs*)—These setae occur on both sides of the dorsal midcranial ridge (mcr) between the postoccipital ridge (por) and the lateral branch of midcranial ridge (lmcr). The fleshy setae, 2 on each side, occur only on the apex of the head in the dorsal vicinity of the lateral branch of the midcranial ridge (lmcr) while the hair-like setae occupy the whole of the aforesaid area and their number is 8 to 10 (av. 9·5) on each side. There are 2-3 (av. 2·5) quadrilocular disc pores, 1 quinquelocular disc pores and 1-4 (av. 2·25) minute sclerotized rings, which probably represent the derm pores, laterally on each side near the base of antenna.

(ii) *Genal Setae* (*gs*)—The genal setae (gs), 3-4 (av. 3·25) on each side, occur on the genae (g) and are all hair-like.

(iii) *Ventral Head Setae* (*vhs*). They occur on the ocular sclerite in between, as well as anterior to and ventral to the ventral eyes (vse). No setae is found on the preocular ridge. The fleshy setae, 1 on each side, are situated laterally on the apex in the vicinity of lateral branch of midcranial ridge (lmcr). The hair-like setae are 25-28 (av. 26·25) in number, of which 10-16 (av.13·5) occur anterior to ventral eyes (vse), 3-4 (av. 3·5) lateral to each ventral eye, one on each lateral branch of the midcranial ridge, 2-4 (av. 2·5) between the ventral eyes and 2-3 (av. 2·25) posterior to the ventral eyes.

2. *Antennae* (Fig. 3) :

The antennae of the male Pseudococcidae have been described by Uichanco and Villanueva (1932). Their description includes the relative lengths and shape of the different segments. Giliomee (1961) has described many morphological details including chaetotaxy of the antennae of three species of the genus *Pseudococcus*. Other papers devoted to the morphology of male Pseudococcidae contain only the brief references to antennae.

The antennae of *S. sacchari* are inserted directly in the membrane in front of the ocelli. The antennae are normally 10 segmented, but in many cases one or both antennae may be found 9 segmented and rarely 8 segmented also. This 9 or 8 segmented condition of antennae is due to the reduction in size of one or more of the segments between fourth and ninth segments and their subsequent merger with the adjacent segment. In some of the well stained mounts this fusion line between two adjacent segments is easily recognised (Figs. 12 A, 13 A). Similar conditions have also been reported by Giliomee (1961) and Ghauri (1959) in three species of *Pseudococcus* and in Diaspididae respectively. From an examination of the adult from the puparium it was invariably found that, in all cases, the antennae of the future adult were undoubtedly ten segmented.

The general appearance of the antenna is filiform. The total length is 346·85-428·10 (av. 393·85) μ. The length and width of different segments in microns are given in the following table:

TABLE 4

		SEGMENTS										Formula of the average
		I	II	III	IV	V	VI	VII	VIII	IX	X	
Length	Max.	30·36	45·54	58·19	32·89	35·42	40·48	45·54	55·66	48·07	63·25	10,8,3,9,2,7,6,5,1,4
	Min.	25·30	40·48	40·48	22·77	25·30	32·89	32·89	43·01	37·95	45·54	
	Mean	28·46	42·58	47·86	27·60	29·44	35·42	40·25	48·07	43·26	56·42	
	S.E.	0·55	0·465	1·478	1·044	1·027	0·843	1·101	1·476	1·230	1·725	
	S.D.	1·908	1·611	5·120	3·464	3·406	2·796	3·652	4·77	3·892	5·456	
	C.V.	6·704	3·783	10·698	12·55	11·569	7·893	9·073	9·923	8·955	9·670	
Width	Max.	40·48	30·36	20·24	22·77	22·77	22·77	22·77	25·30	22·77	25·30	
	Min.	35·42	30·36	17·71	17·71	17·71	20·24	20·24	20·24	20·24	17·71	
	Mean	36·68	30·36	19·22	18·97	19·98	21·25	22·01	23·02	22·52	20·71	
	S.E.	0·600	0	0·402	0·583	0·355	0·425	0·392	0·603	0·262	0·751	
	S.D.	1·899	0	1·273	1·846	1·123	1·342	1·241	1·907	0·830	2·375	
	C.V.	5·177	0	6·623	9·730	5·620	6·315	5·638	8·284	3·730	11·467	

Width of the scape (across centre) 35·42-40·48 (av. 36·89) μ, pedicel 30·36 (av. 30·36) μ and length of flagellar segments 151·80-179·63 (av. 167·74) μ. Ratio antennal length to body length 1 : 2·54-3·15 (av. 2·87). The setae and other dermal structures of the antennal segments are :—

TABLE 5

Description		SEGMENTS									
		I	II	III	IV	V	VI	VII	VIII	IX	X
Fleshy setae	Max.	1	15	10	12	16	17	15	13	13	18
	Min.	1	7	6	2	4	4	9	8	7	5
	Mean	1	10·2	7	5·1	8	9·6	12	10·8	10·14	10·43
	S.E.	0	0·77	0·63	0·92	1·38	1·203	0·75	0·45	0·85	1·702
	S.D.	0	2·44	2·0	2·92	4·37	3·806	2·0	1·54	2·27	4·504
	C.V.	0	23·92	28·57	57·25	54·62	39·64	16·66	14·26	22·38	42·22
Hair-like setae	Max.	5	11	4	3	4	5	5	5	9	14
	Min.	5	5	1	1	0	2	2	1	1	6
	Mean	5	8·6	1·7	1·6	1·6	3·4	3·57	3·5	4·43	9·14
	S.E.	0	0·618	0·297	0·218	0·425	0·26	0·36	0·47	1·13	1·098
	S.D.	0	1·955	0·94	0·69	4·37	0·84	0·97	1·508	2·99	2·905
	C.V.	0	22·73	55·29	43·12	84·37	24·07	27·17	43·08	67·49	31·78
Sensilla basiconica	Max.	...	...	2	...	1	...	...	...	...	2
	Min.	...	...	1	...	0	...	...	...	...	2
	Mean	...	...	1·3	...	0·30	...	...	...	...	2
	S.E.	...	...	0·151	...	0·15	...	...	...	...	0
	S.D.	...	...	0·48	...	0·48	...	...	...	...	0
	C.V.	...	...	36·92	...	160	...	...	...	...	0
Sensillum placodeum	Max.	...	1	...	...	...	...	...	...	...	...
	Min.	...	1	...	...	...	...	...	...	...	...
	Mean	...	1	...	...	...	...	...	...	...	...
	S.E.	...	0	...	...	...	...	...	...	...	...
	S.D.	...	0	...	...	...	...	...	...	...	...
	C.V.	...	0	...	...	...	...	...	...	...	...

The scape (scp) is a short and sub-rectangular segment and is broader than long. This is the widest segment of the antenna and is sclerotized except distally and laterally. Basally the scape bears a strong sclerotized ridge with a lateral small stumpy process which articulates with a similar process of the preocular ridge. Distally the ventral sclerotization of the scape is produced into a distinct process which articulates with the basal ridge of the pedicel (pdc). This type of articulation of scape and pedicel has also been described in other pseudococcids. There occurs only one long slender fleshy seta (fs) dorsolaterally towards the distal end. Hair-like setae (hs) are 5, the 4 of which are on the ventral side. Out of the 4 hair-like ventral setae, 2 are remarkably slender and smaller than others.

The pedicel (pdc) is club-shaped and sclerotized and is reticulated distally. It is less broad than the scape. The basal ridge of the pedicel is well developed ventrally but not dorsally and articulates with the ventral process of the scape. The pedicel is beset with both fleshy (7-15, av. 10·2) and hair-like (5-11, av. 8·6) setae (see the above table). Some of the fleshy setae are characteristically stouter and smaller than others. Distally there is a circular sensillum placodeum (spl) on the dorsolateral aspect.

The flagellum (f III—X) is composed of seven segments which are elongated, cylindrical and slightly constricted at either ends. They are all well sclerotized except for the constricted apical part which is membranous. The relative lengths of the different segments vary considerably (see the above table). The tenth segment is always the largest. The diameter of these segments remains apparently constant.

The setae are more common on the distal half of each flagellar segment than the proximal half. 1-2 (av. 1·3) sensilla basiconica occur ventrodistally on the third segment and 0-1 (av. 0·3) ventrodistally on the 5th. Ventrally on the distal half of each of the 8th and 9th segment, one fleshy seta becomes larger than other. The terminal segment (Xth) is tubularly constricted at the apex as in *P. adonidum* and *P. maritimus* (Giliomee, 1961). This is further beset with 5-18 (av. 10·43) fleshy and 2-10 (av. 5·14) hair-like setae including one apical seta, length 15·18-17·72 (av. 16·86) μ, not apically knobbed; two thick spine-like sub-apical setae, length 32·89—35·42 (av. 33·73) μ, dorsally; two long apically knobbed setae, sub-apical sensory (set. scla.) (seta semi-claviformes—(set. scla) of Sulc, 1943), length 40·48—43·01 (av. 42·16) μ, ventrally; two sensilla vasiconica, one at the apex and the other one a short distance behind, ventrally.

B. The Thorax : (Figs. 1, 2, 4, 5 & 6)

The thorax of Pseudococcidae is described in detail by Mäkel (1942) and to a lesser extent by Berlese (1893) and Beardsley (1960) and is figured by Ezzat (1956). Papers of Vaney and Conte (1908), Uichanco and Villanueva (1932), Cottier (1936), Betrem (1937), Sulc (1943) and Jancke (1955) contain no significant information on the morphology of the thorax.

Theron (1958) has made a detailed study of the thorax and established the homologies of various parts and sclerites. Giliomee (1961) has made an elaborate and comprehensive study of the morphology, including chaetotaxy, of the three species of genus *Pseudococcus*.

The thorax of *S. sacchari* resembles the typical homopteran thorax much more than its head resembles the typical homopteran head. The most striking features of the thorax, of the species studied, are :

(i) Marked sclerite degeneration of the pro- and metathorax;
(ii) The replacement of the hind wings by halteres and resultant reduction of the metathorax;
(iii) Reinforcement of secondary ridges.

Length and width of the thorax in microns are as follows :—

TABLE 6

	Length				Width			
	From cervical groove to the meso-post-phragma	Pres-cutum	Scute-llum	Basis-ternum	Meso-thorax	Pres-cutum (across widest)	Scute-llum (across widest)	Basis-ternum (across widest)
Max.	450·8	91·08	53·13	144·21	303·6	118·91	103·73	172·04
Min.	395·6	73·37	40·48	131·16	240·04	108·78	88·55	141·68
Mean	413·8	82·22	45·54	139·08	276·4	114·69	94·69	156·43
S.E.	10·55	2·02	1·51	1·31	22·98	1·164	2·156	4·38
S.D.	23·53	4·95	4·01	3·21	32·506	2·851	5·705	10·69
C.V.	5·68	6·02	8·80	2·309	11·76	2·485	6·024	6·83

1. *Prothorax* (Figs. 1, 2, 4, 5 & 6):

This is separated from the head by a deep cervical groove (cv) and is largely membranous. There are two narrow transverse ridge-like sclerites (prnr) immediately behind the cervical groove (cv) and are regarded as the cervical sclerites by Mäkel (1942) and as the prothoracic sutures by Ezzat (1956). Theron (1958) regards them representing part of the pronotum and calls them as pronotal ridges (prnr). These sclerites are separated dorsally and each continues ventrally to articulate with a sclerite, the proepisternum+cervical sclerite (pepcv), which is described by Theron as propleuron+cervical sclerite. Giliomee (1961) calls it as proepisternum+cervical sclerite and Ezzat (1956) refers to this as the pleural sclerite of the prothorax.

Each of the pronotal ridges dorsolaterally bears a less sclerotized area, the pronotal ridge (prn), the "Cervicalast" of Mäkel (1942). According to Theron (1958) these two sclerites (prn) resemble the dorsal lobes of the pronotal ridge in *Steingelia*. The two sclerites (prn) are homologous with the lateral pronotal sclerites described by Ghauri (1959) in the Diaspididae. Further back there is a pair of weakly sclerotized plates (pt), which are regarded by Theron (1958) as vestiges of the posttergites (pt). Mäkel (1942) overlooks them.

The pleural region of prothorax of *S. sacchari* is almost similar to that of other pseudococcids. The proepisternum + cervical sclerite (pepcv) is reduced to a strong lateral capitate ridge-like structure, which anteriorly articulates with the postocular ridge (pocr) of its side, and posteriorly becomes fused with the pro-pleural ridge (plr_1) and forms a small internal propleural apophysis (pla_1). Mäkel (1942) calls this structure the propleuron and describes that a small first cervical sclerite is anteriorly separated from it. But this separation of a small cervical sclerite from the anterior portion of this ridge has been shown by Theron (1958) to be incorrect. According to Giliomee (1961) the weakening of this ridge (pepcv) near its anterior end convinced Mäkel (1942) to regard the anterior part as a definite detached cervical sclerite. But as the weakening of anterior part of the ridge (pepcv) does not occur in the primitive Coccoidea (Theron, 1958), this may be of secondary nature. Theron (1958) calls this ridge propleuron+cervical sclerite, but Giliomee (1961) prefers to call it proepisternum+cervical sclerite (pepcv) advocating that although the hind margin of pleural sclerite is formed by propleural ridge (plr_1) and propleural apophysis (pla_1) in pseudococcids, as well as in the Coccoidea studied by Theron (1958), an epimeron has been described by Ghauri (1959) in some Diaspididae; thus making the term proepisternum + cervical sclerite (pepcv) more appropriate for the anterior part of the ridge (representing the cervical and pleural sclerites) than propleuron+cervical sclerite. The propleural ridge (plr_1) is a short process which extends downwards from the propleural apophysis (pla_1) to articulate with the basal process of the coxa (bpc).

Ventrally there is a small prosternum (stn_1), which consists of a small median triangular sclerite bounded posteriorly by a transverse ridge (stn_1r). The prosternum is not correctly figured by Mäkel (1942), who calls it the ventral sclerite. Ezzat (1956) names it as the basisternum and Beardsley (1960) as a remnant of the prothoracic poststernum, while Theron (1958) and Giliomee (1961) both correctly call it prosternum (stn_1).

Dermal Structures : (Figs. 1, 2 & 3)—In the prothorax only hair-like setae are found. Disc pores, which are usually quadrilocular, but sometimes trilocular or quinquelocular or hexalocular, and some minute sclerotized rings representing probably the simple derm pores, are associated with the setae. Minute dermal denticulations are also found here and there near these setae. The setae and other dermal structures of the prothorax are given in the table 7 (on page 84):

TABLE 7

Regions		Dermal Structures					
		Hair-like setae	Simple derm pores	Trilocular disc pores	Quadrilocular disc pores	Quinquelocular disc pores	Hexalocular disc pores
Medial pronotal (mpns)	Max.	12	2	...	4	2	...
	Min.	10	0	...	0	0	...
	Mean	10·5	1	...	2	0·5	...
	S.E.	0·5	0·575	...	0·815	0·500	...
	S.D.	1·0	1·15	...	1·63	1·0	...
	C.V.	9·52	115	...	81·5	200	...
Lateral pronotal (lps) (On each side)	Max.	8	2	...	4	2	...
	Min.	3	0	...	2	1	...
	Mean	5·5	1·25	...	2·5	1·25	...
	S.E.	1·04	0·475	...	0·50	0·25	...
	S.D.	2·08	0·95	...	1·0	0·50	...
	C.V.	37·81	76·0	...	40·0	40·0	...
Posttergital (pts) (On each side)	Max.	6	...	...	1	...	...
	Min.	4	...	...	0	...	...
	Mean	5	...	...	0·5	...	...
	S.E.	0·575	...	...	0·284	...	...
	S.D.	1·15	...	...	0·568	...	...
	C.V.	23·0	...	...	113	...	...
Antespiracular dorsal (asds) (On each side)	Max.	8	...	...	2	1	1
	Min.	2	...	...	0	0	0
	Mean	5	...	...	0·5	0·25	0·5
	S.E.	1·47	...	...	0·500	0·25	0·288
	S.D.	2·94	...	...	1·0	0·50	0·577
	C.V.	58·80	...	...	200	200	115·40
Prosternal (stn/s)	Max.	8	3	...	...	...	...
	Min.	4	0	...	...	...	...
	Mean	6	2·25	...	...	...	...

(*Contd. on page* 85)

Regions		Dermal Structures					
		Hair-like setae	Simple derm pores	Trilocular disc pores	Quadrilocular disc pores	Quinquelocular disc pores	Hexalocular disc pores
	S.E.	0·815	0·750	...	...	...	...
	S.D.	1·63	1·50	...	...	...	...
	C.V.	27·16	66·66	...	...	...	...
Antespiracular ventral (asvs) (On each side)	Max.	4	1	1	2	1	...
	Min.	2	0	0	1	1	...
	Mean	3	0·5	0·25	1·5	1	...
	S.E.	0·408	0·288	0·250	0·288	0	...
	S.D.	0·816	0·577	0·50	0·577	0	...
	C.V.	27·20	115·40	200·0	38·46	0	...

Prothoracic setae may be arranged in the following groups:—

(*i*) *Medial pronotal setae* (*mpns*)—They occur dorsally on each side of the median line anterior to posttergite sclerite (pt). No fleshy setae are found.

(*ii*) *Lateral pronotal setae* (*lps*)—These are found in the area dorsal to the proepisternum+ cervical sclerite (pepcv). They are all hair-like setae and are 3-8 (av. 5·5) on each side. 1-2 (av. 1·25) quinquelocular, 2-4 (av. 2·5) quadrilocular, and 0-2 (av. 1·25) simple derm pores are found on each side.

(*iii*) *Posttergital setae* (*pts*)—They occur on and behind the posttergite sclerite (pt) and are all hair-like. They are 4-6 (av. 5) on each side, out of which 2 are situated on each posttergite sclerite (pt). 0-1 (av. 0·5) quinquelocular and 0-1 (av. 0·75) quadrilocular disc pores; and 0-1 (av. 0·5) simple derm pores occur on each side in this region.

(*iv*) *Antespiracular dorsal setae* (*asds*)—They are situated dorsal to an imaginary line drawn between the propleural apophysis (pla_1) and the mesothoracic spiracular opening. They are 2-8 (av. 5) on each side and all are hair-like. 0-1 (av. 0·25) hexalocular, 1 quinquelocular and 1-2 (av. 1·5) quadrilocular disc pores; and 0·1 (av. 0·25)simple derm pores occur on each side.

(*v*) *Antespiracular Ventral Setae* (*asvs*)—These are found ventral to the imaginary line drawn between the propleural apophysis (pla_1) and the mesothoracic spiracular opening. The number of setae, which are all hair-like, in this region is 2-4 (av. 3) and that of quinquelocular disc pores 0-1 (av. 0·75), quadrilocular 0-2 (av. 1·25), trilocular 0-1 (av. 0·25) and simple derm pores 0-1 (av. 0·5) on each side.

(*vi*) *Prosternal setae* (stn_1s)—They are hardly distinguishable from antespiracular ventral setae (asvs) and are found between the anterior coxae (cx_1), anterior to the transverse ridge of the prosternum (stn_1r). They are all hair-like with the total number 4-8 (av. 6). There are no disc pores, only 0-3 (av. 2·25) simple derm pores are met with.

2. *Mesothorax* (Fig. 1, 2, 4, 5 & 6) :

Mesothorax, being the principal centre of flight, is well developed and is characteristically reinforced by strong sclerotized ridges.

(*I*) *Mesotergum :*

The tergal region of the mesothorax is well sclerotized. This is divided into an alinotum or mesonotum and a postnotum.

(*i*) *The Alinotum*—This consists of a prescutum (prsc), scutum (sct) and scutellum (scl).

(a) *The Prescutum* (*prsc*)—Length 73·37-91·08 (av. 82·22) μ; Width (across widest) 108·78-118·91 (av. 114·7) μ. Its anterior margin curves inwards and becomes continuous with the mesoprephragma. This is strongly arched and is bounded laterally by the prescutal ridges (pscr) and posteriorly by a slight groove which represents the median part of the prescutal sulcus (pscs). The prescutal ridges are strongly developed and anteriorly fused with the mesoprephragma, which is slightly emerginate medially.

Berlese (1893) describes the prescutum as the oval anterior part of the mesonotum. Mäkel (1942) correctly calls it as the prescutum, while Jancke (1955) wrongly names it as the proscutum. The structure, described by Ezzat (1956) as the prescutum, is really the mesoprephragma.

According to Mäkel (1942) the prescutum (prsc) gives rise laterally to the prealare (pra), whereas latter is clearly the lateral extension of the scutum (sct) in *S. sacchari*, and other pseudococcids studied by Theron (1958) and Giliomee (1961), as the prescutal ridges, which bound the prescutum laterally, have shifted far medially.

(*b*) *The Scutum* (*sct*)—This is very large and weakly sclerotized medially. Laterally it is produced into anterior and posterior extensions which extend lateral to the prescutum (prsc) and scutellum (scl) respectively. Each anterior extension extends lateroventrally to form the so-called prealare (pra). Each prealare (pra) is separated from the rest of the scutum by a well developed secondary ridge, the scutal ridge (sctr), which anteriorly forms a finger-like apodeme (ap) and posteriorly extends upto the anterior notal wing process (anp). Distally each prealare terminates into a sclerotized convex triangular plate (tp), posterior margin of which curves inwards forming a distinct apodeme at its base and articulates with the mesepisternum (eps_1). The lateral margin of the scutum is produced into a very well developed anterior notal wing process (anp) which curves upwards. The lateral margin of the scutum is folded downwards; the deflection being indicated by a small notch immediately posterior to the anterior notal wing process (anp). Posterior to the line of this deflection the posterior extensions of the scutum are inflected downwards, for a short distance, and then upwards to form the posterior notal wing process(pnp).

Medially a longitudinal less sclerotized depressed area is present on the scutum. Like other mealybugs a lateral emergination is present and is followed by the posterior notal wing process (pnp). According to Berlese (1893) the prescutum+scutum is pronotum, and he as well as Mäkel (1942) and Jancke (1955) regard the posterior extensions of the scutum (sct) as part of the scutellum (scl), but Theron (1958) and Giliomee (1961) hold that they belong to the scutum.

(c) *The Scutellum* (*scl*)—Length 40·48-53·13 (av. 45·54) μ; width 88·55-103·73 (av. 94·69) μ. This is a subrectangular sclerite. Its anterior and posterior edges are curved inwards giving it a sub-cylindrical appearance. Anteriorly it is separated from the scutum by a distinct scutoscutellar sulcus (scts) and is posteriorly bounded by a ridge (rd) which probably corresponds to the posterior marginal fold of the alinotum (Theron, 1958). Berlese (1893) calls the scutellum as the mesonotum. Medially there is a less sclerotized area which is called the membranous area by Ezzat (1956).

(ii) *The Postnotum*—This is a well developed area. A large subtriangular membranous area, which is called the "Postscutellum or scutellum of the metanotum" by Berlese(1893) and the postscutellum by Jancke (1955), separates the posterior part of the postnotum from the scutellum (scl). Posteriorly it stretches for a considerable distance and curves inwards extending within the metathoracic cavity. Its posterior part becomes overlapped by the deeply involuted metanotum. Beardsley (1960) erroneously describes that the posterior part of the mesonotum is situated externally. Internally where the mesopostnotum and metanotum meet, a slightly emerginate mesopostphragma is formed. Laterally the postnotum gives rise to the two postnotal apophyses (pna), which are described by Berlese (1893) as the "corniculate apophyses of the metanotum" and by Mäkel (1942) as the wedge shaped apophyses. Anterolaterally the postnotum is produced into a postalare (pa) which articulates with the pleuron anterior to the mesopleural ridge (plr_2). The anterodorsal margin of the postalare is strengthened by a ridge, the anterior postalare ridge (apar), which Mäkel (1942) wrongly considered to be fused with the pleural ridge. The posterior margin of the postalare is also reinforced by a ridge, the posterior postalare ridge (ppar). Mäkel (1942) describes this ridge without naming it and holds that it originates at the pleural ridge and extends posteriorly upto the metathoracic pleural wing process (pwp_2). Ezzat (1956) also regards that the postalare is fused with the mesopleural ridge (plr_2).

(II) *Mesopleuron :*

The mesopleuron of *S. sacchari* is somewhat modified due to sclerite degeneration and reinforcement of the secondary ridges. The mesopleural ridge (plr_2) articulates ventrally with the coxa and terminates dorsally in the mesopleural wing process (pwp_1). The mesopleural ridge, at a point where it is overlapped by the anterior part of the postalare (pa), gives out an internal pleural apophysis (pla_2). The sclerotized area anterior to the mesopleural ridge represents the mesepisternum (eps_1), which is divided by a triangular membranous area into dorsal and ventral parts. The dorsal part of the mesepisternum is convex and its posterodorsal edge (called the tendon plate by Mäkel, 1942) projects internally underneath the basalare (bas) and is not visible externally. The triangular plate (tp) of the prealare (pra) partly overlaps the anterodorsal margin of the mesepisternum (eps_1). The mesepisternum is bounded anteriorly by a well developed secondary ridge, the subepisternal ridge (ser) and ventrally by the marginal ridge (mr) of the basisternum (stn_2). The subepisternal ridge (ser) extends from the marginal ridge (mr) of the basisternum to the triangular plate (tp), but is not fused with either. Ezzat (1956) refers to it as the pleural bridge. Dorsally a fairly developed basalare sclerite (bas) extends between the mesepisternum and the mesopleural wing process (pwp_1). Mäkel (1942) refers to this sclerite without naming it. A narrow sclerite (ns) connects the mesopleural wing process with the costal complex of wing veins (ccx). Dorsally a distinct subalare (sa) is present behind the mesopleural wing process. Mäkel (1942) found this sclerite but did not name it. Anteroventral to the subepisternal ridge (ser), immediately above the marginal ridge (mr), a small area extends anteriorly, which, according to Weber (1928) and Theron (1958), is the lateropleurite (lpl), and seems to be a part of the mesepisternum (eps_1). A small sclerotized area, behind the pleural ridge (plr_2) and above the coxal articulation, represents the vestige of the mesepimeron (epm_1). Anterior to the coxal articulation there is a narrow sclerite which extends downwards but does not articulate with the coxa. According to Giliomee (1961) it represents the trochantin (tn_1). This sclerite is not described by Berlese (1893), Theron (1958), Beardsley (1960) and Ezzat (1956), but is described by Weber (1928) and Roberti (1946) for *Aphis* and Kramer (1950) in some auchenorhynchous Homoptera. Mäkel (1942) found it but did not name it as trochantin.

The mesothoracic spiracle (sp_1), with its supporting peritreme (ptr_1), is situated in the membrane anterior to the mesepisternum (eps_1).

(III) *Mesosternum :*

The mesosternum of *S. sacchari* is in the form of a large sclerotized plate, the mesobasisternum (stn_2). This is situated anterior to the mesofurcal pit (fp). Mäkel (1942) recognises it as such, but Ezzat (1956) incorrectly called it as furcasternum. Mäkel (1942) further regards the base of furca

(f) as the furcasternite. The mesobasisternum (stn_2) is separated on each side from the pleuron by a strong marginal ridge (mr). Anteriorly this ridge bends medially and becomes fused with its fellow of opposite side forming the anterior margin of the mesobasisternum (stn_2). Posteriorly it stretches dorsally and becomes fused with the pleural ridge (plr_2) above and anterior to the coxal articulation. The posterior margin of the basisternum is bounded on each side by a ridge, the precoxal ridge (pcr_1), which posteriorly runs to get fused with its fellow of the opposite side, and anteriorly with the marginal ridge (mr) anterior to the coxa (cx_2). The basisternum (stn_2) extends laterodorsally and becomes fused with the mesepisternum in front of the coxa (cx_2), thus forming a precoxal bridge. A postcoxal bridge is altogether wanting. The furcal pit (fp) is situated medially immediately behind the point where the two precoxal ridges (pcr_1) meet. The furca (f) is well developed and consists of a broad base and two furcal arms extending anterolaterally. Berlese (1893) and Larsén (1945) wrongly regard the furca (f) as the metasternal apophysis.

(*IV*) *Wing Articulation* (Figs. 1, 4, 6 & 8):

The articulation of the wings of *S. Sacchari* agrees closely with that of the Coccoidea studied so far. The pteralia taking part in the wing articulation are : the tegula (teg), the first, second and third axillary sclerites (ax_1, ax_2 and ax_3), the first median (m_1), and second median (m_2) plates and the humeral plate (hp). The other thoracic structures involved are; the anterior notal wing process (anp), the mesopleural wing process (pwp_1), the basalare (bas), and the subalare (sa).

(i) The tegula is a small meniscate sclerite which is situated dorsally on a buldged membranous area, anterior to the wing base. According to Theron (1958) a muscle extends posteriorly from it to the anterior margin of the mesopleural wing process (pwp_1), and becomes attached to the latter by a tendon like apodeme (t).

(ii) The first axillary sclerite (ax_1) is small and triangular in shape. Its anterior tip, which is supported by the pleural wing process, articulates with the costal complex of wing veins (ccx). Medially it articulates with the lateral margin of the scutum (sct) near the notch formed by the deflection of the lateral region of the scutum behind the anterior notal wing process (anp). The posterolateral margin of this sclerite is long and produced in the form of a posterior arm, which lies over the second axillary sclerite (ax_2) articulating with the latter. The similar condition of the posterolateral margin is described by Giliomee (1961) in *Pseudococcus,* Ghauri (1959) in the Diaspididae and Theron in the Margarodidae (but not in *Pseudococcus citri*).

(iii) The second axillary sclerite (ax_2) is larger than the first axillary sclerite and is somewhat subrectangular with its anterior end elongated and acute. The elongated anterior end is directed towards the costal complex of wing veins and articulates with the anterior tip of the first axillary. The posterior part of this sclerite is expanded and articulates with the third axillary sclerite (ax_3).

(iv) The third axillary sclerite (ax_3) is the largest of all the three sclerites. It lies immediately behind the second axillary sclerite (ax_2) with which its anterior margin articulates. The anterior portion of this sclerite is somewhat triangular and less sclerotized. The anterior margin of this triangular portion is elongated and lies over the second axillary sclerite (ax_2), and its basal margin is sclerotized and is completely fused to the posterior heavily sclerotized portion. Giliomee's interpretation that this triangular less sclerotized area represents the median plate, as defined by Snodgrass (1935), is erroneous. As the anterior triangular portion does not seem to be a separate sclerite in any of the specimens examined, and the first and second median plates (m_1 & m_2), as defined by Snodgrass (1935) are found here at their right topography, I am not convinced with Giliomee's interpretation. Posteriorly this sclerite gives rise to a heavily sclerotized extension which apparently represents the axillary cord (axc) and has become fused with it. The axillary cord (axc) is connected to the postalare (pa) by means of a sclerotized band, immediately anterior to the point where the sclerotized band from scutellum (scl) is attached. The posterior marginal fold of the notum is, therefore, not directly connected to the wing membrane or axillary cord (axc). Distally the cord merges into the hind margin of the wing.

(v) An additional and less sclerotized sclerite, which possibly represents the first median plate (m_1), as defined by Snodgrass (1935), lies distal to the second and third axillary sclerites. This is sub-triangular in shape with its distal margin somewhat rounded. The proximal part of the anterior margin of it lies overlapped by the second axillary sclerite (ax_2); the posterior margin articulates with the third axillary (ax_3). This is not described by Mäkel (1942), Ezzat (1956), Theron (1958), Beardsley (1960) and Giliomee (1961).

(vi) Another very weakly sclerotized sclerite, which represents the second median plate (m_2), as defined by Snodgrass (1935), is found distal to the first median sclerite. This is referred to by Theron (1958) and Giliomee (1961) as the additional plate. Giliomee (1961) very correctly regards it to represent the second median plate as defined by Snodgrass (1935). This resembles the so-called "Zusatzstuck" which Weber (1929) describes in *Psylla.*

(vii) A triangular weakly sclerotized plate is found anterior to the distal part of the costal complex of wing veins. This possible represents the humeral plate (hp), as defined by Snodgrass (1935). This is not described by Mäkel (1942), Ezzat (1956), Theron (1958) and Beardsley (1960). A humeral plate has been described by Ghauri (1959) in the Diaspididae. Mäkel (1942) rightly recognised this sclerite and called it as circular sclerite. Giliomee (1961) found it anterior to the distal part of the costal complex but failed to recognise it as such.

Mäkel (1942) has also studied the pteralia of *Pseudococcus*, but she has mistaken the costal complex of veins (ccx) for the second axillary sclerite and regards the true second axillary (ax_2) as being part of the third axillary sclerite (ax_3).

Dermal Structures (Figs. 1, 2 &6): Hair-like setae, as well as disc pores are present. Fleshy setae are wanting. The setae are found on the prescutum, scutum, scutellum, and the tegula, the basisternum and on the membranous area anterior to the basisternum (stn_2) and subepisternal ridges (ser). The mesothoracic dermal structures are as follows:—

TABLE 8

Specific Regions		Dermal Structures					
		Hair-like setae	Simple derm pores	Trilocular disc pores	Quadrilocular disc pores	Quinquelocular disc pores	Hexalocular disc pores
Prescutal (pscse)	Max.	6	...	...	...	...	...
	Min.	4	...	...	...	...	...
	Mean	4·5	...	...	...	...	...
	S.E.	0·50	...	...	...	...	...
	S.D.	1·0	...	...	...	...	...
	C.V.	22·22	...	...	...	...	...
Scutal (sctse)	Max.	13	...	...	...	...	...
	Min.	10	...	...	...	...	...
	Mean	11·25	...	...	...	...	...
	S.E.	0·75	...	...	...	...	...
	S.D.	1·50	...	..	...	...	...
	C.V.	13·333	...	...	...	...	...
Scutellar (scls)	Max.	6	...	...	...	...	...
	Min.	4	...	...	...	...	...
	Mean	4·50	...	...	...	...	...
	S.E.	0·50	...	...	...	...	...
	S.D.	1·0	...	...	...	...	...
	C.V.	22·22	...	...	...	...	...

(*Contd. on page* 92)

Specific Regions		Dermal Structures					
		Hair-like setae	Simple derm pores	Trilocular disc pores	Quadrilocular disc pores	Quinque locular disc pores	Hexalocular disc pores
Tegular (tegs) (on each side).	Max.	4	...	...	...	...	...
	Min.	3	...	...	...	...	...
	Mean	3·25	...	...	...	...	...
	S.E.	0·250	...	...	...	...	...
	S.D.	0·500	...	...	...	...	...
	C.V.	15·38	...	...	...	...	...
Postmesostigmatal (pms) (on each side)	Max.	10	1	...	3	1	...
	Min.	6	0	...	1	0	...
	Mean	7·5	0·75	...	1·5	2·5	...
	S.E.	0·365	0·250	...	0·50	0·250	...
	S.D.	1·73	0·50	...	1·0	0·50	...
	C.V.	23·06	66·666	...	66·666	200	...
Basisternal (stn_2s)	Max.	16	...	...	...	...	...
	Min.	11	...	...	...	...	...
	Mean	13·33	...	...	...	...	...
	S.E.	1·442	...	...	...	...	...
	S.D.	2·519	...	...	...	...	...
	C.V.	18·89	...	...	...	...	...

They can be arranged in the following groups :—

(i) *Prescutal Setae* (*pscse*)—A number of hair-like setae are found on each side of the median line on the prescutum. Their number is 2-3 (av. 2·33) on each side. Disc pores are not found.

(ii) *Scutal Setae* (*sctse*)—These occur on each side of the median line and a few near the anterior notal wing process (anp). They are all hair-like and 5-7 (av. 6) in number on each side. Other dermal structures are lacking.

(iii) *Scutellar setae* (*scls*)—They are found on each side of the median line and are 2-3 (av. 2·33), and all hair-like. Disc pores are absent. There are 2-3 (av. 2·66) minute membranous spots, somewhat reminiscent of vacant hair sockets (Giliomee, 1961) on each side.

(iv) *Tegular Setae* (*tegs*)—These include the hair-like setae only and occur on the anterodistal portion of each tegular buldge (teg). Their number is 3-4 (av. 3·33). The fleshy setae and other dermal structures are absent.

(v) *Postmesostigmatal setae* (*pms*)—These occur on the membrane posterior to the mesospiracles (sp_1). They are 12-20 (av. 15) and all hair-like. No fleshy setae are met with. There are 0-2 (av. 0·5) quinquelocular, 2-6 (av. 3) quadrilocular disc pores and 2-4 (av. 2·66) simple derm pores.

(vi) *Basisternal setae* (*stn_2s*)—These are all hair-like and occur mostly on the anterior portion of the basisternum, only one seta is found posteriorly near the precoxal ridge (pcr_1). They are 11-16 (av. 13·33) in number. No fleshy setae or disc pores are found.

3. *Metathorax* : (Figs. 1, 2, 4, 5 & 6) :

Due to the loss of functional hind wings, which have been replaced by halteres, the metathorax of *S. sacchari* is considerably reduced.

(a) *Metanotum*—This originates morphologically posterior to the mesopostphragma, but as it does not extend dorsally and posteriorly beyond the metathoracic fold, which overlaps the mesopostnotum, it is not visible externally. Dorsally the two small sclerities, which are known as suspensorial sclerites (ss), represent the metanotum and each of them is connected to the haltere (h) of its side by means of a sclerotized tendon (ht). These sclerites are not described by Mäkel (1942), Ezzat (1956) and Beardsley (1960). The only other parts of the metanotum which are visible dorsally, are the two weakly sclerotized transverse plates (pn_3) of irregular shape which are found in the membrane posterior to the metanotum. Each sclerite possibly represents the metapostnotum (pn_3). They have been overlooked by Mäkel (1942) and Ezzat (1956).

(*b*) *Metapleuron*—In the metapleuron there is a distinct metapleural sulcus and a corresponding internal ridge, the metapleural ridge (plr_3), which ventrally articulates with the coxa (cx_3) and extends anterodorsally across the pleuron ultimately terminating in a meta-pleural wing process (pwp_2). The metapleural wing process articulates with the base of the haltere (h). The pleural ridge (plr_3) in the middle, fades out and is produced inwardly forming a small metapleural apophysis (pla_3). In this respect it is very similar to the condition described by Giliomee (1961) in the three species of *Pseudococcus*. This condition has not been described by Mäkel (1942), Theron (1958) and Beardsley (1960). Anterior to the ventral part of the metapleural ridge and coxal articulation, there is a moderately sclerotized area, which represents the metepisternum (eps_2), from the ventral part of which a short precoxal ridge (pcr_2) extends ventromedially. Between this ridge (pcr_2) and the coxal articulation the metepisternum (eps_2) bears a short ventral extension which represents the reminiscent of the metathoracic trochantin (tn_2). Posterodorsal to the coxal articulation, behind the precoxal ridge (pcr_2) is an irregular sclerotized area, the metepimeron (epm_2).

The metathoracic spiracle (sp_2) is situated in the membrane anterior to the metepisternum (eps_2). It has a well developed peritreme (ptr_2), which gives support to the spiracle.

(*c*) *Metasternum*—Two metasternal apophyses (sta) are found posteromedially to the ventral ends of the precoxal ridges (pcr_2). Mäkel (1942) has figured them, though incorrectly, without any description. They have been overlooked by Theron (1958) in *P. citri* and Beardsley (1960) in *P. adonidum* and *S. sacchari*. No sternal plates are met with.

Dermal Structures (Figs. 1, 2 & 6)—Only the hair-like setae are found. In addition to the setae, disc pores and sclerotized rings representing the simple derm pores occur in association with the setae. The setae and other dermal structures of metathorax are given in the following table:—

TABLE 9

Specific Regions		Dermal Structures					
		Hair-like setae	Simple derm pores	Trilocular disc pores	Quadrilocular disc pores	Quinquelocular disc pores	Hexalocular disc pores
Metatergal (mts)	Max.	13	...	...	...	...	...
	Min.	12	...	...	...	...	...
	Mean	12·33	...	...	...	...	...
	S.E.	0·33	...	...	...	...	...
	S.D.	0·578	...	...	...	...	...
	C.V.	4·78	...	...	...	...	...
Metapleural (mps) (On each side)	Max.	4	2	...	6	3	...
	Min.	3	1	...	2	0	...
	Mean	3·25	1·75	...	3·75	1	...
	S.E.	0·250	0·250	...	0·8535	0·7071	...
	S.D.	0·50	0·50	...	1·707	1·4142	...
	C.V.	15·38	28·57	...	45·51	141·42	...
Anterior metasternal (amss)	Max.	10	4	...	4	...	...
	Min.	6	2	...	2	...	...
	Mean	8	2·666	...	2·666	...	...
	S.E.	1·154	0·665	...	0·665	...	...
	S.D.	2·00	1·150	...	1·150	...	...
	C.V.	25·0	43·23	...	43·23	...	...

(*Contd. on page* 95)

Specific Regions		Dermal Structures					
		Hair-like setae	Simple derm pores	Trilocular disc pores	Quadrilocular disc pores	Quinquelocular disc pores	Hexalocular disc pores
Posterior metasternal (pmss)	Max.	4	...	...	...	...	...
	Min.	4	...	...	...	...	...
	Mean	4	...	...	...	...	...
	S.E.	0	...	...	...	...	...
	S.D.	0	...	...	...	...	...
	C.V.	0	...	...	...	...	...

The setae of the metathorax can be grouped as follows :—

(i) *Metatergal setae* (*mts*)—These occur on the dorsum in between the two suspensorial sclerites (ss) and all hair-like. They are 6 on each side, 5 of which are grouped together and occur near the suspensorial sclerite (ss) and the remaining on the side of the median line. There are no fleshy setae or disc pores.

(ii) *Metapleural setae* (*mps*)—These occur on the membrane anterior to the metapleural ridge (plr_3) and posterior and posterodorsal to the metaspiracle (sp_2), anterodorsal to the metaprecoxal ridge (pcr_2). They are all hair-like and 3-4 (av. 3·25) on each side. 0-3 (av. 1) quinquelocular and 2-6 (av. 3·75) quadrilocular disc pores and 1-2 (av. 1·75) simple derm pores are associated with these setae on each side.

(iii) *Anterior metasternal setae* (*amss*)—They occur on the membrane between the mesosternum and the metasternum. These are 6-10 (av. 8) in number, and all hair-like, 2-4 (av. 2·66) quadrilocular disc pores and 2-3 (av. 2·33) simple derm pores are met with in this region. Fleshy setae are altogether wanting.

(iv) *Posterior metasternal setae* (*pmss*)—They are found posterior to the metaprecoxal ridge (pcr_2), and are all hair-like and 4 in number. The fleshy setae and disc pores are absent.

4. *Wings and Halteres* (Figs. 1, 4, 6 & 8) :

As a rule only the fore pair of wings are present and are functional; the hind pair being replaced by halteres (h).

The wings are wholy membranous and are attached to the mesothorax. The length and width of the wing and haltere in microns are as follows :—

TABLE 10

	Length			Width	
	Wing	Haltere	Apical hooked seta of haltere	Wing	Haltere
Max.	809·6	70·84	48·07	322·0	15·18
Min.	763·6	63·25	45·54	230·0	12·65
Mean	787·3	67·95	46·55	286·5	14·09
S.E.	5·29	1·21	0·444	15·16	0·510
S.D.	13·99	3·21	0·994	40·105	1·350
C.V.	1·77	4·72	2·13	13·99	9·58

When at rest, the wings are folded in a horizontal position over the abdomen and overlap each other. Its base is narrow, but the distal (posterior) part is much expanded with the posterior margin and the wing tip rounded. There is no notch in the anterior margin of the wing as is indicated by Beardsley (1960). The entire wing surface is covered by minute microtrichia with those on the margins somewhat longer than elsewhere. There is a small pouch near the wing base which is formed by the dilation of the posterior margin of the wing. The hooked tip of the apical seta (a) of the haltere hooks into the ventral invagination of this pouch. This simple type of wing coupling mechanism is common in other Coccoidea also.

Basally on the dorsal surface of the wing, immediately anterior to the common stem of the radius (R) and media (M), are found 3—4 (av. 3·66) hair-like setae, which are known as alar setae (as). Besides, a short row of 2 circular sensilla occurs along the anterior margin of the radius (R), distad to the point where radius and media meet.

Venation :

As in other mealybugs, the venation in *S. sacchari* is also very much reduced. There are only two distinct veins, which, according to Patch (1909), represent the radius (R) and media (M). The radius (R) runs parallel to the anterior margin of the wing, and the media (M), widely separated from the radius, runs along the posterior margin. The two veins converge anteriorly very closely but visibly do not meet. The part of the radius, basal to the point where two veins come very close, possibly represents the common stem of the radius (R) and media (M). Anterior to this commom stem a short independent line extends for about 3/4 of its length. This is called subcosta (Sc) by Patch (1909). The anterior margin of the wing basally merges into an elongated highly sclerotized structure, the costal complex of wing veins (ccx), which Mäkel (1942) calls "Pterale

2". It is divided basally into a pointed upper part and a broad lower part. The latter articulates with the mesopleural wing process (pwp_1).

Halteres (*h*):

The basal half of the haltere is broad and the distal half tapering. Each haltere bears a long hooked apical seta (a) which hooks into the ventral invagination of the pouch of the fore wing. The haltere is membranous except the anterior and posterior margins of the basal part which are sclerotized. Basally each haltere articulates with the metapleural wing process (pwp_2) and also carries a minute process which is connected with the suspensorial sclerite (ss) of its side by means of a sclerotized tendon (ht).

5. *Legs* (Figs. 5, 7, 14, 15 & 16):

In general appearance the legs are long, slender and well suited for locomotion. The middle legs are the shortest and the hind legs the longest. Each leg is composed of a stout coxa (cx), trochanter (tr), long and stout femur (fm), long and slender tibia (tib), and a two-segmented tarsus (tar_1 and tar_2) which carries a single claw (cl). Lengths of the various segments of the leg in microns are given in the table on page 99.

The setae are mainly of the two basic types which occur on the antennae, *i. e.*, fleshy and hair-like setae. Nearly all the segments of the leg possess both the types of setae, the hair-like setae being more in number. Some of the hair-like setae become converted into thick-set, sharp-pointed, spine-like setae, which occur ventrally on the tibia and tarsus. Ventrally the distal end of the tibia bears 4 thick, stout, sharp-pointed spurs, the two of which are longer and thicker than the remaining two. A pair of digitules (tdgt), *i. e.*, long, apically knobbed setae, each with a circular basal ring, occurs dorsally near the distal end of each tarsus. Each claw bears two very much reduced digitules (udgt). The setae and other dermal structures of the legs are given in the table on page 100.

(i) *Coxa* (*cx*)—The coxa (cx) is broadly conical in appearance. Its broad base is strengthened by a highly sclerotized basal ridge (basr), which gives off a short basal process (bpc) articulating with the pleural ridge (plr). The distal margin is also well sclerotized bearing an inverted U-shaped dorsal ridge, the arms of which, after running ventrally more than half the width of the coxa, stretch back more than half the length of the latter. The coxa is mostly sclerotized except the distal half of the venter which is membranous. The U-shaped distal ridge of each coxa bears a posterior and an anterior process which articulate with the corresponding processes of the trochanter. Two types of setae, *i. e.*, hair-like and fleshy setae, are found on the coxa. Only one fleshy seta is found on the base of the basal process of each of the middle and hind coxae and the remainder of the coxa is beset with hair-like setae, which are 9 for the fore, 8-12 (av. 10) for the middle, and 9-10 (av. 9·66) for the hind coxa. One hair-like seta is always found on the basal process of the fore coxa while the basal processes of the middle and hind each bears a fleshy seta. Two hair-like setae are found near the basal ridge and 2 in close proximity of each arm of the U-shaped ridge.

(ii) *Trochanter* (*tr*)—This is short and somewhat bent anteriorly. Its anterior margin is short and concave, and the posterior margin is much longer than the anterior and is rounded. It has two distinct parts, separated by a narrow ridge, *i.e.*, basal narrow, subrectangular, and broad, triangular distal. Basally it is strengthened by a well-sclerotized basal ridge which bears an anterior and a posterior process articulating with the corresponding processes of the coxa. Its distal triangular part is separated from the femur by a narrow articular membrane.

The trochanter is beset with both types of the setae, *i. e.*, fleshy and hair-like. A small hair-like seta occurs on each of the anterior and posterior process of the basal ridge. There are 4-5 (av. 4·33) hair-like and 1-2 (av. 1·66) fleshy setae on the basal half, 1-2 (av. 1·66) hair-like and one fleshy seta on the distal half of the fore trochanter; 4-5 (av. 4·66) hair-like and 1 fleshy setae on the basal half and 2 hair-like and 1 fleshy seta on the distal half of the middle trochanter; and 4-6 (av. 5) hair-like and 1 fleshy seta on the basal half, and two hair-like and 1-2 (av. 1·33) fleshy setae on the distal half of the hind trochanter. There are 3 circular sensilla in a triangle on each of the anterior and posterior faces of the basal half of the trochanter. Giliomee (1961) noted the similar arrangement of these sensilla in the tree species of *Pseudococcus*, but Beardsley (1959) describes only 5 of them.

(iii) *Femur* (*fm*)—This is long and stout. Its distal margin is provided with a well sclerotized ridge, which bears an anterior and a posterior process, each of which articulates with the corresponding processes on the tibia. Basally it is connected with the distal triangular part of the trochanter by a narrow membrane.

Both types of setae are distributed over the entire surface except the distal half of the ventral surface which is bare. The setae are more common on the dorsal surface than on the ventral. Two hair-like setae are always found dorsally near the apex of the femur of all the three legs. There occur 9-12 (av. 10·66) hair-like and 4-7 (av. 5·66) fleshy setae on the fore; 6-10 (av. 8·33) hair-like and 4-3 (av. 5·66) fleshy setae on the middle; and 8-10 (av. 9·33) hair-like and 6-7 (av. 6·66) fleshy setae on the hind femur.

(*iv*) *Tibia* (*tib*)—This is the longest segment of the leg and is comparatively slender. Basally it possesses a highly sclerotized basal ridge, bearing a posterior and an anterior process which articulate with the corresponding processes on the femur. Distally there is a short median ridge at its apex which articulates with the tarsus. Except for a basal articular membrane, it is fairly sclerotized.

The fleshy type setae are more numerous on the tibia. 8-9 (av. 3·66) hair-like and 9-11 (av. 10·33) fleshy type setae occur on the fore, 7-10

TABLE 11

	FORE LEG							MIDDLE LEG							HIND LEG						
	Coxa	Trochanter		Femur (Anterior face)	Tibia	Tarsus	Claw	Coxa	Trochanter		Femur (Anterior face)	Tibia	Tarsus	Claw	Coxa	Trochanter		Femur (Anterior face)	Tibia	Tarsus	Claw
		Anterior face	Posterior face						Anterior face	Posterior face						Anterior face	Posterior face				
Max.	53·13	20·24	60·72	141·68	151·80	70·84	25·30	45·54	20·24	55·66	139·15	146·74	68·31	30·36	55·66	22·77	60·72	161·72	187·22	78·43	30·36
Min.	40·48	17·71	50·60	131·56	134·09	65·78	20·24	40·48	15·18	50·66	126·50	136·62	63·25	25·30	50·60	17·71	55·66	141·68	161·92	70·84	27·83
Mean	46·16	19·29	57·24	137·60	141·99	66·72	24·35	42·44	16·86	52·56	133·80	141·96	64·65	26·42	52·56	19·95	58·19	147·86	171·47	73·93	29·79
S.E.	1·482	0·48	1·283	1·87	2·05	0·717	0·67	0·726	0·593	0·606	0·446	1·51	0·74	0·623	0·82	0·52	0·84	1·03	2·57	0·08	0·346
S.D.	4·191	1·37	3·629	5·29	5·809	2·028	1·90	2·18	1·78	1·82	1·34	4·53	2·22	1·87	2·48	1·56	2·53	4·12	8·73	3·26	1·04
C.V.	9·079	7·102	6·339	3·84	4·09	3·037	7·80	5·13	10·55	3·47	1·001	3·19	3·43	7·07	4·71	7·87	4·34	2·71	5·08	4·41	3·49

TABLE 12

		FORE LEG						MIDDLE LEG						HIND LEG					
		Coxa	Tro-chanter	Femur	Tibia	Tarsus	Claw	Coxa	Tro-chanter	Femur	Tibia	Tarsus	Claw	Coxa	Tro-chanter	Femur	Tibia	Tarsus	Claw
Fleshy setae	Max.	...	3	7	11	6	...	1	2	8	10	6	...	1	3	7	14	2	...
	Min.	...	2	4	9	4	...	1	2	4	8	3	...	1	2	6	12	2	...
	Mean	...	2·66	5·66	10·33	5	...	1	2	5·66	8·66	4·33	...	1	2·66	6·66	12·66	2	...
	S.E.	...	0·329	0·877	0·666	0·577	...	0	0	1·19	0·663	0·881	...	0	0·333	0·333	0·663	0	...
	S.D.	...	0·5708	1·52	1·155	1·0	...	0	0	2·07	1·150	1·527	...	0	0·577	0·578	1·150	0	...
	C.V.	...	21·45	26·85	11·18	20·0	...	0	0	36·57	13·27	329·56	...	0	21·691	8·678	9·083	0	...
Hair-like setae	Max.	9	6	1[illegible]	9	16	2	12	7	10	10	13	2	10	8	10	11	12	2
	Min.	9	6	9	8	11	2	8	6	6	8	12	2	8	6	8	8	9	2
	Mean	9	6	10·66	8·66	12·66	2	10	6·66	8·33	9·33	12·66	2	9·33	7	9·33	9·33	10·66	2
	S.E.	0	0	1·666	0·333	1·66	0	1·413	0·333	1·19	0·663	0·333	0	0·663	0·577	0·663	0·881	0·881	0
	S.D.	0	0	2·887	0·578	2·887	0	2·448	0·578	2·07	1·150	0·577	0	1·150	1·00	1·150	1·527	1·527	0
	C.V.	0	0	27·08	6·67	22·802	0	24·48	8·67	24·84	12·325	4·55	0	12·325	14·285	12·325	16·366	14·324	0
Sensilla	Max.	...	6	...	...	1	...	...	6	...	...	1	...	...	6	...	...	1	...
	Min.	...	6	...	...	1	...	...	6	...	...	1	...	...	6	...	...	1	...
	Mean	...	6	...	...	1	...	...	6	...	...	1	...	...	6	...	...	1	...
	S.E.	...	0	...	...	0	...	...	0	...	...	0	...	...	0	...	...	0	...
	S.D.	...	0	...	...	0	...	...	0	...	...	0	...	...	0	...	...	0	...
	C.V.	...	0	...	...	0	...	...	0	...	...	0	...	...	0	...	...	0	...
Spurs	Max.	...	...	...	4	...	...	...	...	...	4	...	...	...	...	...	4	...	...
	Min.	...	...	...	4	...	...	...	...	...	4	...	...	...	...	...	4	...	...
	Mean	...	...	...	4	...	...	...	...	...	4	...	...	...	...	...	4	...	...
	S.E.	...	...	...	0	...	...	...	...	...	0	...	...	...	...	...	0	...	...
	S.D.	...	...	...	0	...	...	...	...	...	0	...	...	...	...	...	0	...	...
	C.V.	...	...	...	0	...	...	...	...	...	0	...	...	...	...	...	0	...	...

(av. 8·33) hair-like and 8—10 (av. 8·66) fleshy type on the middle, and 8-11 (av. 9·33) hair-like and 12-14 (av. 12·66) fleshy type setae on the hind tibia. Ventrally and laterally, towards the apex, comparatively long hair-like setae are found. 4 strong, thick spurs are found distally on the ventrolateral surface. Two of these spurs are longer and thicker than the others.

(v) *Tarsus* (tar_1 and tar_2)—This is the shortest segment of the leg and is composed of two tarsomeres. The first (tar_1) is a sclerotized ring with enlarged ventral part. It is connected to the tibia by an articular membrane basally, and distally by another articular membrane to second tarsal segment (tar_2). The latter is well sclerotized and elongated. Distally it possesses a short ridge, at the point where it articulates with the claw. Ventrodistally there is an incised area on it. Lobdell (1937) has described two segmented tarsi for a number of Pseudococcidae while Mäkel (1942) overlooked the first segment.

Most of the setae, distributed on the tarsus, form distinct rows on the dorsal and ventral surfaces. The hair-like setae are more numerous. On the ventral surface there is a distinct double row of thick-set, sharp-pointed stout hair-like setae. The first segment (tar_1) is devoid of any seta, all the dermal structures are confined to the distal segment (tar_2) only. There are 9-14 (av. 11) hair-like and 4-6 (av. 5) fleshy setae on the fore, 10-11 (av. 10·33) hair-like and 3-6 (av. 4·33) fleshy setae on the middle, and 9-11 (av. 10) hair-like and 2 fleshy setate on the hind tarsus. Distally just dorsal to the incised area, two long and apically knobbed tarsal digitules (tdgt) are present. There is always a circular companiform sensillum (cams) on the dorsal proximal surface of the distal segment (tar_2).

(*vi*) *Claw* (*cl*)—This is well developed, curved and pointed. It articulates basally with the apical ridge of the tarsus. A very small ungual digitule (udgt) is found on each of the anterior and posterior surfaces. These digitules are described by Cottier (1936), but Mäkel (1942), has overlooked them.

C. THE ABDOMEN : (Figs. 1, 2 & 6):

The abdomen is largely membranous and the segmental boundaries, as well as the line separating it from the metathorax, are seldom distinct in clear preparations. The abdomen, being membranous, gets easily distorted when mounted. It is, therefore, difficult to figure and describe its outline correctly. The segmentation of the abdomen is indicated largely by the segmental arrangement of the setae and the dermal denticulations as well as by shallow intersegmental grooves. The length and width of the abdomen in microns are as follows :—

TABLE 13

	Length					Width
	From mesopostphragma to the basal ridge of penial sheath	Genital segment	Stylus	Aedeagus	Long setae of the glandular plate	(Across 3rd abdominal segment)
Max.	524·4	106·26	27·83	88·55	322·0	303·6
Min.	404·8	83·49	25·30	70·84	285·2	266·8
Mean	456·55	95·38	27·26	78·43	308·2	283·88
S.E.	16·91	1·96	0·38	3·75	5·35	5·71
S.D.	47·70	6·22	1·14	7·51	16·93	15·11
C.V.	10·44	6·52	4·18	9·57	5·49	5·32

1. *The Pregenital Segments* :

In *S. sacchari* the abdomen has eight pregenital segments. The same number of the pregenital segments has been described by Berlese (1893), Mäkel (1942), Theron (1958) and Giliomee (1961) in Pseudococcidae. Beardsley (1960) fails to recognise the first abdominal segment and incorrectly describes only seven segments in the abdomen.

The first abdominal segment is not developed ventrally and according to Stickney (1934), Snodgrass holds that in coccids the metathoracic legs have crowded out in the first abdominal segment. Dorsally two small sclerites represent reminiscences of the first abdominal tergum (at$_1$). Two small sclerites are also found on each of the second and third segments (at$_2$ and at$_3$). The 8th tergum is represented by a fairly large tergal plate (at$_8$), 7th by a somewhat transversely elongated tergal plate (at$_7$), and 6th by a small narrow tergal plate (at$_6$). Ventrally the sclerotization is completely absent, except for a narrow, small sternite (ast$_7$) on the 7th and two small sternites (ast$_8$) on the eighth abdominal segment. The ventral invaginations of the intersegmental boundary between the third and fourth segments are not fairly demarcated. These invaginations correspond to the lateral extremities of the circulus which is present in the larvae and adult females (Giliomee, 1961). Beardsley (1960) did not describe them at all. The first to third abdominal segments are broad, and width gradually decreases posteriorly towards the seventh segment and abruptly narrows at the eighth abdominal segment.

Dorsally at the posterolateral margin of the 6th abdominal segment a pair of slit-like openings (ost) occurs. They are homologous with the posterior dorsal ostiole of the adult female.

The segmental position of the circulus and ostiole is still a matter of controversy. The manner in which Balachowsky (1937) and Borkhsenius (1949) count the abdominal segments of the adult female, circulus is situated between the third and fourth segments and ostioles on the 6th segment. According to Ferris (1950) and Ezzat and McConnel (1956), the circulus is situated between the fourth and fifth abdominal segments and the ostioles in the seventh. Beardsley (1960) contends that the ostioles are situated on the seventh segment, and that the first abdominal segment is absent. But the position of these structures in the larvae and adult male, however, suggests that circulus is situated in the inter-segmental membrane between third and fourth segments, and ostioles in the sixth segment, as also found by Giliomee (1961) in the three species of genus *Pseudococcus*.

Dermal Structures—The abdominal segments are beset with hair-like setae only; the fleshy setae being absent. These setae are always segmentally arranged. Dorsally and ventrally the setae are arranged in a transverse row across the middle of each segment, while the pleural setae (aps) are in a group. The latter are distinctly separated from the dorsal and ventral setae of the respective segment. A number of disc pores occur on the pleuron and some on the ventral surface, in the vicinity of the setae. They are usually quadrilocular, but may be tri- or quinquelocular. There are also minute simple derm pores and tiny dermal denticulations near by these setae and disc pores. Laterally on the posterior margin of the 8th abdominal segment there is a cluster of pores, called the glandular plate (glp), on each side. From each glandular plate (glp) two long setae, about 1/3 to 1/4 of the length of the body, arise and serve as supporting cores around which wax is secreted. Besides, two shorter setae, but longer than the body setae, are found on each glandular plate. These setae are called setae of the glandular plate (glps). The wax is secreted by the pores which are actually wax glands (Pflugfelder, 1939). Number of abdominal dorsal setae (ads), abdominal ventral setae (avs), abdominal pleural setae (aps) and disc pores is as follows :—

TABLE 14

Region	Description		SEGMENTS							
			I	II	III	IV	V	VI	VII	VIII
Dorsal (ads)	Hair-like setae	Max.	9	8	9	9	8	10	7	8
		Min.	8	8	8	6	7	7	5	6
		Mean	8·33	8	8·33	7·66	7·66	8·33	6	6·66
		S.E.	0·333	0	0·333	0·881	0·333	0·881	0·577	0·663
		S.D.	0·577	0	0·577	1·527	0·577	1·527	1·0	1·150
		C.V.	6·926	0	6·926	19·934	7·532	18·33	16·666	17·267
	Simple derm pores	Max.	...	2	1	1	1	1	...	...
		Min.	...	0	0	0	0	0	...	...
		Mean	...	0·50	0·250	0·250	0·250	0·25	...	...
		S.E.	...	0·663	0·333	0·333	0·333	0·333	...	...
		S.D.	...	1·150	0·577	0·577	0·577	0·577	...	...
		C.V.	...	230·0	230·80	230·80	230·80	230·80	...	...
	Trilocular disc pores		...	...	...	...	...	...	...	...
	Quadrilocular disc pores		...	...	...	...	...	...	...	...

(*Contd. on page* 105)

Region	Description		SEGMENTS							
			I	II	III	IV	V	VI	VII	VIII
Dorsal (ads)	Quinquelocular disc pores		...	...	...	...	...	...	...	...
	Hexalocular disc pores		...	...	...	...	...	...	...	...
Pleural (aps)	Hair-like setae	Max.	8	7	8	8	9	8	7	2
		Min.	3	5	5	5	4	6	5	2
		Mean	5·25	6·25	7	6·5	6·5	6·5	6	2
		S.E.	1·108	0·478	0·707	0·645	1·040	0·50	0·577	0
		S.D.	2·217	0·957	1·414	1·291	2·081	1·00	1·154	0
		C.V.	42·22	15·312	20·20	19·861	32·015	15·384	19·233	0
	Simple derm pores	Max.	3	2	3	2	2	2	2	...
		Min.	2	0	0	1	1	0	0	...
		Mean	2·5	1·25	1·75	1·5	1·75	1·25	1	...
		S.E.	0·288	0·478	0·628	0·288	0·250	0·478	0·408	...
		S.D.	0·577	0·957	1·257	0·577	0·50	0·957	0·816	...
		C.V.	23·08	76·56	71·82	38·466	28·57	76·56	81·60	...

(*Contd. on page* 106)

Region	Description		SEGMENTS							
			I	II	III	IV	V	VI	VII	VIII
	Trilocular disc pores	Max.	1	1	1	...	...	1	...	...
		Min.	0	0	0	...	...	0	...	...
		Mean	0·25	0·25	0·25	...	...	0·25	...	...
		S.E.	0·250	0·250	0·250	...	...	0·250	...	...
		S.D.	0·50	0·50	0·50	...	...	0·50	...	...
		C.V.	200·0	200·0	200·0	...	...	200·0	...	...
	Quadrilocular disc pores	Max.	3	1	3	2	2	2	1	...
		Min.	2	1	1	1	1	1	0	...
		Mean	2·25	1	1·5	1·25	1·5	1·25	0·75	...
		S.E.	0·25	0	0·50	0·25	0·288	0·25	0·25	...
		S.D.	0·50	0	1·0	0·50	0·577	0·50	0·50	...
		C.V.	22·22	0	66·66	40·0	38·466	40·0	66·66	...

(*Contd. on page* 107)

Region	Description		SEGMENTS							
			I	II	III	IV	V	VI	VII	VIII
	Quinquelocular disc pores	Max.	1	1	1	1	1	1	1	...
		Min.	1	1	1	1	0	0	0	...
		Mean	1	1	1	1	0·75	0·50	0·50	...
		S.E.	0	0	0	0	0·25	0·288	0·288	...
		S.D.	0	0	0	0	0·50	0·577	0·577	...
		C.V.	0	0	0	0	66·66	115·4	115·4	...
	Hexalocular disc pores		...	...	...	...	...	...	...	...
Ventral (avs)	Hair-like setae	Max.		3	8	4	6	6	4	...
		Min.		3	5	4	4	4	4	...
		Mean		3	6·33	4	5·33	4·66	4	...
		S.E.		0	0·881	0	0·663	0·663	0	...
		S.D.		0	1·527	0	1·15	1·150	0	...
		C.V.		0	24·123	0	21·57	24·65	0	...

(*Contd. on page* 108)

Region	Description		SEGMENTS							
			I	II	III	IV	V	VI	VII	VIII
	Simple derm pores	Max.		2	2	5	4	2	2	...
		Min.		2	0	4	3	2	0	...
		Mean		2	1·33	4·33	3·33	2	1·33	...
		S.E.		0	0·663	0·333	0·333	0	0·663	...
		S.D.		0	1·15	0·578	0·578	0	1·15	...
		C.V.		0	86·46	13·348	17·35	0	86·466	...
	Trilocular disc pores			...	...	...	...	...	...	...
	Quadrilocular disc pores	Max.		...	2	2	2	1	...	...
		Min.		...	0	1	0	0	...	...
		Mean		...	1	1·66	0·66	0·66	...	...
		S.E.		...	0·577	0·333	0·663	0·333	...	...
		S.D.		...	1·0	0·578	1·15	0·578	...	...
		C.V.		...	100	34·819	174·24	87·50	...	...
	Quinquelocular disc pores				...	...	...	...	...	...
	Hexalocular disc pores				...	...	...	...	...	...

2. The Genital Segments and External Genitalia : (Figs. 9 & 10):

The genital segment, posterior to 8th abdominal segment, consists of a dorsal membranous part and a sclerotized ventral or lower part. Berlese (1893) and Mäkel (1942) regard the 9th abdominal segment as the genital segment. Posteriorly on the dorsal membranous part of the genital segment, is situated a small weakly sclerotized area (at 9+10), which possibly represents the fused 9th tergite and 10th segment. The anus (an) is situated behind this sclerite. The sclerotized lower part forms the penial sheath (ps) which is fairly developed. The dorsal membrane slops steeply downwards to the penial sheath (ps) behind the anus (an). The penial sheath (ps), which is called the genital valve by Berlese (1893), represents the lateral parts of the 9th abdominal sternum which have become fused posteriorly and are called pygofers by Singh-Pruthi (1925) and Karshaw and Muir (1922). According to Theron (1958), Morrison's (1928) suggestion that the penial sheath represents fused 'gonapophyses' is not convincing in view of the fact that the anterior border of the sheath is in almost immediate contact with the 8th sternite and it is rather improbable that the whole penial sheath (ps) could represent the harpagones (claspers) or parameres. Theron (1958) refers to the following possibilities of the homology of external genitalia :—

(i) Sheath composed entirely of 9th sternum; parameres absent, penis forms intromittent organ.

(ii) Sheath composed entirely of 9th sternum; parameres indistinguishably fused with penis.

(iii) Sheath formed from 9th sternum fused with parameres; penis forms intromittent organ.

In view of Qadri's (1949) contention that the harpagones have disappeared in other Sternorrhyncha, where the aedeagus is a tripartite structure consisting of penis+parameres, the incorporation of the harpagones is rather unlikely and so the last, (iii) possibility. The (i) and (ii) alternatives do not differ much. However, the homology of external genitalia remains a matter of controversy.

The sheath distally forms a short stylus (st) which is curved upwards and is truncate. The length of stylus (st) is 25·30-27·83 (av. 27·26) μ. Anteriorly the lateral and ventral margins of the penial sheath are provided with basal ridge (brps) which is partly overlapped by the membrane of the 8th segment, forming an internal projection of the basal ridge (pr) on each side. Each valve of the penial sheath posteromedially terminates in a short heavily sclerotized process (pro) which is called the apophysis of the genital valve by Berlese (1893), paramere-like projections by Mäkel (1942), lobular extensions by Theron (1958) and median lobes by Beardsley (1960). They perhaps function as claspers during copulation (Theron, 1958). Between them is a small membrane containing the ventral slit through which the penis protrudes. This slit extends anteriorly upto the point where the basal rod of the penis is fused to the narrow sclerotized anteroventral wall of the penial sheath.

The aedeagus (aed) consists of a wide dorsal tube which narrows abruptly posteriorly and then opens at the flattened tip of a heavily sclerotized curved bar, which runs along the ventral wall of the dorsal tube and extends anteriorly to the point where the ductus ejaculatorius (dej) enters the dorsal tube. This aperture or opening is called the internal genital aperture (iga) by Theron (1958) and the basal foramen by Singh-Pruthi (1925). From the internal genital aperture (iga) the bar continues as a short basal rod (bra) which eventually fuses medially with the ventral wall of the penial sheath. The distal part of the aedeagus is sharp in dorsal as well as in lateral view.

Dermal Structures—5-6 (av. 5·66) hair-like setae are found on the lateral and ventral surfaces on each side. At the apex of each of the processes of the penial sheath (pro) are found 2 tiny setae (pros). They are possibly sensilla and they seem to be connected with the act of copulation. At the apex of stylus some very weakly sclerotized spots are found which are probably the sensilla. There are no disc pores or dermal denticulations.

DISCUSSION

The morphology of male mealybugs provides a considerable amount of material for considering the phylogenetic relationship of the Superfamily Coccoidea with other Sternorrhyncha as well as of the family Pseudococcidae with other subdivisions of the Coccoidea. The affinities of the Coccoidea within the series Sternorrhyncha have been discussed by Osborn (1895), Handlirsch (1908), Kirkaldy (1910^a, 1910^b). Tillyard (1919), Singh-Pruthi (1925), Borner (1904, 1934), Heymons (1915), Spooner (1938) and Theron (1958), and the relationship of the Pseudococcidae within the Coccoidea by Balachowsky (1937, 1942), Jancke (1955), Theron (1958) and Giliomee (1961).

The Pseudococcidae as well as the Coccoidea as a whole, as also referred to by previous workers, exhibit many specialized characters and are more closely related to Aleurodoidea. The specialized morphological characters of *Saccharicoccus sacchari* are nearly that of a generalized pseudococcid. The head of this species is specialized in many respects. The most important of these are as follows:—

(i) The vertex and frons are fused together to form the epicranium ; the latter occupies most of the dorsal part of the head.

(ii) The median part of the epicranium is separated from the lateral parts bearing the simple eyes and ocelli, by membranous areas.

(iii) The typical condition of the head has changed profoundly due to the loss of functional mouth parts and their musculature.

(iv) The presence of a distinct cervical groove separating the head from the prothorax. This, according to Theron (1958), is a type of specialization which has evolved from the primitive condition found in aphids and aleyrodids. But this specialization is not accompanied by the degeneration of the post occipital ridge as described by Theron (1958) in *Pseudococcus*, and a distinct and fairly developed postoccipital ridge is present in the species studied.

(v) The fairly advanced sclerite degeneration is also a specialization. Except for the dorsomedial part of the epicranium and the ocular sclerite and ridges, the whole of the cephalic region is membranous.

(vi) The sclerite-degeneration obviously also necessitated the development of secondary ridges, like pre- and postocular ridges, postoccipital ridge and preoral ridge, for reinforcing the head capsule.

The thoracic region of *S. sacchari* seems to be fairly less specialized than the head. However, few of the specializations of the thorax are equally striking as those of the head.

(i) The most important and obvious of the thoracic specializations is the transformation of the hind wing into halteres and consequent reduction of the metathorax.

(ii) The postnotum is highly specialized. It is infolded into the metathoracic cavity, drawing the metanotum along with it. Consequently the latter is not visible externally.

(iii) The presence of the postnotal apophysis is also a specialization.

(iv) The articulation of postalare with the pleural region, as also found in *Aphis* (Weber, 1928), indicates the specialization of pleuron.

(v) The separation of the scutellum from the postnotum, is a specialized character apparently confined to male Coccoidea.

(vi) The mesonotum presents no specialization except the discontinuity between the posterior marginal fold of the notum and the wing margin, and the sclerotized band formed by the posterior marginal ridge of the notum, connecting the scutellum with postalare.

(vii) The only specialization of the mesopleuron seems to be the reduction in size of the epimeron. This is perhaps due to sclerite degeneration.

(viii) The specializations of the notum of the prothorax are its much reduction and presence of a pair of posttergites.

(ix) The propleuron is much specialized in having the cervical sclerite and pleurite completely fused into an elongated ridge-like structure, the proepisternum+cervical sclerite.

(x) The absence of the pleural sulcus dorsal to the pleural apophysis, so that the weakly sclerotized pleuron is not completely divided into an episternum and an epimeron, represents another feature of specialization.

(xi) The sternal region of the thorax is very much reduced and the sternal plates show no sign of the primary segmentation. The prosternum is provided with a fairly long transverse ridge, but there is no sternal apophysis (as found in *Pseudaspidoproctus*), and no median internal spine (as in *Margarodes*).

(xii) The reinforcement of the secondary ridges, necessitated by the pronounced sclerite degeneration in the thorax is also a specialization.

(xiii) The reduction of the pretarsus to a single claw-like structure is also a specialization.

The abdomen and the genitalia also present many specialized features. The sclerite degeneration is very much pronounced in the abdomen, which is mostly membranous. The elimination of the sternal region of the first abdominal segment is a specialization which *S. sacchari* shares with other mealybugs and also with Coccoidea as well as *Aphidoidea*. The loss of abdominal spiracles is another specialized feature of this species.

The external genitalia lacks any periphallic structure and is simple. This has been regarded by Singh-Pruthi (1925) as the primitive condition. But contrary to this Qadri (1949) refers to the simplicity of the external genitalia as not a primitive condition. The harpagones and other accessory periphallic structures have secondarily been lost. The simplicity of the penis and the absence of parameres and other periphallic structures is thus a specialization. An important specialization is the caudal prolongation of the penial sheath into a stylus. This is possibly co-related with the development of a "scale" in the female; the copulatory stylus becomes inserted underneath the scale during copulation.

RELATIONSHIP OF THE PSEUDOCOCCIDAE WITH OTHER SUB-DIVISIONS OF THE COCCOIDEA

Balachowsky (1937, 1942) studied the anatomy of the male Coccoidea and divided them into three distinct groups according to the following key :—

(1) Abdominal spiracles present.... ....
phylum ..... Margaroidae.
Abdominal spiracles absent 2
(2) Head separated from the thorax by neck .. phylum .. Lecanoidae.
Head fused with thorax ....
phylum .... Diaspidoidae.

The arrangement of Balachowsky (1937, 1942) has been followed by Jancke (1955) and discussed by Theron (1958). Ghauri (1959) and Giliomee (1961) have discussed the relationships of the diaspidoid and pseudococcid males respectively and both have supplemented and improved Theron's findings. The male mealybug, which I have studied, belongs to the lecanoid type and most of the lecanoid characters, as described by Theron (1958), are exhibited by this species. But the following observations recorded here, however, make the inclusion of *S. sacchari* in the lecanoid type problematic:—

(i) In comparing the lecanoid type in which *S. sacchari* is included (on the basis of absence of abdominal spiracles and separation of the head from the thorax by a cervical groove) with the diaspidoid and margaroid types, the absence of a postoccipital ridge is listed by Theron (1958) as one of the specialized characters of the lecanoid type. A distinct "V" shaped postoccipital ridge is undoubtedly present in the species studied and has also been observed by Giliomee (1961) in the three species of *Pseudococcus*. In this respect, thus, the pseudococcids share with both margaroid and diaspidoid types.

(ii) The absence of metasternal apophyses has been considered by Theron as the specialized character of the lecanoid type. In the mealybug studied by me a pair of metasternal apophyses are undoubtedly present. In this respect *S. sacchari* comes close to the margaroid type.

(iii) The presence of vestigeal metapleural apophyses is a primitive character of *S. sacchari*. These apophyses are also described by Ghauri (1959) in more specialized Diaspididae and Giliomee (1961) in the three species of *Pseudococcus*, but is neither observed by Theron (1958) in *Pseudococcus citri* nor Beardsley (1960) in *P. adonidum* and other Hawaiian mealybugs studied by him.

(iv) The presence of a weakly sclerotized trochantin is a primitive feature of the Pseudococcidae not shared by any other Coccoidea.

(v) The presence of the second median sclerite (m_2) and the humeral plate (hp) possibly indicates a primitive character of the species studied. These two sclerites have not been described by any of the workers who studied Coccoidea including Pseudococcidae in the past, except Ghauri (1959), who has described the humeral plate in the Diaspididae.

The above observations reveal that the Pseudococcidae are more primitive than the Lecaniidae and are probably more closely related to the Margarodidae than is indicated by Theron (1958).

SUMMARY

1. The external morphology of the macropterous male pink sugarcane mealybug, *Saccharicoccus sacchari* Cockerell is described in detail and findings are compared with those of other workers.

2. The mealybug is specialized and is characterized by the pronounced sclerite degeneration, the loss of functional mouth parts and dorsal ocelli, and the reduction of the hind wings to halteres.

3. The epicranium consists of a medial part and two lateral ocular sclerites.

4. Compound eyes are replaced by the simple eyes, and larval eyes persist as the lateral ocelli.

5. The head capsule is reinforced by preocular, postocular, postoccipital and preoral ridges, which are secondary in nature.

6. Tentorium is present.

7. The prothoracic pleuron is poorly developed. The episterna and epimera are not distinguished.

8. The mesothorax is fairly similar to other Homoptera.

9. The pteralia taking part in the articulation of the wing are, the tegula, the first, second and third axillary sclerites, the first and second median sclerities, and the humeral plate.

10. The mesopostnotum is overlapped by the metathorax and possesses internal postnotal apophyses and elongate postalares, the latter articulating with the mesopleural ridges.

11. The mesosternal plate represents a basisternum and posetriorly bears a well developed furca.

12. The mesothoracic sternopleural region is strengthened by subepisternal, marginal and precoxal ridges.

13. The matathorax is very much reduced and dorsally two small suspensorial sclerites are met with near the base of the halteres.

14. The presence of metasternal apophyses, vestigial metapleural apophyses and the meso- and metatrochantin is established.

15. The abdomen is largely membranous.

16. The first abdominal segment is not developed ventrally. There are eight pregenital segments.

17. The ostioles are situated in the 6th abdominal segment.

18. The external genitalia consist mainly of a penis (aedeagus) and penial sheath; the periphallic structures are absent.

19. The evidence is presented which supports the view that the Pseudococcidae are distinctly more primitive than the Lecaniidae and are closely related to the Margarodidae.

ACKNOWLEDGEMENTS

I wish to acknowledge my sincere gratitude to Dr. B. Singh Chandel, Asstt. Professor of Zoology for his interest and guidance throughout the course of this investigation, and to the C.S.I.R., New Delhi for sanctioning the Junior Research Fellowship. I am also much indebted to Mr. M. D. Dandwate, Professor of Statistics for the help rendered in the preparation of statistical data. An additional note of thanks is also due to Dr. M. S. K. Ghauri, Commonwealth Institute of Entomology, London, for going through the manuscript and giving useful comments and suggestions.

BIBLIOGRAPHY

1. *Balachowsky, A. 1937. Les Cochenilles de France, d'Europe, du Nord de l'Afrique et du bassin mediterraneen. I. Caracteres generaux des cochenilles, morphologie externe. *Actualites sci. industr.*, **526**, 50 pp.

2. Balachowsky, A. 1942. Essay sur la classification des Cochenilles (Homoptera-Coccoidea). *Ann. Ec. Agric. Grignon*, Serie **3**, Tome III, 34-48.
3. Beardsley, J. W. 1960. A preliminary study of the Males of Some Hawaiian Mealybugs (Homoptera : Pseudococcidae). *Proc. Hawaii. Ent. Soc.*, **17** (2) : 199-243.
4. Beardsley, J. W. 1962. Descriptions and notes on male mealybugs (Homoptera: Pseudococcidae). *Proc. Hawaii. Ent. Soc.*, **18** (1): 125-141.
5. Berlese, A. 1893. Le Cocciniglie Italiane viventi sugli Agrumi. Parte I. I *Dactylopius*. *Riv. Patol. veg.*, **2** : 1-106.
6. *Berlese, A. 1896. Le Cocciniglie Italiane viventi sugli Agrumi. Parte III. I Diaspiti. *Riv. Patol. veg.*, **4** : 203-477.
7. *Betrem, J. G. 1937. De Morphologie eu Systematiek van enkele van de voornaamste Witteluizensoorten van Jawa. *Arch. v. Koffiecult Nederland Indie* **11** : 1-118.
8. Borkhsenius, N. S. 1949. Fauna of the U. S. S. R. Homoptera, Coccoidea, Pseudococcidae. Biological Institute of the Academy of Sciences. U. S. S. R., Moscow, New Series, No. 38, 383 pp.
9. *Borner, C. 1904. Zur Systematik der Hexapoden. *Zool. Anz.*, **27** : 511-533.
10. Borner, C. 1934. Uber System und Stammgeschichte der Schnabelkerfe. *Ent. Beih. Berl. Dahlem*, **I** : 138-144.
11. Cannon, H. G. 1941. On Chlorozol Black E and some other new stains. *J. R. micr. Soc.*, **61** : 88-94.
12. Cottier, W. 1936. A redescription of *Pseudococcus cocotis* Maskell, including a description of the male (Hem.). *Proc. R. ent. Soc. Lond.* (B), **5** : 25-31.
13. Crampton, G. C. 1922. The genitalia of the males of certain Hemiptera (Heteroptera) and Homoptera. *Bull. Brooklyn ent. Soc.*, **17** : 46-55.
14. Du Porte, E. M. 1946. Observations on the morphology of the face in insects. *J. Morph.*, **79** : 371-417.
15. Ezzat, Y. M. 1956. The thoracic sclerotization of coccid adult males as a promising taxonomic character (Coccoidea). *Bull. Soc. ent. Egypte*, **40** : 357-363.
16. Ezzat, Y. M. & Mc Connel, H. S. 1956. A classification of the Mealybug Tribe Planococcini (Pseudococcidae; Homoptera). *Md. Agri. Expt. Sta. Bull.*, **A-84**, 108 pp.
17. Evans, J. W. 1942. The phylogeny of the Homoptera. *Pap. roy. Soc. Tasm.*, 1941, pp. 37-40.
18. Ferris, G. F. 1942. Atlas of the scale insects of North America. Series IV. Stanford University Press, Stanford.
19. Ferris, G. W. 1950. Atlas of the scale insects of North America. Series V. The Pseudococcidae (Part I). Stanford University Press, Stanford.
20. *Geier, P. 1949. Contribution a letude de la Cochenille Rouge du Poirier (*Epidiaspis leperii* Sign.) en Suisse. *Rev. Path. veg.*, **28** : 177-261.
21. Giliomee, J. H. 1961. Morphological and Taxonomic studies on the males of three species of the genus *Pseudococcus* (Hemiptera : Coccoidea). *Ann. Univ. Stellenbosch*, **36** (A, 6) : 243-296.
22. Ghauri, M. S. K. 1959. Studies on the morphology of the scale insects (Homoptera: Coccoidea) with special reference to the texonomic characters of the males. Natural History Museum, London.
23. Habib, A. 1956. The male *Eulecanium corni* Bouche (Homoptera: Coccoidea: Coccidae). *Bull. Soc. Ent. Egypte*, **40** : 119-126.
24. *Handlirsch, A. 1908. Die fossilen Insekten und die Phylogenie der rezenten Formen. *Leipzig*, 1430 pp.
25. *Heymons, R. 1915. 24. Insekten. Brehms Tierleben.
26. Jancke, G. D. 1955. Zur Morphologie der männlichen Cocciden. *Z. angew. Ent.*, **37**: 265-314.
27. Kershaw, J. C. & Muir, F. 1922. The genitalia of the Auchenorhynchous Homoptera. *Ann. ent. Soc. Amer.*, **15** : 201-212.

28. Kirkaldy, G. W. 1910a. A note on Mr Jackson's synopsis of the genus *Pemphigus*. *Canad. Ent.*, **42** : 83-84.

29. Kirkaldy, G. W. 1910b. Note on the ancestry of the Hemiptera. *Proc. Hawaii. ent. Soc.*, **2**: 116-118.

30. Kramer, S. 1950. The morphology and phylogeny of Auchenorhynchous Homoptera (Insecta). *Illinois biol. Monogr.*, **20**, 4 : 111.

31. Krecker, F. H. 1909. The eyes of *Dactylopius*. *Ztschr. f. wiss. Zool.*, **93** : 73-89.

32. *Larsen, O. 1945. Das thorakale Skelett muskel system der Heteropteren. Ein. Beitrag zur vergleichenden Morphologie des Insektenthorax. *Acta Univ. lund.*, **41**, Nr. 11, 83 pp.

33. Lobdell, G. H. 1937. Two segmented tarsi in coccids: other notes (Homoptera). *Ann. ent. Soc. Amer.*, **30** : 75-80.

34. Mac Gillivray, A. D. 1921. The Coccidae. Urbana, Illinois.

35. Mahdihassan, S. 1931. The males of lac and pseudo-lac insects. *Z. wiss. Zool.*, **138**: 371-385.

36. Mäkel, M. 1942. Metamorphose und Morphologie des *Pseudococcus* Männchens mit besonderer Berucksichtigung des Skelettmuskel systems. *Zool. Jb.*, *Anat.*, **67** : 461-512.

37. Marks, E. P. 1951. Comparative studies of the male genitalia of the Hemiptera (Homoptera-Heteroptera). *J. Kansas ent. Soc.*, **24** : 134-141.

38. Misra, A. B. 1931. On the internal anatomy of the male lac insect, *Laccifer lacca* Kerr. (Homoptera : Coccidae). *Proc. Zool. Soc. Lond.*, **4** : 1359-1381.

39. Morrison, H. 1928. A classification of the higher groups and genera of the coccid family Margarodidae. *Bull. U. S. Bur. Ent.*, **52**, 240 pp.

40. Moulton, D. 1907. The Monterey pine scale, *Physokermes insignicola* (Craw). *Proc. Devenport Acad. Sci.*, **12** : 1-26.

41. Nel, R. G. 1933. A comparison of *Aonidiella aurantii* and *Aonidiella citrina*, including a study of the internal anatomy of the latter. *Hilgardia*, **7** : 417-466.

42. Oguma, K. 1919. A new scale insect, *Xylococcus alni*, on alder, with special reference to its metamorphosis and anatomy. *J. Coll. Agric. Sapporo*, **8** : 77-109.

43. Osborn, H. 1895. The phylogeny of Hemiptera. *Proc. ent. Soc. Wash.*, **3** : 185-190.

44. Patch, E. M. 1909. Homologies of the wing veins of the Aphididae, Psyllidae, Aleurodidae and Coccidae. *Ann. ent. Soc. Amer.*, **2** : 101-136.

45. Pesson, P. 1941. Description du male de *Pulvinaria mesembryanthemi* Vallot et observations biologiques sur cette espece (Hemipt: Coccidae). *Ann. Soc. ent. Fr.*, **110** : 71-77.

46. Pflugfelder, O. 1936. Bau und morphologische Bedeutung der sog. Ocellen der Schildlaus-Männchen (*Lecanium corni* March.) *Zool. Anz.* **114**: 49-55.

47. Pflugfelder, O. 1937. Vergleichend-anatomische, experimentelle und embrylogische Unter-suchungen uber das Nervensystem und die Sinnesorganen der Rhynchoten. *Zoologica, Stuttgart*, **34**: Heft 93, 102 pp.

48. Pflugfelder, O. 1939. Arthropoda, Insecta. Coccina Bronns Klassen, Bd. 5, Abt. 3, 1939, Buch 8, Teil b. e. pp. 1-121.

49. Qadri, M.A.H. 1949. On the morphology and post-embryonic development of the male genitalia and their ducts in Hemiptera (Insecta). *J. Zool. Soc. India*, **1**: 129-143.

50. *Reh, L. 1901. Ueber die postembryonale Ent-wicklung der Schildläuse. *Alg. Z. Ent.*, **6**: 51-54, 65-69, 85-89.

51. *Roberti, D. 1946. Monografia dell' *Aphis* (*Dorsalis*) *frangulae* Koch. Parte I Morfolo gia, Anatomia, Istologia. *Boll. Lab. Ent. agr. Portici*, **6** : 125-312.

52. Singh-Pruthi, H. 1925. The morphology of the male genitalia in Rhynchota. *Trans. R. ent. Soc. Lond.*, 1925, pp. 127-267.

53. Snodgrass, R. E. 1935. Principles of insect morphology. McGraw-Hill Book Co., New York.

54. Spooner, C. S. 1938. The phylogeny of the Hemiptera Based on a study of the head capsule. *Illinois biol. Monogr.*, **35** 70 : 102.

55. Stickney, F. S. 1934. The external anatomy of the Parlatoria date scale. *Parlatoria blanchoardi* Targioni-Tozzetti, with studies of the head skeleton and associated parts. *Bull. U. S. Bur. Ent.*, **421**: 67.

56. *Sulc, K. 1932. Ceskoslovenske' druhy rodu puklice (gn.*Lecanium*, Coccidae; Homoptera). *Acta. Soc. Sci. nat. Morav.*, **7**: 1-134.

57. Sulc, K. 1943. Zevni morfologie, metamorfosa a ben zivota cervce *Phenacoccus aceris* Sign. *Acta Soc. Sci. nat. Morav.*, **15**: 1-52.

58. *Suter, P. 1932. Untersuchungen uber Korperbau, Entwicklungsgang und Rassendifferenzierung der Kommaschildlaus, *Lepidosaphes ulmi*. L.*Mitt. schweiz. ent. Ges.*, **15**: 347-420.

59. Theron, J. G. 1958. Comparative studies on the morphology of male scale insects (Hemiptera : Coccoidea). *Ann. Univ. Stellenbosch*, **34** (A, 1) : 71.

60. Tillyard, R. J. 1919. Mesozoic insects of Queensland. No. 7. Hemiptera : Homoptera; with a note on the phylogeny of the Suborder. *Proc. Linn, Soc. N.S.W.*, **44** : 857-896.

61. Uichanco, L. B. & Villanueva, F. E. 1932. Biology of the pink mealybug of sugarcane, *Trionymus sacchari* (Cockerell), in the Philippines. *Philippine Agr.*, **21** : 205-276.

62. *Vaney, C. & Conte, A. 1908. La farme male du *Pseudococcus platani* Sign. *C. R. Ass. franc. Av. Sci.*, **36** : 620-621.

63. Weber, H. 1928. Skelett, Muskulatur und Darm der schwarzen Blattläus *Aphis fabae* Scop. *Zoologica, Stuttgart*, **28**, Heft 76 : 1-120.

64. *Weber, H. 1930. Biologie der Hemipteren. Verlag von Julius Springer, Berlin.

65. *Weber, H. 1935a. Der Bau der Imago der Aleurodinen. *Zoologica, Stuttgart*, **33**, Heft 89, 71 pp.

66. *Weber, H. 1935b. Aphidina. Blattläuse (=Aphidoidea). *Biol. Tiere Dtschl.*, **31** : 209-355.

---

* Originals not seen.

LIST OF FIGURES

Fig. 1. Dorsal View.
Fig. 2. Ventral View.
Fig. 3. Dorsal View of the Right Antenna.
Fig. 4. Dorsal View of the Head and Thorax.
Fig. 5. Ventral View of the Head and Thorax.
Fig. 6. Lateral View.
Fig. 7. Posterior View of the Hind Leg.
Fig. 8. Dorsal View of the Right Wing.
Fig. 9 Lateral View of the Genital Segment and Genitalia.
Fig. 10. Ventral View of the 7th, 8th, 9th Segments and Genitalia, etc.
Fig. 11. Dorsal View of the Terminal Segment of the Right Antenna.
Fig. 12-A Dorsal View of the Right Antenna Showing Fusion of the 4th Segment with the 3rd Segment.
Fig. 12-B Ventral View of the Right Antenna Showing Abnormally Elongated 3rd Segment.
Fig. 13-A Dorsal View of the Left Antenna of the Male No. 4, Showing Fusion of 6th Segment with the 5th Segment.
Fig. 13-B Dorsal View of the Right Antenna of the Male No. 4 Possessing the Normal Number of Segments.
Fig. 14 Posterior View of the Tarsus and Claw of the Left Hind Leg.
Fig. 15 Trilocular disc pore.
Fig. 16 Quadrilocular disc pore.
Fig. 17. Quinquelocular disc pore.
Fig. 18. Hexalocular disc pore.
Fig. 19. Glandular disc pore.

ABBREVIATIONS

a	apical seta of haltere.
aVI, aVII, aVIII	6th, 7th, 8th abdominal segments.
ads	abdominal dorsal setae.
aed	aedeagus.
ams	anterior metasternal setae.
an	anus.
anp	anterior notal wing process.
ap	finger like apodeme.
apar	anterior postalare ridge.
aps	abdominal pleural setae.
as	alar setae.
asds	antespiracular dorsal setae.
ast	abdominal sternite.
asvs	antespiracular ventral setae.
at	abdominal tergite.
ata	anterior tentorial arm.
avs	abdominal ventral setae.
ax_1	first axillary sclerite.
ax_2	second axillary sclerite.
ax_3	third axillary sclerite.
axc	axillary cord.
bas	basalare.
basr	basal ridge of coxa.
bpc	process of basal ridge of coxa.
bra	basal rod of penis.

brps	basal ridge of penial sheath.
bs	sensilla basiconica.
ca	cranial apophysis.
cams	campaniform sensillum.
ccx	costal complex of wing veins.
cl	claw.
cv	cervical groove.
cx	coxa.
dej	ductus ejeculatorius.
dhs	dorsal head setae.
dmep	dorsomedial part of epicranium.
dse	dorsal simple eye.
epm_1	mesepimeron.
epm_2	metepimeron.
eps_1	mesepisternum.
eps_2	metepisternum.
f	furca.
f III-X	segments of flagellum—3rd to 10th.
fm	femur.
fp	furcal pit.
fs	fleshy setae.
g	gena.
glp	glandular plate.
glps	setae of the glandular plate.
gs	genal setae.
gts	setae on genital segment.
h	haltere.
hs	hair-like seta.
ht	tendon attached to haltere.
hp	humeral plate.
iga	internal genital aperture.
ip	intermediate plate.
lmcr	lateral branch of midcranial ridge.
lpl	lateropleurite.
lps	lateral pronotal setae.
M	media.
m_1	first median plate.
m_2	second median plate.
mcr	midcranial ridge.
mo	vestigial mouth opening.
mpns	median pronotal setae.
mps	metapleural setae.
mr	marginal ridge.
mts	metatergal setae.
ns	narrow sclerite attached to costal complex of wing veins.
o	lateral ocellus.
ocr	ocellar ridge.
ocs	ocular sclerite.
ost	ostiole.
pa	postalare.
pcr_1	precoxal ridge of mesothorax.
pcr_2	precoxal ridge of metathorax.
pdc	pedicel.

pepcv	proepisternum + cervical sclerite.
pla$_1$	propleural apophysis.
pla$_2$	mesopleural apophysis.
pla$_3$	vestigial metapleural apophysis.
plr$_1$	propleural ridge.
plr$_2$	mesopleural ridge.
plr$_3$	metapleural ridge.
pms	postmesostigmatal setae.
pmss	posterior metasternal setae.
pn	vestigial metapostnotal sclerite.
pna	mesopostnotal apophysis.
pnao	external opening of postnotal apophysis.
pnp	posterior notal wing process.
pocr	postocular ridge.
por	remnant of postoccipital ridge.
ppar	posterior postalare ridge.
pr	projection of basal ridge.
pra	prealare.
pra	pronotal sclerite.
prnr	pronotal ridge.
pro	process of the penial sheath.
procr	preocular ridge.
pror	preoral ridge.
pros	setal sensilla on the process of the penial sheath.
prsc	prescutum.
ps	penial sheath.
pscr	prescutal ridge.
pscs	prescutal sulcus.
pscse	prescutal setae.
pt	posttergite.
pta	posterior tentorial arm.
ptp	posterior tentorial pit.
ptr$_1$	peritreme of mesothoracic spiracle.
ptr$_2$	peritreme of metathoracic spiracle.
pts	posttergital setae.
pwp$_1$	mesopleuralwing process.
pwp$_2$	vestigial of metapleural wing process.
R	radius.
rd	posterior marginal fold of the alinotum.
sa	subalare.
sc	subcosta.
scl	scutellum.
scls	scutellar setae.
scp	scape.
sct	scutum.
sctr	scutal ridge.
scts	scutoscutellar sulcus.
sctse	scutal setae.
ser	subepisternal ridge.
set.scla	subapical sensory setae.
sp$_1$	mesothoracic spiracle.
sp$_2$	metathoracic spiracle.

spl	sensillum placodeum.
ss	suspensorial sclerite.
st	stylus.
sta	metasternal apophysis.
stn$_1$	prosternum.
stn$_2$	mesobasisternum.
stn$_1$r	prosternal ridge.
stn$_1$s	prosternal setae.
stn$_2$s	basisternal setae.
t	tendon like apodeme.
tar$_1$	first segment of tarsus.
tar$_2$	second segment of tarsus.
tb	tentorial bridge.
tdgt	tarsal digitule.
teg	tegula.
tegs	tegular setae.
tib	tibia.
tn$_1$	mesothoracic trochantin.
tn$_2$	metathoracic trochantin.
tp	triangular plate of prealare.
tr	trochanter.
udgt	ungual digitule.
vc	ventral cavity.
vhs	ventral head setae.
vse	ventral simple eye.

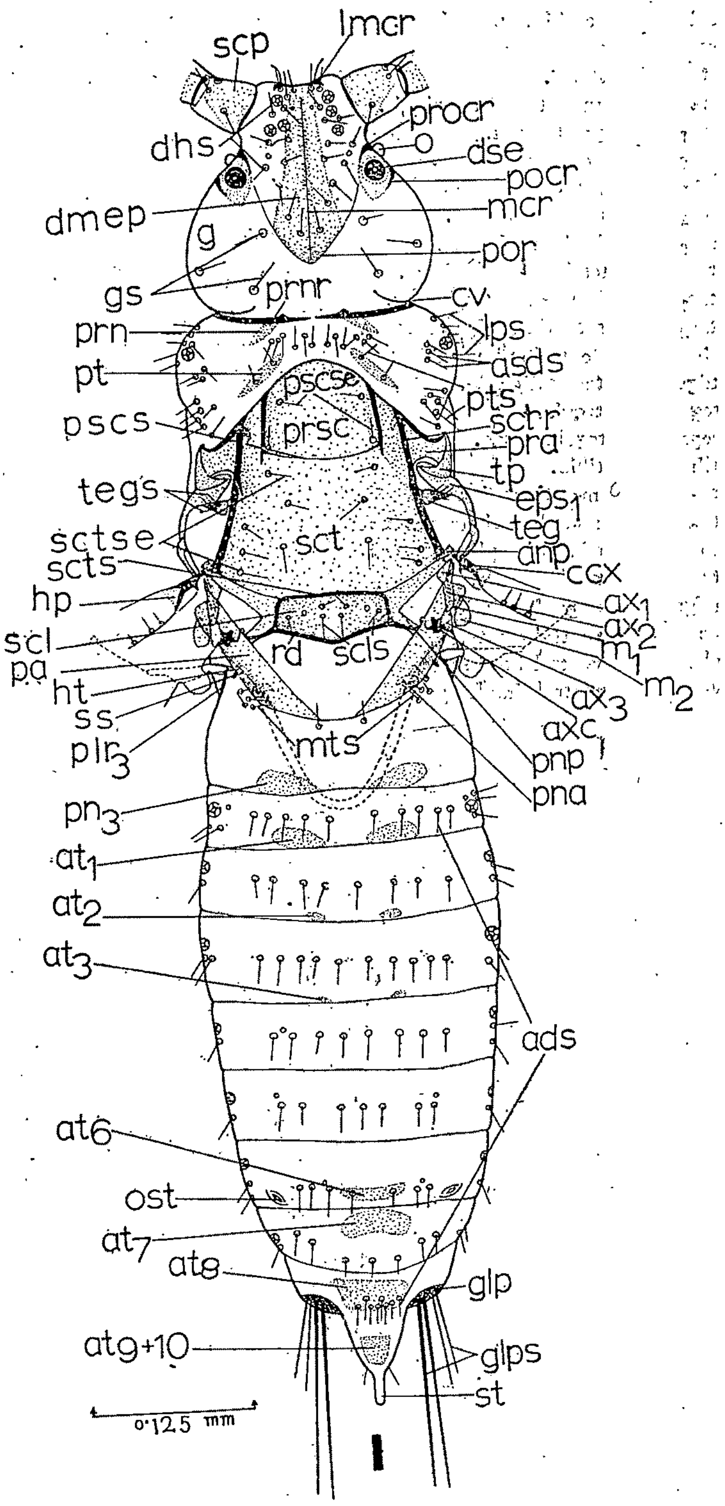
scp
lmcr
procr
o
dhs
dse
pocr
dmep
mcr
g
por
gs
prnr
cv
prn
lps
asds
pt
pscse
pts
pscs
prsc
sctr
pra
tp
tegs
eps1
teg
sctse
scts
sct
anp
ccx
hp
ax1
ax2
scl
m1
rd
scls
m2
pa
ht
ax3
ss
axc1
plr3
mts
pnp
pna
pn3
at1
at2
at3
ads
at6
ost
at7
at8
glp
at9+10
glps
st
0·125 mm

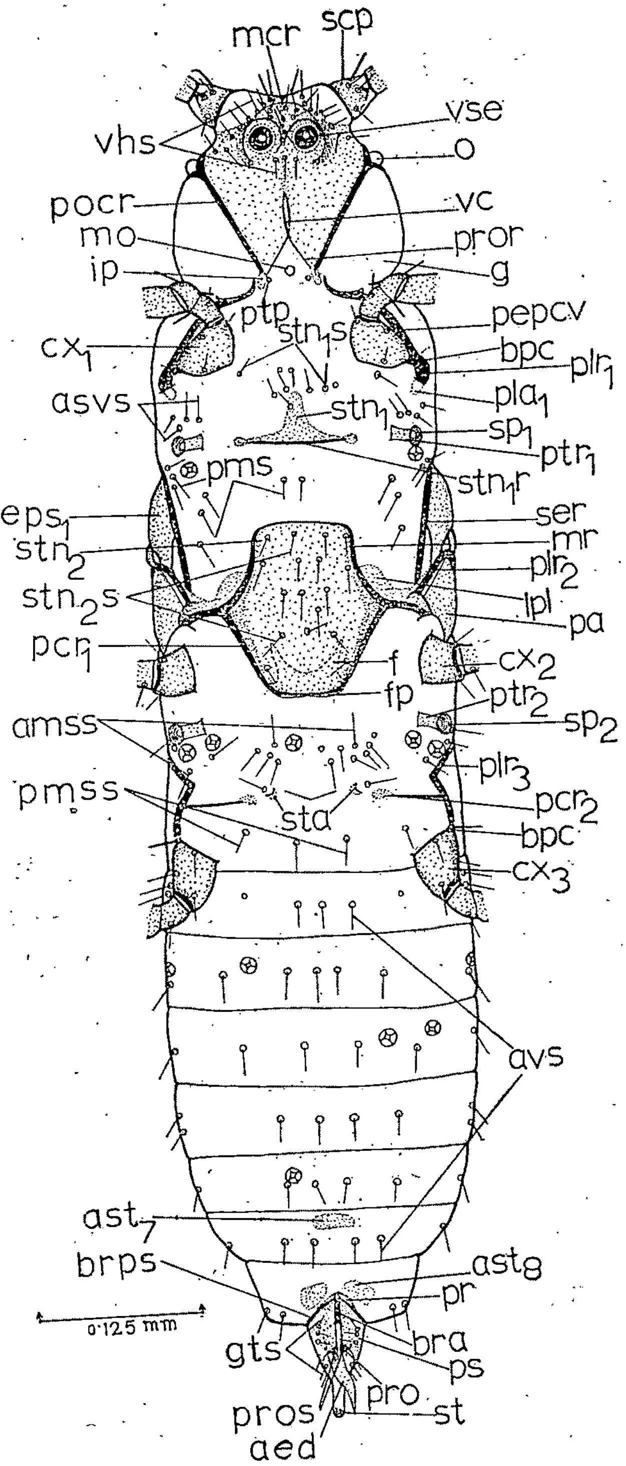
mcr
scp
vse
vhs
o
pocr
vc
mo
pror
ip
g
ptp
stn_1s
pepcv
cx_1
bpc
plr_1
asvs
pla_1
stn_1
sp_1
ptr_1
pms
stn_1r
eps_1
ser
stn_2
mr
plr_2
stn_2s
lpl
pa
pcr_1
f
cx_2
fp
ptr_2
amss
sp_2
plr_3
pmss
pcr_2
sta
bpc
cx_3
avs
ast_7
brps
ast_8
pr
0·125 mm
bra
gts
ps
pro
st
pros
aed

2

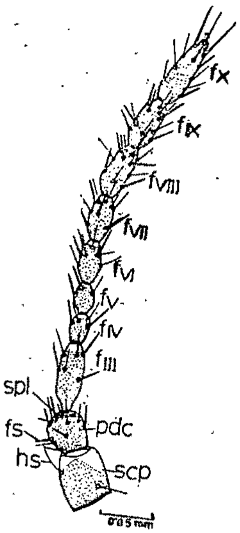
fx
fix
fviii
fvii
fvi
fv
fiv
fiii
spl
pdc
fs
hs
scp
0·05 mm

3

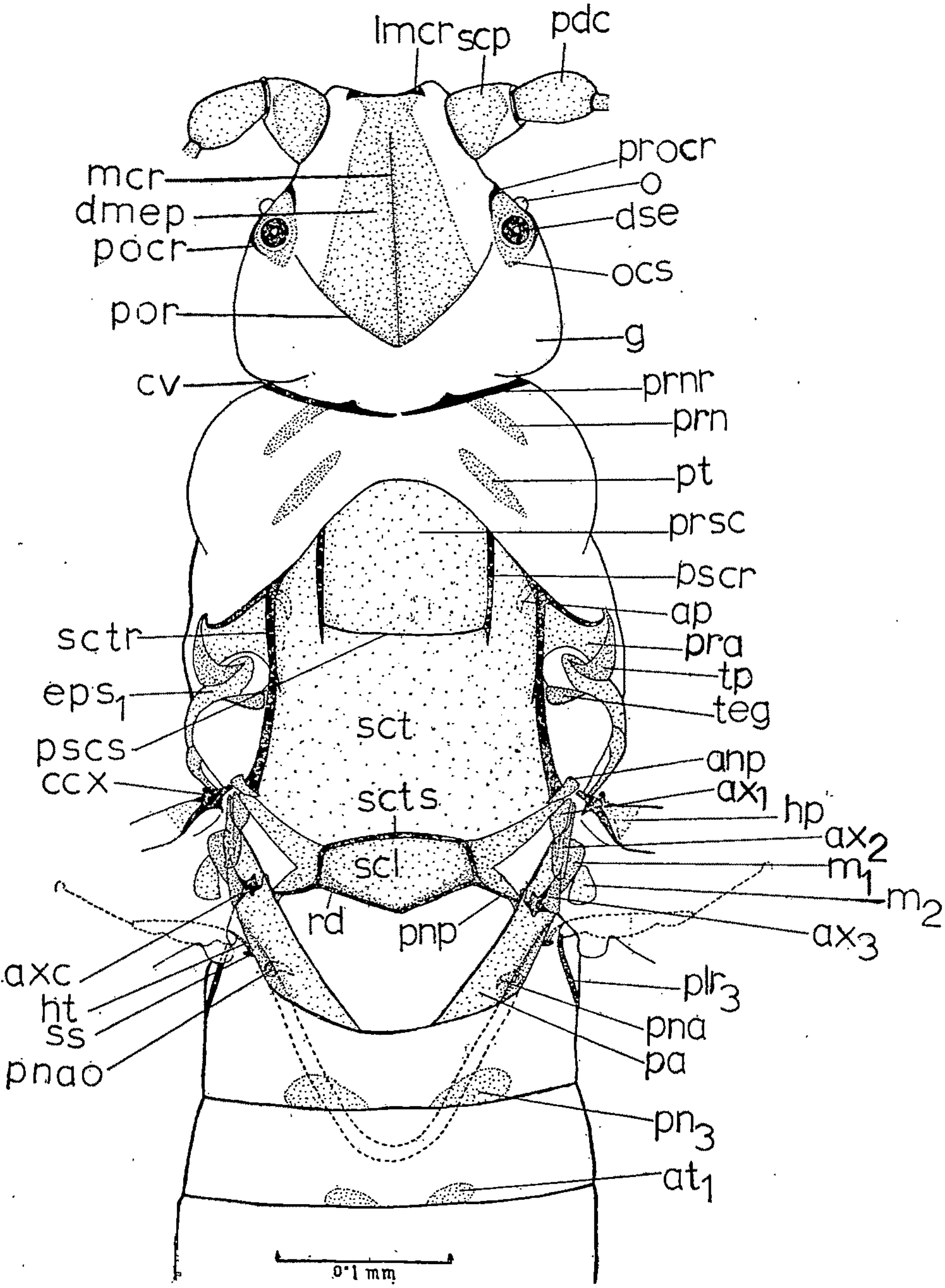
lmcr
scp
pdc
procr
mcr
o
dmep
dse
pocr
ocs
por
g
cv
prnr
prn
pt
prsc
pscr
ap
sctr
pra
tp
eps1
teg
sct
pscs
anp
ccx
ax1
scts
hp
ax2
scl
m1
m2
rd
pnp
ax3
axc
plr3
ht
ss
pna
pnao
pa
pn3
at1
0·1 mm

4

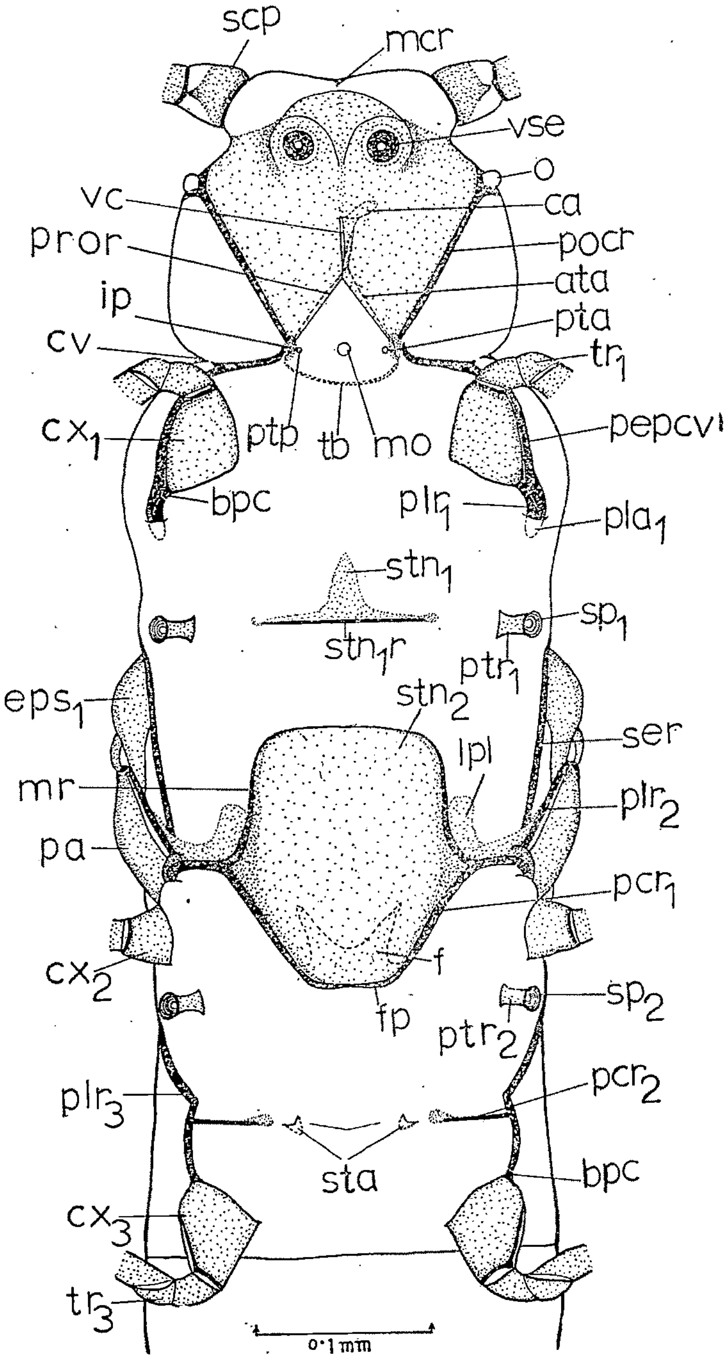
scp
mcr
vse
o
vc
ca
pror
pocr
ata
ip
pta
cv
tr_1
cx_1
ptp
tb
mo
pepcvi
bpc
plr_1
pla_1
stn_1
sp_1
stn_1r
ptr_1
stn_2
eps_1
ser
lpl
mr
plr_2
pa
pcr_1
cx_2
f
sp_2
fp
ptr_2
plr_3
pcr_2
sta
bpc
cx_3
tr_3
0·1 mm

5

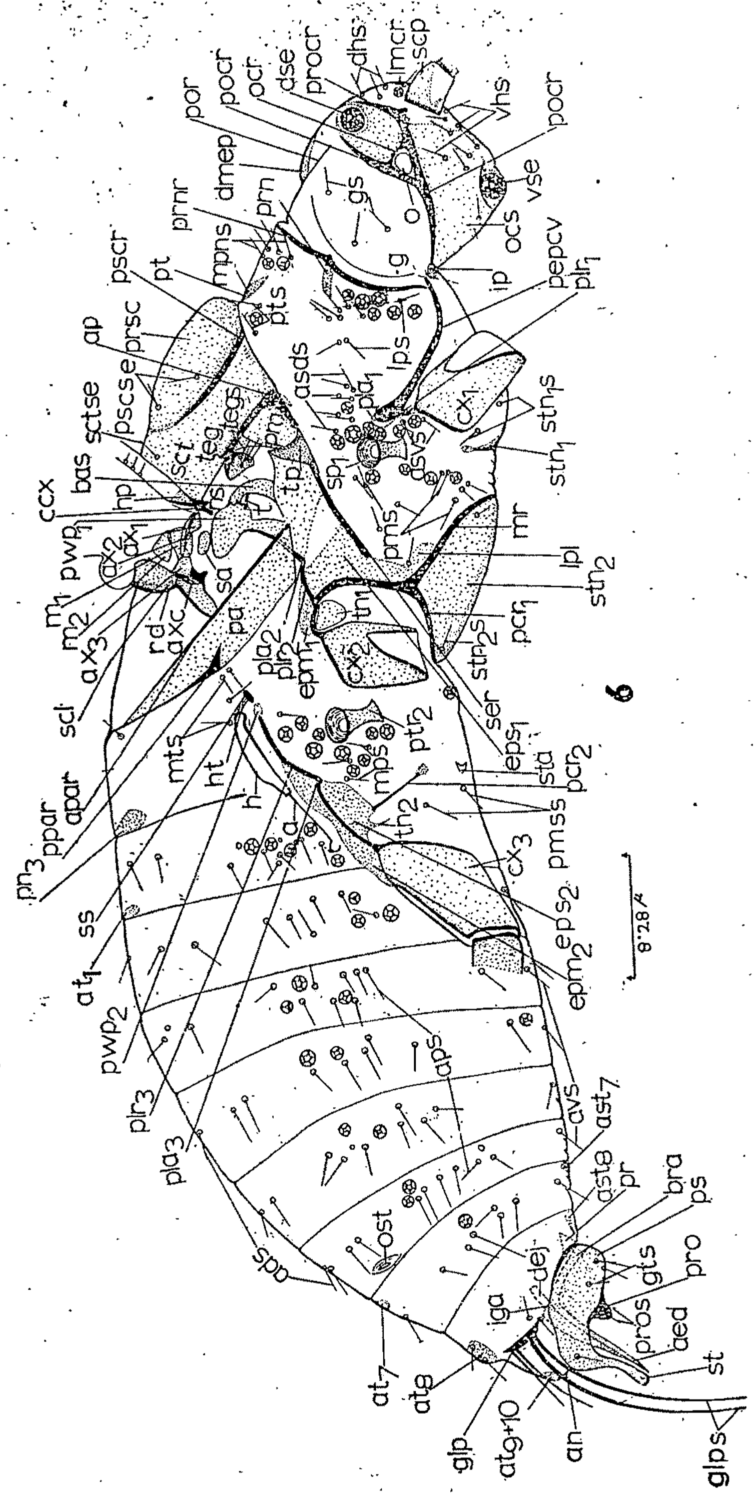
6
dhs
lmcr
scp
procr
dse
ocr
pocr
por
vhs
pocr
vse
dmep
prnr
prn
gs
o
g
ocs
ip
pepcv
plr1
mpns
pt
pscr
pts
prsc
ap
lps
asds
pla1
cx1
stn1s
stn1
sctse
pscse
sct
teg
tegs
pn
sp1
asvs
bas
hp
ccx
pwp1
ax1
ax2
ts
t
tp
pms
mr
lpl
stn2
m1
m2
ax3
rd
axc
sa
pa
tn
pcr1
stn2s
pla2
plr2
epm1
cx2
scl
ser
eps1
ptr2
mps
sta
pcr2
mts
ht
h
a
c
th2
ppar
apar
pn3
ss
pmss
cx3
eps2
at1
0·28 μ
epm2
pwp2
aps
plr3
avs
ast7
pla3
ast8
pr
bra
ps
spa
ost
dej
gts
pro
pros
iga
aed
st
at7
at8
glp
at9+10
an
glps

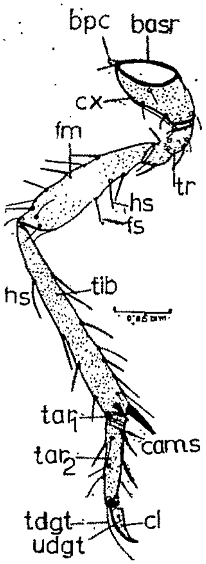
bpc
basr
cx
fm
tr
hs
fs
hs
tib
0·05 mm
tar1
cams
tar2
tdgt
cl
udgt

7

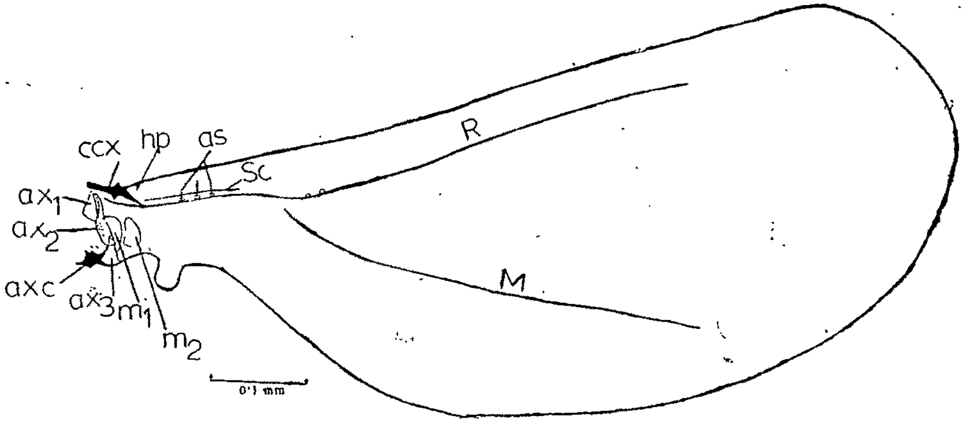
ccx
hp
as
Sc
R
ax1
ax2
axc
ax3
m1
m2
M
0·1 mm

8

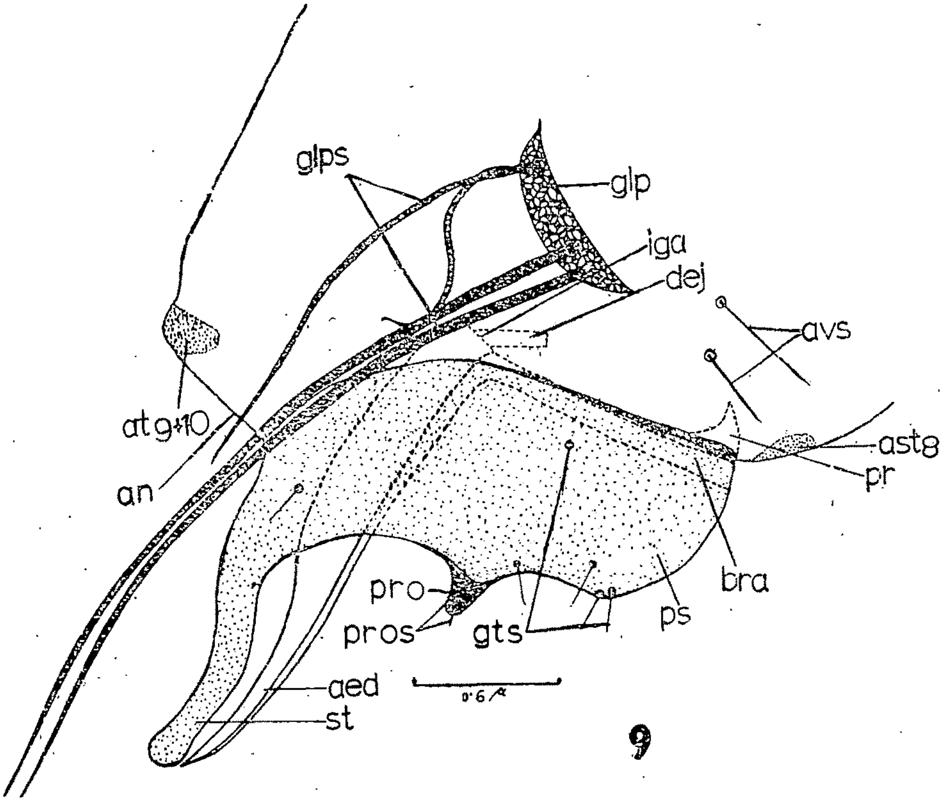
glps
glp
iga
dej
avs
atg9+10
an
astg
pr
bra
pro
pros
gts
ps
aed
st
0·6 μ

9

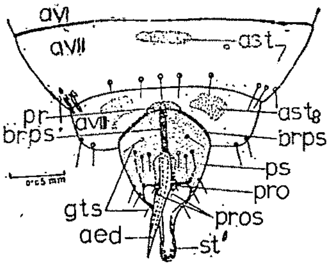

10

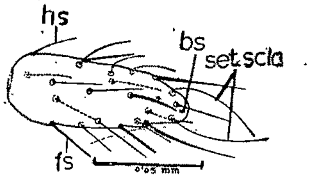

11

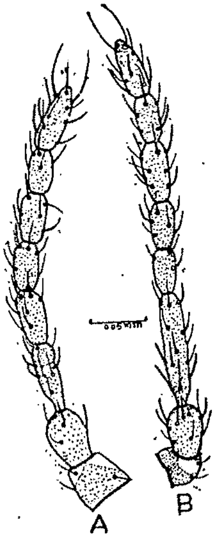

12

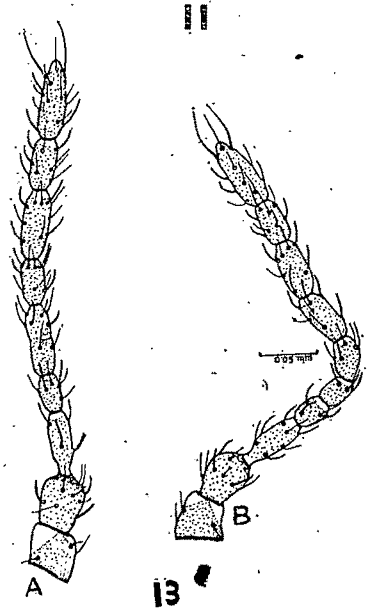

13

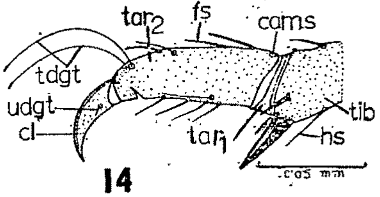

14

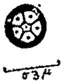

17

16

19

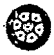

18

15

STRESS DISTRIBUTION IN A NON-NEWTONIAN LIQUID IN THE PRESENCE OF A LINE SOURCE

Prem Dayal Narang*

Introduction

Rivlin[1] has proposed that the macroscopic behaviour of a certain fairly dilute solutions of high polymers can be represented by equations of state in the form

$$p_{ik} = -P\,\delta_{ik} + 2\eta\, e_{ik} + 4\zeta\, e_{ij}\, e_{jk} \qquad ..(1)$$

where η and ρ are coefficients of viscosity and the normal stress coefficient; and p_{ik} and e_{ik} are the stress and rate of strain tensors; P is an undetermined isotropic pressure; δ_{ik} is the kronecker delta

$$(\delta_{ik} = 1, \text{ if } i = k \text{ and } \delta_{ik} = 0 \text{ if } i \neq k)$$

It is proposed here to consider a line source in a non-newtonian liquid satisfying equation (1) and extending to infinity in all directions.

Let us take cylindrical coordinates (r, ϕ, z) taking the axis of Z along the line source; the corresponding velocity components are (u, v, w). Since there is a radial flow in a plane perpendicular to the axis of Z, it is assumed that v and w are both equal to zero and u is a function of r only, and the motion is steady. We shall assume that η and ζ are functions of r only.

Rate of Strain Components

For cylindrical coordinates we have

$$(ds)^2 = (dr)^2 + (rd\phi)^2 + (dz)^2$$

so that

$$h_1 = 1,\ h_2 = r \text{ and } h_3 = 1$$

For the rate of strain components.

We have

$$\left.\begin{aligned} e_{rr} &= \frac{\partial u}{\partial r} = \frac{du}{dr}, & e_{r\phi} &= 0 \\ e_{\phi\phi} &= \frac{u}{r}, & e_{\phi z} &= 0 \\ e_{zz} &= 0 & e_{zr} &= 0 \end{aligned}\right\} \qquad ..(2)$$

---

* Research Scholar, Agra College, Agra and Lecturer in Mathematics at St. John's College, Agra.

STRESS TENSOR COMPONENTS

From (1) and (2) we have

$$\left.\begin{aligned}
p_{rz} &= 2\eta\, e_{rz} + 4\zeta\, \{e_{rr}\, e_{rz} + e_{r\phi}\, e_{z\phi} + e_{r\phi}\, e_{z\phi}\} = 0\\
p_{z\phi} &= 2\eta\, e_{z\phi} + 4\zeta\, \{e_{zr}\, e_{\phi r} + e_{z\phi} e_{\phi\phi} + e_{zz}\, e_{\phi z}\} = 0\\
p_{\phi r} &= 2\eta\, e_{\phi r} + 4\zeta\, \{e_{\phi j}\, e_{rj}\} = 0\\
p_{rr} &= -P + 2\eta \frac{du}{dr} + 4\zeta \left(\frac{du}{dr}\right)^2\\
p_{\phi\phi} &= -P + 2\eta \frac{u}{r} + 4\zeta \frac{u^2}{r^2}\\
p_{zz} &= -P
\end{aligned}\right\} \quad \ldots(3)$$

FORCES DUE TO VISCOUS STRESS

If F_r, F_ϕ, F_z are the components of viscous forces in the directions of $(r.\ \phi,\ z)$ respectively, then from Shih-i-Pai[2] and using (3) we have

$$\left.\begin{aligned}
F_r &= \frac{1}{r}\left[\frac{\partial}{\partial r}\left\{r\left[-P + 2\eta\frac{du}{dr} + 4\zeta\left(\frac{du}{dr}\right)^2\right]\right\}\right]\\
&\qquad - \frac{1}{r}\left[-P + 2\eta\frac{u}{r} + 4\zeta\frac{u^2}{r^2}\right]\\
&= \frac{1}{r}\left[2\eta\left(\frac{du}{dr} - \frac{u}{r}\right) + 4\zeta\left\{\left(\frac{du}{dr}\right)^2 - \frac{u^2}{r^2}\right\}\right]\\
&\qquad + \frac{\partial}{\partial r}\left\{-P + 2\eta\frac{du}{dr} + 4\zeta\left(\frac{du}{dr}\right)^2\right\}\\
F_\phi &= \frac{1}{r}\left[\frac{\partial}{\partial\phi}\left(-P + 2\eta\frac{u}{r} + 4\zeta\frac{u^2}{r^2}\right)\right] = -\frac{1}{r}\frac{\partial P}{\partial\phi}\\
F_z &= \frac{1}{r}\left[\frac{\partial}{\partial z}\left\{r\,(-P)\right\}\right] = -\frac{\partial P}{\partial z}
\end{aligned}\right\} \quad \ldots(4)$$

FLUID ACCELERATION COMPONENTS

If f_r, f_ϕ, f_z denote the acceleration components in the directions of $(r,\ \phi,\ z)$ respectively, then we have

$$f_r = u\frac{du}{dr},\ f_\phi = 0,\ f_z = 0 \qquad \ldots(5)$$

EQUATION OF MOTION

From (4) and (5) in the absence of external forces, the equation of motion are

$$\left.\begin{aligned}
\rho u\frac{du}{dr} &= \frac{1}{r}\left[2\eta\left(\frac{du}{dr} - \frac{u}{r}\right) + 4\zeta\left\{\left(\frac{du}{dr}\right)^2 - \frac{u^2}{r^2}\right\}\right]\\
&\qquad + \frac{d}{dr}\left[-P + 2\eta\frac{du}{dr} + 4\zeta\left(\frac{du}{dr}\right)^2\right]
\end{aligned}\right\} \quad \ldots(6)$$

$$-\frac{1}{r}\frac{\partial P}{\partial \phi}=0 \qquad ..(7)$$

$$-\frac{\partial P}{\partial z}=0 \qquad ..(8)$$

and the equation of continuity is

$$\frac{\partial}{\partial r}(ur)=0 \qquad ..(9)$$

SOLUTION OF EQUATIONS

From (7) and (8) it follows that P is a function of r only.

From (9) we have

$$ur=\text{constant}=A$$

$$\text{or} \quad u=A/r \qquad ..(10)$$

Suppose the output of the line source, per unit length is $2\pi m\rho$ then we have $2\pi m\rho=\rho\times 2\pi ru$

Hence $A=m$

Substituting (10) in (6) and assuming that $\eta=f(r)$ and $\zeta=F(r)$ we get.

$$-\rho\frac{m^2}{r^3}=\frac{d}{dr}\left[-P+2f(r)\left(-\frac{m}{r^2}\right)+4F(r)\frac{m^2}{r^4}\right]-\frac{4mf(r)}{r^3}$$

$$\frac{dP}{dr}=\rho\frac{m^2}{r^3}+\frac{d}{dr}\left[4F(r)\frac{m^2}{r^4}-\frac{2mf(r)}{r^2}\right]-\frac{4mf(r)}{r^3} \qquad ..(11)$$

Integrating both sides we have

$$P=\frac{4m^2}{r^4}F(r)-\frac{2m}{r^2}f(r)-\frac{\rho m^2}{2r^2}-4m\int\frac{f(r)}{r^3}dr+H \qquad ..(12)$$

where H is a constant.

Hence from (3) the stress distribution is given by

$$p_{rz}=0 \quad p_{z\phi}=0, \quad p_{\phi r}=0$$

$$p_{zz}=\left[\frac{4mf(r)+\rho m^2}{2}\right]\frac{1}{r^2}-\frac{4mF(r)}{r^4}-H+4m\int\frac{f(r)}{r^3}dr$$

$$p_{\phi\phi}=\frac{1}{r^2}\left[\frac{4mf(r]+\rho m^2}{2}\right]+\frac{2m}{r^2}f(r)-H+4m\int\frac{f(r)}{r^3}dr$$

$$p_{rr}=\frac{\rho m^2}{2r^2}-H+4m\int\frac{f(r)}{r^3}dr.$$

ACKNOWLEDGEMENT

I thank Dr. J. P. Agarwal for guidance.

REFERENCES

1. Rivlin, R. S. 1948. *Proc. Roy. Soc.*, A **193** : 260 ; 1949. *Trans. Faraday Soc.*, **45** : 739.
2. Shih-i-Pai, Viscous Flow Theory. eq. 3·52 p. 47.

STUDIES ON THE ENERGY EXPONENT OF THE PRIMERY COSMIC RAY SPECTRUM IN THE ENERGY INTERVAL $10^{14}-10^{16}$E. VOLTS THROUGH THE MEDIUM OF AIR SHOWERS AT NAINITAL

B. N. SRIVASTAVA
Professor of Physics, D. S. B. Govt. College, Naini Tal.

INTRODUCTION

There is a great interest in the form of the energy spectrum in the region $10^{14}-10^{16}$ e. volts as the theories of accelerations and trapping of protons in the galactic magnetic fields find an experimental evidence and test from these observations. The integral frequency energy spectrum gives a remarkable straight line on a logrithmic plot with an exponent 1·5 and can be expressed as a power law of the form;

$$n(E)_A = K_A . E^{-\gamma} \text{ particles/cm.}^2\text{/sterad.} \qquad \ldots\ldots(1)$$

where $n(E)_A$ is the flux of Primaries of mass A and energy E and γ is the energy exponent.

The energy exponent γ is found to be 1·5 upto 10^{13} e. volts. Primaries which are studied by direct observations as shown by Ginzburg *et al* (1961) in his review of the available data. The flux of primaries above 10^{14} e. volts is so small that the direct methods become inefficient. Extensive Air Showers of charged particles produced by these primary particles are therefore used to determine the flux of high energy primaries. These showers are spread over a large area and are easy to detect with the help of coincidence counter arrays. For the measurements of the flux of these particles, the data of counting rates of these arrays is combined with the zenith angle distribution or pressure coefficient. This is done because the counter arryas are sensitive to the showers coming from all the directions and the cosmic ray primaries also are coming towards the earth from all directions isotropically.

We have recorded showers in the interval $10^{14}-10^{16}$ e. volts and have also recorded atmospheric pressure variations continuously for a long period. Pressure coefficients have been calculated for showers in this range and the primary flux has been determined.

EXPERIMENTAL SET-UP FOR RECORDING THE RATE OF AIR SHOWERS

Details of the experimental arrangement of the Air Shower Arrays has already been reported (Srivastava—1963)[6]. Showers have been recorded by triple coincidence G. M. Counter arrays in seven different alignments. Each array was sensitive to a particular energy. It was shown earlier that the average density recorded by each Tray with a sensitive area A sq. cm. is given as :—

$\overline{\Delta} = \frac{1}{A}$ where $\overline{\Delta}$ is the average density of particles recorded in a tray/meter². The average number of particles in a shower is on the other hand related to the average density recorded as shown below:—

$$\bar{N} = \frac{2\pi R_0 d \overline{\Delta}}{\sqrt{3}} \cdot e \frac{d}{\sqrt{3 R_0}}$$

$$\bar{N} = \frac{2\pi R_0 d}{A\sqrt{3}} \cdot e \frac{d}{\sqrt{3 R_0}} \quad \ldots\ldots (2)$$

Where d is the distance of separation of counters in an array and R_0 is the cascade length.

The energy E of the Primery producing a shower of an average number ($\bar{N}$) of particles is proportional to $\bar{N}$ and is expressed as ;

$E = f(N) \cdot \bar{N}$ E. Volts., $f(N)$ is very nearly equal to 10^{10} e. volts/particle.[8]........Gailbraith—1958

$$\text{Hence ; } E = 10^{10} \cdot \bar{N} \text{ E. Volts,} \quad \ldots\ldots (3)$$

The experimental arrangement of the counters in various Arrays was as shown in the Fig. 1.

Counter trays of 500 sq. cm. area were arranged in triangular lattice with a separation of 8 m., 20 m., 30 m., and 45 m. and the rate of showers was measured in each array. The energy of showers recorded in these arrays was $5{\cdot}44 \; 10^{14}$ e. v., $3{\cdot}07 \; 10^{15}$ e. v., $5{\cdot}07 \; 10^{15}$ e. v., and $8{\cdot}9 \; 10^{15}$ e. v. respectively. The area of each tray was subsequently reduced to 250 sq. cm. so that the average density of showers recorded by the trays was increased to 40 particles per m.² and the energy to which each tray was sensitive was increased to twice the original value. Counting rate was recorded in this manner in seven energy groups and was used for the determination of flux.

EVALUATION OF THE EFFECTIVE AREA AND SOLID ANGLE

The effective area within which the shower axes fall so as to get recorded by a group of counters in a particular array has been taken to be the area enclosed by a circle drawn with three trays on its circumference. This assumption is justified because the density of particles falls off rapidly as the distance is increased from the cores as indicated by ;

$$\Delta(r) = \frac{N}{2\pi R_0} \cdot \frac{r/R_0}{r} \quad \ldots\ldots (4)$$

The average solid angle from which showers arrive at the recording apparatus has been estimated from the zenith angle distribution of showers and its correlation with pressure coefficient of showers which has been measured by the author in this context. It has been shown by Gailbraith—1958 that ;

$$\bar{\omega} = \frac{2\pi}{(Bt_0+2)} \text{ Sterad.} \qquad \ldots. \quad (5)$$

where $\bar{\omega}$ is the average solid angle from which showers are received in the array, B is the pressure coefficient in per cm. of Hg. and t_0 is the average atmospheric pressure over the recording apparatus. B was found to be 15% cm^{-1} of Hg. and the local pressure over Nainital is=60 cms. of Hg. With above constants $\bar{\omega}$ comes out to be 0·57 steradians. This shows that the arrays record showers from a small solid angle around the zenith and large angle showers are not permitted as these get progressively absorbed in the atmosphere with increasing zenith angle. The zenith angle distribution of showers as calculated from the pressure coefficient comes out to be of the form;

$$J_\theta = J_v \operatorname{Cos}^9\theta \qquad \ldots. \quad (6)$$

where J_θ is the intensity corresponding to a zenith angle θ and J_v is the vertical intensity of shower rates.

The details of the flux values corresponding to a particular energy of the shower is given in table 1.

TABLE 1

Flux of Primeries in number of particles per cm² per sec. per steradians

S. No.	Area of G.M. Counter Trays	Separation of Trays in Meters	Energy of Showers in E. Volts.	Rate of Showers per hour	Flux of Primeries
1.	500	8	$5{\cdot}44\times10^{14}$	$15{\cdot}74\pm{\cdot}14$	$7{\cdot}60\times10^{-9}$
2.	500	20	$3{\cdot}07\times10^{15}$	$16{\cdot}28\pm{\cdot}145$	$1{\cdot}53\times10^{-9}$
3.	500	30	$5{\cdot}07\times10^{15}$	$15{\cdot}55\pm{\cdot}143$	$6{\cdot}30\times10^{-10}$
4.	500	45	$6{\cdot}14\times10^{15}$	$7{\cdot}05\pm{\cdot}095$	$2{\cdot}99\times10^{-10}$
5.	250	20	$8{\cdot}9\times10^{15}$	$7{\cdot}78\pm{\cdot}159$	$1{\cdot}45\times10^{-10}$
6.	250	30	$1{\cdot}02\times10^{16}$	$6{\cdot}37\pm{\cdot}155$	$1{\cdot}06\times10^{-10}$
7.	250	45	$1{\cdot}78\times10^{16}$	$3{\cdot}11\pm{\cdot}113$	$2{\cdot}79\times10^{-11}$

The spectrum has been plotted in the Fig. 2. It gives the integral frequency energy spectrum of the integrated charge groups of primaries producing air showers. The selection system does not distinguish between the different charge groups of primaries and measures only the total energy contained by the primary. The data if fitted into a power law variation of energy with the frequency of showers comes out to be of the form :—

$$n(E)_A = K_A E^{-\gamma} cm.^{-2} \; sec.^{-1} \; sterad.^{-1}$$

The value of γ is found to increase from $1\cdot71$ to $2\cdot15$ in the region $3\cdot07\times10^{15}$ E. Volts. to $1\cdot8\times10^{16}$ E. Volts.

Discussions of the Result

In these measurements the effective area of the arrays in which showers are supposed to strike for efficient selection has been arbitrarily fixed for there are always certain number of showers of higher energy, having their cores at larger distance, also coming into the selection system. However, the actual number of such showers is very small due to the form of the energy spectrum being a power law. The solid angle factor has been calculated from the average value of the pressure coefficient *i. e.*, 15% per cm. of Hg. The pressure coefficient shows a trend of decrease at lower energies and an increase at higher energies. These considerations might introduce some small errors in the estimation of the absolute values of flux. These values, however, are not in error by a large factor. The measured spectrum gives a fairly good estimation of the energy exponent γ. The change in the energy exponent found in this laboratory is similar to that found by B. Rossi and Clark earlier 1959-61.[3,4,5].

Since the air showers measure the total energy contained by a primary of a mass number A, the spectrum as given by the equation (1) can be written as :—

$$n(E)_A = K_A \, (E_A)^{-\gamma} / A^{-\gamma} \ \text{cm}^{-2} \ \text{sec}^{-1} \ \text{sterad}^{-1} .$$

$$= K_A \, A^{\gamma} \, E^{-\gamma} \quad ,, \quad ,, \quad ,, \quad \ldots\ldots\ldots(7)$$

where E represents the energy per particle.

Ginzburg *et al.*, (1961)[1] have estimated the value of the ratio of the contribution of intensity due to higher charge groups to that of the protons from the knowledge of the primary spectrum at lower energies *i. e.*, $\leqslant 10^{13}$ e. v. Table 2 below gives the relative number of nuclei per proton of different charge groups as computed by Ginzburg *et al.*, on the basis of the experimental data.

TABLE 2

Values of the number of nuclei per proton in Primaries below 10^{13} e. v.

S. No.	Group of Nuclei	A	$A^{1\cdot5}$	$\frac{n_A(E)}{n_p(E)}$
1.	Protons	1	1	1
2.	α – Particles	4	8	0·54
3.	L – group	10	32	0·05
4.	M – group	14	53	0·23

The above table indicates that more than half of the cosmic ray intensity in a particular energy region is contributed by particles of average nuclear mass (A) equal to four. If the exponent increases from 1·5 at lower energies *i. e.*, 10^{13} e. v. to 1·7 or 2·15 at larger energies in the region 10^{14} to 10^{16} e. v., the spectrum becomes more steep. This steepness of the spectrum at a certain stage of energy will tend to increase the average of the nuclear mass (A) in the above analysis. A change in the exponent is an indication in this direcion.

Before drawing the above conclusion one has to examine the energy selection criterian in order to get an insight into the invisible errors which might have changed the value of γ. The recording apparatus measures the average number of particles $\overline{N}$ at the place of observation. The energy of showers is calculated on the criterion that the energy is proportional to the total number of charged particles associated with it at the level of maximum which is close to the level of observation in the present case. The ratio of energy to the number of particles in the shower is $=10^{10}$ e. v. per particle.

$$i.\ e.,\qquad f(N)=\frac{E}{\overline{N}}\ \text{E. Volts./particle.}$$

If this ratio remains constant for all the energies, then the exponent should not change due to the structural causes of the cascade. From the considerations of the electromagnetic cascade theory, the energy exponent is given as:—

$$-\gamma=\frac{d\log n(E)}{d\log E}=S\times\frac{d\log n\ (N)}{d\log\ \overline{N}}\ \text{where n (N or E) gives}$$

the flux and S is the age parameter. It is known that the age parameter S remains nearly constant *i. e.* $S=1{\cdot}3$. The changes in γ are therefore independent of the structural properties of the cascade process.

This singularity in the primary spectrum in the region $10^{15}-10^{16}$ E. Volts. is very likely due to the fact that the Primary Protons of the energy 10^{16} e. v. cannot be trapped in the galactic magnetic fields which are $=6\times10^{-6}$ gauss. These particles start escaping out of the galaxy. This tends to increase the relative abundance of the higher charge group of particles since these particles with larger Z number will have a higher cut off energy than Protons. The cut off energies for higher z-number particles might be 10^{17} or 10^{18} e. v. At energies much higher than this, particles of extagalactic origin might also start getting into our galaxy and make the spectrum smooth upto a large energy. Observations on the sidereal anisotropy taken by the author in this laboratory indicate that if the atmospheric variations in the shower rates are systematically eliminated and shower rates are recorded with penetrating particles which are less sensitive to atmospheric variations, then a small sidereal anisotropy of 2·1% is found at 5×10^{15} E. Volts energy[7,8]. This observation also indicates that the primary protons start escaping out of the galaxy at these energies.

ACKNOWLEDGEMENT

The author is much indebted to Dr. D. D. Pant for his constant interest and general guidance.

REFERENCES

1. Gailbraith, W. 1958. Extensive Air Showers, Butterworths Scientific Publications.
2. Ginzburg *et. al.,* 1961. Prog. of theor. *Phys. Suppl., Japan,* **2** : 10.
3. Rossi, B. 1960. *Proc. Moscow Cosmic Ray Conference,* **II** : 18.
4. Rossi, *et al.,* 1959. *Sci. American.* 201.
5. Rossi, *et al.,* 1961. *Phys. Rev.,* 122, 637.
6. Srivastava, B. N. 1963. *Agra Univ. J. Res.* (*Sci*), **XII,** (III) : 13-28.
7. Srivastava, B. N. 1964. Thesis for Ph. D. Agra University.
8. Srivastava, B. N. 1966. Communicated to the Indian Jr. of Pure & Appl. Phys.

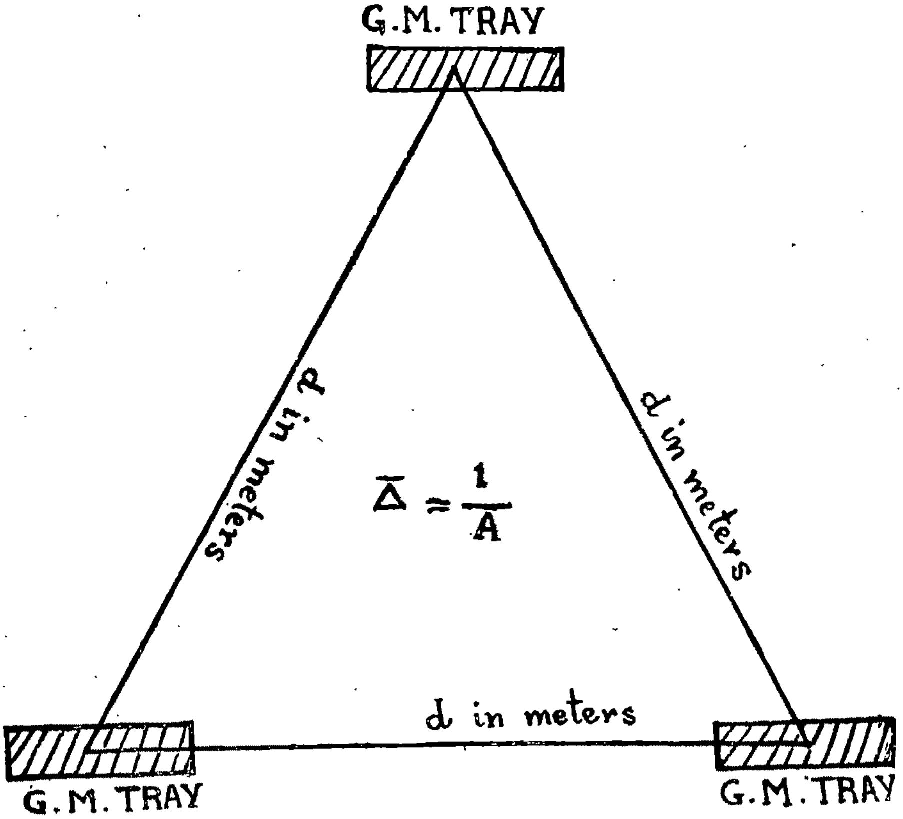

Fig. 1. Arrangement of triple coincidence Arrays.

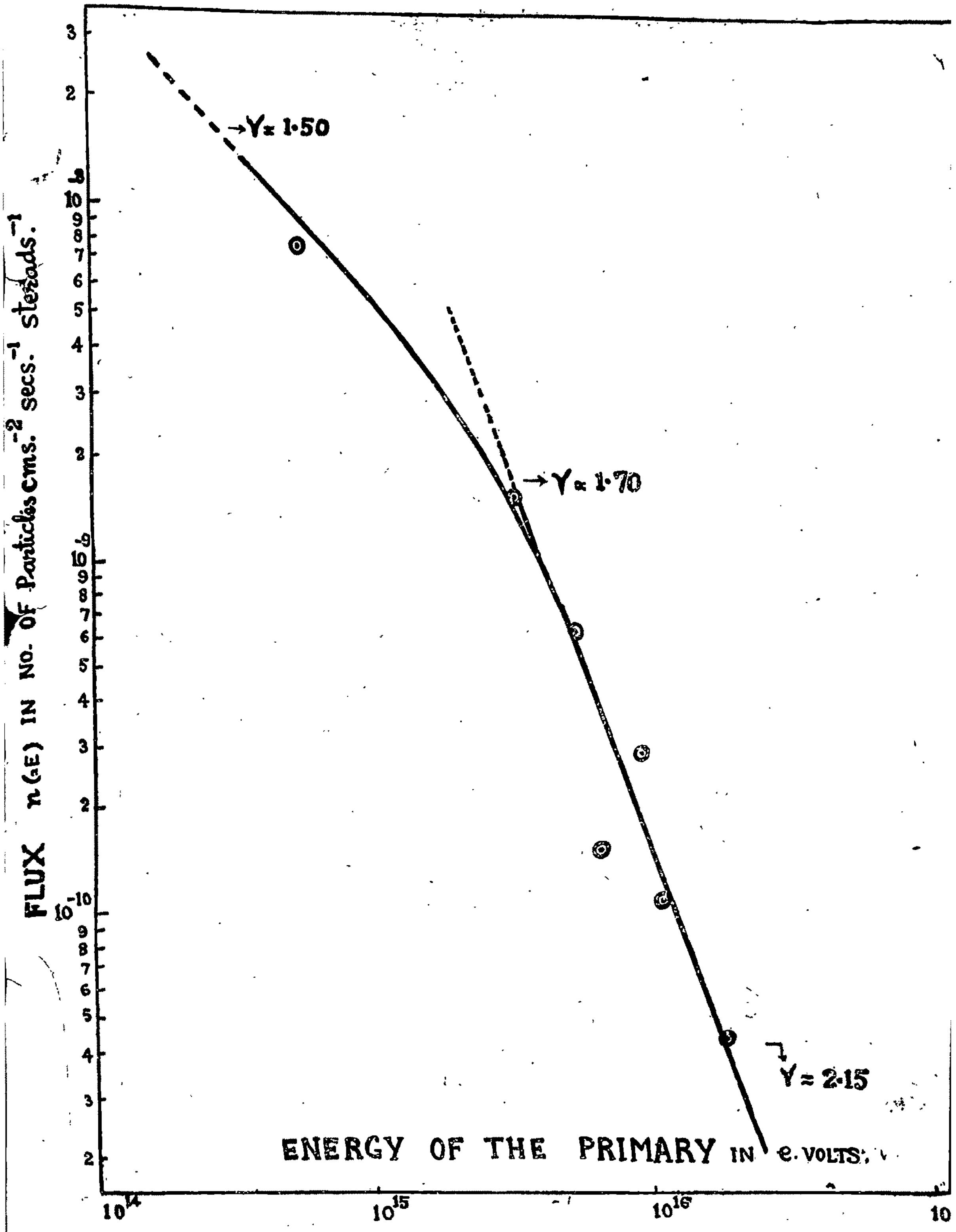

Fig. 2. Integral frequency energy spectrums in the range 10^{14}—10^{16}e. volts Primary Energy.

MAXIMUM ACCELARATION IN TWO DIMENSIONAL IDEAL FLUID FLOW

K. M. Agrawal
Department of Mathematics, B. S. A. College, Mathura.
AND
S. M. Garg
Vaish (P. G.) College, Shamli (Muzaffarnagar).

Yih has established that in a domain free from singularities, the maximum speed in irrotational flows of an incompressible fluid occurs on the boundary of the domain and also that for two dimensional irrotational flows of an incompressible fluid, the maximum magnitude of the accelaration in any singularity-free domain must also occur on its boundary provided the flows are steady. The paper supplies an alternative proof of the later result.

Introduction

It has been shown by Yih[1] that the maximum accelaration in two dimensional steady irrotational flow of an ideal fluid in a singularity free region can occur only on the boundary. The proof given by him makes use of the theory of complex variables and as such his method of proof is not capable of establishing a similar result for the three dimensional potential steady flow of an ideal fluid which is expected to be possibly true. The proof given in the following pages does not make use of the complex variable theory but a method employed by Yih[2] to establish that the maximum speed in a subsonic, isentropic, irrotational, steady flow of a compressible fluid in a singularity free region occurs on the boundary, and this technique is capable of being extended to establish a corresponding possible result for the maximum magnitude of accelaration in the irrotational, steady flow of an ideal fluid in three dimensions. For a proof it is sufficient to show that the Laplacian of a^2 (where a is the magnitude of accelaration) is non-negative[2]. For three dimensions this will be taken up in later communications.

The Proof

In the following presentation the summation convention[3] has been used and the suffixes take up the values 1, 2 and as usual a comma denotes a partial differentiation.

Let ϕ be the velocity potential for the flow in two dimensions then the condition of incompressibility is

$$\phi_{,jj}=0 \qquad \ldots(1)$$

---

[1] Chia Shun Yih, *Quart. Appl. Math.*, **XIII** (2), July 1955, pp. 202-203.
[2] *Ibid.*, July 1958, pp. 178-180.
[3] Tensor Calculus by Bary Spain (Oliver and Boyd, 1953) p. 3.

and if q is speed, then

$$q^2=\phi,_{\alpha}\,\phi,_{\alpha} \qquad \ldots(2)$$

From these we get

$$(q^2),_l=2\phi,_{\alpha l}\,\phi,_{\alpha} \qquad \ldots(3)$$

Equation (3) gives

$$\begin{aligned}(q^2),_{ii}&=2\phi,_{\alpha ii}\,\phi,_{\alpha}+2\phi,_{\alpha i}\,\phi,_{\alpha i}\\&=2\phi,_{\alpha i}\,\phi,_{\alpha i}\end{aligned} \qquad \ldots(4)$$

For $\phi,_{ii}=0$ from (1). This again gives

$$(q^2),_{iil}=4\,\phi,_{\alpha il}\,\phi,_{\alpha i} \qquad \ldots(5)$$

Now if a is the magnitude of the accelaration then

$$\begin{aligned}a^2&=\phi,_{lm}\,\phi,_m\,\phi,_{ln}\,\phi,_n\\&=\frac{1}{4}(q^2),_l\,(q^2),_l\end{aligned} \qquad \ldots(6)$$

using (2). From equation (6) and using the previous results we get

$$(a^2),_i=\tfrac{1}{2}\,(q^2),_{il}\,(q^2),_l \qquad \ldots(7)$$

and

$$(a^2),_{ii}=\tfrac{1}{2}\,(q^2),_{iil}\,(q^2),_l+\tfrac{1}{2}\,(q^2),_{il}\,(q^2),_{il} \qquad \ldots(8)$$

From equation (3)

$$(q^2),_{il}=2\left(\phi,_{\alpha il}\,\phi,_{\alpha}+\phi,_{\alpha i}\,\phi,_{\alpha l}\right) \qquad \ldots(9)$$

Now at all points where

$$(a^2),_i\neq 0$$

the accelaration can not be maximum and hence we concentrate on the case

$$(a^2),_i=\tfrac{1}{2}\,(q^2),_{il}\,(q^2),_l=0. \qquad \ldots(10)$$

On using (9) and (3) condition (10) can be written as

$$\phi,_{\alpha il}\,\phi,_{\alpha}\,\phi,_{lm}\,\phi,_m=-\phi,_{i\alpha}\,\phi,_{\alpha l}\,\phi,_{lm}\,\phi,_m \qquad \ldots(11)$$

From (1) we have after differentiation

$$\phi,_{kkn}=0 \qquad \ldots(12)$$

Let

$$\left.\begin{aligned}&\alpha_1=\phi,_{1m}\,\phi,_m &&\alpha_2=\phi,_{2m}\,\phi,_m\\&A_1=\phi,_2\,d_2-\phi,_1\,d_1 &\text{and}\quad &A_2=\phi,_1\,d_2+\phi,_2\,d_1\end{aligned}\right\} \qquad \ldots(13)$$

Equation (11) then gives

$$\left.\begin{aligned}A_1\,\phi,_{221}+A_2\,\phi,_{112}&=-d_1\,(\phi^2,_{11}+\phi^2,_{12})\\A_2\,\phi,_{221}-A_1\,\phi,_{112}&=-d_2\,(\phi^2,_{11}+\phi^2,_{12})\end{aligned}\right\} \qquad \ldots(14)$$

Solving these for $\phi_{,221}$ and $\phi_{,112}$, we obtain

$$\left.\begin{aligned} &\phi_{,221} = -(d_1A_1+d_2A_2)\ (\phi_{,11}{}^2+\phi_{,12}{}^2)/(A_1{}^2+A_2{}^2) \\ \text{and}\quad &\phi_{,112} = -(d_1A_2-d_2A_1)\ (\phi_{,11}{}^2+\phi_{,12}{}^2)/(A_1{}^2+A_2{}^2 \end{aligned}\right\} \quad \ldots(15)$$

Next equations (5) and (3) give

$$(q^2)_{,iil}\ (q^2)_{,l} = 8\,\phi_{,i\alpha l}\ \phi_{,\alpha i}\ \phi_{,lm}\ \phi_{,m}$$

Writing the right hand side here in full and using the first two relations of (13) we have

$$\begin{aligned} (q^2)_{,iil}\ (q^2)_{,l} &= 8[\phi_{,111}\,\phi_{,11}\,d_1+\phi_{,222}\,\phi_{,22}\,d_2+\phi_{,112}\,(\phi_{,11}\,d_2+2\phi_{,12}\,d_1) \\ &\qquad +\phi_{,221}\,(\phi_{,22}\,d_1+2\,\phi_{,12}\,d_2)] \\ &= -16\ (\phi_{,11}{}^2+\phi_{,12}{}^2)[(d_1A_2-d_2A_1)(\phi_{,11}\,d_2+\phi_{,12}\,d_1)+(d_1A_1+d_2A_2) \\ &\qquad (\phi_{,12}\,d_2-\phi_{,11}\,d_1)]/(A_1{}^2+A_2{}^2) \\ &= -16\ (\phi^2_{,11}+\phi^2_{,12})\ (d_1{}^2+d_2{}^2)\ (\phi_{,12}\,A_2-\phi_{,11}\,A_1)/(A_1{}^2+A_2{}^2) \\ &= -16\ (\phi_{,11}{}^2+\phi_{,12}{}^2)\ (d_1{}^2+d_2{}^2)^2/(A_1{}^2+A_2{}^2) \qquad \ldots(16) \end{aligned}$$

Using (12) and the last relations of (13).

Now,

$$A_1{}^2+A_2{}^2=(d_1{}^2+d_2{}^2)\ (\phi_{,1}{}^2+\phi_{,2}{}^2) \qquad \ldots(17)$$

and

$$d_1{}^2+d_2{}^2 = (\phi_{,11}{}^2+\phi_{,12}{}^2)\ (\phi_{,1}{}^2+\phi_{,2}{}^2) \qquad \ldots(18)$$

Thus from (16) using (17) and (18)

$$(q^2)_{,iil}\ (q^2)_{,l} = -16\ (\phi_{,11}{}^2+\phi_{,12}{}^2)^2 \qquad \ldots(19)$$

Next from (9)

$$\begin{aligned} (q^2)_{,il}\,(q^2)_{,il} = 4\Big(&\phi_{,i\alpha l}\ \phi_{,i\beta_1}\ \phi_{,\alpha}\,\phi_{,\beta} + 2\phi_{,i\alpha l}\ \phi_{,\beta i}\ \phi_{,\beta l}\ \phi_{,\alpha} \\ &+\phi_{,\alpha i}\ \phi_{,\alpha l}\ \phi_{,\beta i}\ \phi_{,\beta l}\Big) \end{aligned}$$

Also $\phi_{,i\alpha l}\ \phi_{,\beta i}\ \phi_{,\beta l}\ \phi_{,\alpha} = 0$ from (2) and hence

$$(q^2)_{,il}\,(q^2)_{,il} = 4(\phi_{,i\alpha l}\ \phi_{,i\beta l}\ \phi_{,\alpha}\ \phi_{,\beta} + \phi_{,\alpha i}\,\phi_{,\alpha l}\ \phi_{,\beta i}\ \phi_{,\beta l})$$

From (12), (15) and (1)

$$\phi_{,i\alpha l}\ \phi_{,i\beta l}\ \phi_{,\alpha}\ \phi_{,\beta} = 2\ (\phi_{,11}{}^2+\phi_{,12}{}^2)^2$$

and from (1)

$$\phi_{,\alpha i}\ \phi_{,\alpha l}\ \phi_{,\beta i}\ \phi_{,\beta l} = 2(\phi_{,11}{}^2+\phi_{,12}{}^2)^2$$

Hence

$$(q^2)_{,il}\,(q^2)_{il} = 16\ (\phi_{,11}{}^2+\phi_{,12}{}^2)^2 \qquad \ldots(20)$$

Therefore from (8), (19) and (20)

$(a^2)_{,11}=0$ whenever $(a^2)_{,1}=0$. ...(21)

MORPHOLOGICAL STUDIES IN APOCYNACEAE
I. *LOCHNERA PUSILLA* K. SCHUM*

Y. S. MURTY AND T. S. CHAUHAN
School of Plant Morphology, Meerut College, Meerut.

INTRODUCTION

Woodson in a series of interesting contributions (*see* 1930, 35,38) on the taxonomy and morphology of members of Apocynaceae, has thrown more light on this family than any one else. Some contributions have also appeared on floral anatomy (Woodson and Moore, 1938; Saunders, 1939 and Rao and Ganguli, 1963) and embryology (Schnarf, 1931; Pannocchia-laj, 1938; Rau 1940 and Periasamy, 1963) of some members while Woodson and Moore (1938) described the anatomy of the carpel and nectaries of *Lochnera rosea.* The development of a normal 8-celled female gametophyte (Pannocchia-laj, 1938) and shoot apex and initiation of floral organs (Boke, 1947, 48, 49) are also described in the same species.

Lochnera pusilla is a common weed of sugarcane fields in this locality. It remained practically unworked out except for a brief account of the anatomical features of its vegetative part by Sayeedud-Din (1941). It is, therefore, felt worthwhile to study the morphology of this common weed. The present paper deals with the nodal and floral anatomy, embryology and seed coat structure.

MATERIAL AND METHODS

The material of *L. pusilla* was collected from the neighbouring fields of Meerut and was immediately fixed in F.A.A. The material was processed in the usual way, after dehydration and passing through alcohol-xylol grades and was finally embedded in paraffin wax. Serial microtome sections were cut at 8-10 microns thick. Safranin-fast green and crystal violet and erythrosin combinations gave satisfactory results.

Some flowers were also treated with 5% KOH for few hours and cleared in lactic acid and stained with basic fuchsin for the study of vasculature of the flowers.

OBSERVATIONS

External Morphology—Lochnera Pusilla is a small annual latex containing branched herb with quadrangular branches bearing opposite, simple leaves. The flowers are mostly solitary and axillary. The sepals are almost free. The white and salvershaped corolla tube is inflated just below the mouth where the short anthers are attached. Numerous hairs are present at the mouth of the corolla tube. The gynoecium is slightly semi-inferior and the carpels become free from one another at the very base *i. e.*, just above the level of the base of the corolla but they again fuse at the top and hence, the style is single with a prominent stigma bearing a reflexed membranous expansion. Two elongate linear nectaries are present alternating with the carpels (Fig. 6). The paired follicles contain numerous seeds and they have an outer ribbed surface.

---

* Research contribution No. 80 from the School of Plant Morphology, Meerut College, Meerut.

Nodal Anatomy—An internode, in a cross section, appears quadrangular with a continuous ring of vascular tissue in the centre (Fig. 1). Just below the node two traces in opposite direction depart from the central stele leaving a gap each. These are the two leaf traces for the two opposite leaves at the node (Fig. 2). Each of the leaf traces is followed by two more traces which supply the axillary branch (Figs. 3-4). The gaps caused by the departure of leaf traces are filled up. Within the leaf base the bundle becomes arc like and prominent. Sinnott (1914) also described a unilacunar node in Apocynaceae.

Some glandular structures are observed on either side of the leaf base (Figs. 4-5). Similar structures in some other members of the family have earlier been interpreted as stipules (Glück, 1919; Woodson and Moore, 1938). These structures are devoid of any vascular supply but from their position by the side of the leaf base, give the impression of stipular nature.

Floral Anatomy—The pedicel is short and in a cross-section it shows a complete ring of amphiphloic siphonostele (Fig. 9) and many layered cortex. Laticeferous canals are present in both cortex and pith. At the base of the receptacle ten traces diverge out from the ring of amphiphloic siphonostele (Fig. 10). Alternately these are the sepal-stamen and petal-sepal strands (Fig. 11). As these strands move into the cortex of the receptacle the central vascular tissue organises into eight bundles (Fig. 12). While each of the sepal-stamen strands splits tangentially into an outer sepal median and an inner stamen bundle, each petal-sepal strand splits into an outer fused sepal lateral and an inner petal median (Figs. 13-14). A fused sepal lateral divides into two sepal laterals of the adjacent sepals. Whereas the sepal medians and sepal laterals form an outer ring of vascular bundles, the petal and stamen bundles organise into an inner ring (Fig. 15). At about this level of the receptacle, two locules make there appearance (Figs. 13-14). Of the eight bundles in the centre the two bundles at the back of the locules, are the carpellary dorsals and the two placed at right angles to the locules are the nectary medians (Fig. 13). The remaining four bundles alternate with the carpellary dorsals and nectary medians. Each of these four bundles first cuts off a carpellary ventral towards inside and also gives out a nectary lateral towards the nectary bundle before finally splitting into many carpellary laterals (Figs. 13,14, 15).

Even before the level of separation of the calyx from the receptacle, ovules make their appearance in each locule. A space that appears in the centre of the two carpels widens and as a result, the two carpels are delimited from each other as well as from the alternating nectaries (Figs. 15, 16). At about this level the calyx with its mid rib and lateral bundles and the corolla containing the petal medians and stamen bundles get delimited from one another and from the receptacle (Fig. 16). The calyx splits into five valvate sepals appearing triangular in cross-section each having a median and two laterals. The corolla tube contains ten bundles representing alternately petal and stamen bundles (Fig.17).

When the nectaries separate from the carpels they appear flattened, and triangular in cross-section. Of the three bundles which are present at the base of the nectary before its separation from the receptacle only the median bundle continues almost to its tip (Figs. 8 & 16). Each carpel has many bundles in its wall and the two ventrals of each carpel supply the ovules on their sides (Fig. 17). Only the carpellary dorsals continue into the style and reach the stigma (Figs. 7, 18, 19, 20 & 21).

At about the level of the stigma the petal medians give out two laterals one on each side. At the back of each stamen bundle a space that appears, enlarges and delimits the filament from the corolla tube (Fig. 22). Just at this level the corolla tube becomes hairy inside and splits into five twisted lobes where the petal laterals branch further (Figs. 23-24).

In one of the flowers examined the nectary median bundles although formed, are not observed even at the level of the appearance of locules. Therefore, only the two laterals are seen at the base of the nectary. However, of these two laterals only one continues to the tip of the nectary (Figs. 25-28).

EMBRYOLOGY

Microsporogenesis—A transection of a young anther is ovoid (Fig. 29). A layer of epidermis surrounds a mass of homogenous cells. At four corners of a slightly older anther 2-3 rows of hypodermal archesporial cells differenciate (Figs. 29-30). Later, anther becomes slightly four lobed. Each of the hypodermal archesporial cells divides periclinally into an outer parietal and an inner sporogenous cell. The parietal cells further divide to give rise to the endothecium, middle layer and tapetum. The sporogenous cells divide to form a mass of cells (Figs. 31-32). The anther wall thus becomes four layered. The tapetal cells as well as the sporogenous cells stain more deeply. The tapetal cells remain uninucleate (Fig. 32). The sporogenous cells show meiotic divisions each forming a tetrad of four microspores (Figs. 33,34,35). Depending on the position of the spindle, the tetrads formed may be tetrahedral or decussate (Figs. 35-36). The microspores to begin with, are uninucleate and as a result of one division each microspore becomes two celled at the shedding stage. The mature pollen grain is tricolporate or tetracolporate with a thick exine (Figs. 37, 38, 39 & 40). In a mature anther the tapetum and middle layers degenerate while the endothecium develops fibrous thickening (Fig. 41).

At the time of dehiscence the partition wall between two microsporangia breaks up forming a single chamber and then opens to outside. The dehiscence is longitudinal (Figs. 42, 43). Rarely one of the pollen grains is observed to germinate while within the microsporangium (Fig. 41).

Megasporogenesis and female gametophyte—The ovules are unitegmic and their initiation begins at the time of the appearance of the archesporial cell. The archesporial cell is hypodermal and functions directly as megaspore mother cell (Figs. 44, 45). As a result of meiotic divisions a linear row of four megaspores are formed (Figs. 46-47). Although the chalazal megaspore alone gives rise to the embryosac, occasionally enlargement of one of the other megaspores has been observed. But no instance of development of embryosac from other than the chalazal megaspore is noticed (Figs. 48, 49, 50). By the time the tetrad of megaspores is formed, the epidermis above begins to disappear and therefore, there is no epidermis above the embryo sac at the micropylar region. But the integument elongates sufficiently to cover the embryo sac and leaves a narrow micropyle. All but the chalazal megaspore finally degenerate (Fig. 51). The chalazal megaspore enlarges and its nucleus divides into two. The two nuclei get separated due to vacuolization and they occupy the two opposite poles in the developing embryosac (Fig.52). There they divide twice and thus eight nuclei are formed (Figs. 53-54). At this stage the position of ovules is anatropous (Fig. 55). One nucleus from each pole migrates to the centre. They fuse forming a secondary nucleus (Figs. 56-57). The remaining three nuclei at the micropylar end organise into an egg apparatus and the three at the chalazal end into antipodal cells (Fig. 57). The micropylar end of the embryosac may be slightly broader than the chalazal end. Thus the embryosac is monosporic; 8-nucleate polygonum type. The antipodals disappear completely after fertilization (Fig.58).

Endosperm –The secondary nucleus moves nearer the egg apparatus prior to fertilization. Just after double fertilization the primary endosperm nucleus divides repeatedly resulting in several free nuclei even before the first division of the zygote has taken place (Figs. 58-59). By the time the first division of the zygote is completed, the endosperm shows foldings and caecae like growths at the chalazal end (Figs. 61, 62). The free endosperm nuclei are scattered throughout the endosperm almost uniformly except in the haustoria like diverticulae or caecae where they are comparatively more crowded (Figs. 63-64). The endosperm remains free nuclear till the embryo becomes heart shaped and finally cell walls are formed starting from the periphery resulting in a number of uninucleate endosperm cells (Fig. 62).

The Embryo—The first division of the zygote is transverse resulting (Fig. 60) in a terminal cell (ca) and basal cell (cb). While the latter divides transversely into two cells (ci) and (m) (Fig. 65), the former shows a longitudinal division into two, thus resulting in a four celled stage of proembryo where the cells are ⊥ shaped in arrangement (Fig.66). The next division is again longitudinal in the two cells of (ca) but at right angle to the first and hence a quadrant is formed (Fig. 67). A transverse division of all the cells of the quadrant results in an octant (Fig. 68). By now (ci) divides transversely into a basal (n′) and a middle (n) (Fig. 67). Later both (n′) and (n) divide once forming a four celled suspensor, the basal cell of which is more prominent (Fig. 72). The original middle cell (m) divides transversely and the resulting two cells divide longitudinally (Figs. 69-70). The octant has by now divided repeatedly forming first the globular stage of the embryo and later heart shaped embryo (Figs. 70-73). It is from this heart shaped body the two cotyledons, plumule and radicle are differenciated (Fig. 74).

The embryo development follows that of crucifer type (Maheshwari, 1950). Johansen (1950) suggested the term "onagrad type" for crucifer type since the embryos of onagraceae are more typical.

The Seed Coat—The integument at the time of fertilization is about 5-layers thick (Fig. 75). It becomes more layered as the embryo grows. As the embryo gets differentiated into cotyledons etc., the inner layers of the integument begin to lose their contents and shrival as a result of the development of the endosperm (Fig. 76-77). Finally in a mature seed only the outer epidermis of the integument is left and all other layers are completely crushed and disappear (Fig. 78). The cells of the epidermal layer in a seed show tooth like projections which are characteristic of the seed in this species (Figs. 78-80). While outermost 4-5 layers of endosperm cells acquire conspicuous thickening and persist (Fig. 80), the remaining portion of endosperm is utilised by the developing embryo.

DISCUSSION

The Calyx—In *Lochnera pusilla* the calyx is supplied by five medrib traces and five commissural traces which branch and supply adjacent sepal margins. The commissural bundles are fused with the petal medians at the base forming the petal-sepal strands.

Woodson and Moore (1938) from their study of vascular organisation of calyx in this family, classified the members under four types. The present study indicates that the vascularization of calyx in *L. pusilla* falls under Woodson and Moore's type II which includes all those species where adjoining lateral traces of adjacent sepals are adnate to the petal midribs. Members of both the sub-families Plumerioideae and Echitoideae are equally represented in this category. The adjacent sepal laterals in some cases are found to be adnate separately with the petal median while in the others they remain fused for some distance and this common bundle is adnate to the petal median. Woodson and Moore (1938) did not give much importance to this point as they found both conditions even in the same species. However, Rao and Ganguli (1963) found this condition only in three out of eight members of plumerioideae (*Carissa congesta, Alstonia scholaris, Tabernaemontana devericata*) they studied.

The Corolla—Boke (1948) from developmental studies regards the corolla tube of *Vinca rosea* as consisting of two parts differing in origin. The lower corolla tube (portion below the stamen insertion) is considered as arising due to toral growth while the upper one (portion above the insertion of stamens) as appendicular in nature. The present anatomical studies do not support such a consideration in *Lochnera pusilla.* Rao and Ganguli (1963) reached a similar conclusion from their anatomical study of members of Apocynaceae.

Nectaries—The gynoecium in *Lochnera pusilla* is bicarpellary with the nectaries alternating with two carpels. After the departure of sepal, petal and stamen supplies, the receptacular stele organises into eight bundles. It may be recalled that of these, the alternating four bundles do not branch and function alternately as carpellary dorsals and medians of the two nectaries. The other four bundles first give off a ventral bundle each towards the centre and one lateral bundle to the nectary before splitting to form a number of carpellary laterals. Only the carpellary dorsal continues into the style.

Woodson and Moore (1938) described the vascular anatomy of the ovaries and associated nectaries in members of Apocynaceae, with selected types of which *Lochnera* is one. In *Lochnera rosea* they describe two ovuliferous carpels, alternating with two nectaries. The receptacular stele consists of about twenty bundles. From these, four placental bundles migrate towards the centre constituting the placental supply of the two ovuliferous carpels. The remaining intervening bundles supply the two nectaries that alternate with the ovuliferous carpels. The same condition they observed in *Vinca major* and *Vinca minor.* From this vascular supply and also from comparison of similar structures in *Pleiocarpa,* they interpreted the nectaries as carpellodes.

Rao and Ganguli (1963) have described a more orless similar condition in *Kopsia fruticosa*. The two alternating nectaries are described as receiving basically similar vascular supply as those of the carpels which are fertile. Therefore, they accepted the interpretation given by Woodson and Moore (1938) for the nectaries in *Lochnera rosea, Vinca minor, V. major* and *Pleiocarpa mutica.* Therefore, the nectaries in *Kopsia fruticosa* are similarly regarded as carpellodes. Boke (1949) from the mode of initiation and other morphological characters interprets the carpellodes (nectaries) in *Vinca rosea* as reduced carpels.

In the present study it is observed that the carpellary dorsals and nectary bundles are organised at the same level. Like the carpellary dorsals, the nectary medians also alternate with the bundles that give out placental bundles, carpellary laterals, and nectary laterals. The nectary laterals are short and only the nectary median continues almost to the tip of the nectary. Therefore, the vascular supply of a carpel and nectary is basically on the same pattern except for the absence of bundle comparable to the carpellary ventrals in the nectary. Hence the interpretation of Woodson and Moore (1938) that the nectaries are the carpellodes is supported.

Placentation—The placentation in Apocynaceae is variously described as parietal (Rendle, 1938) and axile and parietal (Woodson and Moore, 1938; Lawrence, 1951; Hutchinson, 1959). Woodson and Moore (1938) from their observations on different species concluded that the unilocular condition is derived from a bilocular one. They also explained from the orientation of vascular bundles, that the parietal placentation is derived from axile placentation. Rao and Ganguli (1963) supported these conclusions from their observations also specially in the presence of bilocular condition with axile placentation at the base and apex of the ovary and with unilocular condition and parietal placentation in the middle. It may be recalled that in *Lochnera pusilla* each of the two carpels shows a carpellary dorsal and two ventral bundles besides many laterals distributed in the wall of the carpels. The two ventrals are inversely oriented and are arranged in the same radius as that of the carpellary dorsal. The ovary is bilocular at the base and ovules are observed even before the delimitation of the two carpels. The ventrals are completely consumed in supplying the numerous ovules and only the carpellary dorsals of the two carpels continue through the length of the single style.

Applying the various characteristic features mentioned for differentiation of the marginal, axile and parietal placentation by Puri (1952), the placentation in *Lochnera pusilla* has to be described as axile because of the bilocular condition at the base, presence of inverted ventral bundles arranged on the same radius as carpellary dorsals, and also because the ovules borne on the fused margins of the same carpel receive their vascular supply from the inverted ventral bundles. Therefore, from vascular anatomy the placentation should be described as axile in *Lochnera pusilla.*

Embryology—As reported in *Vinca rosea* (Täckholm and Söderberg, 1918) and also in some other members of Apocynaceae (Rau, 1940) the development of the microspores follows simultaneous type and both tetrahedral and decussate tetrads are observed.

As has been reported by Rau (1940) in six members of Apocynaceae the archesporial cell is hypodermal and no parietal cell is cut off in *Lochnera pusilla* also. Further in the formation of a linear tetrad of megaspores of which the chalazal one alone is potential and disappearence of epidermis above the typical polygonum type of embryo sac, this species resembles other members of the family (Rau, 1940). However, occasionally enlargement of other megaspores is also observed but they have not been found to develop further. The polar nuclei as observed in *Vinca minor* and *Allamanda nereiifolia* (Anderson, (1931) and *Vallaris Heyneii* (Rau, 1940) fuse before fertilization. The antipodals start degenerating at the time of fertilization.

As in other members of Apocynaceae the endosperm is free nuclear. Cell walls are laid down when the embryo is many celled. It is interesting to note in this species the formation of endosperm haustoria on the chalazal side in the form of diverticulae or caecae. Endosperm haustoria have already been reported from several families (*see* Maheshwari, 1950, Chopra & Sachar, 1963) but do not appear to have been recorded from Apocynaceae. The embryo development follows that of 'crucifer type' (onagrad type of Johansen, 1950).

SUMMARY

The anatomy of the node, flower and embryology including the seed coat structure of *Lochnera pusilla* are described. The node is unilacunar, and the leaf is single traced. At the base of the receptacle sepal median and stamen traces and similarly petal median and fused sepal laterals of adjacent sepals remain conjoint. From the vascular anatomy the nectaries which alternate with the carpels are interpreted as carpellodes. Anatomically the placentation is considered axile. It is observed that besides the chalazal megaspore, any one of the other megaspores also may enlarge, although only the chalazal one develops into the 8-nucleate polygonum type of embryo sac. Endosperm is free nuclear. Diverticulae or caecae like endosperm haustoria are reported for the first time in this family. 'Crucifer' type of embryo development is observed.

ACKNOWLEDGEMENTS

The authors are highly grateful to Prof. V. Puri, D. Sc., F. A. Sc., F. N. I., for his valuable guidance, constant help and encouragement.

REFERENCES

1. Anderson, A. 1931. "Studien uber die Embryologie der Familien Celastraceae, Oleaceae und Apocynaceae," *Acta. Univ. Lund., Avd.*, (2) **27**: 1-12.
2. Boke, N. H. 1947. Development of the adult shoot apex and floral initiation in *Vinca rosea* L., *Amer. Jour. Bot.*, **34**: 433-439.
3. Boke, N. H. 1948. Development of the parianth in *Vinca rosea* L., *Amer. Jour. Bot.*, **35**: 413-423.
4. Boke, N. H. 1949. Development of the stamens and carpels in *Vinca rosea* L., *Amer. Jour. Bot.*, **36**: 535-547.
5. Chopra, R. N.; Sachar, R. C. 1963. Endosperm. In recent advances in the embryology of Angiosperms. Editor P. Maheshwari. Delhi.
6. *Gluck, H. 1919. Blattund Bluthenmorphologische studien. Jena.
7. Hutchinson, J. 1959. The families of Flowering plants. Vol. 1. Oxford.
8. Johansen, D. A. 1950. Plant Embryology, Waltham, U. S. A.
9. Lawrence, G.H.M. 1951. Taxonomy of vascular plants. Macmillan, New York.
10. Maheshwari, P. 1950. An introduction to the embryology of Angiosperms. McGraw-Hill, New York.
11. *Pannocchia-Laj, 1938. Embryologiae cariologia di *Lochnera rosea*, Nuovo, *Gior. Bot. Ital.*, **45** (2): 122-130.

---

*Not seen in originals.

12. Periasamy, K. 1963. Studies on seeds with ruminate endosperm. 3. Development of rumination in certain members of Apocynaceae, *Proc. Indian Acad. Sci.*, Sec. B, **58**: 325-332.

13. Puri, V. 1952. "Placentation in Angiosperms," *Bot. Rev.*, **18**: 603-651.

14. Rao, V. S. & Ganguli, A. 1963. Studies in the floral anatomy of the Apocynaceae, *Jour. Indian Bot. Soc.*, **42**: 419-435.

15. Rau, M. A. 1940. Studies in the Apocynaceae, *Jour. Indian Bot. Soc.*, **19**: 33-44.

16. Rendle, A. B. 1938. The classification of flowering plants, Vol. II, Cambridge.

17. Saunders, E. R. 1939. Floral morphology, Vol. II, Cambridge.

18. Sayeedud-din, M. 1941. Some common Indian herbs with notes on their anatomical characters Pt. VI. *Lochnera pusilla* K. Schum, *Jour. Bom. Nat. Hist. Soc.*, **42**: 1-3.

19. Schnarf, K. 1931. Vergleichende Embryologie der Angiospermen, Berlin.

20. Sinnott, E. W. 1914. Investigations on the phylogeny of the angiosperms. I. The anatomy of the node as an aid in the classification of angiosperms. *Amer. Jour. Bot.*, **1**: 303-322.

21. *Tackholm, G. Und Soderberg, 1918. "Neue Beispiele der simultanen und sukzessiven Wandbildung in den Pollenmutterellen," *Svensk. Bot. Tidskr.*, **12**: 189-201.

22. Woodson, R. E. (JR.) 1930. Studies in the Apocynaceae I. *Ann. Misso. Bot. Gard.*, **17**: 1-212.

23. Woodson, R. E. (JR.)1935. The floral anatomy and probable affinities of the genus *Grisebachiella* Lorentz. *Bull. Torrey Bot. Club.*, **62**: 471-478.

24. Woodson, R. E. (JR.) & Moore, J. A. 1938. The vascular anatomy and comparative morphology of Apocynaceous flowers, *Ibid.*, **65**: 35-166:

EXPLANATION OF FIGURES

Figs. 1-5. Serial transverse sections of the node of *L. Pusilla* (ax. b. t., axillary branch trace; g., glandular structure; l. t., leaf trace).

Figs. 6-28. Anatomy of the flower of *L. pusilla.* Fig. 6., Entire cleared flower. Fig. 7 A semi-diagrammatic longitudinal section of the flower. Fig. 8. Receptacular portion enlarged to show the vascular supply to nectary. Fig. 9-24. Serial transverse sections of the flower from the base upward. Figs. 25-28. Transverse sections of the flower showing vascular supply to nectary different from the normal flower (c. d., carpellary dorsal; c. l., carpellary lateral; c. v., carpellary ventral; n., nectary; n. d., nectary dorsal; n. l., nectary lateral; p. m., petal median; p. s. str., petal-sepal-strand; s. l., sepal lateral; s. m., sepal median; s. st. str., sepal-stamen-strand; st. t., stamen trace.).

Figs. 29-57. Embryology of *L. pusilla.* Figs. 29—43. Microsporogensis Fig. 29. Transverse section of a young anther showing hypodermal archesporial cells. Fig. 30. Archesporial cells enlarged. Figs. 31—32. Differentiation of sporogenous tissue and formation of parietal layers and showing uninucleate tapetal cells. Figs. 33-36. Dividing sporogenous cells and tetrahedral (Fig. 35) and decussate (Fig. 36) tetrads of microspores. Figs. 37-40. Maturation of microspores into 2-celled pollen grains. Fig. 41. Anther wall showing fibrous thickening and also the germination of one pollen grain inside the the microsporangium. Fig. 42-43. Showing dehiscence of anthers. Figs. 47-57. Megasporogenesis. Figs. 44-45. Showing one celled archesporium functioning directly as megaspore mother cell and development of integuments. Figs. 46-47. Showing the formation of linear tetrad. Figs. 48-53. Degeneration of a few megaspores. Figs. 51. Functioning megaspore Figs. 52-54. Formation of two, four and eight-nucleate embryo sacs. Fig. 55. Position of ovule at 8-nucleate embryo sac stage Fig. 56. Organized embryo sac. Fig. 57. Formation of secondary nucleus (fb. t., fibrous thickening; fun. m., functioning megaspere; m. m. c.. megaspore mother cell; pol. pollen; pol. t., pollen tube; sec. nu., secondary nucleus; sp. t., sporogenous tissue; t., tapetum. Scale 'a' for Fig. 29; 'b' for Figs. 30-32; 'c' for Figs. 33-40; 'd' for Fig. 41; 'e' for Figs. 42-43; 'f' for Figs. 44-45; 'g' for Figs. 46-51; 'h' for Figs. 52-54; 'i' for Fig. 55 and 'j' for Figs. 56-57.

---

* Not seen in original.

Figs. 58-74. Development of endosperm and embryo Figs. 58-59. Showing fertilized egg, one synergid, pollen tube and formation of free nuclear endosperm. Fig. 60. 2-celled embryo. Fig. 61. Semi-diagrammatic longitudinal section of ovule showing endosperm haustoria at bi-celled stage of embryo. Fig. 62. Showing endosperm diverticulae. Figs. 63-64. Endosperm haustoria. Figs. 65-67. Quadrant formation. Fig. 68. Octant. Figs. 69-72. Formation of globular embryo with suspensor. Fig. 73. Heart-shaped embryo. Fig. 74. Semi-diagrammatic longitudinal section of a seed showing mature embryo and ribbed epidermal layer (ca., apical cell; cb., basal cell; cot., cotyledon; div., diverticulae; e., endosperm; e. hau; endosperm haustorium; em., embryo; em. s., embryo sac; fr. egg., fertilized egg., int., integument; plu., plumule; pol. t., pollen tube; r., redicle; syn., synergid). Scale 'k' for Figs. 58-60 & 65; 'l' for Fig. 61; 'm' for Fig. 62; 'n' for Fig. 63; 'o' for Figs. 68-70; 'p' for Figs. 71-72, 'q' for Fig. 73, 'r' for Fig. 74;).

Figs. 75-80. Development of seed coat. Fig. 75. Very young integument. Figs. 76-77. Degeneration of inner layers of the integument and enlargement of endosperm. Fig. 78. Degeneration of endosperm cells. Figs. 79-80. Showing ribbed epidermis and endosperm thickening which acts as seed coat.

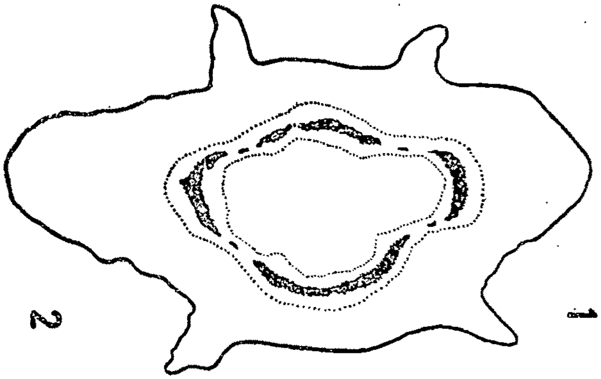

2

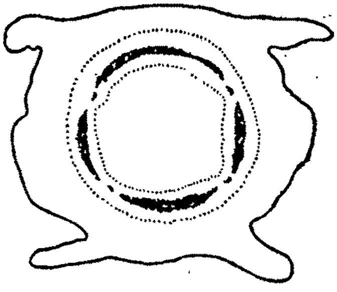

1

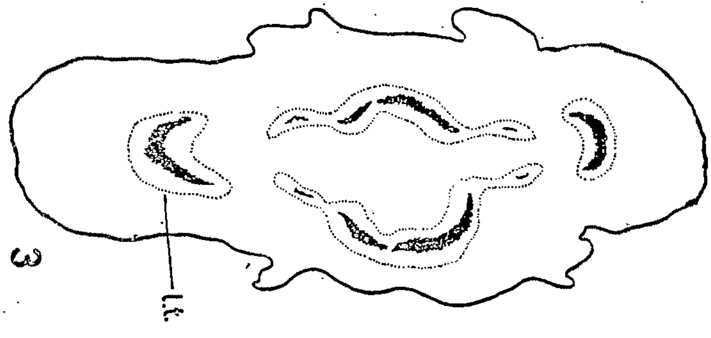

3

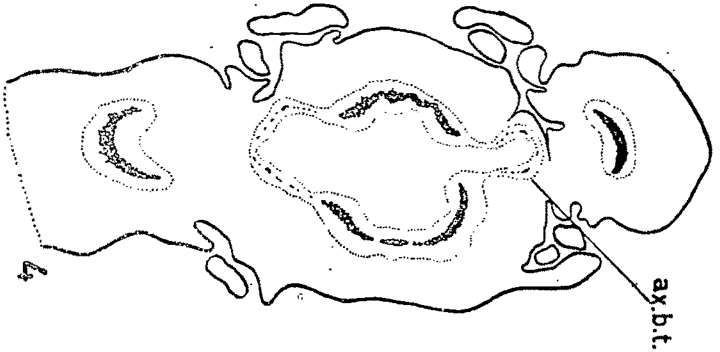

4

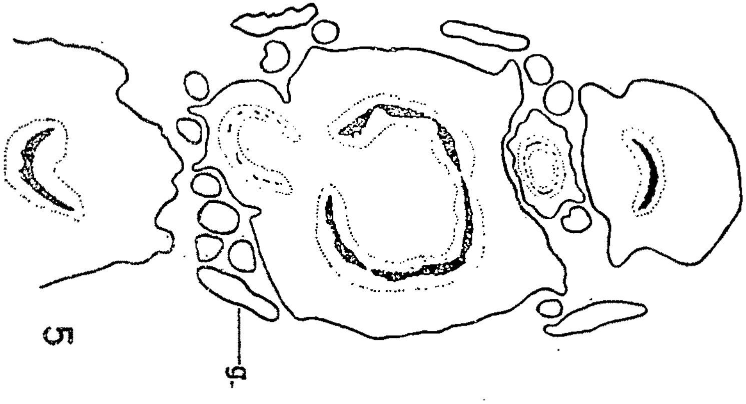

5

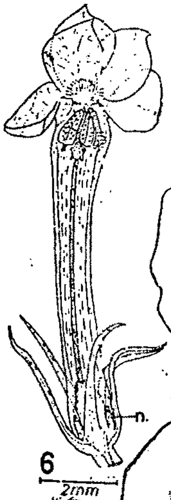

6

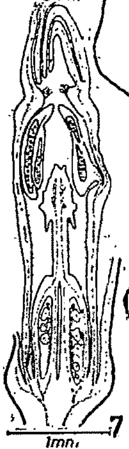

7

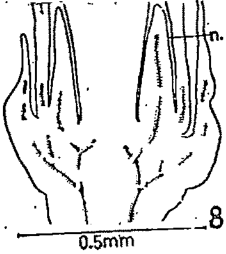

8

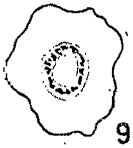

9

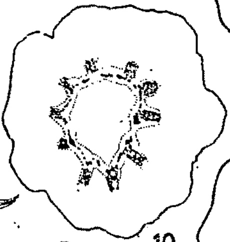

10

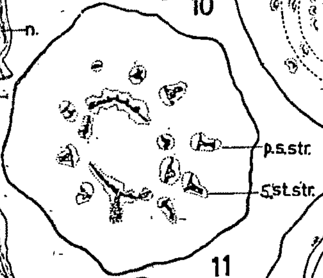

11

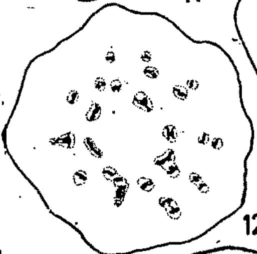

12

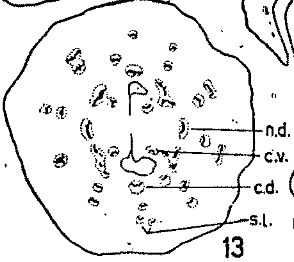

13

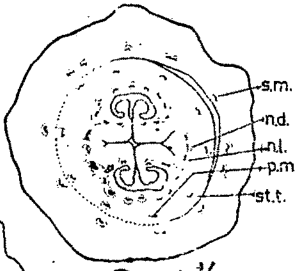

14

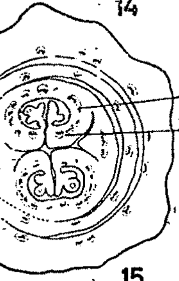

15

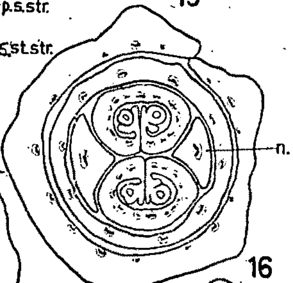

16

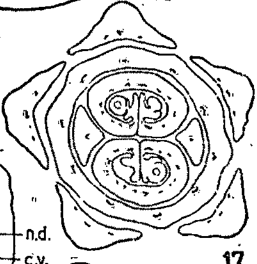

17

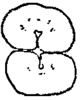

18

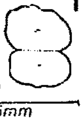

19

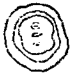

20

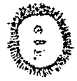

21

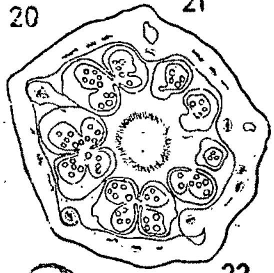

22

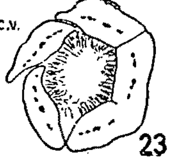

23

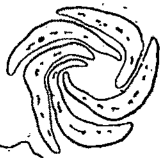

24

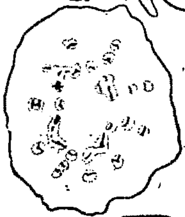

25

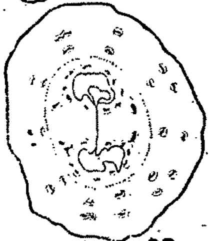

26

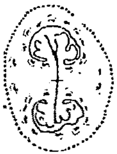

27

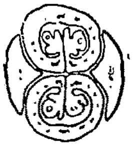

28

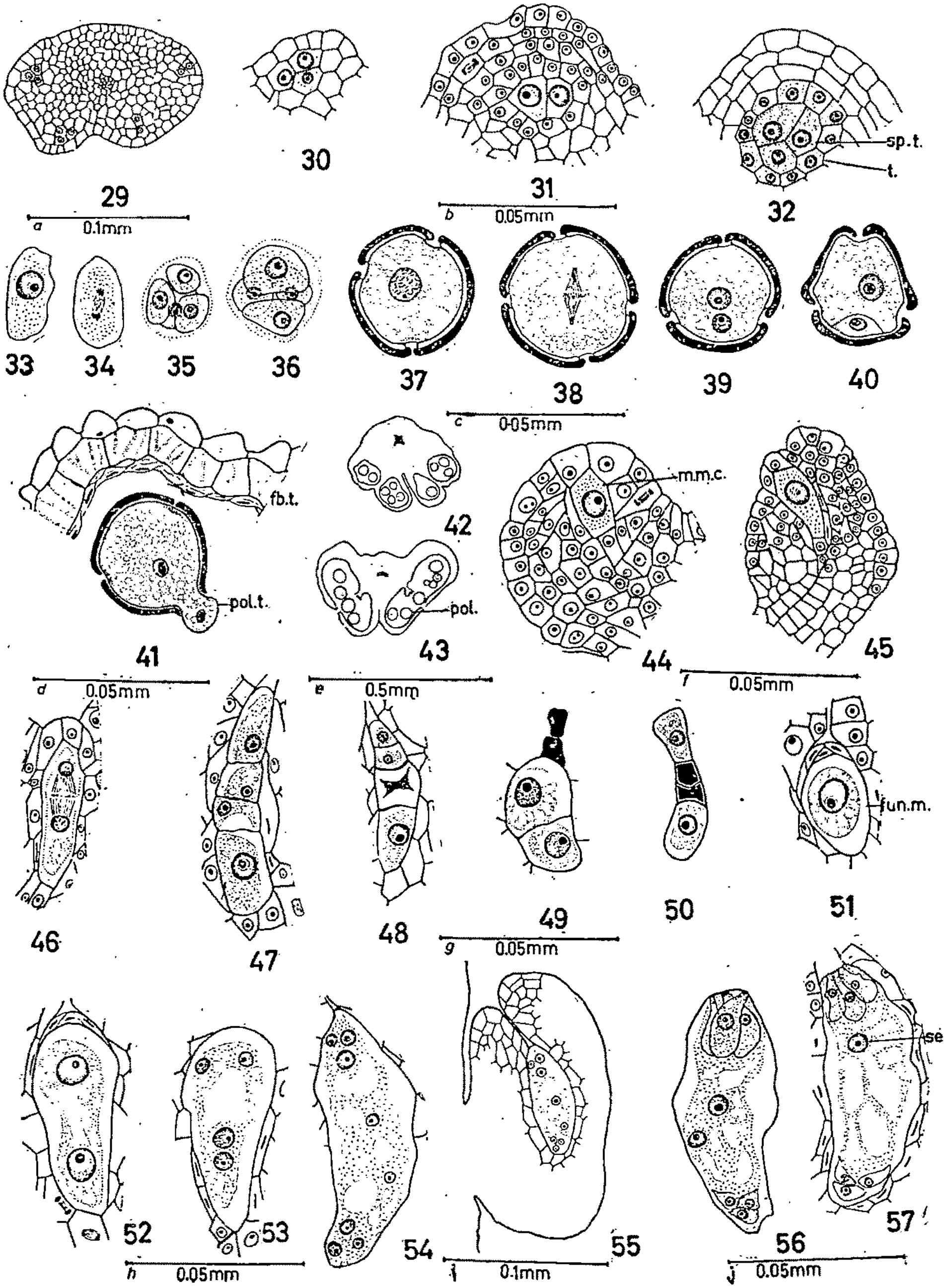
sp.t.
t.
a 0.1mm
b 0.05mm
c 0.05mm
fb.t.
pol.t.
pol.
m.m.c.
d 0.05mm
e 0.5mm
f 0.05mm
fun.m.
g 0.05mm
sec.nu.
h 0.05mm
i 0.1mm
j 0.05mm

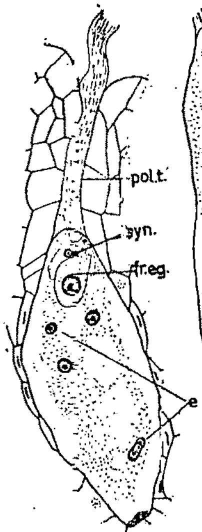

58

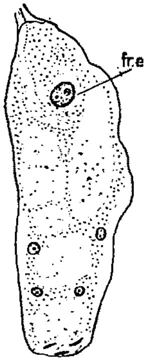

59

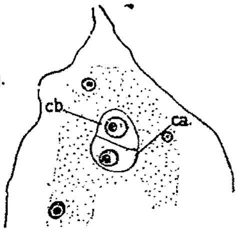

60

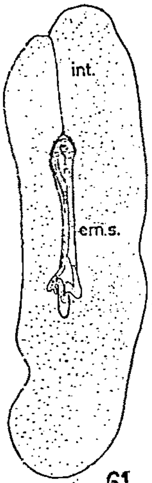

61

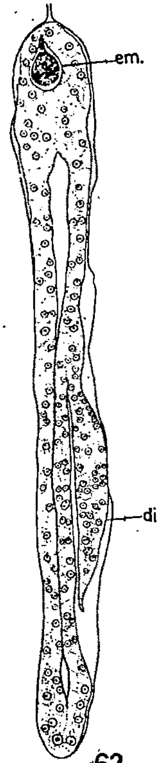

62

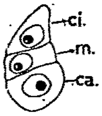

65

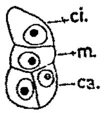

66

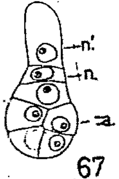

67

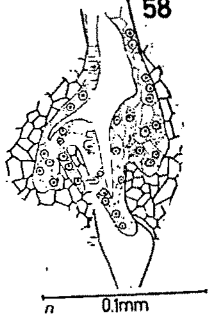

63

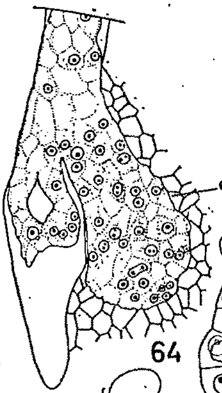

64

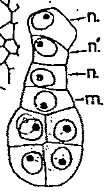

68

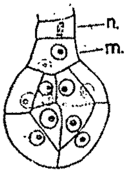

69

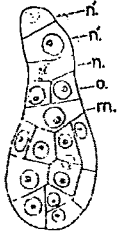

70

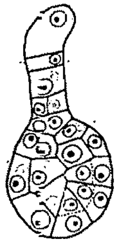

71

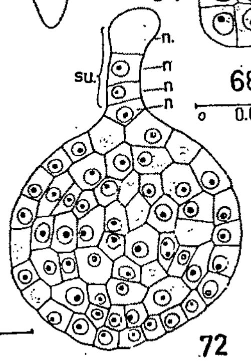

72

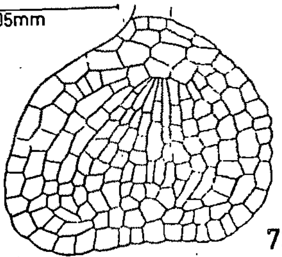

73

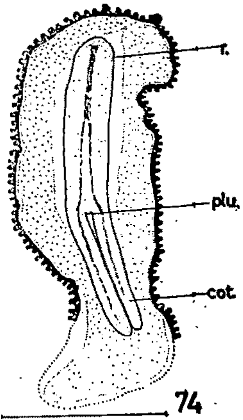

74

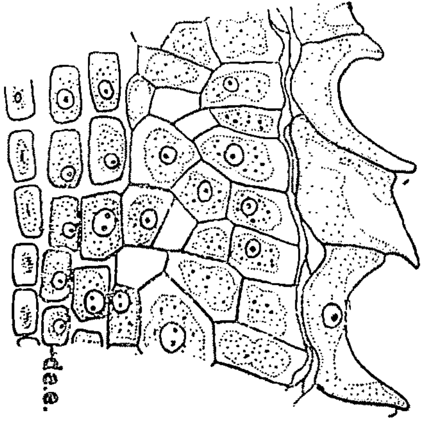

78

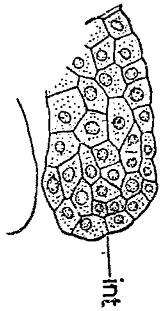

75

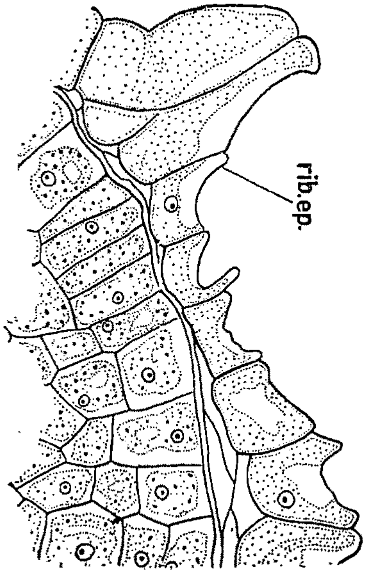

79

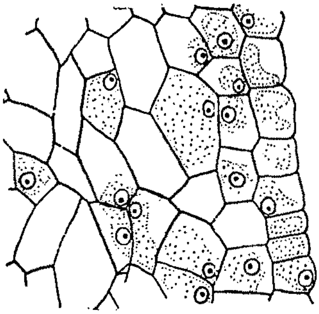

76

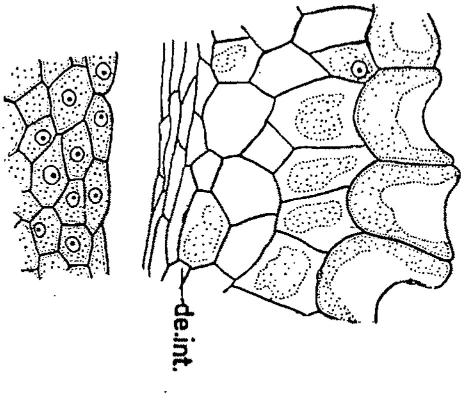

77

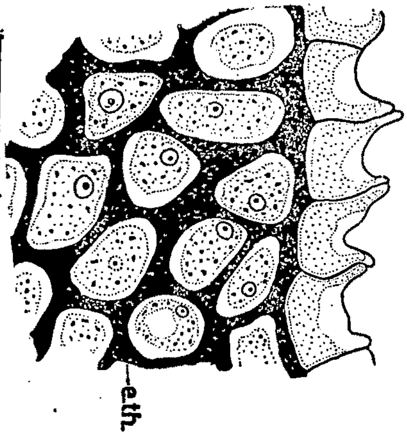

80

ABSORPTION SPECTRA OF SOME NEW KETONES

PART III—SYNTHESIS AND ABSORPTION SPECTRA OF P-CHLORO AND P-BROMO ANILIDES OF BROMO-OXYMETHYLENE ACETOPHENONE.

D. D. PANT, O. N. PERTI*, K. P. VARMA† AND G. C. SINGHAL
Physical and Chemical Laboratories, D. S. B. Govt. College, Nainital.

ABSTRACT

(Absorption spectra of p-chloro and p-bromo anilides of bromo-oxymethylene acetophenone has been studied in n-hexane. The bathochromic shift observed appears to be due to -NHC_6H_4X (X=Br or Cl) group attached to formyl carbon atom.)

INTRODUCTION

Earlier workers [3,4] have reported the UV absorption spectra of halogen formyl esters and halogen formyl acetophenones in different solvents. In the present paper we have described the UV absorption spectrum of p-chloro anilide of bromo-oxymethylene acetophenone and p-bromo anilide of bromo-oxymethylene acetophenone in n-hexane.

EXPERIMENTAL

Bromo-oxymethylene Acetophenone was prepared by the method already reported by Bokadia and Deshapande[2]. A yellow crystalline compound was obtained which was recrystallised from benzene-carbontetra chloride mixture to yield a white solid which melted at 110°C-111°C.

P-Chloro anilide of bromo-oxymethylene acetophenone was prepared from a mixture of bromo-oxymethylene acetophenone (2·2 g) and p-chloro aniline (1·27 g) in a 250 ml conical flask. Absolute alcohol (30 ml) was added to it. A sufficient quantity of anhydrous sodium acetate was added and the whole was refluxed over water bath for three hours. A yellow solid was obtained on cooling. It was separated, washed with a little aqueous alcohol and then finally with water. It was recrystallised from absolute alcohol-water mixture. Yield=2·9 g; M. P. 165·5 C. (Found : C, 53·6%; H, 3·24%; N, 4·32% Cl+Br, 34·6%; $C_{15}H_{11}OBrClN$ requires C, 53·4%; H,3·23%; N, 4·13% Cl+Br, 34·2%). It gave no colour with alcoholic ferric chloride.

P-Bromo Anilide of bromo-oxymethylene acetophenone was prepared in a manner to that described for p-chloro anilide of bromo-oxymethylene acetophenone. Starting from bromo-oxymethylene acetophenone (1·1g), p-bromo aniline (1·87) and absolute alcohol (15 ml) a dark yellow solid was obtained. It was recrystallised from alcohol water mixture. Yield=1 g; M. P. 175 C. It gave no colour with alcoholic ferric chloride.

---

* Present address—M. L. N. Regional Engineering College, Allahabad, India.

† Present address—Government Degree College, Gopeshwar, Chamoli, India.

(Found: C, 47·5%; H, 3·21%; N, 3·6%; Br,41%; $C_{15}H_{11}OBr_2N$ requires C, 47·24%; H, 2·89%; N, 3·67%; Br,41·9%)

UV absorption spectra measurements were carried out with the help oı Hilger Uvispek photo electric spectrophotometer with quartz optics. Solvent used was purified n-hexane. The strength of solution employed was in all cases $0·5 \times 10^{-4}$M.

Results are recorded in figure 1.

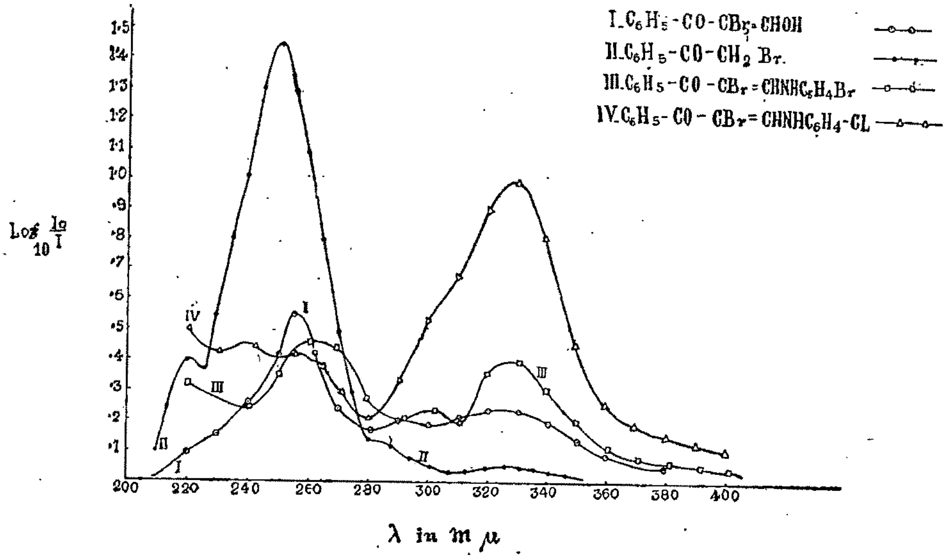

From the graph λ_{max} and ϵ_{max} are recorded in table 1.

TABLE

Compounds	λ_{max} in mμ	ϵ_{max}	λ_{max} in mμ	ϵ_{max}	λ_{max} in mμ	ϵ_{max}	λ_{max} in mμ	ϵ_{max}
I. 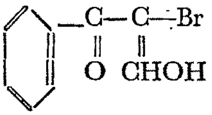	255	11,000	285	3,400	320	4,600	—	—
II. 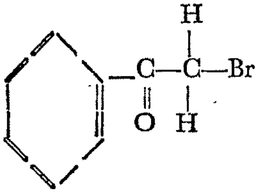	220	8,000	250	29,000	—	—	320	840
III. 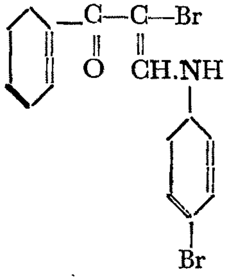 P—bromo anilide of bromo-oxymethylene acetophenone	260	9,000	300	4,600	330	8,000	—	—
IV. 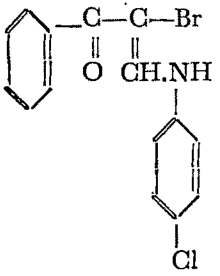 P—chloro-anilide of bromo-oxymethylene acetophenone	240	9,000	255	8,200	297	10,500	330	20,000

Note : I, II studied previously.[1,2]

DISCUSSION

Previously[3,4] we had studied the absorption spectra of α–bromo–α–formyl acetophenone and α–bromo–α–formyl–p–substituted acetophenones in n-hexane. In these compounds a bathochromic shift was observed to be due to the formyl group =CHOH.

The structures of anilides studied are as follows:—

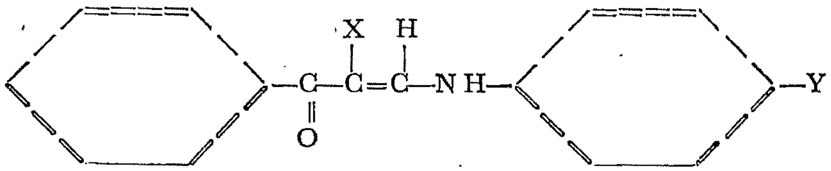

(Compounds III & IV, table ; X=Br, Y=Cl or Br)

They do not exhibit enolic character because they do not give any colour with alcoholic ferric chloride. When we compare the maxima of p-bromo anilide of bromo-oxymethylene acetophenone (III) with the maxima of α–bromo–α–formyl acetophenone (I) and phenacyl bromide it is noticed that the effect is bathochromic. It is due to $\geqslant$C–NHC_6H_4Br group. The π-electrons on the carbonyl group can apparently participate in the conjugated system, which now involves the ring, the N-atom p-electrons, and the π-electrons of the carbonyl group.

Schubert, Craven and Steadly[10] had suggested that the wave length shift was in the order I>Br>Cl>F in α–halogen acetophenones derivatives. Several workers[1,5,6,7,8] have studied extensively α–halogen cycloalkanones and steroid series of ketones and found that the equatorial or chlorine or bromine produces a small hypsochromic shift ($\sim$5 mμ) in the n→π* transition of the unsubstituted ketone; but the axial bromine and chlorine produce 20–30mμ and 11mμ bathochromic shifts, respectively, accompanied by a strong hyperchromic effect. In the case of p-chloro anilide of bromo-oxymethylene acetophenone (IV), in comparison with compounds I, II, and III (table 1) the shift is of the order of 10–20mμ indicating, by analogy, that the halogen is axial.

ACKNOWLEDGEMENTS

Authors are grateful to the authorities of D. S. B. Govt. college, Nainital for providing research facilities and also to the C. S. I. R. for senior fellowship to one of us (G. C. S.).

REFERENCES

1. Bird, C. W., Cookson, R.C. & Dandegaonker, S.H. 1956. *J. Chem. Soc.*, 3675.
2. Bokadia, M.M. & Deshapande, S.S. 1949. *J. Ind. Chem. Soc.*, **26**: 455.
3. Bokadia, M.M. & Varma, K.P. 1957-58. *J. Sci. Res. B.H.U.*, **VIII** (2): 133.
4. Bokadia, M.M. & Varma, K.P. 1958. *Agra Univ. J. Res (Sci)*.**VII** (2),: 119.
5. Cookson, R.C. 1954. *J. Chem. Soc.*, 282.

6. Fieser & M. Fieser. *Steroids*. Reinhold Publishing Corp., New York. 1959. p. 176.
7. Jone, R. N. Ramsay, D.A. Herling, F. & Dobriner, K. 1952. *J.Am. Chem. Soc.*, **74**, 2828.
8. Leonard, N. J. & Owens, F.H. 1958. *J. Am. Chem. Soc.*, **80**, 6039.
9. Pant, Perti, Varma and Singhal. 1966 Agra Univ. J. Res. (Sci.) XV (Part I), 51
10. Schubert, W.M., Craven, J. M. & Steadly, H. 1959. *J: Am. Chem. Soc.*, **81**, 2695.

FLOW OF A NON-NEWTONIAN FLUID THROUGH A RECTILINEAR PIPE

(Section: A Hyperbolic Segment)

RADHEY SHIAM 'SHIAM'
Mathematics Deptt., M. B. College, Udaipur University, Udaipur.

In this paper, the flow of Rivlin Type of liquid through a rectilinear pipe of uniform cross section has been discussed. The section of the pipe is a hyperbolic segment. The distribution of stress due to the flow has been deduced and thrust on the plane wall of the pipe has been calculated.

INTRODUCTION

Rivlin[1,2] has proposed that the rheological behaviour of certain liquids is characterised by the equation of state

$$p_{ik} = -P\delta_{ik} + 2\eta e_{ik} + 4\zeta e_{ij}.e_{ik} \qquad ..(1)$$

where η is the coefficient of viscosity and ζ is the normal stress coefficient.

Also p_{ik} and e_{ik} are stress and rate of strain tensors respectively. P is the undetermined isotropic pressure, which can be superposed on an element of liquid (in any state of motion) without affecting the flow and δ_{ik} is the Kronecker delta ($\delta_{ik}=1$ *if* $i=k$ and $\delta_{ik}=0$ *if* $i \neq k$).

It is proposed here to consider the flow of a Rivilin type of liquid through a rectilinear pipe whose cross section is a hyperbolic segment.

We take the axis of z along the axis of the pipe. Let (u, v, w) be the components of velocity parallel to the axis of x, y, z respectively. It is assumed that u and v are each zero.

The equation of continuity is

$$\frac{\partial u}{\partial x} + \frac{\partial v}{\partial y} + \frac{\partial w}{\partial z} = 0$$

whence, $$\frac{\partial w}{\partial z} = 0$$

which shows that w is a function of x and y only. We shall take η and ζ as physical constants as taken by J. R. Jones[3].

2. Rate of strain components:—

$$\left.\begin{aligned} &e_{xx} = 2\frac{\partial u}{\partial x} = 0, \quad e_{yy} = 2\frac{\partial u}{\partial y} = 0, \quad e_{zz} = 2\frac{\partial w}{\partial z} = 0 \\ &e_{yx} = e_{xy} = \frac{\partial u}{\partial y} + \frac{\partial v}{\partial x} = 0, \quad e_{yz} = e_{zy} = \frac{\partial v}{\partial z} + \frac{\partial w}{\partial y} = \frac{\partial w}{\partial y}, \quad e_{xz} = e_{zx} = \frac{\partial w}{\partial x} + \frac{\partial u}{\partial z} = \frac{\partial w}{\partial x} \end{aligned}\right\} ..(2)$$

3. Components of stress:—

From the rheological equation (1), the stress components are as follows:—

$$\left.\begin{aligned}
p_{xx}&=-P+2\eta e_{xx}+4\zeta\ (e^2_{xx}+e^2_{xy}+e^2_{xz})\\
p_{yy}&=-P+2\eta e_{yy}+4\zeta\ (e^2_{yy}+e^2_{xy}+e^2_{yz})\\
p_{zz}&=-P+2\eta e_{zz}+4\zeta\ (e^2_{zz}+e^2_{xz}+e^2_{zy})\\
p_{xy}&=p_{yx}=2\eta e_{xy}+4\zeta\ (e_{xx}\cdot e_{xy}+e_{xy}\cdot e_{yy}+e_{xz}\cdot e_{zy})\\
p_{xz}&=p_{zx}=2\eta e_{xz}+4\zeta\ (e_{yx}\cdot e_{xz}+e_{yy}\cdot e_{yz}+e_{yz}\cdot e_{zz})\\
p_{yz}&=p_{zy}=2\eta e_{yz}+4\zeta\ (e_{yx}\cdot e_{xz}+e_{yy}\cdot e_{yz}+e_{yz}\cdot e_{zz})
\end{aligned}\right\}\quad ..(3)$$

Now, substituting from equations (2) we have.

$$\left.\begin{aligned}
&p_{xx}=-P+4\zeta\left(\frac{\partial w}{\partial x}\right)^2,\ p_{yy}=-P+4\zeta\left(\frac{\partial w}{\partial y}\right)^2\\
&p_{zz}=-P+4\zeta\left\{\left(\frac{\partial w}{\partial x}\right)^2+\left(\frac{\partial w}{\partial y}\right)^2\right\},\quad p_{xy}=p_{yx}=4\zeta\left(\frac{\partial w}{\partial x}\cdot\frac{\partial w}{\partial y}\right)\\
&p_{xz}=p_{zx}=2\eta\left(\frac{\partial w}{\partial x}\right),\quad p_{yz}=p_{zy}=2\eta\left(\frac{\partial w}{\partial y}\right)
\end{aligned}\right\}\quad ..(4)$$

4. The equations of Motion are:—

$$\rho\left(\frac{\partial u}{\partial t}+u\frac{\partial u}{\partial x}+v\frac{\partial u}{\partial y}+w\frac{\partial u}{\partial z}\right)=\frac{\partial p_{xx}}{\partial x}+\frac{\partial p_{yx}}{\partial y}+\frac{\partial p_{zx}}{\partial z}\quad ...(5)$$

$$\rho\left(\frac{\partial v}{\partial t}+u\frac{\partial v}{\partial x}+v\frac{\partial v}{\partial y}+w\frac{\partial v}{\partial z}\right)=\frac{\partial p_{xy}}{\partial x}+\frac{\partial p_{yy}}{\partial y}+\frac{\partial p_{zy}}{\partial z}\quad ...(6)$$

$$\rho\left(\frac{\partial w}{\partial t}+u\frac{\partial w}{\partial x}+v\frac{\partial w}{\partial y}+w\frac{\partial w}{\partial z}\right)=\frac{\partial p_{xz}}{\partial x}+\frac{\partial p_{yz}}{\partial y}+\frac{\partial p_{zz}}{\partial z}\quad ...(7)$$

Substituting the values of stress components from the equation (4) in the above equations, the equations of motion in the case of steady flow simplify to

$$\frac{\partial P}{\partial x}=4\zeta\left\{2\frac{\partial^2 w}{\partial x^2}\cdot\frac{\partial w}{\partial x}+\frac{\partial^2 w}{\partial x\partial y}\cdot\frac{\partial w}{\partial y}+\frac{\partial^2 w}{\partial y^2}\cdot\frac{\partial w}{\partial x}\right\}\quad ..(8)$$

$$\frac{\partial P}{\partial y}=4\zeta\left\{2\frac{\partial^2 w}{\partial y^2}\cdot\frac{\partial w}{\partial y}+\frac{\partial^2 w}{\partial x\partial y}\cdot\frac{\partial w}{\partial x}+\frac{\partial^2 w}{\partial x^2}\cdot\frac{\partial w}{\partial y}\right\}\quad ..(9)$$

$$\frac{\partial P}{\partial z}=2\eta\left\{\frac{\partial^2 w}{\partial x^2}+\frac{\partial^2 w}{\partial y^2}\right\}\quad ..(10)$$

5. The solutions of the equations of Motion:—

From the equations (8), (9) and (10) it is seen that

$$\frac{\partial P}{\partial x}=f_1\,(x,y),\ \frac{\partial P}{\partial y}=f_2\,(x,y),\ \frac{\partial P}{\partial z}=f_2\,(x,y)$$

Therefore P should be of the form

$$P=Az+f\,(x,y)\quad ..(11)$$

where f is some function of x and y, A is a constant,

$$2\eta\left\{\frac{\partial^2 w}{\partial x^2}+\frac{\partial^2 w}{\partial y^2}\right\}=A\quad ..(12)$$

Boundary conditions are:

$$W=0, \text{ on the boundry chosen.}$$

J. P. Agrawal[4] has discussed flows of Newtonian fluids in pipes whose section is a hyperbolic segment. Following his method we get a solution of this equation (12) as

$$w=\frac{A}{48\eta}\left\{(y^3-3x^2y)+3\,(y^2-x^2)+\quad(x^2+y^2)-10\right\} \qquad ..(13)$$

which vanishes on the boundaries defined by

$$\left.\begin{array}{l} y=1 \\ y^2+10y-3x^2+10=0 \end{array}\right\} \qquad ..(14)$$

We shall investigate whether this value of w together with a suitable value of P satisfies the equations (8) and (9).

Substituting in equations (8) and (9) the values of w and P from equations (13) and (11) respectively, we get

$$\frac{\partial f}{\partial x}=4\zeta\left(\frac{A}{48\eta}\right)^2\left\{180x-324xy+18xy^2+18x^3\right\} \qquad ..(15)$$

$$\frac{\partial f}{\partial y}=4\zeta\left(\frac{A}{48\eta}\right)^2\left\{756y+234y^2-162x^2+18x^2y+18y^3\right\} \qquad ..(16)$$

To test, whether these equations are competible.

From equation (15), $\dfrac{\partial^2 f}{\partial x\partial y}=36xy-324x$

From equation (16), $\dfrac{\partial^2 f}{\partial x\partial y}=36x-324x$

which shows that a value of f exists which satisfies the equations (15) and (16).

From equations (15) and (16)

$$f=4\zeta\left(\frac{A}{48\eta}\right)^2\left\{90x^2+378y^2+78y^3-162x^2y+9x^2y^2+\frac{9}{2}(x^4+y^4)\right\}+C \qquad ..(17)$$

Whence,

$$P=Az+4\zeta\left(\frac{A}{48\eta}\right)^2\left\{90x^2+378y^2+78y^3-162x^2y+9x^2y^2+\frac{9}{2}(x^4+y^4)\right\}+C \qquad ..(18)$$

To determine the constants A and C, let us assume

$$P=p_1,\ z=0,\ x=0=y$$
$$P=p_2,\ z=0,\ x=0=y$$

Therefore, $A=\dfrac{p_2-p_1}{l}$ and $C=p_r$

Hence,

$$P=\frac{p_2-p_1}{l}z+4\zeta\left(\frac{p_2-p_1}{48\eta l}\right)^2\left\{\frac{9}{2}(x^4+y^4)+9x^2y^2+78y^3-162x^2y+90x^2 +371y^2\right\}+p_1 \qquad ..(19)$$

6. Values of the stress components:—

Substituting the values of P in the equations (4), the values of stress components are:—

$$\left.\begin{aligned}
p_{xx}&=4\zeta\left(\frac{p_2-p_1}{48\eta l}\right)^2\left\{27x^2y^2-\frac{9}{2}(x^4+y^4)+90x^2y-78y^3-54x^2-378y^2\right\}\\
&\qquad-\frac{p_2-p_1}{l}z-p_1\\
p_{yy}&=4\zeta\left(\frac{p_2-p_1}{48\eta l}\right)^2\left\{\frac{9}{2}(x^4+y^4)-27x^2y^2+30y^3+54x^2y-90x^2-54y^2\right\}\\
&\qquad-\frac{p_2-p_1}{l}z-p_1\\
p_{zz}&=4\zeta\left(\frac{p_2-p_1}{48\eta l}\right)^2\left\{\frac{9}{2}(x^4+y^4)+9x^2y^2-18x^2y+30y^3-54y^2-54x^2\right\}\\
&\qquad-\frac{p_2-p_1}{l}z-p_1\\
p_{xy}&=p_{yx}=4\zeta\left(\frac{p_2-p_1}{48\eta l}\right)\left\{6x^3y-90xy^2-18x^3+108xy-18xy^3\right\}\\
p_{xz}&=p_{zx}=2\eta\left(\frac{p_2-p_1}{48\eta l}\right)(6x-6xy)\\
p_{yz}&=p_{zy}=2\eta\left(\frac{p_2-p_1}{48\eta l}\right)(3y^2-3x^2+18y)
\end{aligned}\right\}\quad ..(20)$$

7. Calculations of thrust on the plane wall of the pipe.

On $y=1$

$$p_{yy}=4\zeta\left(\frac{p_2-p_1}{48\eta l}\right)^2\left\{\frac{9}{2}x^4-63x^2-\frac{39}{2}\right\}-\frac{p_2-p_1}{l}z-p_1 \qquad ..(21)$$

In accordance with the well known convention[5] regarding sign of stress, the the sign of p_{yy} is to be changed to find out thrust.

Hence, Thrust on the plane wall

$$=-\int_0^l\int_{-\sqrt{7}}^{\sqrt{7}} p_{yy}\ dxdz$$

$$=-\int_0^l\int_{-\sqrt{7}}^{\sqrt{7}}\left[4\zeta\left(\frac{p_2-p_1}{48\eta l}\right)^2\left(\frac{9}{2}x^4-63x^2-\frac{39}{2}\right)-\frac{p_2-p_1}{l}z-p_1\right]dxdz$$

$$=\sqrt{7}\int_0^l\left[4\zeta\left(\frac{p_2-p_1}{48\eta l}\right)^2\left(\frac{1224}{5}\right)+2\left(\frac{p_2-p_1}{l}\right)z+2p_1\right]dz$$

$$=\sqrt{7}\,l\left[4\zeta\left(\frac{p_2-p_1}{48\eta l}\right)^2\left(\frac{1224}{5}\right)+(p_2+p_1)\right]$$

ACKNOWLEDGMENT

I want to express my gratitude to Dr. J. P. Agrawal for his guidance.

REFERENCES

1. Rivilin, R. S., 1948. *Proc. Roy. Soc.* A. 193, 260.
2. Rivilin, R. S., 1949. *Trans. Faraday Soc.* 45, 739.
3. Jones, J. R., 1960. *Quart. Jour. Mech. & Applied Maths.* Vol. XIII, 4. 429.
4. Agrawal, J. P., 1959- *Uttara Bharti*, Vol. VI, 2, 117.
5. Ramsay. *Treatise on Hydromachanics*, p. **365**, Art. 13-21.

VARIATIONAL PRINCIPLE FOR SCALAR WAVE EQUATION LAGRANGE FORMALISM

S. C. GUPTA

Department of Mathematics, Roorkee University, Roorkee.

SUMMARY

A variational principle for the scalar wave equation has been formulated along the lines of Biot (for heat conduction). The Lagrange formalism in generalized coordinates leads to equations which are of the same form as are encountered in classical mechanics. Defining quantities here called pseudo-momenta, the equations for canonical conjugates have been obtained and they are exactly of the same form as are come across in Hamiltonian treatment of classical dynamics. This leads to the formulation of a Liouville's theorem for the development of statistical mechanics for phenomena governed by the wave equation in continuous media. Some general procedures and methods for solving problems in special cases have been given together with an illustrative one dimensional example.

INTRODUCTION

The scalar wave equation occurs in many branches of mathematical physics. The propagation of sound waves of small amplitudes in compressible media, vibrations of thin elastic membranes, propagation of electric and magnetic intensities in electromagnetic wave and a host of other phenomena are governed by this equation.

A variational principle for the wave equation corresponding to the requirement that the difference between the total kinetic energy and the potential energy may be as small as possible and using the concept of Hamiltonian density, already exists in literature[6]. The canonical equations for the conjugates are not as simple as those encountered in classical mechanics. The dependence of the Hamiltonian explicitly on the space variables x, y, z introduces the complexity. It is clear that the canonical formalism is not suited for the development of statistical mechanics for phenomena governed by the wave equation in continuous media.

The variational principle of Leech[4] is the analogue of the Lagrangian formulation in classical mechanics of discrete particles. The generalised coordinates q_r are functions of x, y, z and t (not of t alone). The variational principle of Leech is

$$\delta \int_{t_0}^{t_1} \int_{\tau} a \; d\tau . \; dt = 0$$

where

$$\alpha=\tfrac{1}{2}\left[\left(\frac{\partial\phi}{\partial t}\right)^2-c^2\left\{\left(\frac{\partial\phi}{\partial x}\right)^2+\left(\frac{\partial\phi}{\partial y}\right)^2+\left(\frac{\partial\phi}{\partial z}\right)^2\right\}\right].$$

Taking account of the variation $\delta\phi$ and regarding x, y, z and t as the field parameters one obtains the wave equation from the variational principle. The variation of the integral is to be carried out by varying the path of integration in such a way that the end points $(\phi_0, x_0, y_0, z_0, t_0)$ and $(\phi_1, x_1, y_1, z_1, t_1)$ are fixed for each particle. If

$$L=\int_\tau \alpha\, d\tau,\quad d\tau=dx.\,dy.\,dz, \qquad \ldots(1.1)$$

where τ is the region where the wave disturbance ϕ exists, then using the notation of a functional derivative.

$$\frac{\delta L}{\delta q_r}=\frac{\partial\alpha}{\partial q_r}-\Sigma\frac{d}{dx}\frac{\partial\alpha}{\partial q_{r,x}}, \qquad \ldots(1.2)$$

where

$$\frac{d}{dt}\equiv\frac{\partial}{\partial t}+\frac{\partial\phi}{\partial t}\frac{\partial}{\partial\phi}+\Sigma\frac{\partial\phi_{,x}}{\partial t}.\frac{\partial}{\partial\phi_{,x}}+\frac{\partial\dot{\phi}}{\partial t}.\frac{\partial}{\partial\dot{\phi}}, \qquad \ldots(1.3)$$

and similar expressions for d/dx, d/dy, d/dz, a canonical form of the equations is obtained as below.

$$\frac{\partial\alpha}{\partial q_r}-\frac{d}{dt}\frac{\partial\alpha}{\partial\dot{q}_r}-\Sigma\frac{d}{dx}\frac{\partial\alpha}{\partial q_{r,x}}=0, \qquad \ldots(1.4)$$

or

$$\frac{d}{dt}\frac{\delta L}{\delta\dot{q}_r}=\frac{\partial L}{\partial q_r}. \qquad \ldots(1.5)$$

Admittedly this is a concise relation analogous in form to the corresponding one in classical particle dynamics, but it conveys no further information than (1.4). This formalism also is not suitable for the development of statistical mechanics.

This paper deals with the formulation of a variational principle based on the concept of generalised coordinates and is slightly different from that of Leech. We consider q_r which are functions of t alone. A vector field H and a scalar point function V related to the wave function ϕ are introduced. The variation δH (depending on δq_r) leads to the Lagrangian form of equations for q_r which are identical with the equations in classical dynamics. This procedure has been developed by Biot[1] in his treatment of the transient heat conduction phenomena. This formulation has a distinct advantage over the principles mentioned earlier because in this case Liouville's Theorem[3] of a permanent flow in the phase space can be readily proved. Moreover all the general methods developed in classical statistical mechanics are at once applicable to the wave phenomena. The essential point of difference would be that the phenomena may depend on a countably infinite number of generalised coordinates. This approach is being followed by Joshi and Nigam*.

---

* N. E. Joshi and S. D. Nigam are making an attempt to develop a statistical mechanics based on this variational formulation at I. I. T.. Kharagpur, INDIA.

THE SCALAR WAVE EQUATION AND THE VARIATIONAL PRINCIPLE

Attention here will be confined only to the three dimensional scalar wave equation. The results arrived at can easily be extended to any number of dimensions. The equation is

$$\frac{\partial^2\phi}{\partial t^2}=c^2\left(\frac{\partial^2\phi}{\partial x^2}+\frac{\partial^2\phi}{\partial y^2}+\frac{\partial^2\phi}{\partial z^2}\right), \qquad \ldots(2.1)$$

where c is the wave velocity and in general is a function of x, y, z. The wave transmission takes place in an isotropic medium.

Define a vector field H by

$$\frac{\phi}{c^2}=-\nabla . \mathrm{H},\ \nabla\equiv i\frac{\partial}{\partial x}+j\frac{\partial}{\partial y}+k\frac{\partial}{\partial z}, \qquad \ldots(2.2)$$

a scalar function of position V by

$$\mathrm{V}=\tfrac{1}{2}\int_\tau \frac{\phi^2}{c^2}\,d\tau, \qquad \ldots(2.3)$$

and a variational invariant δD by

$$\delta \mathrm{D}=\int_\tau \frac{\partial^2 \mathrm{H}}{\partial t^2}.\ \delta \mathrm{H}\ d\tau. \qquad \ldots(2.4)$$

Also take

$$\frac{\partial^2 \mathrm{H}}{\partial t^2}=-\nabla\phi. \qquad \ldots(2.5)$$

The variational principle is stated as

$$\delta \mathrm{V}+\delta \mathrm{D}=\int_s \phi n.\ \delta \mathrm{H}\ ds, \qquad \ldots(2.6)$$

where the surface integral extends over the surface S bounding the region τ and n is a unit inward drawn normal to an element of S.

For an arbitrary variation δH, (2.6) must lead to (2.1). From equations (2.3) and (2.2)

$$\delta \mathrm{V}=\int_\tau \frac{\phi}{c^2}\,\delta\phi\ d\tau=-\int_\tau \phi\delta\ (\nabla . \mathrm{H})\ d\tau$$

for ∇ and δ commute. Integration by parts leads to

$$\delta \mathrm{V}=\int_\tau \nabla\phi .\ \delta \mathrm{H}\ a\tau+\int_s \phi n.\ \delta \mathrm{H}\, ds. \qquad \ldots(2.7)$$

Substituting the values of δD from (2.4) and δV from (2.7) in the variational principle (2.6) one obtains

$$\int_\tau \left[\nabla\ \phi+\frac{\partial^2 \mathrm{H}}{\partial t^2}\right].\ \delta \mathrm{H}\ a\tau=0. \qquad \ldots(2.8)$$

Since δH is arbitrary, we must have

$$\nabla\ \phi+\frac{\partial^2 \mathrm{H}}{\partial t^2}=0. \qquad \ldots(2.9)$$

Taking divergence of (2.9) and using (2.2) we obtain the equation (2.1). Hence the variational principle is valid.

LAGRANGE FORMALISM

At this stage we introduce generalised coordinates in association with the variational principle. There are many ways in which this can be done. The vector H can be expressed in terms of the generalised coordinates q_l ($l=1, 2, 3, \ldots\ldots\ldots, m$) by means of the relation

$$H=H\,(q_1, q_2, q_3, \ldots\ldots\ldots q_m\,;\, x, y, z). \qquad \ldots(3.1)$$

Here the generalised coordinates are simply a set of m parameters defining the field configuration and are all functions of t only. There are physical situations in which the vector H is linearly connected with the coordinates q_l. (The explicit dependence of H on t is excluded). In order to cover a wider case we assume here a general dependence of H on q_l's. Sometimes it proves advantageous even in linear problems to choose generalised coordinates which are related non-linearly to the unknown variables[1].

The variations δH arise entirely on account of the variations in q_l's and hence

$$\delta H=\sum_{r=1}^{m} \frac{\partial H}{\partial q_r}\,\delta q_r \qquad \ldots(3.2)$$

and we can also write

$$\frac{\partial H}{\partial t}=\sum_{r=1}^{m} \frac{\partial H}{\partial q_r}\cdot \dot{q}_r, \qquad \ldots(3.3)$$

where a dot denotes differentiation with respect to time. Differentiating (3 3) with respect to $\dot{q}_r$

$$\frac{\partial}{\partial \dot{q}_r}\left(\frac{\partial H}{\partial t}\right)=\frac{\partial H}{\partial q_r}. \qquad \ldots(3.4)$$

The invariant

$$\delta D= \int_\tau \frac{\partial^2 H}{\partial t^2}\cdot \delta H.\, d\tau$$

$$=\int_\tau \frac{\partial^2 H}{\partial t^2}\cdot \sum_{r=1}^{m} \frac{\partial}{\partial \dot{q}_r}\left(\frac{\partial H}{\partial t}\right)\delta q_r\, d\tau. \qquad \ldots(3.5)$$

Let

$$I=\tfrac{1}{2}\left(\frac{\partial H}{\partial t}\right)^2=\tfrac{1}{2}\sum_{rs} \frac{\partial H}{\partial q_r}\cdot\frac{\partial H}{\partial q_s}\dot{q}_r\,\dot{q}_s. \qquad \ldots(3.6)$$

This gives

$$\frac{\partial I}{\partial \dot{q}_r}=\sum_s \frac{\partial H}{\partial q_r}\cdot \frac{\partial H}{\partial q_s}\dot{q}_s. \qquad \ldots(3.7)$$

Differentiating (3.7) with respect to t, we have

$$\frac{d}{dt}\left(\frac{\partial I}{\partial \dot{q}_r}\right)=\sum_s \ddot{q}_s\,\frac{\partial H}{\partial q_r}\cdot\frac{\partial H}{\partial q_s}+\sum_s\left[\sum_k\left(\frac{\partial H}{\partial q_s}\cdot\frac{\partial^2 H}{\partial q_k\,\partial q_r}+\frac{\partial H}{\partial q_r}\cdot\frac{\partial^2 H}{\partial q_s \partial q_k}\right)\dot{q}_k\right]\dot{q}_s$$

$$=\sum_s \ddot{q}_s\,\frac{\partial H}{\partial q_r}\cdot\frac{\partial H}{\partial q_s}+2\sum_{sk}\frac{\partial H}{\partial q_s}\cdot\frac{\partial^2 H}{\partial q_k \partial q_r}\dot{q}_s\,\dot{q}_k \qquad \ldots(3.8)$$

Again

$$\frac{\partial \mathrm{I}}{\partial q_r} = \tfrac{1}{2}\left(\sum_{sk} \frac{\partial^2 \mathrm{H}}{\partial q_r \partial q_k} \cdot \frac{\partial \mathrm{H}}{\partial q_s} + \sum_{sk} \frac{\partial \mathrm{H}}{\partial q_r} \cdot \frac{\partial^2 \mathrm{H}}{\partial q_s \partial q_k}\right) \dot{q}_k \dot{q}_s$$

$$= \sum_{sk} \frac{\partial^2 \mathrm{H}}{\partial q_r \partial q_k} \cdot \frac{\partial \mathrm{H}}{\partial q_s} \dot{q}_k \dot{q}_s. \qquad \ldots(3.9)$$

Equations (3.8) and (3.9) give

$$\frac{d}{dt}\left(\frac{\partial \mathrm{I}}{\partial \dot{q}_r}\right) - \frac{\partial \mathrm{I}}{\partial q_r} = \sum_s \ddot{q}_s \frac{\partial \mathrm{H}}{\partial q_s} \cdot \frac{\partial \mathrm{H}}{\partial q_r} + \sum_{sk} \frac{\partial \mathrm{H}}{\partial q_r} \cdot \frac{\partial^2 \mathrm{H}}{\partial q_k \partial q_s} \dot{q}_s \dot{q}_k. \qquad \ldots(3.10)$$

Differentiating (3.3) with respect to t (replacing r by s)

$$\frac{\partial^2 \mathrm{H}}{\partial t^2} = \sum_s \left(\ddot{q}_s \frac{\partial \mathrm{H}}{\partial q_s} + \sum_k \frac{\partial^2 \mathrm{H}}{\partial q_s \partial q_k} \dot{q}_s \dot{q}_k\right).$$

Multiplying this by $\frac{\partial \mathrm{H}}{\partial q_r}$ by a dot product and using (3.4)

$$\frac{\partial^2 \mathrm{H}}{\partial t^2} \cdot \frac{\partial}{\partial \dot{q}_r}\left(\frac{\partial \mathrm{H}}{\partial t}\right) = \sum_s \ddot{q}_s \frac{\partial \mathrm{H}}{\partial q_s} \cdot \frac{\partial \mathrm{H}}{\partial q_r} + \sum_{sk} \frac{\partial^2 \mathrm{H}}{\partial q_s \partial q_k} \cdot \frac{\partial \mathrm{H}}{\partial q_r} \dot{q}_s \dot{q}_k$$

$$= \frac{d}{dt}\left(\frac{\partial \mathrm{I}}{\partial \dot{q}_r}\right) - \frac{\partial \mathrm{I}}{\partial q_r}. \qquad \ldots(3.11)$$

Therefore if

$$\mathrm{L} = \tfrac{1}{2} \int_\tau \left(\frac{\partial \mathrm{H}}{\partial t}\right)^2 d\tau, \qquad \ldots(3.12)$$

then

$$\delta \mathrm{D} = \int_\tau \frac{\partial^2 \mathrm{H}}{\partial t^2} \cdot \sum_r \frac{\partial}{\partial \dot{q}_r}\left(\frac{\partial \mathrm{H}}{\partial t}\right) \delta q_r .\, d\tau$$

$$= \sum_r \left[\frac{d}{dt}\left(\frac{\partial \mathrm{L}}{\partial \dot{q}_r}\right) - \frac{\partial \mathrm{L}}{\partial q_r}\right] \delta qr \qquad \ldots(3.13)$$

Next we put

$$\int_s \phi n .\, \delta \mathrm{H}\, ds = \sum_r \mathrm{Q}_r\, \delta q_r, \qquad \ldots(3.14)$$

where

$$\mathrm{Q}_r = \int_s \phi \frac{\partial \mathrm{H}_n}{\partial q_r} ds. \qquad \ldots(3.15)$$

H_n denoting the inward normal component of H at the boundary S. Further

$$\delta \mathrm{V} = \sum_r \frac{\partial \mathrm{V}}{\partial q_r} \delta q_r. \qquad \ldots(3.16)$$

Substituting the values of δV from (3.16), δD from (3.13) in equation (2.6) and using (3.14) one obtains

$$\sum_r \left[\frac{d}{dt}\left(\frac{\partial \mathrm{L}}{\partial \dot{q}_r}\right) - \frac{\partial \mathrm{L}}{\partial q_r} + \frac{\partial \mathrm{V}}{\partial q_r} - \mathrm{Q}_r\right] \delta q_r = 0. \qquad \ldots(3.17)$$

Here, since δq_r are arbitrary and independent, we get the following equations

$$\frac{d}{dt}\left(\frac{\partial \mathrm{L}}{\partial \dot{q}_r}\right) - \frac{\partial \mathrm{L}}{\partial \dot{q}_r} + \frac{\partial \mathrm{V}}{\partial q_r} - \mathrm{Q}_r = 0, \ (r = 1, 2, \ldots\ldots, m.) \qquad \ldots(3.18)$$

These equations are analogous in form to the Lagrangian equations of classical mechanics but the quantities L and V do not have the dimensions of kinetic energy and potential energy respectively. They can be called the pseudo kinetic and potential energies. The quantity Q_r will be called pseudo generalised external force or external cause.

An Alternative Variational Formulation

In the special case when the quantities Q_r analogous to external impressed forces, are either zero or derivable from a potential function and c is a constant (c will be assumed constant in the rest of this paper), an alternative variational formulation can be given. Here we assume $Q_r=0$. The case when Q_r can be expressed as $-\partial U/\partial q_r$ can be easily considered by a slight modification of the procedure given below:

The variational principle is

$$\delta\int_{t_0}^{t_1}(L-V)\,dt=0. \qquad \dots(4.1)$$

All variations are zero at times t_0 and t_1, and also at the boundary S of the region occupied by the medium in which wave propagation takes place. L is given by (3.12) and

$$V=\tfrac{1}{2}\int_{\tau} c^2\,(\nabla.\,H)^2\,d\tau, \qquad \dots(4.2)$$

the vector H having the same definition as before. Equation (4.1) gives

$$\delta\int_{t_0}^{t_1}dt\int_{\tau}\left[\left(\frac{\partial H}{\partial t}\right)^2-c^2\,(\nabla.\,H)^2\right]d\tau=0$$

or

$$\int_{t_0}^{t_1}dt\int_{\tau}\left[\frac{\partial H}{\partial t}.\frac{\partial \delta H}{\partial t}-c^2\,(\nabla.\,H)(\nabla.\,\delta H)\right]d\tau=0.$$

Integrating the first term by parts with regard to time (since the variables t, x, y, z are independent and the region of integration fixed, order of integration does not matter) one obtains

$$\int_{\tau}\left[\delta H.\,\frac{\partial H}{dt}\right]_{t_0}^{t_1}d\tau-\int_{t_0}^{t_1}\int_{\tau}\frac{\partial^2 H}{\partial t^2}.\,\delta H.\,d\tau\,dt-\int_{t_0}^{t_1}\int_{\tau}c^2\,(\nabla.H)(\nabla.\delta H)\,d\tau\,dt=0$$

The first term vanishes, since $\delta H=0$ at times t_0 and t_1. Thus

$$\int_{t_0}^{t_1}\int_{\tau}\left[c^2(\nabla.H)(\nabla.\delta H)+\frac{\partial^2 H}{\partial t^2}.\,\delta H\right]d\tau.\,dt=0.$$

Integrating the first term by parts with respect to the space variables x, y, z one finds that the surface integral vanishes on account of the variations being zero at the boundary, and the following result is obtained

$$\int_{t_0}^{t_1}\int_{\tau}\delta H.\left[\frac{\partial^2 H}{\partial t^2}-c^2\,\nabla(\nabla.H)\right]d\tau.\,dt=0. \qquad \dots(4.3)$$

Since δH is arbitrary, using (2.2) this yields

$$\nabla\phi+\frac{\partial^2 H}{\partial t^2}=0 \qquad \ldots(4.4)$$

Taking the divergence of this equation we get the wave equation showing the validity of the variational principle.

CANONICAL EQUATIONS AND LIOUVILLE'S THEOREM

The system will be called conservative when the quantities Q_r are either zero or derivable from a function by differentiating it with respect to the generalized coordinates. For simplicity Q_r will be taken to be zero. The quantity W (here called the Hamiltonian when expressed in terms of q_r and p_r (the generalized pseudo momenta to be defined presently) is given by

$$W=L+V \qquad \ldots(5.1)$$

and remains constant as the system undergoes transformation.

The Lagrangian density function is $L-V=P$ say. We can write $W=2L-P$. The variational principle can then be expressed as $\delta\int(2L-P)\,dt=0$. The generalized pseudo momentum p_r is defined as

$$p_r=\frac{\partial L}{\partial \dot{q}_r}=\frac{\partial P}{\partial \dot{q}r}, \qquad \ldots(5.2)$$

since V is not a function of $\dot{q}_r$'s.

From (6.4) [Here the linear relationship between H and q_r is not necessary],

$$p_r=\sum_s b_{rs}\,\dot{q}_s. \qquad \ldots(5.3)$$

Therefore

$$2L=\sum_r p_r\,\dot{q}r=P+W. \qquad \ldots(5.4)$$

This gives

$$W=\Sigma p\dot{q}-P.$$

For a small change in p's and q's

$$dW=\Sigma p\,d\dot{q}+\Sigma\dot{q}\,dp-\Sigma\frac{\partial P}{\partial\dot{q}}\,d\dot{q}-\Sigma\frac{\partial P}{\partial q}dq$$

$$=\Sigma\dot{q}\,dp-\Sigma\frac{\partial P}{\partial q}dq, \qquad \ldots(5.5)$$

using (5.2). Thus W can be expressed in terms of p and q. The variation of $\int P\,dt$ gives

$$\delta\int_{t_0}^{t_1}(2L-W)dt=\int_{t_0}^{t_1}\sum_r\left[p_r\,\delta\dot{q}_r+\dot{q}_r\,\delta p_r-\frac{\partial W}{\partial q_r}\delta q_r-\frac{\partial W}{\partial p_r}\delta p_r\right]dt.$$

Here δq_r and δp_r are the variations in q_r and p_r. Integrating the terms

$p_r \cdot \delta\dot{q}_r \left[= p_r \frac{d}{dt}(\delta q_r) \right]$ by parts we obtain from the variational principle

$$\int_{t_0}^{t_1} \sum_r \left[\left(-\dot{p}_r - \frac{\partial W}{\partial q_r}\right) \delta q_r + \left(\dot{q}_r - \frac{\partial W}{\partial p_r}\right) \delta p_r \right] dt = 0. \qquad ..(5.6)$$

Varying p's and q's independently, from (5.6) we obtain the following canonical equations

$$\dot{q}_r = \frac{\partial W}{\partial p_r}, \ \dot{\beta}_r = -\frac{\partial W}{\partial q_r}. \qquad ..(5.7)$$

It can easily be seen that the Hamiltonian W is independent of time. For

$$\frac{dW}{dt} = \sum_r \left(\frac{\partial W}{\partial q_r} \frac{dq_r}{dt} + \frac{\partial W}{\partial p_r} \cdot \frac{dp_r}{dt} \right) = 0, \qquad ..(5.8)$$

by the use of (5.7). The formulation of a parallel theorem to that of Liouville in statistical mechanics is a simple matter[3].

Some General Considerations when the Vector Field H is Linearly Dependent on q_r: Normal and Ignorable Coordinates

We shall assume that the vector field H depends linearly on the generalized coordinates. Thus let

$$H = \sum_r q_r H_r, \qquad ..(6.1)$$

where H_r (x, y, z) are fixed configurations. Here

$$V = \tfrac{1}{2} \int_\tau \frac{\dot{\phi}^2}{c^2} d\tau = \tfrac{1}{2} c^2 \int_\tau (\nabla \cdot H)^2 \, d\tau$$

$$= \tfrac{1}{2} c^2 \int_\tau \left(\sum_r q_r \nabla \cdot H_r \right)^2 d\tau = \tfrac{1}{2} \sum_{rs} a_{rs} \, q_r \, q_s, \qquad ..(6.2)$$

where

$$a_{rs} = c^2 \int_\tau (\nabla \cdot H_r)(\nabla \cdot H_s) \, d\tau. \qquad ..(6.3)$$

The quadratic form $\sum_{rs} a_{rs} q_r q_s$ is positive definite and the matrix $[a_{rs}]$ is symmetric. Similarly

$$L = \tfrac{1}{2} \int_\tau \left(\frac{\partial H}{\partial t} \right)^2 d\tau = \tfrac{1}{2} \int_\tau \left(\sum_r \dot{q}_r H_r \right)^2 d\tau$$

$$= \tfrac{1}{2} \sum_{rs} b_{rs} \, \dot{q}_r \, \dot{q}_s, \qquad ..(6.4)$$

where

$$b_{rs} = \int_\tau H_r \cdot H_s \, d\tau. \qquad ..(6.5)$$

It is obvious that

$$\frac{\partial L}{\partial q_r} = 0. \qquad ..(6.6)$$

The quadratic form $\sum_{rs} b_{rs}\, \dot{q}_r\, \dot{q}_s$ is positive definite and the matrix $[b_{rs}]$ is symmetric. In order to write down the Lagrangian equation (3.18) for the unknown generalized coordinates q_r, making use of the above results one obtains

$$\sum_s (b_{rs}\, \ddot{q}_s + a_{rs}\, q_s) = Q_r, \ (r=1, 2, \ldots, m)$$

$$\sum_s (b_{rs}\, p^2 + a_{rs})\ q_s = Q_r, \ p \equiv \frac{d}{dt}. \qquad ..(6.7)$$

We first study the solutions of the equations (6.7) in the special case $Q_r=0$. These equations then become

$$\sum_s (b_{rs}\, p^2 + a_{rs})\, q_s = 0. \qquad ..(6.8)$$

Eliminating q_s's from these equations one arrives at the determinantal equation in p

$$\det |\, p^2\, b_{rs} + a_{rs}\, | = 0. \qquad ..(6.9)$$

This is an equation of degree m in p^2. After calculating the values of p^2, those of p can be easily obtained and their number will be $2m$.

In order that the results may be generally applicable we shall attribute m roots to (6.9) in p^2, despite the fact that some of the roots may be repeated and some others infinite. From a well-known theorem in the theory of matrices[2] we know that the roots of (6.9) in p^2, are all real and never positive. Let the roots be $-\lambda^2_u$ $(u=1, 2, \ldots\ldots, m)$; the quantities λ_u are either positive or zero. Two or more of them may be equal. The values of p then are

$$p = -i\lambda_u, +i\lambda_u, \text{ where } i=\sqrt{-1}, \ (u=1, 2, \ldots\ldots, m). \qquad ..(6.10)$$

The general solutions of equations (6.8) which are periodic are

$$q_r = \sum_u \Big[\psi^{(u)}_{r_1} \sin \lambda_u t + \psi^{(u)}_{r_2} \cos \lambda_u t], \qquad ..(6.11)$$

the summation extending over all the roots taken all distinct. The result in (6.11) may be written as

$$q_r = \sum_u \chi^{(u)}_{r_1} \cos (\lambda_u t + \chi^{(u)}_{r_2}). \qquad ..(6.12)$$

where

$$\chi^{(u)}_{r_1} \cos \chi^{(u)}_{r_2} = \psi^{(u)}_{r_1}, -\chi^{(u)}_{r_1} \sin \chi^{(u)}_{r_2} = \psi^{(u)}_{r_2}. \qquad ..(6.13)$$

To each value of λ_u there will correspond a normal mode of the system. They will be called characteristic solutions. Since there is no essential difference between a sine and a cosine function (as far as the following discussion is concerned) excepting that one differs from the other in phase (by $\pi/2$), we take for convenience in further discussion $\chi_{r_2}^{(u)}=0$, in which case the right hand side of (6.12) will consist of cosines only and when $\chi_{r_2}^{(u)}=-\pi/2$, it will contain sines only. Taking two normal solutions corresponding to $i\lambda_u$, $i\lambda_v$ *viz.*,

$$q_r^{(u)} = \chi_r^{(u)} \cos \lambda_u t, \quad q_r^{(v)} = \chi_r^{(v)} \cos \lambda_v t; \; (r=1, 2, \ldots\ldots, m) \qquad ..(6.14)$$

where $\chi_{r_1}^{(u)}$, has been replaced by $\chi_r^{(u)}$ for simplicity. Substituting them in (6.8)

$$\left.\begin{aligned} &\sum_s a_{rs}\,\chi_r^{(u)} - \lambda_u^2 \sum_s b_{rs}\,\chi_r^{(u)} = 0 \\ \text{and} \quad &\sum_s a_{rs}\,\chi_r^{(u)} - \lambda_v^2 \sum_s b_{rs}\,\chi_r^{(v)} = 0 \end{aligned}\right\} \qquad ..(6.15)$$

Multiplying the first of (6.15) by $\chi_s^{(v)}$ and the second by $\chi_s^{(u)}$ and summing each one of them over the index r

$$\left.\begin{aligned} &\sum_{rs} a_{rs}\,\chi_r^{(u)}\,\chi_s^{(v)} - \lambda_u^2 \sum_{rs} \chi_r^{(u)}\,\chi_s^{(v)}\,b_{rs} = 0 \\ \text{and} \quad &\sum_{rs} a_{rs}\,\chi_r^{(v)}\,\chi_s^{(u)} - \lambda_v^2 \sum_{rs} b_{rs}\,\chi_r^{(v)}\,\chi_s^{(u)} = 0 \end{aligned}\right\} \qquad ..(6.16)$$

Subtracting the second of these from the first and noticing that the matrices $[b_{rs}]$, $[a_{rs}]$ are symmetric and λ_u and λ_v are distinct, we get

$$(\lambda_u + \lambda_v) \sum_{rs} b_{rs}\,\chi_r^{(v)}\,\chi_s^{(u)} = 0. \qquad ..(6.17)$$

Since at least one of them is not zero (one of λ_u or λ_v), we conclude

$$\sum_{rs} b_{rs}\,\chi_r^{(v)}\,\chi_s^{(u)} = 0, \qquad ..(6.18)$$

and hence from (6.16)

$$\sum_{rs} a_{rs}\,\chi_r^{(v)}\,\chi_s^{(u)} = 0. \qquad ..(6.19)$$

These relations establish the orthogonality of $\chi_r^{(u)}$'s.

In an analogous fashion, these results can be extended to the case of multiple roots (multiplicity may be of order k in which case we can determine k different orthogonal modes corresponding to the multiple root). In case of a zero root we have a solution of the type

$$q_r^{(v)} = \chi_r^{(v)} t. \qquad ..(6.20)$$

In a large class of physical problems, a number of generalized coordinates remain hidden. The external causes applied to the system do not excite all the generalized coordinates but influence only l or the coordinates, *viz.*, $q_1, q_2, \ldots, q_l$ and the remaining $m-l$, $(q_{l+1}, \ldots, q_m)$ form the set of ignorable coordinates. The latter do not influence the physical interest in the problem. It is easily seen that zero values of λ_u correspond to ignorable coordinates. If in equation (6.16) we make $u=v$

$$\lambda_u^2 = \frac{\Sigma\, a_{rs}\, \chi_r^{(u)}\, x_s^{(u)}}{\Sigma\, b_{rs}\, \chi_r^{(u)}\, \chi_s^{(u)}} \quad \ldots (6.21)$$

Introduce normal coordinates ξ_u by means of

$$q_r = \sum_u \chi_r^{(u)}\, \xi_u. \quad \ldots (6.22)$$

Normalize $\chi_r^{(u)}$'s such that for each u

$$\sum_{rs} b_{rs}\, \chi_r^{(u)}\, \chi_s^{(u)} = 1. \quad \ldots (6.23)$$

Using these results

$$V = \tfrac{1}{2} \sum_u \lambda^2\, \xi_u^2,\ L = \tfrac{1}{2} \Sigma\, \dot{\xi}_u^2. \quad \ldots (6.24)$$

The quantities corresponding to Q_r in normal coordinates become

$$Z_u = \sum_r \chi_r^{(u)} Q_r. \quad (6.25)$$

The Lagrangian equations corresponding to the normal coordinates are

$$(\lambda_u^2 - p^2)\ \xi_u = Z_u. \quad \ldots (6.26)$$

The operational solution is then

$$\xi_u = \frac{1}{\lambda_u^2 - p^2}\ .\ Z_u, \quad \ldots (6.27)$$

and

$$q_r = \sum_u \frac{\chi_r^{(u)}}{\lambda_u^2 - p^2}\ .\ Z_u. \quad \ldots (6.28)$$

When multiple roots are present all the terms on the right of (6.28) will be treated separately and the summation is considered extending over distinct roots only.

When a general solution of (6.11) having sine and cosine terms is considered the above results can be easily extended.

SOME GENERAL PROCEDURES

In case of linear dependence of H on q_r, some general procedures can be given which will throw some light on the manner of solving problems in special cases.

The vector H in the most general case can consist of two parts. One which is divergence free and the other which is not. The divergence free part will correspond to ignorable coordinates. Let the divergence free part be denoted by H_0 and the remaining by H_1. Thus

$$H=H_0+H_1. \quad ..(7.1)$$

Let the ignorable coordinates be denoted by η_r and the remaining by qr then

$$H_0=\sum_r X_r\eta_r, \quad ..(7.2)$$

and

$$H_1=\Sigma\, Y_r\, q_r. \quad ..(7.3)$$

From the remarks above it follows that

$$\nabla . H_0=\nabla . Xr=0. \quad ...(7.4)$$

V is therefore independent of η_r for

$$\phi=-c^2 (\nabla . H)=-c^2\sum_r q_r (\nabla . Y_r). \quad ...(7.5)$$

Here

$$L=\tfrac{1}{2}\int_\tau \left(\frac{\partial H}{\partial t}\right)^2 d\tau.$$

$$=\tfrac{1}{2}\sum_{rs} b''_{rs}\ \dot\eta_r\ \dot\eta_s+\tfrac{1}{2}\sum_{rs} b'_{rs}\ \dot\eta_r\ \dot q_s+\tfrac{1}{2}\sum_{rs} b_{rs}\ \dot q_r\ \dot q_s, \quad ..(7.6)$$

where

$$\left.\begin{aligned} b''_{rs} &= \int_\tau X_r . X_s d\tau \\ b'_{rs} &= \int_\tau X_r . Y_s d\tau \\ \text{and}\quad b_{rs} &= \int_\tau Y_r . Y_s d\tau \end{aligned}\right\} \quad ...(7.7)$$

If we choose the vectors X and Y mutually orthogonal, then

$$b'_{rs}=0. \quad ...(7.8)$$

Again

$$V=\tfrac{1}{2} c^2 \int_\tau (\nabla . H)^2\, d\tau$$

$$=\tfrac{1}{2}\sum_{rs} a_{rs}\ q_r\ q_s. \quad ..(7.9)$$

No η_r occur in V and a_{rs} is given by

$$a_{rs}= \int_\tau C^2(\nabla . Y_r)\ (\nabla . Y_s) d\tau. \quad ..(7.10)$$

The equations for q_r which are now uncoupled from η_r are

$$\sum_s \left(b_{rs}\ \ddot q_s+ ars\ q_s\right)=Q'_r, \quad ..(7.11)$$

where Q'_r are the external causes corresponding to excited coordinates.

The equations for ignorable coordinates η_r can be studied if the interest lies in the whole of the vector H.

The set of equations (7.11) now has less unknowns as η's do not occur here. But they have the same properties as the corresponding equations in section 6.

AN ILLUSTRATIVE EXAMPLE : CASE OF ONE-DIMENSIONAL WAVEPROPAGATION ALONG A STRING FIXED AT BOTH ENDS

This example will suffice to show the applicability of the ideas developed in the previous sections. The example studied is one dimensional. This is simply for the sake of avoiding tedious algebra. However it is evident that a problem can be worked out provided a proper choice is made for vector field.

Consider a string of length l fixed at its ends under a tension T. The mass per unit length of the string is m. The symbol ϕ is the transverse displacement of any point x (one end of the string is taken as origin, the x-axis along the undisturbed position of its length, the other end being $x=l$). The equation for the wave motion is

$$\frac{\partial^2\phi}{\partial t^2} = c^2\frac{\partial^2\phi}{\partial x^2}, \qquad ..(8.1)$$

where

$$c^2 = \frac{\mathrm{T}}{m}. \qquad ..(8.2)$$

We select a Fourier series representation (which constitutes the normal modes) for the vector field H, taking account of the fact that the transverse displacement is zero at $x=0$, and $x=l$ for all time t. Thus in normal coordinates q_n

$$\mathrm{H}=\sum_1^\infty \frac{lq_n}{n\pi\, c^2} \cos\frac{n\pi x}{l}, \qquad ..(8.3)$$

where q_n are generalized normal coordinates. The multiplier $l/n\pi\, c^2$ for q_n has been so taken, that it may give a simple expression for ϕ *viz*.,

$$\phi=-c^2\frac{\partial \mathrm{H}}{\partial x}=\sum_1^\infty q_n \sin\frac{n\pi x}{l}. \qquad ..(8.4)$$

Using the expression for H and ϕ

$$\mathrm{V}=\frac{1}{2\,c^2}\int_0^l \phi^2\, dx=\frac{l}{4\,c^2}\sum_1^\infty q_n^2. \qquad ..(8.5)$$

$$\mathrm{L}=\tfrac{1}{2}\int_0^l \left(\frac{\partial \mathrm{H}}{\partial t}\right)^2 = dx\frac{l^3}{4\pi^2 c^4}\sum_1^\infty \frac{\dot{q}_n^{\,2}}{n^2}. \qquad ..(8.6)$$

Lagrange equations for q_n in the absence of any external cause is

$$\ddot{q}_n+\frac{\pi^2c^2n^2}{l^2}q_n=0. \qquad ..(8.7)$$

The solution of this equation is

$$q_n=A_n\cos\frac{\pi cnt}{l}+B_n\sin\frac{\pi cnt}{l}, \qquad ..(8.8)$$

and then the expression for ϕ is

$$\phi=\sum_1^\infty\left(A_n\cos\frac{\pi cnt}{l}+B_n\sin\frac{n\pi ct}{l}\right)\sin\frac{n\pi x}{l}. \qquad ..(8.9)$$

This is in complete agreement with the known solution of the problem[5]. The constants A_n and B_n can be determined from the initial conditions on the position of the string and the velocities of its different elements.

ACKNOWLEDGEMENT

My thanks are due to Dr. S. D. Nigam, Senior Scientific Officer, I.I.T. Kharagpur, India, for his guidance during the preparation of this paper.

REFERENCES

1. Biot, M. A. 1957. *Jour. Aero. Sci.*, 24,12 : 857-873.
2. Frazer, R. A.; Duncan, W. J. & Collar, A. R. 1950. Elementary Matrices and some Applications to Dynamics and Differential Equations. *Camb. Univ. Press.*
3. Khinchin, A. I. 1949. Mathematical Foundations of Statistical Mechanics, p. 15 Dover.
4. Leech, J. W. 1958. Classical Mechanics, Chap. 9, Methuen.
5. Mac Robert, T. M. 1947. Spherical Harmonics, Chap. III, Methuen.
6. Morse, P. M. & Feshbach, H. 1953. Methods of Theoretical Physics, Vol. I, McGrawhill.

STUDIES IN FLORAL ANATOMY. VIII. VASCULAR ANATOMY OF THE FLOWER OF CERTAIN SPECIES OF THE ASCLEPIADACEAE WITH SPECIAL REFERENCE TO CORONA*

V. Puri and R. Shiam
School of Plant Morphology, Meerut College, Meerut, India.

Introduction

Asclepiadaceae is one of a small group of families which, while still retaining the actinomorphy of the flower, exhibits considerable variation in floral form. This is brought about chiefly by coronal structures that are so diverse that Woodson (1941) a well-known asclepiadologist, was once obliged to label them as "demnably variable". Again, in the estimation of the genera in this family, Woodson had relied to a very great extent upon the characters of the corona. If his conclusions are accepted we shall have not more than 100 genera in the Asclepiadaceae (Lawrence, 1951) in marked contrast to earlier figures of 280 (Rendle, 1925) and 320 (Willis, 1951). Such a situation definitely calls for a detailed investigations of the flower in general and the coronal structures in particular.

Material and Methods

In the present study some 20 species belonging to 14 genera have been studied. While several species were collected locally, the material of *Sarcostemma* and *Stapelia* was very kindly sent to us by Dr. B. Tiagi of Jaipur and that of some species of Asclepias and two species of *Hoya* (Puri, Nos. 597 & 728) was collected by one of us in the U.S.A. and in Nepal respectively. Flowers of *Oxystelma* were collected from Hastinapur, and preserved material of *Matelia caroliniana* and a few flower buds of some species of *Gonolobus* from herbarium sheets were very kindly spared and sent to us by the late Dr. R. E. Woodson Jr. of St. Louis M. O., U. S. A. The material of *Secamone* was collected and preserved for us by Dr. K. Subramanyam, Joint Director, Botanical Survey of India.

The material was prepared and studied in the usual manner. Schumann (1895) distinguishes two sub-families, Periplocoideae with a single tribe and Cynanchoideae with four tribes. Representatives of all these five tribes have been studied and described.

Observations

Periploceae—The species studied under this tribe are : *Hemidesmus indicus* R. Br. and *Cryptostegia grandiflora* R. Br. These are very similar to one another

---

[*] Research contribution No. 79 from the School of Plant Morphology, Meerut College, Meerut, India.

in the general construction and vasculature of the flower. The sepals are imbricate and leathery. As they separate off, each of the margins of two innermost sepals and the overlapped margin of the third sepal bear a small glandular process. In all there are five such processes in *Hemidesmus* and they appear to alternate with the sepals (Figs. 2-3). They project inward a little and consist of a central parenchymatous core surrounded by densely staining columnar epidermal cells. In *Cryptostegia,* however, every sepal margin bears a glandular process which may divide once giving rise to about twenty processes in five groups (Figs. 9-10). Obviously these are squamules corresponding to similar structures in the Apocynaceae (Woodson and Moore, 1938).

Ten vascular traces diverge from the parent stele for the sepals. These divide once or twice or more often (*Cryptostegia*) and then pass out into sepals each of which receives 3, 4 or more bundles (Figs. 2, 8 and 9).

The petals, though appear valvate in the lower region, are actually twisted as in other asclepiads, the over-lapping being nominal in *Hemidesmus* (Figs. 5 and 6) but very extensive in *Cryptostegia.* They arise conjoint with the stamens (Figs. 1 and 7). Out of the ten large bundles that reorganize themselves after the separation of the sepals, five supply the petals and the alternating five the stamens, all leaving behind some vascular tissue for the gynoecium. As the petal traces diverge they divide into three (*Hemidesmus*) or more (*Cryptostegia*) each and occupy positions in the outer region of the petal-staminal tube (Figs. 4,11 and 12). In *Cryptostegia* the petal regions of the petal-staminal tube that is more elongated, are very richly vascularized and contain numerous vascular branches scattered irregularly on the inner side (Figs. 13 and 14).

The corona in both these species, as also in *Cryptolepis* (Rao and Ganguli, 1963), is petaline in nature. It consists of five parenchymatous lobes that arise from the commissural regions of the corolla. In fact it is in these regions that the corolla remains connected with the staminal tube (*Hemidesmus*) or distinct stamens (*Cryptostegia*) for longer distance. These lobes are first detached from the stamens (Figs. 5 and 13), although Rao and Ganguli (1963) describe and figure them as detached from the corolla first and then from the stamens. Simultaneously with their separation, the petals also become free in *Hemidesmus* but in *Cryptostegia* they separate much higher up. These coronal outgrowths receive their vascular supply from the marginal bundles of petals. They are bilobed or deeply cleft radially into two each in *Cryptostegia.*

The five stamens are free as they arise in *Cryptostegia* but in *Hemidesmus* their bases are fused for a short distance. The filaments are short and the anthers which lie closely appressed to themselves and to the gynostegium are four-lobed having the pollen granular and in tetrads. The upper sterile parts of the anthers arch over the gynostegium before disappearing. Each stamen receives a single trace that traverses undivided throughout its course. It is significant to note that there is no staminal corona in these species except the apical appendages of the anthers.

The gynoecium that is somewhat sub-inferior consists of two carpels that are free from one another in the basal region and fused together in the upper stylar and stigmatic region (Figs. 1, 4, 7 and 13). Each carpel has a massive placenta that is distinctly bilobed and bears numerous ovules closely appressed to one another. The vascular supply of the gynoecium is derived from numerous small branches that are left behind in the centre by the ten prominent traces for the petal-staminal tube. Each carpel receives a continuous band of vascular tissue that follows its contour faithfully and thus illustrates rather clearly its foliar nature (Figs. 4 and 10). Each placental region has two small bundles, *A*' *B*' one in each half (Figs. 4 and 8). These furnish ovular traces and may occasionally be reinforced by small supplies from the main bands of vascular tissue, *A* and *B*.

Beyond the ovule bearing region the vascular bands start disappearing and ultimately only some tissue remains in the positions of the dorsal bundles. Upwards as the gynostegium is reached these bundles become arc-shaped and finally form a complete cylinder of vascular tissue in the upper part of the gynostegium (Figs. 6, 13 and 14). The gynostegium has columnar epidermis that stains densely alternating with the stamens. Upward it narrows, becomes circular in outline and finally disappears before the disappearance of the microsporangia.

Secamoneae—Secamone emetica R. Br. is the only species of this tribe studied here. Recently Safwat (1962) has given an excellent account of floral morphology of some 11 species of this genus (excluding *S. emetica*) and some other genera. Without resorting to a detailed description we shall, therefore, just draw attention to some salient features in the floral morphology of this species primarily from the point of view of comparison with other tribes.

There are five sepals that are very minute and imbricate. Both the margins of the two innermost sepals and the overlapped margins of the third sepal bear glandular outgrowths as in *Hemidesmus* (Fig. 17). The sepals receive a number of vascular branches each derived as a result of ramifications of the five original traces (cf. *Secamone stenophylla*-type of Safwat, 1962).

The petal-staminal tube is short and irregularly lobed on the outer surface (Fig. 18). As usual it contains ten bundles, five for the petals and five for the stamens. Each petal bundle divides into three or more branches that enter the petal as it separates.

There is no distinct petaline corona in so far as nothing separates from the petal surface. But it will be seen that the commissural regions of the petaline tube are considerably produced inward on staminal radii (Fig. 19). Even when the petals separate from one another their margins are considerably swollen (Fig. 20). All this seems to indicate that a petaline corona of the type met with in *Hemidesmus*, is formed but it does not separate, nor does it get any vascular supply.

On the inner side of the petaline corona and getting into its groove there is a blunt, more or less sickle-shaped ridge arising from the back of each stamen (Figs. 20, 23 and 24). This too is non-vascular and is part of the staminal corona. Besides, there are two anther wings from each stamen one on either side and an apical sterile appendage bent inward (Figs. 15 and 22).

The stamens are fused together into a tube that separates higher up into five laterally extended and very small filaments. The anthers are 4-locular and contain four pollinia each (Fig. 22). This is a unique feature for Cynanchoideae which essentially has 2-locular anthers with two pollinia each.

As usual the gynoecium is bicarpellary, the two carpels being free in the basal region, receiving many bundles besides one dorsal and four bundles in the placental region. Of these latter the two outer ones A' and B' furnish ovular traces and disappear in doing so. The other two bundles A and B continue into the style for some distance but disappear when the gynostegium is reached. Thus the gynostegium receives only two dorsals which in the column above form a continuous cylinder of vascular tissue that splits into two arcs before finally disappearing.

In *Secamone* the gynoecium also presents some interesting features. As pointed out by Safwat (1962), the ovary here is somewhat sub-inferior, a feature not recorded in any other Cynanchoideae* but usual in Periplocoideae as described above and in the Apocynaceae (Woodson, 1935). Another very significant feature is the occurrence of thin lateral flaps of parenchymatous tissue, one on either side of a placenta all along its length and forming a sort of peripheral veil for it as it were (Fig. 18). In transverse sections their epidermis is seen continuous with that of the ovary wall on one side and that of the placenta on the other. Safwat (1962), who also records them, considers them as extreme, sterile portions of carpellary margins. We shall revert to a discussion of their morphology at a later stage.

Beyond the ovule-bearing region the two styles, each with a dorsal bundle, fuse together and form a pentagonal gynostegium that is as much swollen as the ovary (Figs. 15 and 21). Upward it constricts abruptly, as if to accommodate the swollen tetralocular anthers and then proceeds up in the form of a column with two vascular arcs (Fig. 22). Higher up it splits into two diverging arms occupying carinal positions and having each an arc of vascular tissue (Fig. 15). These are devoid of any glandular tissue and their presence constitutes an important feature in *Secamone emetica*. Safwat (1962) does not refer to them in the species he investigated.

Gonolobeae—The species studied in this tribe are : (1) *Gonolobus barbatus* (2) *G. cteniphorus* and (3) *Metelea caroliniana*. All these are the

---

* Rao and Ganguli (1963) speak of semi-inferior ovary in many Asclepiadaceae but this situation is brought about by adnation of petal-staminal tube only with the ovary wall, the sepals separating from the base of the ovary.

New World species. The flowers are of medium size and have five sepals that are almost free and appear to be valvate (Figs. 29 and 37). At their bases the sepals have one large (*G. cteniphorus*) or a couple of small (*Matelea caroliniana*) glandular squamulae in each commissural region. In *Matelea* the sepals are sparsely hairy on their back. Five (*Matelea*) or ten (*G. cteniphorus*) traces depart successively for them. As they deverge they divide, so that by the time they enter the free sepals they form five or more small branches, which may undergo further branching within the sepals.

The petals are large, leathery and rotate. They are fused with the staminal column for a longer (*Matelea*) or shorter (*Gonolobus*) distance (Figs. 27, 34 and 35). In *Matelea* they remain fused together for some distance above their separation from the staminal column (Fig. 38); but in *Gonolobus* they detach separately from it. Each petal receives a large number of vascular branches derived by splitting of a single trace (Figs. 29 and 38). A petaline corona that is present only in *Gonolobus* consists of a raised hairy ridge running all around at the base of petals (Figs. 27 and 34). This is non-vascular and may appear in *G. cteniphorus* to be borne on the staminal column rather than on the petals on account of the latter having somewhat saccate bases (Fig.30). The fact that it is absent in *Matelea* restricts the systematic value of this character.

The five stamens are fused by their filaments which are rather short except in *G. barbatus*. The anthers are more or less free from one another. In *Gonolobus* the staminal column at the base is minutely lobed on its outside and has a continuous cylinder of vascular tissue (*G. cteniphorus*) (Fig. 30). A little higher up this latter cylinder breaks up into five staminal bundles that occupy a more central place (Fig. 31), and the coronal skirt diminishing in prominance continues up into five bifid lobes on the backs of the stamens and finally seems to break off as non-vascular structures. Thereafter the five anthers begin to appear and develop more (*G. barbatus*) or less (*G. cteniphorus*) prominent dorsal appendages that hang down a little and consist of compact tissue (Figs. 27 and 34). The staminal bundles dip a little into these appendages, and get cut thrice in transverse section and then proceed up in the connective outside the two locules. The sterile tips of the anthers are produced into membranous flaps that arch over and remain appressed to the stigma head which in turn covers the main parts of the anthers (Figs. 27 and 34).

In *Matelea* the staminal column has smooth outer surface. It separates into a coronal skirt and a stipe (Fig. 35). The coronal skirt consists of five prominent segments on staminal radii fused end to end. Beyond the gynostegium this skirt breaks up into five large lobes alternating with five small ones. The latter may split into two each before disappearing finally. It will be seen that although the cornal structures are much larger here they have no vascular supply other than a sharp bend in the course of the staminal bundles.

The two carpels, as usual, are free in the basal region and fuse only in the stigma head which is larger in *Gonolobus* than in *Malelea* (Figs. 33 and 39). The surface of the carpels in *Matelea* are prominently tubercled in the fertile region (Fig. 37). It will be noted that in both the genera the carpels separate from one another earlier than they do from the adjoining tissue (Fig. 29).

Each carpel, as usual, has a dorsal bundle, a number of lateral bundles and two bundles in the placental region A′ & B′ for supplying ovular traces (Figs. 29 and 37). The gynostegium receives only the two dorsal bundles that enlarge and branch profusely to form a more or less complete cylinder before disappearing (Fig. 33).

Tylophoreae—The species studied under this tribe are: *Leptadenia reticulata* Wight, *Stapelia variegata* L., *Hoya arnottiana* Wight and *H. lanceolata* Wall. The basic plan of construction and vasculature of the flower are the same in all the species. There are five small thick, free sepals that appear to be imbricate (Figs. 41, 51). In between them there are five minute squamulae that are as usual glandular and non-vascular. Five or ten (*Hoya*) traces depart for the sepals. They branch so that the sepals as they separate receive three (*Leptadenia*) five or more (*Stapelia*) bundles (Figs. 41, 47 and 51).

After the departure of sepal traces the central stele may again become a complete cylinder as in *Stapelia*. This shows there is a distinct anatomical internode between sepals and petals. The petals are thick and leathery, fusing at the base with the staminal tube and then for some distance among themselves (Figs. 43, 53). The free lobes may be rotate (Fig. 44), or faintly so (Fig. 56). As usual they get one trace each which invariably divides into a number of small branches before entering the petal.

There is no distinct petaline corona in these species except perhaps in *Hoya* where the corolla tube is slightly ridged opposite the stamens (Fig. 53). In *Gymnema sylvestris*, however, Rao and Ganguli (1963) report prominent coronal lobes separating from commissural regions of the corolla tube and receiving supply from petal marginals.

The filaments of the stamens are short and fused together into a column (Figs. 43, 54). The anthers are small, more or less free and curiously enough occur above (*Stapelia, Hoya*) or on the sides (*Leptadenia*) of the gynostegium and not beneath it as in many other species and are incumbent over it (Figs. 40, 45 and 50). They are bicelled and have one erect compressed and sessile (*Stapelia*) or pedicelled (*Hoya, Leptadenia*) pollinium in each cell (Figs. 49, 56). The anther wings are small and not well defined (Figs. 48, 55).

The staminal corona is very variable. In *Leptadenia* it is very simple, consisting of just five small hump like hoods from the back of every stamen (Figs. 40, 43). The staminal bundle deflects a little outward in this region.

In *Hoya* these outgrowths are much larger covering almost the entire back of the filaments (Fig. 50). Their free margins are recurved outward more (*H. lanceolata*) or less (*H. arnottiana*) and many appear to enclose a space in longitudinal sections (Fig. 50). Besides, the inner apical parts of these hoods are often produced into a tooth-like process each, that covers the anther proper from above. The staminal bundle kneels out into it for a short distance.

The corona in *Stapelia* is most elaborate. As the staminal tube separates from the corolla the backs of the fused filaments begin to be produced out into vertically compressed ridges that project obliquely outward (Figs. 26, 45). In their bases, that are tangentially flattened the staminal bundles appear to spread out a little into them. In transverse sections they appear as Ts, the shorter arms of which guard the passage to anther sacs (Fig. 49). Above these prominent ridges that obviously correspond to hoods, there are five club-shaped processes one from the base of each anther. These, on the other hand, converge over their respective anthers and seem to correspond to horns of *Asclepias.*

Alternating with the hoods there are five prominent boat-shaped *lobules* that also form a sort of covering for the openings to the anther sacs. They are fairly long, parenchymatous, nonvascular structures that have somewhat recurved tips that may be cut twice in transeverse sections (Figs. 48,49).

The structure and vasculature of the gynoecium are the same as described for other species with the difference that the style is very short so much so that in *Stapelia* the stigma head is almost sessile on the ovary (Fig. 45).

Asclepiadeae—The species studied under this tribe are: *Acerates auriculata* Engelm., *Asclepias tuberosa* Linn., *A. subulata* Dcne., *A. syriaca* Linn., *A. sp.*, *Calotropis gigentea* R. Br., *C. procera* R. Br., *Daemia extensa* R. Br., *Oxystelma esculentum* R. Br., and *Sarcostemma brevistigma* Wight & Arn. It is perhaps here in this tribe that a most glorified and complicated corona is met with. In order to save space we shall give a general account and refer to particular species wherever necessary.

The flowers in this tribe are usually large and showy and arranged in umbels or corymbose cymes. The sepals are thick, leathery small, free and imbricate (Fig. 62). In *Acerates auriculata* they are fused slightly at the base and somewhat saccate. As usual they have glandular squmulae arising from their bases on the inner side of their margin. Rao and Ganguli (1963) also describe them as arising from the sepals in many species they have studied but in *Holostemma rheedianum* and *Marsdenia volubilis* they have found them to be receptacular. These squamulae may occur singly as in *Daemia* and *Sarcostemma* or in groups as in *Asclepias tuberosa*, *Calotropis* and *Oxystelma* (Fig. 62). Sometimes they may show some radial splitting.

In all these species ten traces diverge successively for the sepals, five dorsals and five conjoint commissurals of adjacent margins. Immediately after separation the conjoint commissurals split into two each. These may be followed by branching of the dorsals so that each sepal receives three (*Sarcostemma*), five(*Oxystelma, Daemia*) or more (*Asclepias, Calotropis*) bundles. Within the sepals they usually undergo further splitting.

The petals are larger than the sepals, they are thick, leathery, reflexed (*Asclepias. Acerates, Calotropis gigentea*) or erect (*Calotropis procera, Oxystelma, Daemia*, etc.) and rotate. They are usually fused at the base into a short tube (Figs. 79 and 83), although in *Sarcostemma brevistigma* they are free to the base. The corolla tube may be free from the staminal tube (*Asclepias, Calotropis*, etc.) or it may be fused with it for a short distance, the fusion being usually most pronounced on the staminal radii (*Daemia*).

After the departure of the calyx vascular supplies, five prominent bundles differentiate to supply the corolla. Each of these divides into three or more branches that occupy positions in the peripheral region and finally enter their respective petals. Within the petals they may undergo further splitting.

It is significant to note that in this tribe where the corona is best developed there is hardly anything that can be designated as petaline corona. The only remnant of it is perhaps seen in *Oxystelma esculentum* in the form of an annular rim that separates from the corolla tube a little above its detachment from the staminal column. It is too small to appear in the form of a complete annular ring, and is mainly recognized by the thickness of the corolla tube that suddenly becomes thin after its disappearance (Fig. 79). *Daemia,* also has such an *annulus* but this separates from the staminal column rather than from the corolla (Fig. 83). In *Sarcostemma* it clearly separates from the staminal column some distance above the separation of petals (Fig. 87). These three cases seem to form a series where the *annulus* belonging to the petals (*Oxystelma*) appears to be gradually shifting, as it were, on to the staminal column. In *Asclepias* and *Calotropis*, however, there is no *annulus.*

There are five stamens whose filaments are tangentially flattened and fused together either ventrally as in *Oxystelma* and *Daemia* (Figs. 79 and 83) or throughout their thickness to form a short column* (Figs. 59, 63 and 77). The anthers are also flattened tantentially and fuse together and with the fleshy stigmahead to form the gynostegium. They are bicelled as each cell has a pendulous pollinium within it (Figs. 60, 64, 76, 81, 85 and 88). In the upper region, the stamens become free for a short distance and their apical hyaline appendages arch over the stigma head (Figs. 57, 61, 72 and 77).

As pointed out by Woodson (1954, P. 9) "The fascination of the asclepiad flower resides in the stamens". They form a more or less prominent corona consisting usually of (1) *Hood,* (2) *Horn,* (3) *Lobules,* (4) *Anther wings* and (5) *Anther appendages.*

---

* Woodson (1941) distinguishes two regions of the staminal column : that below the attachment of the corona as the "column" and that above, between the corona and anther proper as the "stipe".

The hood is the most promient part of the corona. It is so variable in form and structure that Woodson (1954), who has studied it in detail in North American species of *Asclepias*, was led to admit that "its variations almost defy description". It is a sort of outgrowth from the back of stamen filaments and usually consists of thin walled spongy parenchyma. Woodson (1954) described it to be glandular. Although we have also seen it full of some sort of fluid, we have not seen any glandular or secretary tissue in it. It may be solid (*Oxystelma, Sarcostemma, Daemia*) or hollow (*Calotropis, Asclepias*). In *Asclepias* the hood is open on top as well as on the inner sides, and its thin margins are involutely folded (Fig. 64). In *Acerates* they may be recurved outward (Fig. 59). The hood in *Calotropis gignatea* is laterally and conduplicately flattened and is open on the back (Fig. 74). The hood in *Calotropis* is constructed on a different plan. Its bottom is heavy and is laterally and conduplicately flattened. At the base it has a prominent 'tail' that is coiled outward (Figs. 72 and 77). Above this the cavity of the hood narrows and ultimately becomes a slit that opens on the back (Fig. 74).

The vasculature of the hood is not distinct from that of the stamen. In *Oxystelma, Daemia* and *Sarcostemma* the staminal bundles show some bendings in their course for the hood but the free parts of it are always non-vascular (Figs. 78, 82 and 86). In *Acerates* and *Asclepias* species, however, the staminal bundle goes up for considerable distance in the hood and then returns on its inner side to re-enter the stamen (Figs. 57 and 61). After traversing a short distance up it negotiates a sharp down-turning in its course and goes up again to supply the anther (Fig. 61). At this level the same staminal bundle may be seen cut four or five times in transverse sections (Fig. 63). It disappears in the upper part of the anther while the bundle in the hood may continue much higher.

In *Calotropis* the situation is somewhat different. After the basal outpushing for the 'tail' of the hood the staminal bundle still appears to run in the inner part of the hood (Figs. 72 and 75). It is only in the upper region that it enters the filament proper and after negotiating a sharp down-turning (cf. *Asclepias*) enters the anther region.

Inside the hood there arises in *Asclepias* a slender incurved acicular process, the *horn* that may at maturity be longer (*Asclepias tuberosa*) or shorter (*A. syriaca, A. subulata*) than the hood (Figs. 66, 67 and 68). It is completely lacking in *Acerates auriculata* and is always non-vascular and non-glandular.

The *alternating lobules* (Woodson, 1954) are thin flaps, occurring in between the hoods on the upper half of the column in *Asclepias* and *Calotropis* (Figs. 66, 69 and 71). Upward they become free and bifid due to the *anther wings* that cut down through their middle. These are also non-vascular and non-glandular.

The *anther wings* are thin flaps arising one from either side of an anther in all the genera studied here. Those of adjacent anthers stand close and parallel to one another, and enclose a vertical slit that at its upper extremity bears the 'gland' with two translator arms attached to two pollinia in different anthers. The anther wings may be stiff cartilagenous structures as in *Asclepias* (Fig. 63) or they may be just parenchymatous structures as in *Oxystelma* (Fig. 80) or *Sarcostemma* (Fig. 88). The *apical appendages* of the anthers are membranous flaps that are upward sterile continuations of the anthers and that arch over the gynostegium. They are also non-vascular.

The structure and vasculature of the ovary is similar to that of *Cryptostegia*. The two carpels are free from one another in the basal region, and bear massive placentae each of which is distinguishable into two halves. On either side of a placenta there is a small outgrowth that looks similar to an ovule primordium but never develops into one. These are sterile outgrowths probably of the same nature as those seen in *Secamone*. The gynostegium is pentagonal. It is somewhat obconical and may have a flat or somewhat depressed top (Fig. 69).

Each carpel receives a prominent dorsal bundle and many other lateral bundles on either side of it. The two most distal of these bundles, *A B* (Fig.79) occur just outside the placenta. Corresponding to these each placenta has two small bundles, A′, B′ one in each half placenta. These latter are consumed in supplying ovular traces. At the base, several bundles enter the style but as the gynostegium is reached all except the dorsal bundle disappear. The two dorsals divide and redivide in the upper part of the gynostegium and form a small cylinder of vascular tissue that ultimately breaks up into two before finally disappearing (Fig. 65).

Discussion

There are several points in the present study that deserve some attention here. But before this is done we would like to say a word about the terminology employed. In all the earlier accounts including that of Schumann (1895) all outgrowths from petals and stamens have been described under *Corona* which has been distinguished into *outer corona, middle corona* and *inner corona*. Woodson (1941) has taken exception to such a treatment, as in his opinion, it has led to much confusion in literature. For instance, according to him, the "Outer corona" of one group may easily be mistaken for the "Inner corona" of another in cases of suppression of one or the other corona whorls. Consequently he advocates a rather restricted use of the term 'corona'. True corona, according to him, "consists of various elaborations or enations from the *staminal filaments only*" (italics is ours). Outgrowths from the corolla are described as *faucal annulus* and those from the apices of the anthers as *sterile appendages*.

Such a classification has subsequently been accepted by certain taxonomists, *e.g.*, Holm (1950), Lawrence (1951), Safwat (1962), etc. But to a student of morphology who is familier with the conditions in the Passifloraceae, Caryophyllaceae, Amaryllidaceae, etc., such a restriction on the use of the term corona appears to be rather superfluous and uncalled for. Corona is essentially an outgrowth from the corolla, this is so atleast in the Amaryllidaceae (Arber, 1937), Caryophyllaceae (Arber, 1939) and Passifloraceae (Puri, 1948). Excluding corolline structures from the scope of this term when used in connection with Asclepiadaceae will be very much confusing.

Woodson's only argument for enforcing this restriction is that the adjectives *outer*, *middle* and *inner* used in literature for describing the various parts of the corona are inappropriate and inaccurate. Middle corona, for instance, may be outer or inner depending upon which one of the three coronal series is suppressed. For taxonomists interested in key characters this may be a somewhat serious situation but it can be got over in other ways without in any way restricting the scope of the term corona. After all in a detailled scientific account of the corona we have got to name each and every component of it and not feel content with mere adjectives of position (outer, middle and inner).

In view of these considerations we have avoided the use of the expression *faucal annulus* of Woodson (1941) and have preferred to call that part of the corona as *petaline corona* as distinct from *staminal corona*. Other terms used by Woodson have been profitably employed here too.

The Corona—There are thus two types of corona in the Asclepiadaceae —the petaline and the staminal. The former, when present, is either in the form of finger-like processes arising from the commissural regions of petals and deriving their vascular supply from their marginal bundles or it may be just an annular rim or isolated ridges developing from the base of the corolla and without any vascular supply.

The staminal corona, on the other hand, is usually very elaborate and may be further distinguished into filament corona consisting of *hood*, *horn* and *lobules* and *anther corona* of *anther wing*, *dorsal appendages* and *apical appendages*. All these donot necessarily occur together in the same species; they may vary considerably in form and extent of development. For instance, the *hood* which is perhaps the most universally occuring constituent of the corona in Cynanchoideae may be solid, or hollow opening on the inside or outside. Whereas in *Asclepias* it usually has a more or less well developed horn, it may be without it in *Acerates* and other genera. Other components of the corona donot have any vascular supply.

With regard to relative development and elaboration of the petaline and the staminal corona, in different taxonomic groups, there appears to be at play a certain significant correlation. For instance, in the closely related family Apocynaceae there is marked tendency for the elaboration of the petaline corona and more or less complete suppression of the staminal corona. In the Asclepiadaceae, on the other hand, this tendency seems to be reversed and one finds here the greatest elaboration of the staminal corona accompanied by little or no differentiation of petaline corona. The tribes of the Asclepiadaceae that are less specialized in coronal elaboration, may show greater similarity with one condition or the other. In Periploceae, for instance, in all the species studied the petaline corona is comparatively well developed, it is even vascularized but there is no staminal corona worth the name except the apical appendages of the anthers.

In the tribe Secamoneae, *Secamone astephana* is reported to be without staminal corona (*See* Safwat, 1962). In *S. stenophylla* there are "both a steminal and a corolline corona" (Safwat, 1962), but in *S. emetica* studied here the staminal corona is well developed while the petaline one is very rudimentary and without any vascular supply. So the accent here seems to be on the staminal corona. In the same way in *Gonolobus* the staminal corona is well-developed and although a petaline corona is present it is very rudimentary and non-vascular. In the species of Tylophoreae a petaline corona is lacking and so is the case in *Asclepiadeae.* Here in this last tribe a very rudimentary annular rim separates from the base of the corolla tube in *Oxystelma esculentum.* A more or less similar rim is present in *Daemia* and *Sarcostemma* but this separates from the staminal tube rather than from the corolline tube. So in these species one notices a shift of emphasis from petaline corona to staminal corona as one proceeds from the Apocynaceae to the most specialized tribe Cynanchoideae of the Asclepiadaceae.

In genera like *Asclepias, Calotropis, Stapelia,* etc., where the staminal corona is most elaborate and prominent, the petaline corona is entirely lacking. It seems, therefore, logical to conclude that a well-developed petaline corona and a well-developed staminal one donot co-exist together in nature. They are the expression of two different tendencies of specialization that have their culmination in different groups. The petaline corona attains its maximum development in the Apocynaceae and the staminal corona in the Cynanchoideae of the Asclepiadaceae. A most perfect expression of this tendency of specialization is perhaps seen in *Asclepias* where not only the petals have no trace of any corona but they become recurved down at maturity surrendering, as it were, the entire field of activity to the staminal corona that is very well developed.

The Gynoecium—It will be recalled that the two carpels, that are free from one another in the basal region, fuse together in the stylar region to form a pentagonal stigma—head which together with the anthers form the characteristic gynostegium of the family. The stigma head is variously shaped and has five receptive region. Besides, it has much larger amount of vascular tissue than is present in the regioni mmediately beneath it. The significance of a pentagonal stigma on top of a bicarpellary ovary is every body's guess. But it may be pointed out here that in the closely related family Apocynaceae the tribe Pleiocarpeae of the sub-family Plumerioideae usually have two to five carpels. The African genus *Pleiocarpa* is said to be very prolific in this connection (Woodson and More, 1938). The ovary in all the polycarpellary genera is always apocarpous but the component carpels are united in the stylar region. In the present study we have also come across a condition in *Asclepias syriaca* where two carpellodes alternate with the two fertile carpels. It is quite likely, therefore, that the stigmatic region still retains remnants of those additional carpels that appear to have been lost completely from the ovary region. A similar condition is believed to exist in certain Myrtaceae (Gupta, 1962).

The placentation in the Asclepiadaceae also deserves some attention. It is obviously marginal (Puri, 1952) and each placenta that is bilobed receives two small bundles A' and B' that give off ovular traces (See Fig. 4). On the adaxial side of these there are two other bundles A and B, which together with the lateral bundles (whenever present) and the dorsal bundle form a more or less continuous band of vascular tissue. A clear understanding of the status of bundles A, B and A', B' is of some consequence for it may affect the interpretation of the placenta and hence of the carpel. There are obviously two possible ways in which they can be interpreted :

1. Bundles A and B are true ventrals and bundles A' and B' are branches thereof for supplying ovular traces.
2. Bundles A and B are secondary marginals and bundles A' and B' are true ventrals supplying ovular traces.

Let us analyse the implications of these interpretations in some detail. If we regard the bundles A' and B' as branches of the ventrals and not true ventrals themselves, then we have to consider placenta as an *outgrowth* from the carpellary margin. The classical concept of the carpel to which we subscribe enjoins upon us to assume that ovules are borne on carpellary margins themselves, and not on any outgrowth from them and that they receive their supply ordinarily from the ventral bundles. In view of this it is incumbent upon us to interpret A' and B' as true ventral bundles and the bundles A and B as secondary marginals. Such an interpretation which is undoubtedly as plausable as the other does not clash with the classical concept and hence it is accepted here.

Another feature that has been brought out in the anatomy of the placenta in certain genera is the occurrence of sterile leafy or globular structures one on either side of a swollen placenta. These structures are most prominent in *Secamone* where they are leafy and tapering distally. Safwat (1962) who has also reported them in his study interpreted them as representing extreme and portions of carpellary margins. This means that the carpellary margins in these cases swing inward into the locule and bear ovules on their *dorsal* surface rather than on the *ventral* (see Fig. 89). Safwat fully appreciated this position and described the placentation as submarginal. Earlier Baum (1949) also reported a similar situation in certain asclepiads. She cites some previous literature also on the subject.

This dorsal position of the ovules is really a very unique situation in angiosperm. It will be too dogmatic on our part to suggest that such a situation does not exist anywhere in this group. But with regard to Asclepiadeceae we can say with some amount of confidence that it is a case of misinterpretation. The ovules here are actually borne on the ventral surface of the carpellary margins and that the placentation is really marginal.

In order to appreciate this it is necessary to understand clearly the structure and magnitude of carpellary margins. As emphasized by one of us (Puri, 1962) earlier, a carpellary margin (unlike leaf margin) is, perhaps in response to its ovule bearing function, a well developed structure having some thickness. This latter is represented by what has been called the *lateral face* of the carpellary margin. It is the surface by which the margins of a carpel meet or fuse together. In addition to this a carpellary margin has a portion of the dorsal surface and a portion of the ventral surface bearing ovules.

This concept of carpellary margin if applied to asclepiad gynoecium readily makes it conform to any ordinary type of gynoecium where the ovules are borne on ventral surface of the carpellary margin and the placentation is marginal (*see* Figs. 90 and 91). There is, therefore, no justification for assuming that the ovules in the Asclepiadaceae are borne on the dorsal surface of the carpellary margins and that the placentation is submarginal.

Systematic Considerations—We have just seen that while the corona is too variable to be of much value in systematics the gynoecium is too uniform to be of much consequence. However, there are certain major trends or tendencies in the development and elaboration of the corona and of the anthers that prompt us to some speculation regarding the systematics of the Asclepiadaceae. It will be recalled that there are two recent views on the subject, those of Bullock (1956) and Safwat (1962). Bullock advocates that the two sub-families Periplocoideae and Asclepiadoideae should be regarded as distinct families and that Asclepiadaceae (*sensu restricto*) should be further distinguished into two sub-families, Secamonoideae and Asclepiadaceae (*sensu restricto*). This last sub-family is further recognized into four tribes Asclepiadeae, Marsdenieae, Gonolobeae and Ceropegieae. Recently Mulay *et al* (1965) on the basis of floral anatomical and embryological differences justify the separation of the sub-families Periplocoideae and Cynanchoideae, the former was raised to the rank of the family Periplocaceae and the latter representing Asclepiadaceae proper.

Safwat (1962) who is apparently not familier with Bullock's interest in the family, is, on the other hand, "inclined to believe that phylogeny is better portrayed by combining Asclepiadaceae and Apocynaceae into a single family and re-subdividing the group into five sub-families Plumeroideae, Echitoideae (or Apocynoideae), Periplocoideae, Secamonoideae and Asclepioideae".

Based on judicious weighing of considerable amount of data, both these suggestions are valuable in their own way. We are, however, inclined to believe that ends of consistency are better served by adopting Bullock's treatment.

Periplocaceae stands intermediate between Apocynaceae and Asclepiadaceae. As emphasized by Bullock (1956) it is characterised by filaments free, anthers without horny wings; pollen granular in tetrads, transported on a spathulate carrier. Besides, this is the group in which petaline corona is dominant over the staminal one which is rather rudimentary—a tendency in common with the Apocynaceae. Further, as in the Apocynaceae (Woodson, 1935) there is a tendency in this family towards epigyny, a condition not seen in any Asclepiadaceae (*sensu restricto*) except *Secamone*. Again, Periplocaceae has 4-sporangiate anthers and the meiotic divisions of the microspore mother cells are *simultaneous* (*cf.* Apocynaceae) and not successive as in many members of the Cynanchoideae (*see* Safwat, 1962).

We also feel that the status given to *Secamone* as a subfamily Secamonoideae is well justified. It stands aloof from the Asclepiadoideae (*sensu restricto*) in having 4-sporangiate anthers and in microspore mother cells dividing *simultaneously* as in Periplocaceae and Apocynaceae and in showing a tendency to epigyny (*see* also Safwat, 1962), and in having the stigma head ending in two stigmatic arms.

SUMMARY

The floral anatomy of some twenty species representing all the tribes of the Asclepiadaceae has been studied. Like the calyx and the corolla the gynoecium also is too uniform to be of any help in systematics. There are, however, certain points that are of special morphological interest *e. g.*, the occurrence of a pentagonal stigma head over a bicarpellary ovary, a tendency towards epigyny in the Periplocoideae and Secamoneae, the occurrence of sterile flaps on either side of a placenta is *Secamone* and some others. Regarding this last point that has been discussed at some length it has been suggested that these sterile flaps represent the extreme ends of the placentae and not the carpellary margins as was asserted earlier. There is, therefore, no justification for an earlier suggestion that the ovules in the Asclepiadaceae are borne on the dorsal surface and that the placentation is sub-marginal. In this connection the concept of carpellary margins put forward by one of us earlier has been re-emphasized.

The corona, on the other hand, is too variable to be of any systematic value. Even in the same tribe it shows considerable range of variation. There is, however, one important trend in its elaboration that may be useful. While in the Apocynaceae the petaline corona is well developed and the staminal corona is almost lacking, in the Asclepiadaceae it is the staminal corona that is most elaborate and the petaline one is almost supressed. Since Periplocoideae shows only petaline corona and since it differs from other Ascle-

piadaceae in many other characters, particularly of the stamens, it is considered proper to support its raising to the status of a family, Periplocaceae. On similar grounds another suggestion of Bullock to raise *Secamone* to sub-family Secamonoideae is supported.

ACKNOWLEDGEMENTS

We take this opportunity of thanking all those who have helped us with the material, particularly the late Mr. Manmohan Lal Garg who started this work in 1952 and Dr. V. P. Dube (Modinagar) who cut the material of several species and made rough sketches. We are especially grateful to the late Dr. R. E. Woodson Jr. on whose deep knowledge and understanding of the subject we have drawn freely.

LITERATURE CITED

1. Arber, A. 1937. Studies in flower structure. III. On the "Corona" and androecium in certain Amaryllidaceae. *Ann. Bot.*, **1**: 293-304.
2. Arber, A. 1939. Studies in flower structure. V. On the interpretation of the petal and 'corona' in *Lychnis*. *Ann. Bot.*, *N. S.* **3**: 337-346.
3. Baum, H. 1949. Die Stellung der Samenanlagen am karpell bie *Asclepias syriaca, Cynanchum vinectoxicum,* und *Erythraea centaurium.* Osterreich *Bot. Zeit.*, **95**: 231-256.
4. Bullock, A. A. 1956. Notes on African Asclepiadaceae. VIII. *Kew Bull.*, 1956: 503-522.
5. Gupta, I. 1962. Morphological studies of the flower of Myrtaceae, Unpublished Ph. D. Thesis, Agra University.
6. Holm, Richard, W. 1950. The American Species of *Sarcostemma* R. Br. (Asclepiadaceae). *Ann. Missouri. Bot. Gard.* **37**: 477-560.
7. Lawrence, G. H. M. 1951. Taxonomy of vascular plants. New York.
8. Mullay, B.N., Deshpande, B.D. & Usha Tolani. 1965. Studies in *Asclepiadaceae.* II. Floral Morphology and Gametogenesis in certain Members of the Asclepiadaceae. *Jour. Ind. Bot. Soc.*, **44**: 95-104.
9. Puri, V. 1948. Studies in floral anatomy. V. On the structure and nature of the corona in certain species of the Passifloraceae. *Jour. Indian Bot. Soc.*, **27**: 130-149.
10. Puri, V. 1952. Placentation in Angiosperms. *Bot. Rev.*, **18**: 603-651.
11. Puri, V. 1962. On the concept of carpellary margins. Proc. Summer School of Botany, Darjeeling. p. 326-333.
12. Rao, V. S. & Ganguli, A. 1963. The floral anatomy of some Asclepiadaceae. *Proc. Indian Acad. Sci.*, B. **57**: 15-44.
13 Rendle, A. B. 1925. The classification of flowering plants. Vol. II. Dicotyledons. Cambridge.
14. Safwat, F. M. 1962. The floral morphology of *Secamone* and the evolution of the pollinating apparatus in Asclepiadaceae. *Ann. Missouri Bot. Gard.*, **69**: 95-129.
15. Schumann, K. 1895. Asclepiadaceae, in Engler and Prantl, Die naturlichen Pflanzenfamilien, **IV**(2) : 189-306.
16. Willis, J. C. 1951. A dictionary of flowering Plants and Ferns. Cambridge.
17. Woodson, Robert, E. JR. 1935. The floral anatomy and probable affinities of the genus *Grisebachiella*. *Bull. Torrey Bot. Club.*, **62**: 471-478.
18. Woodson, Robert, E. JR. 1941. The North American Asclepiadaceae. Prospective of the genera. *Ann. Missouri. Bot. Gard.*, **28**: 193-244.
19. Woodson, Robert, E. JR. 1954. The North American Species of *Asclepias* L. *Ann. Missouri Bot. Gard.*, **41**: 1-211.
20. Woodson, Robert, E. JR. & Moore, J.A. 1938. The vascular anatomy and comparative morphology of Apocynaceous flower. *Bull. Torrey, Bot. Club.*, **65**: 135-166.

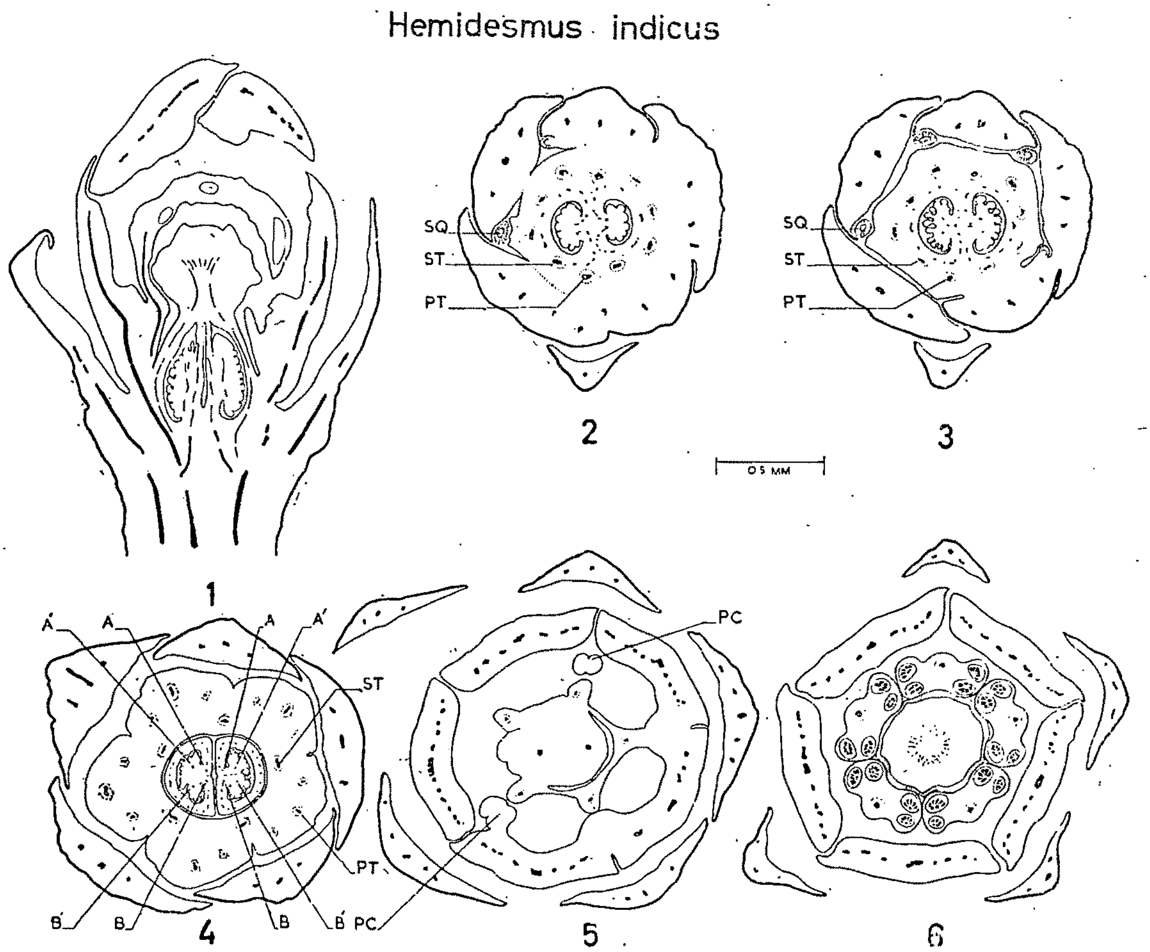

Figs. 1-6. *Hemidesmus indicus.* Fig. 1. L. S. of the flower. Figs. 2-6 Serial transverse sections. A & B=Secondary marginal bundles; A' & B'=Ventral bundles; PC=Petaline Corona; PT=Petal trace; SQ=Squamule; ST=Stamen trace.

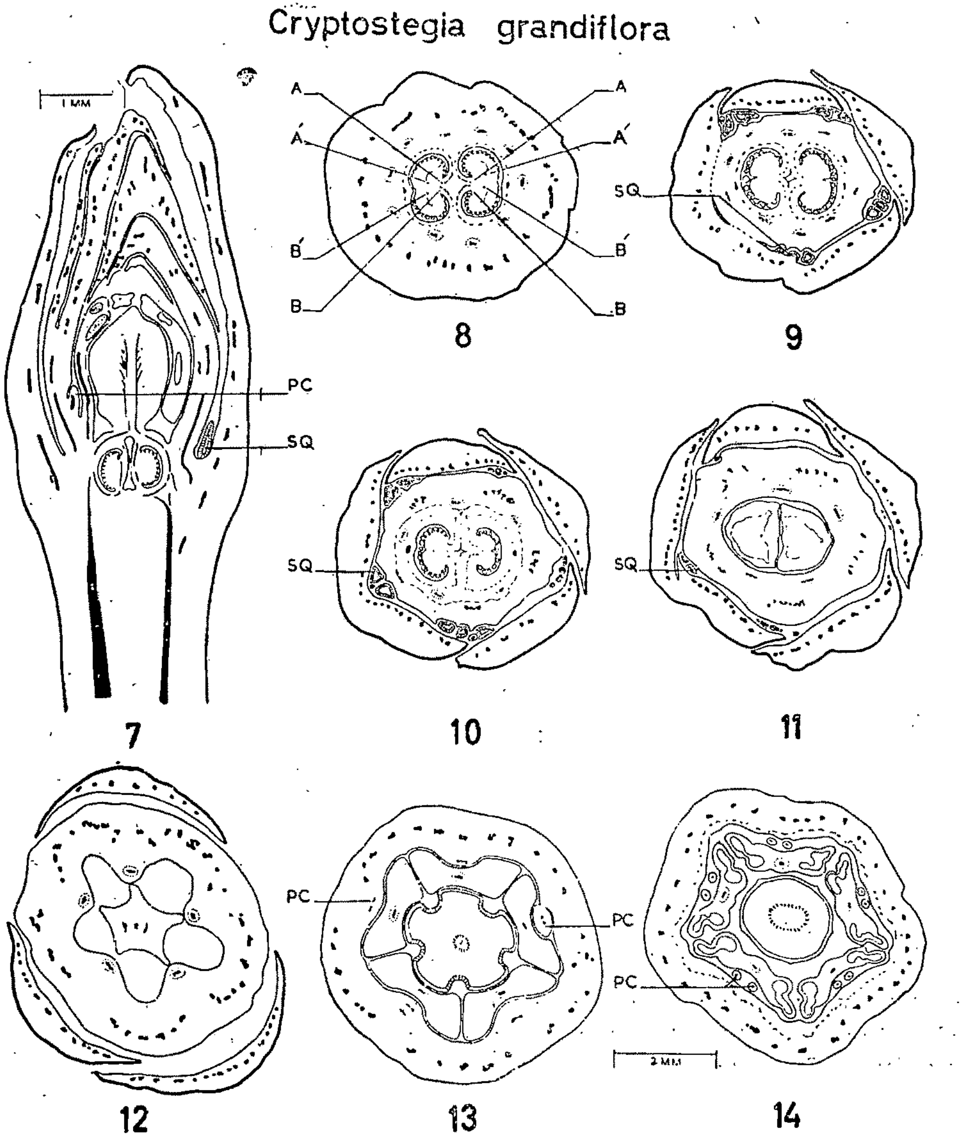

Figs. 7-14. *Cryptostegia grandiflora*. Fig. 7 L. S. of flower. Figs. 8-14. Serial transverse sections from base upwards. A & B=Secondary marginal bundles; A' & B'=Ventral bundles; PC=Petaline corona; SQ=Squamule.

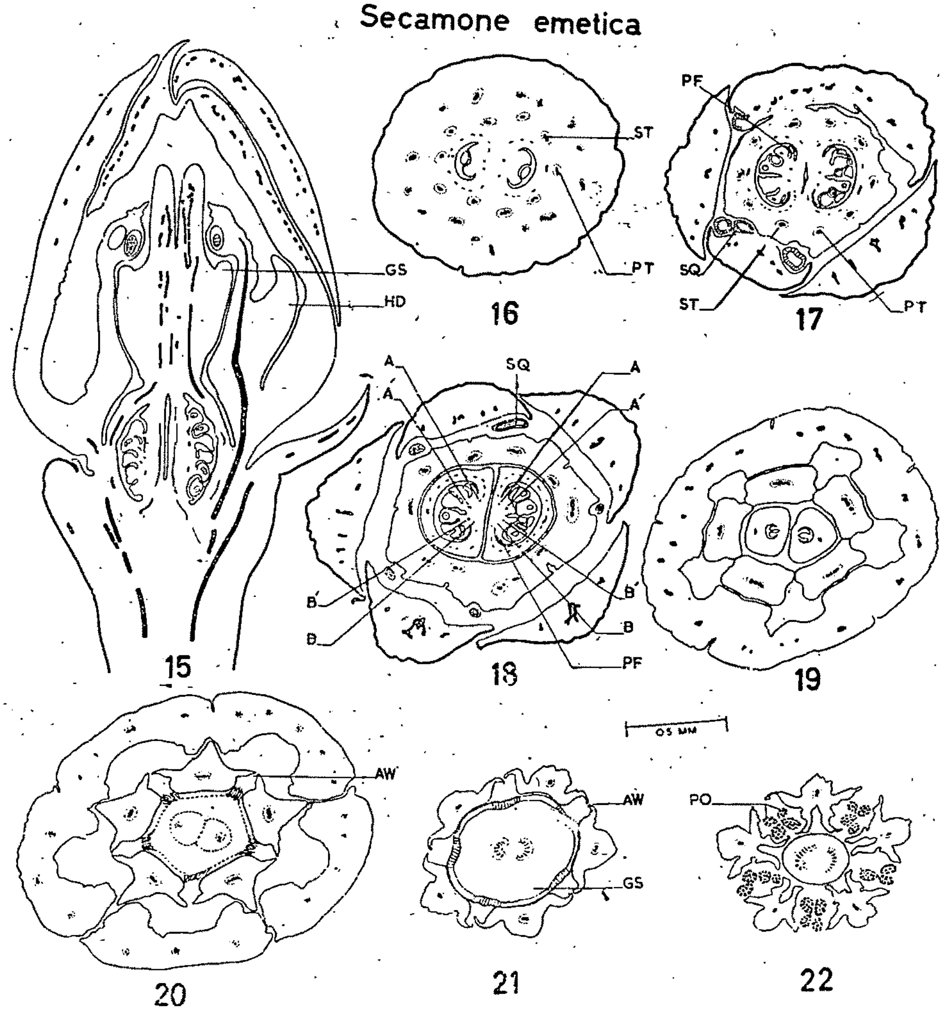

Figs. 15–22. *Secamone emetica*. Fig. 15. L.S. of flower showing a bifurcating style. Figs. 16–22. Serial transverse sections of the same from base upwards. A & B=Secondary marginal bundles; AW=Anther wings; A' & B'=Ventral bundles; GS=Gynosteguim; HD=Hood; PF=Placental flap; PO=Pollinia; PT=Petal trace; SQ=Squamule; ST=Stamen trace.

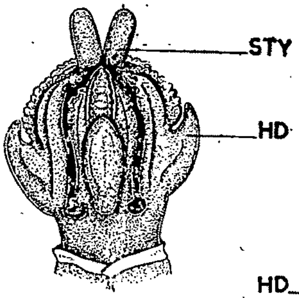

23

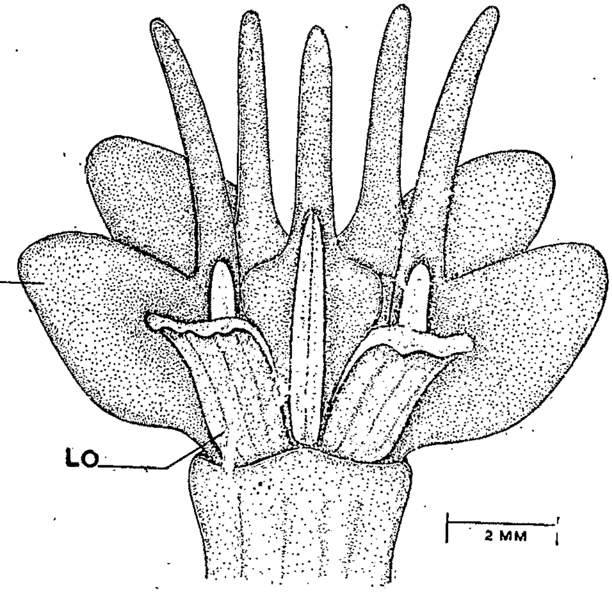

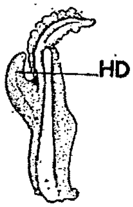

24

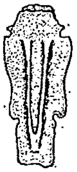

25

26

Figs. 23. Flower of *Secamone emetica* showing the bifurcating style surrounded by steminal corona. Fig. 24. Single hood segment in lateral view. Fig. 25. The same from inner side. Fig. 26. Flower of *Stapelia variegate* showing coronary structures, petals removed. HD=Hood; LO=Lobule; STY=Style.

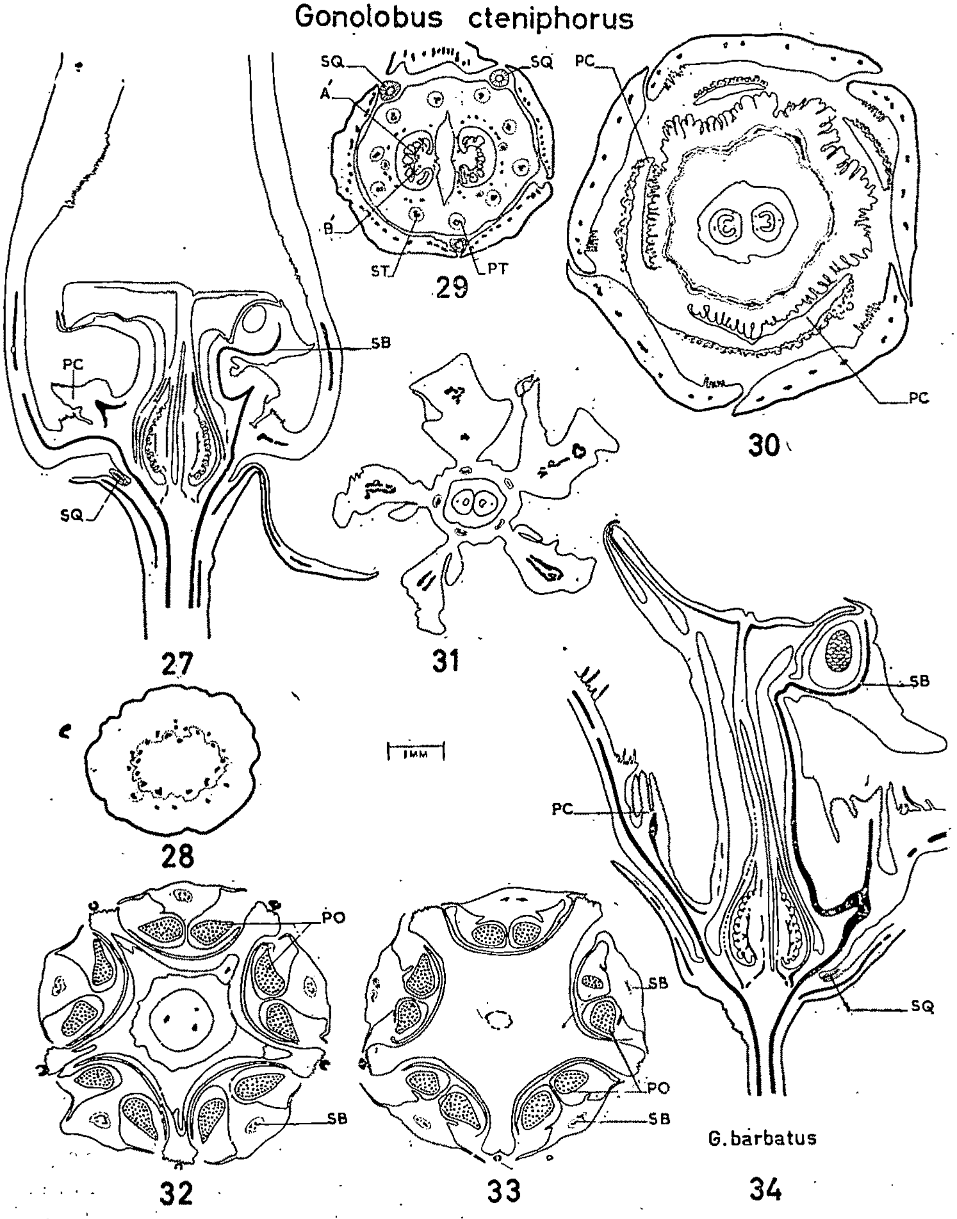

Fig. 27. L. S. Flower of *Gonolubus cteniphours*. Figs. 28-33. Serial transverse sections of the same from base upwards. Fig. 34. L. S. of flower of *G. barbatus* showing the apical and dorsal appendages. A' & B'=Ventral bundles; PC=Petaline corona; PT=Petal trace; PO=Pollinia; SB=Stamen bundle; SQ=Squamule; ST=Stamen trace.

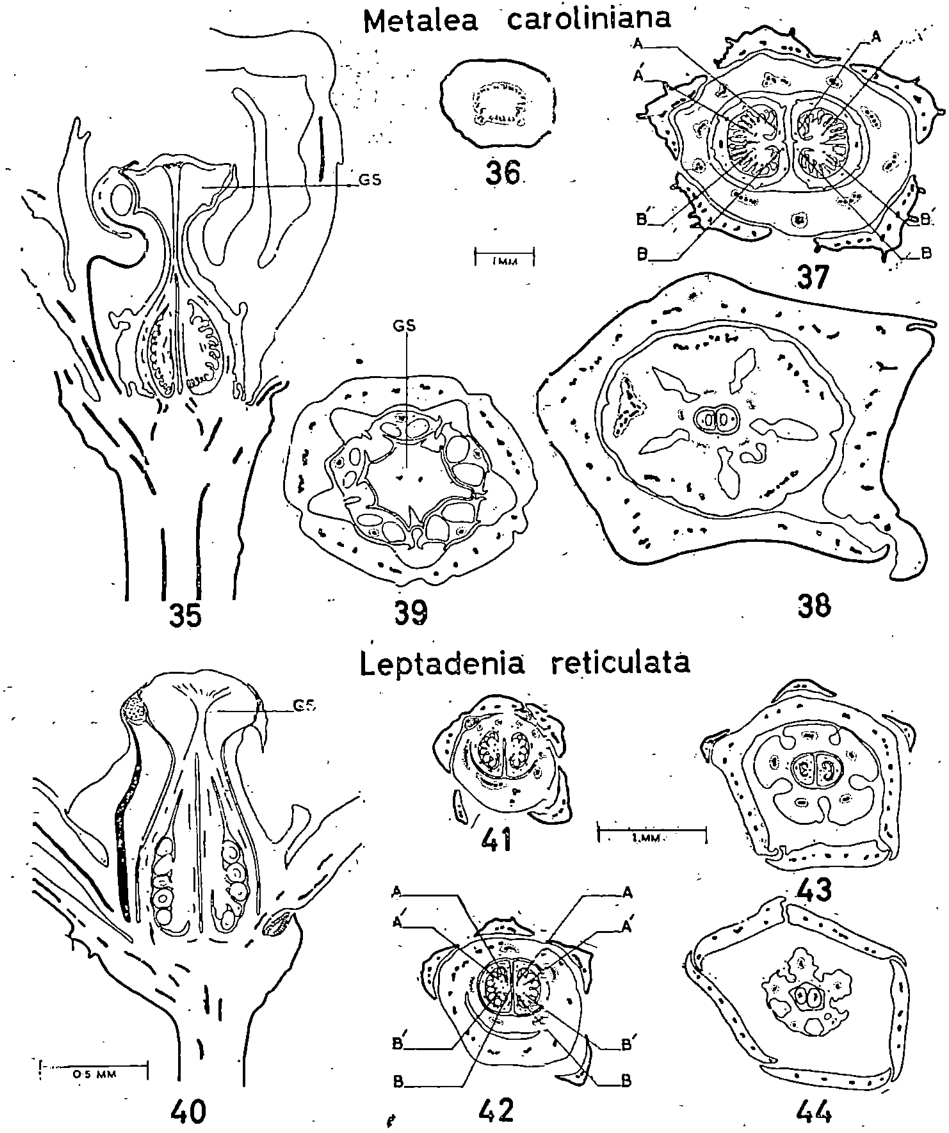

Figs. 35-39. *Metalea caroliniana*. Figs. 35. L. S. of the flower. Figs. 36-39. Serial transverse sections of the same. Figs. 40-44. *Leptadenia reticulata*. Fig. 40. L. S. of the flower. Figs. 41-44. Serial transverse sections of the same. A & B=Secondary marginal bundles; A' & B'=Ventral bundles; GS=Gynostegium.

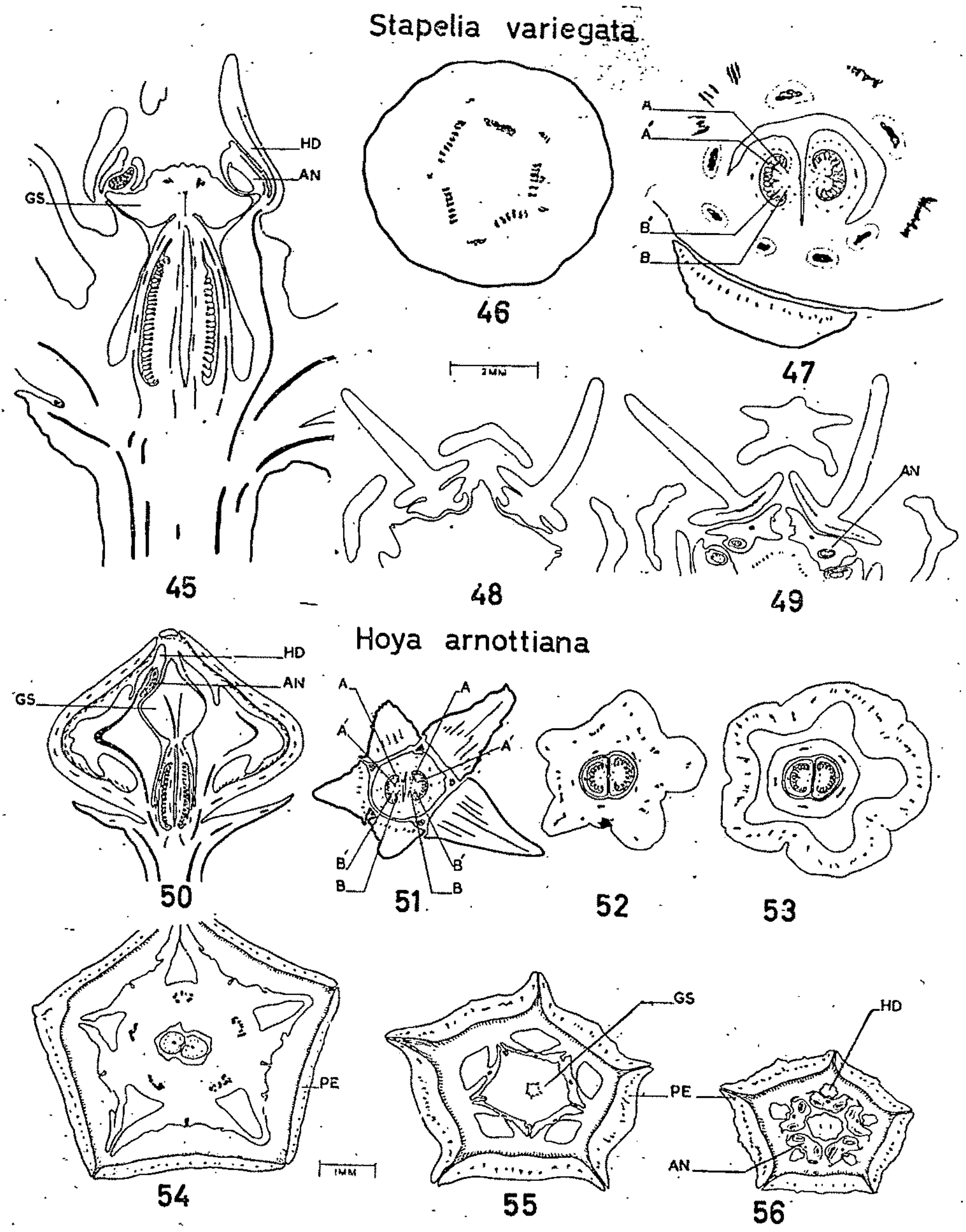

Figs. 45-49. *Stapelia* sp. Fig. 45. L. S. of the flower. Figs. 46-49. Serial transverse sections of the flower. Figs. 50-56. *Hoya arnottina*. Fig. 50. L.S. of the flower. Figs. 51-56. Serial transverse sections of the same. A & B=Sccondary marginal bundles; A' & B'=Ventral bundles; GS=Gynostegium; HD=Hood; PE=Petal.

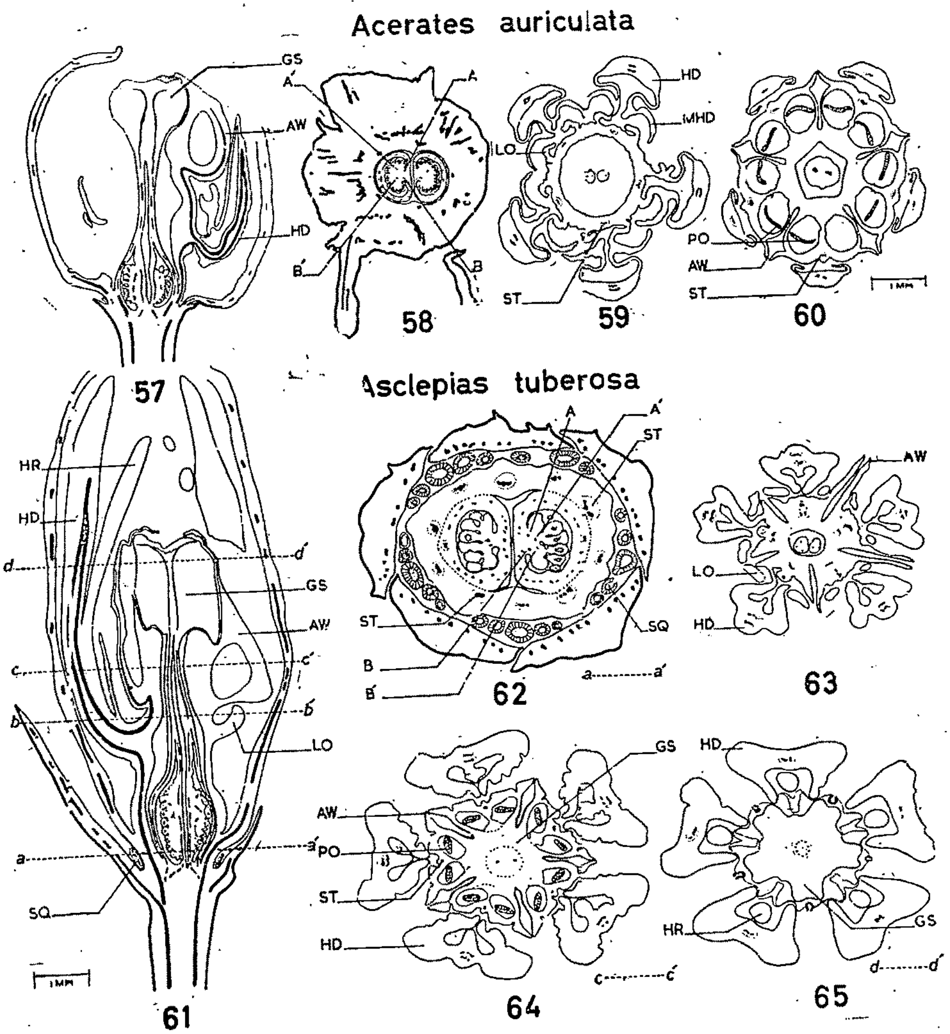

Figs. 57-60. *Acerates auriculata.* Fig. 57. L. S. of the flower. Figs. 58-60. Serial transverse sections of the same. Figs. 61-65. *Asclepias tuberosa.* Fig. 61. L. S. of flower. Figs. 62-65. Serial transverse sections of the same from base upwards. A & B=Secondary marginal bundles; A' & B'=Ventral bundles; AW=Anther wings; GS=Gynosteguism; HD=Hood; HR=Horn; LO=lobule; MHD=Margin of the hood; PO=Pollinia; SQ=Squamule; St=Stamen trace.

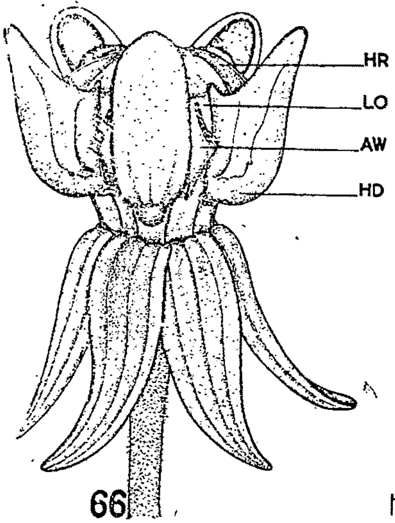

66

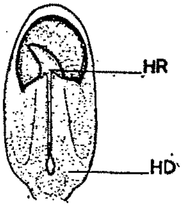

67

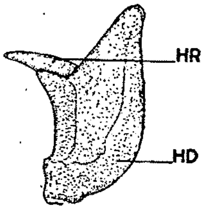

68

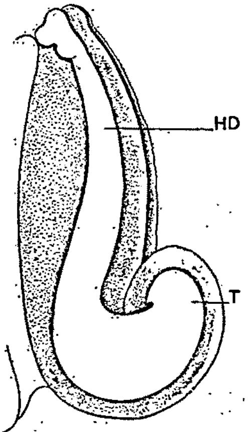

70

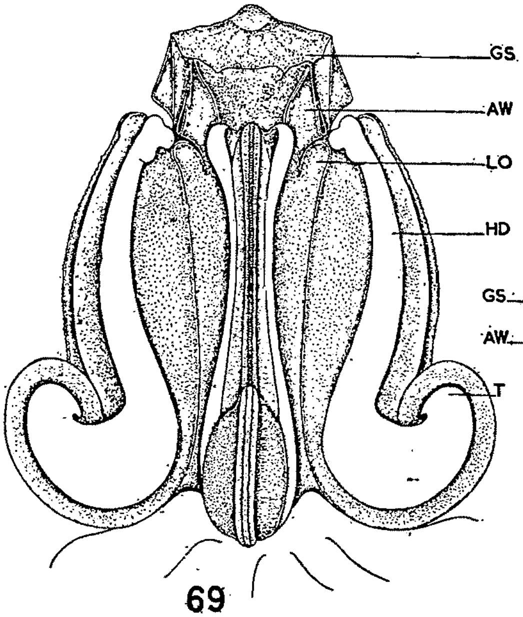

69

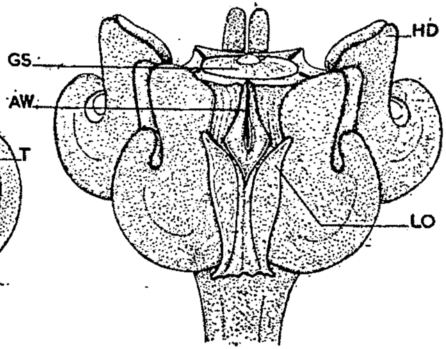

71

Fig. 66. A flower of *Asclepias syriaca* showing five hoods with horns and two anther wings with lobule. Fig. 67. Inner view of a single hood with a horn. Fig. 68. The same in lateral view. Fig. 69. A flower of *Calotropis gigentea* showing the different coronary structures. Fig. 70. A single hood in lateral view. Fig. 71. A flower of *Calotropis procera* with petals removed. AW=Anther wings; GS=Gynostegium; HD=Hood; HR=Horn; LO=Lobule; T=Tail.

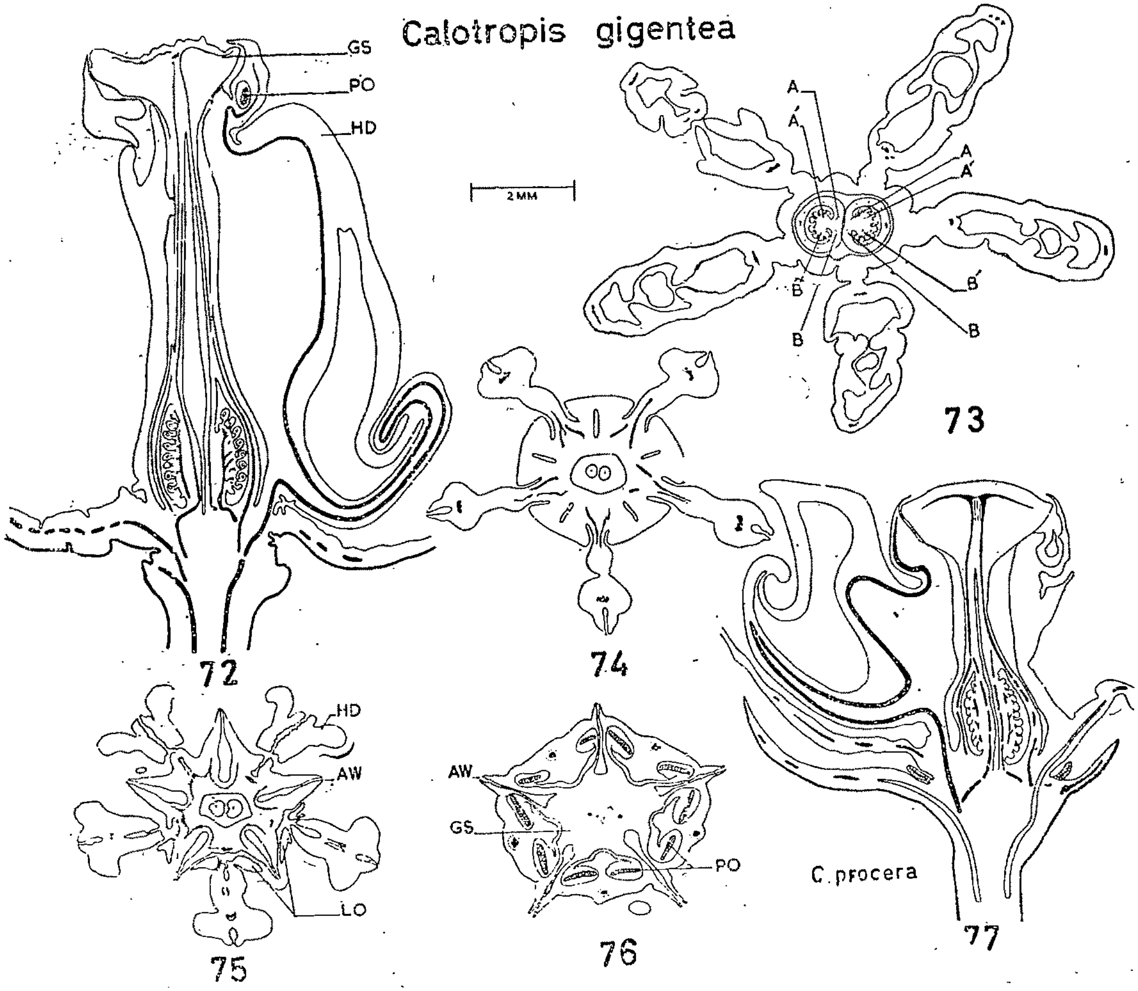

Fig. 72-76. *Calotropis gigentea.* Fig. 72. L. S. of the flower of *Calotropis gigentea.* Figs. 73–76. Serial transverse sections of the same from base upwards. Fig. 77. L. S. of flower of *Calotropis procera.* A & B=Secondary marginal bundles; A' & B'=Ventral bundles; AW=Anther wings; GS=Gynostegium; HD=Hood; LO=Lobule; PO=Pollinia.

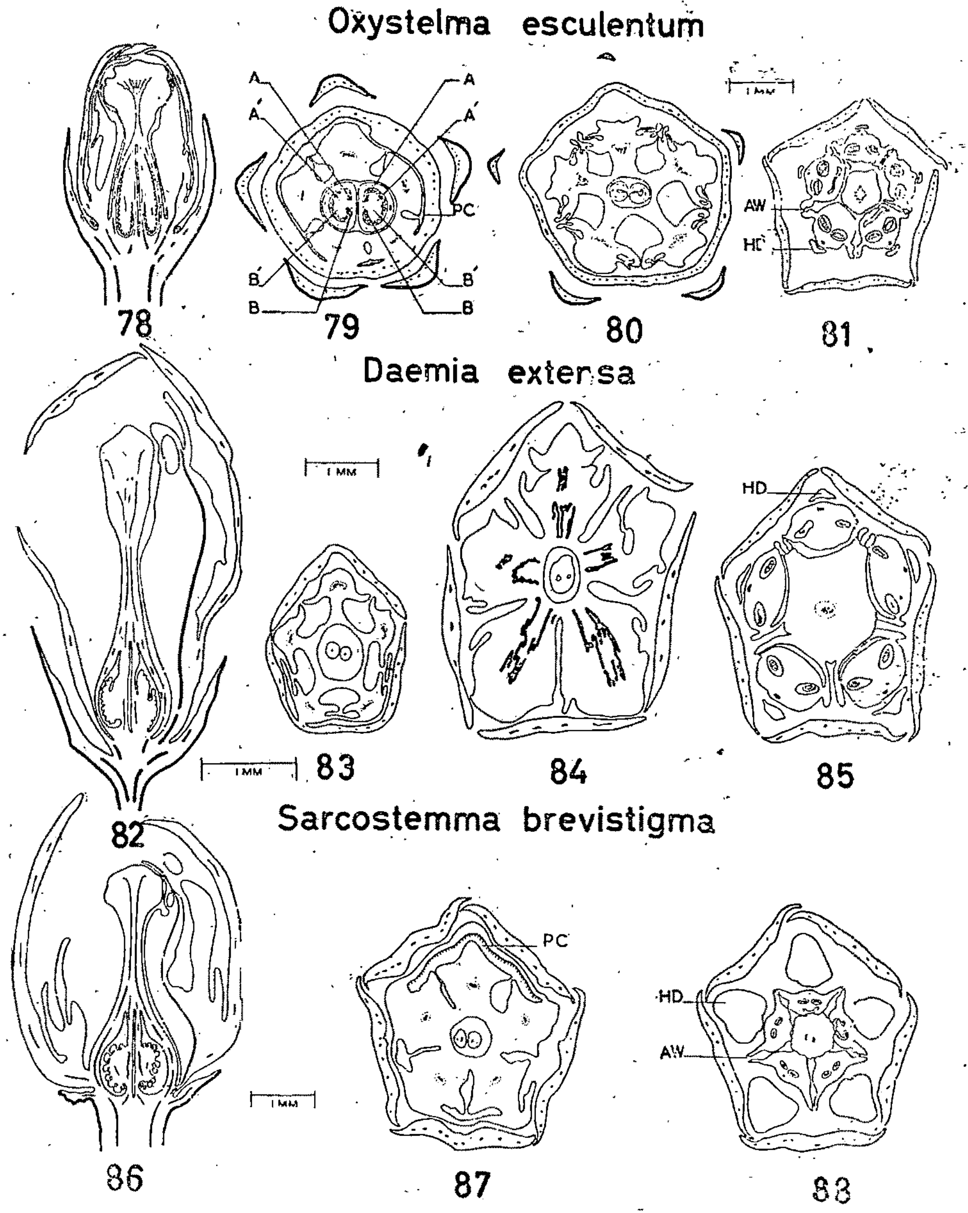

Figs. 78-81. *Oxystelma esculentum.* Fig. 78. L. S. of Flower. Figs. 79-81. Serial transverse sections of the same from base upwards. Figs. 82-85. *Daemia extensa.* Fig. 82. L.S. of the flower. Figs. 83-85. Serial transverse sections of the same from upwards. Figs. 86-88. *Sarcostemma brevistigma.* Fig. 86. L. S. of the flower. Figs. 87-88. Serial transverse sections of the flower from base upwards. A & B=Secondary marginal bundles; A' & B'=Ventral bundles; AW=Anther wings; HD=Hood; PC=Petaline corona.

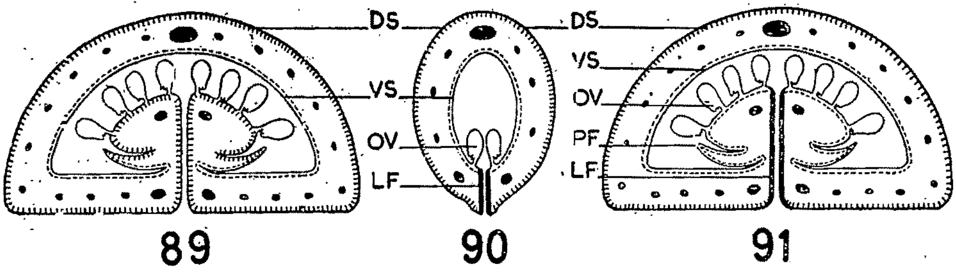

Fig. 89. Theoretical diagram to illustrate Safwats' view on the position of ovules and the nature of placental flaps. Figs. 90 & 91. illustrate our views on the same subject. DS=Dorsal surface; LF=Lateral face; PF=Placental flap;VS=ventral surface.

K° MESON PRODUCTION FROM K^+-P INTERACTIONS AT 2.26 BEV/C*

RANDHIR SINGH
Head of the Physics Department,
R. K. Degree College, Shamli (Muzaffarnagar).

The 20 inch hydrogen buble chamber of Brookhaven National Laboratory was exposed to a separated beam of K^+-mesons of momentum 2·26 Bev/C. The reaction $K^+ + P \rightarrow K^\circ + \pi^+ + P$ was studied. In a study of 30,000 pictures 317 events were found which fit the above reaction.

The reaction was found to be dominated by the production of two resonances, the $I=\frac{1}{2}$ K-π resonance, K* (888), and the I=3/2 pion nucleon isobar N* (1238). In about 62% of the cases the reaction proceeds by the production of one or the other of these resonances, their relative production cross-sections being equal.

Both K* and N* were produced by a peripheral collision mechanism. Production of N* was consistent with the exchange of a ρ meson. Production of K* was found to be inconsistent with the exchange of a single pion at the production vertex.

The evidence for the production of K′ (730) in this reaction is not positive. A suggestion for further study is made, for a few events grouped with invariant masses above 1600 MeV in the $P-\pi^+$ system and around 1540 MeV of the $P-K^\circ$ system.

The partial cross-sections for the reactions which have the topology of two positive prongs and a V° are also determined. It is found that the cross-section for the reaction $K^+ + P \rightarrow K^\circ + \pi^+ + P$ at this energy is less than that reported at a slightly lower energy.

In recent years a large number of strongly interacting particles have been discovered[1]. These resonant particles or resonant states are exceedingly short-lived. Their life times are of the order of 5×10^{-24} to 5×10^{-18} sec. The first such state found was the p-wave pion nucleon resonance, $N^*_{3,3}$ (1238).[1,2] Theoretical calculations[3] indicated the presence of another possible p-wave resonance in $\pi-K$ scattering. Such a resonant state, K* (888), has been discovered[4] in bubble chamber studies, and subsequently examined by various experimenters.[5,6,7] Another $\pi-K$ resonance at 730 Mev, K′ (730), has also been observed[8] in a bubble chamber experiment. In the text, for simpli-

---

* Supported by the Air Force Office of Scientific Research and the National Science Foundation of the U.S.A.

city, $N^*_{3,3}{}^{++}$ (1238) will be referred to as N^* or N^{*++}. Similarly K^{*+} (888) will be written as K^* (888) or simply K^*.

The purpose of the present experiment was to study the interaction of K^+ mesons of momentum 2·26 Bev/c, with protons in the reaction,

$$K^+ + P \rightarrow K^\circ + \pi^+ + P \qquad \text{..(1)}$$

This includes study of mass ranges, central values and widths of K^{*+} and N^{*++}, their relative production cross-sections at this energy, and a study of their production mechanism with a particular emphasis on the one particle exchange model. The partial cross-sections also were determined for the reactions which have the same topology as reaction (1), *viz.*, two positive prongs at the production vertex and an associated V°. In addition, the reaction (1) was examined to see if the K′ (730) or any other resonance between the final state particles might be present.

The film for the experiment was obtained from the 20-inch BNL (Brookhaven National Laboratory of U.S.A.) hydrogen bubble chamber exposed to K^+ mesons of 2·26 Bev/C in the BNL-Yale separated beam[13] at the AGS (Alternating Gradient Synchrotron) of BNL.[14] The momentum spread of the beam was ±1%.

The analysis of the film and reduction of the data was done at the High Energy Laboratory of The Johns Hopkins University. The scanning of the film for the required interactions was done on Prevost-type scanning projectors. Measurement of the events was made on a Brower digitized microscope with Datex encoders and digital system.

The data from the measuring engines were processed through the BNL TRED-KICK system of geometrical reconstruction and kinematical fitting program on IBM 7094 digital computers. An event was accepted as fitting hypothesis (1) if it had a goodness of fit (χ^2) of less than 13·27 as determined by the kinematic fitting program. This corresponded to a probability of greater than 99 per cent.

Of the 30,000 pictures which were analysed, 317 events were found which fit reaction (1). The film was scanned twice with a total scanning efficiency of 97·5 per cent.

The beam of K^+ mesons of 2·26 Bev/C entering the bubble chamber was contaminated by positive pions, muons and electrons. The percentage of K^+ mesons in the beam was determined to be 66·7±3·3% by counting the number of tau decays in the sample and also, independently by counting characteristic delta rays along the track.

Reaction (1) above may proceed via the following four channels;

(a) $K^+ + P \rightarrow K^{*+} + P$

$$\quad\quad \lfloor\!\!\longrightarrow K^\circ + \pi^+$$

$$\text{(b)}\quad K^+ + P \rightarrow K^\circ + N^{*++}$$
$$\qquad\qquad\qquad\qquad \lfloor\!\rightarrow P + \pi^+$$

$$\text{(c)}\quad K^+ + P \longrightarrow \text{interference between processes (a) and (b)}$$

$$\text{(d)}\quad K^+ + P \longrightarrow K^\circ + \pi^+ + P \text{ (not resonating)}, \qquad ..(2)$$

or by some other resonant state.

In what follows, unless otherwise stated, the term center of mass (c.m.) will refer to the center of mass of the incident K+ mesons and the target proton, and the word proton will mean the final state proton. The invariant mass or the effective mass ($M_{1,2}$) of the possible 2-particle combinations is given by,

$$M^2_{1,2} = (E_1 + E_2)^2 - (p_1 + p_2)^2$$

where E_i is the total energy, p_i is the three momentum vector and m_i the rest mass of the i-th particle. We have, also

$$E_i^2 = p_i^2 + m_i^2$$

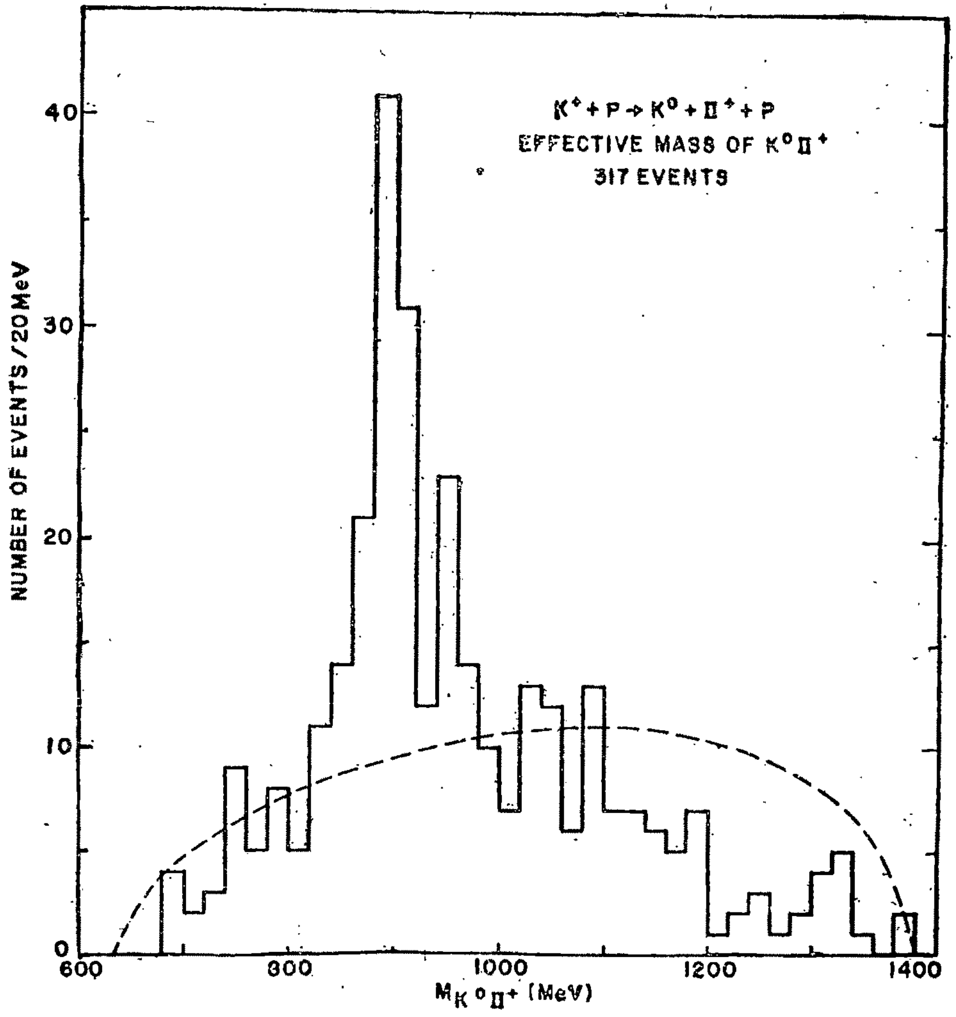

Fig. 1

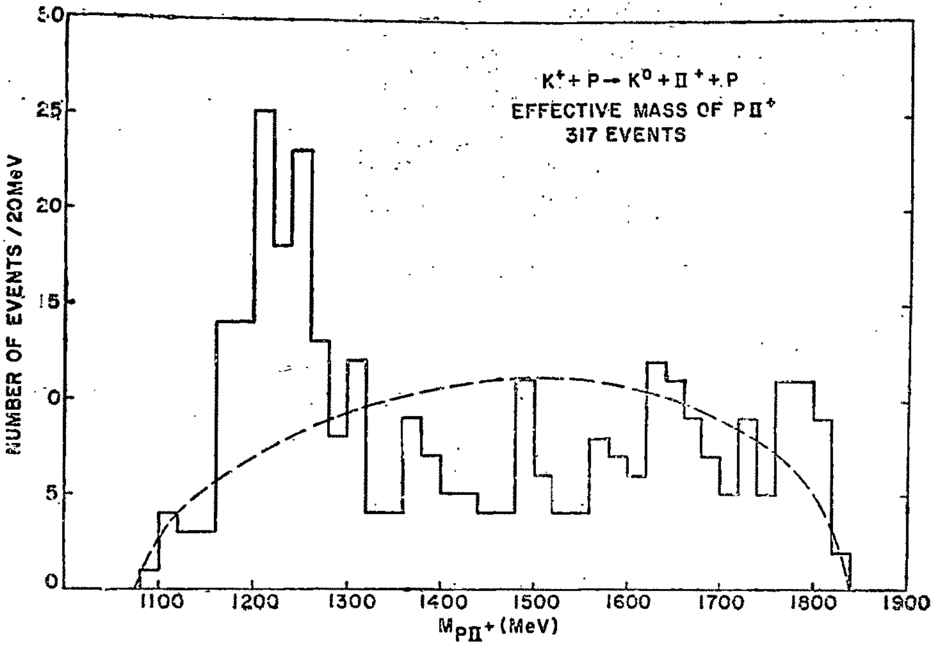
K⁺+ P → K⁰ + Π⁺ + P
EFFECTIVE MASS OF PΠ⁺
317 EVENTS
NUMBER OF EVENTS / 20MeV
30
25
20
15
10
5
0
1100
1200
1300
1400
1500
1600
1700
1800
1900
M_PΠ⁺ (MeV)

Fig. 2

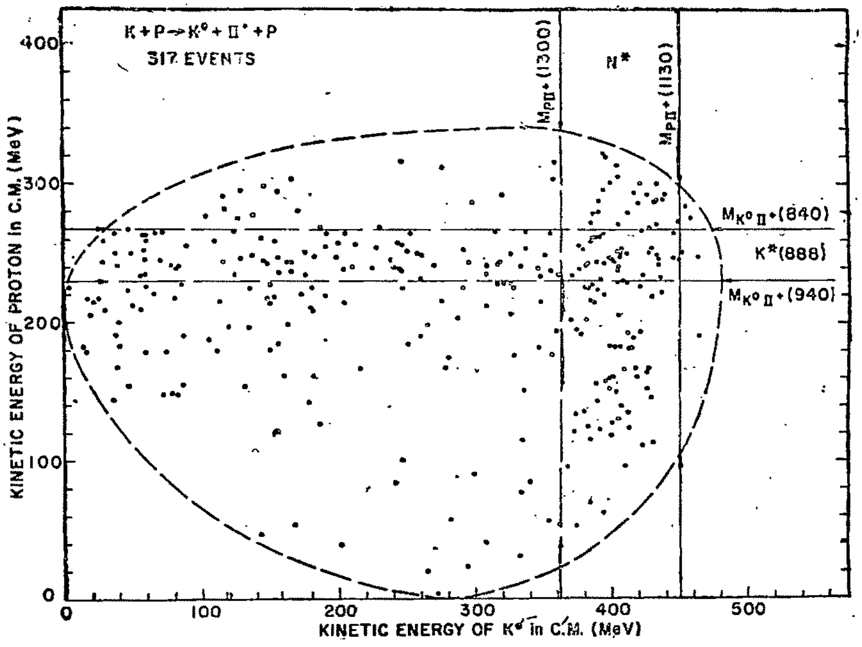
K + P → K⁰ + Π⁺ + P
317 EVENTS
M_PΠ⁺ (1300)
N*
M_PΠ⁺ (1130)
M_K⁰Π⁺ (840)
K*(888)
M_K⁰Π⁺ (940)
KINETIC ENERGY OF PROTON in C.M. (MeV)
400
300
200
100
0
0
100
200
300
400
500
KINETIC ENERGY OF K⁰ in C.M. (MeV)

Fig. 3

Fig. 1 is a histogram of the effective mass of the K°—π^+ system ($M_{K^\circ\pi^+}$) in which a peak corresponding to the K* resonance is evident above the phase space representing the expected distribution in the absence of any final state interaction between the particles. Similarly, in Fig. 2, which is a histogram of the effective mass of the P—π^+ system, a peak corresponding to N* production appears above the phase space. Fig. 3 is a Dalitz plot of the kinetic energy of P versus kinetic energy of K° in the center of mass, where the dotted envelope of the Dalitz plot represents the kinematic limits for the reaction in this experiment. In the absence of any resonances in the final state particles, events should be evenly populated inside the envelope. The condensation of events in the banded regions indicates that the π^+ resonates with the K° or the proton a large fraction of the time to form either a K* or an N*, respectively.

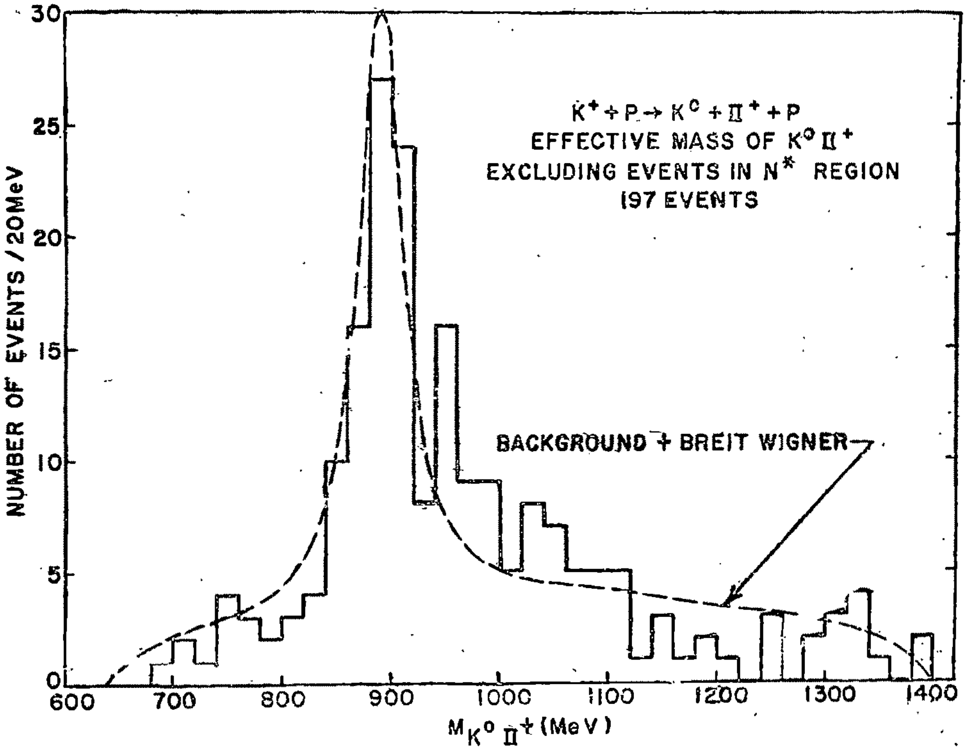

Fig. 4

Fig. 4 is a histogram of the effective mass of the K°—π^+ system ($M_{K^\circ\pi^+}$) excluding events for which the effective mass of the P—π^+ system lay in the N* mass range ($1130 \leqslant M_{P\pi^+} \leqslant 1300$), on this plot, the dotted line is a Breit-Wigner resonance curve, and the phase space is fitted to the background events. There are 85 events in the K* mass region. On both the histograms (figs. 1 and 4) for the effective mass of the K°—π^+ system, a shoulder

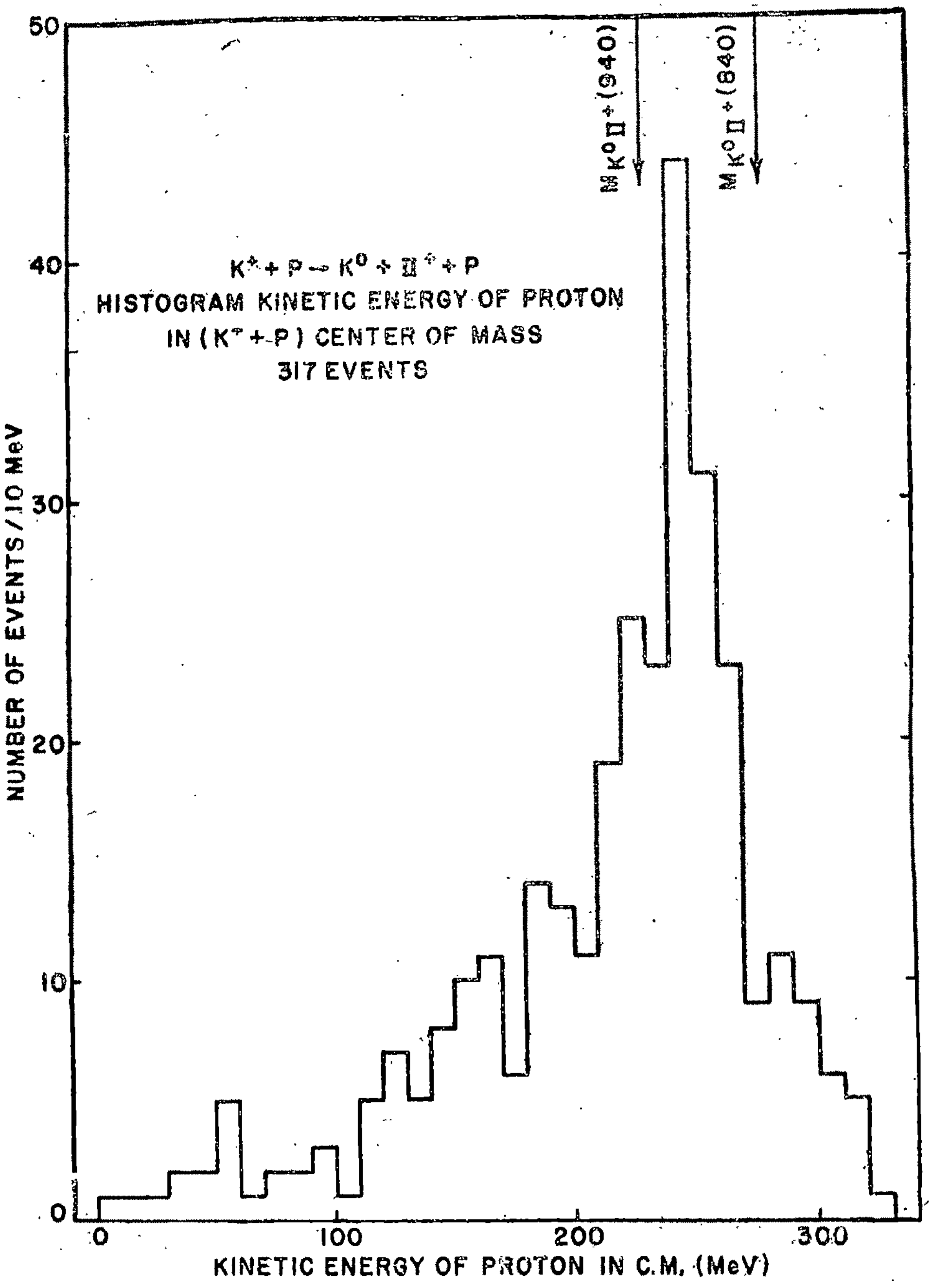

Fig. 5

between $940 \leqslant M_{K^\circ \pi^+} \leqslant 960$ is noticeable above the phase space. Fig. 5 is a histogram of the kinetic energy of P in the center of the mass for all events. In this plot we do not see any bump corresponding to the shoulder noted above. We conclude that this shoulder is only a statistical effect and is not due to any other resonance in the K°—π^+ system. From fig. 4 we take the mass range of the K* resonance to be between $840 \leqslant M_{K^\circ\pi^+} \leqslant 940$ Mev. with full width at half maximum of 50 MeV centered at 888±5. Figs. 1 and 4 do not yield any positive evidence for the existence of the K′ (730) resonance.

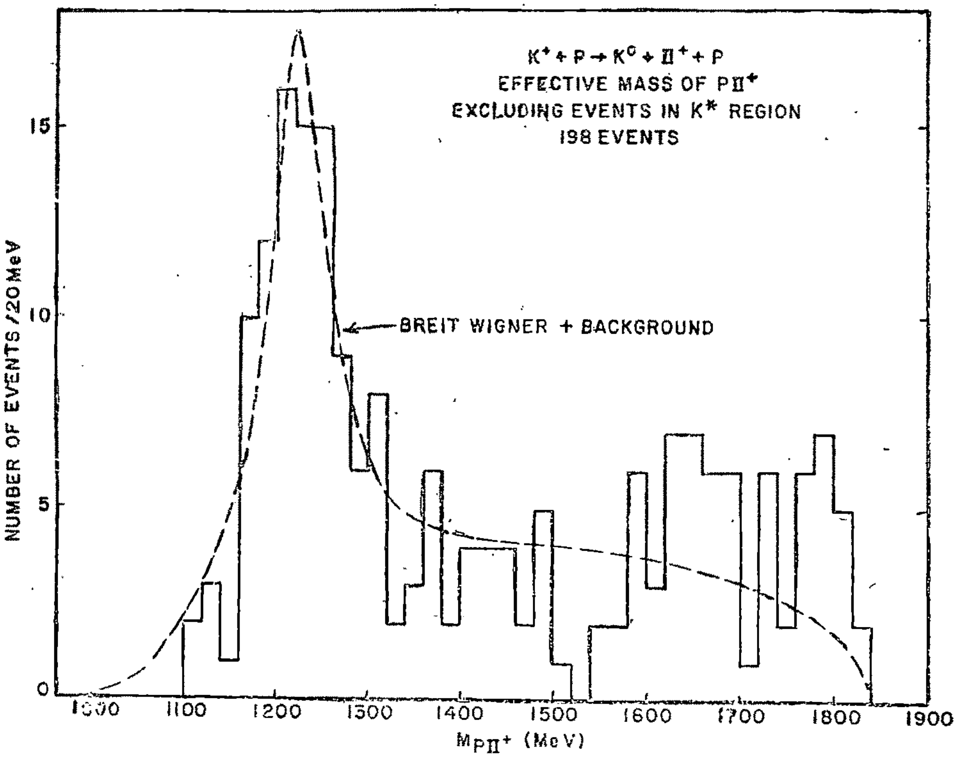

Fig. 6

Fig. 6 is a histogram of the effective mass of the P—π^+ system ($M_{P\pi^+}$) excluding events in the mass range of the K* resonance ($840 \leqslant M_{K^\circ\pi^+} \leqslant 940$). The dotted curve on this plot is again a Breit-Wigner resonance curve and the phase space is fitted to background events. There are 86 events in the N* mass range. From this fit we define the mass range of N* resonance as $1130 \leqslant M_{P\pi^+} \leqslant 1300$ MeV. with full width at half maximum of 80 MeV. and central value of 1225±9 MeV. This result of the central value of N* at 1225 MeV agrees with the results of J. Duboc[7], but differs from the accepted value 1238 MeV.[2] This may be because the statistics is very limited.

Fig. 7 is a scatter plot of the cosine of the π^+ in the center of mass ($\cos\theta_{\pi^+}$) versus effective mass of the K°—π^+ system. We notice that the pion from the K* events goes predominantly forward in the center of mass. Fig. 8

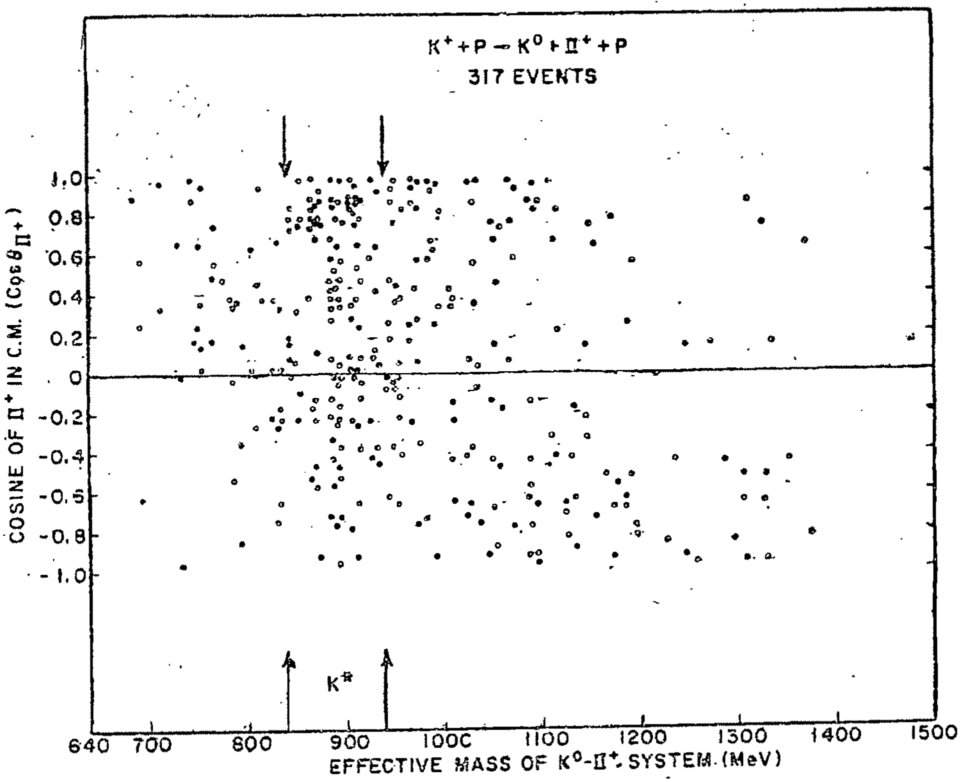
K⁺+P → K⁰+Π⁺+P
317 EVENTS
K*
COSINE OF Π⁺ IN C.M. (Cos θ_Π⁺)
1.0
0.8
0.6
0.4
0.2
0
-0.2
-0.4
-0.6
-0.8
-1.0
640
700
800
900
1000
1100
1200
1300
1400
1500
EFFECTIVE MASS OF K⁰-Π⁺ SYSTEM (MeV)

Fig. 7

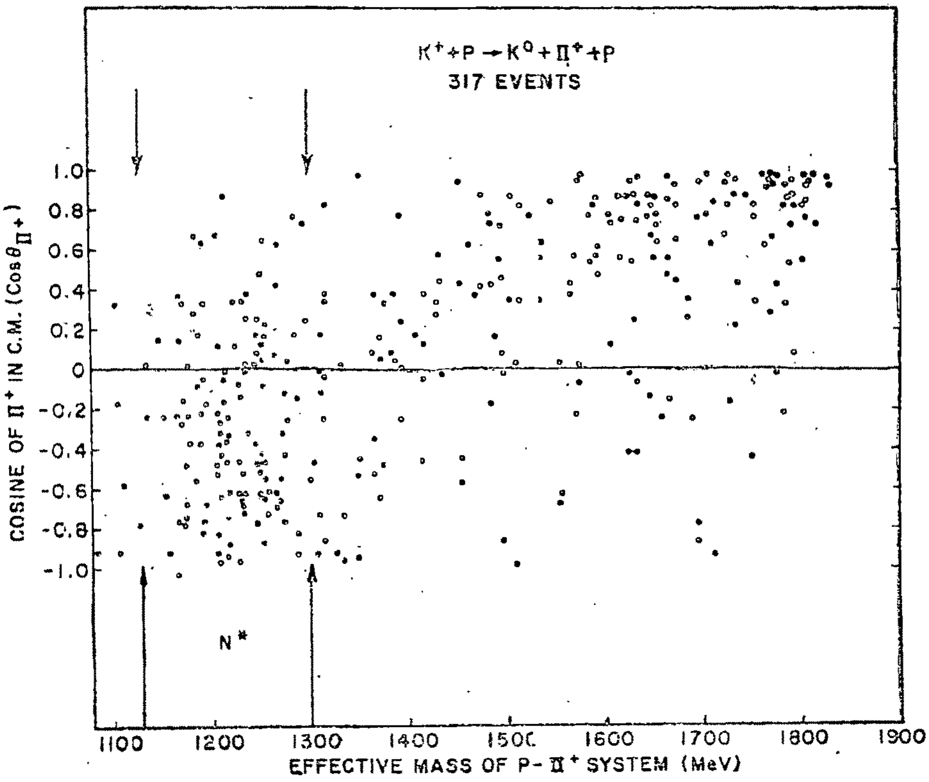
K⁺+P → K⁰+Π⁺+P
317 EVENTS
N*
COSINE OF Π⁺ IN C.M. (Cos θ_Π⁺)
1.0
0.8
0.6
0.4
0.2
0
-0.2
-0.4
-0.6
-0.8
-1.0
1100
1200
1300
1400
1500
1600
1700
1800
1900
EFFECTIVE MASS OF P-Π⁺ SYSTEM (MeV)

Fig. 8

is a similar scatter plot between the cosine of the π^+ in the center of mass versus the effective mass of the P—π^+ system. We notice that the pion from the N* events goes preferentially backward in the center of mass. In addition we notice that above the mass range $M_{P\pi^+} \geqslant 1600$ MeV more pions go forward in the center of mass. Fig. 9 is a plot of the cosine of the π^+ in the center of mass for events which are neither K* nor N*. We notice that the distribution is not isotropic, since more events are going in the for-

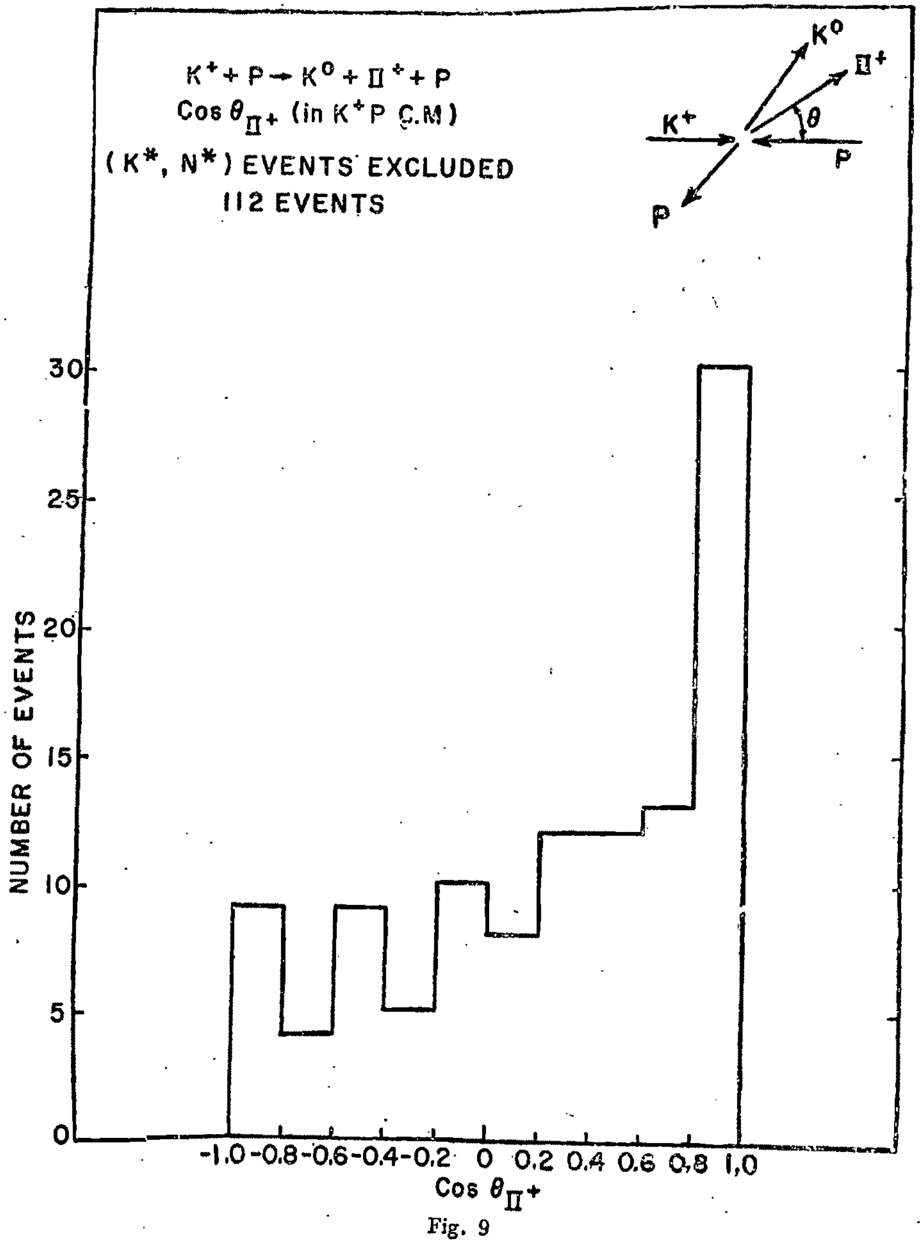

Fig. 9

ward direction than in the backward direction. This effect may be due to those K* events which lie just outside of the mass limits that have been assigned for K*.

The apparent grouping of the events in the mass range $M_{P\pi^+} \geqslant 1600$ MeV (figs. 2 and 6) was studied in detail. In Fig. 10, which is a Dalitz plot of the kinetic energy of the π^+ versus the kinetic energy of P in the center of mass, these events appear to form a band parallel to the N* band. Although a possible I=3/2 nuclean-pion resonance at 1640 MeV has been reported from scattering experiments,[2] the data in this experiment are too meager to draw any conclusion.

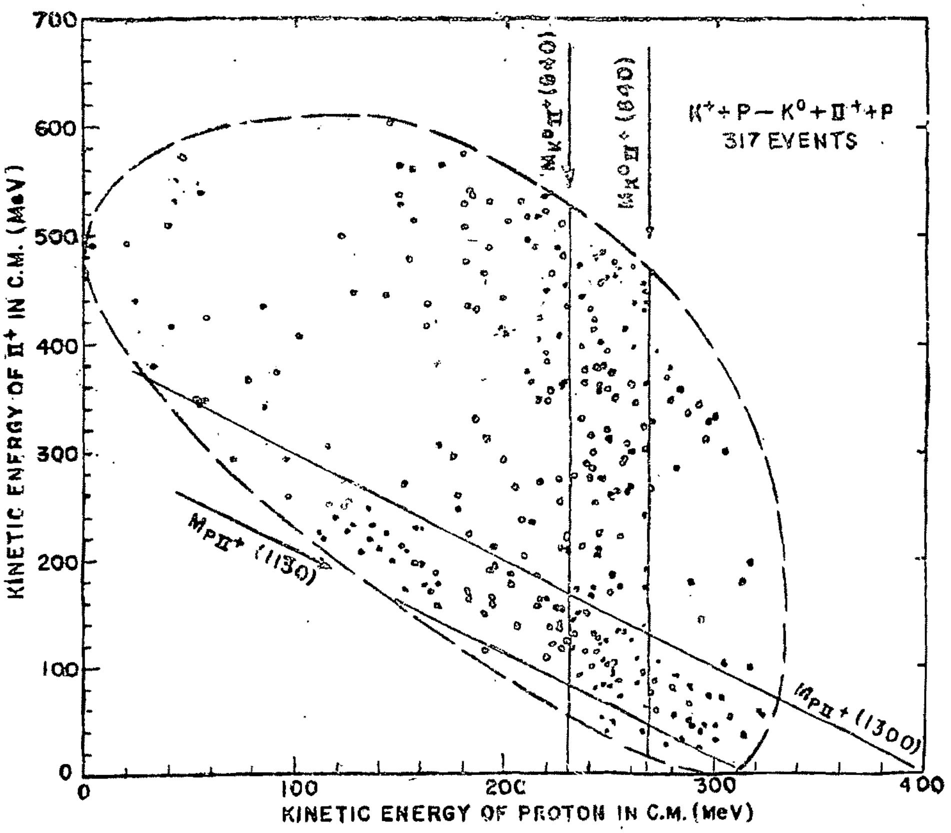

Fig. 10

Fig. 11 is a histogram of the effective mass of the P—K° system excluding the events in the K* and N* mass range. There is no obvious evidence for a resonance in this system, although the grouping around 1540 MeV should be studied when better statistics are available.

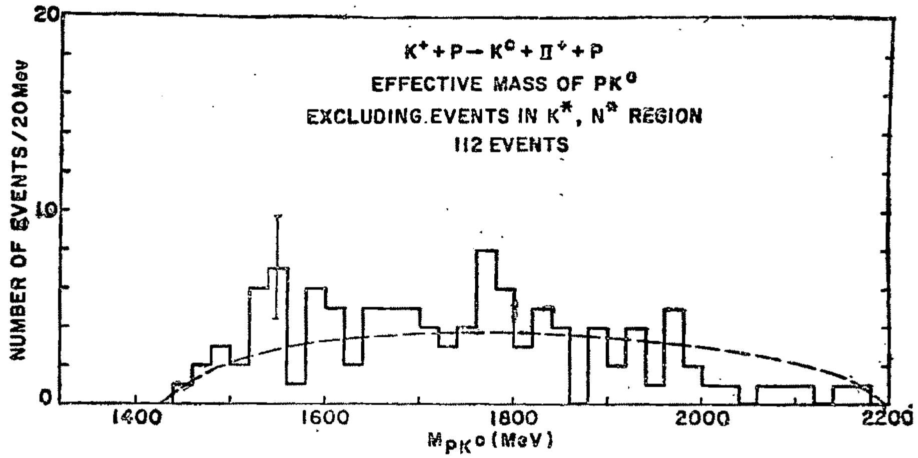

Fig. 11

In the sample of 317 events which fit the reaction (1), only 85 events lay in the mass range of K*, and not in the mass range of N*, 86 events lay in the mass range of N* and not in the mass range of K*. Events in the overlap region, *i.e.*, for which $M_{K^0\pi^+}$ fell in the mass range of K* and $M_{P\pi^+}$ fell in the mass region of N* could have been produced via any of the four channels previously mentioned (2). In order to determine the relative cross-sections for production of K* and N* in reaction (1), the correct number of K* and N* events is needed. Therefore it is necessary to separate the events in the overlap region in categories (2). There are 34 events in this overlap region of K* and N*. The number is consistent with the expected intensities from the superposition of N* and K* bands, therefore we do not see evidence of interference between channels (2a) and (2b). Separation of events from the overlap region was made on the basis of the direction of π^+t in the center of mass and a comparison of the $M_{K^0\pi^+}$ and $M_{P\pi^+}$ with respect to the nominal central value of K* and N* masses. The analysis results in a total of 103 events in the K* mass region and a total of 102 events in the N* mass region. Therefore, 31·9 ± 3·1 per cent of reaction(1) proceeds via the production of N* and 31·9 ± 3·1 per cent proceeds via the production of K*.

Peripheral interactions play an important role in high energy physics.[9],[10] The word "peripheral" usually refers to an interaction which is transmitted by the least massive system that may be exchanged between the colliding particles. In most of the strong interactions this system consists of a single pion. However, in recent years, the meaning of the word "peripheral" has been extended[10] so that any interaction which is transmitted through the exchange of a single virtual particle is called a "peripheral" interaction. This kind of interaction is more properly denoted as a one particle exchange interaction.

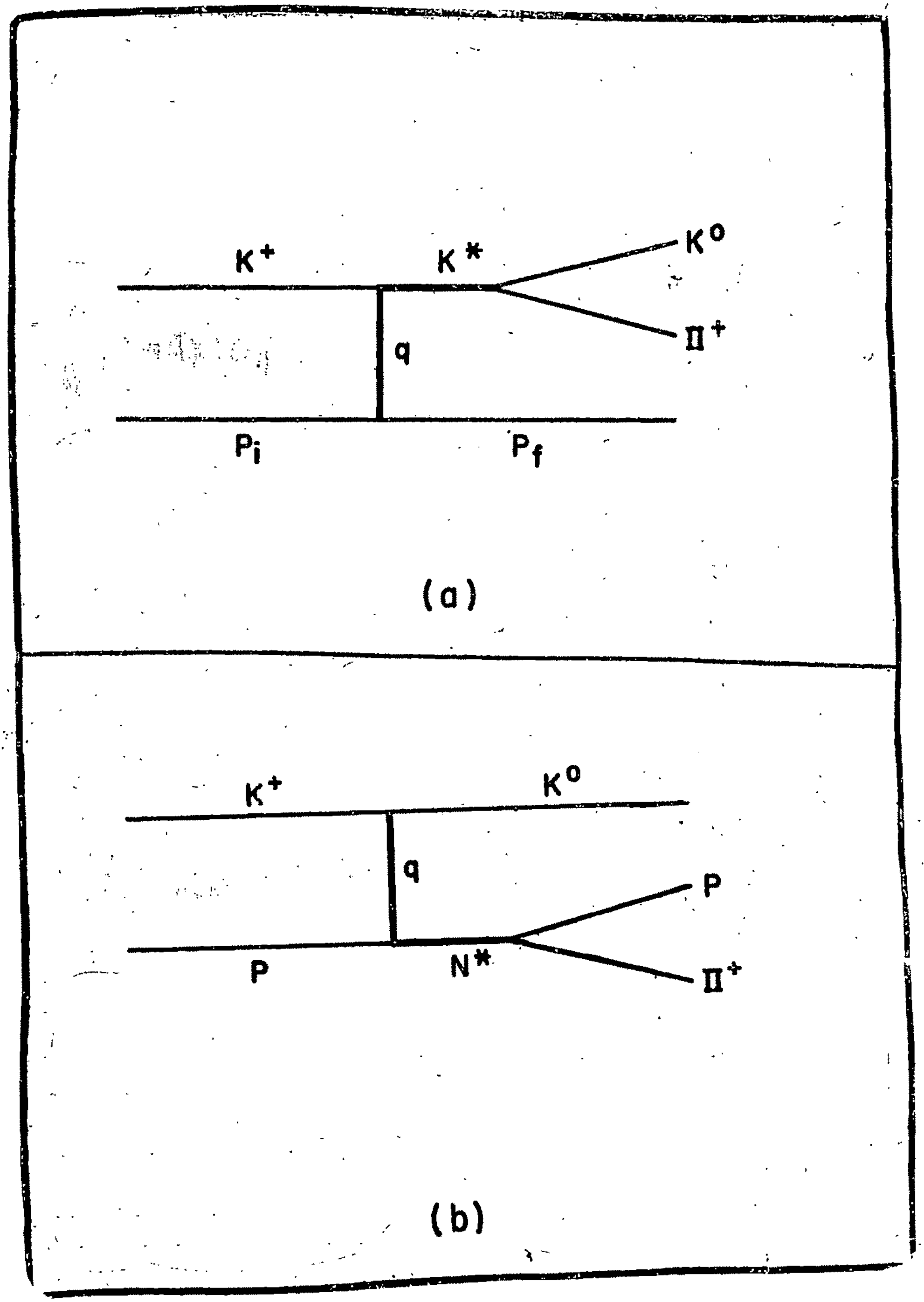

Fig. 12

Various theoretical approaches[9],[10] have been proposed to test the one particle exchange model. Such a model can be tested best in those cases in which the final state particles resulting from the collision of two particles, can be partitioned into two groups, and the invariant momentum transfer at the

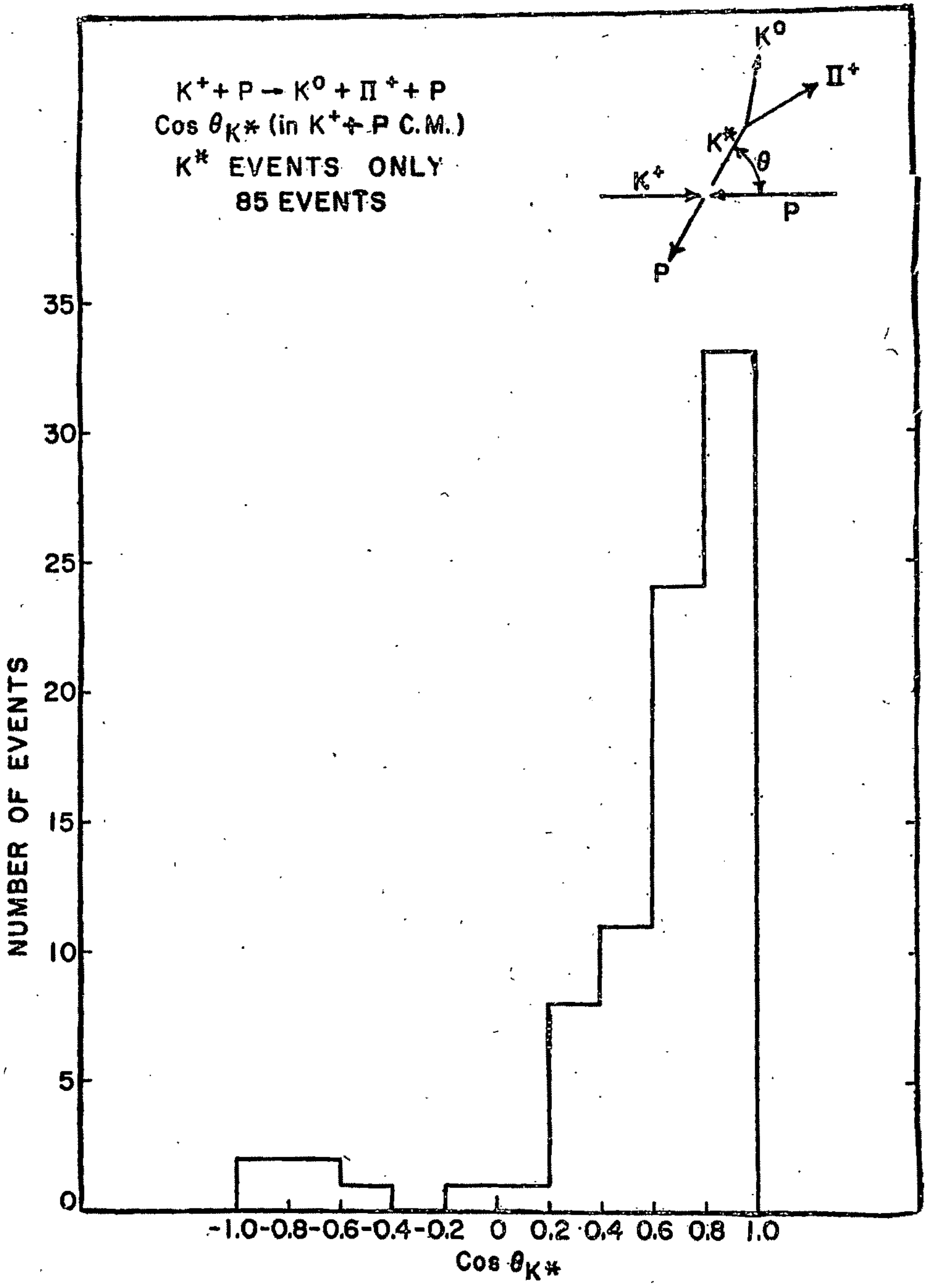

Fig. 13

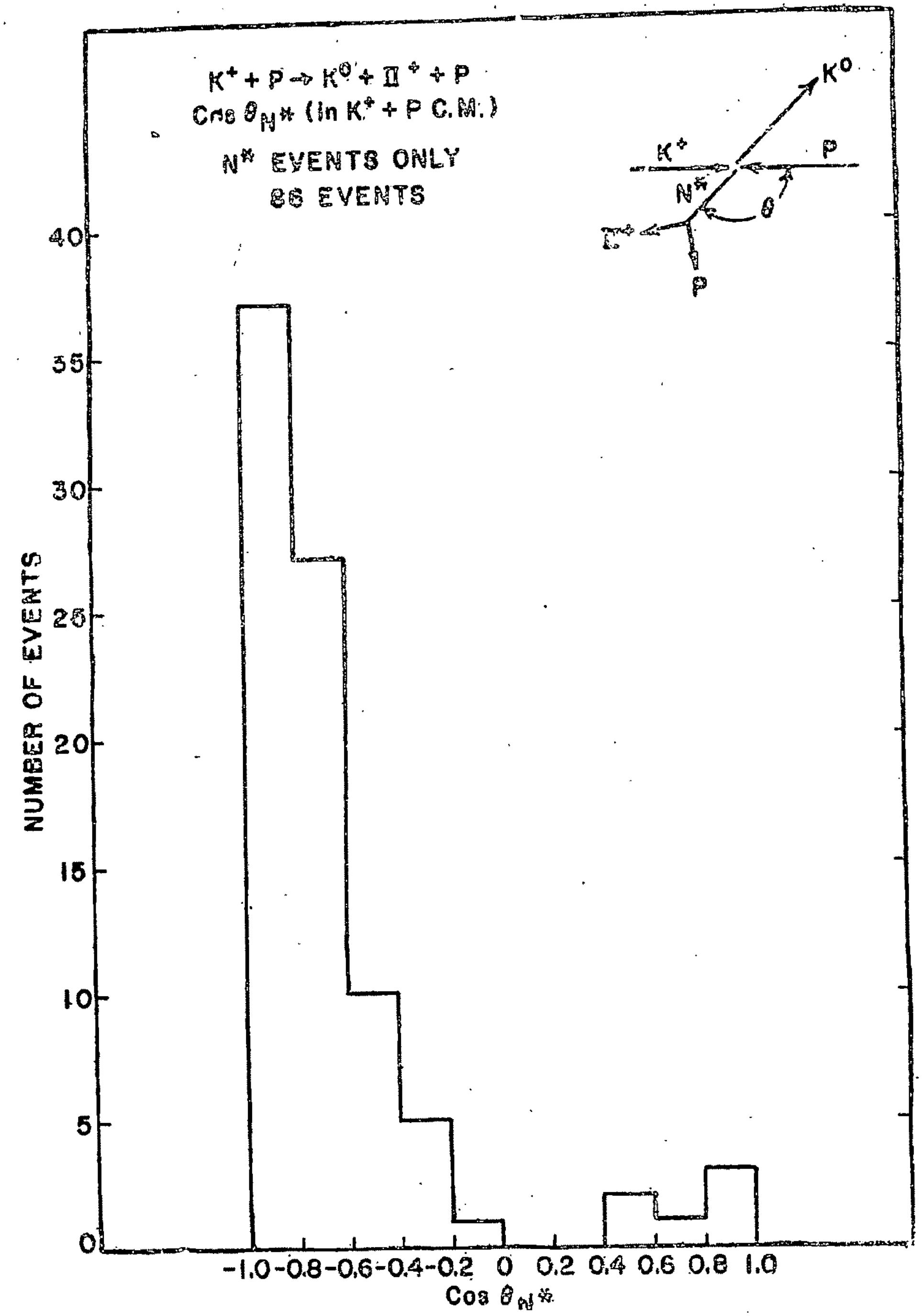

Fig. 14

production vertex is not too large. In the production of K* and N* resonances in reaction (1), the final state particles from two groups, *viz.*, K* and P in the production of K*, and K° and N* in the production of N* (Fig. 12).

Further in the analysis of the data it was found that in the overall center of mass K* goes predominantly forward (Fig. 13) and N* backwards (Fig. 14), suggesting peripheral production of both K* and N*. Therefore an investigation has been made to see whether the one particle exchange model is valid for processes (2a) and (2b).

Fig. 15 shows the distribution in four momentum transfer squared (Δ^2) associated with production of K*. A similar distribution for N* is shown in fig. 16. If P_j represents the four vector, m_j the rest mass, E_j the total energy, and p_j the three momentum vector of the j-th particle, then

$$P_j^2=(p_j,\, iE_j)^2+p_j^2-E_j^2=-m_j^2$$

The invariant four momentum transferred squarred for K* production, fig. 12a is given by

$$\Delta^2_{K^*}=-(P_i-P_f)^2$$

where P is four vector for the initial and final state proton.

Similarly, the invariant four momentum transfer squarred for N* production fig. 12b is given by

$$\Delta^2_{N^*}=-(P_{K^\circ}-P_{K^+})^2$$

In both distribution plots, (figs. 15 and 16), Δ^2 is expressed in terms of pion mass (m_π^2) in an interval of $5m_\pi^2$. From these plots we notice that for production of both K* and N*, Δ^2 is peaked at low values $\{(\Delta/m_\pi)^2\leqslant 25\}$. The low four momentum transfer indicates that both K* and N* are produced in a peripheral collision.

In the production of K* the exchange of a single virtual pion is allowed by the conservation of strangeness, isotopic spin and parity. Exchange of a ρ meson is also allowed. Since the exchange of a scalar meson along 'q' (Fig. 12) does not carry any angular information, no correlation between the directions defined by the plane $(P_i\times P_f)$ and $(K^\circ\times\pi^+)$ is expected. This means that the distribution in the Treiman-Yang angle[11] (ϕ_{K^*}) must be isotropic. The Treiman-Yang angle is given by,

$$\phi_{K^*}=\cos^{-1}\frac{(P_i\times P_f).(K^\circ\times\pi^+)}{|(P_i\times P_f)|.|K^\circ\times\pi^+)|}. \qquad ..(3)$$

where the momentum vectors P_i, P_f, K° and π^+ of the respective particles are evaluated in the rest frame of the initial Kaon. 'i' and 'f' refer to initial and final state particle respectively.

Fig. 17 presents the distribution in the Treiman-Yang angle for K* events only. We observe a strong anisotropy. This anisotropy in the distribution in the Treiman-Yang angle in the production of the K* weighs heavily against the exchange of only a single pion.

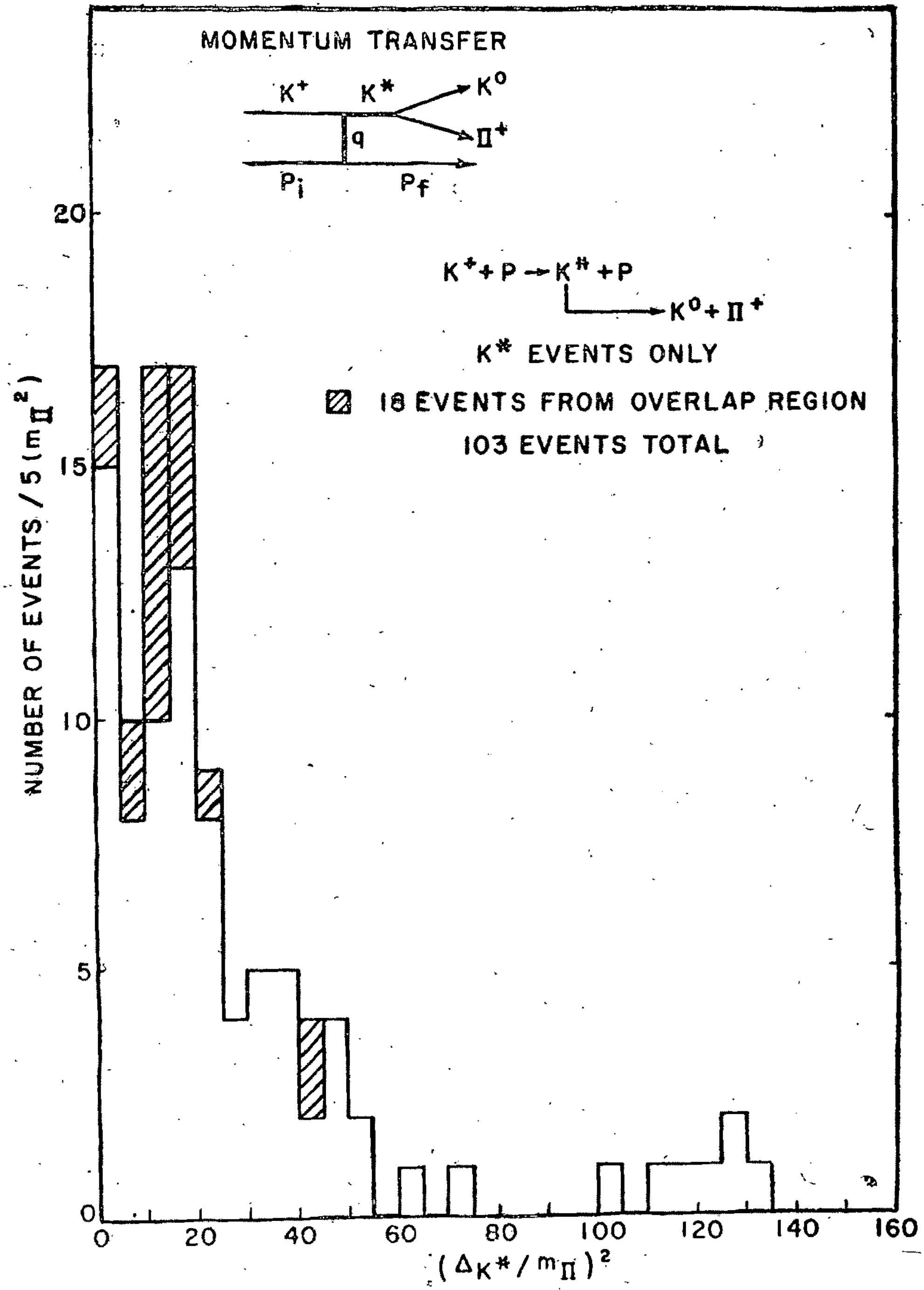
MOMENTUM TRANSFER
K⁺
K*
K⁰
q
Π⁺
Pᵢ
P_f
K⁺+P → K* +P
→ K⁰+ Π⁺
K* EVENTS ONLY
▨ 18 EVENTS FROM OVERLAP REGION
103 EVENTS TOTAL
NUMBER OF EVENTS / 5 (m_Π²)
0
5
10
15
20
0
20
40
60
80
100
120
140
160
(Δ_K* / m_Π)²

Fig. 15

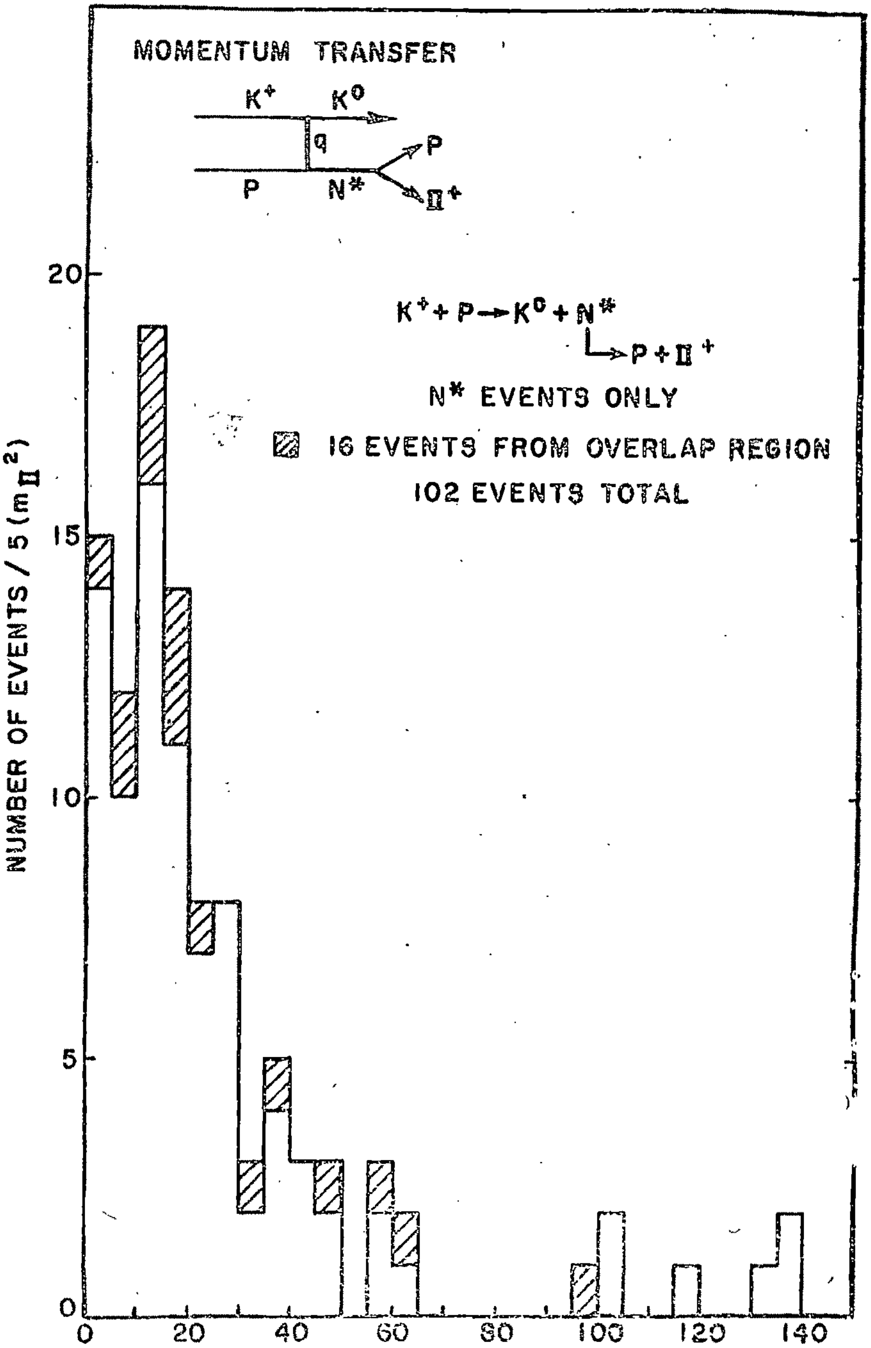
MOMENTUM TRANSFER
K^+
K^0
q
P
P
N^*
π^+
$K^+ + P \rightarrow K^0 + N^*$
$\hookrightarrow P + \pi^+$
N^* EVENTS ONLY
▨ 16 EVENTS FROM OVERLAP REGION
102 EVENTS TOTAL
NUMBER OF EVENTS / 5 $(m_\pi{}^2)$
0
5
10
15
20
0
20
40
60
80
100
120
140
$(\Delta_{N^*}/m_\pi)^2$

Fig. 16

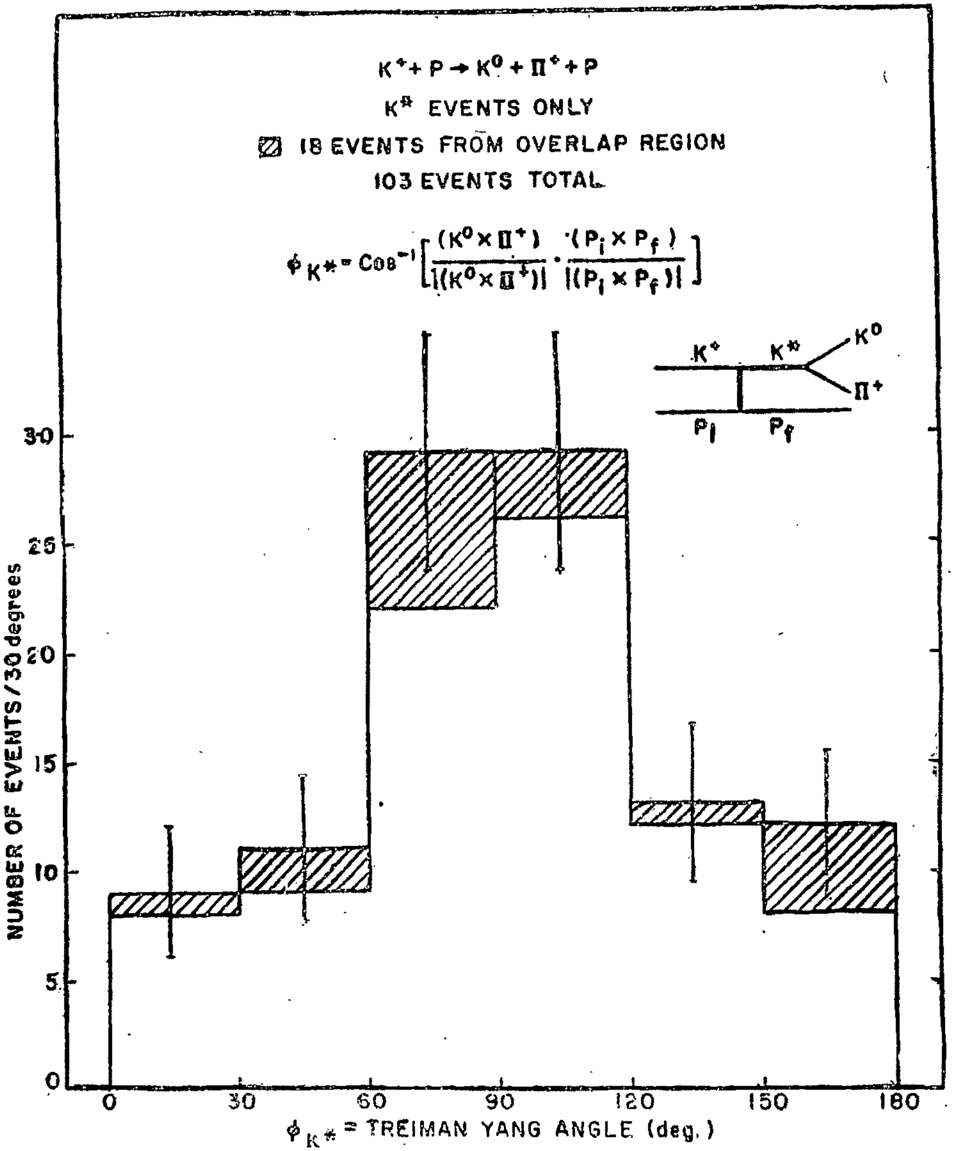

Fig. 17

In terms of the one particle exchange model, if K* was produced via the one pion exchange mechanism the four momentum transfer squared should be less than the four momentum transfer squared associated with the production of N* in which exchange of a particle heavier than a pion is necessary. From figs. 15 and 16 we notice that the four momentum transfer squared associated with production of both the resonances are almost equal. This also shows that our results are not consistent with the production of K* via only a one pion exchange mechanism.

The production of an N* via a one pion exchange is prohibited by the parity conservation at the K+–K° vertex, (fig. 12). The lightest single particle exchange allowed is a ρ meson (spin 1^-, mass 750 MeV). Fig. 18 shows the distribution in Treiman-Yang angle (ϕ_{N*}) for N* events. The Treiman-Yang angle (ϕ_{N*}) for this case is given by,

$$\phi_{N*} = \cos^{-1} \frac{(P \times \pi^+).(K^+ \times K^\circ)}{|(P \times \pi^+)|.|(K^+ + K^\circ)|} \qquad ..(4)$$

K^+, K°, P, π^+ are momentum vectors of the respective particles in the lab. A strong anisotropy in the distribution of (ϕ_{N*}) manifests the possibility of exchange of a vector particle along '*q*'.

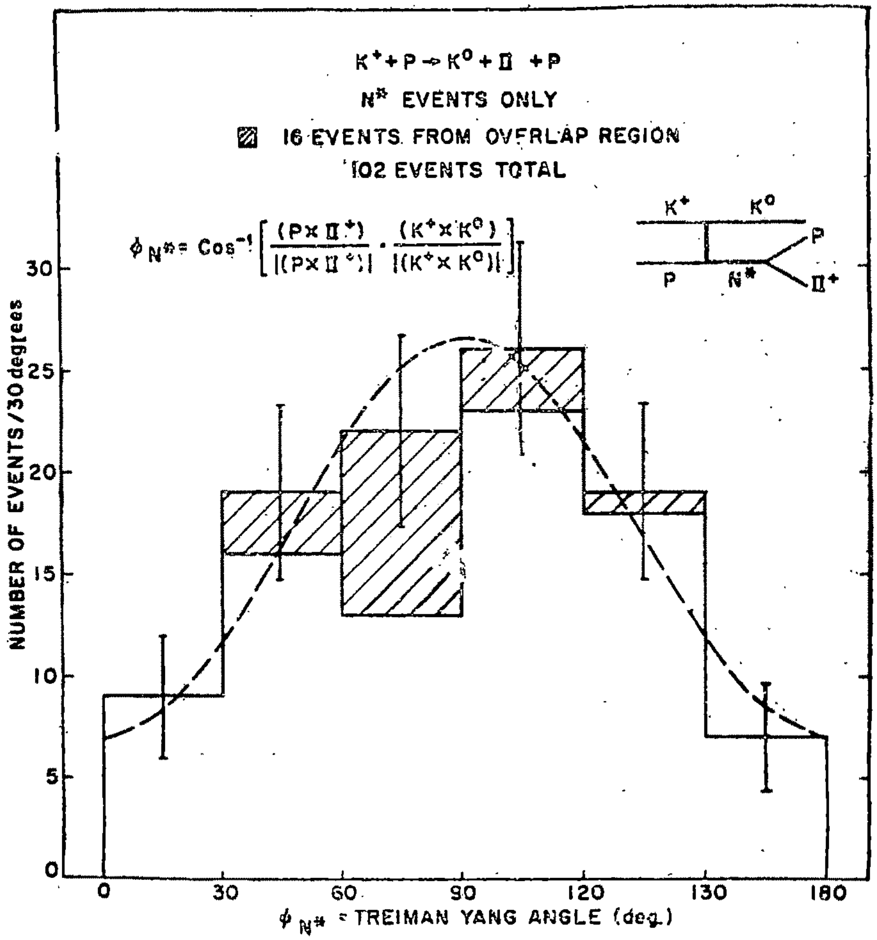

Fig. 18

Stodolsky and Sakurai[12] have suggested that for the production of N* by exchange of a ρ meson the distribution in Treiman-Yang angle (ϕ_{N*}) should be of the form $1+2\sin^2\phi$. The dotted curve superimposed on the experimental distribution (Fig. 18) is of the form $A+B\sin^2\phi$ where $A=7{\cdot}03$

$\pm$·64 and B/A$=$2·77$\pm$1·46. The χ^2 for four degrees of freedom is 1·32. This result is consistent with ρ exchange in the production of N^{*++}.

Stodolsky and Sakurai[12] have also proposed a model for isobar production by vector meson exchange. According to this model for production of N* in (2) via exchange of a ρ meson the model predicts that the decay angular distribution for the isobar relative to the production normal n should be of the form $1+3\cos^2\theta$, where

$$\hat{n}=\frac{(K^+\times K^\circ)}{|(K^+\times K^\circ)|}$$

$$\cos\theta_S=\frac{\hat{n}\,.\,\pi^+}{|(\hat{n})|\,.\,|(\pi^+)|} \qquad ..(5)$$

where K$^+$, K$^\circ$, and π^+ are the respective momentum vectors of K$^+$, K$^\circ$ and π^+, all are evaluated in the rest frame of the isobar.

Stodolsky and Sakurai have also suggested another test. According to this test distribution in the angle ϕ_S *viz.*,

$$\cos\phi_S=\hat{n}.\,\frac{(K^+-K^\circ)\times\pi^+}{|\,(K^+-K^\circ)\times\pi^+\,|} \qquad ..(6)$$

should be of the form: $A+B\cos\phi+C\cos^2\phi$. Whereas before K$^+$, K$^\circ$, π^+ and N are evaluated in the rest frame of the isobar.

The distribution in θ_S for N* events is presented in fig. 19. The least square fit to the data of a form $A+B\cos\theta$ is shown by the dotted curve which yields A$=$4·45$\pm$2·1, B/A$=$3·22$\pm$1·65. The χ^2 for this fit is 7·583 for 8 degrees of freedom. The distribution fits equally well to a curve of the form $A+B\cos\theta+C\cos^2\theta$, where A$=$4·45$\pm$2·1, B/A$=$0·51$\pm$0·35 and C/A$=$3·4$\pm$0·07. The χ^2 fit is 6·226 for 7 degrees of freedom. We notice that the linear term is small and the result is consistent with production of N^{*++} via a ρ meson exchange.

The distribution in ϕ_S is presented in fig. 20. The least squares fit to the data in ϕ_S gives B/A$=-$0·04$\pm$0·23 and C/A$=$0·69$\pm$0·42. Such results have also been reported by Kehoe.[15]

Partial cross-sections for the reactions which have the same topology as reaction (1) are listed below:—

Partial Cross-Sections; K$^+$+P at 2·26 BeV/c

Reaction	Cross-section in milli-barns
$K^++P\rightarrow K^\circ+\pi^++P$	2·59$\pm$0·13
$K^++P\rightarrow K^\circ+\pi^++P+\pi^\circ$	1·50$\pm$0·07
$K^++P\rightarrow K^\circ+\pi^++\pi^++n$	0·39$\pm$0·02
$K^++P\rightarrow \Lambda^\circ+K^++K^+$	0·018$\pm$0·001
NO FIT ($K^++P\rightarrow K^\circ+$ (2 positive particles) +neutrals	0·58$\pm$0·03

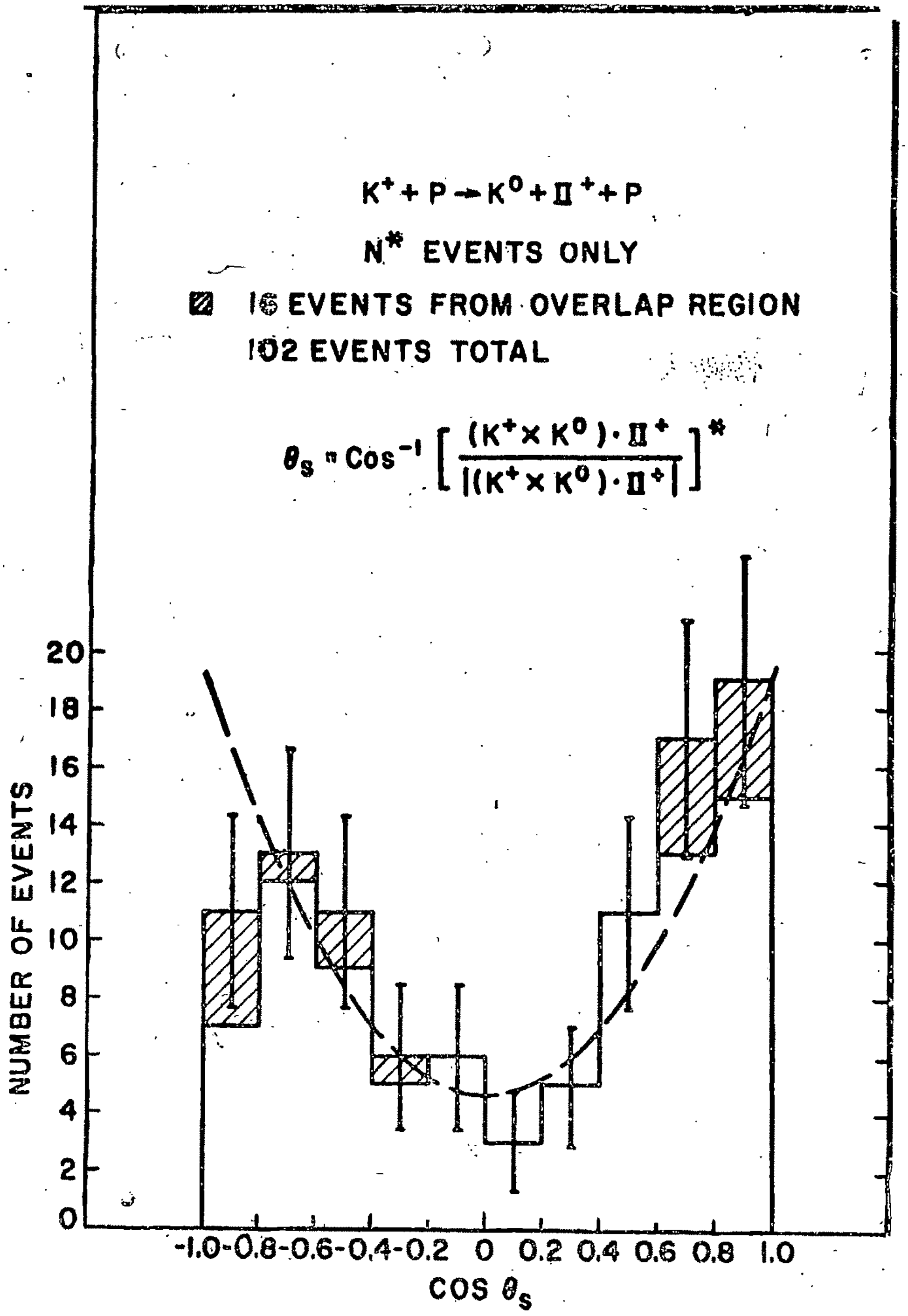
$K^+ + P \rightarrow K^0 + \pi^+ + P$
N* EVENTS ONLY
▨ 16 EVENTS FROM OVERLAP REGION
102 EVENTS TOTAL
$\theta_S = \text{Cos}^{-1}\left[\frac{(K^+ \times K^0)\cdot\pi^+}{|(K^+ \times K^0)\cdot\pi^+|}\right]^*$
NUMBER OF EVENTS
0
2
4
6
8
10
12
14
16
18
20
-1.0 -0.8 -0.6 -0.4 -0.2 0 0.2 0.4 0.6 0.8 1.0
COS θ_S

Fig. 19

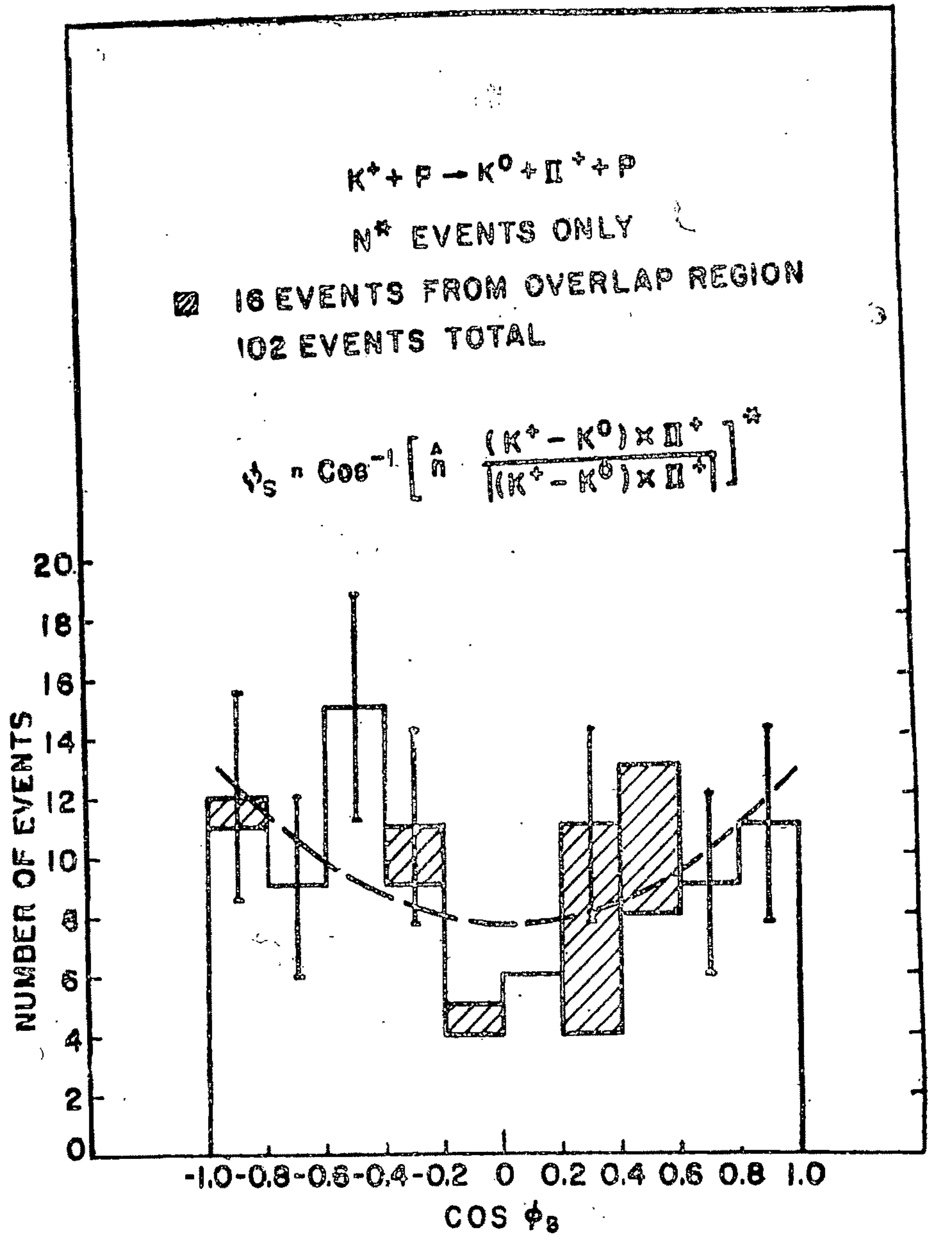

Fig. 20

It is noticed that partial cross-section for the reaction

$$K^+ + P \rightarrow K^\circ + \pi^+ + P$$

is less than that reported at 1·19 BeV/c[5].

ACKNOWLEDGEMENTS

The author would like to thank Prof. A. Pevsner of the Johns Hopkins' University, Baltimore (U.S.A.) for allowing him to work on the problem, for continuous help, and for providing the facilities of the High Energy Physics Group, without which the work could not have been carried out. He also wishes to thank the Air Force Office of Scientific Research and the National Science Foundation of the U.S.A for supporting the experiment.

REFERENCES

1. Proceedings of the Topical Conference on Recently Discovered Resonant Particles, Athens, Ohio, April 26-27, 1963. This Reference presents an up to date survey of the current state of particle resonances.

   Rosenfeld, A. H. "*Strongly Interacting Particles*", UCRL 10492 (unpublished)

   Rosenfeld, A. H. "*Baryon Spectroscopy*", UCRL-10897 (unpublished).

2. Rosenfeld, A. H. & Barkas, W. H. "*Data for Elementary Particle Physics*". UCRL 8030 Rev. (April 1963). (For $T=3/2\pi$-P state at 1640 MeV, see note under N*, p. 25.)

   Moyer, B. J. 1961. *Revs. Mod. Phys.*, **33** : 377.

3. Lee, W. H. 1960. *Phys. Rev.*, **120**: 325.

   Gourdon, M.; Nocrol, Y. 1960. Nuovo Cimento **18** : 651 (Theoretical calculations using dispersion relation techniques showed the possibility of a p-wave resonance in π-K scattering).

4. Alston, M.; Alvarez, L. W.; Eberhard, P.; Good, M. L.; Graziano, W.; Ticho, H. K. & Wojeicki S.

   ———1960. *Phys. Rev.* Letters **5** : 520.

   ———1961. *Phys. Rev.* Letters **6** : 300.

   ———1962. International Conference on High Energy Physics at CERN, p. 291.

5. Chinowsky, W.; Goldhaber, G.; Goldhaber, S.; Lee, W. & O'-Halloran, T.

   ———1962. International Conference on High Energy Physics at CERN, p. 380.

   ———1962. *Phys. Rev.* Letters **9** : 330.

   Chinowsky, W.; Goldhaber, G.; Goldhaber, S.; Lee, W. & O'Halloran, T. *Athens* (cf. ref. 1) p. **80**.

   ———*Athens* p. 104 (cf. ref. 1)

6. Kraemer, R.; Madansky, L.; Miller, I.; Pevsner, A.; Richardson, C.; Singh, R.; Zdanis, R. *Athens*, p. **130** (cf. ref. 1)

7. Duboc, J.; Guong, N. H.; Eberhard, P.; George, R.; Henry, V. P.; Levy, F.; Poyen J. & Pristein, M. Crussard, J. 1963. *A. Tran, Phys. Rev.* Letters **6** : 233.

8. Alexander, G.; Kalbfleisch, G. R.; Miller, D. H. & Smith, G. A. 1962. *Phys. Rev.* Letters **8** : 447.

   ———1962. International Conference on High Energy Physics as CERN, P. **320**.

9. Drell, S. D. 1961. *Rev. of Mod.* Phys. **33** : 458.

   Drell S. D. & Hiida, K. 1961. *Phys. Rev.* Letters **7** : 387.

   Chew G. F. & Low, F. E. 1959. *Phys. Rev.* **113** : 1640.

10. Ferrari, E. & Selleri, F. 1962. *Suppl. Nuovo Cimento* **24** : 453.

    Excellent review of one particle exchange model, gives references a list of theoretical and experimental papers.

11. Treiman, S. B.; Yang, C. N. 1962. *Phys. Rev.* Letters **8** : 140.

12. Stodolsky, L. S. & Sakurai, J. J. 1963. *Phys. Rev.* Letters **11** : 90.

13. Baltay, C.; Sandweiss J. & Sanford, J.; Brown, H.; Webster, W. & Yamamoto, S. 1962. *Proc. of the Int. Conf.* on High-Energy Accelerators and Instrumentation, CERN. Published in Nucl.

Instruments and Methods, Vol. 20, 1963. The separated beam at the AGS, Performance with anti-protons); Leitner, J.; Moneti, G ; Samios, N. P. (performance of the AGS separated beam with high energy Kaons).

14. Livingston, M. S. & Blewett, J. P. 1962. "*Particle Accelerators*", p. **112**. New York, McGraw-Hill.

15. Kehoe, B. 1963. *Phys. Rev.* Letters **11** : 93.

Abstract of Theses

THE THEORY OF HANKEL TRANSFORM*

RAGHUNATH PRASAD GUPTA
Asstt. Prof. of Mathematics,
Th. D. S. B. Govt. College, Naini Tal.

SUMMARY

The thesis consists of ten chapters with the following headings :—

(1) The Theory of Hankel Transform and self-reciprocal functions.
(A brief historical survey)

(2) Hankel transform in two variables of certain functions.

(3) Elementary definitions and properties in Hankel transform of two variables and their applications.

(4) Recurrence relations among Hankel transform in two variables.

(5) Some self-reciprocal functions involving two variables.

(6) Some theorems on self-reciprocal functions of different orders.

(7) Some kernels in the Hankel transform of two variables.

(8) Some properties of $\chi\nu, k, m$—and J_{λ}^{μ} —transforms.

(9) Generalized Hankel Transform and self-reciprocal functions.

(10) Theorems on self-reciprocal functions and resultant kernels in one variable.

A bibliography of 152 references has been given at the end.

In chapter I, I have given an account of the development in the theory of Hankel transform since 1937, the year of publication of the remarkable treatise "Theory of Fourier Integrals" by Professor Titchmarsh and that of the self-reciprocal functions from the year 1930, the year in which Bailey, Hardy and Titchmarsh initiated the subject.

If $f(x)$ and $g(y)$ are two functions connected by the integral equation

$$f(x)=\int_{0}^{\infty} \sqrt{xy}\, J_{\nu}\,(xy)\, g(y)\, dy, \tag{1}$$

---

* Abstract of the thesis approved for the degree of Doctor of Philosophy of the Agra University.

we say that $f(x)$ is the Hankel transform or J_ν —transform of order ν of the function $g(y)$. The kernel $\sqrt{x}\, J_\nu(x)$ of (1) is a Fourier kernel and the inversion formula

$$g(x)=\int_0^\infty \sqrt{xy}\, J_\nu(xy)\, f(y)\, dy, \tag{2}$$

holds under quite general conditions. For $\nu=\pm\frac{1}{2}$, the above relations yield the classical Fourier sine and cosine transforms respectively.

A function is said to be self-reciprocal or skew reciprocal in the Hankel transform of order ν, according as it satisfies the integral equation

$$f(x)=\int_0^\infty \sqrt{xy}\, J_\nu(xy)\, f(y)\, dy,$$

or
$$f(x)=-\int_0^\infty \sqrt{xy}\, J_\nu(xy)\, f(y)\, dy.$$

The theory of Hankel transform has been mainly studied under the following four heads :—

(1) The study by means of fractional integration.
(2) The study by means of operational calculus.
(3) Miscellaneous investigations.
(4) Generalizations.

In chapter II, I have determined the Hankel transform in two variables (denoted hereafter as $J_{\nu,\rho}$ —transform) of certain functions defined by the following integral equation

$$g(x,y)=\int_0^\infty\int_0^\infty \sqrt{y\eta x\xi}\, J_\rho(\eta y)\, J_\nu(\xi x)\, f(\xi,\eta)\, d\xi\, d\eta,$$

The types of functions considered are fairly large and include Algebraic, Exponential, Legendre, Bessel functions and related functions, Parabolic cylinder, confluent Hypergeometric and Generalized Hypergeometric functions. These results have been used in the systematic study of the Hankel transform of two variables in subsequent chapters. Some of the examples are given below in a tabular form.

S.N.	$f(\xi,\eta)$	$g(x,y)=\int_0^\infty\int_0^\infty \sqrt{\eta\, y\, \xi x}\, J_\rho(\eta y) J_\nu(\xi x)\, f(\xi,\eta)\, d\xi\, d\eta$
1.	$\eta^{a}\,\xi^{-\mu-\frac{1}{2}}\left(\eta^2+\xi^2\right)^{-\frac{1}{2}}\left[\left(\xi^2+\eta^2\right)^{\frac{1}{2}}+\eta\right]^{\mu}$ Re $(\nu-\mu)>-1$, Re $(a+\rho)>-3/2$, Re $(a+\rho+\nu)>-3/2$, Re $(a+\mu)<1$	$2^{a-\frac{1}{2}}\, x^{-\frac{1}{2}}\, y^{-a}\times$ $\times\, G^{2,3}_{4,4}\left(y^2x^{-2}\middle\vert\begin{matrix}\frac{1}{2},\, 0,\, \frac{1}{2}-\frac{1}{2}\nu,\, \frac{1}{2}+\frac{1}{2}\nu\\ \frac{1}{2}a+\frac{\rho}{2}+\frac{1}{4},\, -\frac{1}{2}\mu,\, \frac{1}{2}\mu,\, \frac{1}{2}a-\frac{1}{2}\rho+\frac{1}{4}\end{matrix}\right)$
2.	$\eta^{-3/2}\,\xi^{\frac{1}{2}}\,P_{\mu}^{-\frac{1}{2}\nu}\left[\left(1+\xi^2\eta^{-2}\right)^{\frac{1}{2}}\right]Q_{\mu}^{-\frac{1}{2}\nu}\left[\left(1+\frac{\xi^2}{\eta^2}\right)^{\frac{1}{2}}\right]$ Re $\mu>-\frac{3}{4}$, Re $\nu>-1$, Rc $\rho>-1$, Re $(\rho+2\mu)>-2$	$\dfrac{e^{(\mu-\frac{1}{2}\nu+\frac{1}{2})\pi i}\quad \Gamma(1+\mu+\frac{1}{2}\nu)\,\Gamma(1+\mu+\frac{1}{2}\rho)}{\Gamma(1+\mu-\frac{1}{2}\nu)\,\Gamma(\frac{1}{2}\rho-\mu)\,(xy)^{\frac{1}{2}}}$ $\times\, P^{-\mu-\frac{1}{2}}_{\frac{1}{2}\rho-\frac{1}{2}}\left[(1+x^2y^{-2})^{\frac{1}{2}}\right]Q^{-\mu-\frac{1}{2}}_{\frac{1}{2}\rho-\frac{1}{2}}\left[(1+x^2y^{-2})^{\frac{1}{2}}\right]$
3.	$\eta^{2\nu-\rho+\frac{1}{2}}\,\xi^{\frac{1}{2}-\nu}\left[J_\nu(\frac{1}{2}\eta\xi)\right]^2$ Re $\nu>-\frac{1}{2}$, Re $(\rho-2\nu)>-\frac{1}{2}$	$2^{\frac{1}{2}}\,(\pi)^{-\frac{1}{2}}\,x^{2\nu-\rho}\,y^{-\nu}J_{\rho-\nu-\frac{1}{2}}(xy)$
4.	$\eta^{-\frac{1}{2}}\,\xi^{\frac{1}{2}}\,I_{\frac{1}{2}(\nu-\mu)}(\frac{1}{2}\eta\xi)K_{\frac{1}{2}(\nu-\mu)}(\frac{1}{2}\eta\xi)$ Re $\nu>-1$, Re $(\nu-\mu)>-2$, Re $(\rho-\mu)>-1$	$\dfrac{\Gamma(\frac{1}{2}+\frac{1}{2}\rho-\frac{1}{2}\mu)}{\Gamma(\rho+1)}x^{-3/2}\,y^{-\frac{1}{2}}$ $\times\, W_{\frac{1}{2}\mu,\,\frac{1}{2}\rho}(xy)\,M_{-\frac{1}{2}\mu,\,\frac{1}{2}\rho}(xy)$

S.N.	$f(\xi,\eta)$	$g(x,y)=\int_0^\infty\int_0^\infty \sqrt{\eta y\,\xi x}\; J_\rho(\eta y)\, J_\nu(\xi x)\, f(\xi,\eta)\, d\xi\, d\eta$
5.	$\eta^\alpha\ \xi^{-\nu-\frac{1}{2}} K_{2\nu+1}\left[(2\eta\xi)^{\frac{1}{2}}\ e^{\frac{1}{4}\pi i}\right] K_{2\nu+1}\left[(2\eta\xi)^{\frac{1}{2}} e^{\frac{-\pi i}{4}}\right]$ $-1<\mathrm{Re}\,\nu<0,\ \mathrm{Re}\,\alpha<1,$ $\mathrm{Re}\,(\alpha+\rho-\nu)>\lvert\mathrm{Re}\,\nu\rvert-\frac{1}{2}$	$\frac{2}{\sqrt{\pi}}^{\alpha-\nu-5/2}\ x^{2\nu}\ y^{-\alpha+\nu-\frac{1}{2}}$ $\times\, G^{2,3}_{3,3}\left(x^2y^2 \middle\vert \begin{matrix} \frac{1}{4}-\frac{1}{2}\nu,\ \frac{3}{4}-\frac{1}{2}\nu,\ \frac{1}{2}\nu+5/4 \\ \frac{1}{2}(\alpha+\rho-\nu+1),\ \frac{1}{4}-\frac{1}{2}\nu,\ \frac{\alpha-\rho-\nu+1}{2} \end{matrix}\right)$
6.	$\eta^\alpha\xi^\lambda\left[\ I_\mu(\eta\xi)-\ L_\mu(\eta\xi)\ \right]$ $-\mathrm{Re}\,\nu-3/2<\mathrm{Re}\,(\lambda+\mu)<0$ $\mathrm{Re}\,(\alpha+\mu+\rho)>-3/2,\ \mathrm{Re}\,(\alpha+\mu)<0$ $\mathrm{Re}\,(\alpha-\nu-\lambda)<\frac{1}{2}$	$2^{\alpha+\lambda+1}\ (\pi)^{-1}\ x^{-\lambda-1}\ y^{-\alpha-1}$ $\times\, G^{3,2}_{3,5}\left(\frac{x^2\ y^2}{4} \middle\vert \begin{matrix} 1-\frac{1}{2}\mu,\ \frac{1}{2}-\frac{1}{2}\mu,\ 1+\frac{1}{2}\mu \\ \frac{3}{4}+\frac{1}{2}\alpha+\frac{1}{2}\rho,\ \frac{3}{4}+\frac{1}{2}\nu+\frac{1}{2}\lambda,\frac{1}{2}-\frac{1}{2}\mu,\frac{3}{4}+\frac{\lambda-\nu}{2},\frac{3}{4}+\frac{\alpha-\rho}{2} \end{matrix}\right)$
7.	$\eta^\alpha\xi^\lambda\exp(-\xi^2/4\,\eta^2)\, D_\mu(\xi/\eta)$ $\mathrm{Re}\,(\lambda+\nu)>-3/2,$ $-3-\mathrm{Re}\,(\rho+\nu+\lambda)<\mathrm{Re}\,\alpha<0$	$2^{\alpha+\frac{1}{2}\mu+\frac{3\lambda}{2}+\frac{1}{2}\nu+7/4}\ x^{\nu+\frac{1}{2}}\ y^{-\alpha-\lambda-\nu-5/2}$ $G^{3,1}_{3,4}\left(\frac{1}{2}x^{-2}y^2 \middle\vert \begin{matrix} 1,\ \nu+1,\ \frac{1}{2}\lambda\quad \frac{1}{2}\mu\ \vert\ 5/4 \\ \frac{\alpha+\lambda+\nu+\rho+3}{3},\frac{3}{4}+\frac{\lambda+\nu}{2},\frac{5}{4}+\frac{\lambda+\nu}{2}, \\ \frac{\alpha+\lambda+\nu-\rho+3}{2} \end{matrix}\right)$
8.	$\eta^\alpha\xi^{2\lambda-\nu-5/2} W_{k,\mu}(\xi\eta)\ M_{-k,\mu}(\xi\eta)$ $\mathrm{Re}\,\lambda>0,\ \mathrm{Re}\,(\lambda+\mu)>0,$ $\mathrm{Re}\,(2\lambda+2k-\nu)<5/2,\ \mathrm{Re}\,(\alpha+\rho)>-5/2,$ $\mathrm{Re}\,(\alpha+\rho+2\mu)>-5/2,\ \mathrm{Re}\,(\alpha+2k)<-1$ $\mathrm{Re}\,(\lambda-2\alpha)>2$	$\frac{2^{\alpha+2\lambda-\nu-3/2}\ \Gamma(1+2\mu)\ x^{\nu-2\lambda+3/2}\ y^{-\alpha-1}}{\Gamma\left(\frac{1}{2}-k+\mu\right)\ \sqrt{\pi}}\times$ $G^{3,3}_{4,6}\left(\frac{1}{4}x^2y^2 \middle\vert \begin{matrix} \frac{1}{2},\ 0,\ \frac{1}{2}-\mu,\ \frac{1}{2}+\mu \\ \frac{3}{4}+\frac{1}{2}\alpha+\frac{1}{2}\rho,\ \lambda-\frac{1}{2},-k,\ k,\ \lambda-\nu-\frac{1}{2},\frac{3}{4}+\frac{\alpha+\rho}{2} \end{matrix}\right)$

In chapter III, some elementary definitions and few notations have been defined. Later on certain rules for obtaining the Hankel transform in two variables have been investigated. Among these rules are similarity rule, multiplication rules, images of integrals and derivatives, rules involving change of order and rules involving change of order and change of power in the variables.

Some of the rules are as follows :—

If the image of $f(\xi, \eta)$ is $g_{\nu,\rho}(x, y)$,

(*i*) the image of $f(\xi a, \eta b)$ is

$$(ab)^{-1}\, g_{\nu,\rho}(x/a, y/b) \qquad \text{Similarity rule}$$

(*ii*) the images of $\xi^m \eta^n f(\xi, \eta)$ are

$$(\alpha)\ x^{\frac{1}{2}-\nu}\, y^{\frac{1}{2}-\rho}\, (\partial/x\,\partial x)^m (\partial/y\,\partial y)^n \left[x^{-\frac{1}{2}+\nu+m}\, y^{-\frac{1}{2}+\rho+n}\, g_{\nu+m,\rho+n}(xy) \right]$$

$$(\beta)(-)^{m+n} x^{\frac{1}{2}+\nu} y^{\frac{1}{2}+\rho} \left[(\partial/x\partial x)^m (\partial/y\,\partial y)^n \right] \left[x^{-\frac{1}{2}-\nu+m}\, y^{-\frac{1}{2}-\rho+n}\, g_{\nu-m,\rho-n}(xy) \right]$$

(*iii*) the image of

$$(\alpha)\ \eta^{\frac{1}{2}-\rho}\xi^{\frac{1}{2}-\nu}\int_0^\eta\int_0^\xi z^{\rho-\lambda+\frac{1}{2}}\, t^{\nu-\mu+\frac{1}{2}}(\eta^2-z^2)^{\lambda-1}(\xi^2-t^2)^{\mu-1} f(t,z)\, dt\, dz$$

is $2^{\lambda+\mu-2}\,\Gamma(\lambda)\;\Gamma(\mu) x^{-\mu}\, y^{-\lambda}\, g_{\nu-\mu,\,\rho-\lambda}(xy)$

$$(\beta)\ \eta^{\frac{1}{2}+\rho}\xi^{\frac{1}{2}+\nu}\int_\eta^\infty\int_\xi^\infty z^{\frac{1}{2}-\lambda-\rho}\, t^{\frac{1}{2}-\mu-\nu}\, (z^2-\eta^2)^{\lambda-1}(t^2-\xi^2)^{\mu-1} f(t,z)\, dt dz$$

is $2^{\lambda+\mu-2}\Gamma(\lambda)\;\Gamma(\mu)\; x^{-\mu}\, y^{-\lambda}\, g_{\nu+\mu,\,\rho+\lambda}(xy)$

(*iv*) the image of

$$\eta^{\frac{1}{2}-\rho}\ \xi^{\frac{1}{2}-\nu}(\partial/\eta\,\partial\eta)(\partial/\xi\,\partial\xi)\left[\ \eta^{\frac{1}{2}+\rho}\ \xi^{\frac{1}{2}+\nu} f(\xi, \eta)\ \right]$$

is $xy\ g_{\nu+1,\,\rho+1}(xy)$

(*v*) $J_{\nu-\mu-1,\,\rho-\lambda-1}$ —transform of $\xi^{-\mu-1}\ \eta^{-\lambda-1} f(\xi, \eta)$

is $\dfrac{2^{-\mu-\lambda}}{\Gamma(\mu+1)\ \Gamma(\lambda+1)} x^{\nu-\mu-\frac{1}{2}}\, y^{\rho-\lambda-\frac{1}{2}} \times$

$$\int_y^\infty\ \int_x^\infty t^{\frac{1}{2}-\rho} z^{\frac{1}{2}-\nu}\ (z^2-x^2)^\mu\ (t^2-y^2)^\lambda g_{\nu,\,\rho}(z, t)\ dzdt$$

(*vi*) $J_{\nu,\,\rho}$—transform of $\xi^{-2}\,\eta^{-2}\,f(\xi^{-1}/4,\,\eta^{-1}/4)$

is $4(xy)^{\frac{1}{2}}\int_0^\infty\int_0^\infty (zt)^{-\frac{1}{2}}\,J_{2\nu}(\sqrt{xz})\,J_{2\rho}(\sqrt{ty})\;g_{\nu,\,\rho}(zt)\,dz\,dt$

These rules have been used to evaluate certain integrals. An illustrative example is given below :—

$$\int_0^\infty\int_0^\infty (zt)^{-\frac{1}{2}}\,J_{2\nu}(\sqrt{xz})J_{2\rho}(\sqrt{ty})\;t^{-a-1}z^{-\lambda-1}$$

$$\times G^{4,\,2}_{3,\,5}\left(\tfrac{1}{4}t^2\,z^{-2}\,\middle|\,\begin{matrix}\frac{1}{4}-\frac{\lambda+\nu}{2},\,\frac{1}{2}+\frac{1}{2}\mu,\,\frac{1}{4}-\frac{\lambda-\nu}{2}\\ -\frac{1}{4}+\frac{\nu-\lambda}{2},\frac{1+\mu}{2},\frac{-\mu}{2},\frac{\mu}{2},\frac{1}{4}-\frac{\lambda+\nu}{2}\end{matrix}\right)dz\,dt$$

$$=2^{-4(\alpha+\lambda+3/2)}\;x^{\lambda+\frac{1}{2}}\;y^{\alpha+\frac{1}{2}}$$

$$G^{4,\,2}_{3,\,5}\left(\tfrac{1}{2}y^2\,x^{-2}\,\middle|\,\begin{matrix}\frac{1}{2}\alpha-\frac{1}{2}\rho+5/4,\,\frac{1}{2}+\frac{1}{2}\mu,\,\frac{1}{2}\alpha+\frac{1}{2}\rho+5/4\\ -\frac{1}{4}+\frac{1}{2}\nu-\frac{1}{2}\lambda,\,\frac{1}{2}+\frac{1}{2}\mu,-\frac{1}{2}\mu,\,\frac{1}{2}\mu-\frac{1}{4}-\frac{1}{2}\lambda-\frac{1}{2}\nu\end{matrix}\right)$$

provided

$$\left.\begin{matrix}\text{Re }(\rho+2\beta)>\text{Re }\alpha+\frac{1}{2}\\ \text{Re }(\lambda+2\,\beta)>-\frac{3}{4}\end{matrix}\right\}\text{ where }\beta=\max\left(\tfrac{3}{4}+\tfrac{1}{2}\alpha+\tfrac{1}{2}\rho,\,\tfrac{1}{2}+\tfrac{1}{2}\mu,\,\tfrac{1}{2}\mu,-\tfrac{1}{2}\mu\right)$$

and

$$\left.\begin{matrix}\text{Re }(\nu+2\gamma)>\text{Re }\lambda+\frac{1}{2}\\ \text{Re }(\alpha+2\gamma)>-\frac{3}{4}\end{matrix}\right\}\text{ where }\gamma=\max\left(\tfrac{3}{4}+\tfrac{1}{2}\,\lambda+\tfrac{1}{2}\nu,\,\tfrac{1}{2}-\tfrac{1}{2}\mu\right)$$

Besides these rules, I have also obtained two theorems.

Theorem 1. If $\phi_\lambda\,(u,v)$ are the images of $f_\lambda\,(x,y)$, $[\lambda=1,2]$ in the Hankel transform of two variables, then

$$(pq)^{-1}\int_0^\infty\int_0^\infty \phi_1\,(u/p,\,v/q)\,f_2\,(su,\,rv)\;du\,dv=$$

$$(rs)^{-1}\int_0^\infty\int_0^\infty \phi_2\,(u/s,\,v/r)\,f_1\,(pu,\,qv)\;du\,dv$$

provided the integrals involved are absolutely convergent.

For $p=q=r=s=1$, this theorem corresponds to the Parseval's theorem in functions of one variable.

This theorem has been used to evaluate certain single and double integrals. By way of illustration, an example is given below :—

$$\int_0^\infty t^{a+\rho+2\lambda-2\nu-3/2}\times$$

$$\times{}_4F_3\left[\begin{matrix}\lambda-\nu,\ \lambda-\nu+\tfrac{1}{2},\ \lambda-\nu+\mu,\ \lambda-\nu-\mu\ ; \\ \tfrac{1}{2}-k+\lambda-\nu,\ \rho+\tfrac{1}{2},\ \tfrac{1}{2}+k+\lambda-\nu\ ;\end{matrix}-(r^2q^2t^4/s^2p^2)\right]dt$$

$$=\frac{2^{2\lambda-2\nu-3}\underset{*}{\Gamma}(\tfrac{1}{2}\pm k+\lambda-\nu)\,\Gamma(\tfrac{1}{2}+\rho)\,\Gamma(-\tfrac{1}{8}-\tfrac{1}{2}\nu+\tfrac{1}{4}a+\tfrac{1}{2}\lambda+\tfrac{1}{4}\rho)}{\sqrt{\pi}\,(ps)^{\nu+\lambda-\frac{1}{2}a-\frac{1}{2}\rho-\frac{3}{4}}(rs)(rq)^{\frac{1}{2}a+\lambda-\nu+\frac{1}{2}\rho-5/4}}$$

$$\times\frac{\Gamma(\tfrac{1}{8}-\tfrac{1}{4}a-\tfrac{1}{2}\nu-\tfrac{1}{4}\rho+\tfrac{1}{2}\lambda)}{\underset{*}{\Gamma}(\lambda-\nu\pm\mu)\,\Gamma(2\lambda-2\nu)}$$

$$\times\frac{\Gamma(\tfrac{1}{2}\lambda-\tfrac{1}{4}a-\tfrac{1}{2}\nu-\tfrac{1}{4}\rho+9/8)\,\underset{*}{\Gamma}(\tfrac{1}{8}-\tfrac{1}{4}a-\tfrac{1}{2}\nu-\tfrac{1}{4}\rho\pm\mu+\tfrac{1}{2}\lambda)}{\Gamma(\tfrac{5}{8}+\tfrac{3}{4}\rho+\tfrac{1}{2}\nu-\tfrac{1}{4}a-\tfrac{1}{2}\lambda)\,\underset{*}{\Gamma}(\tfrac{5}{8}-\tfrac{1}{4}a-\tfrac{1}{2}\nu-\tfrac{1}{4}\rho\pm k+\tfrac{1}{2}\lambda)}$$

provided Re $(\lambda-\nu)>|\text{Re}\,\mu|$, $\text{Re}(a+\rho+2\lambda-2\nu)>\frac{1}{2}$, Re $(a+\rho+2\lambda-2\nu-4\beta)<\frac{1}{2}$ where $\beta=\min(\lambda-\nu,\ \lambda-\nu+\frac{1}{2},\ \lambda-\nu-\mu,\ \lambda-\nu+\mu)$ and $\underset{*}{\Gamma}(a\pm b)=\Gamma(a+b)\Gamma(a-b)$

Theorem 2. To prove that the functions $(1/x)\,f(y/x)$ and $(1/y)\,f(x/y)$ are $J_{\nu,\,\nu}$ —transforms of each other.

This theorem has been used to establish 17 relations between special functions and to find out certain integrals. Some of these results are known results, but the method with which they have been obtained is new and probably simpler too, while others can be claimed to be new.

By way of illustration, two results are given below :—

Example 1. $$G^{1,\,3}_{3,\,3}\left(y^2x^{-2}\,\middle|\,\begin{matrix}\tfrac{1}{2},\ 0,\ \tfrac{1}{2}-\tfrac{1}{2}\nu \\ -\tfrac{1}{2}\mu,\ \tfrac{1}{2}\mu,\ \tfrac{1}{2}-\tfrac{1}{2}\nu\end{matrix}\right)=(\pi)^{\frac{1}{2}}xy^{-\mu}(x^2+y^2)^{-\frac{1}{2}}\times\left[\,x+(x^2+y^2)^{\frac{1}{2}}\right]^{\mu}$$

Example 2. $$Q^{-\mu-\frac{1}{2}}_{\frac{1}{2}\nu}\left[1+x^2y^{-2})^{\frac{1}{2}}\right]Q^{-\mu-\frac{1}{2}}_{\frac{1}{2}\nu-1}\left[(1+x^2y^{-2})^{\frac{1}{2}}\right]$$

$$=\pi\Gamma_*(\tfrac{1}{2}\nu-\mu\pm\tfrac{1}{2})e^{-2(\mu+\frac{1}{2})\pi i}x^{-1}P^{-\frac{1}{2}-\frac{1}{2}\nu}_{\mu}\left[(1+y^2x^{-2})^{\frac{1}{2}}\right]P^{\frac{1}{2}-\frac{1}{2}\nu}_{\mu}\left(1+\frac{y^2}{x^2}\right)^{\frac{1}{2}}\Bigg]$$

In chapter IV, sixteen recurrence relations among Hankel transform of two variables have been obtained by making use of some of the rules and properties of the Hankel transform of two variables obtained in chapter III. We below give two of them :—

(*i*) $(\rho-\frac{1}{2}+y\,D_y\,)\,g_{\nu,\,\rho}=(\rho-y\,D_y\,-3/2)\,g_{\nu,\,\rho-2}$

$$(ii)\quad \Big[(\tfrac{1}{2}+\nu)(\tfrac{1}{2}+\rho)-xy\ \ D_x D_y\Big]\ g_{\nu,\rho}$$
$$=\Big[(\nu+3/2)(\rho+\tfrac{1}{2})+(\rho+\tfrac{1}{2})\ \ xD_x\Big]\ g_{\nu+2,\ \rho}$$
$$+\Big[(\rho+3/2)(\nu+\tfrac{1}{2})+(\nu+\tfrac{1}{2})\ \ yD_y\Big]\ g_{\nu,\ \rho+2}$$
$$-\Big[(\nu+3/2)(\rho+3/2)+(\nu+3/2)\ \ yD_y+(\rho+\tfrac{3}{2})xD_x+xy\ D_x D_y\Big]\ g_{\nu+2,\ \rho+2}$$

These recurrence relations have been used to obtain certain interesting and useful relations in Struve, Bessel, Modified Bessel, Whittaker, Meijer functions and associated Legendre Polynomials. Most of the relations obtained can be claimed to be new.

As an illustration we give below one of the results obtained in this chapter :—

$$\frac{\Gamma\,(1+\mu+\tfrac{1}{2}\rho)}{\Gamma\,(1-\mu+\tfrac{1}{2}\rho)}\Big\{(\rho-2\mu)(xy)^{-\frac{1}{2}}P^{-\mu-\frac{1}{2}}_{\frac{1}{2}\rho-\frac{1}{2}}\Big[(1+x^2y^{-2})^{\frac{1}{2}}\Big]\ Q^{-\mu-\frac{1}{2}}_{\frac{1}{2}\rho-\frac{1}{2}}\Big[(1+x^2y^{-2})^{\frac{1}{2}}\Big]$$
$$+x^{\frac{1}{2}}y^{-3/2}\ e^{-\frac{1}{2}\pi i}\ (1+x^2y^{-2})^{-\frac{1}{2}}\Big[P^{-\mu+\frac{1}{2}}_{\frac{1}{2}\rho-\frac{1}{2}}(1+x^2y^{-2})^{\frac{1}{2}}\,Q^{-\mu-\frac{1}{2}}_{\frac{1}{2}\rho-\frac{1}{2}}(1+x^2y^{-2})^{\frac{1}{2}}$$
$$+\ P^{-\mu-\frac{1}{2}}_{\frac{1}{2}\rho-\frac{1}{2}}\ (1+x^2y^{-2})^{\frac{1}{2}}\,Q^{-\mu+\frac{1}{2}}_{\frac{1}{2}\rho-\frac{1}{2}}(1+x^2y^{-2})^{\frac{1}{2}}\Big]\Big\}$$
$$=\frac{\Gamma\,(2+\mu+\tfrac{1}{2}\rho)}{\Gamma\,(2-\mu+\tfrac{1}{2}\rho)}\Big\{(\rho+2\mu+2)\ \ (xy)^{-\frac{1}{2}}\ F^{-\mu-\frac{1}{2}}_{\frac{1}{2}\rho+\frac{1}{2}}\ (1+x^2y^{-2})^{\frac{1}{2}}\times\ Q^{-\mu-\frac{1}{2}}_{\frac{1}{2}\rho+\frac{1}{2}}\ (1+x^2y^{-2})^{\frac{1}{2}}$$
$$-x^{\frac{1}{2}}y^{-3/2}\,e^{-\frac{1}{2}\pi i}\ \ (1+x^2y^{-2})^{-\frac{1}{2}}\Big[\ P^{-\mu+\frac{1}{2}}_{\frac{1}{2}\rho+\frac{1}{2}}\ (1+x^2y^{-2})^{\frac{1}{2}}\times\ Q^{-\mu-\frac{1}{2}}_{\frac{1}{2}\rho+\frac{1}{2}}\ (1+x^2y^{-2})^{\frac{1}{2}}$$
$$+\ P^{-\mu-\frac{1}{2}}_{\frac{1}{2}\rho+\frac{1}{2}}\ (1+x^2y^{-2})^{\frac{1}{2}}\,Q^{-\mu+\frac{1}{2}}_{\frac{1}{2}\rho+\frac{1}{2}}\ (1+x^2y^{-2})^{\frac{1}{2}}\Big]\Big\}$$

In the next chapters, *viz.*, V, VI and VII, the theory of Hankel transform in two variables have been extended by determining certain properties of self-reciprocal functions in two variables.

In chapter V, eleven new self-reciprocal functions in two variables have been obtained. These functions involve Algebraic, Bessel, Modified Bessel functions, related functions, Meijer G—and generalized Hypergeometric functions. In order to obtain these functions two methods have been employed. In one of them $J_{\nu,\,\rho}$ —transform of certain functions have been first determined and then the self-reciprocal functions have been deduced as particular cases by giving suitable values to the parameters. In the other case, we have made use of the theorem due to R. P. Agarwal, which connects the different classes of self-reciprocal functions.

Some of the results are stated below :—

Self-reciprocal Functions	Order	Valid under conditions
$x^{\frac{1}{2}-\nu}y^{\frac{1}{2}+\rho}(x^2-y^2)^{-1+\frac{1}{2}\nu-\frac{1}{2}\rho}$	$R_{\nu,\,\rho}$	$-1<\mathrm{Re}\,\rho<\mathrm{Re}\,\nu$
$(xy)^{\frac{1}{2}\nu}\left[I_{\frac{1}{2}(\nu+1)}(xy)-L_{-\frac{1}{2}(\nu+1)}(xy)\right]$	$R_{\nu,\,1}$	$\mathrm{Re}\,\nu>-\frac{1}{2}$
$G^{4,\,2}_{2,\,4}\left(\frac{1}{4}x^2y^2\middle\vert\begin{matrix}\frac{1}{4}-\frac{1}{2}\rho,\ \frac{1}{4}\\ \frac{1}{4}+\frac{1}{2}\lambda,\ \frac{1}{4},\ \frac{1}{4}+\frac{1}{2}\rho,\ \frac{1}{4}+\frac{1}{2}\mu\end{matrix}\right)$	$R_{\mu,\,\lambda}$	$\mathrm{Re}\,\rho>-1$, $\mathrm{Re}\,(\rho+\mu)>-2$ $\mathrm{Re}\,\lambda>-1$

In chapter VI, the theory of self-reciprocal functions in two variables have been extended by establishing certain theorems on self-reciprocal functions of different orders. In particular we have generalized theorems due to R. P. Agarwal and given new theorems in two variables.

Theorem 1. If

$$P(xy)=\frac{1}{(2\pi i)^2}\int_{C'-i\infty}^{C'+i\infty}\int_{C-i\infty}^{C+i\infty}2^{(b+\frac{1}{2})r+(c+\frac{1}{2})s}\,\Gamma(\tfrac{1}{4}+\tfrac{1}{2}\nu+\tfrac{1}{2}r)\,\Gamma(\tfrac{1}{4}+\tfrac{1}{2}\mu+\tfrac{1}{2}r)\times$$

$$\Gamma\left(\tfrac{1}{4}+\frac{\rho}{2}+\tfrac{1}{2}s\right)\Gamma(\tfrac{1}{4}+\tfrac{1}{2}\mu_1+\tfrac{1}{2}s)\times\Gamma\left(\frac{1}{4}+\frac{\lambda}{2}+\frac{r}{2}\right)\Gamma\left(\frac{1}{4}+\frac{\lambda_1}{2}+\frac{s}{2}\right)$$

$$\psi(r,s)\,x^{-r}y^{-s}\,dr\,ds$$

$$f(x,y)=\frac{1}{(2\pi i)^2}\int_{K'-i\infty}^{K'+i\infty}\int_{K-i\infty}^{K+i\infty}2^{br+cs}\,\Gamma(\tfrac{1}{4}+\tfrac{1}{2}\nu+\tfrac{1}{2}r)\,\Gamma(\tfrac{1}{4}+\tfrac{1}{2}\mu+\tfrac{1}{2}r)$$
$$\Gamma(\tfrac{1}{4}+\tfrac{1}{2}\rho+\tfrac{1}{2}s)\,\Gamma(\tfrac{1}{4}+\tfrac{1}{2}\mu_1+\tfrac{1}{2}s)$$

$$\chi(r,s)\,x^{-r}y^{-s}\,dr\,ds$$

where $\psi(r,s)=\psi(1-r,1-s)$ and $\chi(r,s)=\chi(1-r,1-s)$ and

$$\psi(r,s)=0\left\{e^{[(3\pi/2)-3\alpha+3\eta][|t|+|\lambda|]}\right\}$$

$$\chi(r,s)=0\left\{e^{(\pi-2\alpha+2\eta)[|t|+|\lambda|]}\right\}$$

then

$$g(x,y)=\int_0^\infty\int_0^\infty P\,(ux,\,u'y)\,f\,(u,u')\,du\,du'$$

is $R_{\lambda,\,\lambda_1}$

Theorem 2. If

$$P\,(x,y)=\frac{1}{(2\pi i)^2}\int_{C'-i\infty}^{C'+i\infty}\int_{C-i\infty}^{C+i\infty}2^{br+cs}\,\Gamma(\tfrac{1}{4}+\tfrac{1}{2}\nu+\tfrac{1}{2}r)\Gamma(\tfrac{1}{4}+\tfrac{1}{2}\mu+\tfrac{1}{2}r)\,\Gamma(\tfrac{3}{4}+\tfrac{1}{2}\lambda-\tfrac{1}{2}r)\Gamma\tfrac{1}{4}+\tfrac{1}{2}\rho+\tfrac{1}{2}s)$$
$$\times\Gamma(\tfrac{1}{4}+\tfrac{1}{2}\mu_1+\tfrac{1}{2}s)\Gamma(\tfrac{3}{4}+\tfrac{1}{2}\lambda_1-\tfrac{1}{2}s)\psi(r,s)x^{-r}y^{-s}\,dr\,ds$$

and

$$f\,(x,y)=\frac{1}{(2\pi i)^2}\int_{K'-i\infty}^{K'+i\infty}\int_{K-i\infty}^{K+i\infty}2^{(b+\frac{1}{2})r+(c+\frac{1}{2})s}\,\Gamma(\tfrac{1}{4}+\tfrac{1}{2}\nu+\tfrac{1}{2}r)\Gamma(\tfrac{1}{4}+\tfrac{1}{2}\mu+\tfrac{1}{2}r)\,\Gamma(\tfrac{1}{4}+\tfrac{1}{2}\rho+\tfrac{1}{2}s)$$
$$\times\Gamma(\tfrac{1}{4}+\tfrac{1}{2}\mu_1+\tfrac{1}{2}s)\,\chi(r,\,s)x^{-r}y^{-s}\,dr\,ds$$

then

$$g(x,y)=\int_0^\infty\int_0^\infty P\,(u,\,u')\,f\,(ux,\,u'y)\,du\,du'$$

is $R_{\lambda,\,\lambda_1}$

The theorems 1 and 2 have been generalized in the following two theorems.

Theorem 3. If

$$P\,(x,y)=\frac{1}{(2\pi i)^2}\int_{C'-i\infty}^{C'+i\infty}\int_{C-i\infty}^{C+i\infty}2^{(b+\frac{1}{2})r+(c+\frac{1}{2})s}\,\Gamma(\tfrac{1}{4}+\tfrac{1}{2}\rho_1+\tfrac{1}{2}r)\,\Gamma(\tfrac{1}{4}+\tfrac{1}{2}\rho_2+\tfrac{1}{2}r)\ldots\ldots\ldots\Gamma(\tfrac{1}{4}+\tfrac{1}{2}\rho_n+\tfrac{1}{2}r)$$
$$\times\Gamma(\tfrac{1}{4}+\tfrac{1}{2}\rho'_1+\tfrac{1}{2}s)\ldots\ldots\Gamma(\tfrac{1}{4}+\tfrac{1}{2}\rho'_n+\tfrac{1}{2}s)\psi(r,s)x^{-r}y^{-s}\,dr\,ds$$

and

$$f\,(x;y)=\frac{1}{(2\pi i)^2}\int_{K'-i\infty}^{K'+i\infty}\int_{K-i\infty}^{K+i\infty}2^{br+cs}\,\Gamma(\tfrac{1}{4}+\tfrac{1}{2}\rho_1+\tfrac{1}{2}r)\ldots\ldots\Gamma(\tfrac{1}{4}+\tfrac{1}{2}\rho_{n-1}+\tfrac{1}{2}r)\,\Gamma(\tfrac{1}{4}+\tfrac{1}{2}\rho'_1+\tfrac{1}{2}s)\ldots\ldots$$
$$\Gamma(\tfrac{1}{4}+\tfrac{1}{2}\rho'_{n-1}+\tfrac{1}{2}s)\chi(r,\,s)x^{-r}y^{-s}\,dr\,ds$$

then

$$g\,(x,y)=\int_0^\infty\int_0^\infty P\,(ux,\,u'y)\,du\,du'$$

is $R_{\rho_n,\,\rho'_n}$

Theorem 4. If

$$P\,(x,y)=\frac{1}{(2\pi i)^2}\int_{C'-i\infty}^{C'+i\infty}\int_{C-i\infty}^{C+i\infty}2^{br+cs}\,\Gamma(\tfrac{1}{4}+\tfrac{1}{2}\rho_1+\tfrac{1}{2}r)\ldots\ldots\Gamma(\tfrac{1}{4}+\tfrac{1}{2}\rho_{n-1}+\tfrac{1}{2}r)\,\Gamma(\tfrac{3}{4}+\tfrac{1}{2}\rho_n-\tfrac{1}{2}r)$$
$$\times\Gamma(\tfrac{1}{4}+\tfrac{1}{2}\rho'_1+\tfrac{1}{2}s)\Gamma(\tfrac{1}{4}+\tfrac{1}{2}\rho'_2+\tfrac{1}{2}s)\ldots\ldots$$
$$\Gamma(\tfrac{1}{4}+\tfrac{1}{2}\rho'_{n-1}+\tfrac{1}{2}s)\Gamma(\tfrac{3}{4}+\tfrac{1}{2}\rho'_n-\tfrac{1}{2}s)\;\psi\,(r,\,s)x^{-r}y^{-s}\,dr\,ds$$

$$f(x,y)=\frac{1}{(2\pi i)^2}\int_{K'-i\infty}^{K'+i\infty}\int_{K-i\infty}^{K+i\infty}2^{(b+\frac{1}{2})r+(c+\frac{1}{2})s}\Gamma\left(\frac{1}{4}+\frac{\rho_1}{2}+\frac{\gamma}{2}\right)\ldots\ldots\Gamma\left(\frac{1}{4}+\frac{\rho_{n-1}}{2}+\frac{\gamma}{2}\right)\Gamma\left(\frac{1}{4}+\frac{\rho'_1}{2}+\frac{s}{2}\right)\ldots\Gamma\left(\frac{1}{4}+\frac{\rho'_{n-1}}{2}+\frac{s}{2}\right.\quad r,s)\,x^{-r}y^{-s}\,dr\,ds$$

then

$$g(x,y)=\int_0^\infty\int_0^\infty P\,(u,u')\,f\,(ux,u'y)\;du\,du'$$

is R_{ρ_n,ρ'_n}

Theorem 2 is being used to obtain a new self-reciprocal function

$$x^{\frac{1}{2}+\rho_1}y^{\frac{1}{2}+\rho'_1}F\left[\begin{array}{l|l|l}1 & \frac{1}{2}\rho_1+\frac{1}{2}\rho'_1-\frac{1}{2}\lambda+5/4 & \frac{1}{2}x^2\\ 2 & 1+\rho_1,\,1-\frac{1}{2}\rho_2+\frac{1}{2}\rho_1,\,1+\rho'_1,\,1-\frac{1}{2}\rho'_2+\frac{1}{2}\rho'_1 & \\ 1 & \frac{1}{2}\lambda+\frac{1}{2}\rho_1+\frac{1}{2}\rho'_1+7/4 & \\ 2 & 1+\frac{1}{2}\rho_1+\frac{1}{2}\rho_2,\,1-\frac{1}{2}\rho_3+\frac{1}{2}\rho_1,\,1+\frac{1}{2}\rho'_1+\frac{1}{2}\rho'_2,\,1-\frac{1}{2}\rho'_3+\frac{1}{2}\rho'_1 & \frac{1}{2}y^2\end{array}\right]$$

as R_{ρ_3,ρ'_3}, by using the calculus of residues and certain properties of the hypergeometric functions in two variables.

Other theorems obtained in this chapter are as follows:—

Theorem 1. If the function $f(x,y)$ is $R_{\nu,\rho}$, then it is of the form

$$f(x,y)=\frac{x^{\frac{1}{2}-\nu}\,y^{\frac{1}{2}-\rho}}{(2\pi i)^2}\int_{C'-i\infty}^{C'+i\infty}\int_{C-i\infty}^{C+i\infty}r^{-\frac{1}{2}(1+\nu)}\;s^{-\frac{1}{2}(1+\rho)}\;e^{\frac{1}{2}(rx^2+sy^2)}\,\mu(r,s)\,dr\,ds$$

where $\mu(r,s)=\mu(1/r,1/s)$.

Four cases have been also discussed arising due to the form of $\mu(r,s)$.

Theorem 2. If $f(x,y)$ is $R_{\mu,\nu}$, the function

$$g(x,y)=(xy)^{-1}\int_0^x\int_0^y Q\left[\log\,(x/u,y/u')\right]f\,(u,u')\,du\,du'$$

is $R_{\lambda,t}$, provided

$$Q\,(x,y)=\frac{1}{(2\pi i)^2}\int_{C'-i\infty}^{C'+i\infty}\int_{C-i\infty}^{C+i\infty}\Gamma(\tfrac{1}{4}+\tfrac{1}{2}\mu+\tfrac{1}{2}r)\Gamma(\tfrac{3}{4}+\tfrac{1}{2}\lambda-\tfrac{1}{2}r)\Gamma(\tfrac{1}{4}+\tfrac{1}{2}\nu+\tfrac{1}{2}s)\Gamma(\tfrac{3}{4}+\tfrac{1}{2}t-\tfrac{1}{2}s)\chi(r,s)\times e^{rx+sy}\,dr\,ds\qquad \begin{array}{l}x>0,y>0\\ x<0,y<0\end{array}$$

$$=0$$

where $\chi(r,s)=\chi(1-r,1-s)$.

Some corollaries of this theorem have also been discussed.

Theorem 3. If the function $f(x,y)$ is $R_{\mu,\nu}$, the function

$$g(x,y)=\int_0^{\frac{1}{x}}\int_0^{\frac{1}{y}} Q\left[\log\,(1/xu,\,1/yu')\right] f(u,u')\,du\,du'$$

is $R_{\lambda,t}$, provided

$$\begin{aligned}Q(x,y)&=\frac{1}{(2\pi i)^2}\int_{C'-i\infty}^{C'+i\infty}\int_{C-i\infty}^{C+i\infty} 2^{r+s}\,\frac{\Gamma(\tfrac{1}{4}+\tfrac{1}{2}\mu+\tfrac{1}{2}r)\Gamma(\tfrac{1}{4}+\tfrac{1}{2}\lambda+\tfrac{1}{2}r)\Gamma(\tfrac{1}{4}+\tfrac{1}{2}\nu+\tfrac{1}{2}s)}{\Gamma(\tfrac{1}{4}+\tfrac{1}{2}t+\tfrac{1}{2}s)}\,\chi(r,s)\,e^{rx+sy}dr\,ds \quad x>0,\ y>0\\ &=0 \quad x<0\ \ y<0\end{aligned}$$

where $\chi(r,s)=\chi(1-r,1-s)$

Theorem 4. If the function

$$\begin{aligned}f(x,y)=\frac{1}{(2\pi i)^2}\int_{C'-i\infty}^{C'+i\infty}\int_{C-i\infty}^{C+i\infty} 2^{(b+\frac{1}{2})(r+s)}\,&\Gamma(\tfrac{1}{4}+\tfrac{1}{2}\mu_1+\tfrac{1}{2}r)\ldots\Gamma(\tfrac{1}{4}+\tfrac{1}{2}\mu_{n-1}+\tfrac{1}{2}r)\\ &\Gamma(\tfrac{1}{4}+\tfrac{1}{2}\mu'_1+\tfrac{1}{2}s)\ldots\ldots\Gamma(\tfrac{1}{4}+\tfrac{1}{2}\mu'_{n-4}+\tfrac{1}{2}s)\ldots\\ &\Gamma(\tfrac{1}{4}+\tfrac{1}{2}\mu'_{n-1}+\tfrac{1}{2}s)\,\chi(r,s)x^{-r}y^{-s}\,dr\,ds,\end{aligned}$$

and

$$\begin{aligned}Q(x,y)&=\frac{1}{(2\pi i)^2}\int_{C'-i\infty}^{C'+i\infty}\int_{C-i\infty}^{C+i\infty} 2^{b(r+s)}\,\frac{\Gamma(\tfrac{1}{4}+\tfrac{1}{2}\mu_1+\tfrac{1}{2}r)\ldots\Gamma(\tfrac{1}{4}+\tfrac{1}{2}\mu_{n-1}+\tfrac{1}{2}r)\,\Gamma(\tfrac{1}{4}+\tfrac{1}{2}\mu'_1+\tfrac{1}{2}s)\ldots\Gamma(\tfrac{1}{4}+\tfrac{1}{2}\mu'_{n-1}+\tfrac{1}{2}s)}{\Gamma(\tfrac{3}{4}+\tfrac{1}{2}\mu_n-\tfrac{1}{2}r)\Gamma(\tfrac{3}{4}+\tfrac{1}{2}\mu'_n-\tfrac{1}{2}s)}\,w(r,s)\,e^{xr+sy}\,dr\,ds\\ &\qquad\text{when}\quad x>0,\ y>0\\ &=0 \qquad\text{when}\quad x<0,\ y<0\end{aligned}$$

where $\chi(r,s)=\chi(1-r,1-s)$ and $w(r,s)=w(1-r,1-s)$
then the function

$$g(x,y)=(xy)^{-1}\int_0^{y}\int_0^{x} Q\left[\log\,(x/u,\,y/u')\right] f(u,u')\,du\,du'$$

is R_{μ_n,μ'_n},

Theorom 5. If the function

$$\begin{aligned}f(x,y)=\frac{1}{(2\pi i)^2}\int_{C'-i\infty}^{C'+i\infty}\int_{C-i\infty}^{C+i\infty} 2^{(b-\frac{1}{2})r+(c-\frac{1}{2})s}\,&\Gamma(\tfrac{1}{4}+\tfrac{1}{2}\mu_1+\tfrac{1}{2}r)\ldots\ldots\\ &\Gamma(\tfrac{1}{4}+\tfrac{1}{2}\mu_{n-1}+\tfrac{1}{2}r)\ \Gamma(\tfrac{1}{4}+\tfrac{1}{2}\mu'_1+\tfrac{1}{2}s)\ldots\\ &\times\ \Gamma(\tfrac{1}{4}+\tfrac{1}{2}\mu'_{n-1}+\tfrac{1}{2}s)\psi(r,s)x^{-r}y^{-s}\,dr\,ds,\end{aligned}$$

and

$$\begin{aligned}Q(x,y)&=\frac{1}{(2\pi i)^2}\int_{K'-i\infty}^{K'+i\infty}\int_{K-i\infty}^{K+i\infty} 2^{br+cs}\,\frac{\Gamma(\tfrac{1}{4}+\tfrac{1}{2}\mu_1+\tfrac{1}{2}r)\ldots\ldots\Gamma(\tfrac{1}{4}+\tfrac{1}{2}\mu_n+\tfrac{1}{2}r)}{\Gamma(\tfrac{1}{4}+\tfrac{1}{2}\mu'_1+\tfrac{1}{2}s)\ldots\ldots\Gamma(\tfrac{1}{4}+\tfrac{1}{2}\mu'_n+\tfrac{1}{2}s)}\\ &\qquad\times\ w(r,s)e^{xr+ys}\,dr\,ds\\ &\qquad\text{when}\quad x>0,\ y>0\\ &=0 \qquad\text{when}\quad x<0,\ y>0\end{aligned}$$

where $\psi(r,s)=\psi(1-r,1-s)$ and $w(r,s)=w(1-r,1-s)$.

then the function

$$g(x,y)=\int_0^{\frac{1}{x}}\int_0^{\frac{1}{y}} Q\left[\log\ (1/xu,\ 1/yu')\right] f(u,u')\,du\,du'$$

is $R_{\mu n,\ \mu' n}$.

Theorem 6. If the function $f(x,y)$ is $R_{\nu,\ \rho}$ *i. e.*

$$f(x,y)=\frac{1}{(2\pi i)^2}\int_{C'-i\infty}^{C'+i\infty}\int_{C-i\infty}^{C+i\infty} 2^{\frac{1}{2}(r+s)}\Gamma(\tfrac{1}{4}+\tfrac{1}{2}\nu+\tfrac{1}{2}r)\Gamma(\tfrac{1}{4}+\tfrac{1}{2}\rho+\tfrac{1}{2}s)x^{-r}y^{-s}\,\psi(r,s)\,dr\,ds$$

where $\psi(r,s)=\psi(1-r,\ 1-s)$, in the strips

$$a<\sigma<1-a,\ b<\gamma<1-b \qquad (r\equiv\sigma+it,\ s\equiv\gamma+it)$$

and

$$\psi(r,s)=0\left\{e^{(\frac{1}{2}\pi-a+\eta)[\,|t|+|\lambda|\,]}\right\}$$

and

$$E\ f(x,y)\equiv\int_0^{\infty}\int_0^{\infty} g(xt,yz)\,f(x,y)\,dx\,dy$$

where $g(xt,yz)$ is an arbitrary function; then under suitable conditions,

$$E^2 f(x,y)=\int_0^{\infty}\int_0^{\infty} g(pt,qz)\,dt\,dz\int_0^{\infty}\int_0^{\infty} g(xt,yz)\,f(x,y)\,dx\,dy$$

is $R_{\nu,\ \rho}$.

In chapter VII, we have defined the kernel in two variables following the analogy of self-reciprocal functions in one variable, *viz.*, if two functions $f(u,u')$ and $g(x,y)$ are connected by the relation

$$g(x,y)=\int_0^{\infty}\int_0^{\infty} P(xu,yu')\,f(u,u')\,du\,du'$$

where $f(u,u')$ is $R_{\nu,\ \rho}$ and $g(x,y)$ is $R_{\mu,\ \lambda}$; then $P(x,y)$ is called the kernel in two variables for transforming $R_{\nu,\ \rho}$ into an $R_{\mu,\ \lambda}$ and vice-versa.

We have investigated 48 kernels which transform self-reciprocal function of a given order to that of a different order. In order to obtain these kernels we have made use of known double integrals. The results thus obtained in this chapter have been used to obtain some self-reciprocal functions in the form of Meijer's G-function.

Some of the kernels are given below :—

(1) $x^{3\theta-2} e^{-\frac{1}{2}x} {}_1F_1(\theta\,;\,4e-1\,;\,x)\ W_{\frac{1}{2}-\theta,\ 2\theta-1}(x)\ I_{\frac{1}{2}\mu-\frac{1}{4}}(\tfrac{1}{2}x^{n}y) K_{\frac{1}{4}-\frac{1}{2}\mu}(\tfrac{1}{2}x^{n}y)$

is a kernel transforming

$$R_{5\theta-3,\ \mu-1} \text{ to } R_{\theta,\ \mu},\ 2/5<\text{Re}\ \theta<\tfrac{3}{4},\ \text{Re}\ \mu\geqslant\tfrac{1}{2}$$

(2) $x^{2\theta-3} y^{\frac{1}{2}} e^{-\frac{1}{2}x} {}_1F_1(1\,;\,2\theta-1\,;\,x)\ W_{-\theta+3/2,\ \theta-1}(x)\, J_\rho(\sqrt{\tfrac{1}{2}}\, x^{n}y)\ K_\rho(\sqrt{\tfrac{1}{2}}\, x^{n}y)$

is a kernel transforming

$$R_{\theta-1,\ 2\rho} \text{ to } R_{\theta,\ 0}$$

for $\frac{1}{2}<\text{Re}\ \theta<3/2$, $\text{Re}\ \rho>-\frac{1}{2}$.

(3) $x^{b-\theta-\frac{1}{2}}\ e^{-x} {}_1F_1(2\theta-b\,;\,b\,;\,x)\ I_{\frac{1}{2}\mu-\frac{1}{4}}(\tfrac{1}{2}x^{n}y)\ K_{\frac{1}{4}-\frac{1}{2}\mu}(\tfrac{1}{2}x^{n}y)$

is a kernel transforming

$$R_{\theta-1,\ \mu-1} \text{ to } R_{\theta,\ \mu}$$

for $\text{Re}\ \theta<\text{Re}\ b-\frac{1}{2}$, $\text{Re}\ b>0$, $\text{Re}\ \mu\geqslant\frac{1}{2}$.

(4) $x^{\theta-\frac{1}{2}}\ y^{5/2}\ e^{-x} {}_1F_1(-1\,;\,2\theta-2\,;\,x)\ J_\rho(\sqrt{\tfrac{1}{2}}\, x^{n}y)\ \ K_\rho(\sqrt{\tfrac{1}{2}}\, x^{n}y)$

is a kernel transforming

$$R_{\theta-3,\ 2\rho} \text{ to } R_{\theta,\ 2},$$

For $\text{Re}\ \theta>2$, $\text{Re}\ \rho>\frac{1}{2}$.

In chapter VIII, some properties of the Generalized Hankel transforms $\chi_{\nu,\,k,\,m}$ and J_λ^μ-defined by

$$g(x)=\frac{1}{2^\nu}\int_0^\infty (xy)^{\nu+\frac{1}{2}}\chi_{\nu,\,k,\,m}(\tfrac{1}{4}x^2y^2)\,f(y)\,dy,$$

and

$$g(x)=\frac{1}{2^\nu}\int_0^\infty (xy)^{\lambda+\frac{1}{2}}J_\lambda^\mu(\tfrac{1}{4}x^2y^2)\,f(y)\,dy$$

have been investigated. The $\chi_{\nu,\,k,\,m}$—transform was given by Roop Narain and J_λ^μ—transform was given by R. P. Agarwal.

In the investigations of two of these theorems, the properties of the operations of the fractional integration as defined by Kober have been used. With the help of these theorems, we have evaluated certain integrals and have established certain relations between the special functions. Some of the results are known ones while others can be claimed to be new.

Some of the results are as follows :—

Theorem 1. If $f(x)$ and $g(x)$ are $\chi_{\nu,\,k,\,m}$—transforms, then

$$\int_0^\infty x^{-n-\frac12} f(x)\,dx = \frac{2^{-n}\Gamma\frac12(\nu-n+1)\Gamma\frac12(\nu-n+1+4m)\Gamma\frac12(\nu+n+2+2m-2k)}{\Gamma\frac12(\nu-n+2+2m-2k)\Gamma\frac12(\nu+n+1)\Gamma\frac12(\nu+n+1+4m)}$$

$$\int_0^\infty x^{n-\frac12}\, g(x)\,dx$$

provided Re $(\nu+1+4m)>$ Re $\frac12(\nu-n+4m)+\frac12>0$, Re $(\nu+n+2m-2k+2)>0$, Re $(2k+n-\nu-2m)>0$ Re $(\nu+\frac12)>$Re $(\nu-n+1)>0$, $2m$ is not integer or zero and n is any positive integer excluding 0.

Theorem 2. If $1\leqslant p\leqslant 2, f_j\ (t)\ (j=1,2)$ belong to $L_p\ (0,\infty)$

and

$$F_j(x)=2^{-\nu}\int_0^\infty (xy)^{\nu+\frac12}\chi_{\nu,k,m}\left(\tfrac14 x^2y^2\right) f_j(y)\,dy,\ j=1,2$$

then

$$r^{-1}\int_0^\infty F_1\,(x/r)\,f_2\,(sx)\,dx = s^{-1}\int_0^\infty F_2\,(x/s)\,f_1\,(rx)\,dx$$

provided the integrals exist.

Theorem 3. If $f(x)$ and $g(x)$ are $\chi_{\nu,\,k,\,m}$—transforms and $f_1(s)$ and $\phi(s)$ are the Mellin transforms of $f(x)$ and $g(x)$, then

$$\frac{f_1(s)}{\phi(1-s)}=\frac{2^{s-\frac12}\Gamma(\frac14+\frac12\nu+\frac12 s)\Gamma(\frac14+\frac12\nu+\frac12 s+2m)\Gamma(\frac12\nu-\frac12 s+m-k+5/4)}{\Gamma(\frac34+\frac12\nu+\frac12 s+m-k)\ \Gamma(\frac34+\frac12\nu-\frac12 s+2m)\ \Gamma(\frac34+\frac12\nu-\frac12 s)}$$

Two corollaries of the above theorem have also been proved.

Theorem 4. If

$$g^{k,\,m}_{\nu+\frac12,1}(x)=\psi^{k.m}_{\nu+\frac12,\nu}\,f$$

$$g^{+}_{\nu+\frac12,1}(x)=I^{+}_{\nu+\frac12,\,1}\,f,$$

then

$$G^{+}_{\nu+\frac12,\,1}(x)=I^{+}_{\nu+\frac12,\,1}\ g^{k,\,m}_{\nu+\frac12,\,\nu}\,.$$

$$=(x/2)^{\nu+\frac{1}{2}}\int_0^\infty G^{2,\,1}_{2,\,4}\left(\tfrac{1}{4}x^2y^2\,\middle|\,\begin{matrix}-\nu+k-m+\frac{1}{2},-k+m+\frac{1}{2}\\ 0,\,2m,-\nu-2m,-1\end{matrix}\right)$$

$$d\left[y^{\nu+3/2}\,\overset{+}{g}_{\nu+\frac{1}{2},\,1}(y)\right]dy$$

Theorem 5. If

$$\overset{\mu}{g}_{\lambda+\frac{1}{2},\,\lambda}(x)=\overset{\mu}{H}_{\lambda+\frac{1}{2},\,\lambda}\,f$$

$$\overset{+}{g}_{\nu+\frac{1}{2},\,1}(x)=\overset{+}{I}_{\nu+\frac{1}{2},\,1}\,f$$

then

$$-(2/x)^{-1}\,\overset{+}{G}_{\nu+\frac{1}{2},\,1}(x)=\overset{\mu}{H}_{\lambda+\mu+3/2,\;\lambda+\mu+1}\left[y^{\mu-1}\,\overset{+}{g}_{\nu+\frac{1}{2},\,1}(y)\right]$$

In Chapter IX, we have extended the theory of functions which are self-reciprocal in the generalized Hankel transform $\chi_{\nu,\,k,\,m}$.

Theorem 1. If

$$P(x)=\frac{1}{2\pi i}\int_{C-i\infty}^{C+i\infty}2^{(b+\frac{1}{2})s}$$

$$\frac{\underset{*}{\Gamma}(\frac{1}{2}\nu+\frac{1}{2}s+\frac{1}{4}+m\pm m)\,\underset{*}{\Gamma}(\frac{1}{2}\lambda+\frac{1}{2}s+\frac{1}{4}+n\pm n)\,\underset{*}{\Gamma}(\frac{1}{2}\Theta+\frac{1}{2}s+\frac{1}{4}+p\pm p)}{\Gamma(\frac{1}{2}\nu+\frac{1}{2}s+\frac{3}{4}+m-k)\;\Gamma(\frac{1}{2}\lambda+\frac{1}{2}s+\frac{3}{4}+n-1)\;\Gamma(\frac{1}{2}\Theta+\frac{1}{2}s+\frac{3}{4}+p-q)}\,w(s)x^{-s}\,ds$$

where $w(s)=w(1-s)$ and

$$w(s)=0\left\{e^{(\frac{3}{4}\pi-3a+3\eta)\,|t|}\right\}$$

and

$$f(x)=\frac{1}{2\pi i}\int_{C'-i\infty}^{C'+i\infty}2^{bs}\,\frac{\underset{*}{\Gamma}(\frac{1}{2}\nu+\frac{1}{2}s+\frac{1}{4}+m\pm m)\,\underset{*}{\Gamma}(\frac{1}{2}\lambda+\frac{1}{2}s+\frac{1}{4}+n\pm n)}{\Gamma(\frac{1}{2}\nu+\frac{1}{2}s+\frac{3}{4}+m-k)\,\Gamma(\frac{1}{2}\lambda+\frac{1}{2}s+\frac{3}{4}+n-1)}\,\chi(s)x^{-s}\,ds$$

where $\chi(s)=\chi(1-s)$ and

$$\chi(s)=0\left\{e^{(\frac{1}{2}\pi-2a+2\eta)\,|t|}\right\}$$

then the function

$$g(x)=\int_0^\infty P(xy)\,f(y)\,dy$$

is $R_{\Theta}(q,p)$ and belongs to $A(5a,a)$

Similar theorems proved are as follows :—

Theorem 2. If

$$P(x)=\frac{1}{2\pi i}\int_{C-i\infty}^{C+i\infty}2^{(b+\frac{1}{2})s}\frac{\underset{*}{\Gamma}(\frac{1}{2}\nu_1+\frac{1}{2}s+\frac{1}{4}+m_1\pm m_1)\underset{*}{\Gamma}(\frac{1}{2}\nu_2+\frac{1}{2}s+\frac{1}{4}+m_2\pm m_2)\ldots\underset{*}{\Gamma}(\frac{1}{2}\nu_n+\frac{1}{2}s+\frac{1}{4}+m_n\pm m_n)}{\Gamma(\frac{1}{2}\nu_1+\frac{1}{2}s+\frac{3}{4}+m_1-k_1)\Gamma(\frac{1}{2}\nu_2+\frac{1}{2}s+\frac{3}{4}+m_2-k_2)\ldots\Gamma(\frac{1}{2}\nu_n+\frac{1}{2}s+\frac{3}{4}+m_n-k_n)}x^{-s}w(s)\,ds$$

and

$$f(x)=\frac{1}{2\pi i}\int_{C'-i\infty}^{C'+i\infty}2^{bs}\frac{\underset{*}{\Gamma}(\frac{1}{2}\nu_1+\frac{1}{2}s+\frac{1}{4}+m_1\pm m_1)\underset{*}{\Gamma}(\frac{1}{2}\nu_2+\frac{1}{2}s+\frac{1}{4}+m_2\pm m_2)\ldots\underset{*}{\Gamma}(\frac{1}{2}\nu_{n-1}+\frac{1}{2}s+\frac{1}{4}+m_{n-1}\pm m_{n-1})}{\Gamma(\frac{1}{2}\nu_1+\frac{1}{2}s+\frac{3}{4}+m_1-k_1)\Gamma(\frac{1}{2}\nu_2+\frac{1}{2}s+\frac{3}{4}+m_2-k_2)\ldots\Gamma(\frac{1}{2}\nu_{n-1}+\frac{1}{2}s+\frac{3}{4}+m_{n-1}-k_{n-1})}\chi(s)x^{-s}\,ds$$

then the function

$$g(x)=\int_0^\infty P(xy)\,f(y)\,dy$$

is $R_{\nu_n}(k_n, m_n)$

Theorem 3. If

$$P(x)=\frac{1}{2\pi i}\int_{C-i\infty}^{C+i\infty}2^{bs}\frac{\underset{*}{\Gamma}(\frac{1}{2}\nu+\frac{1}{2}s+\frac{1}{4}+m\pm m)\underset{*}{\Gamma}(\frac{1}{2}\lambda+\frac{1}{2}s+\frac{1}{4}+n\pm n)\underset{*}{\Gamma}(\frac{1}{2}\epsilon-\frac{1}{2}s+\frac{3}{4}+p\pm p)}{\Gamma(\frac{1}{2}\nu+\frac{1}{2}s+\frac{3}{4}+m-k)\Gamma(\frac{1}{2}\lambda+\frac{1}{2}s+\frac{3}{4}+n-1)\Gamma(\frac{1}{2}\epsilon-\frac{1}{2}s+p-q+5/4)}w(s)x^{-s}\,ds$$

and

$$f(x)=\frac{1}{2\pi i}\int_{C'-i\infty}^{C'+i\infty}2^{(b+\frac{1}{2})s}\frac{\underset{*}{\Gamma}(\frac{1}{2}\nu+\frac{1}{2}s+\frac{1}{4}+m\pm m)\underset{*}{\Gamma}(\frac{1}{2}\lambda+\frac{1}{2}s+\frac{1}{4}+n\pm n)}{\Gamma(\frac{1}{2}\nu+\frac{1}{2}s+\frac{3}{4}+m-k)\Gamma(\frac{1}{2}\lambda+\frac{1}{2}s+\frac{3}{4}+n-1)}\chi(s)x^{-s}ds$$

then the function

$$g(x)=\int_0^\infty P(x)\,f(xy)\,dy$$

is $R_{\epsilon}(q, p)$.

Theorem 4. If

$$P(x)=\frac{1}{2\pi i}\int_{C-i\infty}^{C+i\infty}2^{bs}$$

$$\frac{\underset{*}{\Gamma}(\tfrac{1}{2}\nu_1+\tfrac{1}{2}s+\tfrac{1}{4}+m_1\pm m_1)\ldots\underset{*}{\Gamma}(\tfrac{1}{2}\nu_{n-1}+\tfrac{1}{2}s+\tfrac{1}{4}+m_{n-1}\pm m_{n-1})\underset{*}{\Gamma}(\tfrac{1}{2}\nu_n-\tfrac{1}{2}s+\tfrac{3}{4}+m_n\pm m_n)}{\Gamma(\tfrac{1}{2}\nu_1+\tfrac{1}{2}s+\tfrac{3}{4}+m_1-k_1)\ldots\Gamma(\tfrac{1}{2}\nu_{n-1}+\tfrac{1}{2}s+\tfrac{3}{4}+m_{n-1}-k_{n-1})\Gamma(\tfrac{1}{2}\nu_n-\tfrac{1}{2}s+m_n-k_n+5/4)}$$

$$\times\, w(s)x^{-s}\,ds$$

and

$$f(x)=\frac{1}{2\pi i}\int_{C'-i\infty}^{C'+i\infty}2^{(b+\frac{1}{2})s}$$

$$\frac{\underset{*}{\Gamma}(\tfrac{1}{2}\nu_1+\tfrac{1}{2}s+\tfrac{1}{4}+m_1\pm m_1)\ldots\underset{*}{\Gamma}(\tfrac{1}{2}\nu_{n-1}+\tfrac{1}{2}s+\tfrac{1}{4}+m_{n-1}\pm m_{n-1})}{\Gamma(\tfrac{1}{2}\nu_1+\tfrac{1}{2}s+\tfrac{3}{4}+m_1-k_1)\ldots\Gamma(\tfrac{1}{2}\nu_{n-1}+\tfrac{1}{2}s+\tfrac{3}{4}+m_{n-1}-k_{n-1})}\chi(s)x^{-s}ds$$

then the function

$$g(x)=\int_0^\infty P\,(y)\,f\,(xy)\;dy$$

is $R_{\nu_n}(k_n,m_n)$.

Theorem 5. If

$$f(x)=\frac{1}{2\pi i}\int_{C'-i\infty}^{C'+i\infty}2^{\frac{1}{2}s}$$

$$\frac{\underset{*}{\Gamma}(\tfrac{1}{2}\nu+\tfrac{1}{4}+\tfrac{1}{2}s+m\pm m)\ldots\underset{*}{\Gamma}(\tfrac{1}{2}\lambda-\tfrac{1}{2}s+\tfrac{3}{4}+n\pm n)\underset{*}{\Gamma}(\tfrac{1}{2}\varepsilon+\tfrac{1}{2}s+\tfrac{1}{4}+p\pm p)}{\Gamma(\tfrac{1}{2}\nu+\tfrac{3}{4}+\tfrac{1}{2}s+m-k)\;\;\Gamma(\tfrac{1}{2}\lambda-\tfrac{1}{2}s+n-1+5/4)\;\;\Gamma(\tfrac{1}{2}\varepsilon+\tfrac{1}{2}s+\tfrac{3}{4}+p-q)}\chi(s)x^{-s}\,ds$$

the function

$$g\,(x)=x^{-1}\int_0^\infty Q\,[\log\,(x/y)]\;f\,(y)\;dy$$

is $R_{\varepsilon}\,(q,\,p)$, where

$$Q\,(x)=\frac{1}{2\pi i}\int_{K-i\infty}^{K+i\infty}\frac{\underset{*}{\Gamma}(\tfrac{1}{2}\nu+\tfrac{1}{4}+\tfrac{1}{2}s+m\pm m)\;\underset{*}{\Gamma}(\tfrac{1}{2}\lambda-\tfrac{1}{2}s+\tfrac{3}{4}+n\pm n)}{\Gamma(\tfrac{1}{2}\nu+\tfrac{3}{4}+\tfrac{1}{2}s+m-k)\;\Gamma(\tfrac{1}{2}\lambda-\tfrac{1}{2}s+n-1+5/4)}\,w(s)\;e^{xs}\,ds \qquad \text{when } x>0$$

$$=0 \qquad \text{when } x<0$$

In the derivation of two theorems we have also made use of the operators

$$E=x^{\lambda-1}\int_0^x dx.\,x^{-\lambda} \qquad \text{and} \qquad E_1=-x^{-\lambda}\int_0^x dx.\,x^{\lambda-1}$$

$$\Delta=\lambda+x\;(d/dx) \qquad \text{and} \qquad \Delta_1=\lambda-1-x\;(d/dx)$$

defined by H. C. Gupta. One of the theorems proved is as follows :—

Theorem. If E and E_1 stand for the operators defined above, Re (λ) lying between a and $1-a$; then $E^m E_1^{\,n} + E^n E_1^{\,m}$ is an operator transforming R_ν (k, p) into another R_ν (k, p) function, where $E^m E^n_1$ stands for the operation of E performed m times and of E_1 performed n times in all in any order.

Another theorem proved is as follows :—

Theorem. If $f(x)$ is R_ν (k, m), the function

$$\phi(x) = a^{a} f(xa^{2a}) \pm a^{-a} f(xa^{-2a})$$

where $a>0$, $a>0$, is $\pm R_\nu$ (k, m).

We have also proved a theorem which establishes a relation between generalized Laplace and Hankel transforms.

Theorem. If

$$f(s^\mu) = s^{a\mu}\int_0^\infty (qs^\mu t)^{c-\frac{1}{2}} e^{-(p-\frac{1}{2}q)s^\mu t} W_{1,\,n}(qs^\mu t)\,\phi(t)\,dt$$

and $t^\lambda\,\phi(t)$ is self-reciprocal in $\chi_{\nu,\,k,\,m}$—transform, *i. e.*,

$$t^\lambda\,\phi(t) = 2^{-\lambda}\int_0^\infty (ty)^{\nu+\frac{1}{2}}\chi_{\nu,\,k,\,m}(\tfrac{1}{4}t^2y^2)\,y^\lambda\,\phi(y)\,dy$$

then

$$f(s^\mu) = \int_0^\infty y^{\lambda+\frac{1}{2}}\left\{\overset{\mu}{\underset{\lambda}{g}}(y/s^\mu) + \overset{\mu}{\underset{\lambda}{G}}(y/s^\mu)\right\}\phi(y)\,dy$$

where
$$\overset{\mu}{\underset{\lambda}{g}}(y/s^\mu) = \frac{\Gamma(2m)\,\Gamma(1-2m)\,s^{\mu(a+\lambda-3/2)}\,q^{\lambda-\nu-3/2}\,(y/4s^\mu)^\nu}{2^{-\nu}\,\Gamma(\frac{1}{2}-k+m)\,\Gamma(\frac{1}{2}+k-m)}$$

$$\times\sum_{r=0}^{\infty}\frac{(-)^r\,\Gamma(\frac{1}{2}+k-m+r)\,\Gamma(\frac{3}{2}+\nu+m-k+r)\,\underset{*}{\Gamma}(c\pm n+\nu-\lambda+2r+3/2)}{r/2^{-2r}\,\Gamma(1-2m+r)\,\underset{*}{\Gamma}(1+\nu+m\pm m+r)\,\Gamma(c+\nu-\lambda+2r-1+2)\,q^{2\nu}}$$

$$\times\ (y/4s^\mu)^{2r}\,{}_2F_1\left[\begin{matrix}c\pm n+\nu-\lambda+2r+3/2\,;\\ c+\nu-\lambda+2r-1+2\,;\end{matrix}\quad 1-(p/q)\right]$$

and

$$\overset{\mu}{\underset{\lambda}{G}}(y/s^{\mu}) = \frac{\Gamma(-2m)\,\Gamma(1+2m)\,s^{\mu(a+\lambda-3/2)}\,q^{\lambda-\nu-4m-3/2}\,{}_{x}(y/4s^\mu)^{\nu+4m}}{\Gamma(\frac{1}{2}-k-m)\,\Gamma(\frac{1}{2}+k+m)\,2^{-\nu-4m}}$$

$$\times\sum_{r=0}^{\infty}\frac{(-)^{r}\,\Gamma(\tfrac{1}{2}+k+m+r)\;\Gamma(v+3m-k+r+3/2)\;\underset{*}{\Gamma}(c\pm n+v-\lambda+2m+2r+3/2)}{r/2^{-2r}\;\Gamma(1+2m+r)\;\underset{*}{\Gamma}(1+v+3m\pm m)\;\Gamma(c-\lambda+v+2m+2r-1+2)\,q^{2r}}$$

$$\times(y/4s^{\mu})^{2r}$$

$$ {}_2F_1\left[\begin{matrix} c\pm n+v-\lambda+2m+2r+\frac{3}{2}\ ; \\ c+v-\lambda+2m+2r-l+2\ ; \end{matrix}\quad\left(1-\frac{p}{q}\right)\right]$$

$$\begin{aligned}\phi(x)&=0(x^{a}) && \text{for small } x \\ &=0(e^{-bx}) && \text{for large } x\end{aligned}\qquad \text{Re } b>0$$

Re $(\lambda+v+a\pm 2m+3/2)>0$. Re $(c+v-\lambda\pm n\pm 2m+3/2)>0$, Re $(v-\lambda+c\pm n+3/2)0$, Re$(ps^{\mu})>0$, $p\geqslant q$ Re $(v+c-\lambda\pm n+4m+3/2)>0$, Re $(c\pm n+a+1)>0$.

From this theorem the results due to S. Masood and Snehlata follow as particular cases.

The last chapter is devoted to the extension of the theory of the self-reciprocal functions in the Hankel transform of one variable, on which a great amount of work has already been done by Bailey, Erdelyi, Hardy Titchmarsh, Brij Mohan, R. S. Varma, H. C. Gupta, Hari Shanker, D. P. Banerji, Shastri Dinesh Chandra, etc., of which a detailed history has been given in the first chapter. In particular I have obtained a few converse theorems on self-reciprocal functions and also, I have obtained 19 new resultant kernels, of which most of them are in the Meijer's G-function. These kernels have been used to derive new self-reciprocal functions.

The kernels obtained in this chapter and self-reciprocal functions deduced therefrom may be claimed to be new.

As an illustration we give a kernel and a self-reciprocal function. The function

$$G^{4,\,2}_{4,\,4}\left(x^{2}\,\middle|\,\begin{matrix}\frac{1}{4},\frac{1}{2},\frac{3}{4},\frac{1}{4}+\frac{1}{2}v \\ \frac{1}{4}+\frac{1}{2}\mu,\frac{1}{4},-\frac{1}{4}+\frac{1}{2}v,0\end{matrix}\right)$$

transforms R_{μ} into R_1, for Re $\mu>-1$, Re $v>0$.

The function

$$G^{4,\,3}_{4,\,5}\left(\tfrac{1}{2}x^{2}\,\middle|\,\begin{matrix}2m-\frac{1}{2}\mu+\frac{1}{4},\frac{1}{4}-\frac{1}{2}\mu,\frac{1}{4},\frac{3}{4} \\ \frac{1}{2}\mu-2m+\frac{1}{4},\frac{1}{4}+\frac{1}{2}v,\frac{1}{4},\frac{1}{4}+\frac{1}{2}v,\frac{1}{4}-\frac{1}{2}\mu\end{matrix}\right)$$

is R_1, provided Re $(\mu+v)>-2$, Re $(\mu-4m)>-1$.

SOME PROBLEMS IN FLUID DYNAMICS*

HAR SWARUP SHARMA
Department of Mathematics, Agra College, Agra.

The thesis contains a number of problems which are separate in themselves. The work has been divided into Chapters each of which is complete in itself.

Chapter I. *Two Dimensional Boundary Flow in a Convergent Channel with Curved Boundaries.*

Pohlausen[13] (1921) gave an exact solution of the boundary layer equations of the problem of two dimensional boundary layer flow which takes place between two converging walls. He assumed that the irrotational flow outside the boundary layer is due to a source or sink at the points towards which the walls converge.

The boundary layer flow in a converging channel formed by two equal circles of radii a and touching each other at the origin was investigated by Sanyal[21] (1955). The irrotational flow outside the boundary layer is due to a dipole at the point of contact of the circles which are eventually the stream lines of irrotational flow. The pressure-gradient calculated from inviscid flow was put into the boundary layer equations which were then integrated by Pohlausen method.

This method can be easily adopted to investigate the boundary flow in a channel which is symmetrical and its curved boundaries are the arcs of the curves

$$r^n = a^n \sin n\theta, \quad 0 \leqslant \theta \leqslant \frac{\pi}{2n}$$

and

$$r^n = -a^n \sin n\theta, \quad -\frac{\pi}{2n} \leqslant \theta \leqslant 0.$$

The irrotational flow outside the boundary layer is due to a multipole at the origin and for this the curved boundaries are the stream lines. The pressure-gradient is calculated from the inviscid solution and then the boundary layer equations have been integrated by Pohlausen's method. For $n=1$, the results agree with those of Sanyal[21] (1955).

Chapter II. *Motion of a Sphere in Rotating Liquid : Motion started Impulsively from Rest.*

Nigam and Rangaswami[11] (1953) discussed the growth of motion in the earlier stages of development, caused by a sphere which at time $t=0$ is suddenly made to rotate with a constant angular spin about a diameter in fluid otherwise undisturbed.

---

* Abstract of the thesis approved by the Agra University for the degree of Doctor of Philosophy in 1965.

In the present problem we have discussed the growth of motion in the earlier stages of its depelopments, caused by a sphere which at time $t=0$ is suddenly made to rotate with a constant angular spin Ω about a diameter in the liquid rotating about the same diameter with an angular spin $\sigma\Omega$. The various cases when σ is greater than 1 or less than 1 have been discussed. We have considered the cases when σ has a negative value *i.e.*, when the sphere rotates in the opposite direction to that of the external liquid.

Chapter III. *Flow of a Compressible Fluid through an Elliptic Pipe.*

Ray[17] (1956), Kapur[5] (1957), Ram Kumar and Warsi[14] (1963) discussed the problem of the Flow of Perfect Gas through a circular pipe by different methods. Here the problem of the flow of perfect gas through an elliptic pipe has been discussed. It has been found that the adiabatic flow is possible but, as pointed out by Kapur, either μ has to be assumed variable or Stoke's condition has to be modified. The solutions have been obtained in terms of Mathieu Functions.

Chapter IV. *Unsteady Motion of a Viscous Incompressible Fluid through Circular and Co-axial Pipes under Pressure-Gradient.*

The problem of the motion of a viscous incompressible fluid in a circular pipe of uniform cross-section has been investigated by many authors. In the case of the steady flow of a viscous fluid, the pressure gradient along the axis of the pipe comes out to be constant. But in the case when the flow is unsteady, the pressure-gradient along the axis of the pipe is not necessarily constant. In general it is a function of time only. In the first part we have discussed the unsteady flow of a viscous incompressible fluid by assuming the pressure gradient to be a suitable function of time.

In the second part the same problem has been extended to the case of flow of a viscous incompressible fluid in a channel bounded by two co-axial circular cylinders under pressure gradient along the axis which is a suitable function of time. The first problem was considered by Mithal[7] (1960) and second by Mittal[8] (1963) using the Laplace's Transforms. Here the problems have been solved by Finite Hankel Transforms. The method used here has this advantage over theirs that it greatly reduces the amount of complicated calculations involved in their solutions.

Chapter V. *Heat Flow through an Infinite Slab with a Face subjected to a Thermal Flux.*

Odier and Leutard[12] (1957) and Bannister[1] (1957) recently considered the problem of the heat flow through an infinite slab in which one face is subjected to a thermal flux, linearly decreasing with time. Their methods are based on Fourier's series, and on the method of images. Newcomb[9]

(1958) found the solution for the same problem using the Laplace's transformation. Gupta[4] (1963) investigated the same problem from a different point of view. Here the same problem has been studied when flux is $-Qf(t)$. The cases when $f(t)=\alpha-\beta t^n$ for all values of n which are multiples of $\frac{1}{2}$ have been considered. If we write $\alpha=1$, $n=1$, our results agree with those of Gupta[4]. His case is only a particular one while ours has general validity. The problem has been investigated in those cases also when $f(t)$ is constant and when $f(t)$ is an exponential function of time.

The analysis has been made by the application of Laplace's Transforms.

Chapter VI. *Flow of a perfect Gas over a Flat Plate under Pressure Gradient.*

Ray[18] (1957) discussed the problem of the steady flow of a perfect gas on a flat plate at zero incidence when σ is not 1. He took the main stream as one of uniform flow parallel to the plate. He did not assume any relation between temperature and viscosity. His assumptions were : (I) the pressure is not an absolute constant but constant along a normal to the plate inside the boundary layer, (ii) the variation of density and temperature from their values in the main stream are small.

In this paper Ray's problem has been solved with the same assumptions but with next approximations, and in doing so we have been able to get better results. Ray[18] (1957) obtained the results by numerical quadratures. But in this paper equations have been solved exactly. We are not to do the complicated process which is involved in Ray's results.

Analysis consists in eliminating pressure and temperature terms from the equations and in getting an equation in u and ρ which has been solved, satisfying the conditions of u and ρ at the edge of the boundary layer. The value of f, to get velocity distribution has been obtained in the form

$$f=\alpha\eta^m \text{ where } m=\frac{1-\sigma}{(\gamma-3)\,\sigma+3},$$

where Ray's relation is in the form

$$(ff')^{(1-\sigma)}\,f^{\sigma\frac{\gamma-1}{e}+1}=\frac{\exp.[f\{1-\sigma(\gamma-1)/2e(1+\frac{1}{4}f^2+\frac{1}{16}f^4+\dots)\}]}{\exp.\{1-0\cdot659\sigma\,(\gamma-1)/e\}}$$

It is evident from the above expressions that the results obtained here are in a better form than Ray's.

Chapter VII. *Linearized Trans-sonic Conical Flows.*

The problem of the flow of a compressible fluid past a cone with axis in the direction of the undisturbed stream has been solved by direct integration of the linearised equation both for supersonic and subsonic flows. Ray[15] (1950) solved the problem by means of a particular substitution for conical boundaries. In this paper it has been solved by means of a general substitution of which Ray's case is a particular one.

Chapter VIII. *Unsteady Flow of a Compressible Fluid around a Corner.*

Durand[3] (1935) studied the Prandtl's problem of the expansion of a uniform two-dimensional stream of gas flowing around a corner at a supersonic speed under adiabatic conditions and he showed that the velocity perpendicular to the radius vector from the corner is always equal to the speed of the sound at the local conditions of pressure and velocity. Bernoulli's equation has been used to find the components of velocity in terms of the angle of deflection and also to find the relation between the pressure and the same angle.

Ray[16] (1955) studied the same problem starting with non-adiabatic conditions, conductivity and viscosity taken into account. He assumed that the velocity, density and pressure are constant along a radius and found that the equations lead to adiabatic conditions and that the transverse velocity is equal to that of sound as before.

In this problem we have discussed the unsteady flow of a compressible fluid around a corner. The equations of motion, the equation of continuity, and the energy equation of unsteady flow of a compressible fluid have been taken and under the assumptions of Ray (velocity, density and pressure are constant along a radius vector) it has been found that the velocity components, density, pressure and enthalpy are independent of time around a corner and depend only on the angle of deflection. Starting with non-adiabatic conditions it is found that the equations lead to adiabatic conditions and that the transverse velocity is equal to the velocity of sound as before.

Chapter IX. *Motion of a Finite Disc in Rotating Fluid : Boundary Layer Growth : Motion started Impulsively from Rest.*

T. V. Kármán[6] (1921) solved the problem of the rotation of an infinite plane lamina in a viscous fluid. Batchelor[2] (195[illegible]), Stewartson[22] (1958), Rogers and Lance[19] (1960) and others investigated the more general problem of a fluid in a rigid body rotation over a rotating disc. The axis symmetric boundary layer on a finite circular disc due to a rotating fluid has been examined numerically by Rogers and Lance[20] (1964). Nigam[10] (1951) discussed the growth of motion in the earlier stages of its development caused by an infinite lamina which is made to rotate.

In this problem we have discussed the case of revolving flow over a rotating finite circular disc. We have considered the growth of motion in the earlier stages of its development caused by a finite circular plane lamina which at $t=0$ is suddenly made to rotate with a constant angular spin. We have discussed the various cases when the angular velocity of the disc is greater or less than the angular velocity of the rotating fluid. The case when the disc rotates in the direction opposite to that of the fluid has also been considered. Results are in error functions, their derivatives and their integrals.

REFERENCES

1. Bannister, F. K. 1957. *Engineering, Lon.*, **9** : 370.
2. Batchelor, G. K. 1951. *Quart. J. Mech. Appl., Math.*, **4** : 29.
3. Durand, W. F. 1935. *Aerodynamics Theory*, **3** : 243.
4. Gupta, R. K. 1963. *Proc. of the National Institute of Sciences of India*, **29, A (1)** : 86.
5. Kapur, J. N. 1957. *Proc. of the third Congress on Theoretical and Applied Mechanics*, 243-250.
6. Kármán, T. V. 1921. *Zeitschr. f. angew. Math. u. Mech.* **1** : 244-247.
7. Mithal, K. G. 1960. *Bull. Cal. Math. Soc.*, **52** : 47.
8. Mittal, M. L. 1963. *App. Sc. Res.*, p. 86-90.
9. Newcomb, T. B. 1958. *Brit. J. Appl. Phys.*, **9** : 370.
10. Nigam, S. D. 1951. *Quart. of Appl. Maths.*, **IX (1)** : 89-91.
11. Nigam, S. D. & Rangaswami, K. S. I. 1953. *Zamp*, **IV** : 221-243.
12. Odier, J. & Leutard, F. 1957. *C. R. Acad. Sci.*, Paris, **244** : 1141.
13. Pohlausen, K. 1921. *Zeits. f. angew. Und Mech.*, **1** : 267.
14. Ram Kumar & Warsi, Z. U. A. 1963. *Bull. Cal. Math. Soc.*, **55 (3)** : 131-137.
15. Ray, M. 1950. *Bull. Cal. Math. Soc.*, **42** : 146.
16. Ray, M. 1955. *Proc. N. I. Sc. of India*, **21 A** (3) : 153-160.
17. Ray, M. 1956. *Proc. Nat. Inst. Sci.* India **22** : 408.
18. Ray, M. 1957. *Bull. Cal. Math. Soc.*, **49** (3).
19. Rogers, M. H. & Lance, G. N. 1960. *J. Fluid Mech.*, **7** : 617.
20. Rogers, M. H. & Lance, G. N. 1964. *Quart. J. Fluid & Appl. Maths.*, **XVII** (3) : 319-330.
21. Sanyal, L. 1955. *Bull. Cal. Math. Soc.*, **47** : 129-133.
22. Stewartson, K. 1958. Boundary Layer Research Symposium, Freiburg Berlin Springer Verlag 59-71.

CHEMICAL EFFECTS OF NUCLEAR TRANSFORMATIONS IN COBALT COMPLEXES*

MANOHAR LAL
Chemistry Division, Atomic Energy Establishment, Trombay,
Block 'L', 414 A, Gadel Road, Bombay—28.

SUMMARY

The kinetic aspects of annealing of recoil species in thermal neutron irradiated solid octahedral cobalt complexes are similar to annealing of radiation damage in solids such as graphite and copper. However, the species formed in (n,γ) reactions are more complex, and chemical and stereochemical factors play important roles in determining the kinetics of annealing.

(n,γ) recoil effects in trisacetylacetone Co(III) have been the subject of detailed study at this laboratory. The present thesis contains work which is a continuation of this comprehensive study. Recoil effects on this complex diluted with the isomorphous trisacetylacetonates of Al(III), Rh(III), and Mn(III) are presented in this thesis.

EFFECT OF DILUTION

Work on (n,γ) reactions in trisacetylacetone Co (III) diluted with isomorphous trisacetylacetone Al (III) clearly indicate that initial retention as well as saturation retention at all temperatures decrease with increasing dilution. The value of initial retention decreases with increasing dilution from about 16% to 2·8%; likewise the extent of annealing decreases with dilution, being negligible for the highest dilution studied. For the latter, this is indicative of absence of post-recoil annealing reactions both during irradiation and in later isothermal annealing runs. One might ascribe this effect to the reduction in the number of available fragments, as the cross-section for $Al^{27}(n,\gamma)Al^{28}$ is very small compared to that for cobalt, the number of fragments created in aluminium-complex-diluted samples due to neutron capture will be much less than in undiluted trisacetylacetone Co(III). In order to check this possibility, similar experiments using isomorphous trisacetylacetone Rh(III), in which the (n,γ) cross-section for the metal is higher than that of Co-59 were carried out.

The data and results of these experiments clearly show that dilution with trisacetylacetone Rh(III) has less effect on initial retention and post-thermal annealing than with the aluminium samples. However, it is evident that the large number of fragments created due to the higher cross-section for $Rh^{103}(n,\gamma)Rh^{104}$ reaction have no effect, since initial retention in general did not show an increase on dilution. As rhodium is a homologue of cobalt the trisacetylacetone Rh(III) is much more closely related to the corresponding cobalt complex than the trisacetylacetone Al(III). Thus the influence appears to be more or less chemical in nature, if other conditions, such as temperature of annealing, are same.

---

* Abstract of the thesis submitted for the degree of Doctor of Philosophy of the University of Agra.

One disadvantage in using aluminium or rhodium complex as diluent lies in the fact that half lives of Al^{28} and Rh^{104} are too short to allow any investigations of recoil effects in the diluent itself. Trisacetylacetone Mn(III), which is also isomorphous with the cobalt complex, was therefore selected as the diluent, the reason being that the half life of Mn^{56} is long enough to permit some experiments with the pure complex.

The initial retention of 4·1 ± 2·0% determined in the case of pure manganese complex is an average of several values. This very well agrees with the "inherent retention" of about 3·5 - 4% (entirely dependent upon physical phenomena) calculated for this complex. A rather sharp increase in retention values has been observed after storage at room temperature.

The situation obtained on dilution of trisacetylacetone Co(III) with trisacetylacetone Mn(III) is radically different in that retention increased on dilution. The extent of thermal annealing is also greater on dilution. Separate experiments by the author showed that Co-60 exchanges with trisacetylacetone Mn(III). In methanol solution more than 80% exchange is observed in about one hour at room temperature.

Initial retention in trisacetylacetone Co(III) :

Consideration of energy transfer processes following (n,γ) reaction in trisacetylacetone Co(III) by Shankar *et al* (1) indicates that in about 2% of recoils the atoms acquire less than the threshold displacement energy (25 ev) and are therefore not displaced from the molecule. This constitutes what may be termed "inherent retention" and is due to reasons other then chemical. Due to compulsory collisions with one or more oxygen atoms and possibly with some carbon atoms an additional 2% of recoil cobalt atoms fall below the limit of 25 ev and will remain within the coordination sphere and as such one may expect the total "inherent retention" to be $\sim$ 4%. However, the experimental data indicates that initial retention in undiluted trisacetylacetone Co(III) is 15-20%. The higher initial retentions observed may be due to the following factors.

(a) Hot radical and epithermal reactions which might lead to formation of parent molecule. One can also visualise certain reactions during the existence of the hot zone.

(b) Irradiation annealing by fast neutrons, energetic electrons and γ-rays which is particularly important in reactor irradiation.

(c) Thermal annealing during reactor irradiation.

The possibility of chemical reactions during the existence of the hot zone in trisacetylacetone Co(III) has been discussed in great detail and it is felt that the contribution of hot zone reactions to retention is negligible.

The other two factors which might contribute to initial retention, namely the thermal and radiation annealing during reactor irradiation have been considered in detail. If these causes can be minimised one can evaluate their contribution towards initial retention. These causes can be minimised by short term and low temperature irradiation. Samples of trisacetylacetone Co(III) were irradiated at dry ice temperature for 1-2 minutes. Initial retention of 4% was obtained for this sample. In another experiment trisacetylacetone Co(III) was irradiated for the same time but without dry ice surrounding the sample. This sample gave an initial retention of 4·8%. The results clearly indicate that values of retention in these experiments agree rather closely with the calculated value of "inherent retention". One more aspect is evident from these experiments. The initial retention decreased by a large amount when time of irradiation and therefore, total γ- and fast neutron flux is reduced. When the temperature of irradiation was simultaneously decreased, not much further lowering of retention was observed. One is tempted to conclude from these experiments that radiation annealing rather than temperature of irradiation plays a prominent role in increasing retention during irradiation.

Examination of kinetics of thermal annealing of recoil effects in trisacetylacetone Co(III) and in diluted system :

Following the classical treatment of Vand (2) and Primak (3) it has been shown by Shankar *et al* (1) that in thermal annealing of recoil damage in trisacetylacetone Co(III), the activation energy shows a spread. In the present work the annealing data in undiluted, aluminium and rhodium diluted samples has been analysed by the above methods. The distribution in activation energy shows a broad shift to lower values on dilution, while it shows shift to higher values in the second of the two stage annealing experiments as compared to the first. However, these methods of analysis are based on certain assumptions and simplifications. This thesis presents a closer scrutiny of these assumptions.

(i) The frequency factor, A was assumed to be 10^{13} sec^{-1} in all the previous studies. As part of this work the value of frequency factor for the kinetic processes has been evaluated by the treatment after Primak (3). Two sets of step annealing experiments were performed and the value of frequency factor obtained as $\sim 4{\cdot}5 \times 10^{11}$ sec^{-1}.

(ii) The application of step-function is a simplification, and this has been avoided in an alternative derivative by Primak (4). Using Laplace transforms the values of po (ε) [po (ε)] is the initial distribution of observable properties p, with activation energy (ε) had been evaluated to a better accuracy than by the method of step function. This method of analysis has not so far been used by other workers to obtain the activation energy spectrum in annealing processes.

Following closely the mathematical formulation by Primak (3) it has been demonstrated that the measured value of property (% separable activity) at any time will always be higher in double stage annealing than in single stage annealing. It may be mentioned in the end that Primak's treatment and therefore the conclusions arrived at in this chapter, are based on the assumption that in all cases of annealing of radiation damage the measured property eventually reaches 100%, that is, complete annealing occurs. It can be shown that after a certain stage the rate of change becomes extremely small so as to make in appear that there is no change of property with time at a given temperatue. This is indeed the case with radiation damage in metals in which annealing consists of combination of vacancies and interstitial atoms.

In the present case the problem is much more complex as annealing cannot obviously be pictured in the same simple manner as in metals. The hot atom which comes out of the coordination sphere gets back in the original molecular form by a series of processes which are not yet clearly understood. Some of these may be chemical in nature. This is supported by the fact that the activation energies are of the same order of magnitude as those encountered in normal chemical reactions. However, the remarkable fact has been brought out that the method of Primak (3,4) can be applied to kinetic data on these complexes. This shows its general nature but the conclusions reached may not be quite exact.

RADIATION ANNEALING

Like thermal annealing, γ- and X-irradiation of neutron irradiated undiluted, aluminium and rhodium diluted trisacetylacetone Co(III) samples increase their initial retention. The extent of radiation annealing decreases with increasing dilution. Isothermal annealing of radiation annealed samples show that in all samples saturation retention ($R\infty$) and reaction half-time ($t_{\frac{1}{2}}$) have decreased.

Increasing γ-dose or heating trisacetylacetone Co(III) prior to (n,γ) reaction results in a lowering of initial retention as well as of the extent of annealing but in an increase of rate of annealing.

The equivalence of thermal and radiation annealing in this complex has been established by closed cycle experiments.

Nature of recoil species and paper electrophoresis studies:

To explain the annealing behaviour of neutron irradiated trisacetylacetone Co(III), Shankar et al (1) have postulated the existance of metastable species. To understand more fully the nature of species formed when irradiated complex is dissolved, paper electrophoresis with undiluted, aluminium and radium dileted trisacetylacetone Co (III) was undertaken. The distinctive features of this study are :—

(i) In all these experiments only two peaks are obtained indicating the presence of only two species in the irradiated complexes on dissolution.

(ii) Most of species produced in (n.γ) reaction in these samples have a positive charge. The distance of migration is the same as that of free Co^{++} ions.

(iii) There is a slight but persistant migration of parent complex towards the negative side of the histogram showing that neutron irradiation might have resulted in the formation of either positively charged degradation species or electron deficient species. It is observed from the histograms of the heated samples (4 hrs at 100°C) that in undiluted and rhodium diluted samples the parent species is restored to the neutral line. This suggests that the positively charged species which might have been produced on neutron irradiation of undiluted and rhodium diluted samples have been stabilised into the original neutral complex on heating.

One way to explain this effect is to postulate positive complex species. Shankar *al et* (1) have suggested that radical deficient species such as [bisacetylacetone Co (III)]$^+$, might exist in irradiated but unannealed systems. This problem has been approached indirectly by studying possible chemical reactions when the irradiated complex is dissolved in acetylacetone itself. Radical deficient species [bisacetylacetone Co (III)]$^+$ takes up an additional acetylacetone ligand and forms the parent complex. The results of the experiments carried out on this aspect clearly indicate that the rate of formation of trisacetylacetone Co (III) is much faster with neutron irradiated complex than with the unirradiated one in (which Co-60 tracer in the form of Co^{++} has been incorporated). The extent of reaction is also more in the former.

The positively charged entities in the irradiated complex need not necessarily be radical deficient species. They may be electron deficient species, such as [trisacetylacetone Co (III)]$^{+n}$. This has been suggested on the basis of the results of experiments carried out which Co-60^m.

As mentioned earlier, independent experiments by author have shown that Co-60 exchanges with trisacetylacetone Mn (III). In view of this fact, the increase in retention on dilution with trisacetylacetone Mn (III) can be easily understood. Thermal exchange mechanism has been suggested for this system. As the observed isotopic exchange between Co^{++} and the cobalt chelate is quite small recombination reactions cannot be possible by thremal exchange. In this thesis the mechanism of 'excited'' exchange has been suggested for the recombination reactions in undiluted and rhodium diluted systems, while in aluminium diluted systems this process is operative only to a slight extent.

In conclusion it has been emphasised that one of the important lines of future research in this field still remains the unambiguous identification of the metastable species in the solid state.

REFERENCES

1. J. Shankar, K. S. Venkateswarlu & Amar Nath. 1960. Proc. of Symposium on Chemical Effects of Nuclear Transformation, IAEA, **1:** 335.
2. V. Vand., 1943. *Proc. Phys. Soc.* (London), **A55:** 222.
3. W. Primak., 1955. *Phys. Rev.,* **100:** 1677.
4. W. Primak., 1960. *J. Appl. Phys.,* **31:** 1524.

STUDIES ON INFECTIOUS LARYNGOTRACHEITIES VIRUS OF POULTRY WITH SPECIAL REFERENCE TO TISSUE CULTURE SYSTEM*

PRAFULLA CHANDRA PANDA†
Department of Pathology and Bacteriology,
U. P. College of Vet. Sci. & Animal Husbandry, Mathura.

This investigation was carried out with an aim to study the characteristics of the Infectious Laryngotracheities virus strain isolated at this Institute and to explore the possibilities of carrying out different diagnostic tests at our present laboratory conditions both in developing embryonated eggs and tissue culture system. To curtail the economic strain incurred by the heavy use of embryonated eggs in virological studies, efforts were directed to study the behaviour and adaptability of the virus especially in tissue culture system.

During the course of this investigation the virus strain was cultivated and propagated in developing embryonated eggs by adopting the dropped chorioallontoic membrane (CAM) technique and in whole chick embryo primary cell culture lines.

The viral agent produced definite pock like lesions to confluent thickenings in the CAM of the infected embryos from the third day onwards, killing most of the embryos between the fifth to sixth day of inoculation. It produced turbidity of the amnionic fluid at times as a result of infection into the amnionic cavity. There was no loss in viral titer by storing the same at four degree centigrade for four days inside the infected embryos. The comparative viral titers achieved by adopting both the dropped CAM and CAS (chorioallontoic sac) route of inoculation indicated that the former method was little superior than the latter.

Successful demonstration of intranuclear inclusion bodies was possible both in infected chorioallontoic membranes and tracheal sections of artificially infected birds during the early stage of infection. Zenker's acetic acid as a fixative was found superior in comparision to formalin.

No adverse effect on the viability of the virus could be observed by treating the same with antibiotics like Penicillin and Streptomycin at the rate of one thousand to five thousand units per cc. and one thousand micrograms to five thousand micrograms per cc. respectively. Successful inactivation of the virus could be done by exposing it to fiftysix degree centigrade for a period of thirty minutes to one hour. A considerable loss in viral titer was noticed as a result of filtration through Seitz filter discs.

---

* This is an abstract of the thesis submitted to and approved by the Agra University in partial fulfilment of the requirements for the award of M. V. Sc. degree in Bacteriology in the year 1964.

† At present the author is working as a Scientist, Central Food Technological Research Institute, Mysore, India.

The viral agent produced distinct cytopathic changes in whole chick embryo primary cell culture lines characterized by the destruction of cell sheet, retraction of cell processes rounding of cells and vacuolization which could be neutralized by treating it with its specific immune antisera.

The viral agent failed to agglutinate chicken red blood cells. Successful serum neutralization tests were performed both in developing embryonated eggs and tissue culture system.

On experimental inoculation, the viral agent failed to set up the violent clinical symptoms of the disease indicating a successful attenuation of the same in developing embryonated eggs. Infection of the susceptible hosts with the viral agent was established by observing a rise in antibody titer between the pre and post inoculation periods and demonstration of intranuclear inclusion bodies during the early stage of infection.

Necessity of further research on the aspects of serological survey, variation of the virus in relation to epizootiology and the possibilities of the production of an egg adopted vaccine and tissue culture vaccine have been discussed.

MORPHOLOGICAL STUDIES IN THE SAPOTACEAE AND SOME ALLIED FAMILIES*

PADAM SARAN KAPOOR
School of Plant Morphology, Meerut College, Meerut.

SUMMARY

Sapotaceae is mainly a tropical family, arborescent in habit and economically important. It has been generally assigned to the order Ebenales, though the Ebenales of different workers is not always similarly constituted. There is a felt of stiff hairs present on the ovary and the sepals, and laticiferous canals and tannin filled cells are abundant throughout the system. The material is difficult to microtome and the techniques are very exacting. From the stand-point of floral anatomy, the family was so far uninvestigated.

The present account is a summary of the results of investigation of sixty species, of which fifty-three belong to Sapotaceae, five to Ebenaceae and two to Symplocaceae. The investigation throws some light on a better understanding of such topics as the relationship between uni- and trilacunar nodes, nature of petal appendages, trends of specialization in the androecium, placentation, etc., reduction in the number of ovules and their relationship with the carpel.

Nodal anatomy of sixteen species (fifteen Sapotaceae and one Ebenaceae) has been worked out. Of the fifteen sapotaceous species fourteen are three-traced, trilacunar and the three traces unite in the nodal cortex to form a single petiolar strand of various types. In only one species the structure has been found to be one traced unilacunar. These results are in disagreement with earlier report of exclusively unilacunar condition. The trilacunar node has been considered to be primitive and the unilacunar derived from it. In the Ebenaceae the node is one-traced unilacunar.

The sepals may be either spiral or in two cycles; they may be three-traced—each trace arising independently, or two of the traces arising conjoint or all the three arising conjoint from a single gap—; two-traced,—two traces arising independently or conjointly—; or one-traced with a trifurcating trace. The one-traced sepals occur very frequently and are believed to have been derived from three-traced ones.

The vascular supply to the sepals in *Lucuma dissepala* shows that the outer two sepals represent a union of two in each. In *Sideroxylon capiri* two of the sepals are sometimes fused in their lower region. These are cases of congenital concrescence.

---

* A summary of the Thesis submitted to and approved by the Agra University in fulfilment of the requirements for the degree of Doctor of Philosophy.

The petals are always one-traced. The petal trace always arises independently except in *Chrysophyllum* (Sapotaceae) and *Diospyros* (Ebenaceae) where it is conjoint respectively with the opposite stamen and stamen fascicle trace. The petals in some genera of the Sapotaceae bear appendages. These may be dorsilateral; ventrolateral or lateral and their method of formation differs in different cases. They are supplied by the lateral branches of the petal bundles and have been interpreted as stipular in nature. The androecium in Sapotaceae may be composed of a single antepetalous whorl or two. In the latter case the alternipetalous whorl may be fertile or staminodal and the condition is normally diplostemonous. In the antepetalous whorl although there is usually a single stamen on each radius, some genera may have fascicles instead of single stamens. The stamens are supplied by an unbranched trace but the staminodes in their form and vasculature are of various description.

The stamens in the alternipetalous whorl are variously modified. The normal condition is represented by *Payera*, *Palaquium*, etc., where a fertile stamen is present on every radius. From this, specialization seems to have progressed along two independent lines, one of them leading to a gradual loss of the staminodes followed by the disappearance of their vascular supply and the other involving a change by gradual stages to large petaloid structures.

The androecium in the Ebenaceae has been found to be obdiplostemonous. It is believed here that the adnation of the antepetalous stamen traces with those of the petals has enabled them to occupy a position outer to that of the alternipetalous stamens. Besides, the carpels as in a case of true obdiplostemony alternate with the alternipetalous stamens which in the changed condition are immediately outer to them.

The hypogynous disc present in the Sapotaceae and Ebenaceae may either be receptacular or carpellary.

The placentation in the Sapotaceae is morphologically always axile although the vascular anatomy in the lower region of the ovary suggests a parietal condition. The ventral strands arise normally oriented on radii alternate to those of the dorsals and are composed of the bundles of adjacent carpels. A reshuffling of the ventral strands takes place in the central column which results in the reformation of an equal number of vascular strands. These are inversely oriented on the radii of the dorsals and composed of ventral bundles of the same carpels. An interesting case is seen in *Lucuma* where no organization of the inverted strands takes place on the radii of the dorsals. The ventral bundles of the split strands on reaching the central column send direct traces to the ovules. The axile placentation in this family is considered to have been derived from parietal placentation.

In the Ebenaceae the placentation is axile. The ventral strands are composed of the ventral bundles of the adjacent carpels and situated in the central column on radii alternate to those of the dorsals. In *Diospyros cordifolia*, however, these ventral strands supply the ovules in the upper unilocular region of the ovary from the disengaged margins of the placentae. This suggests a possible tendency of transition to the parietal condition.

In *Symplocos* (Symplocaceae) the ovules are borne on the disengaged margins of the placentae in the upper unilocular region of the ovary and the placentation is parietal.

The ovules in the Sapotaceae may be either pendulous, horizontal or ascending showing a tendency towards development of basal ovules.

The locules are constantly uniovulate in the Sapotaceae and biovulate in Ebenaceae (exceptionally uniovulate) and Symplocaceae. In the first condition the two marginal bundles jointly supply the single ovules but in the latter they supply the ovules of their respective sides. It has been inferred that the uniovulate condition has been derived from biovulate.

There are many features in the families under investigation that support the view that the ovules are carpellary in nature, *e. g.*, the orientation of the ovules, the unifacial anatomy of the placentae and the definite relationship of the orientation of the placental bundles with that of the dorsals. The ventral strands in some sapotaceous genera, instead of passing straight into the central column, traverse into the ovary wall and diverge in through the septae. This is a further suggestion that the ovules are not axial but carpellary structures.

In the family Symplocaceae the ovary is inferior. Since we have no means of determining if the vascular supply in the ovary wall represents the "traces" or the "bundles" it has not been possible to interpret the exact nature of the ovary wall.

The total anatomical evidence collected in the present study supports independent status for the Sapotaceae, Ebenaceae and Symplocaceae.

ACKNOWLEDGEMENTS

The author is greatly indebted to Prof. V. Puri for valuable guidance and constant encouragement throughout the course of this investigation. Grateful thanks are due to Dr. Y. S. Murty for his een interest in this work and help in several ways.

THE EVERSHED EFFECT IN SUNSPOTS*

ARVIND BHATNAGAR
Kodaikanal Observatory, Kodaikanal-3 (Madras).

In the thesis entitled 'the Evershed Effect in Sunspots', is presented a detailed observational study of the Evershed Effect and associated phenomena in sunpots. The investigation was carried out at the Kodaikanal Observatory with the Solar tower telescope, yielding an image scale of 5″.5 of arc per mm in conjunction with a 18-metre focal length Littrow spectrograph.

In Chapter I, is given a resume of the work done earlier on the Evershed Effect and an outline of the present investigation. It is emphasised that the influence of Zeeman broadening due to the sunspot magnetic field may obliterate the small scale velocity fields. To completely remove the effect of sunspot magnetic field, three Zeeman insensitive lines; 4912·027 A of Ni I, 5576·101 A of Fe I and 5691·508 A of Fe I (Ni) were selected for velocity field determinations in sunspots.

In chapter II, the instrumental arrangement and the observing technique for obtaining the spatial velocity field configuration is described. For a precise determination of small scale Doppler displacements in lines, large spectrographic dispersion and resolution are essential. For obtaining velocity field configurations in sunspots, the fourth and fifth orders of the 18-meter spectrograph, yielding a dispersions of 6 mm per A, and 8 mm per A, respectively were used.

On a high dispersion solar spectrum, of the kind used in this study, it is very difficult to measure precisely the small Doppler displacements. For measuring small Doppler shifts, a modified version of Evershed's positive-on-negative method, using the principle of photographic subtraction was utilized. This modified positive-on-negative method, enables one to precisely and conveniently determine small Doppler displacements of the order of 50 metres per sec. The essential advantage of this method is that it is independent of the width of lines. The technique is described in Chapter II.

The spatial distribution of the sight-line velocities obtained by using the earlier mentioned three Zeeman insensitive lines are given in Chapter II. Variations in the magnitude of velocity vectors in the three lines for the same disk position of the spot are an indication of the depth dependence of the velocity field in spot penumbrae.

---

* Abstract of the thesis submitted to and approved by the Agra University for the degree of Doctor of Philosophy.

To investigate changes in the velocity field pattern with the age of the spot, this investigation was carried out during two successive passages across the disk of the same sunspot group. Spot spectra of Kodaikanal spot No. 12368 for velocity field determinations were obtained before and after a rapid development of the spot group, which occurred during January 14 and January 18, 1963. 167 Spectra were taken using 3 lines for determining the spatial distribution of velocity fields in spots during the two passages. Sight-line velocities were determined at 3,340 points in the spots.

In Chapter III, the mean depths of formation of the two Zeeman insensitive lines, 4912·027 A and 5691·508 A were computed, using a recent sunspot penumbra model of Makita. The three-component velocities (radial, tangential and vertical) obtained from the measured sight-line velocities were calculated using an IBM 1620 computer and are given in this chapter. The radial velocity pattern in sunspots, show a peak around half way across the penumbra. The magnitude of the peak velocity is a function of the line strength and of the disc position of the spot. At each of the nine disk -positions of the spot, the gradient of the maximum radial velocity, Umax with depth is obtained. A mean gradient of Umax in the penumbra was found to be $4{\cdot}0 \times 10^{-3}$ km/sec per km in depth. Small vertical velocities of the order of 0·3 km/sec and less, directed downwards in the spot penumbrae were also found.

These observations show the presence of sizable tangential velocities in the sunspot penumbrae. On six disk positions of spots, a slight systematic pattern in the variation of the tangential component could be seen. Maximum tangential components of the order of 0·6 km/sec were observed on six disk positions. When the spots are close to the centre of the disc, the tangential velocities show large variation in amplitude with no systematic pattern. Evidence for the presence of this important tangential component is not conclusive. However, tangential velocities in spot penumbrae can be expected to exist in the light of the recent measures of orientation and inclination of magnetic lines of force by Adam.

The spatial distribution of magnetic field in spots for which velocity fields were determined, are also given in Chapter III.

In Chapter IV, is presented a photometric study of the phenomenon of asymmetry in lines in the penumbral region. The credit for the discovery of this phenomenon also goes to Evershed. A new parameter called the 'Flag Factor' (F.F) is proposed as a measure of the asymmetry in lines. The variation of the 'Flag Factor' in and around the spot region and also with the disk position of the spots is given in this chapter. The asymmetry varies with the line strength and the magnitude of the maximum asymmetry decreases towards the disk centre positions of the spot. It is suggested that this phenomenon of asymmetry in lines may be due to the relative Doppler displacements occuring in several strata of the line-forming layer.

Spectra obtained under best atmospheric conditions show, besides the large asymmetry in lines in the penumbral region, a diffuse wing in lines in the photospheric region. This phenomenon of diffuse wing in lines in the photospheric regions is more conspicuous in dark spaces between the bright solar granules. Lines acquire their normal shape in the brighter parts of the spectrum. This interesting observation is reported in Chapter IV.

Some of the finest spot spectrograms obtained under very good 'seeing' conditions (better than 1″ of arc), show continuum brightness fluctuations in the penumbral region. A considerable variation in the width of the lines, along the length of the slit, in the penumbral region is observed. A correlation study between the continuum brightness, equivalent width and sight-line velocity is presented in Chapter V. For this study three lines and three slit positions over the spot were used. The correlation study shows that darker (cooler) regions of the penumbra show larger equivalent width while the brighter (hotter) regions show smaller width. It is believed that this spectroscopic observation of brightness variations in the spot penumbral region is reported for the first time. It is proposed that these brightness fluctuations are the manifestation of aggregates of small penumbral filaments, as seen on a good white light photograph of sunspots. The agency responsible for the widening of lines in penumbral region is more efficient in the darker interspaces compared to the brighter parts.

STUDIES ON GROWTH AND YIELD OF TWO VARIETIES OF WHEAT AS INFLUENCED BY VARIATIONS IN PLANT DENSITY AND SOIL FERTILITY*

J. P. AGARWAL
Prof. of Agronomy, R. M. P. College, Narsan (Saharanpur).

Following are the results of a varietal-cum-plant density-cum-soil fertility investigation on wheat conducted at the B. R. College Farm, Bichpuri (Agra) during the *rabi* season (Oct.-April) of two consecutive years (1956-58). The treatments comprised of two varieties (Pb. 591 and N. P. 718), three seedrates 20, (S20) 30, (S30) and 40 Srs. (S40) per acre and four levels of nitrogen (0, (N0) 20, (N20) 40, (N40) and 60, (N60) lb. N. per acre), which were tested in a 'Complex Randomised Block' design of layout with four replications. To ensure a uniform distribution of seeds within rows the spacings of 6", 9" and 12" were adopted in the treatments of 40, 30 and 20 Srs. of seedrate respectively. The full dose of nitrogen in every case was applied broadcast as ammonium sulphate just before sowing. The experimental crop was taken in different fields in the two years—in the first year after fallow and in the second year after a crop of sorghum for green fodder. This difference in the previous cropping caused variation in the initial fertility of the soils on which the experimental crops were sown in the two years. The weather conditions during the two crop seasons also differed greatly resulting in wide variations in the performance of the two crops. The following are the main results and conclusions.

1. In both the years N. P. 718 produced more total dry weight, grain and srtaw per acre than Pb. 591. On an average, over a period of two years N. P. 718 produced 4, 10 and 2 per cent more of dry weight, grain and straw per acre respectively than Pb. 591; the difference between the grain yields was significant.

2. In N.P. 718 a higher plant population per acre (though statistically non-significant) was obtained in both the years. In respect of plant yields the two varieties did not differ much in the first year. However, in the second year, Pb. 591 produced significantly more dry weight, grain and straw per plant than N. P. 718.

3. Among the various characters contributing to plant yields, earlength, weight of 1000 grains and height of the plant was found more in Pb. 591 than N. P. 718 in both the years. The other characters did not show any definite trend.

---

* Abstract of the thesis on which Ph.D. degree of this University has been awarded.

4. The production of total dry weight, grain and straw per acre increased with the increase in rate of seeding, except the grain yield in the second year which showed a little reduction from S_{30} to S_{40}. In all the cases, the yields under S_{30} and S_{40} were significantly superior to these under S_{20}. The increase in the yield of straw, however, increased significantly with every increase in the seedrate. The straw/grain ratio appeared to decrease with the decrease in the seedrate.

5. Plant population increased appreciably with every increase in the seedrate in both the years. In the two years' average the plant population per acre under S_{40} and S_{20} worked out to be 36 and 17 per cent respectively more than that under S_{30}. On the other hand, the plant yields under S_{30} and S_{40} were 88 and 81 per cent dry weight, 89 and 80 per cent grain and 89 and 82 per cent straw respectively that of S_{20}.

6. Among the plant, ear and grain characters, responsible for the yield of grain per plant, it is noted that except the number of ear-bearing shoots per plant in the second year, the three seedrates did not differ significantly among themselves in any case in both the years.

7. The yields of total dry weight, grain and straw per acre increased with every increase in the level of nitrogen in both the years, except from N_{40} to N_{60} in the first year where slight reductions were noted. In the first year the yields of total dry weight and straw per acre under the three levels of nitrogen (N_{20}, N_{40} and N_{60}), among which the differences were non-significant, were significantly higher than those under N_0. However, the yield of grain per acre under N_{20} did not differ significantly from the yield obtained under N_0, but both these yields were significantly lower than the yields under N_{40} and N_{60}, the difference between the latter two was also non-significant. In the second year, on the other hand, the yields per acre increased significantly with every increase in the dose of nitrogen. The straw/grain ratio tended to increase with the increase in the level of nitrogen.

8. The plant population per acre at harvest increased with every increase in the dose of nitrogen in both the years, except from N_{40} to N_{60} in the first year.

9. The total dry weight per acre was affected significantly by varieties x seedrates x levels of nitrogen only in 1957-58. Both the varieties may be seeded at any of the rates (20-40 Srs/acre) under high fertility conditions. However, under low fertility conditions the dry weight per acre increased with increasing seedrates.

10. In both the years the number of shoots per acre increased significantly with every increase in the rate of seeding. The number of shoots per acre also increased with the increase in levels of nitrogen, only with few exceptions. The varieties did not show any conclusive trend.

11. In both the years higher values of leaf Area Index (LAI) due to more number of leaves per sq. yd. and bigger sized leaves were obtained under Pb. 591 than under N.P. 718. The rates of seeding as well as the levels of nitrogen were found to affect favourably the leaf area index, number of leaves per sq. yd. and size of the individual leaf in both the years.

12. As regards the protein content of grain, it was higher in the first year than in the second year. The grains of N. P. 718 variety were richer in protein content than those of Pb. 591. Increasing levels of nitrogen increased the protein content of grain while the rates of seeding showed no definite effect.

13. From the results of this investigation it may be concluded that both the varieties, should be sown at 40 Srs. seed per acre and fertilized with 60 lb. N per acre to get maximum yields, however, under low fertility conditions N.P. 718 can be given preference over pb. 591.

AGRA UNIVERSITY JOURNAL OF RESEARCH

Vol. XV, Part III *SCIENCE* **September, 1966**

Abbr.—*Agra Univ. J. Res. (Sci.)*

PUBLISHED BY
THE REGISTRAR, AGRA UNIVERSITY,
AGRA, 1966.

Annual Subscription : Inland Rs. 15/- ; Foreign Rs. 20/-

Chancellor
Sri Biswanath Das, Governor, Uttar Pradesh State.
Vice-Chancellor
Dr. S. Ranjan, M. Sc. (Cantab), D. Sc. (State France), F.N.I.
Registrar
Sri R. S. Agarwal
Editor
Dr. M. Ray, D. Sc., F. N. I.
Advisory Committee
Dr. S. P. Srivastava, M. S., F.R.C.S.
Dr. S. N. Singh, M. Sc., Ph. D.
Dr. A. Roy, M. Sc., Ph. D.
Dr. D. D. Pant, M. Sc., D. Sc.
Dr. P. I. Ittyerah, M. Sc., Ph. D.
Dr. V. Puri, D. Sc., F.N.I.
Dr. T. Singh, M. Sc., Ph. D.
Dr. Mata Prasad, D. Sc., F. R. I. C., F. N. I.
The Registrar (*Ex-officio*)

Edited by Dr. M. Ray, D. Sc., F. N. I., Principal, Agra College, Agra, Published by Sri R. S. Agarwal, Registrar, Agra University, Agra, and Printed by Mr. H. K. Kapur, Agra University Press, Agra. (J.- 2000)

FACTORS AFFECTING THE RECURRENCE OF POSTPARTUM OESTRUS IN MURRAH BUFFALOES

S. BASU

Balwant Rajput College, Agra.

A buffalo-cow should calve every year for maximum prolificacy and profitable milk production. The recurrence of oestrus after calving is one factor affecting the intercalving period and thus affecting the fertility or productivity of a cow. Many factors, phenotypic and genotypic, as well as individuals, characteristic of strains, etc. are thought to be associated with the breeding of buffaloes. These factors need to be explored so as to bring them under control with improved management and selection techniques. Works had been done to determine the average interval between parturition and the first oestrus (Levine, 1920; Kaleef, 1932; Ocampo, 1939; Hafez, 1954; Rao and Murari, 1956 and Basu, 1962), but no attempt was ever made to find out the factors involved in lengthening the postpartum oestrus period. The present study is designed to investigate whether the factors like, season, milk-yield, age, month of calving, lactation and the dam herself influence the period between the parturition and the first oestrus after calving. The knowledge of such controlling factors may be of value in curtailing the interval which may prove of economic importance to a breeder.

MATERIALS AND METHODS

The data utilised in this study were obtained from the Murrah herd of buffalo, bred and raised at a farm, near Agra. In all 208 parturitions in 86 buffalo-cows were studied.

Teaser bulls were kept in the herd for detection of heat in cows. All animals, however, were examined, individually, for heat. The days from the calving to the recurrence of first oestrus were calculated and compared from the various records, which are maintained with care. The milk yield was worked out for the first 301 days the cow was in milk. Total milk yield was taken in case of cows with lactational length less than 301 days after correction (Correction factor 9·33 lbs. of milk/day). Calves were allowed to suckle one quarter of the udder of their dams. Hence the milk yields of cows always represent the three-fourth of the total milch-ability of the buffaloes.

The age of the animal was calculated in years and months from the date of birth to the date of her first oestrus after each calving. The month during which the animal came in heat and the month of calving were considered for studying their influence. The months were grouped into three distinct seasons —Summer (March to June), Rainy (July to October) and Winter (November to February) to find out their effects.

The animals stayed in the sheds during evening and night and were turned out from 6 a.m. to 3 p.m. every day. All animals were regularly examined as a routine work both for health and reproduction. They were fed on concentrates (equal parts of Barley, Bran and G.N. cake) plus 2% each of salt and mineral mixture, and dry and green fodder as available in different seasons according to body weight and milk production. All animals were tested for tuberculosis and brucellosis at annual intervals.

RESULTS AND DISCUSSION

The average interval between the parturition and first oestrus was found to be 164·93±11·24. The average interval as found by other workers are given in table 1. The interval was larger in this herd than reported so far by other workers. The table 2 shows that maximum number (17·8 per cent) of animals came to heat between 61 to 90 days after calving. Only 4·3 per cent came to heat within 30 days of calving and 66 per cent of animals exhibited heat between 31 to 210 days. In 8 per cent cases the heat recurred beyond 300 days of calving. The range extended from 9 days to 464 days.

TABLE 1

Literature on the interval (in days) between calving and post-partum oestrus of domestic buffaloes.

Race	Range	Mean	Authors
Indian	—	30	Levine (1920).
Bulgarian	14–410	118	Kaleef (1932).
Malayan	30–60	—	Federated Malayan States (1920), Kangaratnam, 1935.
Philippine	24–50	35	Ocampo (1939).
Indian	45–53	50	
Philippine × Indian	35–51	44	
Egyptian	10–76	35	Hafez (1952).
Egyptian	16–76	44	Hafez (1955).
Indian	—	88	Rao and Murari (1956).

TABLE 2

Frequency and average interval between parturition and first oestrus.

Interval (days)	No. of observations	Percentage
1–30	9	4·3
31–60	21	10·1
61–90	37	17·8
91–120	22	10·6
121–150	17	8·1
151–180	21	10·1
181–210	21	10·1
211–240	10	4·8
241–270	9	4·3
271–300	20	9·6
301–330	3	1·4
331–360	3	1·4
361–390	5	2·4
391–420	8	3·8
421–upwards	2	1·0

THE EFFECT OF THE COW ON THE INTERVAL

The data were analysed (Table 3) to find out if the postpartum oestrus interval differed from cow to cow. One hundred and eighty-four observations from 61 cows having at least two calvings were used. The analysis indicates that the difference was highly significant at 1 per cent level of probability. It shows that the postpartum oestrus interval differed significantly among the buffalo-cows. It is suggested that this difference should be reduced for improving the fertility of the buffaloes.

TABLE 3

Effect of the cow on interval from parturition to first oestrus.

Sources of variation	d. f.	M. S.	F
Between cows	60	196426·11	2·50**
Within cows	123	78445·11	

** Highly significant at 1 per cent level.

THE INFLUENCE OF THE SEASON

The study of the month of recurrence of oestrus and the average intervals reveals (Table 4) that the monthly average of the interval was longer for the months June to October and shorter during November to May. The average interval was greatest (230·4 days) in October and shortest (98·3 days) in January. The frequency distribution of the occurrence of oestrus indicated that the number of buffaloes coming in heat were more frequent during the months of August to February *i.e.* during the rainy and winter seasons. The analysis of variance (Table 6) showed that the effect of the season of occurrence of oestrus on the calving-oestrus interval was highly significant. Table 4 also shows that the winter season is very optimum for the occurrence of oestrus and for the least postpartum oestrus interval. Basu (1962) was of the opinion that this increase in sexual activity during winter months was due to ample feeding of Berseem and other luxuriant green fodders.

The influence of the season of calving on the interval (Table 5) indicated that the average interval was longer for calvings in cooler months, *i.e.* from November to April and shorter for calvings in warmer months, *i.e.* from May to October. The different seasons of calvings (Table 6) were found to have a significant effect on the interval from parturition to first oestrus at 1 per cent level of probability.

TABLE 4

The effect of month and season on the length of time from parturition to first oestrus.

Months	n	%	Average Interval
Winter	119	57·2	135·4
November	38	18·3	157·0
December	37	17·8	159·7
January	15	7·2	98·3
February	29	13·9	126·6
Summer	28	13.5	151·8
March	8	3·8	159·4
April	7	3·4	108·6
May	6	2·9	145·2
June	7	3·4	193·0
Rainy	61	29·4	209·4
July	6	2·9	204·0
August	12	5·8	195·3
September	20	9·6	207·8
October	23	11·1	230·4

TABLE 5

The effect of month and season of calving on period between parturition and first oestrus.

Months	n	%	Average interval
Winter	81	38·9	191·7
November	24	11·5	216·6
December	28	13·5	161·3
January	14	6·7	147·5
February	15	7·2	241·2
Summer	30	14·4	162·2
March	15	7·2	192·7
April	5	2·4	167·6
May	6	2·9	144·7
June	4	1·9	143·8
Rainy	97	46·8	135·9
July	11	5·3	119·5
August	26	12·5	158·2
September	35	17·0	136·7
October	25	12·0	129·0

TABLE 6

Analysis of variance showing the effect of season of recurrence of oestrus and the season of calving on the length of postpartum oestrus interval

Sources of variation	d.f.	M.S.	F
Between season of oestrus	2	90440·22	10·72**
Between season of calving	2	72832·08	8·63**
Inter-action	4	48518·01	5·75**
Within Sub-classes	199	8437·14	

** Significant at 1 per cent level.

Villegas (1928), Arunachalam et al (1952), Hafez (1955); Rao and Murari (1956) and Basu (1962) reported high sexual activity during rainy season and cooler months. In the present study it was found buffallo-cows calving from May to October exhibited oestrus earlier. There may be two reasons : First, the later part of this period coincides with availability of large quantity of leguminous and oestrogen containing green fodder which may stimulate the sexual activity. Second, this period being a rainy season and as is also immediately followed by cooler months, the buffalo-cows calving during these months finds a comparatively longer favourable period to exhibit their sexual activity.

THE INFLUENCE OF AGE

The table 7 shows that the postpartum oestrus interval decreases with age, though initially there is an increase from 4 to 6 years of age. The longest interval (208·2 days) was found with animals between 5 to 6 years age group and shortest interval (79·2 days) in 13 to 14 years of age, the oldest group of animals. Two animals above 14 years were not included. The analysis of variance (Table 8) revealed that the age had a significant effect at 5 per cent level of probability on the interval from parturition to first oestrus. Older cows appeared, thus, more fertile than younger cows.

TABLE 7

The influence of age on the interval from parturition to first oestrus.

Age (years)	Frequency	Percentage	Average interval
4–5	10	4·9	160·6
5–6	18	8·7	208·2
6–7	41	19·9	199·3
7–8	35	17·0	169·9
8–9	33	16·0	170·9
9–10	23	11·2	144·0
10–11	22	10·7	122·6
11–12	15	7·3	116·3
12–13	4	1·9	101·0
13–14	5	2·4	79·2

TABLE 8

Analysis of variance showing the effect of age of animals on the interval between parturition and first oestrus.

Sources of Variation	d.f.	M.S.	F
Between age groups	9	27406·72	2·361*
Within age groups	196	11608·87	

* Significant at 5 per cent level.

THE INFLUENCE OF LACTATION NUMBER

The data arranged according to lactation number (Table 9) showed that the first calvers took the longest time (209·5 days) to recur the signs of first oestrus. Thereafter, the post-partum oestrus interval decreased with the increase in the number of lactations. The fifth lactation, an exception, showed a sudden increase in days.

A critical difference test was made using the following formula:—

$$\text{Critical difference} = t_0 \sqrt{\frac{1}{n_a} + \frac{1}{n_b}\ \sigma^2{}_e}$$

where t_0=significance level at P=0·05,

n_a=Number of observations in a-th lactation,

n_b=Number of observations in b-th lactation,

$\sigma^2{}_e$=standard error of the difference.

and then was compared with the La—Lb, (where La and Lb are average intervals in a-th and b-th lactations respectively) to find out if there was any significant contrast between any two of the lactations. For this difference between average postpartum oestrus intervals of all possible pairs of lactations was compared with their corresponding critical difference. The results expressed in bar notation were as follows:—

Lactation No.	L_1	L_2	L_3	L_5	L_4	L_6	L_7
Average interval	209·5	184·1	172·7	149·8	113·8	96·1	83·8

The treatments inside the bars were not significant, but treatments separated by bars were significant.

Analysis of variance (Table 10) showed that there was highly significant difference for the intervals between various lactations. The analysis was limited upto seventh lactation as the 8th lactation contained only three observations.

TABLE 9

The influence of lactation number on the postpartum oestrus interval.

Lactation No.	Frequency	Percentage	Average interval
1st	37	18·0	209·5
2nd	54	26·3	184·1
3rd	49	23·9	172·7
4th	32	15·6	113·8
5th	16	7·8	149·8
6th	10	4·9	96·1
7th	7	3·4	83·8

TABLE 10

Analysis of variance showing the effect of lactation number on the length of period between calving and first oestrus.

Sources of variation	d. f.	M. S.	F
Between lactations	6	47026·64	3·919**
Within lactations	198	12000·06	

** Significant at 1% level.

THE INFLUENCE OF MILK YIELD

A total of 180 lactations in 34 buffalo-cows were studied as only 180 completed lactation records were available. The coefficients of correlation (r) between milk yield and postpartum oestrus interval were significant at 5 per cent level for 3rd and 7th lactations only and the coefficient of regressions (b) were highly significant at 1 per cent level for 3rd, 4th and 7th lactations and significant at 5 per cent level for 1st and 2nd lactations (Table 11). Ragab et al (1956) found significant correlations between service period and milk yields of 2nd, 3rd and 4th lactations. Kohli and Malik (1960) reported a highly significant correlation between service period and 1st lactation only. The coefficients of correlation and regression when studied, taking all lactations together in one pool, were found to be positive and highly significant (Table 12). Kohli and Malik (1960); Ragab et al (1956) and Venkayya and Ananta krishnan (1957) found highly significant correlation with service period and milk yield irrespective of lactations. Then the calving-oestrus intervals were arranged into four groups according to corresponding lactational milk yield. The groups were 0 to 1999 lbs., 2000 to 2999 lbs., 3000 to 3999 lbs and 4000 lbs and upwards (Table 13). It showed that the lowest milk producing group (*i. e.* 0 to 1999 lbs.) had the least postpartum oestrus interval (117·2 days) and the interval increased gradually with higher milk groups. The highest milk producing group had the longest interval (225·5 days). The analysis of variance (Table 14) showed that a highly significant difference exists between the milk groups with regard to the interval between calving and first oestrus.

The above results indicate that high yielding buffalo-cows come to heat late. It may be possible that the nutrients and the ovarian hormone oestrogen during the peak milk yield period go more for the production of milk than for reproduction. So it is not so much the gestation period, which taxes the cow but the lactation period which follows.

TABLE 11

Association of milk yield (y) and the postpartum oestrus period (x) in different lactations.

Lactation No.	n.	x(days)	y(lbs)	r	b
1	36	200·21	2592·00	0·22	2·026*
2	50	199·08	2013·51	0·23	2·201*
3	40	184·17	3039·16	0·359*	3·432**
4	23	124·87	3169·30	0·366	5·275**
5	14	162·78	3171·28	0·098	0·690
6	10	96·10	2162·70	–0·322	–6·567
7	5	97·20	2863·80	0·78*	7·365**

** Significant at 1 per cent level.
* Significant at 5 per cent level.

TABLE 12

Association of postpartum oestrus period and milk yield irrespective of lactation.

Degrees of freedom (d. f.)	179
Average milk yield ($\bar{y}$)	2774·03 lbs.
Average post-partum oestrus period ($\bar{x}$)	173·74 days.
Coefficient of correlation (r)	0·251**
Coefficient of regression (b)	2·424**

** Significant at 1 per cent level.

TABLE 13

The frequency distribution of postpartum oestrus period in relation to milk yield.

Milk yield	No. of observations	Average interval
0 to 1999 lbs.	29	125·0
2000 to 2999 lbs.	68	169·1
3000 to 3999 lbs.	66	186·6
4000 to upwards.	17	225·5

TABLE 14

Analysis of variance showing the effect of milk yield on the calving-oestrus interval.

Sources of variation	d. f.	M. S.	F
Between milk groups	3	48575·72	4·785**
Within milk groups	176	10152·22	

** Significant at 1 per cent level.

SUMMARY

Two hundred and eight parturitions in 86 buffalo-cows had been studied to investigate the nature of influence of various factors on the recurrence of first oestrus after calving. It was found that the cow, season of occurrence of first oestrus, lactation number and milk yield had a highly significant effect on the interval between calving and first heat. The season of calving and age of the cow had only a significant effect at 5 per cent level on the post-partum oestrus interval. The average interval was longer for buffalo-cows whose oestrus occurred during June to October and for calving in cooler months *i. e.* November to April. The interval was shorter in those buffalo-cows whose oestrus recurred during November to May and for calvings during warmer months. It was also revealed that the interval decreased with increase in lactation number and age of the animal. High milk yielding cows had longer interval while low yielding cows had shorter interval.

The average postpartum oestrus interval was calculated to be 164·93 ± 11·24.

REFERENCES

1. Arunachalam, T. V., Lazarus, A. Z. & Anantakrishnan, C. P. 1952. *Indian J. Dairy Sci.*, **5**, 117.
2. Alim, K. A. & Ahmed, I. A. 1954. *Emp. J. Exp. Agric.*, **22**, 37.
3. Asker, A. A. & El-Itriby, A. A. 1951. A.B.A., **26** (1), 272.
4. Basu, S. 1962. *Indian Vet. J.* **39**, 328.
5. Basu, S. 1962. *Ibid.* **39**, 433.
6. Hafez, E.S.E. 1955. *J. Agric. Sci.*, **46**, 137.
7. Kohli, M. L. & Malik, D. D. 1960. *Indian J. Dairy Sci*, **13**, 105.
8. Kohli, M. L. & Malik. D. D. 1960 *Ibid.*, **13** 162.
9. Levine, C. O. 1920. *J. Hered.*, **11**, 51.
10. Ocampo, A. R. 1939 *Philippine Agric.*, **28**, 286.
11. Rao, C. K. & Murari, T. 1956. *Indian Vet. J.* **33**, 54.
12. Ragab, M. T. & Asker, A.A. 1951. *Indian J. Dairy Sci.*, **4**, 159.
13. Ragab, M. T., Asker, A. A. & Hilmy, S. A. 1956. *Ibid.*, **9**, 53.
14. Singh, R. B., Sharma, S. C. & Singh, S. 1958. *Ibid.*, **11**, 154.
15. Vankayya, D. & Anantakrishnan, C. P. 1957. *Ibid.*, **10**, 123.
16. Villegas, V. 1928. *Philippine Agric.*, **17**, 477.

MORPHOLOGICAL, HISTOLOGICAL AND BIOCHEMICAL STUDIES OF CORPUS LUTEUM DURING NORMAL AND ABNORMAL OESTROUS CYCLE IN BUFFALOES

D. J. Roy
Indian Veterinary Research Institute, Izatnagar, U. P.

Summary

The object of the present investigation is directed to elucidation of variations involved in morphological, histological and biochemical aspects of corpus luteum during normal and abnormal oestrous cycle in buffaloes. This would help to give an idea of the functional state of corpus luteum at different stages.

The material included in this study was from a group of 25 experimental buffaloes having records of normal and abnormal oestrous cycles. These studies were also extended to 142 slaughter house animals during non-pregnancy, early pregnancy and during periods of embryonic mortality and post-partum.

The corpora lutea were recovered at 1, 3, 6, 9, 12, 15 and 18 days following oestrus by surgical means from the experimental animals having normal oestrous cycle. Repeated recovery of the corpora lutea at stages from day-9 through day-18 of the cycle were successfully done. The 'regressing' and 'persistent' types of corpora lutea from abnormally long oestrous cycle were recovered similarly and studied.

The corpora lutea in the non-pregnant slaughter house animals were classified into four categories *viz.*, 'developing' (3-9 days), 'developed' (10-15 days), 'regressing' (16-24 days) and 'regressed' (older than 24 days) from morphological appearance and through histological evidences. These types were compared to the corresponding stages of corpora lutea, obtained from normal oestrous cycle.

Early pregnancy corpora lutea were grouped under three stages (within 1, 1-2 and 2-3 months) on the basis of foetal size and weight. The embryonic mortality, which is one of the primary causes of the aberration of oestrous cycle, was accounted within a stage of one month and in fresh cases only. The corpora lutea of the group were compared to that of normal pregnancy at equal stage. Few cases of post-partum corpora lutea were obtained to study the cause of post-partum anoestrus.

Morphological study:

In the animals having normal oestrous cycle, it was found that following ovulation, the ruptured follicle shrunk considerably over the follicular

cavity with little amount of clot at the ruptured point. The organization of corpus luteum (CL) was found to be rather quick. At day-6 after oestrus the CL attained a size of 1·43 cm. in diameter and 0·986 gm. in weight. The maximum size, diameter 1·5 cm. and weight 2·28 gm. were attained by day-12, after which regression, both in size and weight followed. The colour of the CL was at first bright to deep red then turned into pink and at the 'regressing' stage it became red, pink or flesh coloured. The 'regressing' and 'persistent' types of CL in the abnormal oestrous cycle were generally flesh, brick red or chocolate in colour and the mean weights were 1·17 and 1·82 gm. respectively.

The size and weight in the 'developed' and 'regressing' types were lower compared to the corresponding stages of CL obtained from normal oestrous cycle. The rate of regression of CL was found to be slower in slaughter house animals. Significant difference in the weight of CL in all the stages except developing type was observed during breeding and non-breeding parts of the year.

The CL of early pregnancy resembles the 'developed' type in many respects. The variations in size and weight were in significant during the three stages. The colour of pregnancy CL varied from pink to flesh and were more intimately connected to the ovary with the advancement of pregnancy.

The CL of embryonic mortality were indistinguishable from external appearance with the corresponding stages of normal pregnancy CL. The weight of CL in the former group was, however, found to be significantly lower.

The CL of post-partum period were very small in size and weight and resembled the inactive form of corpus albican.

Histological study:

The gradual development of CL from the matured follicle during oestrous cycle has been illustrated. Since after the ovulation, the active organization of CL was observed upto day-3 stage. The compactness of lutein tissue and vascularization were complete by day-6.

The variations in the differential lutein cell count and their density, degree of vascularization and the amount of connective tissue were studied with illustration in different stages of CL during oestrous cycle, pregnancy and embryonic mortality. The CL of post-partum period was devoid of active lutein cells, and the whole tissue was infiltrated with connective tissue.

The lutein cells were identified into five types on the basis of their cytological appearances following the standard classifications made in cow. The average size of lutein cells in case of buffalo was larger than that of cow.

The mean percentages of lutein cell, type I and II, were high in the developing stages and the maximum (81%) was attained by day-9. High percentages of type III, IV and V cells were associated with the regression of CL.

The lutein cells, type I and II, in the 'regressing' and 'persistent' type of CL in abnormal cycle was found to be 8·9% and 13·4% respectively.

The percentage variation of active lutein cells at different stages of CL in non-pregnant slaughter house animal were similar to the corresponding stage of normal oestrous cycle but having lower values.

The histological picture of CL during early pregnancy resembled the fully developed form of cyclic CL excepting that the lutein cells were bigger in size with some cytological variations. The lutein cells, type I and II of CL in embryonic mortality was decidedly lower compared to the corresponding stage of normal CL of pregnancy. Significance of this was discussed.

Biochemical study:

The maximum mean weight of CL was 2·285±0·17 gm. at day-12. At day-6 and day-18, the weights were 0·986±0·09 and 1·176±0·07 gm. respectively. The progesterone concentration estimated at the five stages, 6, 9, 12, 15 and 18 days of cycle were 13·3±2·3, 18·5±2·9, 41·7±6·8, 24·7±2·4 and 17·9±1·3 mcgm./gm. tissue respectively. The corresponding values of ascorbic acid concentration were 0·464±0·13, 1·270±0·18, 1·916±0·15, 0·919±0·07 and 0·758±0·15 mg./gm. tissue. The differential count of lutein cells, type I and II was maximum at day-9 (81·1%) and minimum at day-18 (14·1%). The repeatability was significantly high for the progesterone concentration (0·68), ascorbic acid concentration (0·82) and lutein cell type I and II (0·50) of the CL. The mean weight of 'regressing' and 'persistent' CL were 1·172±0·13 and 1·816±0·12 gm. respectively. The progesterone concentration of the two types were comparable to day-18 stage of normal oestrous cycle. The inhibition of the onset of subsequent oestrous cycle due to the level of progesterone, in these two types of CL was considered to be unlikely. The ascorbic acid concentration was, however, higher in 'persistent' type.

Consistent correlation was obtained for progesterone and ascorbic acid concentration with lutein cells, type I and II. A highly significant correlation ($r=+0·464$) between progesterone and ascorbic acid concentration indicated latter's connection with the synthesis of progesterone. The functional potentialities of CL was highest by day-12 as evidenced from the significant positive inter-correlations of weight, progesterone and ascorbic acid concentration.

Estimation of ascorbic acid was also done in CL of non-pregnancy, early pregnancy, embryonic mortality and post-partum period in the slaughter house animals. The concentrations obtained in 'developing', 'developed', 'regressing' and 'regressed' types of CL in non-pregnant animals were 2·369±

0·18, 1·684±0·23, 0·959±0·10 and 0·664±0·10 mg/gm. tissue respectively. The results are comparable to the similar stages of normal oestrous cycle excepting that the concentration in the 'developing' type was significantly higher.

There was no significant variation obtained in the concentration of ascorbic acid of CL during one, two and three months of pregnancy. The concentration was similar to the 'developed' type of cyclic CL.

Practically, no difference in the concentration of ascorbic acid was observed in the CL of embryonic mortality and normal pregnancy of equal stages. However, total ascorbic acid content was significantly low in case of embryonic mortality.

A consistently high level of ascorbic acid in CL at different stages of oestrous cycle was found to be associated with breeding season in this species.

The percentage distribution of active type of lutein cells (type I and II) during breeding season were relatively higher in 'developing', 'developed', and 'regressing' types of corpus luteum than in the non-breeding season. The mean difference, however, in 'developing' type was only significant at 5% level. Highly significant correlation between active type lutein cells (type I and II) and ascorbic acid concentration was obtained during breeding and non-breeding season.

RESPIRATION AND RECTAL TEMPERATURE AS MEASURES OF ADAPTABILITY OF DIFFERENT BREEDS AND CROSSES OF LAMBS AND KIDS TO TROPICAL ENVIRONMENT

O. N. Seth, K. C. Saraswat and A. Roy
Department of Physiology and Biochemistry,
U. P. College of Vet. Sci. & Ani. Husb., Mathura, (India).

Solar radiation, precipitation, humidity and altitude are some of the climatic factors which affect the animal's physiological processes directly or indirectly. Adaptability may be defined as the animal's ability by alterations in the normal physiological processes to withstand the stress imposed by various climatic factors without its production being undermined. Many exotic breeds of sheep and goat have been and are proposed to be introduced to improve the productivity of the indigenous population through cross breeding. It is implicit that success in the tropics of such a cross breeding programme would be decided by the ability of the cross breds to withstand the stress due to high environmental temperature. Since foraging is the most economic way of maintaining sheep and goat, adaptability to forage in both good and bad weather would be the main condition in determining profitability. The present investigation was undertaken to ascertain the adaptability of lambs and kids of different breeds and crosses during those months of the year when environmental temperature is above 90°F. Respiration, rectal temperature and growth were taken as indices of adaptability.

Materials and Methods

Male lambs and kids were taken for this experiment. Informations regarding the breed composition, average age and weight of the animals at the start of experiment have been given below:—

Lambs			Kids		
Group	Age (days)	Weight (kg.)	Group	Age (days)	Weight (kg.)
Bikaneri	71	13·70	Barbari	64	6·10
Mandia	36	6·21	Sannen	67	11·98
Corriedale	65	13·32	B×S	59	6·15
F_1 cross	168	14·10			
F_2 cross	65	8·12			

(F_1: Bikaneri ♀ × Corriedale ♂, B×S: Barbari ♀ × Sannen ♂).
(F_2: F_1 cross ♀ × Corriedale ♂).

Animals were housed in half wall shed but the space between the pillars were closed by hanging jute curtains in the months of May, June and part of July. Upto three months, 200 gm., and thereafter 250 gm., of crushed gram was given daily as concentrate to the animals. In addition 2000 mg. of T. M-5 (oxytetracycline) was given to each animal. They were allowed grazing for two hours (7·00—9·00 a. m.). Observations were recorded from the first week of May till the end of October. The division of seasons was as follows :—

May-June : Summer
Three weeks of July : Premonsoon
Fourth week of July and August : Monsoon
September-October : Autumn.

Respiration and rectal temperature of each animal was recorded once weekly in the morning (7·00 to 7·30 hours) and in the evening (14·30 to 15·00 hours). Respiration rate was counted for one minute by noting the flank movement. Rectal temperature was determined by a clinical thermometer. Data on the environmental, dry and wet bulb temperature within and outside the shed was also maintained at the time respiration and rectal temperature was recorded.

RESULTS AND DISCUSSION

Respiration rate of lambs—Table 1 shows the mean morning and evening respiration rate of the lambs. Analysis of variance is presented in Table 2. There was significant difference between groups as well as between seasons. Interaction between groups and seasons was also significant.

TABLE 1

Mean values of the respiration rate/minute of lambs of different breeds and crosses during different seasons

	Summer		Premonsoon		Monsoon		Autumn	
Air temperature °F	88·58	103·58	90·16	97·06	86·20	92·40	77·50	92·25
Air humidity %	57·50	38·75	65·66	53·30	78·40	63·80	70·37	53·12
Breeds & Crosses	M	E	M	E	M	E	M	E
Bikaneri	66·08 ±6·08	133·08 ±13·19	81·44 ±3·41	125·80 ±15·09	80·55 ±8·49	100·40 ±8·82	34·59 ±2·01	67·45 ±5·68
Mandia	47·25 ±2·81	82·59 ±6·61	42·18 ±2·05	50·30 ±5·24	31·05 ±7·86	57·70 ±5·15	33·62 ±1·53	44·37 ±2·09
F_1 cross	85·75 ±6·10	135·91 ±11·21	122·44 ±5·24	148·70 ±8·77	95·22 ±18·02	144·10 ±8·76	50·66 ±4·45	77·86 ±5·64
F_2 cross	82·61 ±7·85	132·27 ±9·19	121·33 ±10·19	154·00 ±10·86	101·50 ±12·39	160·50 ±14·87	48·83 ±6·91	92·83 ±10·50
Corriedale	127·50 ±6·20	183·77 ±8·82	117·66 ±13·77	157·33 ±22·34	94·25 ±24·03	151·25 ±12·01	57·06 ±6·86	98·43 ±9·80

M=Morning F_1 cross=Corriedale ♂ × Bikaneri ♀
E=Evening F_2 cross=Corriedale ♂ × F_1 cross ♀.

TABLE 2

Analysis of variance in the respiration rate of lambs

Source of variation	D. F.	Morning		Evening	
		S. S.	M. S.	S. S.	M. S.
Between groups	4	130929·3	32732·32**	276376·4	69094·10**
Between seasons	3	110537·4	36845·80**	200269·2	66756·40**
Interaction group× season	12	47653·7	3971·14**	56847·1	4737·25**
Error	321	283380·3	882·80	581713·6	1812·19
Total	340	572500·7		1115206·3	...

C. D. Between groups : M. R. 12·4, E. R. 17·19
M. R.=Morning respiration, E. R.=Evening respiration,
** Significant at $P<0·01$.

COMPARISON OF RESPIRATION RATE OF DIFFERENT GROUPS IN A PARTICULAR SEASON

Summer—Significant difference was found in the mean value of morning respiration rate of different groups except that of F_1 and F_2 cross. The differences in the mean value of the evening respiration rate were significant for all the groups except Bikaneri, F_1 and F_2 cross. Mandia was found to be the most and Corriedale least heat tolerant with Bikaneri in between them. Significant difference in the mean values of respiration rate of Bikaneri and Mandia lambs suggests that there is a remarkable difference in the heat adaptability of wooly and hairy breeds. All the groups showed an increase in respiration rate with increase in ambient temperature, though the degree of increase differed in different groups. Cross bred lambs tolerated ambient temperature of 103·6°F without showing sign of stress and their respiration rate was same as that of Bikaneri.

Premonsoon—This was the period of high air temperature and high humidity immediately preceeding monsoon rains. Significant difference was found in the mean value of morning as well as evening respiration rate of different groups except Corriedale, F_1 and F_2 cross. In this period morning temperature was 1·58° F and humidity 8·16 per cent more than in the summer and caused a greater increase in the respiration rate of Bikaneri lambs. In the evening there was a drop of 6 5° F in the ambient temperature but humidity increased by 8·16 per cent. Respiration rate in Bikaneri decreased by 7 as compared to summer while the corresponding decline in Corriedale and Mandia was 26 and 32 respectively. High temperature and high humidity were more trying for Bikaneri lambs than high temperature alone. This is supported by the findings of Singh *et al.*, (1963).

It appears that sweating and/or cutaneous evaporation helps thermoregulation in Bikaneri. When humidity is high this mechanism probably fails and the animal takes recourse to thermolysis by more frequent respiration. In Corriedale, increase in humidity, on the other hand has an ameliorative effect.

Monsoon—Significant difference was found in the mean values of morning as well as evening respiration rate of different groups except Corriedale, F_1 and F_2 cross. During monsoon the early hours of the day were highly humid (78·4%) and temperature was 2·3° F less than in the summer. In Mandia and Corriedale, humidity in this particular zone of ambient temperature had an ameliorative effect. Atmospheric temperature in the evening was 11·1° F less than what it was in summer and the humidity was 63·8 per cent. In this atmospheric condition the mean evening respiration rate of Bikaneri was much less than in summer and there was only a difference of 20 in the morning and evening respiration.

Autumn—In all the groups respiration rate was significantly less in this season than in other seasons. No significant difference was found in the mean morning respiration rate of either Bikaneri and Mandia or that of Corriedale, F_1 and F_2 cross. But there was significant difference in the respiration rate of indigenous breeds and that of exotic breeds and its crosses.

Rectal temperature of lambs—Table 3 shows the mean morning and evening rectal temperature of different groups. Analysis of variance (Table 4) showed significant difference between groups and seasons. Interaction between groups and seasons was also significant.

TABLE 3

Mean value of the rectal temperature of lambs of different breeds and crosses during different seasons

Breeds and crosses	Summer		Premonsoon		Monsoon		Autumn	
	M	E	M	E	M	E	M	E
Bikaneri	102·84 ±·086	103·70 ±·521	102·81 ±·184	103·65 ±·526	102·89 ±·135	103·31 ±·485	102·44 ±·128	102·79 ±·079
Mandia	102·79 ±·079	103·53 ±·470	102·56 ±·142	102·30 ±·47	102·67 ±·126	103·07 ±·510	102·22 ±·182	102·89 ±·034
F_1 cross	102·70 ±·13	103·52 ±·489	102·71 ±·184	103·68 ±·55	102·80 ±·126	103·64 ±·762	102·08 ±·143	102·88 ±·112
F_2 cross	102·61 ±·126	103·72 ±·589	102·93 ±·085	104·03 ±·92	102·55 ±·180	103·45 ±·624	102·29 ±·119	102·98 ±·092
Corriedale	103·67 ±·139	104·22 ±·700	103·50 ±·177	103·96 ±·271	102·51 ±·229	103·27 ±·514	102·62 ±·125	103·17 ±·072

TABLE 4

Analysis of variance in the rectal temperature of lambs

Source of variation	D.F.	Morning		Evening	
		S. S.	M. S	S. S.	M. S.
Between groups	4	12·40	3·10**	9.22	2·305
Between seasons	3	20·84	6·946**	35·04	11·680**
Interaction group X Season	12	9·42	·785**	8·29	·6908*
Error	309	92·06	·297	106·03	·3431
Total	328	134·72	...	158·58	...

C. D. : M. T. ·215, E. T. ·237 * Significant at $P < 0·05$ ** Significant at $P < 0·01$

COMPARISON OF RECTAL TEMPERATURE OF DIFFERENT GROUPS IN A PARTICULAR SEASON

Summer—The mean morning and evening rectal temperature was significantly higher only in Corriedale, there being no difference in the other groups. Judged by their rectal temperature Corriedale were found to be less heat adaptable. Bikaneri x Corriedale (F_1 cross) lambs were found to be as efficient in maintaining their body temperature as Bikaneri.

Premonsoon—Though the rectal temperature of Corriedale lambs was higher than the others, relieving effect of humidity on these lambs was evident. Although in the morning, the air temperature was 1·58° and humidity 8·16% more than in summer, the rectal temperature of Corriedale declined by 0·17° F and that of Mandia by 0·23° F. Rectal temperature of Bikaneri and cross breds was the same as recorded in summer.

Monsoon—In the morning rectal temperature of Bikaneri was found to be significantly higher than that of Mandia and Corriedale, while in the evening there was no significant difference in the rectal temperature of these breeds of lambs.

Autumn—There was no significant difference in the mean morning rectal temperature of Corriedale and Bikaneri lambs but the mean evening rectal temperature of Corriedale lambs was significantly higher than that of Bikaneri, F_1 cross and Mandia lambs.

INFLUENCE OF THE CLIMATIC ELEMENTS ON THE RESPIRATION RATE AND RECTAL TEMPERATURE

Correlation and partial correlation coefficients of air temperature and air humidity with rate of respiration and rectal temperature are presented in table 5.

TABLE 5

Correlation Coefficients

Groups	Correlation coefficient with air temperature				Correlation co-fficient with air humidity			
	M.R.	E.R.	M.T.	E.T.	M.R.	E.R.	M.T.	E. T.
Bikaneri	·72813**	·69553**	·48946*	·71283**	–·14546	–·24851	–·02633	–·42068*
Bikaneri × Corriedale	·75421**	·51130**	·56772**	·33423	–·32384	·02584	·10032	–·14297
Corriedale	·81496**	·50104**	·57844**	·80514**	–·41964*	–·18385	–·52702**	–·55341**
Mandia	·40934*	·58364**	·68069**	·54761**	–·23669	–·2353	–·23300	–·29371

Partial correlation coefficients

Groups	Value of partial correlation with air temperature, keeping air humidity constant				Value of partial correlation with air humidity, keeping air temperature constant			
	M.R.	E.R.	M.T.	E.T.	M.R.	E.R.	M.T.	E.T.
Bikaneri	·81067**	·76540**	·52652**	·64997**	·13929	·49807*	·22402	·01833
Bikaneri × Corriedale	·76881**	·75926**	·63760**	·33562	·24423	·65341**	·36488	·00146
Corriedale	·79073**	·53834**	·50714**	70325**	–·28402	·28948	–·44016	–·00555
Mandia	·33946	·61199**	·65781**	·50552**	–·22489	·32198	–·00181	·00168

M. R.=Morning respiration, M. T.=Morning rectal temperature,
E. R.=Evening respiration, E.T.—Evening rectal temperature,
* Significant at $P < 0{\cdot}05$ ** Significant at $P < 0{\cdot}01$.

A highly significant positive correlation was found between air temperature and respiration rate as well as air temperature and rectal temperature of different groups. Correlations of air humidity with respiration rate and rectal temperature were non-significant except that the morning respiration rate of Corriedale was significantly correlated with air humidity and that the Correlation between air humidity and rectal temperature was negative and highly significant both in the morning as, well as in the evening. Partial correlation coefficient of respiration rate and rectal temperature with air temperature were highly significant except for the morning respiration rate of Mandia. Partial correlation coefficient of respiration rate with air humidity was significant for the evening respiration rate of Bikaneri and highly significant for Bikaneri × Corriedale.

Multiple correlations indicate that most of the variations in the respiration rate and rectal temperature of these animals were due to climatic elements.

Multiple correlation coefficient

Groups	M. R.	E. R.	M. T.	E. T.
Bikaneri	·734**	·782**	·527**	·712**
Bikaneri × Corriedale	·771**	·759**	·642**	·334 N. S.
Corriedale	·831**	·560**	·580**	·805**
Mandia	·457*	·639**	·680**	·548**

M. R.=Morning respiration, E. R.=Evening respiration,
M. T.=Morning rectal temperature, E. T.=Evening rectal temperature.
** Significant at P 0·01 * Significant at P 0·05

Multiple regression equations for evening respiration rate of lambs are given below. Y was the estimated value of respiration rate, x_1 the environmental temperature and x_2 the relative humidity.

Y for Bikaneri $= -588{\cdot}09 + 6{\cdot}3778x_1 + 1{\cdot}5279x_2$

Y for Bikaneri × Corriedale $= -730{\cdot}02 + 7{\cdot}4060x_1 + 2{\cdot}7216x_2$

Y for Corriedale $= -520{\cdot}86 + 6{\cdot}1076x_1 + 1{\cdot}4367x_2$

Y for Mandia $= -327{\cdot}11 + 3{\cdot}6050x_1 + {\cdot}7877x_2$

Multiple regression equations for evening rectal temperature of different groups of lambs are given below. Y was the estimated value of rectal temperature, x_1 the environmental temperature and x_2 the relative humidity.

Y for Bikaneri $= 95{\cdot}73 + {\cdot}0743x_1 + {\cdot}008x_2$

Y for Bikaneri × Corriedale $= 98{\cdot}30 + {\cdot}0461x_1 + {\cdot}0118x_2$

Y for Corriedale $= 95{\cdot}67 + {\cdot}0815x_1 + {\cdot}0015x_2$

Y for Mandia $= 97{\cdot}76 + {\cdot}0516x_1 + {\cdot}0074x_2$

Present study indicates that environmental temperature is the main factor in causing variation in respiration and rectal temperature of different breeds and crosses of lambs.

LIVE WEIGHT GROWTH OF LAMBS DURING THE PERIOD OF OBSERVATION

Weekly weights of the three breeds of lambs were recorded during the course of investigation to study adaptability in terms of live weight gain. Regression coefficient of per week gain in live weight and comparison thereof in different breeds of lambs is presented in table 6.

TABLE 6

Regression coefficient of per week gain in live weight and comparison thereof in different breeds of lambs.

Breeds	Regression coefficient (in kg.)	S. E. b.	Comparison of regression in gain in weight
Bikaneri	·457	·024	Between Mandia and Bikaneri**
Mandia	·574	·015	Between Mandia and Corriedale**
Corriedale	·247	·020	Between Bikaneri and Corriedale**

During a period of 26 weeks, live weight gain was 15·10, 12·06 and 6·20 kg. for Mandia, Bikaneri and Corriedale lambs respectively. Daily gain in weight was as follows: Mandia, 83 gm/day; Bikaneri, 66·2 gm/day and Corriedale, 34·0 gm/day.

Though respiration and rectal temperature have been considered as indices of adaptability, from the practical standpoint, it is growth in terms of live weight gain which is most important. The 26 weeks of the investigation, which included the most stressful part of year, show that the effect of this stress was maximum on Corriedale, less so on Bikaneri and minimum on Mandia lambs. Results of respiration and rectal temperature studies indicated a similar trend. These studies indicate that management of Corriedale lambs must be different from that reported here, if growth is to be sustained. Provision should, therefore, be made of a cool room in which they can be kept for the greater part of the day in the months when the environmental temperature is high. Adverse effect of high temperature on growth was shown on Columbia sheep, in which it was found that under cool conditions, lambs weighed about 15 lb. more per head at weaning time than when they were kept in hot condition (Whitchurst *et al.*, 1947).

RESPIRATION RATE OF KIDS

Table 7 shows the mean morning and evening respiration rate of Barbari, Barbari × Sannen and Sannen kids in four different seasons. Analysis of variance is presented in table 8. There was significant difference between the groups as well as between seasons under study.

COMPARISON OF RESPIRATION RATE OF DIFFERENT GROUPS IN A PARTICULAR SEASON

Summer—The analysis shows that mean morning and evening respiration rate of Barbari was significantly less than that of Sannen. In the morning as well as in the evening, there was no significant difference in the respiration rate of Barbari and Barbari × Sannen. Mean evening respiration rate of Barbari × Sannen was significantly less than that of Sannen though no significant difference could be found in the morning. In all the groups there was an increase in the number of respirations with rise in ambient temperature. As the mean ambient temperature rose from 88·58° in morning to 103·58°F in the evening, mean respiration rate increased by 52·26, 28·96 and 24·51 in Sannen, Barbari × Sannen and Barbari respectively. Thus the increase in the respiration rate of Sannen kids was nearly two times that encountered in Barbari and Barbari×Sannen kids.

TABLE 7

Mean values of the respiration rate/minute of kids of two different breeds and their cross during different seasons

Groups	Summer		Premonsoon		Monsoon		Autumn	
	M	E	M	E	M	E	M	E
Barbari	48·37 ±2·06	72·88 ±3·20	41·33 ±3·93	42·66 ±3·26	26·33 ±2·07	34·06 ±1·70	26·20 ±1·38	42·50 ±1·36
Barbari×Sannen	53·16 ±2·78	82·12 ±4·42	31·00 ±2·72	42·83 ±6·41	26·20 ±1·66	32·90 ±2·12	26·06 ±1·56	39·56 ±2·20
Sannen	56·78 ±2·73	109·04 ±9·73	36·50 ±5·00	43·66 ±8·15	28·70 ±2·57	35·60 ±3·03	26·37 ±2·77	61·50 ±1·19

M=Morning E=Evening

TABLE 8

Analysis of variance in the respiration rate of kids

Sources of variation	D.F.	Morning		Evening	
		S. S.	M.S.	S. S.	M. S.
Between groups	2	1431·6	715·8**	19107·1	9553·55**
Between seasons	3	26562·8	8854·28**	95043·6	31681·20**
Interaction group× season	6	40·0	6·66	842·5	140·41
Error	166	17005·2	102·44	75666·9	455·82
Total	177	45039·6	...	190660·1	

C. D. Between group : M. R. 5·86 E. R. 11·6

** Significant at $P<0·01$

Barbari appeared to be the most and Sannen least heat tolerant. No significant difference in the respiration rate of Barbari and Barbari × Sannen indicates that cross breds adapted themselves successfully to heat stress when they were kept in shed.

Premonsoon—There was no significant difference in the respiration rate of different groups, except that the morning respiration rate of Barbari was significantly higher than that of Barbari × Sannen. Kids of all the groups showed a decline in their respiration rate as compared to the respiration rate in summer.

Monsoon—There was no significant difference in the mean morning and evening respiration rate of different groups. Ameliorative effect of humidity was evident in all the groups, most remarkable being on the Sannen kids. In this season the mean evening ambient temperature was 11·18°F less and relative humidity 25·05 per cent more than in summer. Respiration rates were 73·44, 48·06 and 44·98 less than in summer in Sannen, Barbari × Sannen and Barbari kids respectively.

Autumn—No significant difference could be found in the mean morning respiration rate of different groups. Mean evening respiration rate of Sannen was significantly higher than that of Barbari and Barbari × Sannen.

RECTAL TEMPERATURE OF KIDS

Table 9 shows the mean morning and evening rectal temperature of kids. Analysis of variance is presented in table 10. There was significant difference between groups as well as between seasons.

TABLE 9

Mean values of the rectal temperature of kids of two different breeds and their cross during different seasons

Group	Summer		Premonsoon		Monsoon		Autumn	
	M	E	M	E	M	E	M	E
Barbari	102·28 ±·143	103·29 ±·099	102·22 ±·091	102·66 ±·115	102·01 ±·113	102·61 ±·109	101·69 ±·122	102·70 ±·099
Barbari × Sannen	102·83 ±·184	104·00 ±·187	102·46 ±·212	102·88 ±·228	102·05 ±·110	102·58 ±·108	102·01 ±·140	102·91 ±·108
Sannen	102·82 ±·207	104·63 ±·127	103·23 ±·271	104·03 ±·250	102·02 ±·116	102·87 ±·185	102·05 ±·191	102·66 ±·282

M=Morning E=Evening

TABLE 10

Analysis of variance in the rectal temperature of kids

Sources of variation	D. F.	Morning		Evening	
		S. S.	M. S.	S. S.	M. S.
Between groups	2	9·47	4·735**	26·27	13·135**
Between seasons	3	21·42	7·140**	57·78	19·26**
Interaction group× season	6	·70	·116	4·65	·775
Error	164	75·98	·4632	58·17	·3546
Total	175	107·59	...	146·87	...

C. D. between groups; M. T. 0·281. E. T. 0·309

COMPARISON OF RECTAL TEMPERATURE OF DIFFERENT GROUPS IN A PARTICULAR SEASON

Summer—Mean morning and evening rectal temperature of Sannen and Barbari × Sannen kids was significantly higher than that of Barbari kids. No significant difference could be found in the mean morning rectal temperature of Sannen and Barbari × Sannen kids, though in the evening such a difference existed. Diurnal variation in the rectal temperature of different groups was as follows: Sannen, 1·81°; Barberi × Sannen, 1·17°; Barbari, 1·01°F. Rectal temperature study indicates that Barbari is most and Sannen least adaptable to heat stress.

Premonsoon—Mean morning and evening rectal temperature of Sannen kids was significantly higher than that of Barbari and Barbari × Sannen kids. No significant difference could be found in the rectal temperature of Barbari and Barbari × Sannen kids either in the morning or in the evening.

Monsoon—No significant difference was found in the rectal temperature of the different groups in the morning or in the evening.

Autumn—Morning rectal temperature of Barbari kids was found to be significantly less than that of Sannen and Barbari × Sannen kids, there being no difference in the latter two groups. There was no significant difference in the rectal temperature of the different groups in the evening.

INFLUENCE OF CLIMATIC ELEMENTS ON THE RESPIRATION RATE AND RECTAL TEMPERATURE OF KIDS

Correlation and partial correlation coefficients of air temperature and air humidity with rate of respiration and rectal temperature are presented in table 11.

TABLE 11

Correlation Coefficients

Group	Correlation coefficient with air temperature				Correlation coefficient with air humidity			
	M.R.	E·R.	M.T.	E.T.	M.R.	E. R.	M.T.	E. T.
Barbari	·53440*	·84514**	·64464**	·60070**	–·5876**	–·68754**	–·22051	–·52383*
Barbari×Sannen	·46288*	·73875**	·45157*	·59443**	–·43158*	–·71703**	–·49377*	–·41824
Sannen	·22252	·66505**	·73504**	·80052**	–·6599**	–·69797**	–·51866*	–·75853**

Partial correlation coefficient

Group	Value of partial correlation with air temperature, keeping air humidity constant				Value of partial correlation with air humidity, keeping air temperature constant			
	M.R.	E.R.	M.T.	E.T.	M.R.	E.R.	M.T.	E.T.
Barbari	·44950*	·69606**	·62118**	·45621*	–·54149**	–·22074	–·00162	–·01736
Barbari×Sannen	·3786	·46183*	·35451	·46518*	–·3359	–·40025	–·41170	–·00132
Sannen	·01266	·33063	·70105**	·56581**	–·6339**	–·42546	–·43747	–·44298

M. R.=Morning respiration,
E. R.=Evening respiration,
M. T.=Morning rectal temperature.
E. T.=Evening rectal temperature,
** Significant at P<0·01.
* Significant at P<0·05.

A highly significant positive correlation was found between air temperature and evening respiration rate and rectal temperature of kids. Correlation between air temperature and morning respiration rate was positive and significant in Barbari and Barbari × Sannen, while correlation between morning rectal temperature and air temperature was highly significant except for Barbari × Sannen where it was significant at 5% level. Correlation between air humidity and respiration rate was negative and highly significant. A negative significant correlation was found between air humidity and morning rectal temperature in Barbari × Sannen and Sannen kids. Correlation between air humidity and evening rectal temperature was negative and highly significant for Sannen kids and significant for Barbari kids.

Values of partial correlation with air temperature, keeping air humidity constant, were positive and significant for morning respiration rate of Barbari, highly significant for evening respiration rate of Barbari and significant for evening respiration of Barbari × Sannen. Values of partial correlation of rectal temperature with air temperature were positive and highly significant for Barbari and Sannen in the morning and significant in the evening for all the groups.

Values of partial correlation of respiration and rectal temperature with air humidity were negative and non-significant except for the morning respiration rate of Barbari and Sannen in which a negative highly significant value was found.

Multiple correlations indicate that most of the variations in the respiration rate and rectal temperature of these animals were due to climatic elements.

Multiple Correlation Coefficients

Groups	M. R.	E. R.	M. T.	E. T.
Barbari	·703**	·853**	·644**	·600**
Barbari × Sannen	·550**	·780**	·581**	·594**
Sannen	·697**	·737**	·792**	·843**

Multiple regression equations for the evening respiration rate of kids are given below. Y was the estimated value of respiration rate, x_1 the environmental temperature and x_2 the relative humidity.

Y for Barbari $= -142{\cdot}23 + 2{\cdot}1206\, x_1 - {\cdot}2453\, x_2$

Y for Barbari × Sannen $= -83{\cdot}66 + 1{\cdot}7948\, x_1 - {\cdot}7445\, x_2$

Y for Sannen $= -111{\cdot}87 + 2{\cdot}21\, x_1 - {\cdot}61\, x_2$.

Multiple regression equations for the evening rectal temperature of kids are given below. Y was the estimated value of rectal temperature, x_1 the environmental temperature and x_2 the relative humidity.

Y for Barbari $= 99{\cdot}67 + {\cdot}0378\, x_1 - {\cdot}0078\, x_2$

Y for Barbari × Sannen $= 95{\cdot}77 + {\cdot}077\, x_1 + {\cdot}00096\, x_2$

Y for Sannen $= 96{\cdot}44 + {\cdot}087\, x_1 - {\cdot}024\, x_2$

Multiple regression equations indicate that most of the variation in the respiration rate and rectal temperature of kids were due to atmospheric temperature.

Results of present experiment indicate that lambs and kids of exotic breeds were less adaptable as compared to those of indigenous breeds. Cross bred lambs and kids could maintain their thermal equilibrium when maintained in the shed. It is necessary that there should be some change in the management of lambs and kids of exotic breeds and they should be kept in an artificially cooled room to protect them from the thermal stress during the period when atmospheric temperature is high (May to October).

SUMMARY

Adaptability of different breeds and crosses of lambs and kids was ascertained in terms of respiration, rectal temperature and growth during the most stressful part of the year (May to October). Mandia was found to be the most and Corriedale least adaptable of all the breeds and crosses of lambs. In the shed cross bred could withstand thermal stress effectively. Barbari kids were found to be most and Sannen least adaptable to heat stress during summer months. Barbari × Sannen kids could be kept successfully in the shed. In the other seasons there was not much difference in the adaptability of three groups. Environmental temperature was found to be the major factor in causing variation in the respiration rate and rectal temperature of different breeds and crosses of lambs and kids.

ACKNOWLEDGEMENT

Our thanks are due to Mr. C. V. G. Choudary, Principal, U. P. College of Veterinary Science and Animal Husbandry, Mathura for providing necessary facilities.

REFERENCES

1. Singh, B. & Roy, A. 1965. *Ind. J. Vet. Sci. A. H.*, **33** : 128.
2. Whitchurst, V. E., Crown, R. M., Phillips, R. W. & Spencer, D. A. 1947. *Fla. Agric Expt. Sta. Bul.*, **429** (cited by Warwick, E. T. 1958. *J. Heredity*, **49** : 69.)

ACTION OF MILD DOSES OF UV RADIATIONS ON DILUTE AQUEOUS SOLUTION OF GLYCINE

O. N. PERTI
Chemistry Laboratory,
M. L. N. R. E. College, Allahabad.

AND

(MISS) V. PAUL
Chemistry Department,
Agra College, Agra.

ABSTRACT

When a dilute aqueous solution (0·1%) of glycine is exposed to mild doses of UV radiations from a quartz mercury vapour lamp for about 2 minutes presence of other aliphatic amino acids as well as di- and tripeptides of glycine can be detected in the solution. Further exposure apparently destroys all the products formed except alanine whose presence can be detected even after exposure of 30 minutes.

INTRODUCTION

Action of ultraviolet radiations on aqueous solutions of glycine have been studied by several workers who reported evolution of ammonia. [1,2,3,4,5] Easy elimination of ammonia has been explained on the basis of a zwitter ion structure for the amino acid molecule[6,7,8,9] and participation of water leading to formation of glycollic acid.[1] However, the occurrence of a side reaction was also noticed as indicated by the evolution of a gas rich in carbon monoxide.[1] Later Ide[10] also reported the presence of glycollic acid, ammonia and carbon monoxide when aqueous solution of glycine was irradiated by quartz mercury vapour lamp in open air at room temperature.

The source of carbon monoxide in the photolysis of glycine has not been investigated but it could only be the carboxyl group either of glycine or of glycollic acid which is known to be produced. Carboxyl group in simple aliphatic acids (R. COOH) is known to decompose under the impact of UV radiations from a quartz mercury vapour lamp, chief products being CO, CO_2 and R.OH in aqueous solutions. [11,12] Hydroxy acids are also known to undergo photolysis under the influence of UV radiations.[13] All this indicates that when aqueous solution of glycine is exposed to UV radiations several products would be present such as glycine, glycollic acid, carbon monoxide, carbon dioxide, ammonia and methyl alcohol. These can be expected to interact with one another. In this paper are described our preliminary attempts to trace the presence of other amino acids or peptides which might possibly get formed when a dilute aqueous solution of glycine is exposed to mild doses of UV radiation from a quartz mercury vapour lamp.

EXPERIMENTAL

All vessels used in these experiments were thoroughly washed and sterilised by heating them at 200°. They were then placed in an autoclave and were heated at 20 lbs. steam pressure for 30 minutes.

Glycine used was chromatographically pure. Very dilute solution (0·1000g/100 ml) was employed with a view that the products formed during photolysis should as far as possible remain in solution. This solution was placed at a distance of 37 cms. from ELVAK 'Universal' quartz mercury vapour lamp with in-put of 1500 watts. A portion of the solution was also kept apart as control.

Periodically a portion of the solution was taken out and was subjected to chromatographic analysis. Either several drops were used or the solution was concentrated at room temperature under high vacuum and then used.[14,15,16,17] Only a test for amino acids and peptides was made. After a preliminary run the identification of substances was confirmed by co-chromatographic technique using authentic samples. Results are summarised in the table

TABLE

Exposure of dilute aqueous solution of glycine to mild doses of UV radiations
Concentration = 0·1000 g/100 ml—Temperature = 20−25°

Exposure time	Results of chromatographic analysis for amino acids and peptides	
	Unexposed solution	Exposed solution
0 sec.	glycine	glycine
30 ,,	,,	,,
1 min.	,,	glycine+alanine+one spot (faint)
2 ,,	,,	glycine+alanine+glycyl-glycine+glycyl-glycyl-glycine+α-amino-n-butyric acid+valine
7 ,,	,,	glycine+alanine+glycyl-glycyl-glycine
10 ,,	,,	glycine+alanine
15 ,,	,,	,, ,,
20 ,,	,,	,, ,,
25 ,,	,,	,, ,,
30 ,,	,,	,, ,,

DISCUSSION

When dilute aqueous solution of glycine is exposed to short doses of UV radiation, it is found that after about 2 minutes exposure other amino acids like alanine, α-amino-n-butyric acid and valine as well as di- and tri-peptides of glycine can be detected in the solution. Further exposure seems to destroy all other products except alanine which can be detected even after 30 minutes exposure. From the comparison of the intensity of the spots it appears that there is a reduction in the concentration of both glycine and the alanine when exposure is more than 10 minutes.

It was pointed out in the introduction that several compounds such as carbon monoxide, carbon dioxide, methanol, ammonia, glycine, and glycollic acid can be expected to be present in aqueous solution of glycine exposed to UV radiation. Photolysis of methanol can further be expected to give rise to formaldehyde, hydrogen and carbon monoxide.[18,19,20,21] Under the seheterogenous conditions transient formation of other amino acids was not surprising as several workers[22,23,24] have noted formation of amino acids under UV radiation in a mixture of methane and ammonia in contact with water, and, Reid[25] noted formation of glycine, alanine, glutamic acid and leucine when an aqueous mixture of formaldehyde and ammonia through which carbon dioxide was bubbled was kept under an ordinary quartz mercury vapour lamp. Earlier work by one of us[14,15,16,17,26] also suggests possible formation of other amino acids under these conditions. It may further be recalled that in several abiogenic synthesis of amino acids it was noted[22,23,24,25,26] that whenever glycine was formed, the presence of alanine was also detectable. Easy conversion of glycine$\rightleftharpoons$alanine under UV radiations was also noted by Reid.[25]

The presence of peptides is also not surprising as the formation or breakage of a peptide link involves energy change of the order of 2-3 K.Cal. per gram mole,[14] and such links can be formed in aqueous solution of amino acids on exposure to even sunlight.[15]

Preliminary observations recorded in this paper seem to throw significant light on abiogenic formation of amino acids in the pre-biological era of the Earth when atmosphere had no oxygen and consequently there was no ozone layer to cut off UV radiations from sunlight.[27,28,29,30,31] They point out that sunlight rich in UV radiations playing upon dilute aqueous solutions of glycine could have given rise to other amino acids and peptides under suitable conditions.

In this preliminary report no attempt has been made to trace the course of reactions. Further work in this direction is in progress.

ACKNOWLEDGEMENT

Authors are grateful to C. S. I. R. for a research grant and for the award of a Junior Research Fellowship to one of us (V. Paul).

REFERENCES

1. Henri, V., Weizmann, C. & Hirschberg, 1934-35. Y. *Compt. rend.*, **198**, 168; **199**, 1205.
2. Weizmann, C. Hirschberg, Y. & Bergmann, E. 1938. *J. Am. Chem. Soc.*, **60**, 1799.
3. Dale, W. M. & Davis, J. V. 1949-1950. *Nature.*, **163**, 64; **166**, 1121.
4. Dale, W. M., Davis, J. V. & Gilbert, C. W. 1949. *Biochem. J.*, **45**, 93, 543.
5. Vaidyanathan, C. S., Kalyankar, G. D. & Giri, K. V. 1955. *Proc. Natl. Acad. Sci. India*, **24A**, 286.
6. Ley, H. & Zschacke, F. H. 1924. *Ber.*, **57B**, 1700.
7. Ley, H. & Arends, B. 1928. *Ber.*, **61B**, 212.
8. Ueda, H.: 1929. *J. Chem. Soc. Japan*, **50**, 502.
9. Leuthardt, F. & Pfister, M. 1933. *Helv. Chini. Acta.*, **16**, 228.
10. Ide. I. 1960-61. *Nagasaki*, Igakkai Zasshi, **35** : 99 ; Chem. Abst., **55**, 2251 g.

11. Berthelot, D. & Gandechon, H. 1911. *J. Soc. Chem. Ind.*, **29,** 1081; 1913. *Compt. rend.*, **156,** 68.
12. Farkas, L. Wansbrough-Jones, O. H. 1932. *Z. physik. Chem.*, **18B**, 124.
13. Volmar, 1923. *Compt. rend.*, **176**, 742; 1923 *J. Chem. Soc.*, **124**, II, 279; *J.S.C.I.*, **42A**, 423.
14. Perti, O.N. & Pathak, H. D. 1961. *Agra Univ. J. Res.* (*Sci.*). **10**, 265.
15. Perti, O. N. & Bahadur, K. & Pathak, H. D. 1961. *Proc. Natl. Acad. Sci.*, India, **30A**, 206.
16. Perti, O. N., Bahadur, K. & Pathak, H. D. 1962. *Ind. J. Appl. Chem.*, **25**, 90.
17. Perti, O. N., Bahadur, K. & Pathak, H D. 1962. *Biokkimia* (Russian). **27,** 708.
18. Patat, F. *et al.*, 1935. *Anz. Akad. Wiss. Wien. Math-naturw Kl.*, 93, 1933; *Chem. Abs.*, **28**, 6371, 1934; *Z. Electrochem.*, **41,** 494, 1935.
19. Fricke, H. & Hart, E. J. *J. Chem. Physics.*, **4**, 418 1936.
20. Elhart, W. & Orth, O. S. *Anesthesia and Analgesia*, **14,** 15 1935; *Chem. Abs.*, **29,** 3401 1938.
21. Contieni, R., Ber., **69B**, 1101, 1386 (1936) Cf. Milas, N., U.S.P. 2, 115, 206-7, April 26, 1938; *Chem. Abs.*, 4606 (1938).
22. Groth, W. & Weyssenhoff, H. V. *Naturwissenschaften*, 510, 1957.
23. Terenin, A. *The Origin of Life on the Earth* (Eds. F. Clarke and R.L.M. Synge), 136, Pergamon Press 1959.
24. Miller, S. L. *The Origin of Life on the Earth* (Eds. F. Clarke and R.L.M. Synge), footnote on p. 131, Pergamon Press 1959.
25. Reid, C. *The Origin of Life on the Earth* (Eds. F. Clarke and R.L.M. Synge), 619, Pergamon Press 1959.
26. Perti, O N. *Agra Univ. J. Res.* (*Sci.*), **XII** (II): 1-48. 1963.
27. Kuiper, G. P. (Ed.) *Atmospheres of the Earth and Planets*, 2nd edition, University of Chicago Press 1952.
28. Urey, H. C. *The Origin of Life on the Earth* (Eds. F. Clarke and R.L.M. Synge), 16-22, Pergamon Press 1959.
29. Vinogradov, A. P. *The Origin of Life on the Earth* (Eds. F. Clarke and R. L. M. (Synge) 23-37, Pergamon Press 1959.
30. Sokolov, V.A. *The Origin of Life on the Earth* (Eds. F. Clarke and R.L. M Synge) 54-67, Pergamon Press 1959.
31. Miller, S. L. & Urey, H. C. *Science*, **130**, 245, 1959.

STUDIES ON THE ELECTROPHORETIC PATTERN OF PROTEIN FRACTIONS OF COLOSTRUM AND MILK WHEY

T. PRASAD, J. S. RAWAT AND A. ROY
U. P. College of Vet. Sc. & Ani. Husb., Mathura.

Large individual variations and significant breed differences in milk protein production have been reported; it was found that alpha-casein, beta-casein and beta-lactoglobulin values were significantly less in Holstein than in other breeds and that gamma-casein in Holstein was significantly higher (Rolleri *et al* 1956). Studies on variations in protein components of cow milk during lactation revealed that while the relative concentrations of alpha-casein and beta-casein remained almost constant, changes in casein concentrations were apparent only during colostral phase and regression milk phase. In contrast, the changes in whey protein components were more marked. Further during regression phase, immune globulins and albumin components increased progressively while at parturition, the immune globulins formed the most predominent protein component (Gronwall 1947 and McMeekin 1952).

In the investigations under report, milk protein fractions were estimated to observe their variations in the changing phases of lactation and also to correlate the blood serum proteins of zebu and buffalo calves with the milk protein fractions of their respective dams.

MATERIAL AND METHODS

1. *Animals*—The animals used in this investigations comprised of eight newly born zebu (Hariana) and eight newly born buffalo (Murrah) calves together with their dams. Concentrate was fed in accordance with their maintenance and production requirements.

2. *Material*—Samples of colostrum and milk were drawn from all the four teats of the dams at periods (a) at parturition (I period), (b) one and a half to two days after parturition (II period), (c) 10 days after parturition (III period), (d) 30 days after parturition (IV period) and (e) 60 days after parturition (V period). The samples were kept in a refrigerator before use.

3. *Protein fractionation*—Fractionation of whey proteins was done with the help of paper electrophoretic technique.

Whey obtained both from skim milk and colostrum and dialysed as described by Larson and Rolleri (1955) was used with a little modification. As electrophoresis was carried out in phosphate buffer (pH 6·6 and ionic strength 0·1), the third dialysis in veronal buffer (pH 8·6 and ionic strength 0·1) as given in the procedure of Larson and Rolleri (1955) was not done. The dialysing sacks containing samples of milk whey were processed for the purpose of electrophoresis according the method of Larson and Rolleri (1955).

Colostral whey samples were however diluted with phosphate buffer (pH 6·6) in the ratio of 1 : 9.

Analytical and staining procedure adopted and recording of pherograms and calculation of relative concentration of different protein fractions were done in the manner described by Jencks *et al* (1955) for serum proteins.

RESULTS AND DISCUSSIONS

Electrophoretic pattern of colostral and milk whey samples of zebu and buffaloes have been presented in Plates I and II. The relative concentration of different protein components have been shown in table 1.

TABLE 1

Relative percentage of different protein fractions in milk and colostral whey of cows (zebu) and buffalo at different periods from parturition onwards

Periods	Fractions	Cows (Zebu)			Buffaloes		
		Average	S. E.	Coef. of Variance	Average	S. E.	Coef. of Variance
I	Component I	0·0	...	...	0·0	...	...
	Component II	0·0	...	...	0·0	...	...
	Component III	16·0	0·9	14·3	15·7	0·7	12·0
	Component IV	83·9	0·9	2·7	84·3	0·7	2·2
II	Component I	1·2	0·6	140·7*	2·1	0·8	100·0*
	Component II	22·6	2·8	34·7	26·3	1·5	14·8
	Component III	16·7	1·9	32·6	22·3	1·3	15·8
	Component IV	59·4	2·6	12·4	49·3	1·9	10·2
III	Component I	2·4	0·9	110·7*	1·3	0·6	122·7*
	Component II	35·9	3·1	24·6	29·2	1·7	15·1
	Component III	22·2	1·4	17·6	37·8	4·2	29·3
	Component IV	38·9	4·0	29·1	31·6	2·9	24·1
IV	Component I	2·4	0·6	61·1*	3·8	1·1	77·0*
	Component II	41·8	2·1	13·0	31·2	2·7	23·4
	Component III	26·3	2·0	20·3	36·8	3·2	23·2
	Component IV	29·4	2·9	26·3	27·6	3·0	28·5
V	Component I	1·4	0·4	77·4*	1·6	0·7	112·0*
	Component II	44·2	1·8	10·5	35·1	3·0	21·2
	Component III	26·3	0·6	6·4	38·0	0·4	27·6
	Component IV	27·9	2·1	19·4	25·3	2·9	27·9

* High value of coeficient of variation for the fraction may be viewed in the light of its range where zero value is incorporated.

Four protein components (the different protein components I, II, III and IV, have been numbered in order of decreasing mobilities so that component IV was least mobile) were observed in milk whey samples of both the species.

In colostral whey, samples collected at parturition, only two components (III and IV) were discernible (Plates I & II). The other components (I and II) which were absent in the colostral whey samples, collected at parturition, developed after about one and a half to two days in the whey samples of both the species. The relative concentration of component II which was 22·6 per cent at this stage in the mammary secretion of zebu, increased gradually and was 44·2 per cent in 60 days after parturition. In case of buffaloes, increase in the concentration of this component in whey followed the same pattern but the rise was not so sharp as in the case of zebu. Per cent concentration of component I, both in zebu and buffalo whey, always remained at a lower level from parturition onwards. Its relative concentration was never above five per cent.

In case of zebu whey, the concentration of component II was always greater than that of component III, but this was not true in buffalo whey (Table I). The concentration of component II was either equal to or lesser than that of component III in the latter. The mobilities of these two components in zebu whey also differed from that in buffalo whey (Plate III).

Electrophoretic fractionation of proteins in colostral and milk whey was carried out in phosphate buffer. Milk whey proteins were fractionated into three visible band on filter paper strips but on electrophoretic scanning a fourth peak probably corresponding to serum albumin, was also obtained (Plates I and II). The fractions described as component I, II, III and IV are believed to correspond to serum albumin, alpha-lactalbumin, beta-lactoglobulin and immune-globulin fractions in whey proteins (McMeekin 1952). In a few cases of milk whey, a small fraction, stationary at the point of application was noticed. Presence of such unidentified stationary fraction was also reported by Raetskaya (1961) on electrophoresis. In the present investigation, this stationary fraction was found only in few cases. The occasional presence of stationary fractions, in amounts not sufficient for quantitative differentiation, was not believed to be an extra fraction and was grouped alongwith component IV for purposes of expressing relative concentration in this experiment. This might raise the relative concentration of the component only slightly. The possibility that stationary component was a result of protein denaturation, caused by addition of acetic acid for casein precipitation, as has been reported by Perlamann and Kaufman (1949) and Polson (1952) can not be ruled out.

Out of the only two components *i.e.*, III and IV discernible in colostral whey the latter seemed to correspond to immune globulin fraction and had a relative concentration of 83·9 per cent in zebu and 84·3 per cent in buffalo colostral whey. Polson (1952) obtained similar nature of protein peaks in colostrum, though the nomenclature of protein fractions used in his experiments were different from Jenness *et al* (1956). The value for component III corresponding to beta-lactoglobulin was 16·1 per cent and 15·7 per cent in zebu and buffalo colostral whey respectively. This showed remarkable similarity in the relative protein fractions of colostral whey of the two species at this stage; the other fractions, *viz.*, components II and I, were absent in the whey samples in both the species.

As a result of transition from colostrum to milk the relative concentration of individual components changed considerably. The value of component IV, decreased in one and a half to two days and ten days collections and attained the constant level only 30 days post-partum in zebu milk while this constancy was acquired much earlier (ten days post-partum) in buffalo milk. Relative concentration of component III, on the other hand, increased till the thirtieth day in zebu and tenth day samples in buffalo, where after it also became constant. These findings corroborate the observations that the time required for colostrum to attain normal milk composition is shorter in buffalo than in cows, as pointed out by Ghosh and Anant Krishnan (1964).

The pattern of component I, both in zebu and buffalo whey samples, was much variable in individual animals. The average value of this component was very low (less than 5 per cent). This corresponds to the observations of Raetaskaya (1961) who obtained 5·7 per cent serum albumin fraction in the milk samples of grazing cattle.

In all the samples of milk whey studied, conspicuous difference (Table 1 and Plates I & II), both in relative concentration and mobilities of components II and III were observed in zebu and buffalo whey. While the relative concentration of component III in zebu whey was less than that of component II, the same was either equal to or greater than component II in all cases of buffalo whey studied. Conspicuous differences in mobilities of component III with respect to component II was also evident and was greater in zebu than in buffalo whey.

SUMMARY

(i) Electrophoretic studies in skim milk proteins were carried out in buffalo and zebu cows.

(ii) Electrophoretic fractionation of whey proteins gave rise to four protein components, namely component I, II, III and IV probably corresponding to serum albumin, alpha-lactalbumin, beta-lactoglobulin and immune-globulins respectively.

(iii) Out of the four electrophoretic fractions observed in samples of milk whey, component I and II, probably corresponding to serum albumin,

alpha-lactalbumin, respectively, were absent in colostral whey of both zebu and buffalo dams.

(iv) The relative concentration of component I remained always below five per cent in milk whey. Soon after parturition, the concentration of component II increased and reached a constant value in about one and a half to two days in buffalo whey and ten days in zebu whey.

(v) After parturition, the concentration of component IV (corresponding to immune globulins) was maximum and it tended to decrease gradually. Component III (corresponding to beta-lactoglobulin) gradually increased in whey samples of both the species studied.

(vi) Taking into consideration the changes in concentration of the protein components studied in whey it can be said that the transition from the stage of colostrum to the stage of milk, takes lesser time in buffaloes than in the case of zebu.

(vii) The concentration of component II was always greater than that of component III in zebu whey, but was either equal to or lesser than the latter in buffalo whey. Marked difference was also evident in the mobilities of these components in zebu than in buffalo whey.

REFERENCES

1. Ghosh, S. N. & Anant Krishnan, C. P. 1964. *Ind. J. Dairy Sci.*, **17** : 17.
2. Gronwall, A. 1947. *Nature*, 159, 376.
3. Jenness, R., Larson, B. L., McMeekin, T. L., Swanson, A. M., Whitrah, C. H. & Whitney, R. McL. 1956. *J. Dairy Sci.*, **39**: 536.
4. Jencks, W.P., Jetton, M.R. & Durrum, E.L. 1955. *Biochem. J.* **60**: 205.
5. Larson, B.L. & Rolleri, G.D. 1955. *J. Dairy Sci.*, **38**: 351.
6. McMeekin, T.L. 1952. *J. Milk and Food Technol.*, **15**: 57.
7. Perlmann, G.E. & Kaufman 1949. *J. Biol. Chem.* **179**: 133.
8. Polson, A. 1952. *Onderteport, J. Vet. Res.*, **25** (4): 7.
9. Raetskaya, Yu. I. 1961. *Vestn. Sel. Skokhoz Nanki*. **6**: 67 *cited in Dairy Sci. Abstr.* **24**, No. 3348.
10. Rolleri, G.D., Larson, B.L. & Touchberry, R.W. 1956. *J. Dairy Sci.*, **39**: 1683.

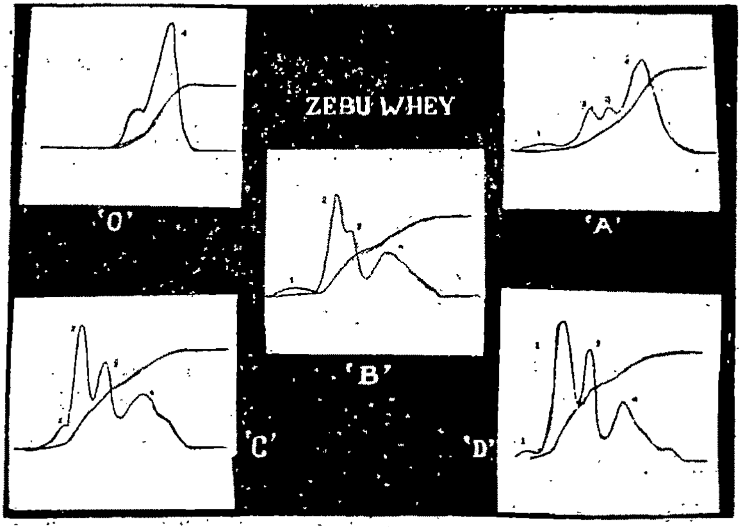

Plate I. Electrophoretic pattern of colostral and milk whey proteins of zebu dam from parturition to 60 days postpartum.
'O'=Samples collected immediately after parturition.
'A'=Samples collected at 1½ to 2 days post-partum.
'B'=Samples collected at 10 days post-partum.
'C'=Samples collected at 30 days post-partum.
'D'=Samples collected at 60 days post-partum.

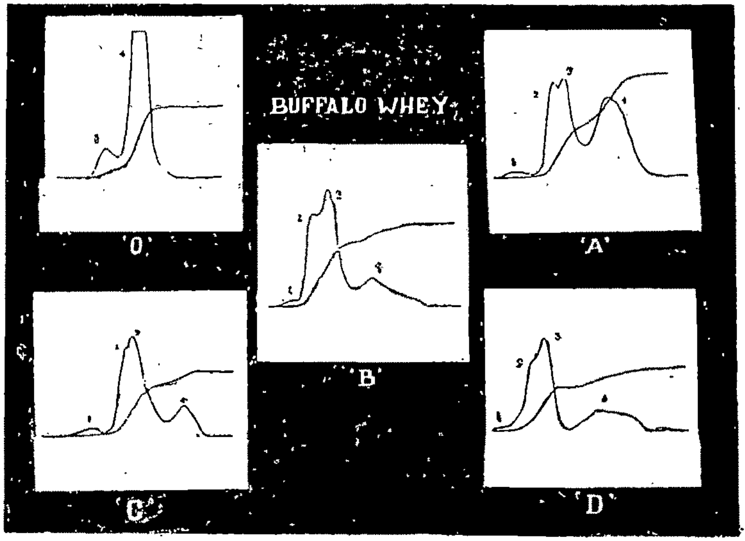

Plate II. Electrophoretic pattern of colostral and milk whey proteins of buffalo dam from parturition to 60 days post-partum.
'O'=Samples collected immediately after parturition.
'A'=Samples collected at 1½ to 2 days post-partum.
'B'=Samples collected at 10 days post-partum.
'C'=Samples collected at 30 days post-partum.
'D'=Samples collected at 60 days post-partum.

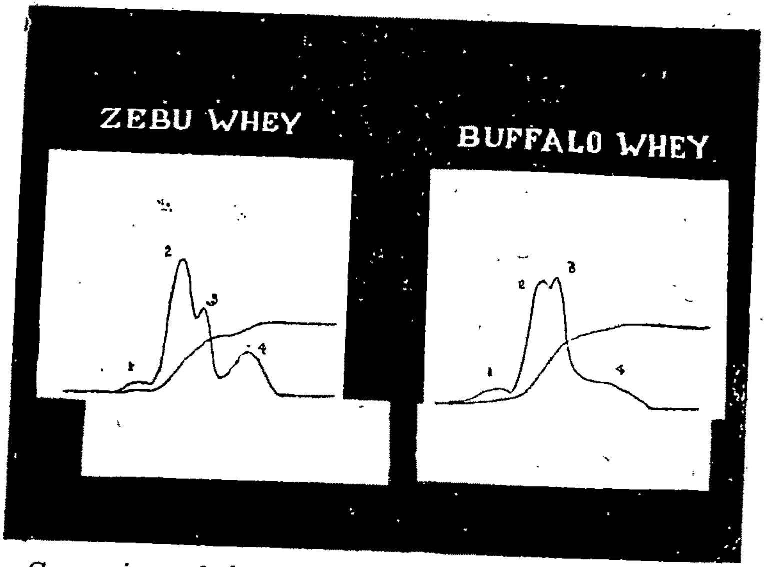

Plate III. Comparison of electrophoretic pattern of zebu and buffalo whey proteins. Difference in relative concentration and mobilities of components 2 and 3 may be seen.

VARIABLE FLOW OF A VISCOUS INCOMPRESSIBLE FLUID THROUGH A PIPE OF RECTANGULAR CROSS-SECTION UNDER A TIME DEPENDENT PRESSURE GRADIENT

PREM DAYAL NARANG*

INTRODUCTION

Drake [1] has discussed approximations of a flow in a rectangular channel due to a periodic-pressure gradient but in the present paper the pressure gradient is taken to be in entirely different forms. We have adopted a different method, namely that of transforms. We have also found out the approximate value of the velocity distribution after the manner of Lachlan [3].

We will consider here the unsteady flow of viscous incompressible fluid through a pipe of rectangular cross-section, under a pressure gradient directly proportional to time.

Let us take the cartesian coordinates (x, y, z), taking the axis of Z along the axis of the pipe, and the axis of x and y along two adjacent sides of the section. The corresponding velocity components are (u, v, w). Assuming u and v to be zero, the equation of continuity gives $\frac{\partial w}{\partial z}=0$, so that $w=f(x, y, t)$. Let us take the sides of the rectangle as $x=0$; $x=b$; $y=0$; $y=a$. [Fig. 1].

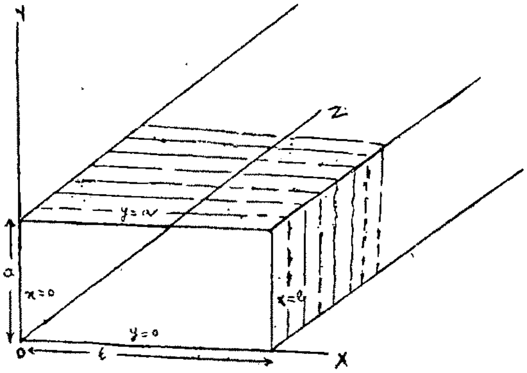

Fig. 1.

EQUATIONS OF MOTION

The equations of motion are

$$0=-\frac{\partial p}{\partial x} \quad ..(1)$$

$$0=-\frac{\partial p}{\partial y} \quad ..(2)$$

and

$$\rho\frac{\partial w}{dt}=-\frac{\partial p}{\partial z}+\mu\left(\frac{\partial^2 w}{\partial x^2}+\frac{\partial^2 w}{\partial y^2}\right) \quad ..(3)$$

---

[*] Research scholar, Agra College, Agra and Lecturer in Mathematics, St. John's College, Agra.

From these equations it is clear that it is a function of t only, here we assume $\frac{d\rho}{dz}=\rho A t$ ..(4)

(where ρ is the density of the fluid and A is a positive constant)

After substituting this in (3) we get

$$\frac{\partial w}{\partial t}=\frac{\mu}{\rho}\left[\frac{\partial^2 w}{\partial x^2}+\frac{\partial^2 w}{\partial y^2}\right]-At \qquad ..(5)$$

The equation (5) is subject to the boundary conditions that

$$\left.\begin{array}{ll}\text{when} & x=0 \text{ or } b,\quad w=0\\ \text{when} & y=0 \text{ or } a,\quad w=0\end{array}\right\} \qquad ..(6)$$

Let us apply Laplace transform to (5) taking $\bar{w}=\int_0^{\infty} w\, e^{-pt}\, dt$, then we get

$$\frac{\mu}{\rho}\left[\frac{\partial^2 \bar{w}}{\partial x^2}+\frac{\partial^2 \bar{w}}{\partial y^2}\right]=A.\frac{1}{p^2}+p\bar{w} \qquad ..(7)$$

subject to the boundary conditions

$$\left.\begin{array}{l}\bar{w}=0,\quad x=0 \text{ or } b\\ \bar{w}=0,\quad y=0 \text{ or } a\end{array}\right\} \qquad ..(8)$$

If we put $y=a/\pi.\eta$ in equation (7) then we get

$$\frac{\mu}{\rho}\left[\frac{\partial^2 \bar{w}}{\partial x^2}+\frac{\pi^2}{a^2}\frac{\partial^2 \bar{w}}{\partial \eta^2}\right]=\frac{A}{p^2}+p\bar{w} \qquad ..(9)$$

$$\left.\begin{array}{l}\bar{w}=0,\quad x=0 \text{ or } b\\ \bar{w}=0,\quad \eta=0 \text{ or } \pi\end{array}\right\} \qquad ..(10)$$

Applying finite Fourier transform to the equation (9), taking

$\bar{w}'=\int_0^{\pi} \bar{w}\sin p'\eta\, d\eta$ we get

$$\frac{\mu}{\rho}\frac{d^2\bar{w}}{dx^2}=\frac{A}{p^2}\cdot\frac{2}{p'}+p\bar{w}'+\frac{\mu}{\rho}p'^2\,\bar{w}'\frac{\pi^2}{a^2} \qquad ...(11a)$$

if p' is an odd number.

and $\frac{\mu}{\rho}\frac{d^2\bar{w}'}{dx^2}=p\,\bar{w}'+\frac{\mu}{\rho}p'^2\,\bar{w}'\frac{\pi^2}{a^2}$ ..(11b)

if p' is an even number

(11a) can be written as

$$\frac{d^2\bar{w}'}{dx^2}=\bar{w}'\left(\frac{p^{2\prime}\pi^2}{a^2}+\frac{p\rho}{\mu}\right)+\frac{A}{\mu}\,\frac{\rho}{p^2}\cdot\frac{2}{p'} \qquad ..(12)$$

or

$$\frac{d^2\bar{w}'}{dx^2}-k^2\bar{w}'=C \qquad ..(13)$$

where $K^2=\left(\frac{p^{2\prime}\pi^2}{a^2}+\frac{p\rho}{\mu}\right)$ and $C=\frac{A}{\mu}\,\frac{\rho}{p^2}\,\frac{2}{p'}$ ..(14)

Let the solution of equation (13) be

$$\bar{w}=Ae^{kx}+Be^{-kx}-C/k^2 \qquad ..(15)$$

subject to the conditions $\bar{w}'=0$ where $x=0$ or b

Hence $$A+B=C/K^2 \qquad ..(16)$$

and $$Ae^{kb}+Be^{-kb}=C/K^2 \qquad ..(17)$$

Solving (16) and (17) we get

$$A=C/K^2\left(\frac{1}{1+e^{bk}}\right),\ B=C/K^2\left(\frac{e^{kb}}{1+e^{bk}}\right)$$

or $$\bar{w}'=C/K^2\left[\frac{e^{kx}+e^{(b-x)k}}{1+e^{kb}}-1\right] \qquad ..(18)$$

Similarly the solution of (11b) is given by

$$\bar{w}'=0, \qquad ..(19)$$

Inversion of (18) by inverse finite Fourier transform gives

$$\bar{w}=\frac{4A\rho}{\pi\mu p^2}\Sigma\ \frac{1}{p'}\ \frac{1}{k^2}\left[\frac{e^{xk}+e^{(b-x)k}}{1+e^{bk}}-1\right]\sin p'\eta$$

p' is an odd positive integer.

i. e., $$\bar{w}=\frac{4A\rho}{\pi\mu p^2}\sum_{n=0}^{n=\propto}\frac{1}{(2n+1)k^2}\left\{\frac{e^{kx}+e^{(b-x)k}}{1+e^{bk}}-1\right\}\sin(2n+1)\eta \qquad ..(20)$$

where $$K^2=\left[\frac{p'^2\pi^2}{a^2}+\frac{p\rho}{\mu}\right]=\left[\frac{\pi^2(2n+1)^2}{a^2}+p\frac{\rho}{\mu}\right]$$

$$=\frac{\rho}{\mu}\left[p+\frac{\pi^2}{a^2}\frac{(2n+1)^2\mu}{\rho}\right]$$

Let $$\frac{\rho}{\mu}=\lambda \text{ and } \frac{\pi^2}{a^2}\frac{(2n+1)^2\mu}{\rho}=\theta \qquad ..(21)$$

$\therefore$ $$K=\sqrt{\lambda}\sqrt{p+\theta}$$

therefore (20) becomes

$$w=\frac{4A}{\pi p^2}\sum_{n=0}^{n=\propto}\frac{1}{(p+\theta)}\left[\frac{e^{\sqrt{\lambda}\sqrt{p+\theta x}}-e^{\sqrt{\lambda}\sqrt{p+\theta}(b-x)}}{1+e^{b\sqrt{\lambda}\sqrt{p+\theta}}}-1\right]\frac{\sin(2n+1)\eta}{(2+1)n} \qquad ...(22)$$

applying the Laplace inversion formula we get

$$w=\frac{4A}{\pi}\frac{1}{2\pi i}\int_{\gamma-i\propto}^{\gamma+i\propto}\sum_{n=0}^{n=\propto}\frac{e^{pt}\,dp}{p^2(p+\theta)}\left\{\frac{e^{\sqrt{\lambda}\sqrt{p+\theta}.x}+e^{\sqrt{\lambda}\sqrt{p+\theta}(b-x)}}{1+e^{b\sqrt{\lambda}\sqrt{p+\theta}}}-1\right\}\frac{\sin(2n+1)\eta}{(2n+1)} \qquad ..(23)$$

where γ is greater than the real parts of all the singularities of the integrand *i. e.* $\gamma>0$

the terms in the Laplace inversion formula 23 are

$$\frac{e^{pt}}{p^2\,(p+\theta)} \qquad ..(24a)$$

and

$$\frac{e^{pt}\left\{e^{\sqrt{\lambda}\,\sqrt{p+\theta}\,x}+e^{\sqrt{\lambda}\,\sqrt{p+\theta}\,(b-x)}\right\}}{p^2\,(p+\theta)\,(1+e^{\sqrt{\lambda}\,\sqrt{p+\theta}.b})} \qquad ..(24b)$$

From tables of Integral transforms [2], the inversion for (24a) is $\frac{1}{\theta^2}\left[e^{-\theta t}+\theta t-1\right]$

CALCULATION FOR 24 B

$$\int_{\gamma-i\infty}^{\gamma+i\infty} e^{pt}\frac{\left\{e^{\sqrt{\lambda}\,\sqrt{p+\theta}\,x}+e^{\sqrt{\lambda}\,\sqrt{p+\theta}\,(b-x)}\right\}}{p^2\,(p+\theta)\left\{1+e^{b\sqrt{\lambda}\,\sqrt{p+\theta}}\right\}}dp$$

Applying the transformation

$$p+\theta=\xi$$
$$dp=d=\xi$$

This is transformed as

$$e^{-\theta t}\int_{\gamma+\theta-i\infty}^{\gamma+\theta+i\infty} e^{\xi t}\frac{\left\{e^{x\sqrt{\lambda}\,\sqrt{\xi}}+e^{(b-x)\,\sqrt{\lambda}\,\sqrt{\xi}}\right\}}{(\xi-\theta)^2\,\xi(1+e^{b\sqrt{\lambda}\,\sqrt{\xi}})}d\xi \qquad ..(25)$$

We now calculate the value of

$$\int_{\gamma+\theta-i\infty}^{\gamma+\theta+i\infty} e^{\xi t}\frac{\left\{e^{x\sqrt{\lambda\xi}}+e^{(b-x)\,\sqrt{\lambda\xi}}\right.}{(\xi-\theta)^2\xi\,(1+e^{b\sqrt{\lambda\xi}})}d\xi \qquad ..(26)$$

(26) has a branch point at $\xi=0$; and singularities at $\xi=\theta$ (double pole) and an infinite number of singularities at $\xi=-\frac{(2m+1)^2}{\lambda}\cdot\frac{\pi^2}{b^2}$ where $m=1, 2, 3, \ldots\ldots \infty$

Considering the value of the integral

$$e^{\xi t}\frac{\left\{e^{x\sqrt{\lambda\xi}}+e^{(b-x)\sqrt{\lambda\xi}}\right\}}{(\xi-\theta)^2\xi\,(1+e^{b\sqrt{\lambda\xi}})}$$

round the countour (ABDEFGA)—see fig. 2. [Where AB is on the right of all the singularities and the Radius of arcs C_1 and C_2 tends to infinity, *i. e.* $(R\to\infty)$; and the radius of arc C_3 tends to zero.]

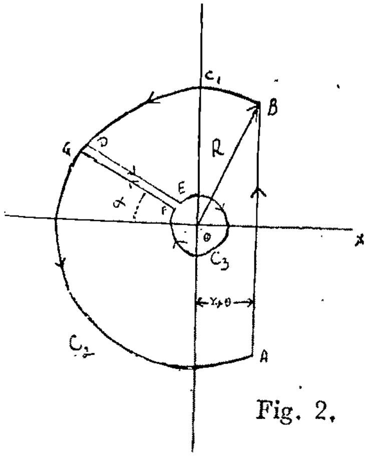

Fig. 2.

We have therefore $\int_{AB} \ldots d\xi + \int_{C_1} \ldots d\xi + \int_{DE} \ldots d\xi + \int_{C_3} \ldots d\xi + \int_{FG} \ldots d\xi + \int_{C_2} \ldots d\xi$

$$= 2\pi i \left[\begin{array}{l} \text{Sum of the residues at the poles } \xi = 0 \\ \text{and at } \xi = -\dfrac{(2m+1)^2}{\lambda} \cdot \dfrac{\pi^2}{b^2} \end{array} \right] \qquad ..(27)$$

$$\int_{C_1} \ldots d\xi + \int_{C_2} \ldots d\xi = 0 \qquad ..(28)$$

Because $\dfrac{1 \left\{ e^{x\sqrt{\lambda\xi}} + e^{(b-x)\sqrt{\lambda\xi}} \right\}}{(\xi-\theta)^2\, \xi (1+e^{b\sqrt{\lambda\xi}})} \to 0$ as $|\xi| \to \infty$ as in [4]

Here $\displaystyle\int_{AB} \ldots d\xi = \int_{\gamma+\theta-i\infty}^{\gamma+\theta+i\infty} e^{\xi t} \frac{\left\{ e^{x\sqrt{\lambda\xi}} + e^{(b-x)\sqrt{\lambda\xi}} \right\}}{(\xi-\theta^2)\xi\, (1+e^{b\sqrt{\lambda\xi}})}\, d\xi$ is the required integral ..(29)

$$\int_{C_3} \ldots d\xi = (-2\pi i) \operatorname*{Lt}_{\xi \to 0} e^{\xi t} \frac{\left\{ e^{x\sqrt{\lambda\xi}} + e^{(b-x)\sqrt{\lambda\xi}} \right\}}{(\xi-\theta)^2\, (1+e^{b\sqrt{\lambda\xi}})}$$

$$= (-2\pi i)\ 1/\theta^2 = -2\pi i/\theta^2 \qquad ..(30)$$

$$\int_{DE} \ldots d\xi = \int_{\infty}^{0} e^{-r e^{-\alpha i}} \frac{\left\{ e^{x\sqrt{\lambda r i e^{-\alpha/2 i}}} + e^{(b-x)\sqrt{\lambda r i e^{-\alpha/2 i}}} \right\}}{(re^{-\alpha i}+\theta)^2\, r e^{-\alpha i}\, (1+e^{b\sqrt{\lambda r i e^{-\alpha/2 i}}})}\, dr\, e^{-\alpha i}$$

as ξ along DE is given by $\xi = r\, e^{(\pi-\alpha)i} = -r\, e^{-\alpha i}$ ..(31)

$$\therefore \quad d\xi = -dr e^{-\alpha i}$$

and $\displaystyle\int_{FG} \ldots d\xi = \int_{0}^{\infty} e^{-r e^{-\alpha i}} \frac{\left\{ e^{(b-x)\sqrt{\lambda r i e^{-\alpha/2 i}}} + e^{x\sqrt{\lambda r i e^{-\alpha/2 i}}} \right\}}{(re^{-\alpha i}+\theta)^2\, r\, e^{-\alpha i}\, (1+e^{b\sqrt{\lambda r i e^{-\alpha/2 i}}})}\, dr e^{-\alpha i}$ ...(32)

as along FG is given by $\xi = r\, e^{-(\pi+\alpha)i} = -r\, e^{-\alpha i}$

$$\therefore \quad d\xi = -dr\, e^{-\alpha i}$$

Hence $\displaystyle\int_{DE} \ldots d\xi + \int_{FG} \ldots d\xi = 0$ ..(33)

Hence the L. H. S. of (27) is equal to

$$\left\{ \int_{\gamma+\theta-i\infty}^{\gamma+\theta+i\infty} e^{\xi t} \frac{\left\{ e^{x\sqrt{\lambda\xi}} + e^{(b-x)\sqrt{\lambda\xi}} \right\}}{(\xi-\theta)^2\, \xi (1+e^{b\sqrt{\lambda\xi}})}\, d\xi - 2\pi i/\theta^2 \right\}$$

Residue at Double Pole

(at $\xi=\theta$) is

$$e^{\theta t}\left[\frac{\left\{e^{x\sqrt{\lambda\theta}}\left(t+\frac{x}{2}\sqrt{\frac{\lambda}{\theta}}\right)+e^{(b-x)\sqrt{\lambda\theta}}\left(t+\frac{b-x}{2}\sqrt{\frac{\lambda}{\theta}}\right)\right\}\theta\left(1+e^{b\sqrt{\lambda\theta}}\right)-}{\theta^2\left(1+e^{b\sqrt{\lambda\theta}}\right)^2}\right.$$

$$\left.\frac{\left\{e^{x\sqrt{\lambda\theta}}+e^{(b-x)\sqrt{\lambda\theta}}\right\}\left\{1+\frac{b\theta+2}{2}\sqrt{\frac{\lambda}{\theta}}\,e^{b\sqrt{\lambda\theta}}\right\}}{}\right] \quad ..(34)$$

Residue at

Infinite Poles at $\xi=-\frac{(2m+1)^2}{\lambda}\cdot\frac{\pi^2}{b^2}$

Sum of the residues

$$=\underset{\xi\to-\frac{(2m+1)^2}{\lambda}\frac{\pi^2}{b^2}}{\mathrm{Lt}}\ \sum_{m=0}^{m=\propto} e^{\xi t}\frac{\left\{e^{x\sqrt{\lambda\xi}}+e^{(b-x)\sqrt{\lambda\xi}}\right\}\left\{\xi+\frac{(2m+1)^2}{\lambda}\frac{\pi^2}{b^2}\right\}}{(\xi-\theta)^2\,\xi\left\{1+e^{b\sqrt{\lambda\xi}}\right\}}$$

$$=\underset{\xi\to-\frac{(2m+1)^2}{\lambda}\frac{\pi^2}{b^2}}{\mathrm{Lt}}\ \sum_{m=0}^{m=\propto} e^{\xi t}\frac{\left\{e^{x\sqrt{\lambda\xi}}+e^{(b-x)\sqrt{\lambda\xi}}\right\}}{(\xi-\theta)^2\,\xi\, b\sqrt{\lambda}\,\frac{1}{2}\,\xi^{-\frac{1}{2}}\,e^{b\sqrt{\lambda\xi}}}$$

$$=\frac{2\lambda^2}{\pi i}\sum_{m=0}^{m=\propto}\frac{e^{-\frac{(2m+1)^2}{\lambda}\frac{\pi^2}{b^2}t}\left\{e^{x(2m+1)\pi/bi}\ e^{-x(2m+1)\pi/e\,i}\right\}}{(2m+1)\left[(2m+1)^2\pi^2/b^2+(2n+1)^2\pi^2/a^2\right]^2}$$

$$=\frac{4\lambda^2}{\pi^5}\sum_{m=0}^{m=\propto}\frac{e-\frac{(2m+1)^2}{\lambda}\frac{\pi^2}{b^2}t\left\{\sin(2m+1)\pi x/b\right\}}{(2m+1)\left\{(2m+1)^2/b^2+(2n+1)^2/a^2\right\}^2} \quad ..(35)$$

Applying (20), (29), (38), (33); (34), (35), on (27) we get

$$\int_{\gamma+\theta-i\infty}^{\gamma+0+i\propto} e^{\xi t}\frac{\left\{e^{x\sqrt{\lambda\xi}}+e^{(b-x)\sqrt{\lambda\xi}}\right\}}{(\xi-\theta)^2\,\xi\left(1+e^{b\sqrt{\lambda\xi}}\right)}d\xi-2\pi i/\theta^2$$

$$=2\pi i\left[\frac{4\lambda^2}{\pi^5}\left\{\sum_{m=0}^{m=\propto}\frac{e^{-\frac{(2m+1)^2}{\lambda}\frac{\pi^2}{b^2}t}}{(2m+1)\left\{(2m+1)^2/b^2+(2n+1)^2/a^2\right\}}\sin(2m+1)\pi x/b\right.\right.$$

$$+\,e\theta t\,\frac{\left\{e^{x\sqrt{\lambda\theta}}\left(t+\frac{x}{2}\sqrt{\frac{\lambda}{\theta}}\right)+e^{(b-x)}\left(t+\frac{b-x}{2}\sqrt{\frac{\lambda}{\theta}}\right)\right\}\theta\left(1+e^{b\sqrt{\lambda\theta}}\right)-}{\theta^2\left(1+eb\sqrt{\lambda\theta}\right)^2}$$

$$\left.\frac{\left\{e^{x\sqrt{\lambda\theta}}+e^{(b-x)\sqrt{\lambda\theta}}\right\}\left\{1+\frac{2+b\theta}{2}\sqrt{\frac{\lambda}{\theta}}\,e^{b\sqrt{\lambda\theta}}\right\}}{}\right] \quad ..(36)$$

Using (25) we have

$$\int_{\gamma-i\propto}^{\gamma+i\propto} e^{pt}\frac{\left\{e^{\sqrt{\lambda}\,\sqrt{p+\theta x}}+e^{\sqrt{\lambda}\sqrt{p+\theta}(b-x)}\right\}}{p^2\;(p+\theta)\{1+e^{b\sqrt{\lambda}\,\sqrt{p+\theta}}\}}\,dp=$$

$$=\Bigg[\frac{2\pi i}{\theta^2}e^{-\theta t}+2\pi i\Bigg\{e^{-\theta t}\frac{4\lambda^2}{\pi^5}\sum_{m=\theta}^{m=\propto}\frac{e^{-\frac{(2m+1)^2}{\lambda}\frac{\pi^2}{b^2}t}\sin(2m+1)\pi x/b}{(2m+1)\;\{(2m+1)^2/b^2+(2n+1)^2/a^2\}^2}$$

$$+\frac{\left\{e^{x\sqrt{\lambda\theta}}\left(t+\frac{x}{2}\sqrt{\frac{\lambda}{\theta}}\right)+e^{(b-x)\sqrt{\lambda\theta}}\left(t+\frac{b-x}{2}\sqrt{\frac{\lambda}{\theta}}\right)\right\}\theta\left(1+e^{b\sqrt{\lambda\theta}}\right)-}{(2m+1)\;\{(2m+1)^2/b^2+(2n+1)^2/a^2\}^2}$$

$$\frac{\left\{e^{x\sqrt{\lambda\theta}}+e^{(b-x)\sqrt{\lambda\theta}}\right\}\left\{1+\frac{2+b\theta}{2}\sqrt{\frac{\lambda}{\theta}}\,e^{b\sqrt{\lambda\theta}}\right\}}{}\Bigg\}\Bigg]\qquad ..(37)$$

Using the values of (24a) and (24b) and substituting for θ and η

We get

$$w=4A/\pi\sum_{n=\nu}^{n=\propto}\Bigg[\frac{4\rho^2}{\mu^2\pi^5}\sum_{m=0}^{m=\propto}\left\{e^{-\left(\frac{(2m+1)^2}{b^2}+\frac{(2n+1)^2}{a^2}\frac{\mu^2}{\rho}\right)\pi^2 t}\sin(2m+1)\pi x/b\right\}$$

$$+\frac{e^{x\,\pi/a(2n+1)}\left\{t+\frac{x}{2}\,\frac{\rho a}{\pi\mu(2n+1)}\right\}+e^{(b-x)\pi/a\,(2n+1)}\left\{t+\frac{b-x}{2}\,\frac{\rho a}{\pi\mu(2n+1)}\right\}}{\pi^2(2n+1)^2\;\mu/\rho a^2\;\{1+e^{b\pi/a\,(2n+1)}\}}$$

$$-\frac{\left\{e^{x\,\pi/a(2n+1)}+e^{(b-x)\pi/a(2n+1)}\right\}\left\{1-\frac{b\pi}{2}\left(\frac{2n+1}{a}\right)e^{\pi b/a\,(2n+1)}+e^{\pi b/a(2n+1)}\right\}}{\pi^4(2n+1)^4\mu^2/\rho^2a^4\{1+e^{b\pi/a(2n+1)}\}^2}$$

$$-\frac{\rho^2a^4}{\pi^4(2n+1)^4\mu^2}\left\{\frac{\pi^2(2n+1)^2\mu}{\rho a^2}\,t-1\right\}\Bigg]\frac{1}{(2n+1)}\sin(2n+1)\pi y/a\qquad ..(38)$$

APPROXIMATE CALCULATION FOR VELOCITY DISTRIBUTION

(*a*) *when t is small*

We have from (23)

$$w=\frac{4A}{\pi}\cdot\frac{1}{2\pi i}\int_{\gamma-i\propto}^{\gamma+i\propto}\sum_{n=\propto}^{n=0}\frac{e^{pt}\,dp}{p^2(p+\theta)}\left\{\frac{e^{\sqrt{\lambda}\sqrt{p+\theta}\,x}+e^{\sqrt{\lambda}\sqrt{p+\theta}(b-x)}}{1+e^{b\sqrt{\lambda}\,\sqrt{p+\theta}}}-1\right\}\frac{\sin(2n+1)\eta}{(2n+1)}$$

which we proceed to calculate as follows :—

(24b) can be written as

$$\frac{e^{pt}}{p^2(p+\theta)}\;\frac{\left\{e^{-\sqrt{\lambda}\,\sqrt{p+\theta}(b-x)}+e^{-x\sqrt{\lambda}\,\sqrt{p+\theta}}\right\}}{\{1+e^{-b\sqrt{\lambda}\sqrt{p+\theta}}\}}$$

which when transformed as in (25), we get

$$e^{-\theta t}\int_{\gamma+\theta-i\infty}^{\gamma+\theta+i\infty} e^{\xi t}\,\frac{\left\{e^{-(b-x)\sqrt{\lambda\xi}}+e^{-x\sqrt{\lambda\xi}}\right\}}{(\xi-\theta)^2\xi\,(1+e^{-b\sqrt{\lambda\xi}})}\,d\xi$$

which tends to zero as in Lachlan [2].

Hence

$$w=\frac{4A}{\pi}\;\frac{1}{2\pi i}\int_{\gamma-i\infty}^{\gamma+i\infty}\sum_{n=0}^{n=\infty}-\frac{e^{pt}\,dp}{p^2(p+\theta)}\cdot\frac{\sin(2n+1)\eta}{(2n+1)} \quad ..(39)$$

where $\eta=\pi y/a$

$$\simeq\frac{4A}{\pi}\sum_{n=0}^{n=\infty}-\frac{t^2}{2}\,\frac{1}{(2n+1)}\sin(2n+1)\frac{\pi y}{a} \quad ..(40)$$

(40) is obtained from (39) by making $|p|$ very large in comparison with θ as in Lachlan [5]

(40) leads to

$$\frac{4A}{\pi}\left(-\frac{t^2}{3}\right)\left(\frac{\theta'-\theta'1}{2}\right)=\left[-\frac{A(\theta'-\theta'1)t^2}{\pi}\right]=-\tfrac{1}{2}At^2$$

$$\left[\text{where }\tan\theta'_1=-\frac{\sin(\pi y/a)}{1-\cos\pi y/a}\text{ and }\tan\theta'=\frac{\sin\pi y/a}{1+\cos\pi y/a}\right] \quad ..(41)$$

i. e. $\tan(\theta'-\theta'_1)=\infty$

(*b*) *when t is very large*

By making t very large in (38) *i. e.*, ($t\rightarrow\infty$) and neglecting other quantities in comparison to t, we have

$$\omega=\frac{4A}{\pi}\sum_{n=0}^{n=\infty}\left\{\frac{e^{(b-x)(2n+1)\pi/a}+e^{x(2n+1)\pi/a}}{1+e^{b(2n+1)\pi/a}}-1\right\}\frac{(t\,a^2\rho)}{\pi^2\mu(2n+1)^3}\sin(2n+1)\pi y/a \quad ..(42)$$

OTHER TIME DEPENDENT PRESSURE GRADIENTS

Let $dP/dz=f(t)$, where $f(t)$ can be (Cos $a't-1$), Sin $a't$, Sinh $a't$, (Cos $a't-1$) Sin $a't$ Erf $(a'^{\frac{1}{2}}.f^{\frac{1}{2}})$ etc.

Here $f(t)$ has been chosen so that dP/dz vanishes at $t=0$

$$\text{Let}\int_0^\infty f(t)e^{-pt}\,dt=\bar{f}(p) \quad ..(43)$$

then proceeding as in the previous sections from (5) to (24a) and (23b) we get $\frac{e^{pt}}{(p+\theta)}\bar{f}\,(p)$ in place of (24a). ..(44a)

and $\frac{e^{pt}}{p+\theta}f'(p)\,\frac{\left\{e^{x\sqrt{\lambda}\sqrt{p+\theta}}+e^{\sqrt{\lambda}\sqrt{p+\theta}(b-x)}\right\}}{\{1+e^{b\sqrt{\lambda}\sqrt{p+\theta}}\}}$ in place of (24b) ..(44b)

and hence in place of (26), we have

$$e^{-\theta t}\int_{\gamma+\theta-i\infty}^{\gamma+\theta+i\infty} e^{\xi t}\frac{f'(\xi-\theta)}{\xi}\,\frac{\left\{e^{x\sqrt{\lambda\xi}}+e^{(b-x)\sqrt{\lambda\xi}}\right\}}{(1+e^{b\sqrt{\lambda}\sqrt{p+\theta}})}d\xi \qquad ..(45)$$

Where γ is greater than all the real parts of the singularities of $\bar{f}\,(\xi)$.

(45) can be easily calculated for the functions given above, because a procedure similar to that of (28) and (33) will apply in these cases also.

Similarly we can also calculate the approximate value of velocity distribution when t is very small or very large.

ACKNOWLEDGEMENT

I am thankful to Dr. J. P. Agarwal, Head of the Mathematics Department, Agra College, Agra for the guidance.

REFERENCES

1. Drake, D. G. Flow in a rectangular channel due to a periodic pressure gradient—*Quart. Jour. Mech.* and *App. Maths.* Feb. 1965.
2. Harry Bateman. Tables of Integral Transforms Calculus Vol. I. Edition 1954 p. 230.
3. Lachlan, N. W. Complex Variable Theory and Transform calculus Article 6.32.
4. Lachlan (*Loc. Cit.*). Article 4.31 p. 77.
5. Lachlan (*Loc. Cit.*). Articles 4.61, 4.62.

A STUDY OF THE FISH FAUNA OF VISAKHAPATNAM DISTRICT (ANDHRA PRADESH)—ITS DISPOSAL AND MARKETING

II. FISHERY STATISTICS OF VISAKHAPATNAM DISTRICT

M. V. SUBBA RAO
Dept, of Zoology,
S. V. University, Tirupati, (A.P.)

AND

RATAN SINGH
Dept, of Zoology,
B. R. College, Agra, (U.P.)

(*Communicated by R. D. Saksena, M. Sc., Ph. D., F. Z. S. I.*)

The collection of accurate fishery statistics for the whole of India is a necessary pre-requisite for a proper scientific plan of exploitation and development of marine and inland fisheries. Until very recently the statistics has been collected in Visakhapatnam district under the auspices of the Village Panchayats.

The fishing industry in Visakhapatnam district is still in a primitive stage and is in the hands of a large number of illiterate fishermen. The degree of development and organisation of the industry vary from district to district. Hence it is clear that any single method of collection of statistics may not be applicable to the whole country but at the same time multiplicity of methods have to be avoided as it leads to complication.

The various types of statistics required to be collected in the present stage of development fall into the following categories.

GENERAL TECHNICAL REQUIREMENTS

(*a*) *Statutory provisions*—Usually there will be need for sound legislative measures, which make it incumbent upon all potential suppliers of statistics, to provide the required data accurately and to supply them promptly.

(*b*) *Accuracy*—There are numerous sources of errors, such as misleading, wrong transfer of figures, arithmetical errors, errors in species identification, mistakes or misunderstandings in measurements of their fish or craft. The correctness of the degree of accuracy should be indicated in all statistical reports.

(*c*) *Priorities*—The traditional way of statistical work is "Collection" of figures, then "Compilation", including tabulation and finally "Interpretation" of the statistics.

(*d*) *Suppliers of Statistics*—The information on catches could come from fishermen direct, but it will be a great saving of labour, if it can be obtained through merchants and processors, as the number of suppliers would be smaller. Direct questioning of fishermen at regular intervals, or a general census, would strengthen the basis of these statistics.

(*e*) *Demarcation of fishing grounds*—A breakdown of statistics according to fishing grounds, would meet the biologists' requirements and also make it easy for the fishermen to report. This demarcation should be such, as to make it relatively easy for a fisherman to state where he took his catch from. Maps could be distributed to fishermen.

(*f*) *Listing of fish species*—Various species have to be listed, standardised and grouped.

(*g*) *Units and conversion factors*—It is easier to let figures in units known to the trade, such units can be used for recording, or estimating original statistics, the quantity caught should be recorded in the actual state of dressing *i. e.*, round, filleted, salted etc., it is the recording the weight which actually entered the trade at first market transaction.

STATISTICS ON CATCHES AND LANDINGS

A proper statistical system will make it possible to calculate, by species, the fish caught per unit of physical input (for fishermen, vessel, set of gear) and according to regions. Statistics on landed quantities should be arranged in such a way, that they can be related to the amount of physical effort spent on primary production. Most accurate figures are obtainable when fish is discharged from fishing craft, for trading or further processing.

MEASUREMENT OF AMOUNT OF EFFORT

(*a*) *The fishermen*—The enumeration of man-power in fisheries is difficult, as the number varies and also as the individual effectiveness will vary according to his skill and ability, the craft and gear he used and the potentiality of the grounds he fishes.

(*b*) *The Craft (Boats)*—There are two types of craft *i.e.*, Catamaran and Masula Boats in use at Visakhapatnam district having variation in their catching capacity, quality, seaworthiness, adaptability for various types of gear, so there is little use in collecting information about the number of fishing craft. But generally in Visakhapatnam district the Catamarans are more popular than Masula boats.

(*c*) *Gear (Nets)*—The types of gear, the number of units of each used on different kinds of craft, catch per unit, effort required on operation in maintenance, cost and durability will vary considerably. Broad classifications should suffice. At Visakhapatnam district there are four types of gears, namely Shore seine, Boat seine, Gill nets and Kuduru nets, generally used. Gill nets and Boat seine are very popular in this district.

So, research workers, administrators, business economists and fishermen all need statistics which, of course, must be based on accuracy, comparability and coordination at every stage.

ACKNOWLEDGEMENT

We are grateful to Dr. R. D. Saksena, Professor and Head of Dept., of Zoology, B. R. College, Agra for providing all facilities during the course of this work.

REFERENCES

1. Gerhardsen, G. M. 1952. "Purpose and Methods in fishery Statistics." F. A. O. Publication.
2. Government of India. 1950. "Report of the Technical Committee Co-ordination of Fisheries Statistics." Government of India, Ministry of Agriculture.
3. Turvey, R & Wisemar, J. 1957. "The Economics of Fisheries" F. A. O. Publication.

TABLE

Statement showing the Fishermen Statistics in Visakhapatnam District

Name of the village	Houses	Population	Active persons	CRAFT Masula boats	 Catamaran	GEAR Shore Seine	 Boat Seine	 Gill nets	 Kuduru nets
1. *Visakhapatnam Taluk*									
Rushikonda	27	72	32	2	28	2	8	20	...
Revedu gollapalam	52	259	80	4	8	4	10	12	...
Mulapalem	175	571	183	10	44	10	63	84	...
Vasupathipalem	164	419	130	6	43	6	52	24	...
Yendada	62	170	71	...	64	...	39	61	...
Jalaripeta	360	1476	552	1	457	1	265	348	...
Kothayatasipeta	481	1915	665	10	282	10	243	514	...
Dibbalapalem	150	415	147	3	54	3	57	107	...
Jalaripallipalem	90	306	102	4	36	4	36	137	...
Gangavaram	420	1857	547	9	195	9	106	304	...
2. *Bhimilipatnam Taluk*									
Chintapalli	158	687	160	16	163	16	94	...	...
Kothasitapalli	36	172	40	4	24	4	11	12	...
Pativada	20	77	25	2	11	2	9	7	...
Puligeddapalem	36	133	30	3	16	3	8	21	...
Kothuru	72	217	94	2	40	2	5	25	...
Pippavalasa	300	872	241	4	110	4	15	55	...
Boddugbrayyapeta	140	462	152	6	82	6	40	84	...

TABLE (*Contd.*)

Statement showing the Fishermen Statistics in Visakhapatnam District

Name of the village	Houses	Population	Active Persons	Masula boats	Catamaran	Shore Seine	Boat Seine	Gill nets	Kuduru nets
				CRAFT		GEAR			
Bodduvenkatapeta	47	121	42	2	68	2	34	50	...
Kondada	112	423	137	...	...	...	...	...	...
Pedakavadigapalem	...	640	269	5	140	5	60	278	...
Kothapalem	120	420	148	66	68	6	30	126	...
Chinkondayapalem	117	360	96	4	42	4	22	52	...
Mukkam	482	2162	682	15	480	15	64	267	...
Chapalakunepuram	182	734	214	4	112	4	38	68	...
Veeravenkayapalem	81	232	62	2	56	2	18	4646	...
Annavaram	21	82	...	...	...	...	...	...	...
Yerrayyapalem	315	1160	432	13	262	13	57	266	...
Chinantogayyapalem	192	895	286	8	136	8	40	98	...
Peddantogayyapalem	300	1696	454	13	247	13	51	160	...
Bhimilipatnam	450	3400	737	17	235	17	178	554	...
Pedauppada	140	643	195	8	77	8	37	97	...
Chinauppada	111	448	123	5	50	9	34	61	...
Paturu	49	241	87	3	37	3	12	34	...
Gangodipalem	110	362	134	3	52	3	21	78	...
Garupeta	75	375	109	4	35	4	30	55	...
Chukkodipalem	90	380	101	3	2	3	20	58	...
Dibbalapalem	115	584	121	5	446	5	27	99	...
Pedamongaripeta	170	684	251	9	74	9	41	130	...
Chinmongaripeta	58	392	212	5	45	7	20	71	...
Kondavarakothuru	60	240	64	2	23	2	14	26	...
3. *Anakapalli Taluk*									
Appakonda	62	272	122	5	30	5	...	51	...
Thikkavaripalem	90	306	102	10	50	10	24	70	...
Jalaripeta	29	121	41	2	17	2	12	6	...
Mutyalapalem	130	677	226	11	59	11	23	41	...
Dibbapalem	120	534	179	6	40	6	18	36	...

TABLE (*Contd.*)

Statement showing the Fishermen Statistics in Visakhapatnam District

Name of the village	Houses	Population	Active persons	Masula boats	Catamaran	Shore Seine	Boat Seine	Gill nets	Kuduru nets
				CRAFT		GEAR			
Thantadi	31	126	38	2	46	2	16	16	...
Kadapalem	208	948	02	14	132	14	63	144	...
Kondapalem	178	799	243	17	96	17	44	128	...
Jalaripalem	64	345	103	...	84	...	18	42	24
Pudiniadana	40	221	65	...	36	...	14	33	...
Lovapalem	114	490	120	3	14	3	15	15	40
Venkayyapalem	104	240	110	2	9	2	...	...	24
Jangaveddipalem	49	196	78	1	8	1	...	...	20
4. *Elamanchili Taluk*									
Rambilli	83	312	130	6	20	6	...	58	40
Narasapuram	127	592	257	8	44	8	...	26	50
Kothapatnam	216	570	248	9	28	9	20	67	130
Bangarammapeta	104	560	238	21	75	21	30	108	35
Revugopalapuram	252	912	335	14	96	14	50	107	200
Chinathunala	127	526	219	5	38	5	18	62	80
Pedathunala	263	1008	453	5	42	5	63	58	...
Dondavaki	47	200	84	2	18	2	12	17	...
Rajayyapeta	379	1450	614	15	270	15	95	275	45
Boyapadu	130	430	183	6	45	6	23	75	40
Amalapuram	85	378	163	2	28	2	...	53	38
Lakshmipuram	34	151	60	2	10	2	5	10	20
Banagarammapeta	126	438	171	11	40	11	40	40	...
Pentakota	317	1540	603	15	130	15	80	48	150
Rayavaram Ganapatinagaram	150	275	144	8	36	18	18	...	...
Venkatanagaram	131	405	153	5	34	5	34	30	48
Rajanagaram	63	276	117	3	22	3	13	...	36
Ratnayyapeta	125	6000	219	8	44	8	36	30	60
Korlayyapeta	61	260	112	2	26	3	13	40	...
Palachetturu	98	380	412	6	62	6	43	...	70

BOUNDARY LAYER
IN SOME UNSEPARATED AXISYMMETRICAL FLOWS

RADHEY SHIAM
Lecturer in Mathematics,
Udaipur University, M. B. College, Udaipur.

SUMMARY

In this paper, the method of Blasius Series has been adopted to consider the boundary layer on two solids namely (i) solid formed by the revolution of the curve $r=\frac{3}{4}$ cosec $\frac{\theta}{2}$ about the initial line and (ii) the paraboloid of revolution. The equations of these surfaces have been taken in such a way that the nose radius is unity in each case. The coefficient of local skin friction has been found out. The convergence of the series has been improved by some devices. Approximate values of local skin friction have been found out in each of these cases.

In Part I, the case of the solid formed by revolving the curve $r=\frac{3}{4}$ cosec $\frac{\theta}{2}$ about the initial line has been discussed.

In Part II, the case of paraboloid of revolution is discussed.

In Part III, comparison of the coefficients of local skin friction for the two solids has been made.

INTRODUCTION

The equation to the curve to be revolved about the initial line is

$$r=a\ \text{cosec}\,\frac{\theta}{2} \qquad \ldots\ \ldots (1)$$

In order that the nose radius may be unity

$$a=\frac{3}{4}\ ;$$

and therefore, the equation to the generating curve is

$$r=\frac{3}{4}\ \text{cosec}\ \frac{\theta}{2} \qquad \ldots\ \ldots (2)$$

The solid formed by revolving this curve about the initial line is placed in an inviscid stream flowing with unit velocity from infinity in the positive direction of the initial line. The stream function for inviscid flow obtained from Milne Thompson [1] is

$$\psi=\left(\frac{9}{16}\cos\theta-\tfrac{1}{2}r^2\sin^2\theta\right) \qquad \ldots \ldots (3)$$

whence
$$q_r=-\frac{1}{r\sin\theta}\cdot\frac{\partial\psi}{r\partial\theta}$$
$$=\left(\frac{9}{16r^2}+\cos\theta\right)$$
$$q_\theta=\frac{1}{r\sin\theta}\cdot\frac{\partial\psi}{\partial r}$$
$$=\sin\theta$$

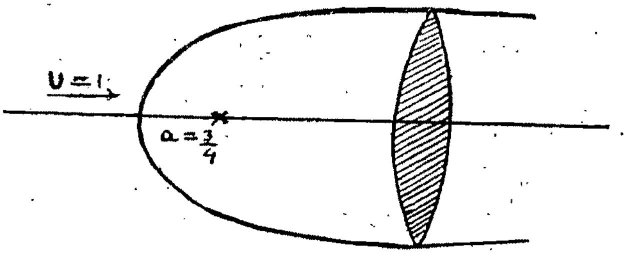

fig 1

If s denotes the length of the arc of generating curve from the vertex and n, the normal distance from the curve, and U_1 (s, o) the surface speed along the wall, then,

$$U_1\ (s,o)=\sqrt{q_r^2+q_\theta^2}\ ,\ \text{for}\ r=\frac{3}{4}\operatorname{cosec}\frac{\theta}{2}$$
$$=\left\{\left(\sin^2\frac{\theta}{2}+\cos\theta\right)^2+\sin^2\theta\right\}^{\frac{1}{2}}$$
$$=\cos\frac{\theta}{2}\left(1+3\sin^2\frac{\theta}{2}\right)^{\frac{1}{2}} \qquad \ldots \ldots (4)$$

To measure s from the stagnation point, we put

$$\theta=\pi-\phi$$

Therefore,
$$U,\ (s,o)=\sin\frac{\phi}{2}\left(1+3\cos^2\frac{\phi}{2}\right)^{\frac{1}{2}} \qquad \ldots \ldots (5)$$
$$=\phi-\frac{13}{96}\phi^3+\frac{241}{30720}\phi^5-\frac{2773}{20643840}\phi^7 \ldots \qquad \ldots \ldots (6)$$

which is convergent for $-\pi\leqslant\phi\leqslant\pi$

Blasius Series

We adopt the approximations of Blasius and Frossling [2] which require an expansion for velocity in the boundary layer in powers of s.

First, we shall find an expansion for ϕ in powers of s, and, then, substitute this expansion in (6)

Now, from equation (2)

$$ds = -\frac{\frac{3}{8}\sqrt{1+3\sin^2\frac{\theta}{2}}}{\sin^2\frac{\theta}{2}}d\theta$$

$$= \frac{\frac{3}{8}\sqrt{1+3\cos^2\frac{\phi}{2}}}{\mathrm{Cos}^2\frac{\phi}{2}}d\phi$$

or

$$\frac{d\phi}{ds}=\frac{8}{3}\sqrt{\frac{\cos^2\frac{\phi}{2}}{1+3\cos^2\frac{\phi}{2}}}$$

$$=\frac{4}{3}\left\{1-\frac{5}{32}\phi^2+\frac{17}{6144}\phi^4+\frac{23}{589824}\phi^6\ldots\ldots\right\} \qquad \ldots\ldots (7)$$

Now, assume,

$$\phi=a_1s+a_3s^3+a_5s^5+a_7s^7 \qquad \ldots\ldots (8)$$

($a_0=a_2=a_4=a_6=\ldots\ldots\ldots\ldots.0$, because, the generating curve is symmetrical about the initial line, also $s=0$ when $\phi=0$)

$$\frac{d\phi}{ds}=a_1+3a_3s^2+5a_5s^4+7a_7s^6 \qquad \ldots\ldots (9)$$

Now, substituting the value of ϕ from (8) into (7)

$$\frac{d\phi}{ds}=\frac{4}{3}\left\{1-\frac{5}{32}a_1^2s^2+\left(\frac{17}{6144}a_1^4-\frac{5}{16}a_1a_3\right)s^4+\left(\frac{23}{589824}a_1^6+\frac{17}{1516}a_1^3a_3-\frac{5}{16}a_1a_5-\frac{5}{32}a_3^2\right)s^6\ldots\right\} \qquad \ldots\ldots (10)$$

Comparing the coefficients of like powers of s in (9) and (10) and finding the values of a_1, a_3, a_5, etc. and substituting them in (8) we have,

$$\phi=\frac{4}{3}s-\frac{10}{81}s^3+\frac{13}{810}s^5-\frac{5995}{918540}s^7 \qquad \ldots\ldots (11)$$

And, therefore, (6) becomes

$$U_1(s,0)=\frac{4}{3}s-\frac{4}{9}s^3+\frac{56}{405}s^5-\frac{3104}{2187\times 35}s^7 \qquad \ldots\ldots (12)$$

From Frossling [3], the Blasius Series for the velocity in the boundary layer is given by the formula

$$u=u_1sf'_1+2u_3s^3f_3'+3u_5s^5f'_5+4u_7s^7f'_7 \qquad \ldots\ldots (13)$$

where u_1, u_3, u_5, u_7,.....are the coefficients of s, s^3, s^5, s^7.....in the expansion of U_1 (s, o) in powers of s and f_1', f_3', f_5', f_7'.....etc. are functional coefficients in terms of dimensionless coordinate N corresponding to n *i.e.*,

$$N = n\sqrt{\frac{2u_1}{\nu}} \qquad \ldots \ldots (14)$$

$$= n\sqrt{\frac{8}{3\nu}} \qquad \ldots \ldots (14a)$$

Hence,

$$u = \frac{4}{3}\, s f_1'(N) - \frac{8}{9} s^3 f_3'(N) + \frac{56}{135} s^5 f_5'(N) - \frac{12416}{2187\times 35} s^7 f_7'(N) \qquad \ldots (15)$$

THE COEFFICIENT OF LOCAL SKIN FRICTION

$$C = \frac{\tau}{\frac{1}{2}\rho U^2}$$

$$= \frac{2\tau}{\rho U^2}$$

$$= 2\nu\left(\frac{\partial u}{\partial n}\right)$$

$$= 2\nu\left(\frac{\partial u}{\partial N}.\frac{\partial N}{\partial n}\right)$$

$$= 4\sqrt{\frac{2\nu}{3}}\left(\frac{\partial u}{\partial N}\right) \qquad \text{From (14a)} \qquad \ldots \ldots (16)$$

Also, R, the Reynold's number $= \frac{U\rho l}{\mu} = \frac{1}{\nu}$

Therefore, $$C_f = 4\sqrt{\frac{2}{3R}}\left(\frac{\partial u}{\partial N}\right)$$

or $$R^{\frac{1}{2}} C_f = 4\sqrt{\frac{2}{3}}\left\{\frac{4}{3} s f_1''(N) - \frac{8}{9} s^3 f_3''(N) + \frac{56}{135} s^5 f_5''(N) - \frac{12416}{2187\times 35} s^7 f_7''(N) \;\ldots\ldots\right\} \qquad \ldots \ldots (17)$$

To utilise the approximations of Frossling [3] we also require expansion of $\overset{\frown}{\omega}$ in powers of s where $\overset{\frown}{\omega}$ is the length of perpendicular from a point on the generating curve to the axis of revolution.

Now, $$\overset{\frown}{\omega} = r \sin\theta$$

$$= \tfrac{3}{4} \operatorname{cosec}\frac{\theta}{2} \sin\theta$$

$$= \frac{3}{2}\cos\frac{\theta}{2}$$

$$= \frac{3}{2}\sin\frac{\phi}{2}$$

$$=\tfrac{3}{4}\left(\phi-\frac{\phi^3}{24}+\frac{\phi^5}{1920}-\frac{\phi^7}{64\times 5040}\cdots\cdots\right)$$

$$=s-\frac{1}{6}\,s^3+\frac{37}{1080}s^5-\frac{12559}{918540}s^7\ldots\ldots\text{from (11)} \qquad \ldots\ldots(18)$$

The functional coefficients $f_1''(N)$, $f_3''(N)$, $f_5''(N)$, $f_7''(N)$....etc. are calculated below by making use of the work of Frossling [3] and also equations (12) and (18).

Therefore, $f_3''=g_3''+\frac{1}{2}h_3''$

$$f_5''=g_5''+\frac{37}{112}h_5''+\frac{15}{14}k_5''+\frac{15}{28}j_5''+\frac{15}{56}q_5''$$

$$f_7''=g_7''+\frac{12559}{36\times 776}h_7''+\frac{35\times 27}{3104}j_7''+\frac{27\times 35}{776}k_7''+\frac{37\times 63}{6208}l_7''+$$
$$\frac{441}{388}p_7''+\frac{27\times 35}{6208}q_7''+\frac{37\times 63}{12416}v_7''+\frac{27\times 35}{1552}t_7''+\frac{441}{776}z_7''\cdots\ \cdots(19)$$

The values of f_1'', g_3'', h_3''......g_5'', h_5'',.........g_7'', h_7''..... ......have been substituted from the tables by Scholkemeir [4] and, therefore,

$$R^{\frac{1}{2}}C_f=4\sqrt{\tfrac{2}{3}}\left[1{\cdot}2369s-{\cdot}9510s^3+{\cdot}4648s^5-{\cdot}1428s^7\ldots\ldots\right]\ \cdots\ \cdots(20)$$
$$=[4{\cdot}0397s-3{\cdot}1060s^3+1{\cdot}5180s^5-{\cdot}4664s^7\ldots\ldots\ldots]\ \cdots\ \cdots(21)$$

THE CONVERGENCE OF THE SERIES (12) AND (21)

From, (7) $$\frac{ds}{d\phi}=\frac{3}{8}\,\frac{\sqrt{1+3\cos^2\dfrac{\phi}{2}}}{\cos^2\dfrac{\phi}{2}}$$

which shows that there are singularities of $\dfrac{ds}{d\phi}$ in the plane of ϕ at $\phi=\pm\pi$ and branch points at $\phi=\pi-i\log 3$, $\pi+i\log 3$, $-\pi-i\log 3$, $-\pi+i\log 3$. Consequently, there will also be the singularities and branch points of s in the plane of ϕ at these points.

Hence, the expansion of s in powers of ϕ will be convergent and the radius of convergence will be $\phi=\pi$.

From reversion of power series, we can say that the expansion of ϕ in powers of s would have a radius of convergence given by the values of s corresponding to $\phi=\pi$ *i. e.*, $s=\infty$. Thus the series (11) will be convergent for all values of s. When we substitute the series (11) in (6) for ϕ, the resulting series (12) will be convergent for all values of s.

Again, the unsigned ratios of successive coefficients in (21) are 1·3, 2·040, 3·25.......... ....which seem to increase without limit so that the radius of convergence of the series (21) may be taken to be infinity as in Van Dyke [7].

PART II

The transformation

$$-x+\tfrac{1}{2}+\bar{\omega}i = \tfrac{1}{2}(\xi+i\eta)^2 \qquad \ldots\ldots(22)$$

gives

$$\left.\begin{aligned} -x+\tfrac{1}{2} &= \tfrac{1}{2}(\xi^2-\eta^2) \\ \bar{\omega} &= \xi\eta \end{aligned}\right\} \qquad \ldots\ldots(23)$$

Elimination of η between these two equations leads to

$$-x+\tfrac{1}{2}-\tfrac{1}{2}\xi^2 = -\frac{\bar{\omega}^2}{2\xi^2}$$

This shows that $\xi=1$ is a parabola

$$x=\frac{\bar{\omega}^2}{2}\text{, with nose radius unity} \qquad \ldots\ldots(24)$$

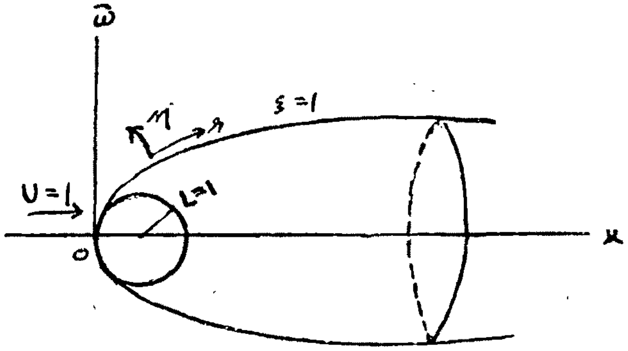

fig 2.

The stream function for the inviscid flow past the paraboloid (obtained by revolving the above parabola about its axis) with free stream velocity U=1 in the positive direction given by Milne Thompson [5] with necessary modification is

$$\psi = -\tfrac{1}{2}(\xi^2-1)\,\eta^2 \qquad \ldots\ldots(25)$$

The surface speed on the boundary from Milne Thompson [6]

is

$$\begin{aligned} U_1(s,o) &= \frac{1}{J\bar{\omega}}\left(\frac{\partial\psi}{\partial\xi}\right)_{\xi=1} \\ &= -\frac{1}{\sqrt{\eta^2+1}}\cdot(-\eta) \\ &= \frac{\eta}{\sqrt{\eta^2+1}} \qquad \ldots\ldots(26) \end{aligned}$$

Again, to utilise the Blasius Series, $U_1(s, o)$ is to be expanded in powers of s

Now, we have,

$$(ds)^2 = (dx)^2 + (d\bar{\omega})^2$$

$$= \left\{\left(\frac{\partial x}{\partial \xi}\right)d\xi + \left(\frac{\partial x}{\partial \eta}\right)d\eta\right\}^2 + \left\{\left(\frac{d\bar{\omega}}{d\xi}\right)d\xi + \left(\frac{d\bar{\omega}}{d\eta}\right)d\eta\right\}^2$$

$$= (\xi^2+\eta^2)\{(d\xi)^2+(d\eta)^2\} \text{ with the help of (23)} \qquad \ldots\ldots(27)$$

Whence; $ds = \sqrt{\eta^2+1}\, d\eta$ on $\xi=1$

Integrating,

$$s = \tfrac{1}{2}\eta\,\{\eta\sqrt{\eta^2+1} + \sinh^{-1}\eta\} + \psi \text{ (taking } s=o \text{ at } =0) \ldots \qquad \ldots(28)$$

Now, $\bar{\omega}=\eta$, on the paraboloid $\xi=1$ $\qquad \ldots\ldots(29)$

Also, let us assume

$$\bar{\omega} = a_1 s + a_3 s^3 + a_5 s^5 + a_7 s^7 \ldots. \qquad \ldots\ldots(30)$$

($a_0=a_2=a_4=a_6=a_8\ldots.=0$, since $s=o$, $\bar{\omega}=0$ and also the parabola is symmetrical about x axis)

Diff. w. *r.* to s

$$\frac{d\bar{\omega}}{ds} = a_1 + 3a_3 s^2 + 5a_5 s^4 \qquad \ldots\ldots(31)$$

Also, replacing η by $\bar{\omega}$ in (28)

$$s = \tfrac{1}{2}\{\bar{w}\sqrt{\bar{\omega}^2+1} + \sinh^{-1}\bar{\omega}\}$$

Diff., this also, *w. r.* to s

$$1 = \frac{d\bar{\omega}}{ds}(\bar{\omega}^2+1)^{\frac{1}{2}}$$

$$\text{or } \left(\frac{d\bar{\omega}}{ds}\right)^2 = \frac{1}{\bar{\omega}^2+1}$$

$$= \frac{1}{1+(a_1 s + a_3 s^3 + a_5 s^5 \ldots.)^2} \quad \text{From (30)} \qquad \ldots\ldots(32)$$

$$= (a_1 + 3a_3 s^2 + 5a_5 s^4 \ldots.)^2 \quad \text{From (31)} \qquad \ldots\ldots(33)$$

Expanding (32) and (33) in powers of s and equating the coefficients of like powers of s in two expansions, the values of the numerical coefficients are found, and therefore,

$$\bar{\omega} = s - \tfrac{1}{6}s^3 + \frac{13}{120}s^5 - \frac{493}{5040}s^7 + \frac{37369}{362880}s^9 \qquad \ldots\ldots(34)$$

And therefore,

$$U_1(s, o) = \frac{\bar{\omega}}{\sqrt{\bar{\omega}^2+1}} \quad \text{From (29)}$$

$$= s - \tfrac{2}{3}s^3 + \frac{11}{15}s^5 - \frac{292}{315}s^7 \qquad \ldots\ldots(35)$$

(by substituting for $\bar{\omega}$ from (34)

BLASIUS SERIES

Substituting, the values of u_1, u_2, u_3, etc. in (13) from (35) we have

$$u = \left[sf_1'(\mathrm{N}) - \tfrac{4}{3} s^3 f_3'(\mathrm{N}) + \frac{11}{5} s^5 f_5'(\mathrm{N}) - \frac{1168}{315} s^7 f_7'(\mathrm{N}) \cdot\cdot \right] \cdot\cdot (36)$$

Where $\mathrm{N} = n\sqrt{\frac{2}{\nu}}$ From (14)

And, therefore,

$$\mathrm{R}^{\frac{1}{2}}\,\mathrm{C}_f = 2\sqrt{2}\left[sf_1''(\mathrm{N}) - \tfrac{4}{3}s^3 f_3''(\mathrm{N}) + \frac{11}{5}s^5 f_5''(\mathrm{N}) - \frac{1168}{315}s^7 f_7''(\mathrm{N}) \cdots\cdots \right]$$

$$= 2\sqrt{2}\left[sf_1''(\mathrm{N}) - \tfrac{4}{3}s^3\left(g_3'' + \tfrac{1}{4}h_3''\right) + \frac{11}{5}s^5\left(g_5'' + \frac{13}{88}h_5'' + \frac{20}{33}k_5'' + \frac{5}{33}j_5'' + \frac{5}{132}q_5''\right) - \frac{1168}{315}s^7\left(g_7'' + \frac{493}{4692}h_7'' + \frac{35}{1752}j_7'' + \frac{70}{219}k_7'' + \frac{91}{1168}l''_7 + \frac{77}{146}p_7'' + \frac{35}{7008}q_7'' + \frac{91}{4672}v_7'' + \frac{35}{438}t_7'' + \frac{77}{584}z_7''\right) \cdots \right]$$

$$= 2\sqrt{2}\,[\cdot 9277\,s - 1\cdot 4116\,s^3 + 2\cdot 2519\,s^5 - 3\cdot 6201\,s^7 \ldots\ldots]$$

$$= 2\cdot 6239\,s - 3\cdot 9926\,s^3 + 6\cdot 3693\,s^5 - 10\cdot 2391\,s^7 \quad \cdot\cdot\ \cdot\cdot\ (37)$$

THE CONVERGENCE OF THE SERIES (37)

$$\mathrm{U}_1(s, o) = \frac{\eta}{\sqrt{\eta^2 + 1}}$$

$$\text{or } \eta = \frac{\mathrm{U}_1}{\sqrt{1 - \mathrm{U}_1^2}}$$

Substituting this value of η in (28)

$$s = \tfrac{1}{2}\left\{ \frac{\mathrm{U}_1}{1 - \mathrm{U}_1^2} + \sinh^{-1}\frac{\mathrm{U}_1}{\sqrt{1 - \mathrm{U}_1^2}} \right\}$$

If now, $\mathrm{U}_1 = \infty$, then

$$s = -\frac{\pi}{4}i$$

This shows that there is a singularity of U_1 at $s = -\frac{\pi}{4}i$, hence, the series for $\mathrm{U}_1(s, o)$ converges for $s < \frac{\pi}{4}$

The unsigned ratios of successive coefficients in series (37) are respectively ·6572, ·6248, ·6225

It seems in this case that these ratios approach $(\frac{1}{4}\pi)^2 = \cdot 6169$, so that we may take that the Blasius Series converges and the radius of convergence may be taken as $s = \frac{\pi}{4}$

Thus, the convergence of Blasius Series is the same as that of the series for inviscid surface speed $U_1(s, o)$.

TRANSFORMATION OF BLASIUS SERIES FOR SKIN FRICTION

To improve the convergence of the series (37) we shall follow the method used by Van Dyke [7]. We see that the series is limited here by a mathematical singularity lying on the imaginary axis in the plane of s regarded as complex variable. It is not limited by any physical singularity in the boundary layer. Therefore, the range of convergence can be enlarged by a change in the variable. Therefore, recasting the series in powers of η by the use of (28)

$$\frac{1}{2\sqrt{2}} R^{\frac{1}{2}} C_f = \cdot9277\,\eta - 1\cdot2570\,\eta^3 + 1\cdot5229\,\eta^5 - 1\cdot7469\,\eta^7 \quad \ldots\ldots \quad (38)$$

The unsigned ratios of the successive coefficients, now, are ·7380, ·8254 ·8718.

In this case, it seems likely, that these ratios approach unity. Therefore the above series converges for η less than one. Thus in terms of s, the radius of convergence has increased, because $\eta = 1$ corresponds to $s = 1\cdot15$ whereas the previous value was $s = \frac{\pi}{4}$ *i. e.*, $s = \cdot75$. We may further enlarge the range of convergence by applying Euler's transformation. Recasting, the series in powers of a new variable z

$$z = \frac{\eta^2}{1+\eta^2}, \text{ or } \eta^2 = \frac{z}{1-z}$$

Now, since, z is an even function of η and C_f is an odd function of η. Therefore, applying Euler's transformation to $\eta\, C_f$ we have

$$\frac{1}{2\sqrt{2}}\left(R^{\frac{1}{2}}\eta\right) C_f = \cdot9277\,\eta^2 - 1\cdot2570\,\eta^4 + 1\cdot5229\,\eta^6 - 1\cdot7469\,\eta^8$$

$$\text{or} \quad \tfrac{1}{2}\,(-Rx)^{\frac{1}{2}} \cdot C_f = \cdot9277z - \cdot3293\, z^2 - \cdot0564\, z^3 - \cdot0005\, z^4 \quad \ldots\ldots (39)$$

The unsigned ratios of successive coefficients are

2·8172, 5·8387, 104·4444

These seem to approach some number greater than unity, and, therefore, it is safe to say that the radius of convergence is some quantity greater than one. This is in accordance with Van Dyke analysis [7].

Thus, the series (39) converges to the correct results upto $Z = 1$ which corresponds to $s = \infty$

PART III

We now proceed to compare the coefficients of local skin friction for the two solids for some given values of s. In the case of paraboloid, the values of $R^{\frac{1}{2}} C_f$ have been calculated for s correct to three decimal places.

s	η	$R^{\frac{1}{2}} C_f$ for paraboloid	s	$R^{\frac{1}{2}} C_f$ for the surface by $r=\frac{3}{4}\mathrm{cosec}\,\frac{\theta}{2}$
·500	×	·9318	·500	1·6754
1·0001	·893	·019	1·000	1·9853
1·5002	1·235	−12·835	1·500	− ·8648
2·0001	1·528	−68·843	2·000	− 27·8918

ACKNOWLEDGEMENT

I want to express my gratitude to Dr. J. P. Agrawal, Mathematics Department Agra College, Agra for his kind help and guidance throughout in the preparation of this paper.

REFERENCES

1. Milne Thompson, 1960. *Theoretical Hydrodynamics*, p. 456-57.
2. Schlichting, H. 1960. *Boundary Layer Theory*, p. 185-7.
3. Schlichting, H. 1960. *Boundary Layer Theory*, p. 186-7.
4. Rosen Head, L. 1963. *Laminar Boundary Layers*, 425.
5. Milne Thompson, 1960. *Theoretical Hydro Dynamics*, p. 478-79.
6. Milne Thompson, 1960. *Theoretical Hydro Dynamics*, p. 474.
7. Van Dyke, 1964. *Journal of Fluid Mechanics*, Part I, May' 1964.

MORPHO-HISTOLOGICAL STUDIES ON THE ALIMENTARY CANAL OF *BAGARIUS BAGARIUS* HAM.

RATAN SINGH
Department of Zoology, B. R. College, Agra.

Bagarius bagarius (Family-Sisoridae) is generally called as a fresh water shark on account of its ugly appearance. It is sluggish by nature and attains a large size. It is difficult to catch the fish as it generally escapes by damaging the tackle. It is interesting to note that this fish moves very quickly and thrusts itself into the mud when shot with a bullet.

Bagarius is a voracious feeder and is fond of live prey which it destroys. The food contents of the fish usually consist of small fishes. A study of the literature on the food, feeding habits and the digestive tract of fishes reveals that the subject has attracted the attention of a large number of workers since very early times. The important references are those of Blake (1930, 1936), Rogick (1931), Sarbahi (1939) and Curry (1939). Al-Hussaini (1946,1949) has discussed in a comparative way the alimentary canal of a few teleosts.

However, there is no work on the gut organisation of this fish which is of great economic importance. To fill up this gap in our knowledge, a detailed study was made on the digestive system of *Bagarius bagarius.*

MATERIAL AND METHODS

A large number of specimens of *Bagarius* were collected from Jumuna river and Kitham lake on the outskirts of Agra. For morphological investigation freshly collected fishes were dissected, the mucosal folds were studied, by giving a median longitudinal incision and fixing in 10% formalin.

The dentition and gill-rakers were examined by making alizarine transparencies which gave a clear picture about the structure and articulation of teeth on different bones.

For histological study, different parts of the alimentary canal were fixed in Bouin's picroformol acetic acid. The material was cleaned either in cedar wood oil or benzene. The sections 8 microns thick were stained with Delafield or Ehlrich's Haematoxyline and counter stained with Eosine. Mallory's triple stain was also tried.

MORPHOLOGY OF ALIMENTARY CANAL

The alimentary canal along with mouth and anus constitute the organs of food capture, digestion and absorption. The alimentary canal of *Bagarius bagarius* is small, almost a straight tube running within the body cavity upto the anus which is situated posteriorly at about two-third the length of the body. It consists of the mouth, buccal cavity, pharynx, oesophagus, stomach, intestine, rectum and anus.

Mouth and Bucco-pharynx :

The mouth is a large crescentic opening, being slightly sub-ventral in position. It is bounded by upper and lower jaws. The upper jaw which is formed by the elongated premaxillaries is slightly longer than the lower jaw which is formed by the dentaries.

The mouth leads into a spacious dorsoventrally flattened buccal cavity. The roof of the buccal cavity is formed by the base of the cranium, the sides and the floor by the branchial arches, the mucosal thickening at the anterior part of the floor of the buccal cavity is suggestive of a tongue-like structure analogous to a true tongue.

Posteriorly the buccal cavity leads into a dorsoventrally compressed pharynx. The roof of the pharynx is arched while the floor is almost flat. The lateral sides of the pharynx are perforated by gill clefts. The roof of the pharynx is supported by the pharyngobranchials and epibranchials while the sides and the floor are supported by ceratobranchials, hypobranchials and basibranchials.

On the surface of each branchial arch, separating the adjacent gill slits, are rows of gill rakers. The arrangement of gill rakers on the different branchial arches is different. The gill rakers of the adjoining arches are so arranged that they provide an interlocking arrangement and serve as a sieve so that food particles are not allowed to escape with the respiratory current.

Arrangement of Teeth:

The dentition in *Bagarius,* as also in most other teleosts, is homodont and polyphyodont. A typical tooth comprises of a pointed apex, the crown and the basal part known as the base by which it is attached to the bone. The tooth is made up of dentine covered over by enamel. The dentine encloses a spacious pulp cavity which contains pulp, connective tissue, blood capillaries, and nerve endings. The dentine is non vascular but is traversed by numerous radiating branches called the dentinal tubules into which extend protoplasmic prolongations from the scleroblasts which secrete the dentine.

Teeth on the roof of Bucco-pharynx :

(a) *Maxillary teeth*—The maxillary teeth are borne by the elongated premaxillaries. These include villiform closely set teeth arranged in several rows. These teeth are unequal in size, those of the outer row are smaller while those of the inner row are large and stout.

(b) *Pharyngeal teeth*—In the middle of the posterior region of the pharynx are present a pair of circular cushion like pharyngeal pads which are beset with sharply pointed teeth which are curved and directed backward.

Teeth on the floor of Bucco-pharynx :

(a) *The mandibular teeth* are arranged in two rows on the dentaries. In addition, there is a cluster of small irregularly arranged teeth on either side of the mandibular symphysis.

(b) *The horny pad teeth* are borne on a pair of triangular horny pads, located on the floor of the bucco-pharynx, immediately behind the fourth gill arch.

All these teeth except those on the infra-pharyngeal pads are situated in depressions and are fixed by fibrous ligaments to the underlying bones. These teeth, in all probabilities are not masticatory in function but only help in the capture of the prey and prevent its escape.

Oesophagus—The pharynx pierces through the septum transversum to open into the short, muscular oesophagus. It serves only as a conducting tube between the pharynx and the stomach. The oesophagus is situated dorsal to the pericardial chamber and emerges into the visceral cavity where it passes over the liver lobes.

Stomach—The oesophagus passes insensibly into the stomach without any external demarcation. However, in the larger specimens, an external circular constriction marks the boundary between the oesophagus and the stomach. The stomach of *Bagarius* is a long, thick walled, cylindrical bag-like structure. It can be divided into three parts: (*i*) the anterior cardiac stomach, (*ii*) posterior blind portion called the fundus and (*iii*) the pyloric region lies on the left side.

Intestine—The intestine originates from the pyloric end of the stomach. It is long, N-shaped in appearance and lies on the right side of the body cavity. Soon after its origin, the intestine curves upwards, crosses below the cardiac stomach and then takes three turns vertically up and down with small coils at each bend. Finally it descends down and becomes dorsal in position and makes a loop below the fundus.

Rectum—The last portion of the intestine which is comparatively thin walled is sometimes known as the rectum. However, there is no external demarcation between the intestine and the rectum.

From the left side of the posterior most region of the rectum, arises a single blind outgrowth known as the rectal gland. Finally the rectum opens to the exterior.

Associated organs—The associated organs of the alimentary canal include liver and pancreas with gall bladder. As the spleen is also found in association with the digestive organs, it has become customary to describe this also with the digestive organs.

Liver—The liver of *Bagarius* is rather large, bilobed organ yellowish in colour. The two lobes cover the anterior part of the stomach. It is attached to the posterior face of the septum transversum by a suspensary ligament. The liver extends backwards along the ventrolateral sides of the stomach, attached by the hepatic omentum.

The gall bladder is thick, oval structure, situated laterally beneath the right lobe of the liver. It is closely applied to the dorsal side of the anterior part of the intestine. The cystic and bile ducts are very short. The bile secreted by the liver is green in colour and is alkaline in reaction. It imparts green colour to the gall bladder.

Pancreas—The Pancreas is in the diffused shape and is embedded in the adipose tissue surrounding the intestine. It is more profusely distributed between the loops of the intestine.

Spleen—The spleen of *Bagarius* is a small, oval structure, brown or chocolate in colour. It is situated along the mid-dorsal line over the anterior part of the stomach.

The mucosal folds—The internal mucosa of the alimentary canal is produced into mucosal folds which are different in the various parts of the gut.

The mucosal epithelium of the buccal cavity is smooth and without any folds. However, a few ill defined folds are seen in the region of the pharynx.

The mucosa of oesophagus is produced into about 25 well defined longitudinal folds which are simply posterior continuations of the pharyngeal folds.

The mucosa at the junction of the oesophagus and the stomach is produced into a deep circular furrow which works as a constrictor valve between the two regions. The mucosa of the cardiac stomach is produced into well developed longitudinal folds which range from 12 to 17 in number.

The pyloric part of the stomach has a few longitudinal folds which gradually decrease towards the fundus.

The internal lining of the stomach is produced into a network of papillae-like structures which run obliquely. They branch and anastamose profusely, thus presenting a velvety appearance.

These papillae continue into the rectum where they become comparatively small. These papillae almost disappear in the posterior most part of the rectum. The papillae are here replaced by a few very fine longitudinal folds.

HISTOLOGY OF THE ALIMENTARY CANAL

Buccal cavity—The buccal cavity is lined by two layers only *i.e.*, the mucosa and submucosa. The mucosa consists of stratified epithelium. Some of these cells tend to become elongated specially towards the submucosa. A few granular, mucus cells and a few oval shaped taste buds are also present.

The submucosa is composed of connective tissue fibres. The inner portion lying immediately beneath the mucosa consists of compactly placed connective tissue. The outer layer has loosely packed tissue which contains blood vessels and nerve fibers.

Pharynx—The mucosa of phyranx is six to seven layers thick. It also contains a few taste buds, mucus cells and a few granular cells. The submucosa which is composed of both compactly packed and loosely arranged connective tissue has a large number of blood vessels and nerve fibers.

A proper muscular layer is absent. However, in the posterior region of the pharynx, a few scattered muscle bundles of both longitudinal and circular nature are present.

Oesophagus—The oesophagus consists of the usual four layers *i.e.*, mucosa, sub-mucosa, muscularis and serosa. The mucosa of the oesophagus consists of columnar epithelial cells with scattered gastric glands. A distinct submucosa is present which consists of loose connective tissue fibers which become compactly placed posteriorly. The submucosa is richly vascular and is provided with nerve fibers.

The muscular layer consists of an outer longitudinal layer and an inner circular layer. Both the layers are of almost uniform thickness. The serosa forms the outermost layer and is formed of thin flattened cells.

Cardiac stomach—The mucosa of the cardiac stomach is made up of columnar cells and gastric crypts. In between the two are to be found a few small rounded granular cells. The crypts are composed of a large number of gastric glands which open into the lumen of the stomach either singly or through a common duct. The submucosa is made up of loose connective tissue fibers. It is continued in the middle of the mucosal folds as there are elongated tunica propria. There is no stratum compactum.

The muscularis layer is very thick. It consists of the outer longitudinal layer and the inner circular layer which is about 3-4 times thicker than the longitudinal layer. The serosa is comparatively thick and is composed of a single layer of columnar cells.

Pyloric stomach—The mucosa is made up of columnar cells, mucus cells and granular cells. Just beneath the columnar cells, there is a region of stratum granulosum which consists of 3 or 4 layers of small rounded cells. The gastric glands are absent in this region. The submucosa is thinner than that of the cardiac stomach. It enters the elongated narrow mucosal folds as very fine tunica propria.

The muscularis is almost similar to that of the cardiac stomach except that the longitudinal layer is thinner while the circular layer is thicker than the cardiac stomach.

Fundus—The posterior blind end of the stomach may be formed as blind sac or fundus. The mucosa of fundus is almost similar to that of the cardiac stomach. The gastric crypts are more elongated and the stratum granulosum is absent. The submucosa is comparatively thick. It is composed of compact connective tissue which is highly vascular. Tunica propria is elongated.

The muscularis is made up of an outer longitudinal layer and an inner circular layer. The thickness of the two layers is in between those of the cardiac and the pyloric stomach. The serosa consists of short, rounded or oval cells.

Intestine—The wall of the intestine is also lined with the usual four layers. The mucosa consists of columnar cells, rounded mucus cells and a few small granular cells. There is no definite stratum granulosum. The submucosa is a thin region of connective tissue fibers which are highly nucleated and richly vascular. The tunica propria is a thin elongated layer. A stratum compactum is absent.

The muscularis of intestine consists of a very thin outer layer of longitudinal muscles and an inner thick layer of circular muscle fibers. The serosa is a very thin layer of longitudinally elongated flattened cells.

Rectum—The histology of rectum is precisely similar to that of the intestine. The mucosa is formed of columnar cells with centrally placed nuclei. Immediately beneath these cells is to be found a layer of granular cells. The submucosa is made up of areolar connective tissue which is highly nucleated and vascularized. The tunica propria enters the mucosal folds.

The outer longitudinal layer of muscularis is thin whereas the inner circular layer is comparatively thick. The serosa is thin and consists of a single layer of vascular flattened cells.

Rectal gland—The rectal gland is a hollow outgrowth of the rectum. The mucosa of rectal gland is thrown into complex mucosal folds which almost obliterate the lumen of the gland. The mucosa consists of stratified cells, rounded granular cells and gland cells. The stratified layer is made up of flattened cells with centrally placed nucleus. Beneath this layer are to be found rounded or oval granular cells. This layer is followed by the presence of numerous glandular cells which are oval or polygonal in shape. These glandular cells usually aggregate together to form granular crypts which somewhat resemble the gastric glands. A top plate is also present. The submucosa is represented only as a thin vascular connective tissue layer which penetrate into the mucosal folds as a very narrow region between the mucosa and muscularis.

The muscularis consists of the usual outer longitudinal layer and inner circular layer. Both the layers are quite thin and are richly vascular. The serosa of rectal gland is rather thicker than that of the rectum.

DISCUSSION

It is expected that the morphology and histology of the alimentary canal of a fish are adapted to the character of food that it takes. Suyehiro (1941) has said that the feeding habit of fishes cannot easily be correlated with the morphological structure of the gut. Authors like Steven (1930) and Martin (1954) have emphasized the view that the fish can adapt itself to the diet available in the particular environment. The observations minimize the chances of a true correlationship between the diet and the morphology and histology of the alimentary canal.

The fish, *Bagarius bagarius* is mainly carnivorous in its feeding habit. Its subventral mouth points to its bottom feeding habit. The presence of a large number of well developed teeth also agree with its carnivorous diet as it usually feeds on large sized animals which are retained in the buccal cavity with the help of well developed teeth.

According to Inms (1904) the gill rakers serve for straining mechanism. The moderate development of the gill rakers can also be correlated with the fact that they feed on large food particles. The small size of the alimentary canal can also be correlated with its carnivorous feeding habit. According to Al-Hussaini (1947), the size of the gut varies according to their feeding habits, it is long in the herbivorous fish and short in the carnivorous fish.

The presence of numerous taste buds specially in the bucco-pharynx suggests that the fish depends on taste buds for the selection of food.

The arrangement of gastric glands has been differently described by different authors. According to Macallum (1886) the glands occur in pyloric stomach while Ghazzawi (1935) reported the presence in the cardiac region. Ishida (1935) has described their absence in either of the region. In *Bagarius bagarius* the gastric glands are present only in the cardiac stomach.

The presence of a rectal caecum in *Bagarius bagarius* is a rare occurrence among the teleosts. According to Brown (1957) the rectal gland is characteristic of selachians. According to Agarwal and Singh (1964) the rectal gland of *Notopterus notopterus* is absorptive in nature.

SUMMARY

Bagarius bagarius of the family Sisoridae is generally called as a fresh water shark. It is sluggish in nature and attains a large size. It is carnivo-

rous in habit and is a voracious feeder. The food contents of the fish mainly include small fishes of other species.

The alimentary canal of *Bagarius* is comparatively small. The bucco-pharynx is provided with maxillary, mandibular, horny pad and pharyngeal teeth which are primarily meant to capture the prey and to prevent its escape. The mucosa of bucco-pharynx is lined with mucous cells and taste buds. The small oesophagus has well developed longitudinal mucosal folds.

The stomach is divisible into cardiac stomach, pyloric stomach and fundus. The mucosa of cardiac stomach has well developed gastric glands while such glands are absent from the pyloric stomach. The muscularis of stomach is quite thick. It has an outer thin, longitudinal layer and inner thick circular layer.

The intestine lies coiled within the body cavity. The posterior part of the intestine may be formed as rectum. Histologically, both intestine and rectum are precisely similar. From the posterior end of the rectum, arises a blind rectal gland which, in all probability serves for the absorption of food.

REFERENCES

1. Agarwal, V. P. & Singh, H. M. 1964. Functional morphology of the rectal caecum of *Notopterus notopterus*. *Curr. Sci.*, **33**: 53-54.
2. Al-Hussaini, A. H. 1946. The anatomy and histology of the alimentary canal of the bottom feeder, *Mulloidis anriflamma*. *J. Morph.*, **78**: 121-154.
3. Al-Hussaini, A. H. 1947. The anatomy and histology of the alimentary tract of plankton feeder. *Atherina forskali Ibid.*, **80**: 251-286.
4. Al-Hussaini, A. H. 1949. On the functional morphology of some fish in relation to differences in their feeding habits, anatomy and histology. *Quart. J. Micr. Sci.*, **90**: 109-139.
5. Blake, I. H. 1930. Studies on the comparative histology of the digestive tube of certain teleost fishes. I. A predaceous fish, the sea bass (*Centropristes striatus*) *J. Morph.*, **50** : 39-70.
6. Blake, I. H. 1936. Studies on the comparative histology of the digestive tube of certain teleost fishes. III. A bottom feeding fish, the sea-robin (*Prionotus carolinus*). *Ibid.*, **60**: 77–102.
7. Brown, M. E. 1957. The physiology of Fishes. Vol. I. Academic Press, New York.
8. Ghazzawi, F. M. 1935. The pharynx and intestinal tract of Egyptian mullets-*Mugil Cephalus* and *Mugil capito*. Notes and Mem. Fish. *Res. Dir. Cairo*. **6**: 1-14.
9. Imms, A. D. 1904. Notes on the gill rakers of the spoon bill sturgeon, *Polyodon spetulus*. *Proc. Zool. Soc. Lond.*, **2**: 239-254.
10. Ishida, J. 1935. Ciliated intestinal epithelium in teleost. *Annot. Zool. Japon*. **15**: 158-160.
11. Macallum, A. B. 1896. The alimentary canal and pancreas of *Acipencer, Amia* and *Lapidosteus*. *Jour. Anat. Phys.*, **20**: 604-636.
12. Martin, N. V. 1954. Catch and winter food of lake trout in certain Algonquin Park Lakes. *J. Fisheries Res. Board. Can.* **11**: 5-10.

13. Rogick, M. D. 1931. Studies on the comparative histology of the digestive system of certain teleost fishes. A minnow (*Compostoma anomalum*). *J. Morph.*, **52**: 1-36.

14. Sarbahi, D. S. 1939. The alimentary canal of *Labeo rohita* (Ham.) *J. Roy. As. Soc. Bengal*, **5**: 87-116.

15. Steven, G. A. 1930. Bottom Fauna and the food of fishes. *J. Marine Biol. Asso. U.K.* **16**: 677-700.

16. Suyehiro, Y. 1941. A study of the digestive system and feeding habits of fish. *Jap. J. Zool.*, **10** : 1-303.

ABBREVIATIONS

A	—Anus
B	—Barbel
BC	—Buccal cavity
GF	—Gill filament
GR	—Gill raker
HP	—Horny pad teeth
INT	—Intestine
JM	—Jaw markings
LIV	—Liver
LJ	—Lower jaw
MAN.T	—Mandibular teeth
O.OE	—Opening of oesophagus
PHP	—Pharyngeal pad
PR.T.	—Premaxillary teeth
REC	—Rectum
ST	—Stomach
T	—Teeth
UJ	—Upper jaw

Plate I—Ventral view of *Bagarious bagarious* showing alimentary canal.

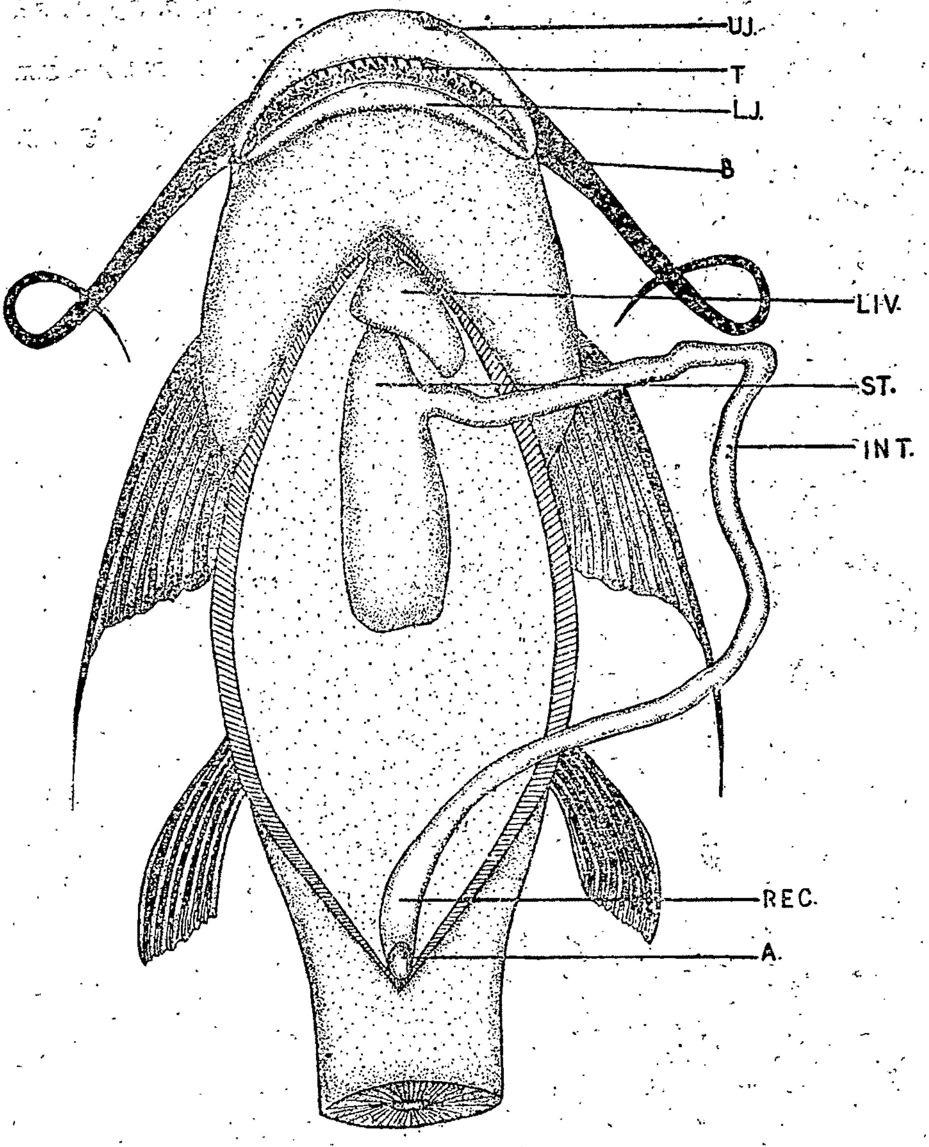

Plate II—Bucco-pharynx of *Bagarious bagarious* showing the arrangement of teeth

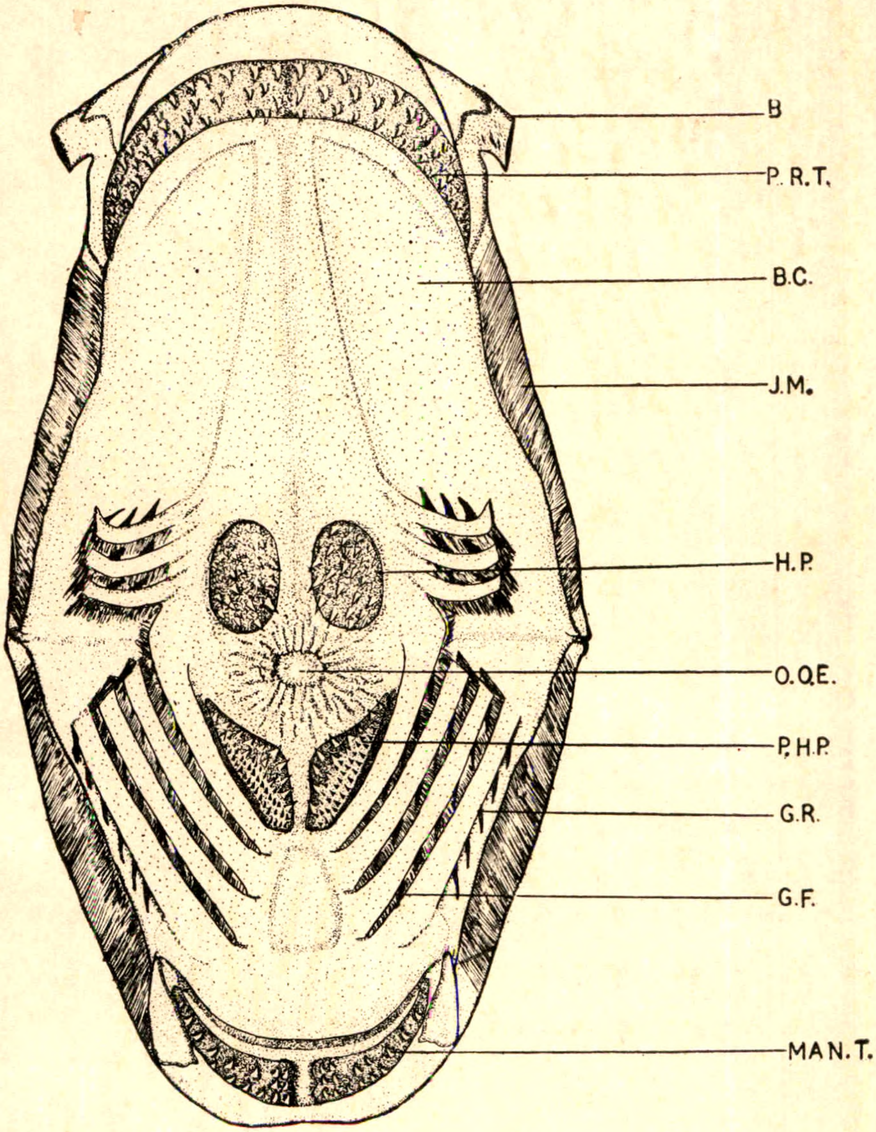

Plate III—*Bagarions bagarious*

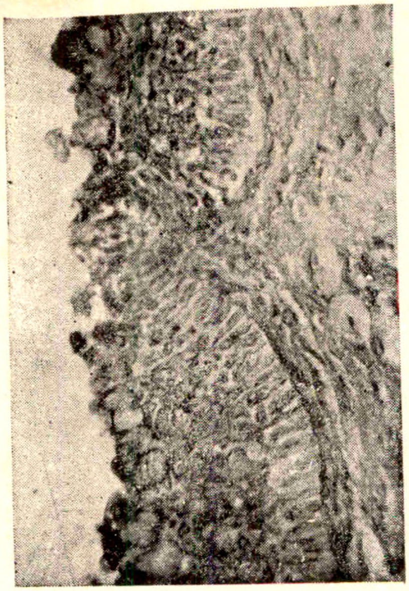

Fig. 1. A part of T. S. of buccal mucosa.

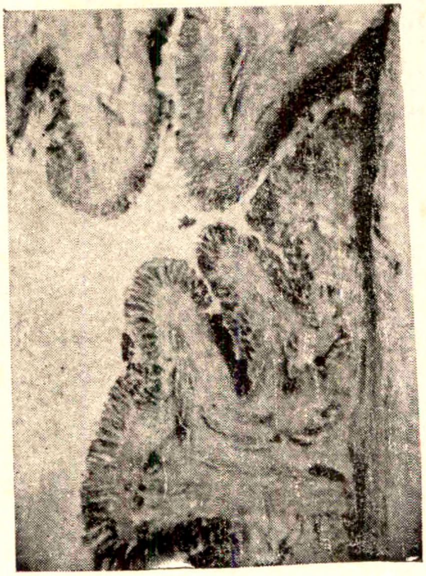

Fig. 2. T. S. of posterior pharynx.

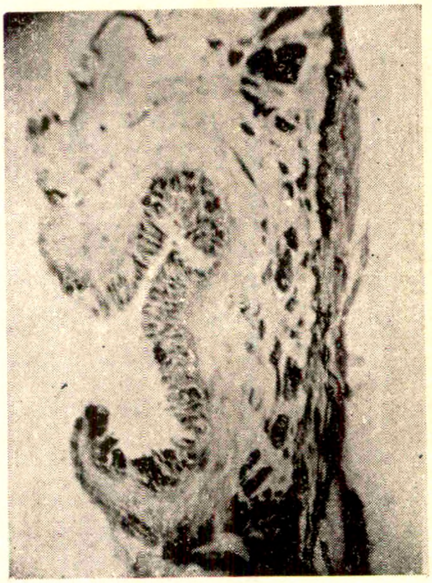

Fig. 3. T. S. of oesophagus.

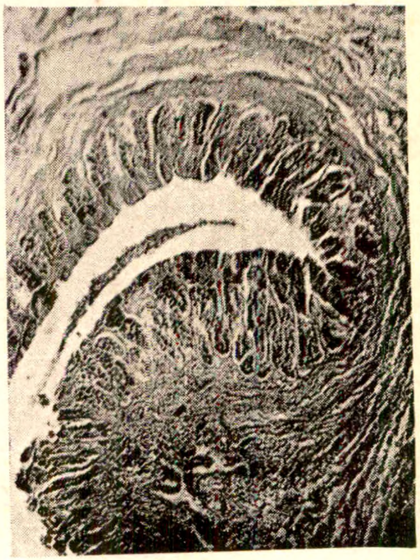

Fig. 4. A part of T. S. of cardiac stomach.

Plate IV—*Bagarious bagarious*

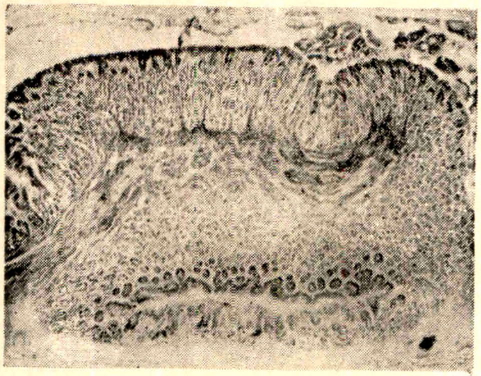

Fig. 1. T. S. of a part of pyloric stomach.

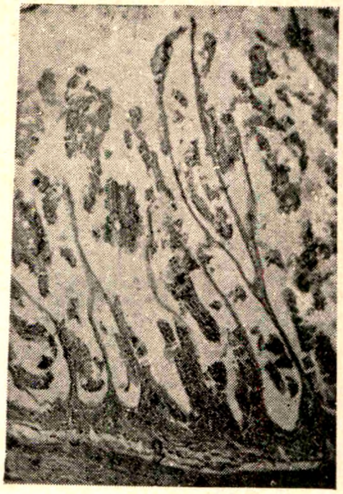

Fig. 2. T. S. of a part of intestine.

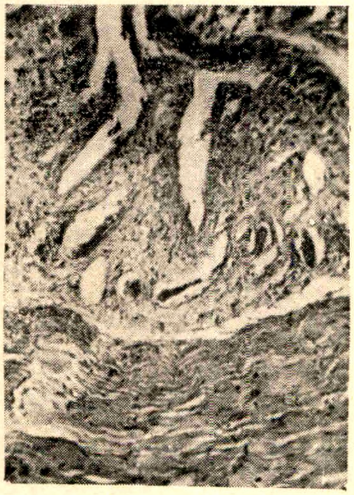

Fig. 3. T. S. of a part of rectum.

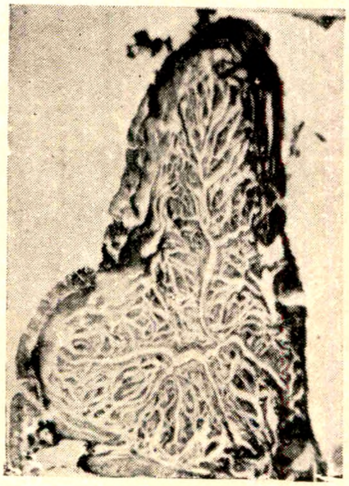

Fig. 4. T. S. of rectal gland.

MORPHOLOGICAL AND ANATOMICAL STUDIES IN HELOBIAE IX.

Vascular Anatomy of the Flower of Hydrocharitaceae— Vallisnerioideae and Halophiloideae*

V. Singh

School of Plant Morphology, Meerut College, Meerut.

Introduction

In the earlier paper of this series (Singh, 1966) the author has described the vascular anatomy of the flower of five species of the tribes Stratioideae and Thalassioideae. The present work deals with the vascular anatomy of the flower of seven species of the tribes Vallisnerioideae and Halophiloideae, and summarizes the results based on the study of some 12 species of the family Hydrocharitaceae.

Material and Methods

Except for the two species that were collected by the author, the material of other species was obtained from various sources (Table 1). Methods of investigation have already been described in the preceding paper of the series.

Table 1

Species	Place	Collector (s)
1. *Blyxa octandra* (Roxb). Planch ex Thw.	Madras	Dr. K. K. Lakshmanan
2. *Blyxa echinosperma* (Clarke) Hook. *f.*	Dehradun	Author
3. *Vallisneria spiralis* Linn.	Meerut Ramchandrapuram (S. India)	Author Dr. G. Gopal Krishna
4. *Vallisneria americana* Michx.	Minnesota (U.S.A.)	Dr. Ernst C. Abbe
5. *Hydrilla verticillata* (Linn. f.) Royle	Meerut Madras	Author Dr. K. K. Lakshmanan
6. *Elodea canadensis* Michx.	Chicago (U.S.A.) Leiden (Netherlands)	Dr. Y. S. Murty Dr. W. A. van Heel
7. *Halophila ovalis* (R. Br.) Hook. f.	Madras	Dr. K. K. Lakshmanan

---

* Research contribution No. 85 from the School of Plant Morphology, Meerut College, Meerut.

OBSERVATIONS

Blyxa Thours

The genus *Blyxa* has got about a dozen species distributed in the warmer parts of the Old World. They are found growing in stagnant water of ponds, lakes and marshes. The two species of the genus studied are *Blyxa octandra* (Roxb.) Planch ex Thw. and *Blyxa echinosperma* (Clarke) Hook.f.

Blyxa octandra is a scapigerous fresh water herb. The plants are dioecious. The spathes are peduncled, tubular and bifid at the tip. The female spathe has a single sessile flower while there are 5-15 pedicellate flowers in a male spathe. In the male flower the outer three perianth segments are linear, green, tinged with red and persistent, and the inner three are white and fringed. The stamens are nine, in three whorls of three each. The filaments are narrow and the anthers are dithecous and dehiscing by lateral slits. The male flower has three slender pistillodes which are connate at the base.

The perianth of the female flower is similar to that of the male flower. The gynoecium is tricarpellary syncarpous with a long, beaked, inferior and unilocular ovary bearing many ovules on three parietal placentae. The styles are three, short and connate at the base, each terminating in a filiform stigma. The fruit is long with a membranous pericarp and included in the ribbed, narrow, ventricose spathe. The seeds are oblong-elliptic, tuberculate and without any tail. The testa has eight longitudinal rows of more or less curved spines.

Anatomy of the Male Inflorescence and Flower—The structure and vascular supply of the scape of the male inflorescence is similar to that of the female (Fig. 82). The vascular supply of the male spathe is also derived in a similar fashion (Figs. 83-85).

The central mass of vascular tissue left after the departure of the traces for the spathe expands very much and then splits into a large number of bundles (Figs. 85, 86). All the male flowers receive three bundles each almost at the same level. Squamulae are present in between the spathe and the pedicels of the male flowers (Fig. 87).

The vascular supply of the pedicel consists of three collateral vascular bundles which generally alternate with three large air cavities (Fig. 88). Several smaller air cavities are also present in the peripheral region of the cortex.

Within the pedicel, each bundle gives off one trace which takes an anticlock direction and lies opposite to an air cavity (Figs. 89, 90). After the departure of these three traces, the bundles expand and extend towards the centre and at the base of the receptacle the three bundles coalesce to form a central mass of vascular tissue from which three traces extend outwards alternating with the first three traces (Fig. 92). These are the median bundles of the three perianth segments of the outer whorl. In the mean time each of the first formed traces branches into two (Fig. 91) and they form the marginal bundles of the two adjacent perianth segments. A little higher up nine traces diverge out from the central mass of the vascular tissue for the three perianth segments of the inner whorl (Figs. 93, 94). The three bundles of each perianth segment extend as such up to the tip. The perianth segments of the inner whorl show irregular foldings on the inner surface in the upper region.

Subsequently nine traces are given off in three successive whorls of three each for the stamens (Fig. 95). The single concentric bundle of each stamen traverses undivided up to the top of the connective. The stamens of the outermost whorl lie opposite the perianth segments of the outer whorl (Fig.98).

The remaining stelar tissue splits into three bundles (Fig. 96). They extend into the three carpellodes which alternate with the stamens of the innermost whorl (Fig. 97).

Anatomy of the Pistillate Flower—The ground tissue of the scape shows a large number of air cavities. The vascular supply consists of two larger bundles in the central and seven smaller bundles in the peripheral region (Fig. 100). The xylem of each bundle is reduced to a cavity. Near the base of the spathe the two central bundles coalasce to form a central mass of vascular tissue (Fig. 101) which gives off two traces in opposite directions for the spathe (Fig. 102). Besides, all the peripheral bundles also enter as such into the spathe. The bundles lie in a single series in the spathe except at the two thickened ends where two bundles lie one above another. In between the spathe and the ovary a large number of squamulae are present (Fig. 103).

After the departure of the traces for the spathe, six traces diverge almost simultaneously from the central mass of the vascular tissue (Fig. 103). Alternately they constitute carpellary dorsals and secondary marginals. The remaining central vascular tissue splits up into three ventral strands (fused ventrals) of the three carpels (Fig. 194). With the departure of the ventral strands three locules make their appearance but they merge into one (Fig. 105). Each placenta has a projecting bilobed structure in the middle marking the limits of the two halves of a placenta. Many anatropous ovules are arranged in two series on each placenta. Each ventral strand supplies ovules of the two half placentae of the two adjacent carpels (Fig. 106). Higher up each ventral strand split into two ventral bundles. The dorsals and the secondary marginals continue as such throughout the ovary wall (Fig. 107).

At the top of the ovary the dorsals and the secondary marginals contribute to the vascular supply of the perianth segments. Each perianth segment of the outer whorl receives three traces—the median derived from the carpellary dorsal and the laterals from the two secondary marginals (Fig. 108). The two traces from a secondary marginal form the laterals of the two adjacent perianth segments. The three bundles of each perianth segment extend unbranched to the tip. At a slightly higher level each dorsal bundle gives off one trace for a perianth segment of the inner whorl (Fig. 109). The single bundle continues up to the tip as such.

After the departure of the perianth traces each secondary marginal splits into two bundles (Fig. 109). At this level there are fifteen bundles in total—6 carpellary ventrals, 6 secondary marginals and 3 carpellary dorsals (Fig. 110). Out of these, 5 bundles (2 ventral, 2 secondary marginals and 1 dorsal) extend into each of the 3 styles (Figs. 99, 111). The ventrals and the secondary marginals disappear at a slightly lower level while the dorsal extends up to the stigma. The three styles are connate at the base but they become free higher up. Each style is grooved on the adaxial side.

Blyxa echinosperma (Clarke) Hook.f. is very similar to *B. octandra* in vegetative characters but differs in floral characters. The flowers are bisexual, solitary and sessile in a spathe. There are three stamens and the ovary is as long as the spathe. The testa of the seed has two longitudinal rows of blunt spines connected by scarious membranes and a long filiform tail at each end.

The vascular ground plan of the flower is almost similar to that of the pistillate flower of *B. octandra* but for minor differences. After the departure of the perianth traces of the outer whorl the secondary marginals are completely used up in supplying to the inner perianth segments (Figs. 112-114). The single bundle of each inner perianth segment traverses branched to the tip. The three dorsal bundles enter the three stamens (Fig. 115). The single staminal bundle extends throughout the length of the filament and the connective unbranched. The ventrals bifurcate at the base of the style and continue up to the base of the stigma (Fig. 116).

Vallisneria Linn.

The genus *Vallisneria* was named after Antonio Vallisneri (1661-1730) an Italian Botanist. Both the species of the genus *viz. V. spiralis* Linn. and *V. americana* Michx. have been studied.

Vallisneria spiralis Linn. is widely distributed in the warmer parts of both hemispheres. It is common throughout India found growing in muddy bottoms of fresh water ponds and slow-running streams. The plants are submerged, stoloniferous, perennial herbs with a creeping root-stock bearing tufts of fibrous roots.

The plants are dioecious. The flowers, which remain submerged arise in the axils of the leaves. The numerous minute staminate flowers are crowded in a head enclosed by an ovoid, 3-lobed, short peduncled spathe. They are arranged in three series of which the lowest are having small pedicels and the uppermost with the longest pedicels. At the opening of the spathe the flowers break off at the base of the pedicel and float on the surface of water. The outer perianth which recurves on opening, is of three segments arranged in a whorl. The inner perianth is reduced to a very small structure lying opposite the staminode. The fertile stamens are two in number with their slender filaments completely free and spreading apart from one another. The basifixed, 2-chambered anthers at dehiscence form a globular coherent mass of pollen at the top of each filament. In addition to the two fertile stamens one staminode is also present in each male flower (Fig. 117) lying opposite the reduced perianth segment of the inner whorl.

The sessile pistillate flowers are borne singly in a 3-toothed tubular spathe terminating on a long peduncle. The flowers are borne under water but at the time of pollination they are raised to the surface of water by elongation of the peduncle. The outer perianth is small and sessile with three, free and obovate lobes. Three small rudimentary perianth segments of the inner whorl, are attached at the top of the ovary inside the outer perianth. The ovary is inferior, cylindrical and unilocular with numerous ascending orthotropous ovules on three parietal placentae. The three bilobed stigmas, densly clothed with hairs, lie opposite the perianth segments of the outer whorl. After pollination the female flowers are dragged under water by spiral twisting of the filiform peduncle. The fruit is partly enclosed in the spathe.

Anatomy of the Male Inflorescence and Flower—There is a single stele like bundle in the centre of the peduncle which expands and gives off three traces for the spathe. In between the spathe, at the base of the pedicles of the male flowers, there are present a large number of squmulae. The remaining vascular tissue gives rise to many traces in an irregular fashion, one for each of the male flowers. The single bundle in the pedicel of the male flower bifurcates into two at the base of the receptacle (Fig. 118). These two resultant bundles form the vascular supply of the two stamens. The single stamen bundle passes up to the top of the connective unbranched (Fig. 119). No vascular supply could be traced to the perianth segments and the staminode.

Anatomy of the Pistillate Flower—The vascular supply of the scape consists of three bundles (Fig. 121), of these one is comparatively larger. The phloem is well-developed and the xylem is represented by a cavity. At the base of the receptacle the bundles coalasce to form a central mass of vascular tissue which expands to give off traces for the spathe (Fig. 122). At first four traces for the spathe are given off, two on either side, almost at the same level (Fig. 123). Slightly higher up two more traces for the spathe are given off, in opposite directions and at right angles to the first traces. Thus the spathe receives six traces (Fig. 124). There are present a large number of squamulae in between the spathe and the base of the ovary (Figs. 125,126).

The vascular tissue left after the departure of the spathe traces splits up into three bundles which constitute the gynoecium supply (Fig. 124). At a slightly higher level from each of these three bundles one small trace pass outward (Fig. 125). These are the dorsal bundles of the carpels. They traverse for a short distance before they fade out at a level where the locule makes its appearance (Fig. 126).

The remaining three vascular bundles are the ventral strands of the carpels. As they extend in the ventral walls of the carpels they give rise to numerous ovular traces (Figs. 120, 127). The cells of the inner layers of ovary wall show starch grains. Tannin cells are also scattered in the ovary wall.

The ventral strands continue up to the top of the ovary and there they flatten and each of them gives off one trace for the perianth segment of the outer whorl (Figs. 128, 129). The single perianth bundle takes the median position and extends as such almost to the tip of the perianth. A large number of lacunae and tannin cells are present in the mesophyll of the perianth segments. Three rudimentary perianth segments have also been observed in the inner whorl (Fig. 130), but no vascular supply could be traced to them.

Each of the ventral bundles after giving rise to traces for the outer perianth segments splits into two which continue one in each of the two fleshy lobes of a stigama (Figs. 130-132).

Vallisneria americana Michx—the American form of *Vallisneria*—is considered only a variety of *V. spiralis* by some authors (*see* Fernald, 1918). The structure of the flower shows some differences from that of *V. spiralis*. In *V. americana* the two stamens in male flower are close together upright in the centre of the flower forming a single mass of pollen grains. Further at the base of the stamens numerous curved hair-like structures are reported by earlier workers which are described by Wylie (1917) as representing the inner whorl of perianth. These statements could not be checked in the absence of male flowers in the material available. In pistillate flowers the ovary is much longer than that of *V. spiralis*. The bifid stigmas are sharply coiled and the coils protrude outside the outer perianth in the open flowers. The staminodia are said to be present in American form by Wylie (1917) and Witmer (1937), but in the material which was available to the author for study from U.S.A. no such structures could be seen.

The vasculature of the flower is essentially same as that of *V. spiralis*.

Hydrilla Rich.

Hydrilla is a monotypic genus. *Hydrilla verticillata* (Linn. f.) Royle is widely distributed in the warmer regions of the Old World occurring gregariously in still or slow running water. It is a submerged herb with slender branched stems often rooting at the nodes.

The plants are dioecious. The sub-sessile, subglobose and muricate male spathes are present solitarily in the axils of the leaves, each containing a single pedicellate male flower. At maturation the male flowers break off and liberate by opening of the spathe and float on the surface of water. The perianth is of six free segments in two whorls of three each. The outer three are green, imbricate while the inner three are small and white. Alternating with the perianth segments of the inner whorl are three stamens with short filaments and large reniform, dithecous and latrorsely dehiscing anthers. The pollen grains are large and globular. The membranous cylinderical female spathes which are bifid at the top are solitary and sessile in the axils of the leaves. Each spathe contains a single sessile female flower. The perianth segments are in two whorls of three each. The inner three are very much reduced. The ovary is inferior, cylindric to narrowly conical, produced beyond the spathe in a filiform beak. It is unilocular with many anatropous ovules on parietal placentae. The styles are three, linear, alternipetalous and each terminating in a fimbriate stigma.

Anatomy of the Staminate Flower—The internal structure of the male scape and vascular supply to the spathe are similar to that of the female (Figs. 133-34).

After supplying the spathe, the stele expands at the base of the receptacle and the xylem cavity is replaced by some lignified elements. Three traces are given off almost simultaneously that enter the three perianth segments of the outer whorl (Fig. 135). The single bundle of each perianth segment continues umbranched to the tip. The outer perianth has tannin cells and air cavities. The three perianth segments of the inner whorl are reduced and without any vascular supply (Figs. 137, 138).

After the departure of the perianth traces the remaining vascular tissue splits into three bundles (Fig. 136) which constitute the androecium supply. Each stamen receives a single concentric bundle which traverses unbranched up to the top of the connective.

Anatomy of the Pistillate Flower—The vascular supply of the scape consists of a centrally disposed vascular cylinder. The xylem is reduced to a cavity lined by a layer of thin walled cells. At the base of the receptacle the stele expands slightly and gives off two traces in opposite directions almost simultaneously. These traces traverse the cortex and enter the spathe which encloses a solitary flower. The two bundles extend unbranched throughout the length of the bifid spathe. Some tannin cells are also present in the spathe. A number of squamulae are present all around in between the spathe and the base of the flower (Fig. 140).

At the base of the ovary the stele expands and becomes somewhat three lobed and soon it splits up into three bundles which constitute the gynoecium supply (Figs. 140-142). These bundles take an outward course and lie against the three rounded angles of a roughly triangular ovary. The single locule makes its appearance in the centre (Fig. 143). The placental region is not well defined but the region of the ovary wall where bundles lie slightly projects inwards. The cells of the internal lining of the ovary take a dense stain. They also show some starch grains. Some tannin filled cells are also scattered in the ovary wall. On each placenta a few anatropous ovules are borne which generally lie in vertical position in the ovary.

Thus, in *Hydrilla* the vascular supply of the ovary is reduced to three bundles. There are no traces of the dorsals. These three bundles continue in the ovary wall against the ill-defined placentae. Each bundle gives off traces for the ovules borne on the placentae against which it lies (Fig. 144). These carpellary bundles continue up to the top of the ovary (Fig. 146). In the upper region of the ovary there are three wing-like outgrowths, each lying against a bundle (Fig. 145). The three bundles extend separately within the beaks of the ovary for a short distance and then fuse to form a central mass of vascular tissue (Fig. 147, 148). At the top of the filliform beak of the ovary three traces arise (Fig. 149) which enter the base of the three perianth segments of the outer whorl. The single bundle traverses unbranched up to the tip. The three perianth segments of the inner whorl which alternate with those of the outer are very small and reduced (Fig. 151). No vascular supply could be traced to the inner perianth.

The remaining vascular tissue after the departure of the traces for the outer perianth soon splits into three bundles (Fig. 150). They extend into three free styles only for a short distance (Figs. 151, 152). Tannin cells and air cavities are present in the perianth segments and styles.

Elodea Michx.

Elodea canadensis Michx., the American water weed, is common in quiet water in N. America. It is a perennial, submerged, dioecious herb sometimes rooting at the nodes. The male spathes which are present in the axils of the upper leaves are sessile and tubular, each with two broad apical teeth. Each spathe encloses four or more male flowers. The perianth is of six segments in two whorls of three each. The outer are sepaloid, and the inner are petaloid and clawed. The stamens are nine, arranged in three whorls of three each. The filaments are short, that of inner most whorl are united into a short column. The anthers are dithecous and introrse.

Only the staminate flowers of *Elodea canadensis* were available for study from the material obtained from U.S.A. and Netherlands.

Anatomy of the Male Inflorescence and Flower—The vascular supply of the peduncle consists of a centrally disposed vascular cylinder (Fig. 153). The xylem of which is reduced to a cavity surrounded by phloem. At the base of the spathe two traces depart simultaneously in opposite directions from the stele (Fig. 154). They traverse the cortex and enter the spathe which encloses the male flowers. The two bundles continue unbranched up to the top of the spathe.

After the departure of the spathe traces the remaining vascular tissue divides into four bundles, one for each flower (Fig. 155). Within the pedicel each bundle splits into three (Fig. 156). Thus the pedicel of each staminate flower has three bundles. At the base of the pedicels in between the spathe a large number of squamulae are present (Figs. 155, 156).

The pedicel of the flower is roughly three-angular in outline in a cross-section. The three bundles lie at the three angles of the pedicel each alternating with a large air cavity (Fig. 157).

As the bundles extend upwards they expand and at the base of the receptacle one trace arises from each of the three bundles (Fig. 158). These traces traverse the cortex and enter the three perianth segments of the outer whorl. After giving rise to these traces the three bundles come closer and anastomose to form an almost complete vascular cylinder from which three more traces arise simultaneously alternating with those of the first (Fig. 159). They form the vascular supply of the three perianth segments of the inner whorl., Thus each perianth segment receives a single bundle which takes the median position and extends up to the tip unbranched. The epidermal cells of the inner whorl of the perianth segments bear numerous small unicellular outgrowths in the upper region.

Before the gaps caused by the perianth traces are filled up, the staminal traces arise from the vascular cylinder (Figs. 160, 161) in three successive whorls. The three traces of a whorl arise simultaneously and those for the successive whorls alternate with each other. The vascular tissue is completely used up in giving rise to traces for the innermost whorl of the stamens. The single stamen bundle is concentric and it extends throughout the length of the filament and the connective unbranched (Figs. 162, 163).

After the separation of filaments of the innermost whorl of stamens a mass of tissue is left in the centre which soon splits into three parts. They are the styllodia which are devoid of any vascular supply (Fig. 162). They continue only for a very short distance.

Halophila Thou.

Halophila ovalis (R. Br.) Hook. f. [Syn. *H. ovata* (non Gaud) Aschers] occurs submerged or often burried in muddy or sandy bottoms in sheltered localities arround the sea coast.

The plants are dioecious. The flowers in both the sexes are enclosed in solitary, sessile, broadly lanceolate spathes which arise between the pairs of leaves. Each spathe is composed of two membranous keeled bracts, one embracing the other. The male flowers are pedicellate and solitary in a spathe. The parianth is of three free, elliptic, spreading and white segments arranged in an imbricate manner. The three stamens which alternate with the perianth segments have sessile and dithecous anthers. The connective projects slightly above the anther lobes. In each chamber the pollen grains are in chains. The ovary is unilocular and beaked, and bears many ovules on parietal placentae. The styles are three, linear and filiform. The ovary is also crowned by three very reduced perianth segments. The fruit is included in the spathe.

Anatomy of the Staminate Flower—The stele of the peduncle is centrally disposed, the xylem of which is represented by a lacuna bounded by a layer of thin-walled cells. In the cortex there are about ten lacunae arranged in a circle. The cells of the cortex show starch grains.

At the base of the spathe the xylem lacuna of the stele is replaced by lignified cells. The stele gives off two traces closely one above another in opposite directions (Figs. 165, 166) These traces traverse the cortex and enter the base of the two sheathing bracts (Figs. 167, 168). The single bundle of each sheathing bract takes a median position and traverses unbranched up to the tip In the axils of each sheathing bract are present two squamulae (Fig. 168).

After the departure of the traces for the sheathing bract xylem cavity makes its appearance again in the centre of the stele. The stele extends into the pedicel of the male flower as such. Once more the xylem cavity is replaced by lignified cells just before the level where traces for the perianth segments are to depart. The three traces for the perianth are given off successively closely one above another (Fig. 169). Each perianth segment receives one bundle which traverses along the median line throughout its length unbranched. Before the perianth separates from the central axis the vascular tissue left reorganises into a three lobed structure (Fig. 170). It soon splits up into three bundles each of which enters the connective of a sessile stamen (Figs. 164, 171, 172).

Anatomy of the Pistillate Flower—The structure and vascular supply of the peduncle of the female flower is similar to that of the male. The vascular supply of the two bracts which enclose a female flower is also derived in a similar manner as in case of male flowers (Figs. 173, 174). In the axil of each bract near the base of the ovary two squamulae, as in male flowers, are also present.

After the traces for the spathe have arisen the xylem cavity of the stele is replaced by some lignified elements and soon the stele becomes somewhat four lobed (Fig. 175). Two traces extend outwards from the two lobes of the stele and they form the dorsal bundles of the carpels. Immediately the remaining vascular tissue splits into two bundles which extend outwards into the receptacle to enter the carpels as their ventral strands. A single locule makes its appearance in the centre of the ovary (Fig. 176). The ovules derive their vascular supply from the two ventral strands which are completely used up in supplying the ovules (Figs. 177, 178). The dorsal bundles extend through the ovary wall and at the top of the ovary one of them splits into two. The three resultant bundles continue into the three styles almost up to the top (Figs. 179-181).

At the top of the ovary three very much reduced perianth segments are present but they do not show any vascular stubs. The styles are covered with small unicellular papillose hairs and are receptive throughout their length.

Discussion and Conclusions

With a few exceptions like *Ottelia* and *Blyxa* the members of this family possess unisexual, usually crowded (staminate) or solitary (pistillate) flowers. They are surrounded by a structure generally described as a spathe. If we consider spathe as a leafy structure which surrounds or subtends a flower cluster then it will be technically incorrect to designate the structure that surrounds a solitary pistillate flower as a spathe. However, in view of the common usage and in view of the fact that it has the same structure and vasculature as the spathe in male inflorescence we have retained the same term for the organ in female flower.

The flowers of Hydrocharitaceae are typically trimerous with two whorls of perianth segments. But reduction in their size, number and vasculature has been observed in the different genera investigated. There are two normal whorls of perianth segments in *Ottelia, Bootia, Hydrocharis, Blyxa, Hydrilla* and *Elodea*. But in the pistillate flowers of *Blyxa octandra* and the bisexual ones of *Blyxa echinosperma* the perianth segments of the inner whorl are reduced and are much smaller in size than those of the outer whorl. The perianth segments of both the whorls are very much reduced in staminate and pistillate flowers of *Hydrilla*. Further reduction is seen in staminate flowers of *Nechamandra* where the inner whorl has only two perianth segments instead of usual three. In the staminate flowers of *Vallisneria* the inner perianth is represented by a single minute segment only. Extreme reduction is seen in the pistillate flowers of *Halophila* where the inner perianth is totally absent and the outer is represented by minute outgrowths at the top of the ovary.

Similar reduction series can be drawn in the vascular supply of the perianth in different genera. Each perianth segment receives five (outer perianth of *Hydrocharis*), three (staminate flowers of *Bootia* and *Blyxa* bisexual flowers of *Ottelia*, pistillate flowers of *Enhalus*, outer perianth of the pistillate flowers of *Blyxa octandra* and bisexual flowers of *Blyxa echinosperma*) or one (staminate flowers of *Elodea* and *Enhalus*, inner whorl in staminate and pistillate flowers of *Hydrilla* and pistillate and bisexual flowers of *Blyxa octandra* and *Blyxa echinosperma* respectively, outer whorl of staminate flowers of *Halophila* and pistillate flowers of *Vallisneria*) trace. The inner perianth segments of staminate and pistillate flowers of *Hydrilla*, outer and inner perianth segments of staminate flowers of *Nechamandra* and *Vallisneria* and the only whorl of perianth segments in pistillate flowers of *Nechamandra* do not show any vascular supply. It is, therefore, interesting to note that during the course of reduction, the organ is not completely reduced but its vascular supply is lost. A number of authors hold the view that the "Vascular bundles are more conservative than the organ they traverse" (Eames, 1931). Arber (1913, 15) in her earlier writings also supported this view but later on she changed her opinion and became a strong opponent of it. She held (Arber, 1933, p. 233) that a "rudimentary form is found to correspond to a vascular system which is equally, or even more, rudimentary; indeed an organ which retains some trace of its external form, may yet show a complete lack of vascular tissue. It thus becomes clear that we have no alternative but to discard the doctrine of conservatism of the vascular bundle". The present observations also seem to lend support to such a view.

Reduction has also been observed in the number of stamens. They are present in trimerous whorls, each alternating with the other, and that the outermost whorl alternating with the inner perianth whorl. There are twelve (*Bootia* and *Blyxa octandra*) or nine (*Elodea* and *Ottelia*) stamens, but in *Ottelia* three of them are reduced to staminodes. Further reduction is seen in *Halophila*, *Enhalus* and *Hydrilla* where there is only a single whorl of three stamens. Only two stamens are present in *Vallisneria* and *Nechamandra*, however, a small staminode devoid of any vascular supply is also present in *Vallisneria*. As usual the stamens are one traced and the single bundle continues unbranched throughout the length of the filament and connective. In *Nechamandra* and *Vallisneria*, however, the bundle traverses only up to the middle of the connective.

Six staminodia have also been observed in the pistillate flower of *Hydrocharis*. They have vascular structure of stamens in somewhat reduced form. Thus they are the vestigial stamens which through reduction have become staminodia.

In the same way reduction in the number of carpels has been observed in different genera. While there are six carpels in *Ottelia*, *Hydrocharis* and *Enhalus* there are three in *Blyxa*, *Vallisneria* and *Hydrilla*. In *Nechamandra* and *Halophila* apparently there are only two carpels. The vascular supply of a carpel normally consists of a dorsal and a ventral strand (placental strand). The ventral strands, each of which is a fusion product of the two ventrals of the two adjacent carpels, are normally oriented, *i.e.*, their xylem faces towards the centre of the flower and they occur on radii different from those of the carpellary dorsals. In *Hydrocharis* and *Enhalus* the ventral bundles divide into many smaller bundles which are distributed in the placental region. Some deviation from this normal condition is seen in some genera. Besides the dorsal and the ventral bundles, secondary marginals are also present in

Hydrocharis and *Enhalus.* On the other hand in *Vallisneria* and *Hydrilla* some reduction in normal vascular supply is seen. In *Vallisneria* though dorsal bundles are present, they continue only for a very short distance and fade out at a level where the locule makes its appearance. In *Hydrilla* the dorsal bundles are totally absent and the vascular supply of the gynoecium consists of only three ventral strands.

The placentae are borne on the fused margins of different carpels in all the genera investigated. In most of them two halves of a placenta are distinct and the ovules borne on them face in opposite directions. In certain genera such as *Hydrocharis, Ottelia* and *Enhalus* and condition becomes rather interesting in that the ovary is incompletely divided into six segments and most of the internal surface of the ovary wall, except along the dorsal line, is covered with ovules, a condition recalling that of *Butomus.* Thus, in the light of the criteria suggested by Puri (1952a) the placentation in all the genera is parietal. Puri (1952a) explains a condition similar to *Hydrocharis, Ottelia* and *Enhalus* in some members of Rafflesiaceae and Papaveraceae that in such cases the placentae enlarge considerably and project toward the centre, there are apparently no true septa but merely placental lamellae and thus he described the placentation as parietal or lamellar.

As pointed out earlier the gynoecium appears to be bicarpellary in *Halophila* and *Nechamandra.* It is evident from the fact that the vascular supply of the gynoecium consists of two dorsal and two placental strands. But there are distinctly three styles and three stigmas in these cases. The placental strands are completely used up in supplying the ovules present on ill-defined placentae. It is interesting that one of the two dorsal bundles splits into two at the top of the ovary and these resultant three bundles extend into the three styles and stigmas. Therefore, it appears that the bicarpellary condition has been brought about by the suppression of one of the carpels in the ovary region, a condition also reported in certain Myrtaceae (Gupta, 1962). Since one of the carpels is suppressed, the placental bundle of the suppressed carpel has also disappeared, but its dorsal bundle become incorporated with the dorsal of the other carpel in the ovary region and becomes separate only in the stylar region.

Further, the tri-carpellary condition in the family also appears to be a derived one. Probably it has been brought about by suppression of three carpels from a hexacarpellary condition, which is prevalent in several genera of the family.

Styllodia are present in the staminate flowers of some genera such as *Bootia* and *Elodea.* In *Bootia* there are six styllodia in two whorls of three each. Each styllodium receives a single bundle which bifurcates higher up. In *Elodea* there are three styllodia in one whorl and they are devoid of any vascular supply.

The presence of staminodia and styllodia in the pistillate and staminate flowers respectively has sometimes been taken to indicate that the unisexual condition in the family is derived from the bisexual one which is still prevalent in some members of the family. If this reasoning is correct then the genera with bisexual flowers are to be considered as more primitive than those with unisexual flowers.

Cushion-shaped nectaries with dark staining cells are present in *Hydrocharis* at the top of the ovary opposite the three perianth segments of the inner whorl. They lie at the base of the styles and are actually fused with them. These structures resemble the nectary found at the summit of the inferior ovary in members of the Umbellales. A number of authors interpreted the nectary of Umbelliferae as representing the expanded bases of the styles (*see* Henslow, 1890; Jackson, 1933; Douglas, 1944; Fernald, 1950; etc.). Recently Fahn (1951) also described the nectary of Umbelliferae as of "stylar type". Mittal (1955, 1958) concludes on the basis of vascular anatomy that the nectary in Umbellales represents the sterile region of the ovary which has grown up a little beyond the style bearing region and has become solidified and taken to secretory function.

The present observations reveal that the nectary in *Hydrocharis* is of "stylar type" and represents the expanded bases of styles as pointed out by a number of workers for Umbelliferae. It is evident from the fact that the nectaries actually remain fused with the bases of styles and derive their vascular supply from the stylar bundles which are left after giving rise to the traces to perianth and staminodes.

On the basis of his extensive study of nectaries in a large number of families Fahn (1953) comments upon the phylogenetical trend of the location of the nectary and concludes that the migration of nectariferous tissue takes place from outer to the inner floral organs and from lower to the upper parts of the pistil. Thus he considers the stylar nectaries to be most highly evolved.

It may be recalled here that the Hydrocharitaceae is the only family of the Helobiae where the ovary is inferior.

In all the species investigated the vascular cylinder of the pedicel generally gives rise to two sets of bundles at the base of the ovary. The inner two, three or six (corresponding to the number of carpels in different species) form the ventral strands of carpels and constitute the placental supply. They are generally completely utilized in furnishing ovular traces except of *Hydrocharis* and *Ottelia* where they extend into the styles. The bundles of the outer set are equal in number to that of the inner set or sometimes double as in *Hydrocharis* and *Enhalus* where secondary marginals are present. They contribute to the perianth traces (also staminodal traces in *Hydrocharis*) and the dorsal bundles of the carpels. Besides these two sets of bundles a ring of peripheral bundles also separates from the very base of the ovary in *Hydrocharis* and *Enhalus*. These bundles extend into the outer region of the ovary wall which is quite distinct from the inner region. They constitute the vascular supply of both the whorls of perianth as in *Enhalus* or only the outer whorl as in *Hydrocharis*.

There is little controversy regarding the nature of the internal region of ovary wall since most of the authors agree that it is truly carpellary. The present study also lends support to it as in some cases (*Hydrocharis* and *Enhalus*) the inner part of ovary "wall" stands apart clearly from the peripheral part containing a large number of air cavities. Similar distinction has also been observed in Umbelliferae and Araliaceae (Mittal, 1955, 1958) and in Myrtaceae (Gupta, 1962).

Regarding the outer region of the ovary "wall", however the opinion is sharply divided and it has been interpreted as appendicular or axial in nature (*see* Douglas, 1944,1957; Puri 1951,1952b; Eames, 1961). According to the appendicular theory the outer part of the ovary "wall" is formed by the fusion of the bases of the outer floral whorls and according to the axial theory it is formed by the fusion of the receptacular cup with the ovary wall.

In *Enhalus* the traces for both the whorls of perianth though fused among themselves are free from the dorsal bundles from the very base and they traverse through the peripheral region of the ovary and supply the perianth at the top. In *Hydrocharis* only the traces for the outer whorl of perianth are free while those of the inner whorl are fused with the carpellary dorsals. In still other cases the bundles traversing the ovary "wall" are the fusion products of the traces of different floral organs occurring on the same radii. However, it may be mentioned here that the placental strands in all the cases are free from the very base of the ovary while the carpellary dorsals separate from those of the other floral organs at the top of the ovary.

Eames (1931) and Mac Daniels (1940) have given series of diagrams in Ericaceae and Rosaceae respectively to show adnation and fusion among the floral organs and their vascular bundles. They conclude that by the cohesion of the basal region of the outer floral organs with the ovary wall, the superior ovary becomes inferior and the outer "wall" is, therefore, interpreted as appendicular in nature. A similar view has been expressed by a number of other workers (*see* Eames and Mac Daniels, 1947; Gauthier, 1950; Eames, 1961). Studies on some monocotyledonous families such as Orchidaceae (Swamy, 1948) and Agavaceae (Wunderleich, 1950) also support such an inference. In regards to fusion and adnation of the bundles the present observations seem to support the appendicular view.

The above authors also consider the bundles which traverse the outer region of ovary wall in free or adnate condition as appendicular. But as pointed out by Puri (1951, 1952a) appendicular bundle has a duel nature, it is a 'trace' when it traverses the cortex of the receptacle and 'bundle, when it enters the organ. Since we can not differentiate where the 'trace' ends and 'bundle' starts, Puri (1952) states that the vascular anatomy can be of little help in determination of the composition of ovary wall and can not offer any suitable explanation of the problem of the inferior ovary.

Troll (1931) expressed doubt regarding the syncarpous nature of the gynoecium in the Hydrocharitaceae. He considered that the gynoecium in this family is really apocarpous and that it seems to be syncarpus apparantly. He designates such a condition as pseudo-coenocarpous. However, the present investigation shows that the gynoecium in the family is truely syncarpous. Not only the ovary is unilocular but the ventral bundles of the two adjacent carpels are also fused to form a ventral strand (placental strand). It may be possible that the present day condition has been derived from apocarpous condition through *Butomus*-like members where the carpels are connate at the base and the perianth is fused with the carpels for some distance.

SUMMARY

In the present investigation vascular anatomy of the flower of 12 species belonging to ten genera—*Ottelia, Bootia, Hydrocharis, Enhalus, Nechamandra, Blyxa, Vallisneria, Hydrilla, Elodea* and *Halophila*—of the family Hydrocharitaceae has been studied.

The flowers are generally unisexual with a few exceptions like *Ottelia* and *Blyxa* where they are bisexual. Several staminate or a solitary pistillate flower is surrounded by a spathe.

The perianth is generally in two whorls of three each, but reduction in their size, number and vascular supply has been observed in different genera investigated. In certain genera like *Nechamandra, Vallisneria* and *Hydrilla* though the perianth segments are present, they do not show any vascular supply. It is, therefore, interesting to note that during the course of reduction, the organ is not completely reduced but its vascular supply is lost. This goes against the doctrine of conservation of the vascular bundle and lends support to Arber's view (Arber, 1933).

Reduction in the number of carpels has been observed in different members of the family studied. While there are six carpels in *Ottelia, Hydrocharis* and *Enhalus* the number is three in *Blyxa, Vallisneria* and *Hydrilla*. In *Nechamandra* and *Halophila* apparently there are only two carpels.

The vascular supply of a carpel normally consists of a dorsal bundle and a ventral (placental) strand, which lie on different radii. In some genera (*Hydrocharis* and *Enhalus*) secondary marginals are also present, on the other hand some reduction in normal vascular supply is also seen. While the dorsals continue only for a very short distance in *Vallisneria* they are totally absent in *Hydrilla*.

The placentation is normal parietal in majority of genera but in some cases such as *Hydrocharis*, *Ottelia* and *Enhalus* the condition becomes rather interesting since the ovary is incompletely divided into six segments and most of the internal surface of ovary wall, except along the dorsal suture, is covered with ovules. This condition has sometimes been described as superficial placentation. But as pointed out by Puri (1952) in such cases the placentae enlarge considerably and project toward the centre, and thus he described the placentation as parietal.

It appears that the bicarpellary condition in *Halophila* and *Nechamandra* has been brought about by the suppression of one of the carpels in the ovary region. Similarly tricarpellary condition in the family also appears to have been derived from hexacarpellary condition which still prevails in several genera of the family.

The present observations reveal that the nectary in *Hydrocharis* is of "stylar type" and represents the expanded bases of styles.

Hydrocharitaceae is the only family of Helobiae where the ovary is inferior. The internal region of the ovary wall is truely carpellary in nature. Regarding the outer region of the ovary wall, which has been a centre of controversy, the present observations give support to appendicular view. But the author is in complete agreement with Puri (1952) that the vascular anatomy can be of little help in determination of the composition of ovary wall and can not offer any suitable explanation of the problem of the inferior ovary.

The present investigation shows that the gynoecium in the family is truely syncarpous and not pseudo-coenocarpous as suggested by Troll (1931).

ACKNOWLEDGEMENTS

It gives me a great pleasure to express my gratitude to Dr. Y. S. Murty for guidance, keen interest and collecting the material of *Elodea canadensis* from Chicago (U. S. A.), and to Professor V. Puri for valuable suggestions and critically going through the manuscript. My grateful thanks are due to Dr. K. K. Lakshmanan (Madras), Dr. W. A. van Heel (Leiden, Netherlands), Professor Ernst C. Abbe (Minnesota, U. S. A.), Mr. Ramji Sharma (Rewa, M. P.) and Dr. G. Gopal Krishna (Ramchandrapuram, A. P.) for their generous help in providing most of the material used in this study.

LITERATURE CITED

1. Arber, A. 1913. "On the structure of the androecium in *Parnassia* and its bearing on the affinities of the genus", *Ann. Bot.*, **27**: 491-510.
2. Arber, A. 1915. "The anatomy of the stamens in certain Indian species of *Parnassia*" *Ann. Bot.*, **29**: 159-160.
3. Arber A. 1933. "Floral anatomy and its morphological interpretation" *New Phyt.*, **32**: 231-242.

4. Douglas, G. E. 1944. "The inferior ovary", *Bot. Rev.*, **10:** 125-186.
5. Douglas, G. E. 1957. "The inferior ovary, *Bot. Rev.*, **23:** 1-46.
6. Eames, A. J. 1931. "The vascular anatomy of the flower with refutation of the theory of carpel polymorphism, *Amer. Jour. Bot.*, **18:** 147, 188.
7. Eames, A. J. 1961. *Morphology of Angiosperm*, New York.
8. Eames, A. J. & MacDaniels, L. H. 1947. *An Introduction to Plant Anatomy*, 2nd ed., New York.
9. Engler, A. & Prantl, K. 1889. *Die naturlichen Pflanzenfamilien*, II, Leipzig.
10. Fahn, A. 1951. "On the structure of floral nectaries, *Bot. Gaz.*, **113:** 464-470.
11. Fahn, A. 1953. "The topography of the nectary in the flower and its phylogenetical trend," *Phytomorphology*, **4:** 424-426.
12. Fernald, M. L. 1950. *Gray's Manual of Botany*, 8th ed., New York.
13. *Gauthier, R. 1950. "The nature of inferior ovary in the genus *Begonia*", *Contr. Inst. Bot. Univ. Montreal*, **66:** 1-93.
14. Gupta, Ishwari. 1962. "Morphological studies of the flower of Myrtaceae with special reference to its vasculature", *Ph. D. Thesis, Agra University* (unpublished).
15. Henslow, G. 1890. "On the vascular systems of floral organs and their importance in the interpretation of the morphology of flowers, *Jour. Linn. Soc. Bot.* London, **28:**151-197.
16. Jackson, G. 1933. "A study of the carpophore of Umbelliferae", *Amer. Jour. Bot.*, **20:** 121-144.
17. Kaushik, S. B, 1940. "Vascular anatomy of the pistillate flowers of *Enhalus acorodies* (L.) Steud., *Curr. Sci.* **2:** 182-184.
18. MacDaniels, L. H. 1940. "The morphology of the apple fruit and other pome fruits, *Cornell. Univ. Agric. Exp. Sta. Mem.* 230.
19. Majumdar, G. P. 1938. "A preliminary note on polystely in *Limnanthemum cristatum* and *Ottelia alismoides*", *Curr. Sci.*, **6:** 383-385.
20. Mittal, S. P. 1955. "A contribution to the morphology of *Centella asiatica* (Linn.) Urban and some other related species", *Jour. Indian Bot. Soc.*, **34:** 248-261.
21. Mittal, S. P. 1958. "Morphological and anatomical studies in Umbellales", *Ph. D. thesis, Agra University* (unpublished).
22. Puri, V. 1951. "The role of floral anatomy in the solution of morphological problems", *Bot. Rev.*, **17:** 471-553.
23. Puri, V. 1952a. "Placentation in angiosperms", *Bot. Rev.*, **18:** 603-651.
24. Puri, V. 1952b. "Floral anatomy and inferior ovary", *Phytomorphology*, **2:** 122-129.
25. Singh, V. 1966. "Morphological and Anatomical Studies in Helobiae VIII. Vascular Anatomy of the Flower of Hydrocharitaceae—Stratioideae and Thalassioideae", *Agra Univ. J. Res. (Sci.)*, **XV :** 43-59.
26. Swamy, B. G. L. 1948. "Vascular anatomy of the orchid flowers", *Bot. Mus. Leafl. Harvard Univ.*, **13:** 61-91.
27. Troll, W. 1931. "Beiträge zur Morphologie des Gynaeceums, I. Über das Gynaeceum der Hydrocharitaceen", *Planta*, **14:** 1.
28. Willis, J. C. 1951. *A dictionary of the flowering plants and ferns*, Cambridge.
29. Wunderleich, R. 1950. "Die Agavaceae Hutchinsons im Lichte ihrer Embryologie, ihres Gynözeum—, Staubblatt—, und Blattbaues," *Oester. Bot. Zeits.*, **97:** 437-502.

---

*Not seen in original.

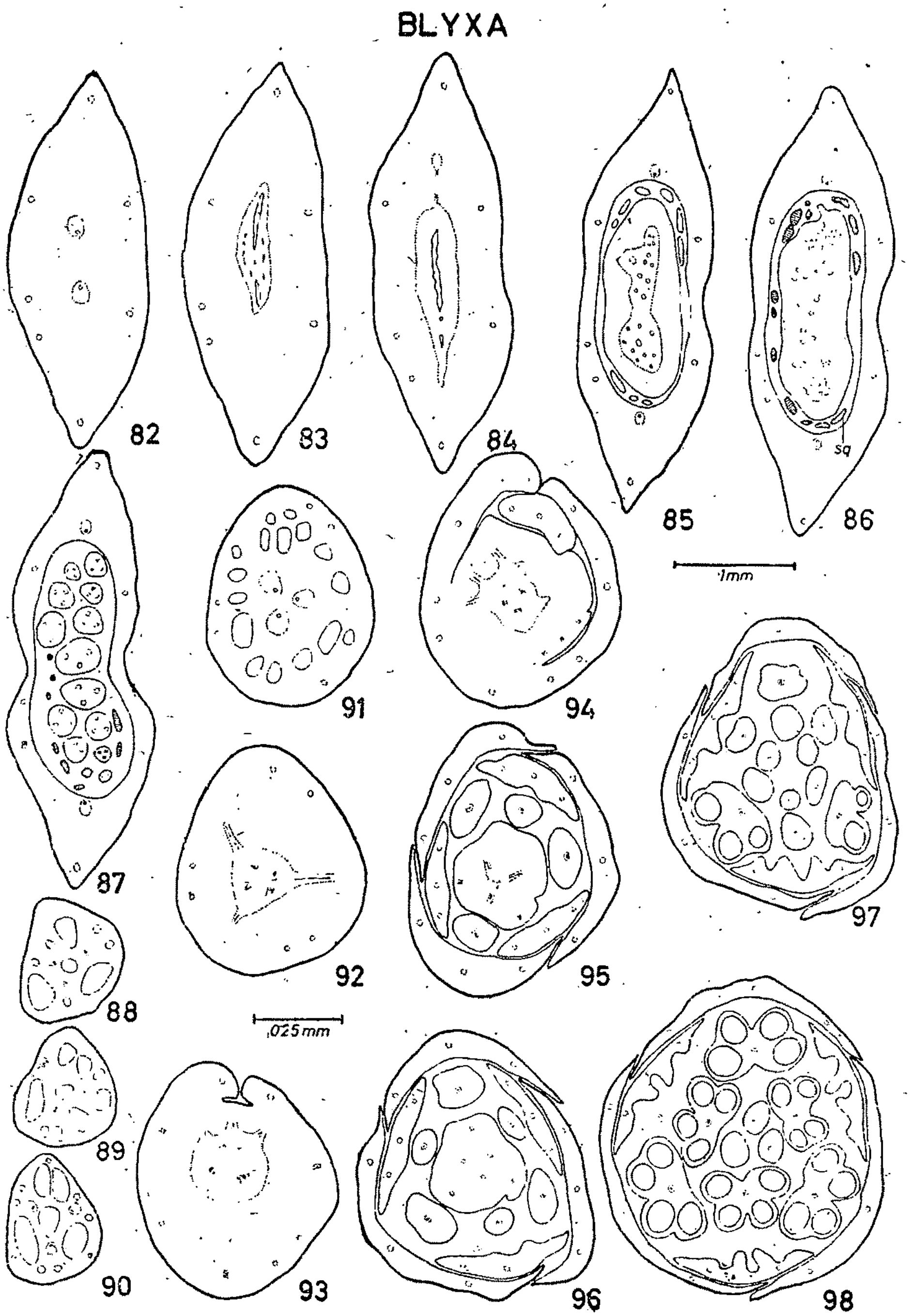

Figs. 82-98. *Blyxa octandra*. Figs. 82-87. Serial cross sections of male inflorescncee from below upward. Figs. 91-98. Serial cross sections of staminate flower from base upward showing vascular supply to different organs.

sq—squamulae.

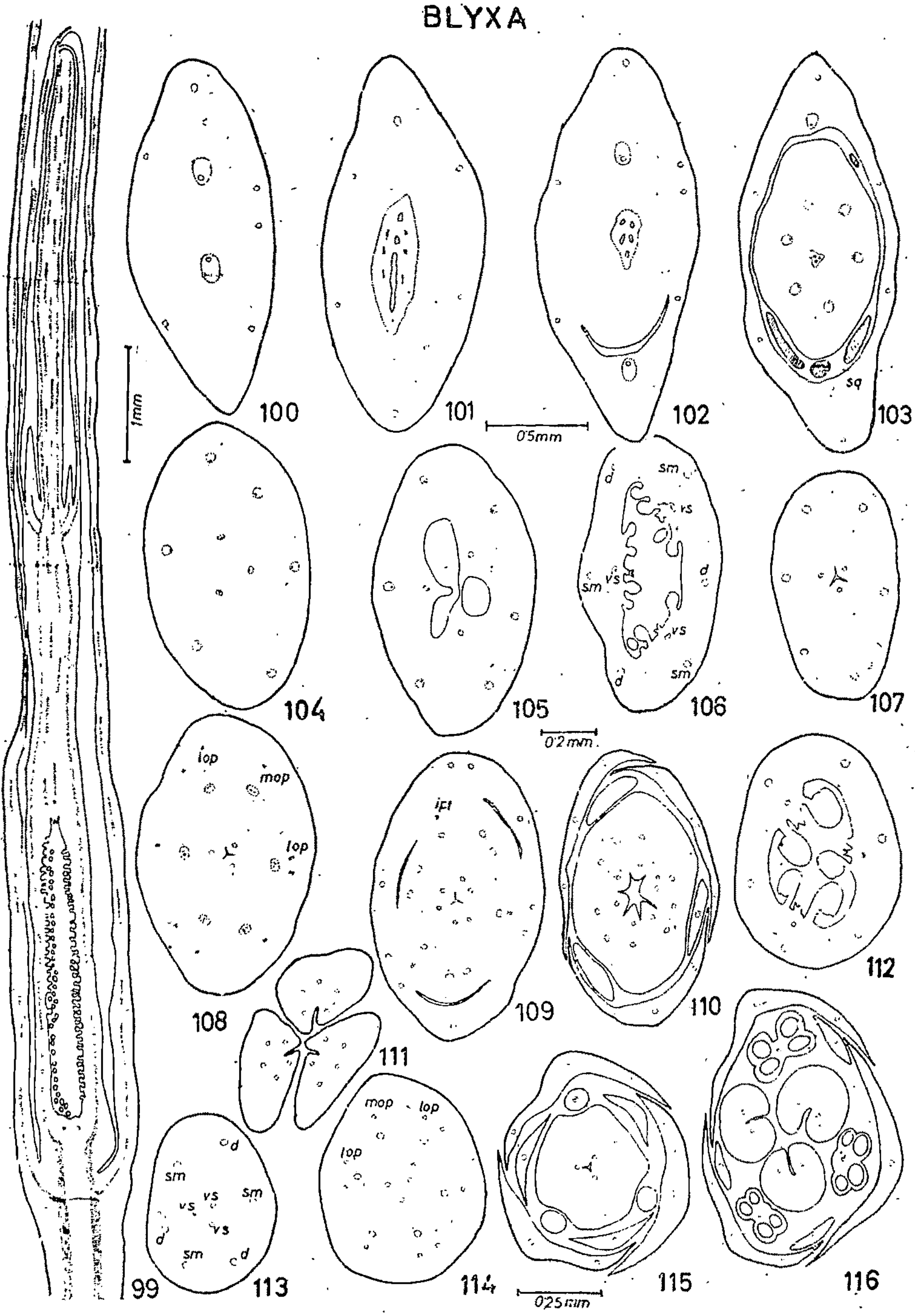

Figs. 99-116. Figs. 99-111. *Blyxa octandra*. Fig. 99. Longitudinal section of pistillate flower showing vascular ground plan—semidiagrammatic. Figs. 100-111. Serial cross sections of the same from base upward showing vascular supply to different organs. Figs. 112-116. *Blyxa echinosperma*. Cross sections of pistillate flower at different levels.

d—dorsal bundle; lop—lateral trace of outer perianth segment; mop—median trace of outer perianth segment; sm—secondary marginal; sq—squamulae; vs—ventral strand.

VALLISNERIA SPIRALIS

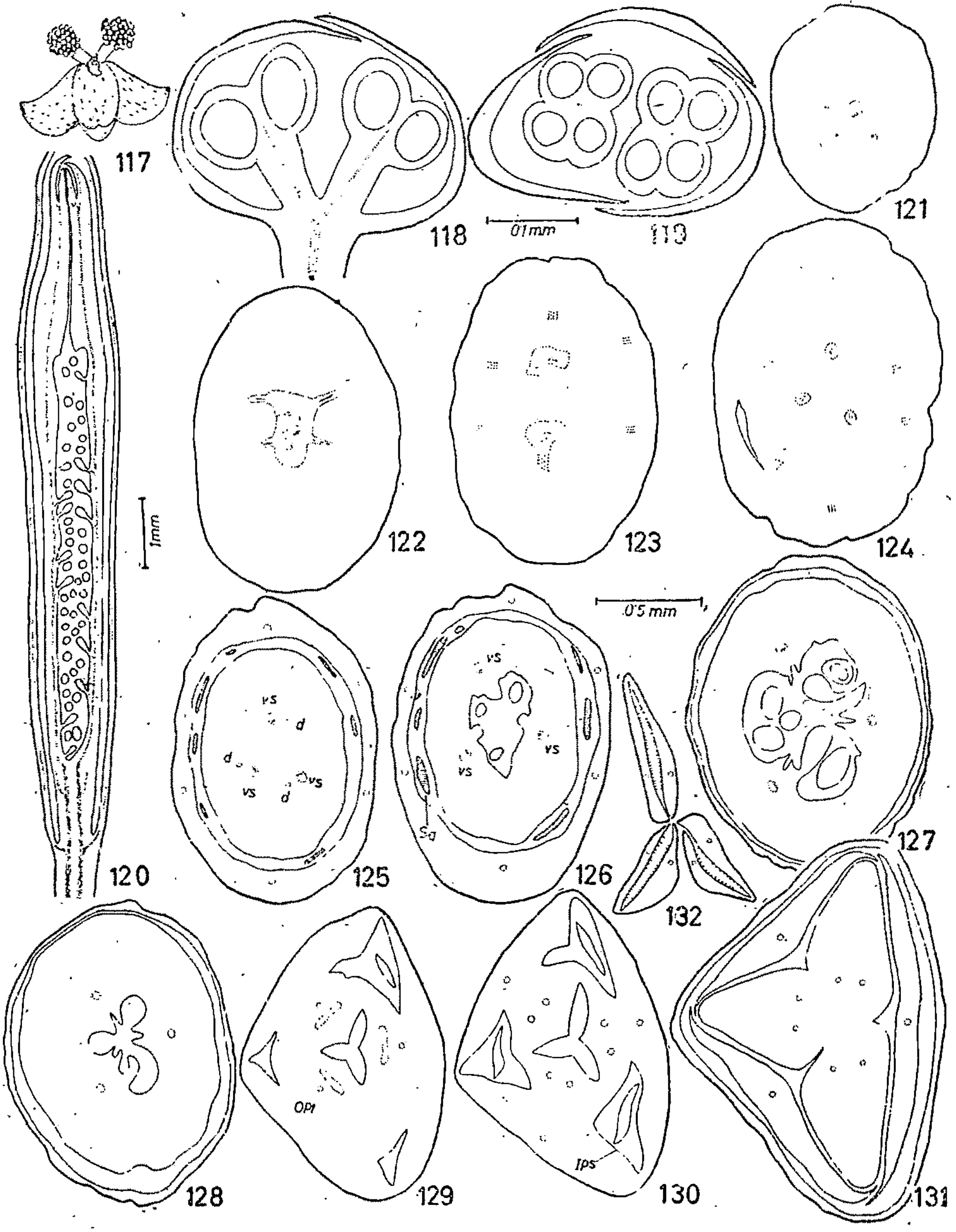

Figs. 117-131. *Vallisneria spiralis.* Fig. 117. External view of a staminate flower. Figs. 118 and 119. Longitudinal and transverse sections of the same respectively. Fig. 120. Semidiagrammatic representation of vascular ground plan of pistillate flower in longitudinal section. Figs. 121-131. Serial cross sections of the same from base upward showing vascular supply to different organs.

d—dorsal bundle; ips—inner perianth segment; opt—outer perianth trace; sq—squamulae; v—ventral strand.

HYDRILLA VERTICILLATA

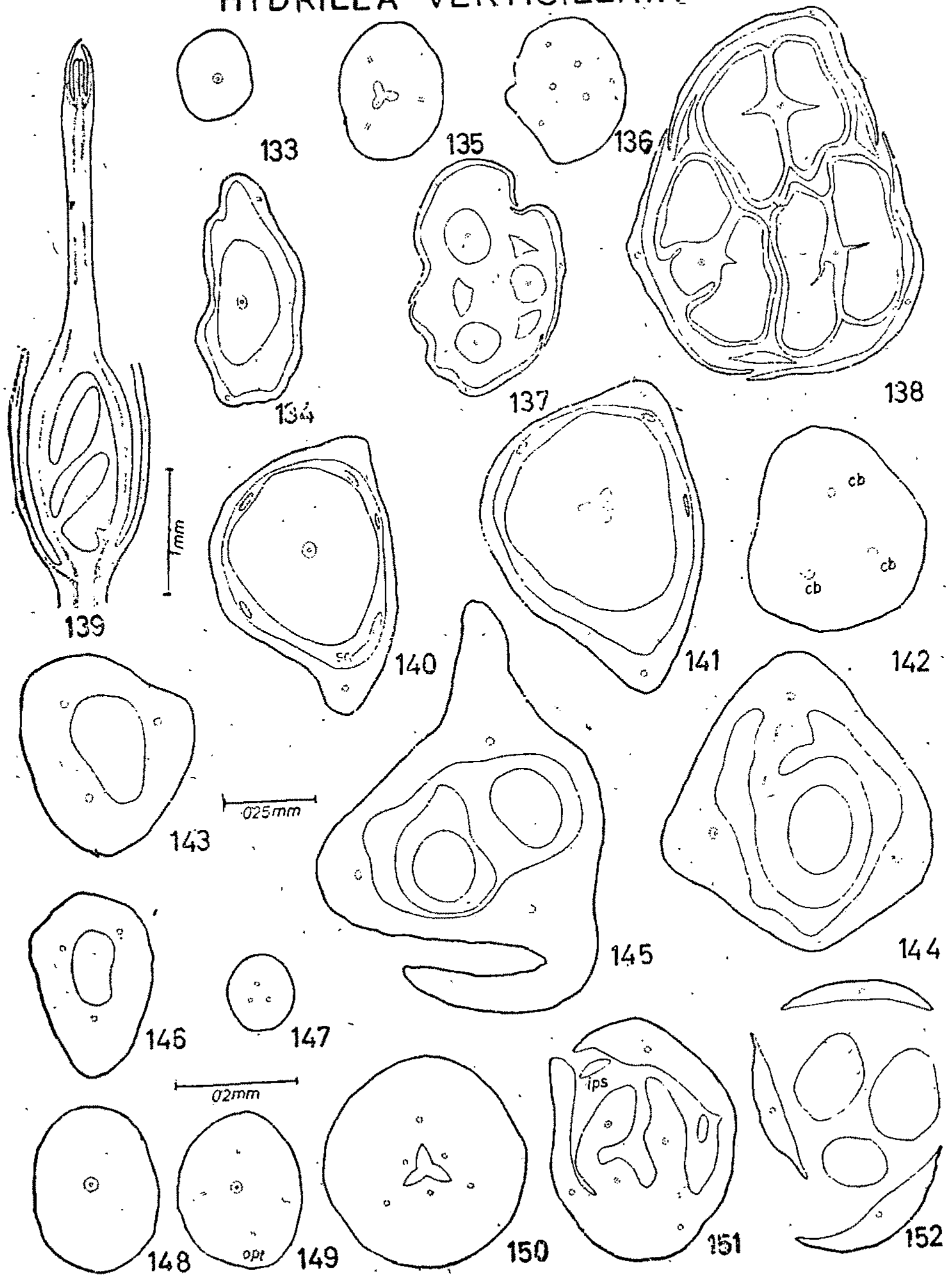

Figs. 133-152. *Hydrilla verticillata.* Figs. 133-138. Serial cross sections of staminate flower from base upward. Fig. 139. Semidiagrammatic longitudinal section of pistillate flower showing vascular ground plan. 140-152. Serial cross sections of the same from base upward.

cb—carpellary bundle; ips—inner perianth segment; opt—outer perianth trace; sq—squamulae.

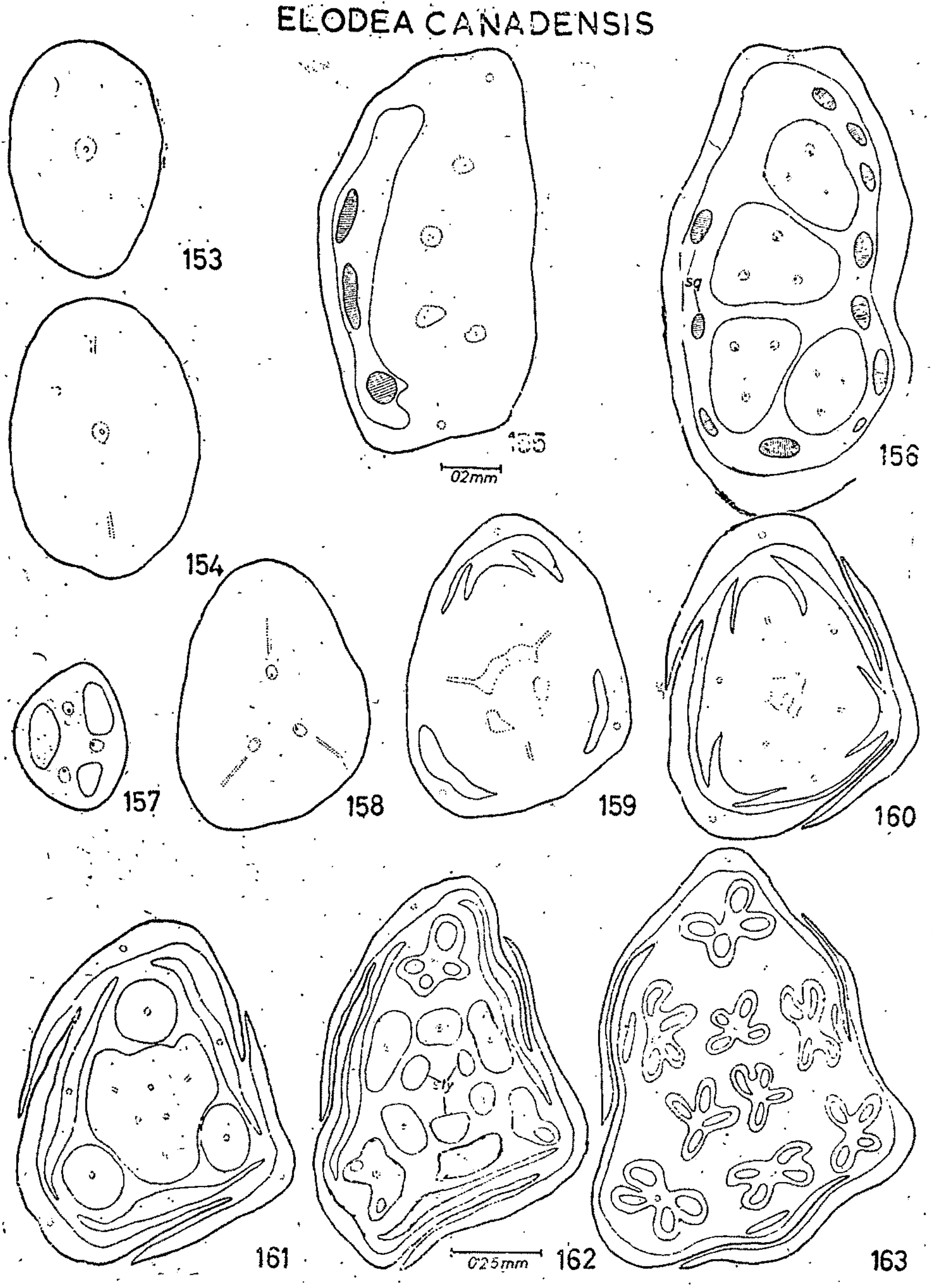

Figs. 153-163. *Elodea canadensis*. Figs. 153-156. Cross sections of male inflorescence at different levels. Figs. 157-163. Serial cross sections of staminate flower from base upward showing vascular supply to different organs.

sq—squamulae; sty—styllodia.

HALOPHILA OVALIS

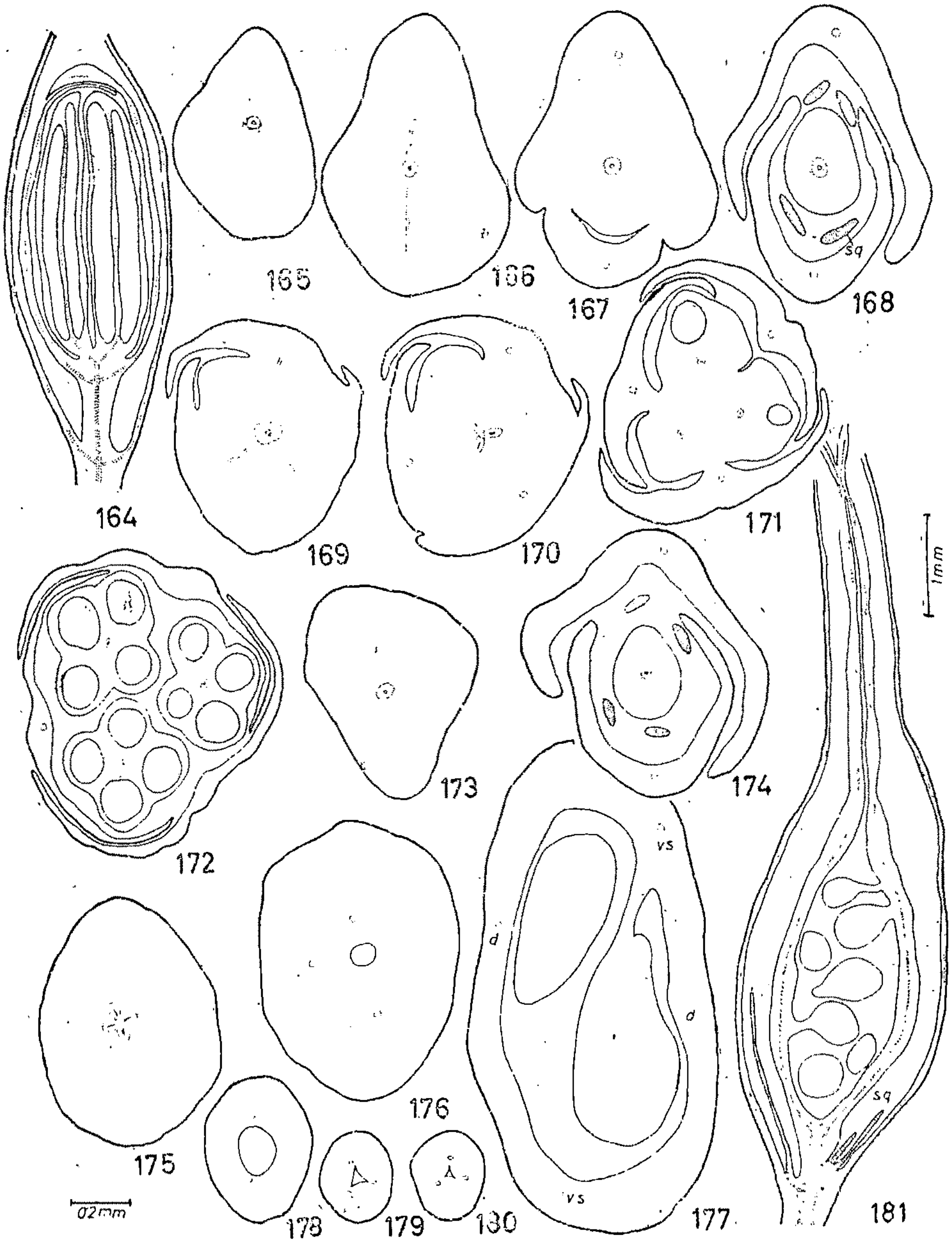

Figs. 164-181. *Halophila ovalis.* Fig. 164. Longitudinal section of staminate flower. Figs. 165-172. Serial cross sections of the same from base upward. Figs. 173-180. Serial cross sections of pistillate flower from base upward showing vascular supply at different levels. Fig. 181. Semidiagrammatic representation of longitudinal section of same.
d—dorsal bundle; sq—squamulae; vs—ventral strand.

DESCRIPTION OF ONE NEW SPECIES OF *PHYTOBIA* LIOY (AGROMYZIDAE: DIPTERA) FROM INDIA*

SANTOKH SINGH AND SANTOSH K. TANDON
School of Entomology, St. John's College, Agra.

In the course of the taxonomic studies of the Indian Agromyzidae, we came across a couple of very interesting specimens of an apparently undescribed species belonging to the genus *Phytobia* Lioy. Of the 15 species of *Phytobia* so far known from the Oriental region, only one, *viz.*—*Phytobia* (*Calycomyza*) *humeralis* (V. Roser) has been recorded from India. A new species *Phytobia* (*Phytobia*) *ipeii* from S. India is being described in this paper.

We thank the authorities of the School of Entomology, for facilities for work and the U. P. Govt. Research Committee for financial assistance in making the collections. The type specimens will be deposited in the national collections at Zoological Survey of India, Calcutta.

PHYTOBIA (PHYTOBIA) IPEII, sp. nov.

Head—(Figs. 1, 2) Frons wider than width of eye (0·34 : 0·25 mm) about one and a half times as long as wide, sides almost parallel. Face vertical with narrow carina; lunule low, approximately semi-circular and extending a little below the bases of second LOR; parafrontals slightly bulged out in profile and slightly more than one-fourth as wide as the frontalia. Ocellar triangle prominent, with apex reaching up to the level of first ORS, distance between lateral ocelli little more than the distance between lateral and median ocellus. FO five pairs, upper FO two and reclinate, first being longer than the second; the lower LFO three, almost equal, first and second lower orbitals upright while the third reclinate; orbital setulae sparse, reclinate. Frons not projecting above eyes in profile, cheeks elongated, about one-fifth the vertical height of the eye; eyes oval, pilose, dorsal margin covered with minute bristles, longer than broad. Antennae adjoining, located below the mid-level of the eye; second antennal segment minutely pubescent; third antennal segment round, pubescent, transverse; arista long, a little less than double the size of antenna (0·30:0·17 mm) and a little more than half the height of the eye, conspicuously pubescent; about six to seven oral vibrissae; peristomal setae absent.

Throax—(Fig. 3) Mesonotum with four pairs of strong dc, one anterior to the suture and three posterior to the suture; first dorso-central about one and a half times as long as the fourth dc, second almost equal to first, third dc slightly smaller than first dc: acr in four irregular rows extending a little above the second dc; prescutellars two, a little more than half the size of the first dc; sa one, strong, at level with the third dc and slightly smaller than first dc; ia one, smaller than sa; pa one strong, slightly longer than the first dc; ps one, about the size of the fourth dc; np two, anterior being slightly smaller than the posterior; humeral one, with minute setulae, longer than the fourth dc. Mesopleura with six, strong bristles pointing posteriorly; sternopleura with five to six bristles pointing dorsally.

---

* Contribution No. 115 from the School of Entomology, St. John's College, Agra.

Wing—(Fig. 4) Costa ending at M_{1+2}, second, third and fourth costal segments as 3·8 : 1·2 : 1; wing apex between termination of R_{4+5} and M_{1+2}, nearer to R_{4+5}; R_{4+5} and M_{1+2} almost parallel; last section of vein M_{1+2} more than four times as long as the penultimate section; r—m little beyond the termination of vein R_1 and slightly beyond the mid-point of discal cell; ultimate segment of M_{3+4} in ratio 1:1 2 with the penultimate.

Abdomen—Broadly ovate, tergites pilosed, with prominent marginal and discal setae; laterals on third segment prominent.

Colour—Frons matt black; parafrontals and ocellar triangle black; lunule dark-grey; cheeks black; antenna and arista dark-brown; proboscis dark-brown; palpi black; eyes dark-brown with red periphery; mesonotum, scutellum and pleurae shining-black; abdomen and legs black; wings hyaline, squammae and its fringe white, veins brown; halteres white.

Male—Similar in colouration to female, differing only in size.

Measurements—

	Body length	Wing length
♂	2·52 mm	2·52 mm
♀	3·23 mm	2·70 mm

Holotype—One female labelled "Kumli (Kerala, India), 27.i.1963. Coll. Ipe M. Ipe; on grass." In the collections of the School of Entomology, St. John's College, Agra.

Paratype—One male on pin, labelled "Kumli (Kerala, India), 27-i-1963, coll. Santosh K. Tandon; on grass." In the collections of the School of Entomology, St, John's College, Agra.

This species resembles *Phytobia* (*Phytobia*) *nigrita* (Malloch) from Formosa but can be readily distinguished by the ocellar triangle being prominent and extending up to the level of first upper orbitals; frons wide; fronto-orbitals being five pairs; third antennal segment pilosed with completely pubescent arista; and the squamal fringe being white.

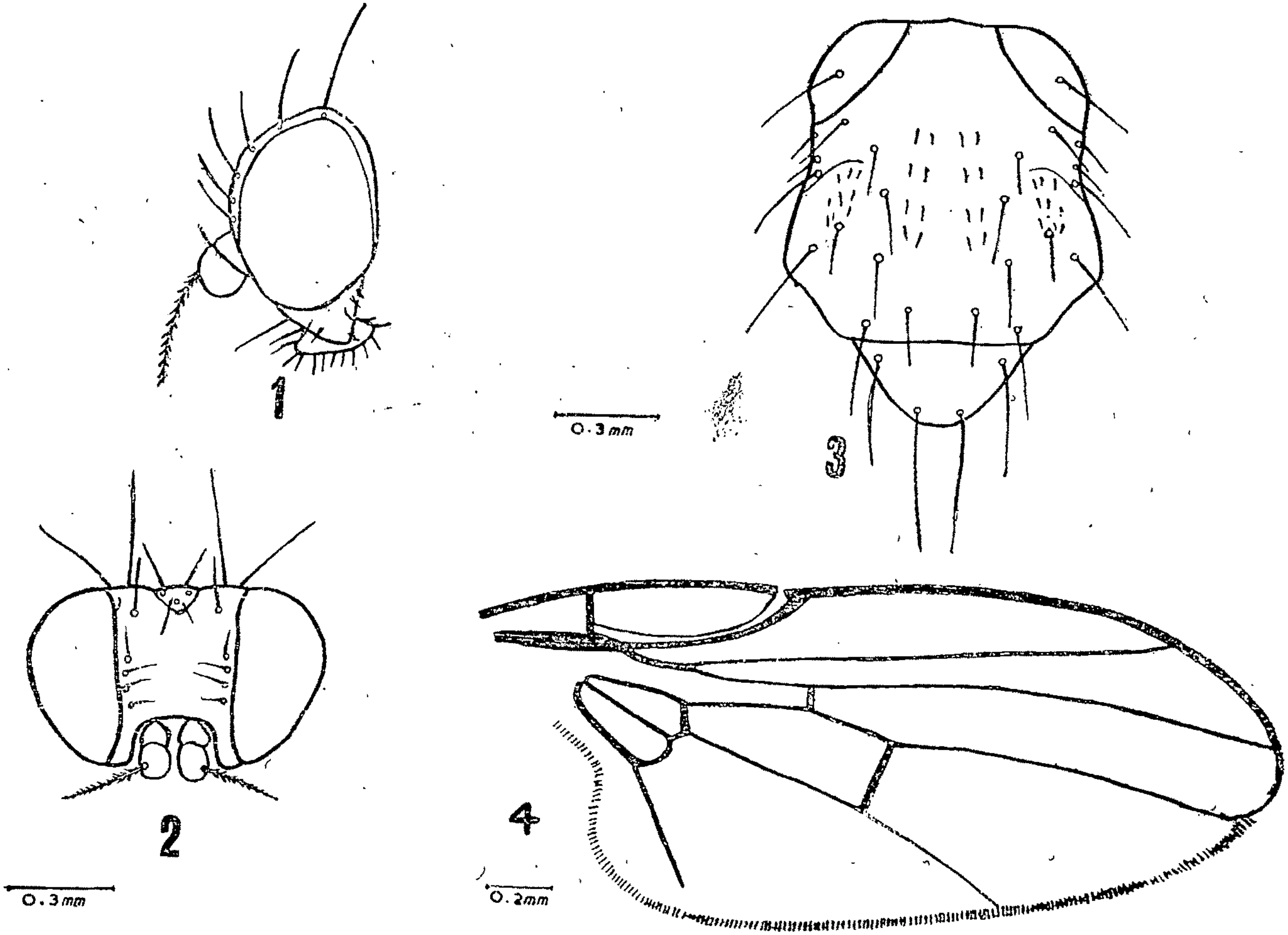

Phytobia (*Phytobia*) *ipeii*, sp. nov. 1. Head in profile; 2. Head anterior view; 3. Mesonotum (dorsal view); 4. Wing.

STUDIES ON INDIAN AGROMYZIDAE (DIPTERA) PART I. DESCRIPTION OF TWO NEW SPECIES OF *PHYTAGROMYZA* HENDEL*

SANTOSH K. TANDON
Senior Research Fellow, C. S. I. R.
School of Entomology, St. John's College, Agra.

In the course of my studies on the Indian Agromyzidae (Diptera), the relatively small genus *Phytagromyza* Hendel, represented hitherto only by a single species from the Oriental region, attracted my attention. Descriptions of two new species *viz.*—*P. keralaensis* sp. nov. and *P. agraensis* sp. nov. are given in this paper, making the total number of species so far known from India to three, along with a diagnostic key for identifying the three species. The type specimens will be deposited in the national collections at Zoological Survey of India, Calcutta.

I offer my grateful thanks to Dr. T. Singh, Professor of Zoology and Entomology for guidance and for facilities for work. Also I thank Dr. Santokh Singh and Dr. J. L. Nayar for help in various ways during the preparation of this paper.

Key to the Oriental species of *Phytagromyza* Hendel:

1.	Arista bare; squamal fringe brown; second costal segment 2:1 with fourth	*atrata* (Malloch)†
—	Arista plumose; squamal fringe not brown; second costal segment unlike as above	2
2.	Frons narrow than the width of eye; squamal fringe dark; second costal segment 2·5:1 with fourth ...	*keralaensis* sp. nov.
—	Frons more than twice the width of eye; squamal fringe white; second costal segment 3:1 with fourth.	*agraensis* sp. nov.

Phytagromyza keralaensis sp. nov.

Head—(Figs. 1 and 2) Frons slightly narrow than the width of eye (0·26:0·28 mm), slightly more than twice as long as wide, sides parallel, lunule white extending up to the level of the second lower orbitals; parafrontals narrow, slightly bulged out in profile and little more than one-fifth as wide as the frontalia; ocellar triangle short extending far above the level of the first upper orbitals; the three ocelli form an equilateral triangle, dorsal side of the ocellar triangle, subequal to the width of the frontalia. Fronto-orbitals

---

* Contribution No. 116 from the School of Entomology, St. Jonn's College, Agra.

† Spencer, K. A. 1961. A synopsis of the Oriental Agromyzidae (Diptera). *Trans. R. ent. Soc. Lond.*, **113** (4) : 90.

four pairs, upper orbitals reclinate, while the lower fronto-orbitals upright; the first upper fronto-orbitals largest; the first lower orbital slightly longer than the second lower orbital and about half the size of the first upper orbital; the distance between the lower orbitals slightly more than the distance between the upper orbitals. Cheeks broad, produced at rear, about one-fourth the vertical height of the eye; oral vibrissae present; eyes oval, sparsely pubescent; antennal grooves separated by carina; second antennal segment minutely pubescent; third antennal segment rounded, slightly longer than broad; arista short, slightly longer than the antenna, about half the vertical height of the eye (0·21:0·41 mm) and conspicuously plumose.

Thorax—(Fig. 3) Mesonotum with three pairs of *dc* posterior to the transverse suture; first slightly longer than the second, *2dc* little below the supra-alar, *3dc* about one-third the first *dc*; *acr* in six regular rows extending up to the level of second *dc*; *ia* one and about one and a half times the second *dc*; *sa* one, smaller than the *ia*; *pa* one, subequal to first *dc*; *h* one with minute setulae; *np* two, posterior being longer than the anterior; *ps* one and equal to the second *dc*. Mesopleura with three bristles pointing posteriorly; one strong sternopleural bristle directed posteriorly.

Wing—(Fig. 4) Costa terminating at R_{4+5}, second, third and fourth costal segments as 2·5:1·9:1; wing apex between termination of vein R_{4+5} and M_{1+2}, the latter two being almost parallel; last section of vein M_{1+2} more than twenty-seven times as long as the penultimate section; ultimate segment of M_{3+4} in ratio (9·3:1) with the penultimate.

Abdomen—Oval, tergites setaceous; the marginal and discal bristles prominent; the third tergite with distinct laterals in addition.

Colour—Para-frontals black; ocellar triangle faintly shining; frontalia matt; antenna and arista black; eyes dark-brown; proboscis brown, palpi black; cheeks black. Mesonotum glossy black; pleurae and scutellum black; legs black, tarsals brown. Abdomen shining black. Wings hyaline, squamae grey, fringe dark; veins brown; halteres white.

Measurements—

	Body length	Wing Length
Male	2·22 mm.	2·00 mm.

Holotype—One male labelled "Kottayam (Kerala, India), 25.1.1963, coll. Santosh K. Tandon; on grass". In the collections of the School of Entomology, St. John's College, Agra.

This species differs from the only Oriental species of this genus, *Phytagromyza atrata* (Malloch), known from Japan, Formosa, Indonesia and India (Calcutta), in arista being plumose, second costal segment about two and a half times the length of fourth costal segment and with differences in colour and size.

Phytagromyza agraensis sp. nov.

Head—(Figs. 5 and 6) Frons broad, more than twice the width of eye (2·3:1), about twice as long as wide (1·1:0·61 mm), sides almost parallel; lunule dark, microscopically pubescent; parafrontals bulged out in profile and about one-fourth as wide as the frontalia. Ocellar triangle short, extending only up to the level of first upper orbital; the three testaceous ocelli form equilateral triangle, dorsal side of the ocellar triangle subequal to the width of the frontalia. Fronto-orbitals four pairs, upper orbitals reclinate and lower orbitals upright; the distance between lower orbitals more than the upper orbitals. In profile, parafrontals raised above eye margin; cheeks broad produced at rear and about one-fourth the vertical height of eye. Four to five marginal setae on the post-frons; one to two strong oral vibrissae accompanied with minute pile; eyes somewhat oval, concave anteriorly and convex posteriorly, sparsely pubescent. The antennal grooves separated by prominent carina; second antennal segment with minute bristles; third antennal segment obtusely pointed; longer than broad; arista slightly longer than the antenna (0·49:0·35 mm) and shorter than the vertical height of eye (0·49:0·67 mm.).

Thorax—(Fig. 7) Mesonotum with four strong *dc*, one being anterodorsocentral and three posterodorsocentrals; first about twice the length of fourth; third and fourth subequal; second about one and a half times the third and fourth. Six irregular rows of *acr* extending up to the level of prescutellars; *la* one; *pa* one, almost equal to *ia*; *sa* one: *Np* two, posterior being shorter than anterior; *h* one with distinct setulae; presutural one, longer than *h*; prescutellar one, equal to second *dc*. Mesopleura with two prominent setulae directed posteriorly.

Wing—(Fig. 8) Costa ending at R_{4+5}, second, third and fourth costal segments as 3·7:1·4:1; wing apex between terminations of R_{4+5} and M_{1+2} but nearer to R_{4+5} and M_{1+2}; but slightly diverging apically; distal section of vein M_{1+2} more than six times as long as the penultimate section; *r-m* slightly distal to the termination of R_1 and beyond the mid point of discal cell; ultimate segment of M_{3+4} in ratio (1:1·4) with penultimate.

Abdomen—Broadly ovate, first tergite sparsely covered with setae, remaining tergite prominently setaceous; marginal, discal and lateral bristles prominent; seventh, eighth and ninth segments form a slender, telescopic, setaceous tube.

Colour—Head black; frontalia matt; parafrontals and ocellar triangle shining black; cheeks and antennae black; arista dark-brown; eyes dark. Mesonotum shining black; scutellum black; pleura matt black. Wings hyaline; calypters with fringe white veins brown; haltere knob conspicuously white, stalk pale; wing base dark.

Measurements—

	Body length	Wing length
Female	3·8 mm.	3·5 mm.

Holotype—Female labelled "Dayalbagh, Agra, 12.iii.1963, coll. Santosh K. Tandon; from Barley leaves." In the collections of the School of Entomology, St. John's College, Agra. Paratypes 3 females with the same data.

This species can easily be separated from *Phytagromyza atrata* (Malloch) from Formosa, by the presence of prescutellar bristles and in the ratio of second and fourth costal segments; and from *Phytagromyza keralaensis* sp. nov. in frons being more than twice the width of the eyes, differences in the ratio of the costal segments and calypters being with white fringe.

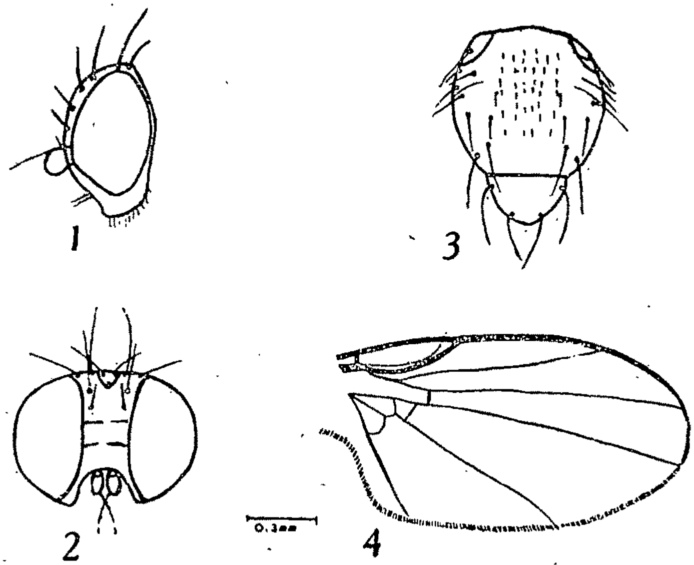

Figs. 1-4. *Phytagromyza keralaensis*, sp. nov.
1. Head in profile, 2. Head (anterior view),
3. Mesonotum (dorsal view). 4. Wing.

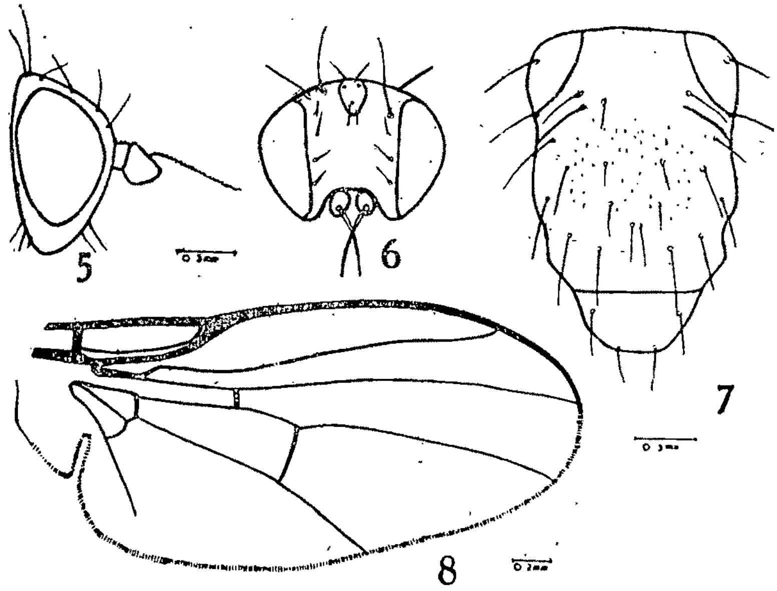

Figs. 5-8. *Phytagromyza agraensis.* sp. nov.
5. Head in profile. 6. Head (anterior view).
7. Mesonotum (dorsal view). 8. Wing.

MONOGRAPHIC STUDIES OF *CYPERUS ESCULENTUS*[*][†]

I. GROWTH HABITS AND TUBERIZATION

R. SHIAM
School of Plant Morphology, Meerut College, Meerut.

INTRODUCTION

From the view point of the traditional economic botany the Cyperaceae, comprising some 4000 species (Koyama, 1961) is of slight value. However, a few species from this family have entered into the service of man to a minor extent. Of all the Cyperaceae, the "Chufa" *Cyperus esculentus* is perhaps of greatest economic importance. Its distribution is worldwide and its popularity as an article of food is almost an extensive. Its edible tubers have long been valued throughout the world as a vegetable delicacy and as a source of starch sugar and oil.

Cultivation of this plant was very much neglected in the past due to some practical difficulties associated with digging. A recent imposition of an embargo in 1950 on commercial shipments of tubers of *Eleocharis dulcis* from Communist China has promoted interest in experimentation in the cultivation of *Eleocharis dulcis* (Hodge, 1956).

Our country has conditions suitable for the growth of *Cyperus esculentus* and hence there is vast scope for the development of its cultivation. It is very likely that with improved methods of cultivation the tubers may increase in size and their food value may be significantly increased. With this object in view a detailed monographic study of this plant has been undertaken under the supervision and guidance of Professor V. Puri.

MATERIAL AND METHODS

The material for the present study of *Cyperus esculentus* was collected from a pond situated by the side of Mawana Road about four miles north of Meerut. A few plants were also collected from a pond near Mansha Devi Mandir by the side of Garh Road. In August young plants were collected and a few of them were also transplanted in the Botanical garden of Meerut College, in a newly constructed *Cyperus* pond, in order to have a close eye on them.

A few tubers were also transplanted in the pond and detailed field studies were carried out involving their sprouting and leaf formation. Weekly observations of stolon formation were also recorded. The depth of soil at which the tuberization is affected was noted and soil from different ponds was collected in order to find out its pH value. All these observations were taken at weekly intervals for more than one season.

---

[*] Based on part of a thesis accepted for the Ph.D. degree of the Agra University, in 1962.

[†] Contribution No. 83 from the School of Plant Morphology, Meerut College, Meerut, India.

OBSERVATIONS

External Morphology—Cyperus esculentus is an erect, glabrous, annual herb propagating vegetatively. The plant is a marshy one, even when submerged during rains a few leaves and culms always remain above water. Under natural habitat it attains a normal height of about 90 cm., but in extreme cases the culms measured upto 276 cm. The axis is underground with creeping slender subterranean stolons. It is roughly cylindrical and varies from 1·0 to 1·5 cm. in diameter, and bears leaves and culms above and roots under soil.

Vegetative propagation is carried out by axillary buds borne on underground axes. These buds usually grow out into long stolons that run horizontally to the surface of the soil, and at right angles to the axis of the plant. Each stolon at its tip bears a bud that generally produces a satellite plantlet or when it goes deep into the soil, forms a tuber that is a small rounded structure.

The plants have an adventitious root system typical of Monocotyledons. The roots arise from the axis, tuber and stolon. They may arise both from the nodal as well as from the internodal regions, and vary in thickness and length. A few rootlets are also given out.

The narrow linear foliage leaves of *Cyperus esculentus* can be distinguished into a sheathing leafbase, a channelled blade and a pointed tip (Fig. 1). The sheathing leafbases enclose the axis for a very short distance. They develop in a regular sequence in three rows and their arrangement is very symmetrical. The vegetative apex of the plant is dome shaped or conical structure, surrounded by a number of small young leaves. The apex remains underground.

The inflorescence axis or the culm is a very long triangular structure with sharp angles and with a few moderately large leaves clustered at its base. It ends in an inflorescence with very large leafy bracts. The culm is formed of a single internode and does not branch except in giving rise to the peduncles of the inflorescence. It is always erect and exceptionally straight.

The inflorescence is in the form of umbellate spike subtended by a number of large leafy bracts. The flowers are arranged in spikelets. They arise in the axils of the glumes which are arranged on the axis of the spikelet. Flowers are pistillate below and hermaphrodite above. Each hermaphrodite flower is typically trimerous, having 5 to 6 perianth members three stamens and a tricarpellary ovary with a dilated style and three stigmatic lobes.

The stigmatic lobes are comparatively very long and are often seen emerging out from the glumes in the spikelet.

Fruit and seed formation has not been observed by the present author although he has examined a very large amount of material over more than one season.

Growth Habit—*Cyperus esculentus* is perhaps the most typically amphibious plant in the family Cyperaceae, and is seen in ditches of marshes or brakish waters occuring associated with *Eleocharis plantaginea*, *Aponogeton natans*, *Sagittaria guayanensis* and *Juncellus species*. At Meerut it occurs in the months of June to March. During this period the weather conditions are very variable. In June the temperature reaches the highest point. In July and August rains set in and we have 80% of the total annual rainfall (about 520 mm. at Meerut). Under these conditions sprouting of tubers takes place. The tuber germinates from its terminal end and produces small band-shaped white leaves which are wholly or partially submerged (Fig. 2). The first leaves produced by the sprouting tuber are scale leaves overlapping each other acropetally. These leaves show rapid elongation and soon attain a fairly long size (Figs. 3-5). Later on the plant produces rosettes of linear elongated foliage leaves that are broader and longer than the scale leaves. The plants dug up carefully in later summer, are found to show a number of white long stolons arising from among the basis of the crowded leaves on the short main axis (Fig. 6). The stolons are distinguished from the roots by their greater size and thickness and in possessing scale leaves at node and a terminal bud. In July they are only 3-7 cm. long but may attain a length of about 60 cm. in some cases in the middle of August. The number of stolons produced from the base of a single plant is variable. As many as 6 stolons were recorded arising from a single plant.

The behaviour of stolons is interesting. In the early August they grow roughly horizontally to the soil surface and approximately at right angles to the axis of the parent plant. After running for a short distance which varies from plant to plant, each stolon produces a satellite plantlet at its tip in the growing season (Fig. 7). All these satellite plantlets show vertical growth and are responsible for all the aerial vegetative growth. This is followed by flowering that starts in September and continues upto the middle of November.

Simultaneously with this some stolons develop approximately at an angle of 45° to the vertical axis of the parent plant. The growing apices of these stolons instead of forming satellite plantlets swell up to form the edible tubers (Fig. 9). As the stolons elongate their tips increase in size until finally they take the shape of mature tubers. The tuberization is over usually by December. The young tubers are white in colour but become brown or black as they mature.

There is still another type of behaviour shown by the stolons. A few stolons arise at an angle of more than 45° from the vertical axis of the plant and produce small tubers. These tubers may sprout in the same season and produce small leaves from their terminal region. But these sprouting tubers remain underground for most of their length. After a certain period their growth ceases and the sprouting tubers remain buried in the soil upto the next growing season. Figure 8 shows a parent plant with three sprouting tubers of the same season.

The tubers are produced at different depths below the soil surface which usually vary from 5 to 45 cm., but the average depth is about 20 cm. The soil is clayey and as such has much water-holding capacity. Its pH during the rains is about 7·5.

With the advent of winter in January and February the leaves become somewhat yellow and dry off along with the inflorescence and its axis. The underground portions of the plant are also affected resulting in the decay of the delicate parts like stolons. This decay sets the tubers free from the parent plant. It is at this time that the tubers are dug off. Those that are left from digging perennate for the next season's growth. But if there is an occasional rainfall or by chance the tubers get sufficient water, they may start sprouting from their terminal end. This, however, does not continue growth for long as in April the ponds are usually dried and no aerial growth is possible.

As the rains approach early in July the terminal buds of the perennating tubers grow out into elongated axes, bearing scale leaves, and carrying bud upto the surface of the soil (Fig. 10). Following this a new adventitious root system is formed from the shoot just below the surface of the soil. At this stage the parent tuber appears to have lost its reserve food-material and it is in a dry, exhausted rotten state. It is possible to find a plant still attached to a parent tuber and this in turn producing satellite plantlets and stolons which will develop into tubers of the next generation.

DISCUSSION

The growth habit of *Cyperus esculentus* presents some points of interest and it will be profitable to discuss them at some length here.

The plant completes its life cycle by means of tubers, which sprout during the favourable period and form the vertical axis. The roots lack cambium and consequently their power to increase in thickness is lost and remain small in cross-section. To compensate for this a large number of roots are formed from vertical axis, stolons and tubers.

The vertical axis is much reduced in *Cyperus esculentus* and remains mostly underground. In a few cases it gives rise to the inflorescence axis or the culm, which does not divide further. But in those cases where the inflorescence axis or the culm is not formed, there are present some axillary buds at the closely placed basal nodes of the vertical axis. The growth of these buds then continues the life of the plant. The axillary buds grow more or less horizontally to form stolons which carry their growing-points away from the vertical axis and then form a region of close root bearing nodes. The production of roots near the tips of the stolons is an indication of the formation of new plants or tubers. Latter on the stolon tips form a few erect foliage leaves, thus forming a number of satellite plantlets in early stages of vegetative growth.

By late August each satellite plantlet forms a number of stolons, which in turn again produce new plantlets with their own root system and erect leaves. All this leads to a kind of irregular sympodial tufted growth. The space is limited for further growth of the plants. In the meantime winter days approach, and available water becomes scarce. Such conditions perhaps lead to the development of the resting organs. And it is at this time that the tips of the stolons which go deep into the soil swell up to form the tubers. These tubers are formed by mere enlargement of the parenchymatous cells of the cortex and the medullary region of the stolon tip. Engler (1884) is of the opinion that since the monocotyledonous axis is more frequently tuberous, there is probably some relation between the tardy development of the stem apex and the accumulation of carbohydrate reserves. The lack of opportunities for translocation may, in some cases, be responsible for tuber formation. Arber (1925) while studying *Arrhenatherum avenaceum* var. *bulbosa* comments that the tuberization is by the swelling of the cortical cells as well as the cells of the pith region. The present study shows that in *Cyperus esculentus* also the tuberization is by swelling or enlargement of the cells of these regions.

With further lowering of temperature and the water drying up the aerial portions of the plant die. But the underground portions like tubers rest until the next growing season, when their terminal buds develop into vertical axes and produce new shoots and their own adventitious root system. Hence we find that *Cyperus esculentus* completes its life-cycle vegetatively without showing any cambial growth. This throws some light on the problem as to why the cambium is lost. There are two views to this problem.

Sargant's (1903) view of monocotyledons in general is that they lost their cambium because it was not necessary. She has emphasized that the production of underground perennating organs was facilitated by a cambium less growth; and that the necessity for the production of such organs, therefore, led to the disappearance of cambium.

Holttum's (1955) viewpoint, however, is somewhat different. He suggests that the lack of cambium led first of a peculiar type of continuous vegetative growth in the moist tropics, namely, sympodial growth. And this sympodial growth proved itself peculiarly adaptable to the production of the resting organs, thus allowing cambium-less plants to spread to seasonal climates.

In view of what has already been said above, Holttum's view appears to be more logical.

SUMMARY

Cyperus esculentus is an erect, glabrous, annual herb and propagates vegetatively. Its growth habits are interesting as it propagates with the help of tubers. The tubers sprout from their terminal ends under favourable conditions and produce the underground vertical axis of the plant. The vertical axis produces the stolons and roots under the soil and leaves and culms above the ground level.

Three types of behaviour are exhibited by stolons. In one type they elongate very much and grow more or less horizontally to the soil surface and produce satellite plantlets at their tips. In second type the stolons which go deeper into the soil, swell at their tips to form the tubers that perennate in the winter and sprout only in the next season when the environmental conditions are favourable. In the third type the stolons that arise at an angle of more than 45° from the vertical axis of the plant produce small tubers that may sprout in the same season. The plant exhibits sympodial growth.

ACKNOWLEDGEMENTS

I am extremely grateful to my respected teacher Professor V. Puri for his valuable guidance, constant help and continuous encouragement received throughout the course of this study. I am also thankful to Dr. Y.S. Murty for his kind help in several ways, and to the authorities of the C. S. I. R., New Delhi, for financial help.

REFERENCES

1. Arber, A. 1955. *Monocotyledons*. A Morphological study. Cambridge.
2. Engler, E. 1884. Beitrage zur Kenntniss der Araceae. *Engler's Bot. Jahrb.*, **5** : 141-188.
3. Hodge, W. H. 1956. Chinese Water chestnut or Matai—*A Paddy crop of China. Eco. Bot.*, **10** : 49-65.
4. Holttum, R. E. 1955. Growth-habits of Monocotyledons-variation on a theme. *Phytomorphology*, **5** : 399-413.
5. Koyama, T. 1961. Classification of the family Cyperaceae (I). *Jour. Fac. Sci. Univ. Tokyo*, III, **10** : 38-86.
6. Sargant, E. 1903. A theory of the origin of monocotyledons founded on the structure of their seedlings. *Ann. Bot.*, **17** : 1-92.

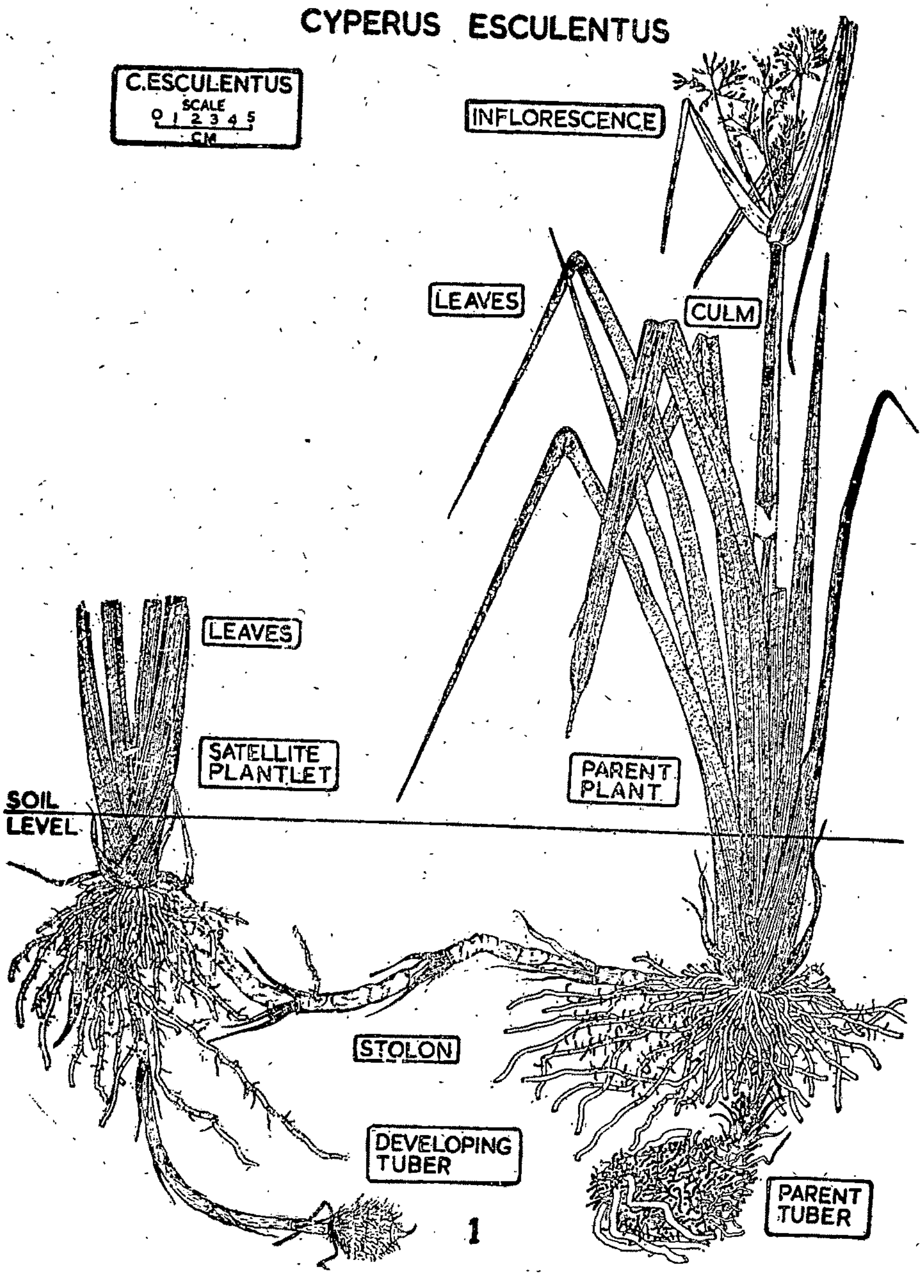

1

Fig. 1. *Cyperus esculentus.* An entire plant with a satellite plantlet.

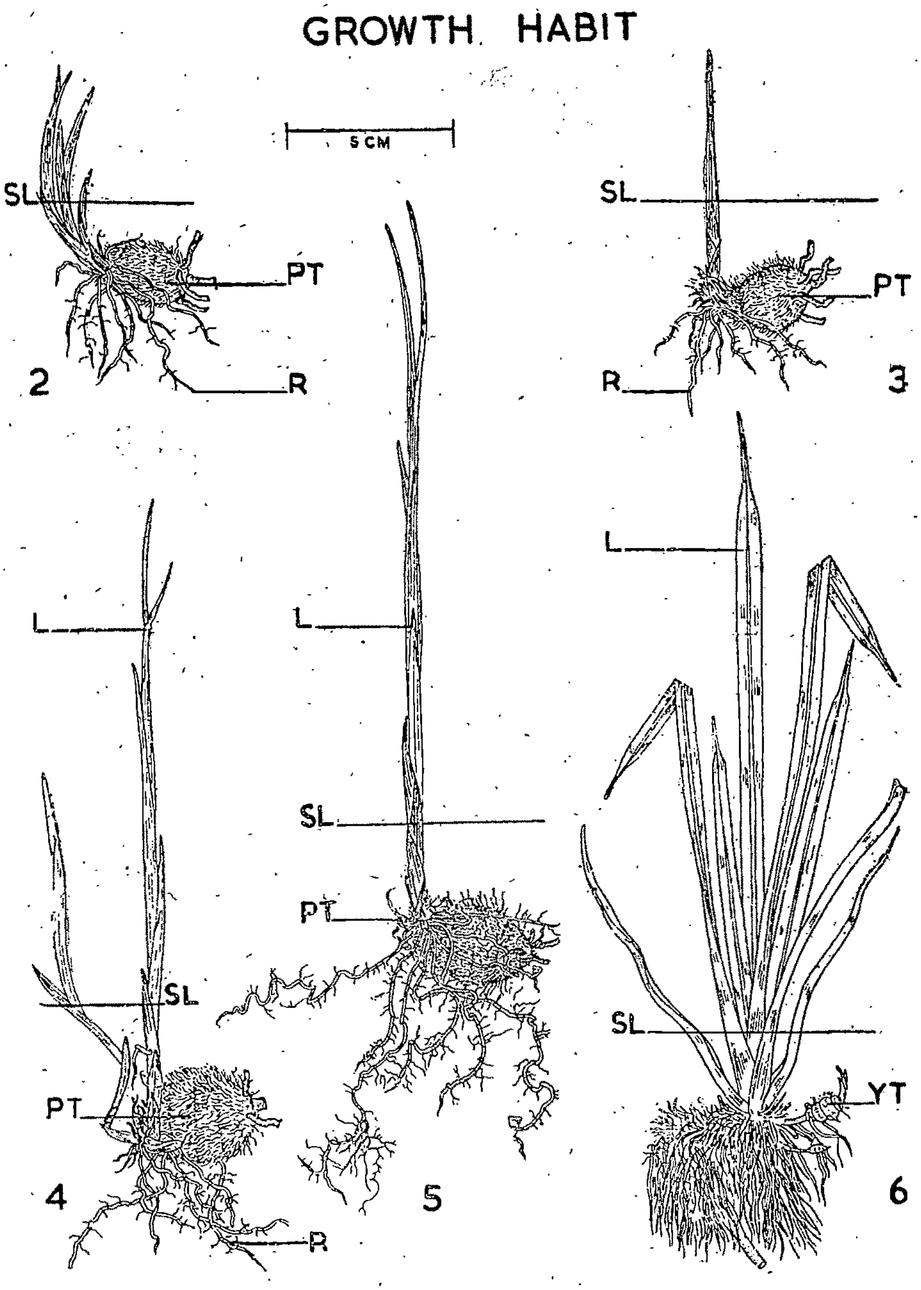

Figs. 2-6. *Cyperus esculentus* growth habit. Figs. 2-5. Sprouting tubers at different developmental stages. Fig. 6. A young plant. L—Leaves; PT—Parent tuber; R—Roots; SL—Soil level; YT—Young tuber.

GROWTH HABIT

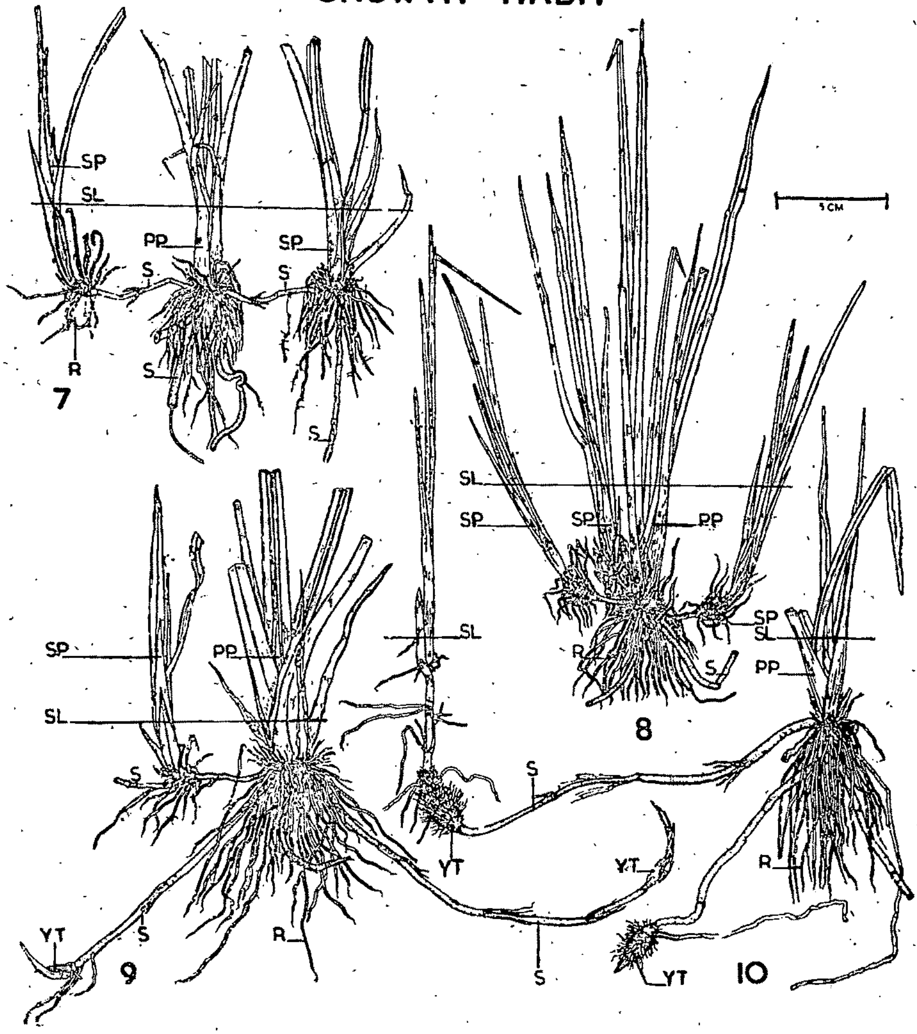

Figs. 7-10. *Cyperus esculentus* growth habit. Fig. 7. A young plant with two satellite plantlets. Fig. 8. A comparatively older plant with three satellite plantlets. Fig. 9. A plant with a single satellite plantlet and with two developing tubers. Fig. 10. A plant with two tubers, one growing into a plant. PP—Parent plant; R—Roots; S—Stolons; SL—Soil level, SP—Satellite plantlet; YT—Young tuber.

VARIABLE FLOW IN A UNIFORM TUBE OF A PARTICULAR TYPE OF SECTION

J. P. Agarwal
Agra College, Agra.

Abstract

In this paper the flow of an incompressible viscous fluid in a long uniform tube due to a periodic pressure gradient has been considered. The section of the tube is a curvilinear quadrilateral bounded by arcs of two concentric circles and the segments of two radii of bigger circle intercepted between those arcs. The exact solution for the velocity has been obtained by the application of Finite Fourier Transform.

Introduction

Richardson and Tyler [2] considered the flow of an incompressible viscous fluid in a long straight uniform tube of circular section due to a periodic pressure gradient. The case of a tube of elliptic section was considered by Khamrui [1].

In the present paper the same problem has been considered when the section of the tube is a curvilinear quadrilateral shown in the figure.

Equations of Motion

Using cylinderical coordinates r, θ and z; taking z in the direction of the tube through the centre of the concentric circles, the walls of the tube are $r=a$, $r=b$, $\theta=0$ and $\theta=\alpha$.

Let w be the velocity in the z-direction and other components of the velocity are assumed to be zero. By reference to the equation of continuity $\frac{\partial w}{\partial z}$ must be zero, so that w is a function of r, θ and t only.

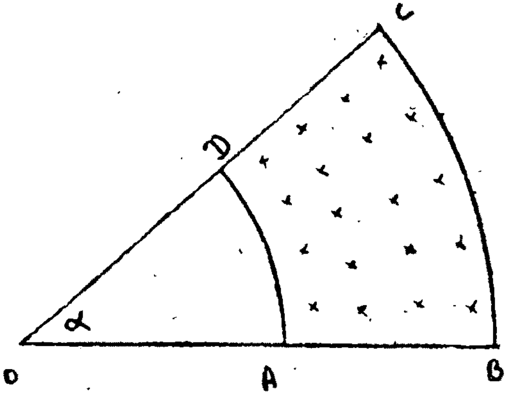

OA=b, OB=a
ABCD is section of the tube.

The equations of motion, in the absence of external forces, reduce to

$$\frac{\partial P}{\partial r}=0, \quad \frac{\partial P}{r\partial \theta}=0,$$

$$\frac{\partial w}{\partial t}=-\frac{1}{\rho}\frac{\partial P}{\partial z}+\nu\left(\frac{\partial^2 w}{\partial r^2}+\frac{1}{r}\frac{\partial w}{\partial r}+\frac{1}{r^2}\frac{\partial^2 w}{\partial \theta^2}\right).$$

It follows that P is independent of r and θ, and that $\dfrac{\partial P}{\partial z}$ is a function of t alone.

If for the problem under consideration,

$$\frac{\partial P}{\partial z}=-k\rho\cos wt, \qquad \text{where } k \text{ is a constant,}$$

then w must satisfy the eq.

$$\frac{\partial w}{\partial t}=k\cos wt+\nu\left(\frac{\partial^2 w}{\partial r^2}+\frac{1}{r}\frac{\partial w}{\partial r}+\frac{1}{r^2}\frac{\partial^2 w}{\partial\theta^2}\right) \qquad \ldots (1)$$

The boundary conditions are

$$\left.\begin{array}{ll} w=0, \text{ when } r=a \text{ and } b, & 0\leqslant\theta\leqslant\alpha \\ w=0, \text{ when } \theta=0 \text{ and } \alpha, & b\leqslant r\leqslant a \end{array}\right\} \qquad \ldots (2)$$

SOLUTION OF THE EQUATION

It is obvious that w=Real part of W, where W satisfies the eq.

$$\frac{\partial W}{\partial t}=k e^{iwt}+\nu\left(\frac{\partial^2 W}{\partial r^2}+\frac{1}{r}\frac{\partial W}{\partial r}+\frac{1}{r^2}\frac{\partial^2 W}{\partial\theta^2}\right) \qquad \ldots (3)$$

It is easy to see that the solution of this equation is

$$W=f(r,\theta)\,e^{iwt}$$

where $f(r,\theta)$ satisfies the eq.

$$\left(\frac{\partial^2}{\partial r^2}+\frac{1}{r}\frac{\partial}{\partial r}+\frac{1}{r^2}\frac{\partial^2}{\partial\theta^2}-\frac{iw}{\nu}\right)f=-\frac{k}{\nu} \qquad \ldots (4)$$

Putting $\theta=\dfrac{\alpha}{\pi}\phi$, this eq. becomes

$$\left(\frac{\partial^2}{\partial r^2}+\frac{1}{r}\frac{\partial}{\partial r}+\frac{1}{r^2}\frac{\pi^2}{\alpha^2}\frac{\partial^2}{\partial\phi^2}-\frac{iw}{\nu}\right)f=-\frac{k}{\nu} \qquad \ldots (5)$$

subject to the conditions

$$\left.\begin{array}{ll} f=0, \text{ when } r=a \text{ and } b, & 0\leqslant\phi\leqslant\pi \\ f=0, \text{ when } \phi=0 \text{ and } \pi, & b\leqslant r\leqslant a \end{array}\right\} \qquad \ldots (6)$$

Now we use a finite sine transform and write

$$\bar{f}=\int_0^\pi f.\sin p\phi\,d\phi,$$

where p is a positive integer.

Since f vanishes at $\phi=0$ and π,

$$\int_0^\pi \frac{\partial^2 f}{\partial\phi^2}\sin p\phi\,d\phi=-p^2\bar{f}.$$

Applying this finite sine transform to the eq. (5), we get

$$\left.\begin{aligned}\left[\frac{d^2}{dr^2}+\frac{1}{r}\frac{d}{dr}-\frac{\pi^2p^2}{a^2r^2}-\frac{iw}{\nu}\right]\bar{f}&=0,\text{ if } p \text{ is even}\\ &=-\frac{2K}{\nu p},\text{ if } p \text{ is odd}\end{aligned}\right\} \qquad \ldots (7)$$

subject to the conditions

$$\bar{f}=0 \quad \text{when } r=b \text{ and } a. \qquad \ldots (7A)$$

For even values of p, the solution of eq. (7) subject to the conditions (7A) is

$$\bar{f}=0$$

We now proceed to find the solution for odd values of p. The complementary function for the eq. (7) is

$$A\, J_{\frac{\pi p}{a}}\left(e^{-\frac{i\pi}{4}}\sqrt{\frac{w}{\nu}}\cdot r\right)+B\, Y_{\frac{\pi p}{a}}\left(e^{-\frac{i\pi}{4}}\sqrt{\frac{w}{\nu}}\cdot r\right) \qquad \ldots (8)$$

Applying the method of variation of parameters, this would also be the complete primitive if

$$\frac{dA}{dr}=\frac{2k\pi}{\nu p}r\, Y_{\frac{\pi p}{a}}\left(e^{-\frac{i\pi}{4}}\sqrt{\frac{w}{\nu}}\cdot r\right)$$

and $$\frac{dB}{dr}=-\frac{2k\pi}{\nu p}r\, J_{\frac{\pi p}{a}}\left(e^{-\frac{i\pi}{4}}\sqrt{\frac{w}{\nu}}\cdot r\right) \qquad \ldots (9)$$

Putting $A=G(r)+C_1$

and $B=F(r)+C_2$ $\qquad \ldots (10)$

where

$$G(r)=\frac{2k\pi}{\nu p}\int_b^r r\, Y_{\frac{\pi p}{a}}\left(e^{-\frac{i\pi}{4}}\sqrt{\frac{w}{\nu}}\cdot r\right)dr$$

$$F(r)=-\frac{2k\pi}{\nu p}\int_b^r r\, J_{\frac{\pi p}{a}}\left(e^{-\frac{i\pi}{4}}\sqrt{\frac{w}{\nu}}\cdot r\right)dr$$

and C_1 and C_2 are arbitrary constants,
we have

$$\bar{f}=[G(r)+C_1]\, J_{\frac{\pi p}{a}}\left(e^{-\frac{i\pi}{4}}\sqrt{\frac{w}{\nu}}\cdot r\right)+\left[F(r)+C_2\right] Y_{\frac{\pi p}{a}}\left(e^{-\frac{i\pi}{4}}\sqrt{\frac{w}{\nu}}\cdot r\right) \qquad \ldots (11)$$

Applying the boundary conditions (7A), we have

$$[G(a)+C_1]\, J_{\frac{\pi p}{a}}\left(e^{-\frac{i\pi}{4}}\sqrt{\frac{w}{\nu}}a\right)+[F(a)+C_2]\, Y_{\frac{\pi p}{a}}\left(e^{-\frac{i\pi}{4}}\sqrt{\frac{w}{\nu}}a\right)=0$$

and

$$[G(b)+C_1]\, J_{\frac{\pi p}{\alpha}}\left(e^{-\frac{i\pi}{4}}\sqrt{\frac{w}{\nu}}.b\right)+[F(b)+C_2]\, Y_{\frac{\pi p}{\alpha}}\left(e^{-\frac{i\pi}{4}}\sqrt{\frac{w}{\nu}}b\right)=0 \quad \text{.. (12)}$$

From these, the values of C_1 and C_2 can be found and inserted in (11) to determine $\bar{f}$ completely.

Now by an inversion of the transform,

$$f = \frac{2}{\pi}\sum_p \bar{f}\sin p\phi, \text{ where } p \text{ is an odd positive integer}$$

$$=\frac{2}{\pi}\sum_p\left[AJ_{\frac{\pi p}{\alpha}}\left(e^{-\frac{i\pi}{4}}\sqrt{\frac{w}{\nu}}.r\right)+B\, Y_{\frac{\pi p}{\alpha}}\left(e^{-\frac{i\pi}{4}}\sqrt{\frac{w}{\nu}}.r\right)\right]\sin\frac{p\pi}{\alpha}\theta \quad \text{.. (13)}$$

Hence

$$w=\frac{2}{\pi}\text{Re}\sum_p\left[AJ_{\frac{\pi p}{\alpha}}\left(e^{-\frac{i\pi}{4}}\sqrt{\frac{w}{\nu}}r\right)+B\, Y_{\frac{\pi p}{\alpha}}\left(e^{-\frac{i\pi}{4}}\sqrt{\frac{w}{\nu}}.r\right)\right]\sin\frac{p\pi}{\alpha}\theta.e^{iwt} \quad \text{.. (14)}$$

where A and B are given by equations (9), (10), (11) and (12).

REFERENCES

1. Khamrui, S. R. 1957, *Bull. Cal. Math. Soc.*, **49** : 57.
2. Richardson, E. G. & Tyler, E. 1929. *Proc. Phys. Soc. London*, **42** : 1

STEADY POISEUILLE FLOWS THROUGH STRAIGHT CHANNELS BOUNDED BY PARABOLIC WALLS

G. C. SHARMA
Agra College, Agra.

ABSTRACT

In this paper steady flow of an incompressible viscous fluid in a long uniform straight channel due to a constant pressure gradient has been considered. The section of the channel is a curvilinear quadrilateral bounded by the arcs of four confocal parabolas. The exact solution for the velocity has been obtained by the application of finite Fourier Transform. Two particular cases have also been derived.

INTRODUCTION

The steady flow of an incompressible viscous fluid in a pipe of rectangular cross-section has been considered experimentally and theoretically by R. J. Cornish [2]. J. P. Agrawal [1] has considered the flow through pipes, section—a hyperbolic segment. In a recent paper the present author [3] has studied the steady flow due to a constant pressure gradient, the section of the tube being the curvilinear quadrilateral bounded by the arcs of two confocal ellipses and two confocal hyperbolas.

In the present paper the steady flow due to a constant pressure gradient has been considered when the section of the channel is the quadrilateral PQRS shown in the figure.

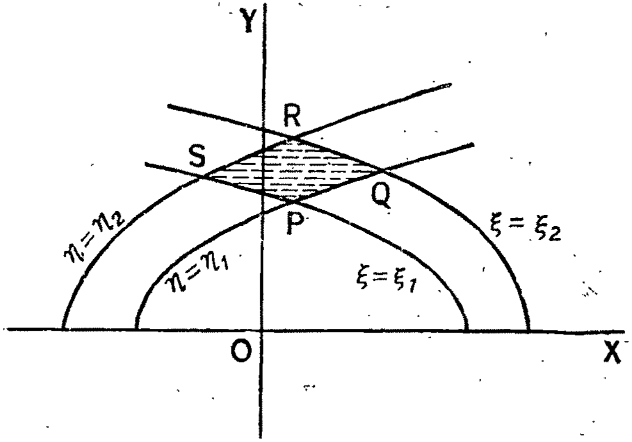

FIG. NO. 1.

Equation of Motion

Using a rectangular cartesian coordinate system the equation of motion for steady flow is

$$\nu\left(\frac{\partial^2 w}{\partial x^2}+\frac{\partial^2 w}{\partial y^2}\right)=\frac{1}{\rho}\,\frac{\partial p}{\partial z} \qquad ..(1)$$

where w is the velocity in the direction of z. Other components of the velocity are assumed to be zero; ν is the kinematic viscosity and $\frac{\partial p}{\partial z}$ is constant.

For the present problem, put $x+iy=(\xi+i\eta)^2$ ..(2)

Then $\xi=\xi_1$, $\xi=\xi_2$, $\eta=\eta_1$ and $\eta=\eta_2$ are four confocal parabolas. We will take ξ to vary from 0 to ∞ to cover the whole plane and η to vary from $-\infty$ to $+\infty$. Then $\eta=$ (positive) represents a parabolic arc above the x—axis and $\eta=$ (negative) represents a parabolic arc below the x—axis.

If the cartesian equations of the confocal parabolas be,

$$y^2=-4a\,(x-a)$$
$$y^2=-4b\,(x-b)$$
$$y^2=4\alpha\,(x+\alpha)$$
$$y^2=4\beta\,(x+\beta)$$

respectively, then the values of ξ_1, ξ_2, η_1 and η_2 will be as follows,

$$\xi_1=\sqrt{a}$$
$$\xi_2=\sqrt{b}$$
$$\eta_1=\pm\sqrt{\alpha}$$
$$\eta_2=\pm\sqrt{\beta}$$

Equation of motion with the help of (2) becomes

$$\frac{\partial^2 w}{\partial \xi^2}+\frac{\partial^2 w}{\partial \eta^2}=\lambda\,[\xi^2+\eta^2] \qquad ..(3)$$

where $\lambda=-\frac{4P}{\nu\rho}$, $-P$ being the value of $\frac{\partial p}{\partial z}$.

The boundary conditions are :—

$$\left.\begin{array}{l} w=0 \text{ when } \xi=\xi_1 \text{ and } \xi=\xi_2 \\ w=0 \text{ when } \eta=\eta_1 \text{ and } \eta=\eta_2 \end{array}\right\} \qquad ..\ (4)$$

Solution of the Equation

Putting $\eta=Aq+B$ where

$$A=\frac{\eta_2-\eta_1}{\pi} \text{ and } B=\eta_1 \qquad ..\ (5)$$

equation (3) becomes

$$\frac{\partial^2 w}{\partial \xi^2}+\frac{1}{A^2}\frac{\partial^2 w}{\partial q^2}=\lambda\Big[\xi^2+(Aq+B)^2\Big] \qquad ..\ (6)$$

subject to the conditions :—

$$w=0 \text{ when } \xi=\xi_1 \text{ and } \xi=\xi_2 \text{ and } 0\leqslant q\leqslant\pi \qquad ..\ (7)$$

$$w=0 \text{ when } q=0 \quad\text{and}\quad q=\pi \quad\text{and}\quad \xi_1\leqslant\xi\leqslant\xi_2 \qquad \ldots (8)$$

Now we use a finite sine transform and write

$$\bar{w}(s)=\int^{\pi} w \sin sq\, dq, \text{ where } s \text{ is a positive integer.}$$

Since w vanishes at $q=0$ and $q=\pi$,

$$\int_0^{\pi} \frac{\partial^2 w}{\partial q^2}\sin sq\, dq=-s^2\bar{w}$$

Applying this finite transform to equation (6) we get,

$$\frac{d^2\bar{w}}{d\xi^2}-\frac{s^2}{A^2}\bar{w}=\lambda\int_0^{\pi}\left\{\xi^2+(Aq+B)^2\right\}\sin sq\, dq.$$

$$\therefore \frac{d^2\bar{w}}{d\xi^2}-\frac{s^2}{A^2}\bar{w}=-\frac{\lambda A\pi}{s}(\pi A+2B), \text{ when } s \text{ is even.} \qquad \ldots (9)$$

$$\frac{d^2\bar{w}}{d\xi^2}-\frac{s^2}{A^2}\bar{w}=\frac{2\lambda\xi^2}{s}+\frac{\lambda}{s}\Big[(A\pi+B)^2+B^2-\Big]\frac{4\lambda A^2}{s^3}, \text{ when } s \text{ is odd.} \quad (10)$$

with conditions $\bar{w}=0$ when $\xi=\xi_1$ and $\xi=\xi_2$ .. (11)

For even values of s the solution of equation (9) is

$$\bar{w}=C_1\, e^{\frac{s}{A}\xi}+C_2 e^{-\frac{s}{A}\xi}+\frac{\pi\lambda A^3}{s^3}(A\pi+2B) \qquad \ldots (12)$$

where C_1 and C_2 are to be determined with the help of conditions (11)

$$\left.\begin{aligned} \therefore\quad C_1 e^{\frac{s}{A}\xi_1}+C_2\, e^{-\frac{s}{A}\xi_1} &= -\frac{\pi\lambda A^3}{s^3}(A\pi+2B)\\ \text{and}\quad C_1\, e^{\frac{s}{A}\xi_2}+C_2 e^{-\frac{s}{A}\xi_2} &= -\frac{\pi\lambda A^3}{s^3}(A\pi+2B)\end{aligned}\right\} \qquad \ldots (13)$$

from (13) the values of C_1 and C_2 can be obtained and inserted in (12) to determine $\bar{w}$ completely.

Now we proceed to find the solution of (10) for odd values of s.

$$\bar{w}=C_3\, e^{\frac{s}{A}\xi}+C_4\, e^{-\frac{s}{A}\xi}-\frac{\lambda A^2}{s^3}[2\xi^2+A^2\pi^2+2\pi AB+2B^2] \qquad \ldots (14)$$

where C_3 and C_4 are to be determined with the help of conditions (11).

$$\left.\begin{aligned} \therefore\quad C_3\, e^{\frac{s}{A}\xi_1}+C_4 e^{-\frac{s}{A}\xi_1} &= \frac{\lambda A^2}{s^3}[2\,\xi_1^2+A^2\pi^2+2\pi\, AB+2B^2]\\ \text{and}\quad C_3\, e^{\frac{s}{A}\xi_2}+C_4 e^{-\frac{s}{A}\xi_2} &= \frac{\lambda A^2}{s^3}[2\,\xi_2^2+A^2\pi^2+2\pi AB+2B^2]\end{aligned}\right\} \qquad \ldots (15)$$

C_3 and C_4 can be determined from (15) and substituted in (14) to determine $\bar{w}$.

Now by inversion of the transform

$$w = \frac{2}{\pi}\sum_s \bar{w} \sin sq, \quad \text{where } s \text{ is a positive integer.}$$

$$= w_1 + w_2$$

where
$$w_1 = \frac{2}{\pi}\sum_s \left[C_1 e^{\frac{s}{A}\xi} + C_2 e^{-\frac{s}{A}\xi} + \frac{\lambda\pi A^3}{s^3}(A\pi + 2B) \right] \sin sq$$

$$= {}^{2} \sum_s \left[C_1 e^{\frac{s}{A}\xi} + C_2 e^{-\frac{s}{A}\xi} + \frac{\lambda\pi A^3}{s^3}(A\pi - 2B) \right] \sin s\, \frac{(\eta - B)}{A} \quad \dots (16)$$

when s is even.

and

$$w_2 = \frac{2}{\pi}\sum_s \left[C_3 e^{\frac{s}{A}\xi} + C_4 e^{-\frac{s}{A}\xi} - \frac{\lambda A^2}{s^3}(2\xi^2 + \pi^2 A^2 + 2\pi AB + 2B^2) \right] \sin sq$$

$$= \frac{2}{\pi}\, {}_s \left[C_3 e^{\frac{s}{A}\xi} + C_4 e^{-\frac{s}{A}\xi} - \frac{\lambda A^2}{s^3}(2\xi^2 + \pi^2 A^2 + 2\pi AB + 2B^2) \right]$$
$$\times \sin s \left(\frac{\eta - B}{A}\right) \quad \dots (17)$$

when s is odd.

Here A and B, C_1 and C_2, C_3 and C_4 are given by (5), (13) and (15) respectively.

PARTICULAR CASES

s **No. 1.** If $\eta_1 = 0$ then $A = \frac{\eta_2}{\pi}$, $B = 0$, $q = \frac{\pi\eta}{\eta_2}$. In this case the section of the channel is in the form of the space bounded by $\xi = \xi_1$, $\xi = \xi_2$, $\eta = 0$ and $\eta = \eta_2$ [See Fig. No. 2.]

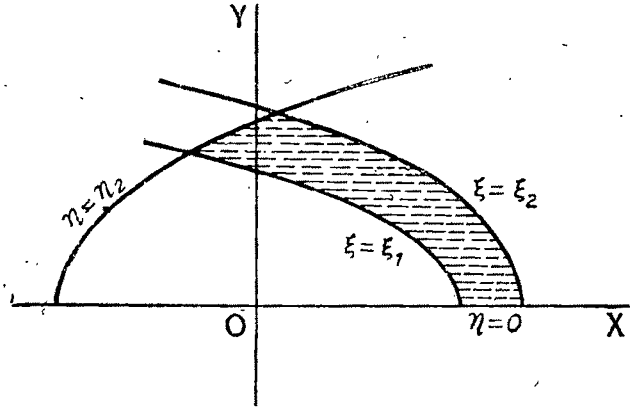

FIG. NO. 2.

$\therefore \quad w = w_1 + w_2$ where

$$w_1 = \frac{2}{\pi} \sum_s \left[C_1 e^{\frac{s\pi}{\eta_2}\xi} + C_2 e^{-\frac{s\pi}{\eta_2}\xi} + \frac{\lambda \eta_2{}^3}{\pi^2 s^3} (\eta_2 + 2B) \right] \sin s \frac{\eta\pi}{\eta_2}$$

when s is even,

and $$w_2 = \frac{2}{\pi} \sum_s \left[C_3 e^{\frac{s\pi}{\eta_2}\xi} + C_4 e^{-\frac{s\pi}{\eta_2}\xi} - \frac{\lambda \eta_2{}^2}{\pi^2 s^3} (2\xi^2 + \eta_2{}^2) \right] \sin s \frac{\eta\pi}{\eta_2}$$

when s is odd,

where C_1, C_2 and C_3, C_4 can be determined from (13) and (15) by putting $A = \frac{\eta_2}{\pi}$ and $B = 0$.

Case No. 2. If we consider the section of the channel to be portion of the parabolic quadrilateral symmetrical about the axis i. e. bounded by $\xi = \xi_1$, $\xi = \xi_2$, $\eta = \eta_1$ (positive), and $\eta = -\eta_1$

Then $A = -\frac{2\eta_1}{\pi}$, $B = \eta_1$, $q = \frac{(\eta - \eta_1)\pi}{-2\eta_1}$ [See Fig. No. 3.]

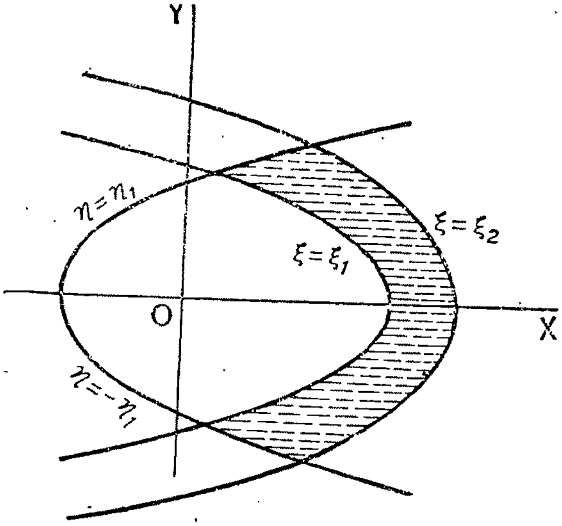

Fig. No. 3

$\therefore \quad w = w_1 + w_2$ where,

$$w_1 = \frac{2}{\pi} \sum_s \left[C_1 e^{-\frac{\pi s}{2\eta_1}\xi} + C_2 e^{\frac{\pi s}{2\eta_1}\xi} + \frac{8\lambda \, \eta_1{}^4}{\pi^2 s^3} \right] \sin s \frac{(\eta_1 - \eta)\pi}{2\eta_1},$$ when s is even,

and $$w_2 = \frac{2}{\pi} \sum_s \left[C_3 e^{-\frac{\pi s}{2\eta_1}\xi} + C_4 e^{\frac{\pi s}{2\eta_1}\xi} - \frac{8\lambda \, \eta_1{}^2}{\pi^2 s^3} (\xi^2 + \eta_1{}^2) \right] \sin s \frac{(\eta_1 - \eta)\pi}{2\eta_1},$$

when s is odd,

where C_1 and C_2, C_3 and C_4 are to be determined from (13) and (15) by putting the values of A and B.

Acknowledgement

In the end I take this opportunity to express my thanks to Dr. J. P. Agarwal for the help in the preparation of this paper.

References

1. Agarwal, J. P. 1959. *Uttar Bharti*, **VI** (2) : 117-126.
2. Cornish, R. J. 1928. *Proc. Royal Soc.*, (**A**) **120** : 619-700.
3. Sharma, G. C. 1966. *Agra Univ. J. Res. (Sci.)* **XV** (1) : 59-66.

APPEARANCE OF SHORT-WAVE RADIO SIGNALS IN THE MORNING HOURS INDICATING THE CONCENTRATION OF THE RECEIVED ENERGY NEAR M. U. F.

R. R. MEHROTRA, J. D. GARG AND B. S. SHUKLA
Physics Laboratory, D. J. College, Baraut (Meerut).

INTRODUCTION

Enhancement of intensity of short-wave radio signals prior to cessation has been reported by a number of ionospheric workers.[1–3] Detailed study of the fading patterns obtained near M.U.F. was, however, taken up by Banerjea and Mehrotra.[1] On the basis of observations recorded at B.H.U., Varanasi, from transmissions mostly from AIR, Delhi, it was reported by Mehrotra[2] that the smoothness of the fading patterns increases as M.U.F. is approached. In another communication Mehrotra and Shukla[3] attributed the enhancement of intensity of short-wave radio signals near M.U.F. to the concentration of received energy as M.U.F. is approached.

The purpose of the present note is firstly to communicate the study of some of the appearance patterns of short-wave radio signals taken at Baraut (29° 6′ N. Lat., 77° 15′ E. Longi.) district Meerut (U.P.) for transmissions from Karachi (24° 50′ N. Lat., 67° 5′ E. Longi.) in the morning hours when the ionic density is increasing, and secondly to discuss the concentration of received energy of the fading patterns near M.U.F.

EXPERIMENTAL ARRANGEMENT

For this study, an automatic fading recording system somewhat similar to that used by Banerjea and Mehrotra has been developed in the Electronics Laboratory of the Physics Department, D.J. College, Baraut (Meerut). The circuit diagram of the developed fading recorder is given in fig. 1. The D. C. voltage developed across the load resistance R_1 in the second detector stage of the superhet-receiver whose AVC has been made inoperative is applied in-between the grid and cathode of the first tube of the amplifier. The plate of the first tube is connected directly to the grid of the second tube and by inserting a suitable resistance between the grid and the cathode of this tube and connecting this cathode to a high voltage point, a negative bias is made available to the grid of the second tube. The plate of the second tube is connected through the recorder to another H. T. point. To obtain different H. T. voltages a rectifier with proper filtering system and two VR-tubes has been used as indicated in the circuit diagram (fig. 1).

Voltage developed across R_1, proportional to the strength of the received signal, makes the grid of the first tube more negative, giving rise to a corresponding decrease in its plate current. As the plate current of the first tube passes through R_2, the grid of the second tube becomes less negative giving rise to a corresponding increase in its plate current.

OBSERVATIONS AND DISCUSSION

In order to collect information regarding concentration of received energy near M.U.F. various types of observations of fading patterns are taken as communicated by Mehrotra.[2] In the present communication the observations of fading of short-wave radio signals representing the appearance of the signal in the morning hours have only been taken for discussion.

With the increase in electronic density in the morning hours the skip distance decreases. And so long as the skip distance is greater than the distance between transmitting and receiving stations, the signal is not received. When the skip distance decreases due to increase in electronic density and becomes equal to the distance between the transmitting and receiving stations, the signal appears. The appearance of the signal is a clear indication that the frequency of transmission at the time of observation for the transmitting and receiving stations under consideration is the maximum usable frequency. Any further increase in the electronic density decreases the skip distance and the frequency of transmission goes away from the M.U.F.

In the presence of the magnetic field, the magneto-ionic splitting of the ray takes place. The condition of reflection of the ordinary ray may be taken to be the same as the condition of reflection of the ray in the absence of the magnetic field. The extra-ordinary ray is reflected from a lower level.

The skip distance for the extra-ordinary ray for any ionospheric condition is less than the skip distance for the ordinary ray. In the morning hours when the electronic density is increasing slowly the distance between the transmitting and receiving stations first becomes equal to the skip distance of the extra-ordinary and as such the extra-ordinary ray appears first. For the ordinary ray, however, the receiving station still lies in the skip zone. With a slight further increase in the electronic density the frequency of transmission goes away from the MUF of the extra-ordinary and as the frequency of transmission becomes equal to the M.U.F. for the ordinary ray appears.

The exact recording of the fading patterns for a few seconds just at the time of appearance of the extra-ordinary is not possible due to the difficulty of tuning in the absence of any signal. The upper extra-ordinary and the lower extra-ordinary interference pattern is, however, observed. As discussed by Mehrotra[2,3], the intensity of the upper extra-ordinary decreases very rapidly due to concentration effect and after a very small interval the strength of the upper extra-ordinary becomes practically zero and the reception continues only due to the lower extra-ordinary ray. When the distance between the transmitter and the receiver becomes just equal to the M.U.F. for the ordinary, the appearance pattern of .the ordinary ray is recorded.. At the time of the appearance of the ordinary ray due to the concentration and focussing effects considerable enhancement of intensity is observed. This fact is evident from the sudden increase in the intensity as indicated in the figures 2, 3, 4, 5 and 6. The patterns recorded at this time are the interference patterns having three interfering components viz., the upper ordinary, the lower ordinary and the lower extra-ordinary. With the increase in the electronic density the frequency of transmission goes away from the M.U.F.S. of ordinary and the extra-ordinary. As a result of this change in the electronic density equivalent paths of the different interfering components change and the interference patterns are observed.

The patterns (figures 2,3,4,5 and 6) obtained at the time of appearance of the ordinary may be said to be the fading patterns obtained as a result of the interference of the three component waves whose strength and path-differences change in different magnitudes. As a result of this a complex pattern having two periodicities of nearly equal periods changes into a periodic pattern having superimposition of ripples.

Just at the time of appearance of the ordinary, as the amplitude of the upper ordinary is large and as the rate of change of path-difference between upper and lower ordinary is least, small portion in the beginning appears to be a mixed pattern different from the periodic patterns having supper-imposition of ripples obtained afterwards. A few such observations are given in the table and the corresponding fading patterns are shown in figures 2, 3, 4, 5 and 6. It is evident from different fading patterns that the intensity of all the three interfering components decreases as the frequency of transmission goes away from M.U.F. Nearer the M.U.F. with respect to the frequency of transmission, greater is the strength of the interfering components. This is attributed to the concentrations of received energy near MUF and can be explained with the help of D-i curve as discussed by Mehrotra and Shukla.[3]

It may further be mentioned that the two periodicities obtained in the fading patterns recorded at the time of x appearance of the ordinary, as a result of change of electronic density can be used for getting an idea of the profile near the maximum electronic density region.

The detailed study in this direction is in progress.

ACKNOWLEDGEMENT

The authors are thankful to Principal A. B. Malkani for his constant interest in the progress of the work.

REFERENCES

1. Banerjea, S. S., & Mehrotra, R. R. 1952. 'Intensity variations of Short-wave radio signals and their bearing on the Ionsphere.' *Jour. of Sc. & Indus. Res.* **11A** (1): 11,
2. Mehrotra, R. R., 1958. 'Smoothness of fading patterns of Short-wave radio signals near M.U.F.', *Agra Univ. Jour of Res. (Sci.)*, **VII** (2) : 133-142.
3. Mehrotra, R. R. & Shukla, B. S. 1965. 'Concentration of Received energy near M. U. F.', *Agra Univ. Jour. of Res. (Sci.)* **XIV**. (3) : 19-23.

TABLE 1

Transmitting Station : Karachi *Receiving Station : Baraut.*

Aerial distance between Karachi & Baraut is 1104 Km.

1 Fig. No.	2 Wave-band Metres	3		4 Sequence of events	5 Remarks
2	25	19.10.1966	0700 Hrs. IST	Transmissions from Karachi on 19 and 25 Metres were going on at the time of observation. Reception on 19 Metres was not possible upto 0723 Hrs. Signal on 25 Metre was, however, received at 0700 Hrs. The strength of the signal was very low in the beginning but after a short time considerable increase in the intensity was observed and the fading pattern changed into a periodic pattern having superimposition of ripples.	The pattern is the appearance patten o the ordinary and is preceded by reception due to the lower extra-ordinary ray.
3	19	30.10.1966	0745 Hrs. IST	Transmissions from Karachi on 19 and 25 Metres were going on at the time of observation. 25 Metres was available but reception on 19 Metres became possible at 0745 Hrs. Considerable enhancement of intensity is observed and the pattern in the beginning is a mixed one which changes subsequently into a periodic pattern having superimposition of ripples.	Just at the time of appearance the frequency of transmission was equal to the M.U.F. and the patten is the interference pattern showing decrease in the strength of the received signal as frequency of transmission goes away from M.U.F.
4	25	3.11.1966	0723 Hrs. IST	Transmissions from Karachi on 19 and 25 Metres were going on at the time of observation. Reception on 19 metres was not possible at the time of observation. It was first received at 0739 Hrs. Signal on 25 metres was received with low intensity. After a short while pattern corresponding to the appearance of the ordinary ray was obtained.	The pattern shows the appearance of the ordinary ray indicating concentration of received energy near M.U.F.

(*Continued on page 141*)

TABLE 1 (*Contd.*)

Transmitting Station : *Karachi* *Receiving Station* : *Baraut*

Aerial distance between Karachi & Baraut is 1104 Km.

1 Fig. No.	2 Wave-band Metres	3 Date & Time of observation		4 Sequency of events	5 Remarks
5	25	7.11.1966	0720 Hrs. IST	Transmissions from Karachi on 19 and 25 metres were going on at the time of observation. Reception on 19 Metre was not possible Signal on 25 metres was first of all received at 0720 Hrs. Shallow periodic fading Pattern was obtained. Depth of fading gradually decreased and ultimately the appearance pattern of the ordinary was obtained. At the time of appearance complex pattern is obtained which changes into a periodic Pattern having suprimposition of ripples.	The pattern is the appearance pattern of the ordinary and is preceded by the reception due to extra-ordinary ray. It indicates considerable spreading of energy as frequency of transmission recedes from M.U.F.
6	25	12.11.1966	0715 Hrs. IST	Transmissions from Karachi on 25 and 31 metres were going on at the time of observation. The signal was first received at 0715 Hrs. and after a short-while the appearance pattern of the ordinary is obtained.	The pattern is the appearance pattern of the ordinary and is preceded by the reception due to extra-ordinary ray.

CIRCUIT DIAGRAM OF FADING RECORDER

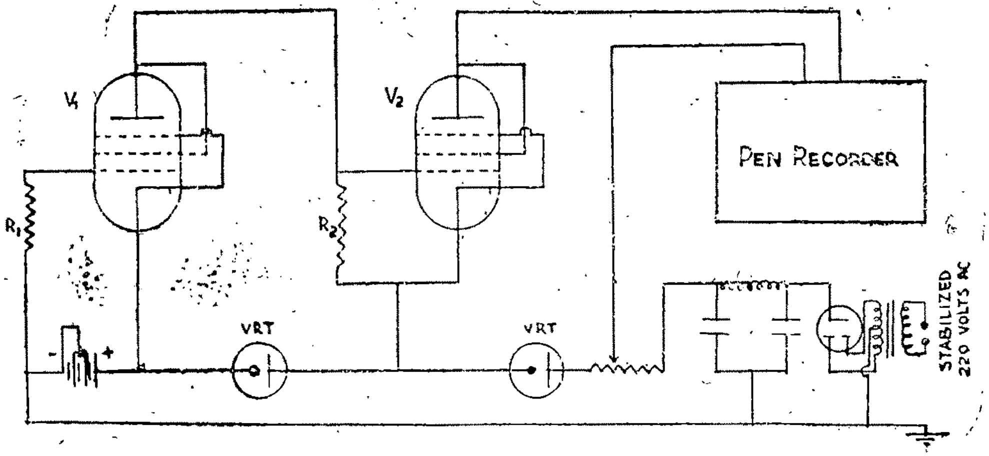

Fig. 1

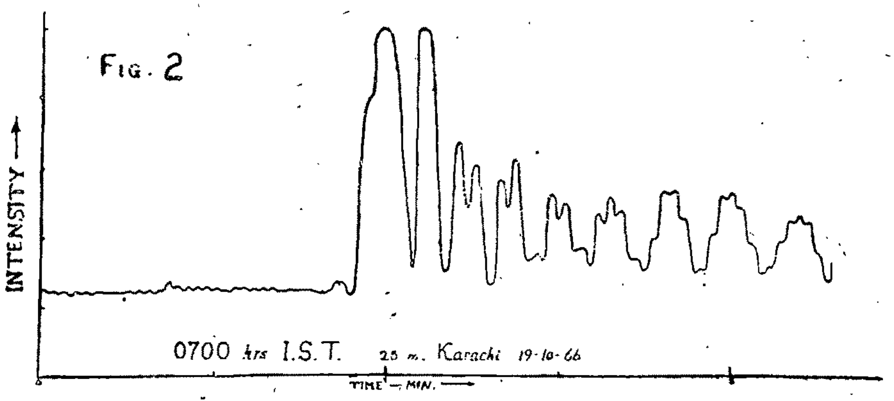

Fig. 2

0700 hrs I.S.T. 25 m. Karachi 19-10-66

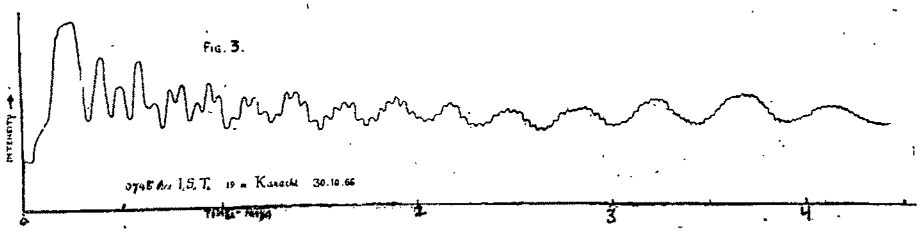

Fig. 3.

0745 hrs I.S.T. 19 m Karachi 30.10.66

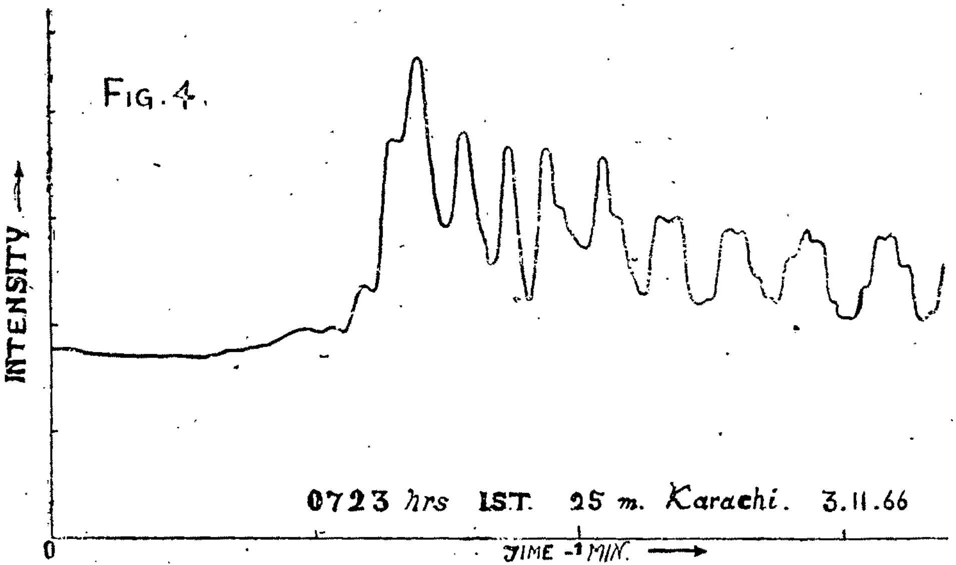
FIG. 4.

0723 hrs IST 25 m. Karachi. 3.11.66

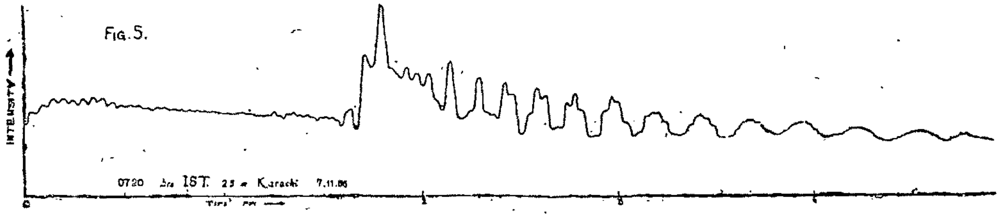
FIG. 5.

0720 hrs IST 25 m Karachi 7.11.66

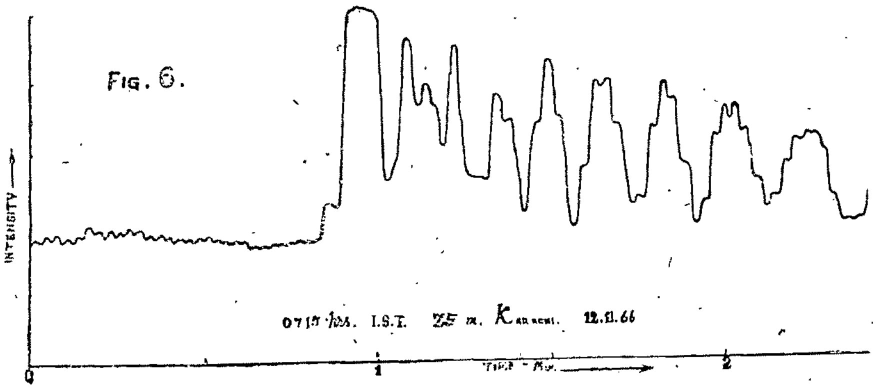
FIG. 6.

0715 hrs. I.S.T. 25 m. Karachi. 12.11.66

A NEW APPARATUS FOR THE MEASUREMENT OF THE RATE OF SYNERESIS BY SOAP GELS FORMED IN ORGANIC LIQUIDS, ALONG WITH A REVIEW OF PREVIOUS LITERATURE

MATA PRASAD AND R. C. SETH
Chemistry Department, St. John's College, Agra.

PREVIOUS LITERATURE

The rate of syneresis was first quantitatively measured by Holmes, Kaufmann and Nicholas[3] in the case of gels of silicic acid. In their method the same gel-forming mixture (water glass of 1·15 sp. gr. and 6N nitric acid) is poured into a plain test-tube and a test-tube of the same diameter vaselined on the inner side. On standing for 8—10 days the gel in the vaselined tube contracts so much that it can be taken out easily. Since syneresis varies directly as the free surface which increases when a gel contracts in vaselined tube, far more liquid separates out in this tube than from the same volume of the gel in the plain tube to which the gel adheres.

Pijper and Kraan[7] have determined the rate of syneresis of agar gels by making gels in a cylindrical form and placing them in a slightly larger cylinder; the liquid exuded by the gel falls into a measuring cylinder from which its volume is read directly at different intervals of time.

The rate of syneresis of geranin gels has been determined quantitatively by Lipatov[4] by a slightly different method. The gels are prepared in a separating funnel or a conical flask and are allowed to synerise for twenty hours. The liquid exuded is then removed by decantation and its volume measured. Later Lipatov[5] modified this method; the gels are prepared in glass cylinders and after the syneresis reaches its maximum, the contents are poured out on a perforated filter funnel and the volume of the filtrate is determined.

Mukoyama[6] has measured the syneresis of viscose gels by placing 20 ml. of its sol in a test-tube which is then sealed and placed in a constant temperature bath at 17°C. The sol sets and after syneresis becomes visible, the liquid exuded is measured by breaking the tube and pouring the synereticum into a measuring cylinder. After determining its volume, the liquid is poured back into the original tube which is then resealed and replaced in the bath. This operation is repeated at definite time intervals.

Prakash and Dhar[8] have measured] the syneresis by taking a known amount of jelly-forming substances in 80 ml. Jena glass conical flasks, and adding to it various amounts of electrolytes of concentrations suitable for the formation of jellies. The total volume is then made upto the same value by the addition of requisite amount of water. The conical flasks are well corked and sealed with wax in order to prevent the evaporation of water. The jellies are allowed to stand for a day or so and then the synerised liquid is carefully poured out into measuring tube graduated to one-tenth of a cubic centimeter. The volume is read correctly upto 0·05 ml. by eye estimation.

Ferguson and Applebey[2] have devised an apparatus (Fig. 1) for the measurement of the rate of syneresis of silica gels. It consists of a piece of burette tubing (A), graduated in 0·1 ml., sealed to a wide piece of glass tubing (B) connected at its lower end to a similar piece of tubing (C) by a narrow bore tube; the upper end of (C) is connected to a short opening tube (E) through a stopcock (D). Gels are prepared in (B) whose inner surface is coated with a thin regular film of petroleum jelly to avoid adherence of gels to the walls of the tube, and CCL_4 is filled in (C) and 3 or 4 cm. deep in (B).

50 ml. of silica sol is introduced in (B) where it floats on the surface of CCl_4 and after a time sets to a gel. At any time after setting, CCl_4 and the syneretic liquid are raised into (A) by blowing gently down (E) and the volume of the liquid exuded, is read to the nearest 0·01 ml. The whole liquid is then sucked back to the original position and the gel is allowed to synerise further. The above procedure, repeated at different intervals, gives the rate of syneresis.

Bonnell[1] has devised another apparatus (Fig. 2), called as synerometer, for measuring the rate of syneresis of silica gels. It mainly consists of two parts (A) and (B) connected to each other by ground glass joint (G) protected by mercury seal (S). (A) consists of a 4 cm. wide glass tube joined at its lower end to a narrow tube (T) carrying a glass stopcock (K) with a tapering bore, and (B) is a 1·2 cm. wide glass tube, graduated in 0·1 ml., and is provided with two capillary side tubes with mercury seal stopcocks (F) and (F′). (A) is closed by a ground glass cap (C) having a central hole (H) of 0·5 cm. diameter and a metal plate (P) having suspension hooks (X) and (Y), and both of them are protected by another cap (D) provided with mercury seal (E) which closes the system completely. A specially prepared filter cone (N) suspended in (A) from (X) by a fine nickel wire, carries the experimental syneretic gel. The whole apparatus is placed in a water-bath maintained at a constant temperature.

The silica gel is prepared in a cone identical in shape and size with the filter cone but with inner surface vaselined to prevent adhesion of the gel to the cone walls; it can be opened and by inverting on a glass plate, the contained gel can be easily removed. A gel-forming mixture is poured into this cone, and after setting, the gel is transfered to the cone (N), previously saturated with the syneretic liquid of the same gel. By attaching the hook (Y) to the beam of a balance, the cone and its contents are weighed at different intervals, and the loss in weight gives very accurately the amount of syneresis in a given time. The cone having been previously saturated with the syneretic liquid, does not retain any liquid exuded by the gel, with the result that the syneretic liquid filters through as it is formed and its volume measured in (B). No loss due to evaporation takes place as the whole apparatus is a closed system. Further, this apparatus permits the measurement of both the volume and the weight of the liquid synerised.

Prasad, Hattiangdi and Mathur[9] and Prasad and Sundaram[10] have measured the syneresis of sodium oleate gels in pinene by a different method. The gel-forming solutions, prepared in several test-tubes of the same internal diameters, are allowed to set in a thermostat. At regular intervals of time, a test-tube is removed from the bath, wiped till completely dry, then allowed to cool to room temperature, and weighed. Then the bulk of the exuded liquid is decanted out by slowly tilting the test-tube; the last traces of synereticum are removed by carefully introducing small rolls of filter paper vertically into the test-tube, and the rolls are changed when they get saturated with the synereticum. The introduction of filter papers is stopped when it is considered that no more exuded liquid remains in the test-tube which is weighed again. The loss in weight gives the amount of the liquid exuded in a given interval. Another test tube is used for the determination of the amount of syneresis in another interval in the same manner. The same method has been used by Seth and Khandelwal[11] to measure the syneresis of sodium oleate gels in a fraction of turpentine.

PRESENT WORK

The authors have designed a new synerometer for the accurate measurement of the rate of syneresis of sodium oleate gels in a fraction of turpentine, called as the liquid A by Seth and Khandelwal[11] who have also given its physical characteristics. The description of the apparatus and the technique of measurement of the amount of syneresis are given below:

(*a*) *Description of the synerometer:*

The synerometer, shown in Fig. 3, consists of an outer jacket (A) which can be closed at its upper end by a quick-fit stopper (B). The lower end of the jacket is connected to a microburette (C) graduated in 0·01 ml., the volume is readable upto 0·005 ml. by eye estimation. The lower end of the microburette is attached to a side-tube (E) having a bulb (F) at its upper end; (D) and (D′) are stopcocks. The jacket (A) carries a sintered glass crucible (H) of specification of Gl through which the synerised liquid passes out into the microburette without applying any pressure.

(*b*) *Preparation of the gels:*

For use in this apparatus gels of sodium oleate in the liquid A are prepared in Pyrex glass tubes, internal diameter 1·6 cm., in an apparatus shown in Fig. 4. One end of the tube (A) is closed by quick-fit stopper (B), and the other end is attached to a two feet long condenser (C) by a ground glass joint to prevent any loss of liquid due to evaporation. Sodium oleate is weighed out in the tube and 10 ml. of the liquid A and some quantity of mercury (D) are added to it, and the air condenser is placed in position. The tube is then placed in a constant temperature bath electrically heated to 140°C, and the contents are stirred from time to time until all the soap is dissolved. The air condenser is then removed and the upper end of the tube is tightly corked. The tube is then placed in an air thermostat maintained at a constant temperature. The solution in the tube sets to gel (J) on the top of mercury after some time.

(*c*) *Measurement of syneresis:*

Mercury is filled in the bulb (F) and set at zero in the microburette. The bed (I) of the crucible (H) is saturated with synerised liquid. After the gel sets in the tube (Fig. 4), the stopper (B) and mercury (D) are removed from the lower end and the gel (J) transfered to the sintered crucible; the set gel easily slides out of the tube. It is then covered by tube (K) of diameter slightly larger than the diameter of the gel, and the jacket is closed by (B). The synerometer is then kept in an air thermostat maintained at a constant temperature. The time of the transference of the gel is taken as the starting time for the measurement of the rate of syneresis. The liquid exuded by the gel drops in the microburette from which its volume is read directly at regular intervals of time.

Sodium oleate gels in the liquid A of concentrations below 2% are soft and hence they do not keep their stiff form on transfer from the tube to its position on (H). Hence gels of concentration above 2% which do not lose their form on transfer are used with this apparatus.

Some of the results obtained are summarised in table in which the following symbols have been used (cf. Seth[12]):

t=time at which the amount of syneresis was measured, in hours;
T=temperature at which gels synerised, in centigrade;
Q=weight of sodium oleate dissolved in 10 ml. of the liquid A, in grams.

Authors are thankful to Dr. P. I. Ittyerah, Head of the Chemistry Department, St. John's College, Agra for giving them all facilities and one of them (RCS) is thankful to the C.S.I.R. for awarding him the Research Fellowship, to carry out this investigation.

REFERENCES

1. Bonnell, D. G. R. 1932. *Trans. Faraday Soc.*, **28**: 1.
2. Ferguson, J. & Applebey, M. P. 1930. *Trans. Faraday Soc.*, **26**: 642.
3. Holmes, H. N., Kaufmann, W. E. & Nicholas, H. O. 1919. *J. Am. Chem. Soc.*, **41**: 1329.
4. Lipatov, S. 1927. Kolloid Z., **41**: 200.
5. Lipatov, S. 1927. Kolloid Z., **43**: 396.
6. Mukoyama, T. 1927. Kolloid Z. **42**: 79.
7. Pijper & Kraan, 1921. *Med. J. of S. Africa*, **16**: 221.
8. Prakash, S. & Dhar, N. R. 1930. *J. Indian Chem. Soc.*, **7**: 417.

9. Prasad, M., Hattiangdi, G. S. & Mathur, K. N. 1945. *Proc. Indian Acad. Sci.*, **21** A: 105.
10. Prasad, M. & Sundaram, V. 1951. *Proc. Indian Acad. Sci.*, **33**: 295.
11. Seth, R. C. & Khandelwal, J. K. 1962. *Agra v.. J. Res.* (*Sci.*), **XI** (2): 237.
12. Seth, R. C. *Ph. D. Thesis, Univ. Agra*, 1 !.

TABLE

Volume of Synerised liquid in ml.

t	T=50°		T=60°	
	Q=0·30	Q=0·40	Q=0·30	Q=0·40
0·25	0·060	0·035	0·055	0·030
0·50	0·100	0·065	0·090	0·050
1·00	0·180	0·105	0·160	0·090
1·50	0·240	0·140	0·230	0·120
2·00	0·280	0·170	0·265	0·140
2·50	0·320	0·190	0·300	0·155
3·00	0·350	0·210	0·330	0·165
3·50	0·385	0·225	0·365	0·180
4·00	0·425	0·235	0·380	0·190
4·50	0·445	0.245	0·400	0·200
5·00	0·455	0·250	0·410	0·210
5·50	0·460	0·255	0·420	0·215
6·00	0·465	0·260	0·425	0·220

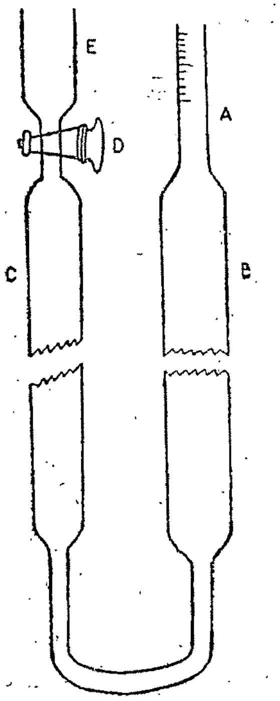

FIG. I.

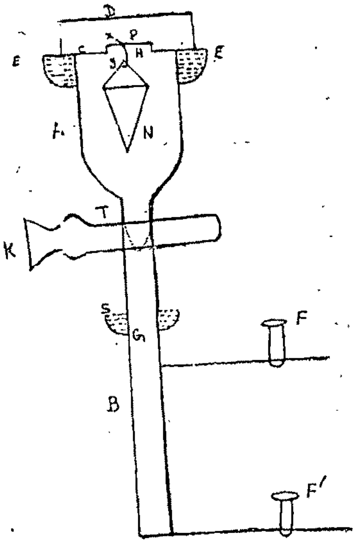

Fig. 2.

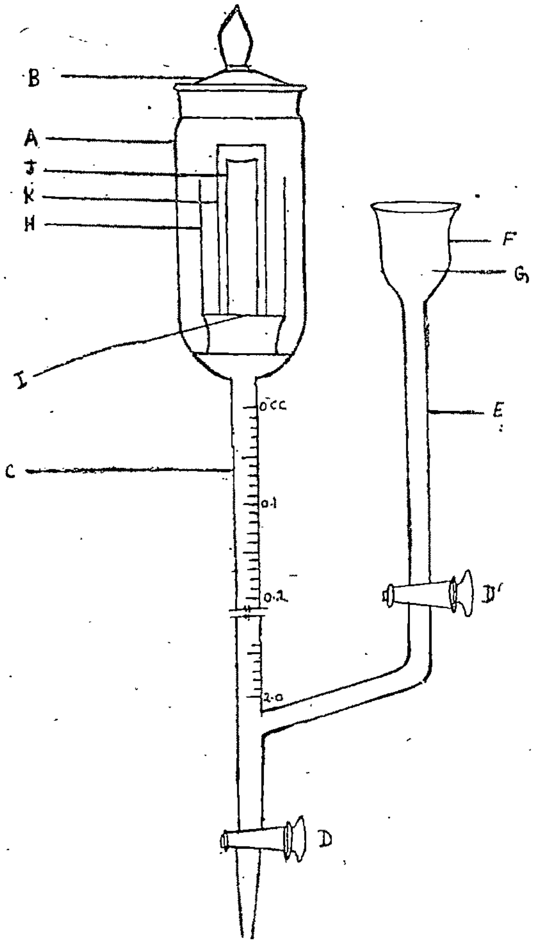

Fig.3

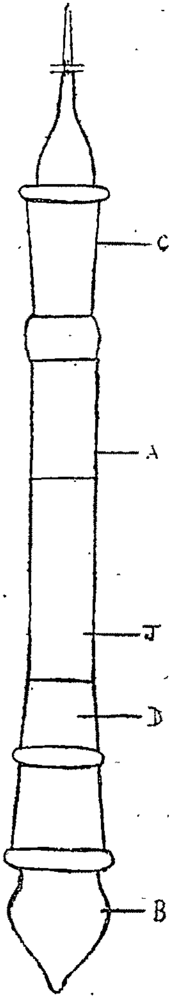

Fig. 4

REACTIONS BETWEEN AMMONIUM CHLORIDE AND AMMONIUM NITRATE IN SOLUTION AND CARBONATES OF MAGNESIUM, CALCIUM, STRONTIUM AND BARIUM

Kali Prasad Gupta[1]* and Suresh Singh†
Department of Chemistry, St. John's College, Agra.

The authors[2,3] have developed a method for the estimation of calcium and magnesium carbonates in their mixtures and in limestones, dolomite and calcareous materials on the basis of Cantoni and Goguelia's observations[1] that magnesium, calcium, strontium and barium carbonates, denoted as MCO_3, react with ammonium chloride in aqueous solution as

$$MCO_3+2NH_4Cl=MCl_2+2NH_3+CO_2+H_2O \quad \ldots(1)$$

and the reactions go to completion at the temperature of boiling water. One of the authors (K.P.G.) has found that these carbonates react with ammonium nitrate as well (see also Vecchiotti[4]) and the reactions go to completion at the boiling water temperature. Presumably these reactions take place as

$$MCO_3+2NH_4NO_3=M(NO_3)_2+2NH_3+CO_2+H_2O \quad \ldots(2)$$

This paper deals with the examination of the truth of equations (1) and (2), and the determination of a relation between the concentrations of NH_4Cl or NH_4NO_3 and the time needed for the completion of the two reactions at the boiling water temperature.

Experimental

(a) *Verification of equations (1) and (2)*

This was done by estimating the amounts of the CO_2, NH_3, and Mg^{++}, Ca^{++}, Sr^{++}, or Ba^{++} ions produced during the reactions.

(1) *Estimation of* NH_3 : A mixture containing 1·0 g. of dried magnesium, calcium, strontium or barium carbonate of A. R. quality, five times of its equivalent of NH_4Cl or NH_4NO_3, calculated according to equation (1) or (2), and 100 ml. of redistilled water, was heated in a round bottom flask to boiling until all the solid disappeared. The gases evolved were passed through a 5% solution of boric acid and the ammonia absorbed was titrated against N/40 solution of HCl.

(2) *Estimation of* CO_2 : In another experiment conducted in the same manner as above, the evolved gases were passed first through concentrated solution of H_2SO_4 and then through a baryta solution, and the amount of CO_2 was estimated by titrating the baryta solution against N/40 solution of HCl.

(3) *Estimation of* Mg^{++} Ca^{++}, Sr^{++} *or* Ba^{++} ions : The solutions left after the completion of the reaction were made upto 250 ml. 1·0 ml. of

---

1. Present address : * Kali Prasad Gupta, C/O Sri Kailash Nath Gupta, Cloth Merchant, Kannauj (Farrukhabad) U.P.
† Dr. Suresh Singh, RK., 54, Rohrabund, Sindri (Bihar).

these solutions was titrated against M/100 disodium salt of EDTA, using pH 10 buffer containing Mg salt of EDTA, and Erichrome Black T as indicator; the end point was indicated by the colour change from red to blue. The titre values were used to calculate the amounts of Mg^{++}, Ca^{++}, Sr^{++} or Ba^{++} ions in the whole solution.

The results obtained, given in Table 1, show that there is a good agreement between the observed and the expected values.

(*b*) *Effects of the concentration of* NH_4Cl *or* NH_4NO_3 *solutions on the time of completion of the reactions :*

For this purpose 1·0 g. of each of the carbonate and different amounts of NH_4Cl or NH_4NO_3 dissolved in 100 ml. of redistilled water were heated in a round bottom-flask and the time taken for the complete dissolution of the solid was noted; the total volume of the reaction mixture was kept constant (100 ml.) throughout the reaction. The results obtained are given in Tables 2 and 3 in which the following notations have been used:

a = amount in grams of NH_4Cl or NH_4NO_3 equivalent to 1·0.g. of each of the carbonate, according to equation (1) or (2),
b = amount in grams of NH_4Cl or NH_4NO_3 used, and
t = time in minutes taken for complete dissolution of the carbonate.

The curves obtained on plotting the values of b against t are shown in Figs. 1 and 2. These curves show that the time taken for the completion of these reactions decreases at first slowly and then rapidly as the concentration of NH_4Cl or NH_4NO_3 is increased.

It has been found that the relation between b and t can be represented by the following empirical equation :

$$t=K_1 . 1/(b-a)+K_2+K_3 (b-a)^3,$$

where K_1, K_2 and K_3 are constants. The values of these constants have been evaluated in individual cases and are given in Tables 4 and 5. These Tables also give the values of t calculated for several values of b along with the corresponding observed values of t read from grahps in Figs. 1 and 2 and bring out that the empirical equation reproduces the observed results very satisfactorily. This conclusion has been further emphasized by plotting the values of b and t (calculated), givin in Tables 4 and 5, on graphs in Figs. 1 and 2 which are seen to lie well on the observed b—t curves.

A comparision of the data given in Figs. 1 and 2 shows that a given quantity of Mg, Ca, Sr or Ba carbonate dissolves in the same quantity of NH_4Cl more quickly (in a shorter time) than in NH_4NO_3. Hence, whenever quickness in the estimation of Ca and Mg is desired, NH_4Cl instead of NH_4NO_3 should be used for bringing the Mg and Ca carbonates into solution.

SUMMARY

The mode of the chemical reaction between NH_4Cl or NH_4NO_3 and carbonates of magnesium, calcium, strontium or barium has been quantita-

tively studied, and an empirical relation between the time required for the completion of these reactions at the temperature of boiling water and the concentrations of solutions of NH_4Cl or NH_4NO_3 in g/100 ml., has been successfully evolved.

ACKNOWLEDGEMENTS

The authors are thankful to Dr. Mata Prasad, D. Sc., F.R.I.C., F.N.I., for suggesting the problem and his guidance throughout the investigation. They are also thankful to Dr. P. I. Ittyerah, Ph. D., F.R.I.C., Head of the Chemistry Department, St. John's College, Agra, for providing the facilities required for the investigation, to Mr. J. K. Ghosh, M. Sc., for assistance in the deduction of the empirical equation, and to U.P.C.S.I.R., and Ministry of Education respectively, for awarding them Research Scholarship.

REFERENCES

1. Cantoni & Goguelia; 1904 *Bull. Soc., Chem.* (3), **31** : 282; 1905. *ibid*, (3), **33** : 13.
2. Suresh Singh & Kali Prasad Gupta, 1963 *Agra Univ., Jour. of Res.* **XII**: 413.
3. Suresh Singh & Kali Prasad Gupta, 1964 *Z. analyt. Chem.* 206, **5**.
4. Vecchiotti, 1907. *Etude de l' action del nitrates alcalins sur le carbonatide baryum*, Geneva.

TABLE 1

Reaction Mixture taken	Ammonia		Carbon di-oxide		Mg^{++}, Ca^{++}, Sr^{++} or Ba^{++} ions	
	Found	Expected	Found	Expected	Found	Expected
1·0 g. $MgCO_3$+5·00 g. NH_4Cl	0·3998 g.	0·4032 g.	0·5193 g.	0·5219 g.	0·2873 g.	0·2884 g.
1·0 g. $CaCO_3$+4·28 g. NH Cl	0·3360 g.	0·3410 g.	0·4350 g.	0·4400 g.	0·3960 g.	0·4000 g.
1·0 g. $SrCO_3$+2·902 g. NH_4Cl	0·2350 g.	0·2300 g.	0·2970 g.	0·2970 g.	0·5900 g.	0·5940 g.
1·0 g. $BaCO_3$+2·168 g. NH_4Cl	0·1740 g.	0·1720 g.	0·2120 g.	0·2200 g.	0·7100 g.	0·6960 g.
1·0 g. $MgCO_3$+5·00 g. NHNO_3	0·4099 g.	0·4032 g.	0·5198 g.	0·5219 g.	0·2869 g.	0·2884 g.
1·0 g. $CaCO_3$+8·00 g. NH_4NO_3	0·3380 g.	0·3400 g.	0·4380 g.	0·4400 g.	0·3890 g.	0·4000 g.
1·0 g. $SrCO_3$+5·42g. NH_4NO_3	0·2250 g.	0·2300 g.	0·2960 g.	0·2980 g.	0·5960 g.	0·5940 g.
1·0 g. $BaCO_3$+4·052 g. NH_4NO_3	0·1760 g.	0·1720 g.	0·2250 g.	0·2250 g.	0·7060 g.	0·6960 g.

TABLE 2

Reaction with NH_4Cl

$MgCO_3$=1·00 a=1·268		$CaCO_3$=1·00 a=1·070		$SrCO_3$=1·00 a=0·725		$BaCO_3$=1·00 a=0·542	
b	t	b	t	b	t	b	t
1·600	27·0	2·140	193	1·500	152	1·084	198
1·900	17·5	2·675	143	1·813	120	1·900	87
2·540	12·0	3·210	110	2·176	103	2·981	50
3·175	10·5	3·500	90	2·902	70	3·253	44
3·810	9·5	4·280	73	4·353	56	4·336	23
5·080	8·0	5·350	60	5·804	43	6·504	18
6·300	7·5	6·420	54	8·706	36	8·672	16
9·525	6·5	7·490	50	11·608	23	10·840	12
15·240	5·0	8·560	47	13.421	20	13·008	6
		10·700	37	17·421	14		
		12·840	34	20·412	11		
		17·120	24				
		21·070	17				

TABLE 3

Reaction with NH_4NO_3

$MgCO_3=1\cdot00$ $a=1\cdot897$		$CaCO_3=1\cdot00$ $a=1\cdot60$		$SrCO_3=1\cdot00$ $a=1\cdot086$		$BaCO_3=1\cdot00$ $a=0\cdot812$	
b	t	b	t	b	t	b	t
2·124	45·00	3·200	300	2·171	110	1·624	54
2·381	25·00	4·000	220	3·256	70	2·436	33
2·057	17·00	4·800	175	3·500	60	3·249	25
3·810	13·00	6·400	120	4·342	54	4·000	22
4·762	11·50	8·000	90	5·000	47	5·000	19
6·667	9·75	9·600	75	6·513	42	6·480	16
8·572	8·50	11·200	54	8·684	34	8·000	14
12·882	7·00	16·000	35	15·197	22	9·746	13
16·000	5·50	19·200	27			13·000	10

TABLE 4
Reaction with NH_4Cl

$MgCO_3$=1·00 a=1·268 K_1=7·239 K_2=6·153 K_3=−0·00059			$CaCO_3$=1·00 a=1·070 K_1=186·900 K_2=18·000 K_3=−0·00130			$SrCO_3$=1·00 a=0·725 K_1=109·400 K_2=22·000 K_3=−0·00200			$BaCO_3$=1·00 a=0·542 K_1=103·800 K_2=3·000 K_3=−0·00270		
b	t cal.	t obs.	b	t cal.	t obs.	b	t cal.	t obs.	b	t cal.	t obs.
13·76	5·6	5·3	21·07	17·0	18·0	15·01	18·0	17·5	11·65	8·6	9·0
11·27	6·3	6·0	17·74	23·2	24·0	13·22	22·9	22·0	10·54	10·7	12·0
8·41	6·8	6·7	15·36	27·2	28·0	11·83	26·3	25·0	8·87	13·9	15·0
6·27	7·5	7·4	13·57	30·4	31·0	10·72	28·9	27·5	6·42	20·1	20·0
5·26	7·9	7·9	11·07	35·4	37·0	9·82	31·0	30·0	5·54	23·4	23·0
4·60	8·3	8·2	7·74	45·6	47·0	7·39	37·2	38·0	3·87	34·0	34·0
3·77	9·0	9·0	6·07	58·2	55·0	5·72	43·4	43·0	3·04	44·5	46·0
2·69	11·2	11·2	5·07	64·6	63·5	4·06	54·7	56·0	2·54	54·9	56·0
1·93	17·0	17·0	4·40	73·9	72·0	2·72	76·4	78·0	1·97	75·6	76·0
1·77	20·6	20·6	3·57	92·7	91·0	2·15	98·5	98·0	1·54	106·8	108·0
			3·07	111·4	111·0	1·72	131·4	130·0	1·37	127·5	128·0
			2·74	130·1	130·0	1·38	156·1	177·0	1·04	210·6	210·0
			2·49	148·8	149·0						

TABLE 5

Reaction with NH_4NO_3

$MgCO_3$=1·00– a=1·897 K_1=8·333 K_2=8·334 K_3=–0·00122			$CaCO_3$=–1·00 a=1·60 K_1=531·100 K_2=1·000 K_3=–0·00021			$SrCO_3$=–1·00 a=1·086 K_1=95·700 K_2=23·000 K_3=–0·00260			$BaCO_3$=–1·00 a=0·812 K_1=36·800 K_2=10·000 K_3=–0·00150		
b	t cal.	t obs.	b	t cal.	t obs.	b	t cal.	t obs.	b	t cal.	t obs.
14·40	6·60	6·25	21·60	25·8	24·0	15·39	22·0	22·0	13·31	10·0	10·0
11·90	7·95	7 25	11·60	52·20	50·0	11·09	30·0	29·0	10·81	12·2	11·5
8·56	9·22	8·75	8·20	80·6	84·0	6·09	40·0	41·5	5·61	17·4	17·0
6·90	9·84	9·50	5·60	134·0	137·0	3·95	56·5	56·0	4·14	21·0	21·0
5·90	10·33	10·25	4·10	213·0	212·0	3·31	66·0	65·0	3·31	24·7	25·0
4·39	11·65	12·00	3·60	266·0	260·0	2·75	80·4	80·0	2·81	28·3	28·0
3·89	12 50	12·75				2·09	119·0	120·0	2·06	39·4	39·0
3·32	14·17	14·25									
2·90	16·66	16·50									

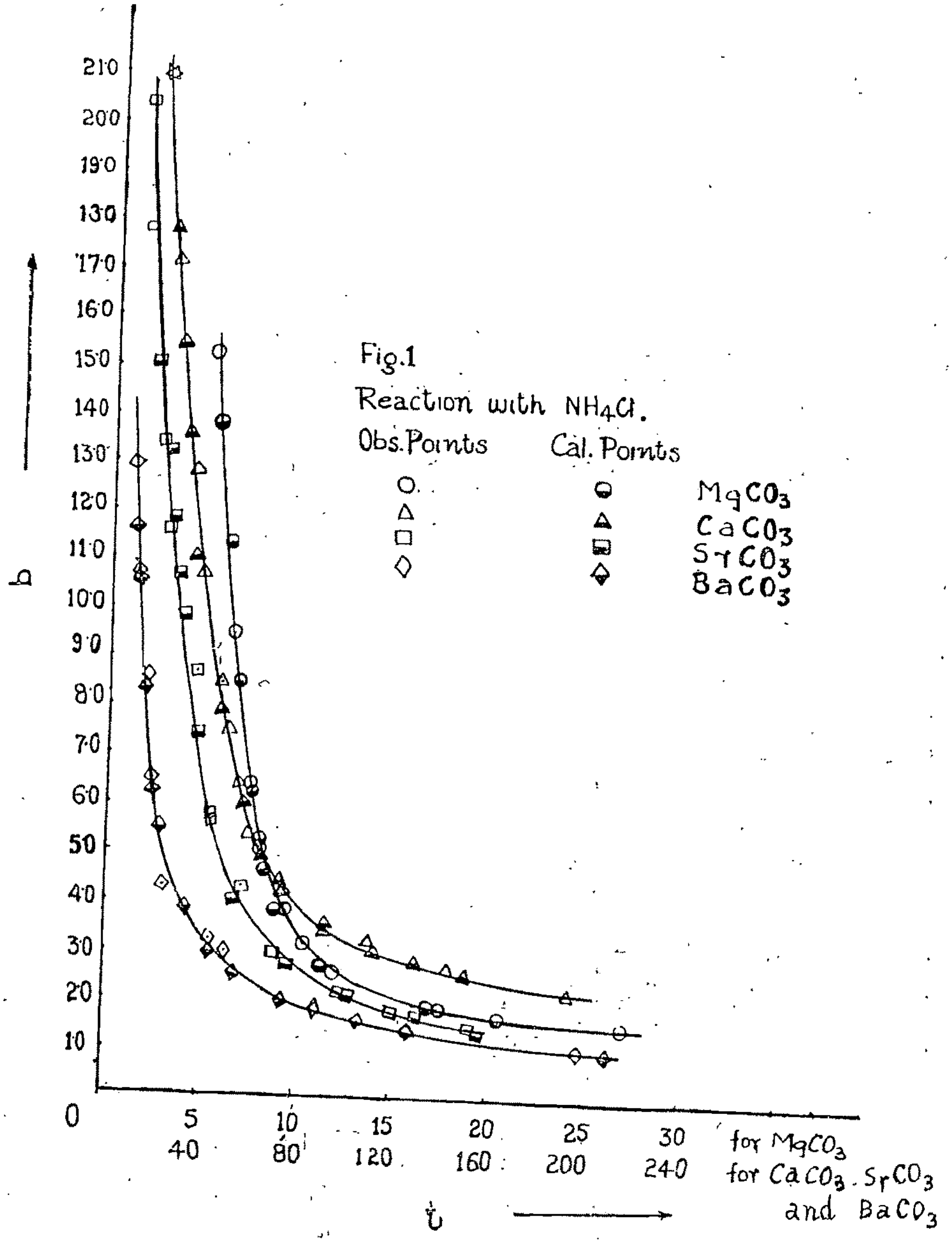

Fig.1
Reaction with NH_4Cl.

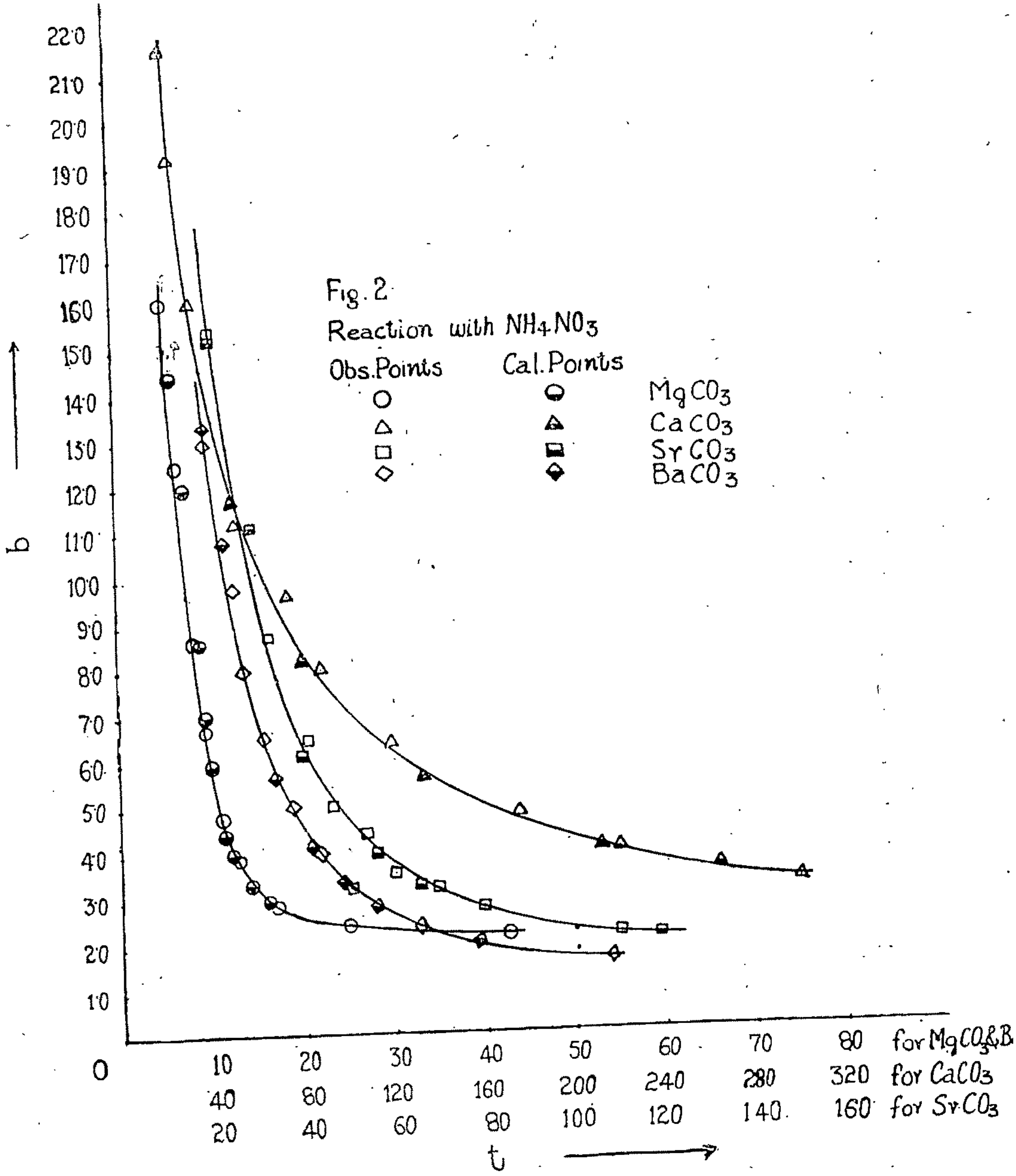

Fig. 2

Reaction with NH_4NO_3

Abstract of Theses

SYNTHETIC STUDIES IN THE CYCLO-OCTANE SERIES*

MAHESH PRAKASH
C/o Prof. G. S. SAHARIA,
Delhi University, Delhi.

The present investigations were undertaken with a view to compare the behaviour of the eight membered ring system with its lower analogues, work on which is being carried out by Saharia and his coworkers. The starting material was the difficulty accessible cyclo-octanone and the entire work carried out is described below.

The earlier part of the work deals with the synthesis of 1-carboxy cyclo-octane-1-acetic acid, its half ester anhydride and 1-phenacyl and substituted phenacyl cyclo-octane-1-carboxylic acids.

1-Carboxy cyclo-octane-1-acetic acid was prepared by the hydrolysis of the potassium salt of the dicyano ester, obtained by adding potassium cyanide to ethyl (—) cyclo-octylidene alpha-cyanoacetate; the latter ester was, however, prepared by condensing cyclo-octanone with ethyl cyanoacetate. The anhydride and the half-ester of 1-carboxy cyclo-octane-1-acetic acid were prepared in the usual way. The condensation of the anhydride with benzene, toluene, o-xylene, m-xylene, chlorobenzene and anisole under the conditions of Friedel and Crafts' reaction gave the respective keto acids; attempts to reduce the keto acids did not succeed.

Synthesis of cyclo-octane-1, 1-dicarboxylic acid was attempted with an idea to isolate the different isomers if any, due to different configurations of the ring by damping down the oscillations, and free rotations of the molecule by introducing electrical, and steric interferences; but the attempts did not materialise. This work was extended to the synthesis of cyclo-octan-1-one-2-carboxylic acids and cyclo-octan-1-ol-2-corboxylic acids.

Ethyl cyclo-octan-1-one-2-carboxylate was prepared by the pyrolysis of cyclo-octan-1-one-2-glyoxalate, the latter was prepared by reacting cyclo-octanone with ethyloxalate in presence of sodium ethoxide.

The condensation of ethyl cyclo-octan-1-one-2-carboxylate with different halo-esters furnished the corresponding diesters which on subsequent hydrolysis gave the respective keto acids. The reduction of these keto acid was carried out with sodium borohydride when in all cases, except cyclo-octan-1-one-2-acetic acid and cyclo-octan-1-one-alpha-methyl-2-acetic acid, hydroxy acids were obtained. These two acids, however, furnished the corresponding lactones thus leading us to conclude that the hydroxy acids were the cis-isomers.

---

* Abstract of the thesis on which Ph. D. degree has been awarded by this University.

The preparation of some cyclo-octane-alpha-substituted acetic acids was then taken up with an idea that these may be pharmacologically active like their cyclohexane analogoues. Side by side is also included the synthesis of alpha-cyclo-octyl succinic acid, which has been resolved into its optical isomers.

These acids were obtained by the hydrolysis of the respective ethyl cyclo-octyl-alpha-cyano-alpha-substituted acetates, these in turn were prepared by condensing ethyl cyclo-octyl-alpha-cyanoacetate with alkyl halides, aryl halides and haloesters in presence of sodium ethoxide.

Further work was taken up with the intention of studying the chemistry of 2-alkyl substituted cyclo-octanones and the stereo-chemistry of 2-benzyl cyclo-octanol.

The ketones were prepared by condensing ethyl cyclo-octan-1-one-2-carboxylate with methyl iodide, ethyl bromide, allyl iodide, and benzyl chloride in presence of sodium ethoxide and subsequent hydrolysis. 2 Benzyl cyclo-octanone on reduction with sodium borohydride furnished 2-benzyl cyclo-octanol confirmed through I. R. to be the cis-isomer.

Later, the syntheses of 1-arylaminocyclo-octane-1-cyanides, 1-arylamino-cyclo-octane-1-carboxylic acid amides and 1-aryl-aminocyclo-octane-1-carboxylic acids were carried out with an idea of preparing some spiro compounds which may throw some light on the configuration of the ring. 1-Arylamino-cyclo-octane-1-cyanides were prepared by condensing cyclo-octanone with various arylamines in presence of glacial acetic acid and potassium-cyanide. Their hydrolyses in two stages furnished the acid amides and the carboxylic acids respectively. Attempts to cyclise the carboxylic acids to the indoxyl-spirocyclo-octanes did not succeed and in this behaviour it resembled the cycloheptane ring.

Finally, the syntheses of condensed ring systems (i) substituted 1, 4 and 1, 2-quinolones and (ii) substituted pyrrol-2-ones are described. This work was taken up with the object of studying the reaction of ethyl cyclo-octan-1-one-2-carboxylate with arylamines at room temperature and at 180-90° and compare the behaviour of the β-keto esters, ethyl cyclonpenta 1-one and ethyl cyclohexan-1-one-2-carboxylates. Condensations at room temperature indicated that the cyclo-octane ring behaved like the lower rings. The reactions at high temperature were carried out for three minutes and there only one product was encountered, while conflicting observations have been made by other workers when similar condensations were carried out with ethyl cyclopentan-1-one-2-carboxylate and ethyl cyclohexan-1-one-2-carboxylate.

The 1, 4-quinolones were prepared by the cyclisation of the respective anils obtained by reacting aromatic bases with ethyl cyclo-octan-1-one-2-carboxylate at room temperature. The 1, 2-quinolones were synthesised from the anilides which were prepared by condensing ethyl cyclo-octan-1-one-2-carboxylate with primary aromatic amines at 180-90°.

Cyclo-octan-1-one-2-acetic acid on condensation with various aromatic amines at high temperature gave 1-aryl 2 : 3-dihydro-4 : 5-hexamethylene pyrrol-2-ones.

CHEMICAL EXAMINATION OF LITSEA CONSIMILIS AND FRAXINUS FLORIBUNDA*

KANAYA LAL DHAR†
Chemical Laboratories, Th. D. S. B. Govt. College, Naini Tal.

The present work deals with the chemical examination of two medicinal plants of Kumaon region, *Litsea consimilis* and *Fraxinus Floribunda*, with special reference to the study of Fats and Oils, Alkaloids and Glycosides.

LITSEA CONSIMILIS

(*a*) *Fats and Oils*—The seeds when extracted with pet. either (40-60) gave a dark brown oil with characteristic smell, which was purified by the usual methods.

The physical and chemical characteristics of the oil are as given below :

1.	Yield of the oil	50%
2.	Specific gravity (30°C)	0·8942
3.	Refractive Index	1·4520
4.	Acid Value	4·18
5.	Iodine value (Hanus Method)	9·40
6.	Saponification value	244·70
7.	Saponification equivalent	229·30
8.	Ester value	240·52
9.	Acetyl value	17·578
10.	Hehner value	96·5%
11.	Reichert-Meisel value	5·87
12.	Unsaponified matter	1·55%
13.	Percentage of Lauric acid	93·13%
14.	Percentage of Oleic acid	5·32%

Though the main constituents of the component fatty acids, as observed were Lauric and Oleic acids, yet some traces of other component acids were also detected by reverse phase paper chromatography. As such following fatty acids were detected on paper (Whatman No. I) impregnated in 12% solution of Olive oil in toluene and developed with 75 per cent alcohol for 48 hrs, (descending type).

	Component acids	*Rf. Value*
1.	Lauric acid	0·49
2.	Oleic acid	0·19
3.	Linoleic acid	0·26
4.	Myristic acid	0·39
5.	Unidentified acid	0·66

---

* Abstract of the thesis on which Ph. D. degree has been awarded by this University.

† Present address—Senior Research Fellow, Regional Research Laboratory, Canal Road, Jammu-Tawi, (J.&K. State).

Trilaurin m.p. 45° was also directly obtained by cooling the alcoholic solution of the oil.

B-sitosterol m.p. 37° was isolated from the unsaponified matter.

(*b*) *Alkaloid*—The petroleum-ether extracted residue of seeds and bark of *Litsea consimilis* was extracted with chloroform and ethanol separately. Both the extracts on usual processing for alkaloids furnished a colourless base, crystallised from acetone (to which a drop of water was added) in needles m.p. 125°.

The base $C_{19}H_{21}NO_4.H_2O$ yielded crystalline hydrochloride m. p. 245°, oxalate m. p. 233°, picrate m. p. 147° dibenzoyl m. p. 169°, thiocarbamide m.p. 154°, dimethyl-methiodide m. p. 209° and dimethyl-methine-methiodide m.p. 276°.

On alkaline $KMNO_4$ oxidation 1 : 2 dimethoxy benzene, 3 : 4 : 5 tricarboxylic acid $C_{11}H_{10}O_8$ m. p. 165°. The base was thus identified as Laurotetanine $C_{19}H_{21}NO_4$. H_2O m.p. 125°.

FRAXINUS FLORIBUNDA

The alcoholic extract of the bark of *F. floribunda* after processing for glycosides, furnished a colourless, non-fluorescent glucoside $C_{15}H_{19}O_9$ m. p. 210°.

The compound when boiled with mineral acids yielded an aglucone $C_9H_6O_4$ m.p. 265-70°. The aglucone which responded to all coumarin tests, formed crystalline diacetyl m.p. 130-31°, benzoyl m. p. 185°, 7-monomethyl ether m.p. 186° and 6 : 7 dimethyl ether m.p. 142°. On alkaline $KMNO_4$ oxidation 2 : 4 : 5 trihydroxy benzoic acid m. p. 217° and on HNO_3 oxidation oxalic acid was obtained.

The spectral data, Rf. value and mixed melting point with authentic sample alongwith the above data confirmed the identity of the aglucone as Aesculetin $C_9H_8O_4$ m.p. 265-70° and that of the glycoside as Cichorin $C_{15}H_{19}O_9$ m.p. 210°. Cichoriin has been previously isolated from the flowers of *Cichorium intybus*.

Besides, Cichoriin, Aesculin $C_{15}H_{19}O_9$ m.p. 201° and Fraxin $C_{16}H_{21}O_{10}$ m.p. 205° the two fluorescent glycosides were also isolated and identified.

BIOLOGICAL AVAILABILITY OF CALCIUM IN GROWING RUMINANTS FROM INDIAN FEEDS*

B. L. Agrawal
Professor of Chemistry, B. S. A. College, Mathura.

An attempt has been made to study the availability of calcium from Indian feeding stuffs that are specially rich in this mineral with young ruminants during the active period of growth.

It is not a difficult affair to prepare a low calcium basal diet with rats and human beings. With cattle, however, the construction of such a diet is undoubtedly beset with many practical difficulties. It is realized that without such a diet it should not be possible to study the availability of calcium. The diet must be otherwise adequate and supply sufficient nutrients for the growth of the ruminants except calcium and at the same time must be palatable to them. After some preliminary trials it has been observed that a diet consisting of 80 per cent low calcium maize and 20 per cent low calcium groundnut-cake should meet the requirement. But since concentrate alone can not constitute the sole diet of ruminants, small quantity of low calcium wheat bhoosa was supplemented to help the peristaltic movement. The total intake of calcium when such a feed was fed varied from 2·55 to 3·20 grams and the balance +0·16±0·13 gram, thus creating an ideal condition for studying the availability of calcium from different feeding stuffs. In addition to calcium, balances of phosphorus, magnesium and nitrogen have also been determined. The plane of nutrition of the experimental animals has been worked out from the average digestibility data obtained under these feeding conditions. The average digestibility of dry matter, crude protein, ether extract, crude fibre, nitrogen-free extract and total carbohydrate was found to be 63·47±2·14, 64·06±1·16, 79·48±2·24, 21·81±2·61, 72·44±1·83 and 73·28± 1·21 per cent respectively. It has been observed that except crude fibre, the digestibility coefficients of other nutrients are not effected at such a low intake of calcium from the basal diet. The average balance of phosphorus, magnesium and nitrogen was quite satisfactory. Having devised with this low calcium basal diet, calcium was supplemented in quantities required to obtain normal growth from various Indian cattle feeds with a view to testing their biological availability.

The calcium rich Pipal (Ficus religiosa) and Burgad (Ficus benghalensis) leaves were selected for determining the availability of calcium, because these are easily available to the farmers. Moreover, these leaves are extensively fed to cattle in our country. It has been observed that on an average intake of 14·39 grams of calcium from pipal leaves, the average balance of the mineral was +6·31±0·675 grams. The balances of phosphorus, magnesium and nitrogen were found to be quite satisfactory. The average digestibility coefficients as determined by conventional procedure with respect to dry matter, crude protein, ether extract, crude fibre, nitrogen-free extract were 70·51±2·24, 67·99±0·68, 65·65±4·33, 57·14±1·68, 75·18±2·62 and 73·33±2·48 respectively.

---

* This is an abstract of the thesis on which Ph. D. degree has been awarded by the Agra University.

The study with Burgad leaves at a little lower intake of 10·69 grams showed on average a positive balance of 4·48±0·20 grams. These investigations further showed that the availability of calcium from pipal and burgad was 55·3 and 52·7 per cent respectively, indicating thereby that these tree leaves are as efficient a source of calcium as any other. The balances of mineral elements phosphorus, magnesium nitrogen and the digestibility coefficients of organic nutrients were found to be quite satisfactory.

Since legumes are highly favoured as a source of calcium, systematic study has been made with two important green legumes, Cowpea (Vigna Catiang) and Berseem (Trifolium Alexandrium), and their availability compared with tree leaves to further confirm the potentiality of the tree leaves as a source of calcium supplement. On an average intake of 14·76 grams of calcium, the balance was 6·04±0·50 grams. Thus it was found that the availability of calcium from cowpea and tree leaves is of the same order. The average digestibility coefficients with respect to D. M., C. P., E. E., C. F., N. F. E. and total carbohydrates were found to be 69·86±1·36, 60·51±1·19, 64·49±1·99, 52·92±3·21, 76·61±1·34 and 73·62±1·34 respectively.

On an average intake of 12·52 grams of calcium in the case of green berseem the balance of 4·48±0·44 grams was obtained indicating thereby that as a source of calcium berseem is slightly inferior to burgad and pipal leaves and cowpea. The average digestibility coefficients with respect to D. M., C. P., E. E., C. F., N. F. E. and total carbohydrates were found to be 70·55±0·25, 73·69±1·32, 56·80±1·08, 72·68±2·57 and 70·90±2·20, respectively. The balances of mineral elements, phosphorus, magnesium and nitrogen in the case of both the legumes were found to be quite satisfactory for the growth of young ruminants.

The efficiency of utilization of calcium from an oil cake has also been studied. Although in general concentrates are very poor in calcium but til-cake is an exception, which contains about 2·7 per cent of the mineral on dry matter basis. On an average total intake of 15·18 grams of calcium, the balance recorded was +6·50 grams. Thus it has been observed that at the same level of total intake there appears to be no difference in the utilization of calcium from til-cake and pipal leaves, further confirming that these leaves are a valuable source of calcium. The balances of other mineral elements phosphorus, magnesium and nitrogen as also the digestibility coefficients of various organic constituents indicate that til-cake is an efficient feed and calcium supplement.

The availability of calcium from di-calcium phosphate and bone meal (tri-calcium phosphate) has also been the subject of detailed study, not only to determine their comparative efficiency, but also to study and investigate the comparative efficiency of calcium availability from organic and inorganic sources. It is quite interesting to note that on an average intake of 14·13 grams of calcium from dicalcium phosphate the balance was +6·17±0·42 grams *i. e.*, almost identical with other sources hitherto discussed. On an average intake of 14·89 grams of calcium from bone-meal the balance was 7·14±0·71 grams. The balances of the mineral elements phosphorus, magnesium and nitrogen were found to be quite satisfactory in both these tests. The average digestibility coefficients with respect to D. M., C. P., E. E., C. F., N. F. E. and total carbohydrate were found to be 70·16±1·89, 68·08+0·95, 72·10±1·64, 39·99±2·93, 79·59 ± 1·57 and 73·90±1·53 for dicalcium phosphate and 67·24±1·84, 68·89±0·74, 63·85±3·87, 36·36±3·97,74·53±1·24 and 69·62±1·69 for bone-meal.

These carefully conducted experiments in which calcium has been superimposed from feeds of various descriptions, *viz.*, tree leaves, leguminous roughages, concentrate and mineral salts on a low calcium basal diet according to the N. R. C. recommendation, therefore, tend to show that the availability of calcium is practically of the same order.

From these studies an attempt has been made to determine the calcium requirement of young Hariana calves from a comprehensive data of 106 metabolism trials. It has been observed that an intake of 13 to 15 grams of calcium fully guarantees an adequate calcium nutrition. Higher intake over this appears to be a waste and is of little consequence.

ORGANIC REAGENTS IN INORGANIC ANALYSIS WITH SPECIAL REFERENCE TO THE USE OF THE DERIVATIVES OF NAPHTHOQUINONES*

KESHAV CHANDRA HAJELA
113/340, Swarup Nagar, Kanpur.

The purpose of the present work has been to investigate the possibility of using 1, 2–naphthoquinone and some derivatives of 1, 4–naphthoquinone in qualitative detections and in gravimetric determinations of the metal ions. The following derivatives of 1, 4–naphthoquinone have been used :—

(1) Phthiocol (2 hydroxy–3 methyl–1, 4–naphthoquinone),
(2) Lawsone (2–hydroxy–1, 4–naphthoquinone),
(3) Lomatiol (2 hydroxy–(γ-methyl–γ hydroxy methyl allyl)–1, 4–naphthoquinone);
(4) Lapachol (2 hydroxy–3–γ–γ–dimethyl allyl–1, 4–naphthoquinone),
(5) Naphthazarin (5, 8–dihydroxy–1, 4–naphthoquinone),
(6) Juglone (5 hydroxy–1, 4–naphthoquinone),
(7) Plumbagin (2 methyl–5 hydroxy 1, 4–naphthoquinone), and
(8) 2 methyl-1, 4–naphthoquinone.

QUALITATIVE APPLICATIONS OF NAPHTHOQUINONES

1. *Phthiocol*—In aqueous alcoholic medium, Phthiocol forms coloured complexes with a number of metal ions. From analytical point of view, this quinone is highly sensitive towards the bivalent cation of lead and is fairly sensitive towards the bivalent cations of palladium, magnesium, calcium, nickel, beryllium, copper and cobalt, monovalent mercury and lithium and tetravalent vanadium and zirconium. Phthiocol can also be used to detect (*a*) beryllium in presence of aluminium, lanthanum, lithium, vanadium, barium, strontium, magnesium, zinc, cadmium, and bismuth, (*b*) zirconium in presence of beryllium, lanthanum, titanium, lithium and palladium, (*c*) calcium in presence of strontium, barium, cadmium, manganese, magnesium, aluminium, iron and nickel; (*d*) cobalt in presence of nickel, calcium and iron; (*e*) copper in presence of cadmium and iron; (*f*) palladium in presence of lanthanum and titanium; (*g*) calcium and lead and calcium and copper can be detected together. Moreover, phthiocol can also be used to detect selenious anions.

In glacial acetic acid medium also, phthiocol can be used as an analytical reagent for detecting monovalent copper, bivalent copper, nickel, cobalt, and palladium and trivalent aluminium and chromium. It is also possible to identify cobalt in presence of iron or nickel; copper in presence of cobalt or iron; and nickel in presence of aluminium.

---

* Abstract of the thesis on which Ph. D. degree has been awarded by the Agra University.

2. *Lawsone*—Lawsone shows colour reactions with a number of metal-ions. Sensitive tests have been discovered for bivalent cations of copper, magnesium, calcium, lead, cobalt and nickel and trivalent iron by using 50% ammonia solution along with lawsone. The reagent would also be a suitable analytical reagent for monovalent mercury, bivalent palladium and trivalent cerium.

3. *Lomatiol*—Lomatiol does form brightly coloured complexes with some metal ions but from analytical point of view, the reagent does not exhibit much analytical value. It can find a limited use for distinguishing calcium from magnesium and cobalt from nickel.

4. *Lapachol*—Lapachol forms coloured complexes with various metal ions but the sensitivity of the reagent is not of good order. It is fairly sensitive towards lithium and its sensitivity towards monovalent silver, bivalent copper, lead, and palladium, trivalent lanthanum and tetravalent zirconium may be considered tolerably satisfactory.

5. *Naphthazarin*—In aqueous medium, naphthazarin displays its high capacity to form brightly coloured metal-complexes with almost all the metal-ions. From analytical point of view, this versatile reagent is very sensitive towards zirconium, aluminium, beryllium, palladium (in Conc. HCl), nickel, calcium, cobalt, manganese, magnesium, lanthanum, cerium (III) and lead (II). It can also be used to detect *aluminium* in presence of beryllium; *zirconium* in presence of beryllium, lanthanum, vanadium, titanium, lithium, manganese, cerium, and selenious anions; *beryllium* in presence of lithium, lanthanum, magnesium, calcium, zinc, cadmium, manganese and selenium; *lanthanum* in presence of tetravalent cerium and bivalent lead, magnesium, calcium, strontium barium, zinc, cadmium and manganese; *lithium* in presence of manganese and palladium; *iron* in presence of palladium; and *palladium* in presence of lanthanum. It is an excellent analytical reagent for zirconium, aluminium, beryllium, palladium, nickel, calcium, manganese, cerium (III) and selenium.

In glacial acetic acid medium, naphthazarin is extremely sensitive towards aluminium, beryllium, zirconium and palladium. In this medium, it provides distinguishing tests for (*a*) trivalent and tetravalent cerium, (*b*) monovalent and bivalent copper, (*c*) bivalent cobalt and nickel. Moreover, *beryllium* can be tested in presence of strontium and barium both of which interfere in aqueous medium; *copper* can be tested in presence of bivalent cations of nickel, cobalt, manganese, calcium and strontium; *cobalt* can be tested in presence of bivalent nickel, calcium, manganese, and trivalent iron; *aluminium* can be tested in presence of silver, magnesium, calcium, cadmium, palladium and bismuth; *silver* can be tested in presence of magnesium and calcium; *beryllium* can be tested in presence of lithium, lanthanum, zirconium bismuth, strontium, barium and silver; and palladium can be tested in presence of beryllium.

6. *Juglone*—In aqueous medium, Juglone forms coloured complexes with a number of metal ions. From analytical point of view, juglone is highly sensitive towards zirconium, palladium, nickel, vanadium (in HCl), and fairly sensitive towards cobalt, manganese, magnesium, copper, calcium and trivalent iron.

In Acetone medium, juglone produces sensitive colour reactions with copper, magnesium, cobalt and iron (III).

7. *Plumbagin*—In aqueous medium, plumbagin forms coloured complexes with common metal ions. Its sensitivity is fairly good towards aluminium and cobalt and sufficiently sensitive towards bivalent nickel, manganese, zinc, copper, and magnesium and trivalent iron. It will be a good reagent for distinguishing magnesium from calcium; zinc from manganese and nickel from cobalt.

8. *1, 2-naphthoquinone*—This quinone forms coloured complexes with the cations of monovalent copper and silver, bivalent copper, tin, cobalt and nickel and trivalent iron in glacial acetic acid medium at 0°C. The sensitivity of the colour reactions is poor and it may be used for detecting monovalent and bivalent copper and for distinguishing between cobalt and nickel. In aqueous medium also it is fairly sensitive towards bivalent copper and can be used to distinguish between cobalt and nickel.

9. *2 methyl 1, 4-naphthoquinone*—In glacial acetic acid medium at zero degree centigrade, this quinone indicates complex formation with the salts of monovalent capper, bivalent copper, cobalt, nickel, and palladium and trivalent chromium and iron. The sensitivity of the reagent is very poor but it may be used for detecting monovalent and bivalent copper and also for distinguishing nickel from cobalt. In ethyl alcoholic medium, this quinone forms a light green complex with bivalent copper.

GRAVIMETRIC DETERMINATIONS AND COMPOSITIONS

Phthiocol is an excellent precipitant for bivalent lead and very accurate results are obtained if the concentration of lead in the salt solution is one mg. or more per c.c. The scarlet red complex is quickly precipitated at low temperatures, easily filtered, washed and dried between 75—85°C. The ratio of the phthiocol molecules to the lead atom in the complex has been found to be in the ratio of 2 : 1 and hence the molecular formula would be $(C_{11}H_7O_3)_2\,Pb$.

Phthiocol is also a good precipitant for bivalent copper from solutions containing at least 0·8 mgs. of copper per cc. of the solution kept at 0°C.

The brick red precipitate is easily filtered, washed and dried at 60-70°C. In the metal-complex, the ratio of bonding of the phthiocol molecules to the copper atom has been found to be 2 : 1 and hence the molecular formula of the complex would be $(C_{11}H_7O_3)_2\,Cu$.

Juglone together with 40% ammonia solution can be used for the gravimetric determination of tetravalent zirconium from solutions containing 2 mgs. of zirconium per c.c. of the solution. The precipitation has been done in an ice-bath at zero degree centigrade and the brownish maroon coloured precipitate has been dried at 75-85°C., and ignited to zirconium dioxide which is then weighed.

Naphthazarin together with 40% ammonia solution has been used for the gravimetric determination of tetravalent zirconium from the salt solution containing at least 1·5 mgs. of zirconium per c.c. of the solution. In this case also the precipitation has been done in an ice bath and the purple coloured precipitate has been washed, dried between 60-70°C., and ignited to zirconium dioxide which is then weighed.

Besides the determination of the compositions of lead-phthiocol and copper-phthiocol complexes, the compositions of lanthanum-naphthazarin complex $(C_{10}H_5O_4)_3\,La$, zirconium-naphthazirin complex $(C_{10}H_5O_4)_4\,Zr$, cadmium-plumbagin complex $(C_{11}H_7O_3)_2$ Cd, nickel-lapachol complex $(C_{15}H_{13}O_3)_2$ Ni, cobalt-lomatiol complex $(C_{15}H_{13}O_4)_2$ Co, Ceric-lawsone complex $(C_{10}H_5O_3)_4$ Ce magnesium-lawsone complex $(C_{10}H_5O_3)_2$ Mg, cadmium-lawsone complex $(C_{10}H_5O_3)_2$ Cd, nickel-phthiocol complex $(C_{11}H_7O_3)_2$ Ni and zirconium-phthiocol complex $(C_{11}H_7O_3)_4$ Zr have also been determined.

Mechanism of reaction—The hydroxy-naphthoquinones are believed to behave as weak acids which yield univalent anions of the weak acids. The complex formation by these compounds is, therefore, essentially a reaction between a cation and an univalent anion and can be represented as :

$$M^{+n} + n(LH) = ML_n + nH^+$$

where M represents the metal ion of valency 'n' and (LH) stands for the molecule of the hydroxy naphthoquinone. The univalent anions of these quinones form 4-co-ordinated complexes of the type MX_2 with bivalent cations, 6-co-ordinated complexes of the type MX_3 with trivalent cations and 8 co-ordinated complexes of the type MX_4 with tetravalent cations of co-ordination number 8; here M stands for the metal atom and X stands for the organic anions. These metal-quinone complexes contain two or three or four ring systems. Phthiocol, Lomatiol, Lapachol and Lawsone form metal complexes which contain two or more five membered rings whereas Juglone, Plumbagin and Naphthazarin form metal complexes containing two or more six membered rings.

Comparative reactivity and sensitivity—It has been found that naphthazarin has a superior sensitivity and reactivity towards various metal ions followed by phthiocol, juglone, lawsone, plumbagin, lapachol and lomatiol so that lomatiol is the least sensitive. As between 1, 2-naphthoquinone, which acts as a bidentate chelating agent and 2 methyl-naphthoquinone, which acts as a mono dentate chelating agent, the former is comparatively more reactive than the latter.

CHEMICAL INVESTIGATION ON THE STRUCTURE OF COMMIPHORA MUKUL GUM AND OTHER PLANT GUMS*

K. C. Gupta

Deptt. of Organic Chemistry, National Sugar Institute, Kanpur.

Isolation and Purification of C. Mukul Gum :

C. Mukul, Hook ex stocks is the source of a gum-resin commonly known as "Guggul" which is well known for its number of uses in indigenous medicine. The present investigation discusses in detail the isolation, purification and composition of the gum occurring in *C. Mukul* gum-resin. Deresinification of *C. Mukul* gum-resin was carried out by extraction with hot ethanol and the powdered resin free crude gum was purified by repeated precipitation from its aqueous acidic solution with ethanol. It was finally purified by treatment with freshly regenerated cation exchange resin Duolite C-25. The pure gum acid on analysis was found to contain sulphated ash, 0·15 ; pentosans, 19·5 ; pentoses, 22·13 ; furfural (estimated as phloroglucide), 11·14 ; methoxyl, 2·17 per cent ; equivalent weight (by direct titration), 1482. Nitrogen, halogens and sulphur were found to be absent.

Homogeneity of the gum :

Homogeneity of the gum was established by the fractional precipitation with ethanol which resulted in three samples. Quantitative hydrolysis of the three gum samples was done and estimation of sugars released was carried out by oxidising with sodium metaperiodate. The result of the analysis showed that the gum was homogenous in character.

Autohydrolysis of the gum :

Autohydrolysis of the gum was carried out by heating the aqueous solution of the gum on a boiling water bath for 80 hours. The autohydrolysate on being worked up was separated in fraction A consisting of neutral sugar mixture and fraction B consisting of the barium salt of the degraded gum. Cellulose column chromatography of fraction A yielded three crystalline components which were identified as D-galactose, L-arabinose and L-fucose.

Graded hydrolysis of degraded gum (Fraction B) :

Acid hydrolysis of fraction B resulted in the production of a neutral sugar identified as D-galactose and an aldobiouronic acid. Further acid hydrolysis of the aldobiouronic acid gave a neutral sugar characterised as D-galactose and an uronic acid identified as 4-0-methyl-D-glucuronic acid.

Complete hydrolysis of the gum:

Complete acid hydrolysis of the gum furnished a mixture of neutral sugars identified as D-galactose, L-arabinose and L-fucose and an uronic acid characterised as 4-0-methyl-D-glucuronic acid.

---

[*] Abstract of the thesis on which Ph. D. degree has been awarded by this University.

Quantitative hydrolysis of the gum and estimatian of galactose and arabinose ratio:

The molecular ratio of D-galactose and L-arabinose present in gum was estimated by carrying out quantitative acid hydrolysis of the gum. The liberated sugars were separated by paper chromatography and were estimated by oxidising with sodium metaperiodate and titrating the liberated formic acid. The results indicated that the two major sugars L-arabinose and D-galactose were present in the gum in the proportion of 1 : 3.

Structure of aldobiouronic acid:

The aldobiouronic acid upon reduction furnished a neutral disaccharide which after hydrolysis yielded two sugars identified as D-galactose and 4-0-methyl-D-glucose. To ascertain the nature and position of the D-galactose and 4-0-methyl-D-glucuronic acid, the aldobiouronic acid was fully methylated which upon hydrolysis yielded 2, 3, 4-tri-0-methyl-D-galactose and 2, 3, 4-tri-0-methyl-D-glucuronic acid in nearly equal amounts. The identification of the methylated sugars together with the specific rotation of the methylated aldobiouronic acid indicated that the aldobiouronic acid is 6-0-(4-0-methyl-β-D-glucopyranosyluronic acid)-D-galactose. The structure of aldobiouronic acid was finally settled by subjecting it to periodate oxidation which resulted in the consumption of 3·05 moles. of periodate with the liberation of 0·96 mol. of formic acid per equivalent of the aldobiouronic acid.

Structure of the degraded C. Mukul gum:

The degraded gum free from arabinose, was completely methylated and the methylated product upon methanolysis and further hydrolysis with aqueous acid furnished acidic and neutral sugar fraction. The acidic fraction was identified as 2, 3, 4-tri-0-methyl-D-glucuronic acid (3 moles.) and the neutral sugar fraction was found to consist of 2, 4, 6-tri-(1 mol.), 2, 3, 4-tri-(6 mols.) and 2,4-di-0-methyl-D-galactose (2 mols.). The isolation of the above acidic and neutral sugars from the methylated degraded gum indicates its branched character and also demonstrates that all the D-galactose and 4-0-methyl-D-glucuronic acid residues are of pyranose structure and are joined by 1—→6 and 1—→3 linkages. From these results it appears that the average repeating unit occuring in the degraded *C. Mukul* gum is composed of nine D-galactose and three 4-0-methyl-D-glucuronic acid residues. Thus a possible structure (I) for the repeating unit of the degraded C. Mukul gum has been suggested.

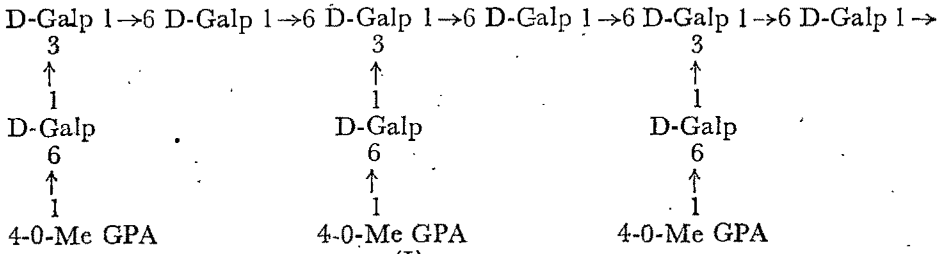

$$\begin{array}{cccccccccccc}
\text{D-Galp} & 1\rightarrow 6 & \text{D-Galp} & 1\rightarrow 6 & \text{D-Galp} & 1\rightarrow 6 & \text{D-Galp} & 1\rightarrow 6 & \text{D-Galp} & 1\rightarrow 6 & \text{D-Galp} & 1\rightarrow \\
3 & & & & 3 & & & & 3 & & & \\
\uparrow & & & & \uparrow & & & & \uparrow & & & \\
1 & & & & 1 & & & & 1 & & & \\
\text{D-Galp} & & & & \text{D-Galp} & & & & \text{D-Galp} & & & \\
6 & & & & 6 & & & & 6 & & & \\
\uparrow & & & & \uparrow & & & & \uparrow & & & \\
1 & & & & 1 & & & & 1 & & & \\
\text{4-0-Me GPA} & & & & \text{4-0-Me GPA} & & & & \text{4-0-Me GPA} & & &
\end{array}$$

(I)

For further confirmation of the structure (I) the degraded gum was subjected to periodate oxidation studies which resulted in the consumption of 5·38 mols. of periodate with liberation of 2·43 moles. of formic acid. The periodate oxidised gum consisting of 1——>3 linked galactopyranose residues furnished on hydrolysis 0·89 mol. of galactose per equivalent of the degraded gum. The above results are in good agreement with that required by the structure (I) proposed for the repeating unit of the degraded gum.

Structural features of the C. Mukul gum :

The general structural features of *C. Mukul* gum has been found out from the results of methylation experiment. The fully methylated gum was hydrolysed and the hydrolysate was separated into ether soluble fraction and ether insoluble fraction. The ether soluble fraction was fractionated on Whatman No. 3 MM filter paper sheets to give four components which were identified as 2, 3, 4, 6-tetra-0-methyl-D-galactose (3 moles.), 2, 3-di-0-methyl-L-arabinose (3 moles.), 2, 3, 4-tri-(3-moles.) and 2, 4-di-0-methyl-D-galactose (6 moles). The ether insoluble fraction was characterised as 2, 3, 4-tri-0-methyl-D-glucuronic acid (3 moles.). To accommodate all the types of linkages mentioned above, a provisional structure (II) for the repeating unit present in *C. Mukul* has been advanced after taking into consideration the structure of the degraded gum.

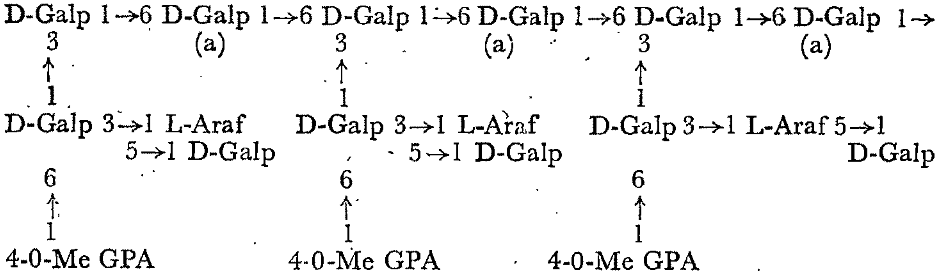

(II)

Galp = Galactopyranose Araf = Arabofuranose

4-0-Me GPA = 4-0-methyl—D—glucopyranosyluronic acid

The tentative structure suggested for the *C. Mukul* gum indicates that the gum is highly branched in nature and contains 1→6, 1→3 and 1→5 types of linkages. The highly branched character and the presence of 1→3 type of linkage is confirmed by periodate oxidation. Upon oxidation with sodium metaperiodate the gum yields 1·24 moles. of formic acid per equivalent of the gum with concomitant consumption of 6·05 moles. of periodate. Analysis of periodate oxidised gum showed that some of the galactose units have escaped oxidation.

SUBSIDIARY THESIS

Sugarcane Wax Part III. An examination of fatty lipid for sterols :

Fatty matter obtained by defatting crude sugarcane wax was saponified and the unsaponifiable portion on fractional crystallisation resulted in the production of sterol fractions whose melting points were observed to be in a long range of 8 to 10°. This demonstrated that the preparations were not homogenous. Direct chromatography over Brockman alumina also failed to resolve the mixture. Attempt was made to separate the stigmasterol from β-sitosterol by applying the classical method of Windaus and Hauth. The above two sterols were obtained in pure state in the yield of 13·37 and 5·60 per cent respectively from unsaponifiable portion of fatty matter.

Direct isolation of sterols from fatty matter by alcohol fractionation procedure was also attempted which furnished crude sterol mixture in an yield of 8·01 per cent. Crude sterol mixture was separated by the procedure described above and the yield of stigamasterol and β-sitosterol was estimated to be 0·69 and 2·66 per cent respectively. During alcohol fractionation of the fatty matter, a higher alcohol namely η-octacosanol was also obtained.